Investigating the heterogeneity of leukaemia kinase networks and the impact of the microenvironment on leukaemic cell signalling

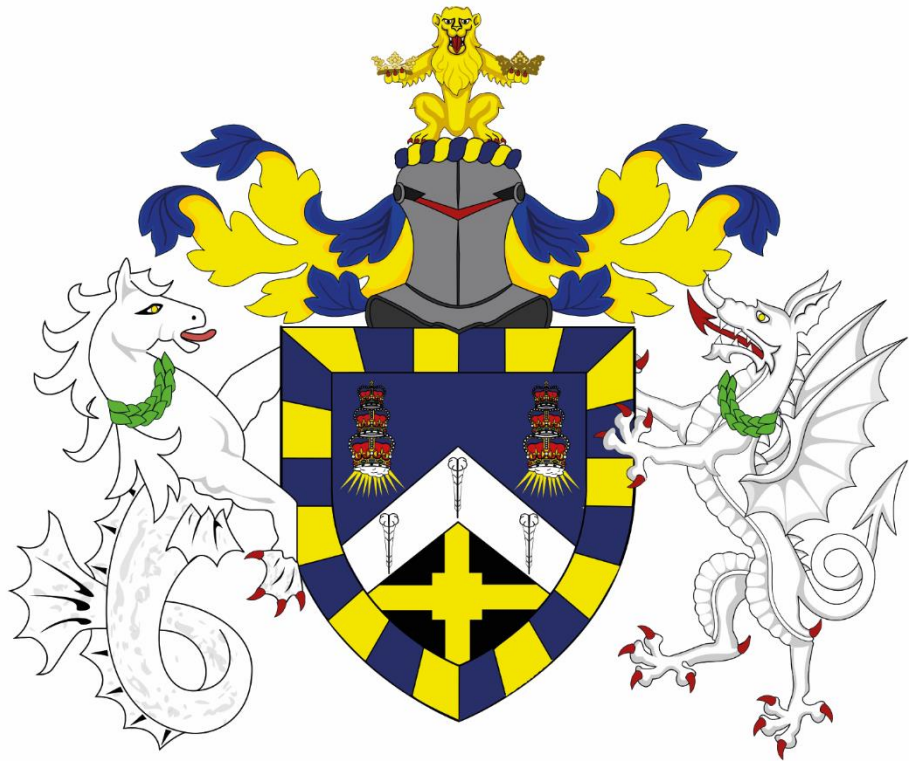

Queen Mary University of London

Barts and The London School of Medicine and Dentistry

Submitted in partial fulfillment of the requirements of the Degree of Doctor of Philosophy

Author: Arran D. Dokal

Principal Supervisor: Dr. Pedro R. Cutillas

Second Supervisor: Prof. John G. Gribben

Statement

I, Arran Dokal, confirm that the research included within this thesis is my own work or that where it has been carried out in collaboration with, or supported by others, that this is duly acknowledged below and my contribution indicated. Previously published material is also acknowledged below.

I attest that I have exercised reasonable care to ensure that the work is original, and does not to the best of my knowledge break any UK law, infringe any third party's copyright or other Intellectual Property Right, or contain any confidential material.

I accept that the College has the right to use plagiarism detection software to check the electronic version of the thesis.

I confirm that this thesis has not been previously submitted for the award of a degree by this or any other university.

Signature: 

Date: 28.12.2017

Details of collaboration and publications:

- The work presented in Chapters 3-5 of this dissertation is currently being submitted to Leukaemia for publication

- Work presented in this thesis has been selected for presentation at,

  9th European Summer School for Advanced Proteomics 2015 in Brixen
  21st European Hematology association congress 2016 in Copenhagen
  British society of proteomic research congress 2016 in Glasgow
  22nd European Hematology association congress 2017 in Madrid
  GTC European Pharma summit 2017 in Berlin

- Other work performed during the course of this research that has been selected for presentation,

  Vilventhraraja E, Edelmann J, Norster F, Braun A, Gribben JG, Cutillas PR and **Dokal A**. Sustained Reduction of Intracellular Calcium Is Important to Maximise GA101-Mediated Direct Cell Death in B-Cell Lymphomas. ASH2017, Abstract no1269.

- Other work performed during the course of this research has also been published,

  Dermit M*, **Dokal A*,** Cutillas PR. Approaches to identify kinase dependencies in cancer signalling networks. FEBS letters. 2017.

  ***** Joint first author

- This thesis has been typeset in 11pt, Calibri font and is 74,484 words (not including references).

Acknowledgements

I would like to thank the generosity of the Barry Reed charity for funding this research, which has provided me a platform by which to explore scientific ideas, while at the same time gain a myriad of new skills. It was also through this charity that I met a friend for life, Emma. We began and will finish our PhDs together, but also jointly established the current PhD forum, and held the position of Barts postgraduate research representatives on the student council. I would not have accomplished these achievements alone, thanks for all your support.

I was very fortunate to be part of a fantastic group of people and scientists, in no particular order I would like to acknowledge and thank Dave, Ed, Ryan, Maru, Pedro Casado, Vinni, Maria, Saul and Federico. I hope to professionally work with these individuals again.

The Haemato-oncology department has been a pleasure to work in, and I would like to thank all members past and present. It would be remiss though not to mention some specific individuals, for creating both great scientific debate and laughter. In no order I thank Rob, Emily, Ana, Hemalvi, Ateeq and Faith. Separate to this group I have to thank the 'coffee club' (Lily, Alex and Caroline) who provided many moments of respite from the trials of the lab, both with coffee or much needed trips to the pub.

Outside of the laboratory I have to mention the enduring support that my family has given me, they never let me get too carried away with anything and are always ready to ground me when required. I separately would like to acknowledge my Dad as he is someone that has always pushed me in life – especially in science. He has always reiterated the need for a strong work ethic and that at times you need to find the answer alone, lessons that I think have been invaluable during my PhD.

To conclude I would like to thank my supervisors, John Gribben for welcoming me into the department and for creating an environment with diverse minds that I feel have in ways influenced the way I undertook this project. Finally, and by no means least I would like to thank my friend and mentor Pedro Cutillas. From our first meeting he has always showed tremendous belief in me, providing the freedom and tools necessary to become the scientist that I am today. I feel truly privileged to have worked for Pedro and represented the Cutillas group. I hope that we shall continue to cross paths in the future.

I dedicate this work to my fiancée Laura who drives me to be the best that I can, while also being the perfect tonic to hard days in the lab.

Abstract

The tumour microenvironment plays a key role in tumour progression. In this thesis acute myeloid leukaemia (AML) was used as a model system to investigate the interplay between stromal and cancer cells. AML is a heterogeneous clonal disorder of haematopoietic undifferentiated progenitor cells or 'blast cells', which accumulate in the bone marrow and lead to the reduced output of crucial haematopoietic elements. Due to its heterogeneity (at least in part), treatment of the disease has not witnessed great innovation in the past 30 years. The bone marrow microenvironment (BMM) has a key role in the haematological malignancies contributing to the survival of leukaemic blasts. Relapse in AML occurs because of residual disease and evidence suggests that this resistance is facilitated through leukaemic cells ability to reside in BMM niches. To understand the precise role of the BMM in AML progression and therefore target any supportive mechanisms requires knowledge of how AML cells communicate with their microenvironment. In the work presented in this thesis I undertook a multi-proteomic approach that utilised liquid chromatography tandem mass spectrometry (LC-MS/MS) to assess the interplay between AML and BMM cell signalling.

This thesis shows the results of a secretomic analysis of stromal cell lines, which identified a previously uncharacterized panel of six stromal secreted proteins (BMP-1, CSF-1, CTGF, HGF, S100-A4 and S100-A11) that support primary AML cell survival and proliferation in culture. Comparison of AML cell signalling (using global phosphoproteomic methods) following treatment with the newly identified growth factors revealed that these signalling proteins elicit multi-nodular activation of signalling networks with known anti-apoptotic activity. Consistent with the cell signalling proteomics data, cell viability studies as a function of pharmacological kinase inhibitor treatment determined that the sensitivity of AML to targeted kinase inhibitors was modulated by the supportive stromal conditioned media.

To investigate heterotypic signalling between cell populations, AML/stromal cell co-cultures were designed, tested and optimised. These studies identified additional activated pathways in AML cells that were only present when AML cells had physical interaction with stroma. Complementary analysis of the stromal cells which had been first cultured with AML cells revealed that despite heterogeneity there is an emerging stromal phospho-proteomic signature that is different in BMM independent AML cells vs BMM interactive AML cells.

Collectively these findings evidence the influence that the BMM can have on AML signalling. Although evidence for the influence of BMM in modulating AML resistance to standard chemotherapy exists, this study highlights specific BMM components that contribute to the ability of AML cells to circumvent current treatments based on kinase targeted drugs. These observations have implications for designing future therapies for AML.

Contents

Statement **2**

Acknowledgements **4**

Abstract **5**

Contents **6**

Abbreviations **11**

List of Figures **15**

List of Tables **19**

Chapter 1: Introduction **20**

1.1 Acute myeloid leukaemia **20**

1.1.1 Overview 20

1.1.2 Pathogenesis 20

1.1.3 Classification 21

1.1.4 Genomic landscape 22

1.1.5 Treatment 26

1.1.6 Treatment resistance and relapse 29

1.2 Tumour microenvironment **30**

1.2.1 Cellular Composition 30

1.2.2 Role of microenvironment in AML progression 30

1.2.3 Leukaemia induced remodelling of the microenvironment 31

1.3 Cell signalling and kinase networks **33**

1.3.1 Cell communication and molecular cross-talk 33

1.3.2 Canonical AML cell signalling 35

1.3.3 Network rewiring and plasticity 37

1.4 Proteomics **40**

1.4.1 Mass spectrometry-based proteomics 40

1.4.2 Mass spectrometry-based secretomics 49

1.5. Phosphoproteomics **52**

1.5.1 The implications of phosphorylation events 52

1.5.2 Phosphopeptide enrichment strategies for MS analysis 53

1.6 Aims **57**

Chapter 2: Materials and Methods 58
2.1 Reagents 58
2.2 Cell lines and primary patient samples 62
2.2.1 Seeding for experimentation 63
2.2.2 Clinical features of primary samples 63
2.3 Stromal secretome production 65
2.4 Cell lysis 66
2.5 Western Blot 67
2.6 Guava ViaCount 67
2.7 Gene expression microarray 68
2.8 CyTOF 68
2.9 Co-immunoprecipitation (co-IP) 68
2.10 Liquid Chromatography – Tandem Mass Spectrometry Sample preparation 69
2.10.1 Secretome solubilisation 69
2.10.2 Tryptic Digestion 69
2.10.3 Peptide desalting utilising solid phase extraction 69
2.10.4 Phosphopeptide enrichment 70
2.11 Liquid Chromatography – Tandem Mass Spectrometry analysis 70
2.11.1 Liquid chromatography separation 70
2.11.2 Mass spectrometry analysis 71
2.12 Data analysis 73
2.12.1 Protein identification 73
2.12.2 Protein quantification 73
2.12.3 Kinase substrate enrichment analysis 73
2.12.4 K-means clustering 74

Chapter 3: Characterising the composition of AML supportive secretomes derived from stromal MS-5 and HS-5 cell lines 75
3.1 Introduction and aims of the study 75
3.2 Validating supportive qualities of the MS-5 and HS-5 cell lines 76
3.3 Optimisation of stromal conditioned media 77
3.4 Optimisation of secretome purification 84
3.5 Western blot analysis of secretome effects on signalling nodes 85
3.6 LC-MS/MS analysis of MS-5 secretome 86
3.7 LC-MS/MS analysis of HS-5 secretome 91

3.8 Co-culture models to induce dynamic stromal protein expression 97

3.9 Co-culture viability assays 98

3.10 LC-MS/MS analysis of co-culture secretomes 99

3.11 Panel of six stromal secretome proteins selected for further investigation 103

3.12 Western blot analysis of S100-A4 and CSF-1 presence in primary co-culture secretomes 106

3.13 Summary 109

Chapter 4: Empirical determination of identified protein components from the BMSM and their role in AML survival 112

4.1 Introduction and aims of the study 112

4.2 Optimisation of recombinant protein stimulation of primary AML cells 115

4.3 Survival assays using purified recombinant forms of identified signalling molecules secreted by stromal cells 119

4.4 Proliferation assays using purified recombinant forms of identified signalling molecules secreted by stromal cells 122

4.5 Gene expression analysis of secretome derived proteins within TCGA AML dataset 124

4.6 Kinase inhibition of common AML signalling nodes are altered following culture with stromal conditioned media 126

4.7 Investigating the influence of stromal derived factors on phenotypic heterogeneity and selection in AML 136

4.7.1 AML cells survive 36 days in culture due to HS-5 conditioned media 136

4.7.2 Mass cytometry (CyTOF) principles 139

4.7.3 Understanding the AML response to stromal conditioned media using AML phenotype antibody panel 140

4.8 Summary 149

Chapter 5: Determining the heterogeneity of AML cell signalling and the response of the phosphoproteome to BMSM stimulation 152

5.1 Introduction and aims of the study 152

5.2 Analysis of AML signalling response to network perturbation following GF stimulation 154

5.2.1 GF response of major signalling nodes 154

5.2.2 Phosphoproteomic analysis of GF stimulated primary AML cells 158

5.3 Characterise kinase activity heterogeneity in patients to bulk HS-5 conditioned media 168

5.3.1 Differential abundance 169

5.3.2 Heterogeneous phosphoproteomic signature 169
5.3.3 Implementation of KSEA reveals temporal effects of HS-5 factors on kinase activity 171
5.3.4 Condensing the global and heterogeneous effects HS-5 conditioning has on seven primary AML phosphoproteomes 173
5.4 AML/Stromal cell co-culture: how MS-5 cells modulate AML signalling networks.. 175
5.4.1 Examination of co-culture induced relationships 176
5.4.2 KSEA analysis of phosphoproteomes identifies three groups of responders ... 177
5.4.3 K-means clustering analysis of primary AML phosphoproteomics to study the influence of MS-5 stromal co-culture on 'ex vivo' leukaemic behaviour 180
5.4.4 Phosphopeptides that are increased in all AML primary samples following MS-5 cell co-cultures 182
5.5 AML/Stromal cell co-culture: identifying patterns of MS-5 response to different primary AML disease 184
5.5.1 Differential abundance 184
5.5.2 Global phosphoproteomic analysis of MS-5 cells following AML co-culture.... 185
5.5.3 KSEA analysis of MS-5 following AML co-cultures reveals two patterns of kinase activity 188
5.5.4 AML blast independence and embedding in MS-5 stromal cells could correlate with PCA observations 189
5.6 Summary 192

Chapter 6: Functional and biochemical characterisation of PAK signalling in AML 197
6.1 Introduction and aims of the study 197
6.2 Meta-analysis of genetic mutations in AML 200
6.3 Western blot analysis of PAK expression in AML cell lines 201
6.4 Co-immunoprecipitation optimisation 202
6.4.1 Principle of approach 203
6.4.2 Effects of detergent type on PAK protein yield 204
6.4.3 On-bead protein digestion 205
6.5 Optimisation of conditions for dynamic complex formation 208
6.5.1 Serum deprivation followed by secretome stimulation 209
6.5.2 PAK pulldown following PAK inhibition treatment 212
6.5.3 Serum deprivation followed by serum stimulation 214
6.6 Investigation of PAK signalling dynamics across isoforms 217
6.7 Summary 220

Chapter 7: Discussion 223

7.1 Characterising the composition of AML supportive secretomes derived from stromal MS-5 and HS-5 cell lines 225

7.1.1 Context and motivation for stromal secretome dissection 225

7.1.2 Variables that characterise conditioned media and secretomes 225

7.1.3 Label free LC-MS/MS based secretomics 226

7.1.4 Technical considerations and limitations of the study 226

7.1.5 Implications and future work 227

7.2 Empirical determination of identified protein components from the BMSM and their role in AML survival 229

7.2.1 Introduction and context of investigations 229

7.2.2 Validation of secretomic protein function in AML 229

7.2.3 Analysis of kinase inhibition to abrogate stromal secretome response 230

7.2.4 Analysis of AML adaption to stromal conditioned medium 232

7.2.5 Technical considerations 232

7.2.6 Implications and future work 233

7.3 Determining the heterogeneity of AML cell signalling and the response of the phosphoproteome to BMSM stimulation 235

7.3.1 Context 235

7.3.2 Analysis of single GF stimulated pathways in AML 236

7.3.3 Analysis of kinase network heterogeneity in response to secretome 237

7.3.4 Analysis of co-culture on AML signalling networks 238

7.3.5 Analysis of co-culture on MS-5 signalling networks 239

7.3.6 Implications and future work 240

7.4 Functional and biochemical characterisation of PAK signalling in AML 242

7.4.1 Context 242

7.4.2 Findings 242

7.4.3 Technical considerations 242

7.4.4 Implications and future work 243

7.5 Concluding remarks 245

Chapter 8: References 247

Abbreviations

4EBP1	Eukaryotic translation initiation factor 4E-binding protein 1
ACN	Acetonitrile
Ab	Antibody
AKT	Protein kinase B
ALL	Acute lymphocytic leukaemia
AML	Acute myeloid leukaemia
APEX	Absolute protein expression
APL	Acute promyelocytic leukaemia
ARHGEF	Rho guanine nucleotide exchange factor
ATR	Serine/threonine-protein kinase ATR
ATRA	All-trans retinoic acid
BARD1	BRCA1-associated RING domain protein 1
BCA	Bicinchoninic acid
BM	Bone marrow
BMM	Bone marrow microenvironment
BMP-1	Bone morphogenic protein-1
BMSC	Bone marrow stromal cell
BMSM	Bone marrow stromal microenvironment
BSA	Bovine serum albumin
c-MET	Tyrosine-protein kinase Met/HGF receptor
CDK	Cyclin-dependent kinase
CHAPS	3-((3-cholamidopropyl) dimethylammonio)-1-propanesulfonate
CID	Collision-induced dissociation
CK1A	Casein kinase 1 subunit alpha 1
CK2A1	Casein kinase 2 subunit alpha 1
CK2A2	Casein kinase 2 subunit alpha 2
CM	Conditioned media
co-IP	Co-immunoprecipitation
COSMIC	Catalogue of somatic mutations in cancer
CR	Complete remission
CSF-1	Colony stimulating factor-1
CSF1R	Colony stimulating factor-1 receptor
CTAM	Compound-target activity markers
CTGF	Connective Tissue Growth Factor
CXCL	Chemokine ligand
CXCR	Chemokine receptor
CyTOF	Cytometry by time of flight
DDA	Data dependent acquisition
DIA	Data independent acquisition
DIGE	Difference gel electrophoresis
DMEM	Dulbecco's modified eagle medium
DNMT3A	DNA (cytosine-5)-methyltransferase 3A
DTT	Dithiothreitol
DYRK2	Dual specificity tyrosine-phosphorylation-regulated kinase 2
EB	Empty bead control

ECM	Extracellular matrix
EGFR	Epidermal growth factor receptor
EN	Endosteal niche
ERK	Extracellular signal-regulated kinase
ESI	Electrospray ionisation
ETD	Electron-transfer dissociation
FA	Formic acid
FAB	French–American–British classification
FBS	Fetal bovine serum
FLT3	Receptor-type tyrosine-protein kinase FLT3
FT-ICR	Fourier transform ion cyclotron resonance
G-CSF	Granulocyte colony stimulating factor
GAPDH	Glyceraldehyde 3-phosphate dehydrogenase
GF	Growth factor
GIT	G-protein-coupled receptor-kinase-interacting proteins
GM-CSF	Granulocyte-macrophage colony-stimulating factor
GO	Gene ontology
GPCR	G-protein-coupled receptor
GSK3β	Glycogen synthase kinase 3 beta
HCD	Higher energy collision-induced dissociation
HGF	Hepatocyte growth factor
HILIC	Hydrophilic interaction chromatography
HSC	Haematopoietic stem cell
IAM	Iodoacetamide
ICAT	Isotope-coded affinity tag
IGF-1R	Insulin-like growth factor 1 receptor
IL	Interleukin
ILK	Integrin linked kinase
IMAC	Immobilised metal ion affinity chromatography
IMDM	Iscove's modified dulbecco's medium
Inv	Inversion
IR	Insulin receptor
ITD	Internal tandem duplication
ITRAQ	Isobaric tags for relative and absolute quantitation
JAK	Janus kinase
KSEA	Kinase-substrate enrichment analysis
LATS1	Serine/threonine-protein kinase LATS1
LC	Liquid chromatography
LC-MS/MS	Liquid chromatography - Tandem mass spectrometry
LIC	Leukaemic initiator cell
LSC	Leukaemic stem cell
LTQ	Linear trap quadrupole
MALDI	Matrix-assisted laser desorption/ionisation
MAPK	Mitogen-activated protein kinase
MAPKAPK2	MAP kinase-activated protein kinase 2
MC	Methanol-chloroform
MDS	Myelodysplasia
MEK	Dual specificity mitogen-activated protein kinase

MEM	Minimum essential Media
Mixed GF	Mixed growth factor condition
MOAC	Metal oxide affinity chromatography
MRD	Minimal residual disease
MS	Mass spectrometry
MSC	Mesenchymal stem cell
mTOR	Mechanistic target of rapamycin
MWCO	Molecular weight cut-off
NF-κβ	Nuclear factor kappa-light-chain-enhancer of activated B cells
NPM1	Nucleophosmin
OS	Overall survival
p70S6K	Ribosomal protein S6 kinase beta-1
PAGE	Polyacrylamide gel electrophoresis
PAK	p21 activated kinase
PB	Peripheral blood
PC	Principal component
PCA	Principal component analysis
PDHK	Pyruvate dehydrogenase (acetyl-transferring)] kinase
PEDF	Pigment epithelium-derived factor
PESCAL	Peak statistic calculator
PI3K	Phosphatidylinositol-4,5-bisphosphate 3-kinase
PKC	Protein kinase C
PKCD	Protein kinase C δ isoform
PLC	Phospholipase C
PTM	Post-translational modification
RAGE	Advanced glycosylation end product-specific receptor
ROCK1	Rho-associated protein kinase 1
RP	Recombinant protein
RPMI	Roswell Park Memorial Institute medium
RT	Room temperature
RTK	Receptor tyrosine kinase
SAGE	Serial analysis of gene expression
SAX	Strong-anion-exchange chromatography
SCT	Stem cell transplant
SCX	Strong-cation-exchange chromatography
SDF-1	Stromal derived factor-1
Sec	Secretome
SILAC	Stable isotope labelling with amino acids in cell culture
SRM	Selected reaction monitoring
STAT	Signal transducers and activators of transcription
t(;)	Translocation
TCGA	The cancer genome atlas
TFA	Trifluoroacetic acid
TIC	Total ion chromatogram
TKD	Tyrosine kinase domain
TGF-β	Transforming growth factor beta
TMT	Tandem mass tag
TNF	Tumour necrosis factor

TOF	Time of flight
TP53	Cellular tumour antigen p53
tR	Retention time
TSP	Thrombospondin
VBA	Visual basic for applications
VEGF	Vascular endothelial growth factor
VLA-4	Vascular cell adhesion molecule-1
VN	Vascular niche
WHO	World health organisation
WT	Wild-type
XIC	Extracted-ion chromatogram

List of Figures

Figure 1.1: AML Pathogenesis p.21
Figure 1.2: Molecular subgroups in AML defined by genomic landscape p.24
Figure 1.3: Bone marrow stromal microenvironment p.31
Figure 1.4: Model of the bone marrow microenvironment and the expansion of AML p.32
Figure 1.5: AML blast and stromal cell "crosstalk" p.34
Figure 1.6: Signalling pathways of significance in AML p.36
Figure 1.7: Models of cell signalling p.39
Figure 1.8: Principles of LC-MS/MS p.44
Figure 1.9: Approaches to study secretome composition p.50
Figure 1.10: Molecular mechanisms that contribute to the activation of kinase signalling p.53
Figure 1.11: Established and alternative strategies for phosphopeptide enrichment p.55

Figure 2.1: Protocol for producing MS-5 and HS-5 conditioned media and enrichment of secretome p.66
Figure 2.2: Schematics of the LTQ Orbitrap-XL and Q-Exactive Plus mass spectrometers p.71

Figure 3.1: Stromal conditioned media extends primary AML cell survival ex vivo p.76
Figure 3.2: Dissection of the supportive role MS-5 secretome plays in AML cell survival p.77
Figure 3.3: Optimising the duration of stromal media conditioning p.78
Figure 3.4: Optimising stromal cell confluency and conditioned media volume p.79
Figure 3.5: Determination of factor loss during filtration p.70
Figure 3.6: Effects of the freeze thaw process on the ability of CM to maintain AML ex vivo p.81
Figure 3.7: HS-5 stromal conditioned media is the optimum means of extending primary AML cell survival ex vivo p.82
Figure 3.8: Controlling for serum utilisation and accumulation of non-supportive components p.84
Figure 3.9: Increase in PAK phosphorylation in MV4-11 cells over secretome time-course p.85
Figure 3.10: MS-5 total ion chromatogram produced during LC-MS/MS analysis p.87
Figure 3.11: Relative abundance of secreted MS-5 proteins following LC-MS/MS analysis p.87
Figure 3.12: Relative abundance of secreted MS-5 proteins to total ion intensity p.89
Figure 3.13: List of the most abundant secreted MS-5 growth factors p.90
Figure 3.14: Panther gene ontology analysis of MS-5 secretome p.91
Figure 3.15: Optimisation of secretome enrichment finds Vivaspin columns best approach p.92
Figure 3.16: List of the most abundant secreted HS-5 growth factors p.94
Figure 3.17: Panther gene ontology analysis of HS-5 secretome p.96
Figure 3.18: Schematic for AML – MS-5 co-culture model p.98
Figure 3.19: AML cell viability over 24 hours following serum starvation in culture alone or in co-culture with MS-5 stromal cells p.99
Figure 3.20: Hierarchical clustering analysis of the changes in protein expression in AML-MS5 co-cultures p.100
Figure 3.21: Volcano plots of stromal factors that significantly increase and decrease following co-culture with P31/FUJ and HL60 cells p.101
Figure 3.22: Volcano plots of stromal factors that significantly increase and decrease following co-culture with MV4-11 and CTS cells p.102

Figure 3.23: Box plots of six chosen stromal proteins that changed dynamically across the co-cultures p.103
Figure 3.24: Co-culture secretomes derived from different AML patients induce variable CSF-1 and S100-A4 abundance p.106
Figure 3.25: Individual and co-culture secretomes produced by 5 AML patients' exhibit variable CSF-1 and S100-A4 abundance p.108

Figure 4.1: Known receptors with specificity to selected secretome derived factors p.113
Figure 4.2: Cell viability assay of high risk primary AML patient cells grown for seven days with growth factors in serum starved or serum stimulated setting p.116
Figure 4.3: Cell growth assay of high risk primary AML patient cells grown for seven days with growth factors in serum starved or serum stimulated setting p.118
Figure 4.4: The effects of stromal derived growth factor panel on ex vivo survival of five primary AML patient samples p.121
Figure 4.5: Cell growth assays reveal that factors induce increase cell growth across patients compared to no growth factor p.122
Figure 4.6: Kaplan Meier curves displaying the difference in AML patient survival with higher or lower expression of growth factor genes p.125
Figure 4.7: Primary AML targeted MEK inhibition with/without HS5 conditioned media p.128
Figure 4.8: Primary AML targeted mTOR inhibition with/without HS5 conditioned media p.130
Figure 4.9: Primary AML pan kinase inhibition with/without HS5 conditioned media p.131
Figure 4.10: Primary AML targeted JAK inhibition with/without HS5 conditioned media p.133
Figure 4.11: Primary AML targeted PAK inhibition with/without HS5 conditioned media p.134
Figure 4.12: HS-5 conditioned media is the most successful at maintaining patient 0 cell viability across seven days p.136
Figure 4.13: Relative primary AML cell proliferation p.137
Figure 4.14: Patient #0 cells during 36 day time-course in culture p.138
Figure 4.15: CyTOF principle p.139
Figure 4.16: ViSNE analysis of markers CD7, CD19, CD16 and CD15 during 36 days in culture p.143
Figure 4.17: ViSNE analysis of markers CD14, CD45, CD144 and CD11b during 36 days in culture p.144
Figure 4.18: ViSNE analysis of markers CD184, CD123 and CD64 during 36 days in culture p.145
Figure 4.19: ViSNE analysis of markers CD3, CD117, CD33 and HLA-DR during 36 days in culture p.146
Figure 4.20: ViSNE analysis of key LIC markers CD34 and CD38 during 36 days in culture p.147
Figure 4.21: Heatmap of surface marker expression during 36 days of ex vivo cell culture p.148

Figure 5.1: Concept of cell signalling and the means of signal transduction p.153
Figure 5.2: MAPK and PI3K-AKT-mTOR signalling axis p.154
Figure 5.3: Western blot analysis of MAPK signalling in P31/FUJ cells p.155
Figure 5.4: Western blot analysis of AKT/mTOR signalling in P31/FUJ cells p.156
Figure 5.5: Western blot analysis of PAK signalling in P31/FUJ cells p.157
Figure 5.6: Patient #1 selected to for phosphoproteomic analysis based on functional response to GF stimulation p.159
Figure 5.7: Experimental design used to define the topology of kinase signalling following growth factor stimulation p.160
Figure 5.8: Quality control of MS data used to analyse the phosphoproteomes of GF stimulated AML cells p.161
Figure 5.9: Differential abundance analysis of the patient #1 phosphoproteomics data following GF stimulation p.162
Figure 5.10: Hierarchical clustering analysis of recombinant factor stimulated phosphopeptide expression in patient #1 cells p.163

Figure 5.11: Heatmap of kinase substrate enrichment analysis (KSEA) p.165
Figure 5.12: Multivariate analysis of GF stimulated patient #1 datasets highlights the distinct effect S100-A4 and Mixed GF conditions can have on the AML phosphorylome p.167
Figure 5.13: Experimental design for to determine the heterogeneity in AML signalling network response to growth with HS-5 conditioned media p.168
Figure 5.14: Differential abundance analysis of the primary AML phosphoproteomics data p.169
Figure 5.15: Heterogeneous response of primary AML to HS-5 conditioning p.170
Figure 5.16: KSEA heatmap of temporal effects of HS-5 derived factors on AML kinase activity p.172
Figure 5.17: Principal component analysis of primary AML cells grown in HS-5 CM p.174
Figure 5.18: Experimental design for MS-5/AML cell co-culture p.175
Figure 5.19: Hierarchical clustering analysis of AML phosphoproteomes following MS-5 cell co-culture p.176
Figure 5.20: PCA of 7 primary AML samples representing the changes in phosphoproteomic expression that co-culture with MS-5 cells induces in these AML cells p.177
Figure 5.21: KSEA of significantly modulated kinases in primary AML cells following MS-5 co-culture p.178
Figure 5.22: K-means clustering analysis comparing AML cells grown in MS-5 co-culture compared to those independently grown p.181
Figure 5.23: K-means analysis reveals that there is enrichment for phosphopeptides that are indicative of AKT2 activity and an increase in anti-apoptotic signalling p.183
Figure 5.24: Differential abundance analysis of MS-5 phosphoproteomes following co-culture p.184
Figure 5.25: Hierarchical clustering of MS-5 phosphopeptide expression fold changes in response to co-culture with patient AML cells p.186
Figure 5.26: Heatmap of enriched gene ontology processes in MS-5 cells following AML co-culture p.187
Figure 5.27: KSEA of significantly modulated kinases in MS-5 cells following co-culture p.188
Figure 5.28: Multivariate analysis of MS-5 cells following co-culture demonstrates AML influence p.189
Figure 5.29: Bright field images of primary AML/MS-5 co-cultures prior to phosphoproteomic analysis p.191

Figure 6.1: Global kinase substrate enrichment analysis (KSEA) reveals substrates of PAK are one the most frequently enriched groups in primary AML cells p.197
Figure 6.2: PAK signalling cascade in a physiological context p.198
Figure 6.3: Oncogenic PAK signalling characterised in solid tumours p.199
Figure 6.4: Meta-analysis of genetic mutations from COSMIC repository of 390 whole genome sequenced AML patients p.201
Figure 6.5: Western blot showing the activity and basal expression of the PAK isoforms AML cell line p.202
Figure 6.6: Optimised co-immunoprecipitation workflow p.204
Figure 6.7: Hepes based CHAPS lysis buffer is optimal for PAK assessment p.205
Figure 6.8: In-gel digestion of PAK co-IP complexes leads to no PAK detected in mass spectrometer p.206
Figure 6.9: Co-Immunoprecipitation optimised pull-down results p.207
Figure 6.10: Proteins identified in pull-down experiments of PAK1, PAK2 and PAK4 p.208
Figure 6.11: PAK co-immunoprecipitation strategy p.209
Figure 6.12: Western blot analysis of PAK1 and PAK2 status during secretome and serum stimulation p.210
Figure 6.13: Co-Immunoprecipitation of PAK in MV4-11 cells following secretome stimulation p.211
Figure 6.14: Comparison between secretome stimulation PAK pulldown and unstimulated reveals no substantial enrichment p.212
Figure 6.15: Heatmap of PAK pull-down in MV4-11 following PAK inhibitor treatment p.213

Figure 6.16: Co-Immunoprecipitation of PAK in MV4-11 cells following both serum starvation and stimulation p.215
Figure 6.17: Comparison of PAK complex co-eluents between serum stimulated and starved cells reveals enrichment for histones p.216
Figure 6.18: Volcano plots of proteins identified in targeted PAK1, 2, 4 pull-downs coupled with LC-MS/MS detection p.218
Figure 6.19: Protein string of PAK4 pull-down proteins that are significantly enriched for in serum stimulated P31/FUJ p.219

Figure 7.1: Theory for bone marrow stromal cell initiated activation of AML cell signalling nodes p.231

List of Tables

Table 1.1: FAB AML classification p.21

Table 1.2: The WHO classification, 2016 update p.22

Table 1.3: Recurrent AML mutations grouped into functional sets p.25

Table 1.4: ELN defined AML risk groups p.27

Table 2.1: A summary of cell culture reagents p.58

Table 2.2: A summary of kinase inhibitors p.58

Table 2.3: A summary of recombinant growth factors used in Chapter 4 experiments p.59

Table 2.4: A summary of antibodies used in western blots (WB) and co-immunoprecipitations (co-IP) p.59

Table 2.5: A summary of antibodies used in Mass Cytometry experiments p.60

Table 2.6: A summary of all miscellaneous materials and reagents used p.61

Table 2.7: A summary of cell lines p.62

Table 2.8: Cytogenetic and molecular features of the primary AML samples used in studies p.64

Table 2.9: Clinical features of the included primary AML samples p.64

Table 2.10: Selected genes that were screened for variants in patients #1, 2, 6-12 p.65

Table 2.11: A summary of lysis buffers used, buffer composition and the applications for which they were applied p.67

Table 3.1: The most abundant proteins in secretome p.88

Table 4.1: Features of the dataset used to compare gene expression of growth factors in AML. p.124

Table 4.2: Panel of targeted kinase inhibitors used in kinase inhibition studies p.127

Table 4.3: Overview of primary AML response to kinase inhibitors across patients p.135

Table 4.4: Panel of CyTOF antibodies used to characterise potential AML clones within patient samples p.141

Table 5.1: Summary table of the PCA scores for the HS-5 phosphoproteomics analysis p.173

Table 6.1: Co-Immunoprecipitation optimisation. p.203

Chapter 1: Introduction

1.1 Acute myeloid leukaemia

1.1.1 Overview

Acute myeloid leukaemia (AML) is a haematopoietic stem cell (HSC) malignancy that is characterised by impaired haematopoiesis and bone marrow failure (1). In the western world this disease accounts for ~25% of all adult-onset leukaemias, with an incidence of 3 to 5 cases per 100,000 people per year and a median age of onset of 69 years (2-5). Once deemed incurable, AML is now considered curable in 35-40% of adults under 60 years of age, however, in patients over 60 years of age, prognosis is bleak with 'cure' rates at 5-15% (1). The reduced survival that older patients experience is representative of current treatment options, where despite significant progress in our understanding of AML biology, there has been little meaningful therapeutic advance. High intensity, poorly tolerated therapies remain the most curative options (6). AML is a cancer, and it is a disease of the elderly who cannot tolerate current therapies, this demonstrates an unmet clinical need for new approaches to treat this disease.

1.1.2 Pathogenesis

AML is a heterogeneous clonal disorder characterised by the expansion of undifferentiated haematopoietic progenitor cells or 'blast cells' (7). These blast cells can exhibit various degrees of stagnated differentiation while accumulating in the bone marrow (BM), which leads to the reduced output of crucial haematopoietic elements (8-10). Their proliferative nature eventually leads to infiltration of the peripheral blood and other tissues (11).

AML blasts are thought to be part of clonal populations that arise from leukaemic stem cells (LSCs), which due to chromosomal aberrations harbour mutations that characterise the phenotype of the disease (12-15). Oncogenic mutations are described as either class I mutations, which confer a proliferative/survival advantage such as the well described FLT3-ITD genotype, or class II mutations, which cause an impairment in haematopoietic differentiation and subsequently prevent apoptosis; class II mutations tend to be loss of function mutations in transcriptional regulators (16, 17). These classes of mutation were thought to occur in a 'two-hit model' where the two mutation types were required to initiate the disease (18). It has since become clear the disease can manifest without class I mutations, while there are also commonly mutations in epigenetic regulators (*DNMT3A, IDH1*) as well as tumour suppressors (*TP53*) (19).

In addition to the successive genomic events in AML propagation, there are also epigenetic factors and external cues from the microenvironment that influence disease

behaviour (19). Finally, it is also possible for multiple malignant clones to co-exist, thus making this a very heterogeneous disease that is prone to treatment resistance (20). These mechanisms of propagation are summarised in Figure 1.1.

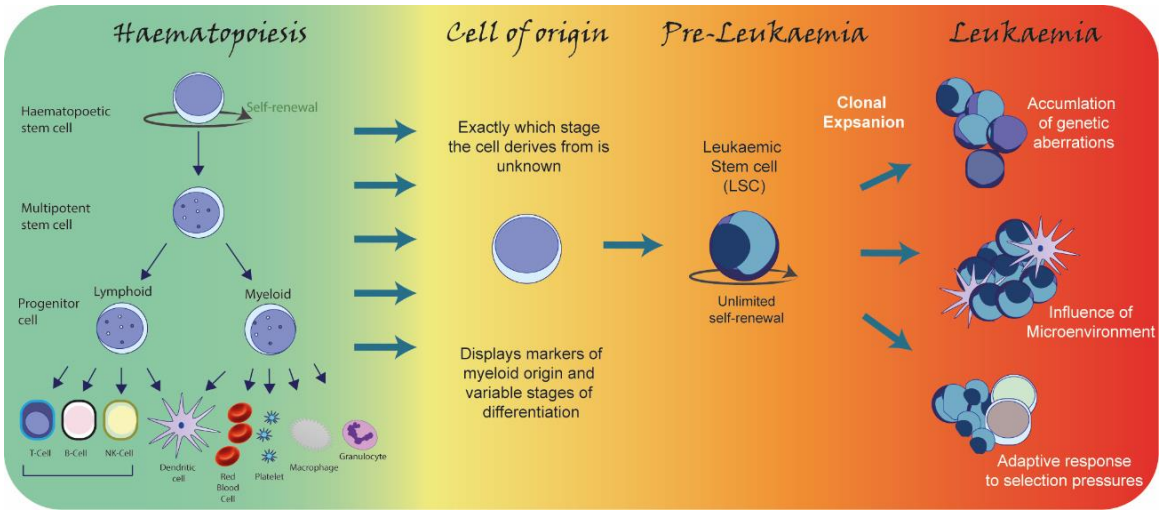

Figure 1.1: AML Pathogenesis. This schema provides a simplified view of the progression that occurs during AML. It reflects the departure from normal blood cell producing haematopoiesis, characterised by a lack of differentiation and an increase in proliferation. This is initiated by a myriad of genetic events that lead to the formation of an LSC that has the potential for self-renewal. Clonal expansion from these leukaemia initiating cells combined with the pressures of the environment lead to the heterogeneous forms of leukaemia that patients present with.

1.1.3 Classification

The criteria for AML diagnosis has evolved over the years with multiple revisions of the classifications. A diagnosis is made if myeloblasts are found to comprise at least 20% of the total number of nucleated cells in the BM (21). Diagnosis can also be determined by morphological assessment of BM specimens and blood smears, these criteria underpinned the previous French American British (FAB) classification (Table 1.1) (8).

Subtype	FAB classification morphological description
M0	Acute non-differentiated leukaemia – immature blast cells with minimal differentiation
M1	Acute myeloblastic leukaemia without maturation – immature blast cells without signs of myeloid differentiation
M2	Acute myeloblastic leukaemia with granulocytic maturation
M3	Promyelocytic or acute promyelocytic leukaemia (APL)
M4	Acute myelomonocytic leukaemia
M4eo	Myelomonocytic leukaemia with bone marrow eosinophilia
M5	M5a – Acute monoblastic leukaemia without maturation M5b – Acute monoblastic leukaemia with partial maturation
M6	Acute erythromyelosis
M7	Acute megakaryoblastic leukaemia

Table 1.1: FAB AML classification. AML was divided into subtypes, M0 (minimally differentiated) through to M7 (differentiated), based on the type of cell from which the leukaemia developed and how differentiated the cells appeared under the microscope (8).

Advances in cytogenetic testing and genetic screening means that the most recent classification according to the World Health Organisation (WHO) of AML builds on the previous FAB criteria, but also incorporates the cytogenetic and molecular understanding that has been garnered over the past 30 years (Table 1.2) (22). The main categories becoming, AML with recurrent genetic abnormalities, AML with myelodysplasia (MDS) related changes, therapy-related AML, and AML not otherwise specified.

WHO classification of AML
AML with recurrent genetic abnormalities
AML with t(8;21)(q22;q22.1);RUNX1-RUNX1T1
AML with inv(16)(p13.1q22) or t(16;16)(p13.1;q22);CBFB-MYH11
APL with PML-RARA
AML with t(9;11)(p21.3;q23.3);MLLT3-KMT2A
AML with t(6;9)(p23;q34.1);DEK-NUP214
AML with inv(3)(q21.3q26.2) or t(3;3)(q21.3;q26.2); GATA2, MECOM
AML (megakaryoblastic) with t(1;22)(p13.3;q13.3);RBM15-MKL1
Provisional entity: AML with BCR-ABL1
AML with mutated NPM1
AML with biallelic mutations of CEBPA
Provisional entity: AML with mutated RUNX1
AML with myelodysplasia-related changes
Therapy-related myeloid neoplasms
AML, Not Otherwise Specified
AML with minimal differentiation
AML without maturation
AML with maturation
Acute myelomonocytic leukaemia
Acute monoblastic/monocytic leukaemia
Pure erythroid leukaemia
Acute megakaryoblastic leukaemia
Acute basophilic leukaemia
Acute panmyelosis with myelofibrosis
Myeloid sarcoma
Myeloid proliferations related to Down syndrome
Transient abnormal myelopoiesis (TAM)
Myeloid leukaemia associated with Down syndrome

Table 1.2: The WHO classification, 2016 update. A more encompassing classification that is based upon a combination of morphology, immune-phenotype, genetics, and clinical features (21).

1.1.4 Genomic landscape

The underlying genetic landscape has to date defined the way this disease is studied and has profoundly influenced the way the disease is classified, managed and targeted (21, 23). Since the introduction of next generation sequencing there have been a number of comprehensive sequencing studies that have collectively identified many leukaemia associated genes; however,

these are infrequent mutations and patients typically present with more than one of them (13, 18, 20, 24). One aspect of AML evolution that could explain this genetic heterogeneity is that most cases of AML exhibit clonal heterogeneity at the time of diagnosis, with at least a founding clone and a further subclone observed (18). The presence of these additional clones is also thought to play a significant role in patient relapse and subsequent resistance to previously effective therapies (19).

Cytogenetics has played a prominent role in diagnosing and managing AML, as non-random chromosomal abnormalities (deletions and translocations) are observed in ~52% of adult AML patients and are thought to be aberrations that significantly contribute to disease severity (25). Cytogenetic abnormalities such as t(8;21)(q22;q22), inv(16) and t(15;17) are predominantly associated with longer remissions and longer patient survival (26). Whereas, deletions in 5q or 7q chromosomes, or the accumulation of >3 alterations (complex) chromosomal abnormalities are often associated with poor treatment responses and adverse patient outcome (27). In contrast, around 40-50% of AML cases exhibit normal cytogenetics and thus, are a very heterogeneous group of patients in terms of treatment response and outcome (28). Although this patient group possess normal cytogenetics, that does not mean they do not harbour molecular abnormalities and these mutations can offer crucial prognostic information (18, 25, 29, 30).

Twenty years ago, cytogenetics determined how AML from a genetic perspective was perceived, since the introduction of next generation sequencing however, the genetic landscape of AML has become more defined, particularly in those individuals that do not possess cytogenetic abnormalities. These studies have come to recognise that each case on average has 13 mutations, with 8 of them typically being randomly accrued mutations that can be termed ‘passenger’ mutations, and 5 that will be recurrent mutations observed in AML, these get termed ‘driver’ mutations (18). This knowledge is now incorporated into the WHO classification and, when possible, it is used to direct patient treatment (23).

The largest study undertaken to date to define the genomic landscape in AML was performed by Papaemmanuil et al., using next generation sequencing, 1540 patients were both screened for 111 cancer genes and cytogenetically screened to profile their genomes (31). This study identified 5234 driver mutations across 76 genes, with 2 or more drivers identified in 86% of the cohort. Patterns of co-mutations could then be grouped into 11 different groups, with class-defining mutations contributing independently and additively to outcome (Figure 1.2). Notably it was found that co-mutations could significantly alter the impact of other mutations (gene-gene interactions): the combination of DNA methyl-transferase-3A (*DNMT3A)* and nucleophosmin 1 (*NPM1)* aberrations did not markedly affect survival, but the addition of a

mutation in FMS-related tyrosine kinase 3 (*FLT3)* to these two mutations significantly reduced survival (31).

Figure 1.2: Molecular subgroups in AML defined by genomic landscape. Genetic profiling of 1540 patients screening 111 cancer genes and cytogenetics defines 13 genomic categories listed along x-axis. Each column represents a patient and rows represent a different genetic lesion, with purple lines denoting observed mutations. Orange lines separate respective genomically defined groups. Colour key represents known function of mutated driver gene. Figure adapted from (31).

There are a number of mutations that are frequently recurrent in AML and these can be classified into functional groups, which collectively go some way to explaining the classical features of AML such as the proliferation, stagnated differentiation and the aversion to cell death, these are summarised in Table 1.3.

Functional class	Specific example mutations
Signalling and kinase pathway	*FLT3, KRAS, NRAS, KIT, NF1, PTPN11*
Epigenetic modifiers	*DNMT3A, IDH1, IDH2, TET2, ASXL1, EZH2, MLL/KMT2A*
Nucleophosmin	*NPM1*
Transcription factors	*CEBPA, RUNX1, GATA2*
Tumour suppressors	*TP53*
Spliceosome complex	*SRSF2, SF3B1, ZRSR2, U2AF1*
Cohesion complex	*STAG1, STAG2, SMC3, SMC1A, RAD21*

Table 1.3: Recurrent AML mutations grouped into functional sets. The five most frequently mutated genes highlighted in red.

Mutations in signalling pathways occur in approximately two-thirds of AML cases (the most common mutational subset) and are believed to contribute to the aberrant activation and proliferation tied to these pathways (32). These mutations are thought to be subclonal, therefore indicating that they are late clonal events in disease evolution, this suggests these are not disease causing alterations (33). The most frequently mutated signalling gene is *FLT3* which is mutated in nearly one-third of all AML patients and presents with either mutations in the tyrosine kinase domain (TKD), thought to be kinase activating events, or internal tandem duplicates (ITD), insertions of variable length in the juxta-membrane domain that render the protein constituently active (34).

The family of RAS oncogenes (*NRAS, KRAS, PTPN11* and *NF1)* are mutated in 10-15% of all AML cases. Like *FLT3* mutations these are believed to cause aberrant proliferative signalling through activation of the RAS/RAF/MEK/ERK pathway, these mutations tend to be associated with poor prognosis due to co-occurrence during MDS transformation to AML – which are always considered to have adverse outcomes (35). KIT mutations are observed in a small subset

of AML patients - in 20% of patients that have core binding factor translocations and these are frequently associated with poor prognosis (36).

The high frequency of mutations in signalling proteins (such as FLT3, c-KIT and RAS) whose functions correlate with the characteristic features of AML coupled with the adverse prognosis that has been associated with such events has led these proteins to become the focus of AML targeted therapies (37). Additionally, many large-scale genome projects conclude that awareness of the complete genomic landscape will be necessary to stratify patients and know when to target such drivers (31, 38-40).

1.1.5 Treatment

Treatment of the AML has not witnessed great innovation in the past 40 years, with the standard treatment of cytarabine-based chemotherapy (41, 42) and allogeneic stem cell transplant (SCT) remaining relatively constant (8, 43). This approach is considered appropriate for all "medically fit" individuals (including older patients); for older "medically unfit" patients - traditionally the cohort with least treatment options, due to treatment related morbidity - hypomethylating agent strategies as a frontline therapy are looking very promising with Azacitidine treatment providing better outcomes now than no leukaemia-directed therapy (44, 45).

Current therapy eventually fails for most patients as it preferentially targets rapidly dividing cells, while exerting minimal effects on the leukaemic and pre-leukaemic stem cells due to their quiescent nature (42, 46-48). LSCs are thought to be responsible for disease initiation and relapse, and therefore there is a need for novel therapies that can target the LSCs thus maintaining remission and ultimately improving survival (20).

The notable exception in AML therapy is for a subtype named acute promyelocytic leukaemia (APL) where the introduction of All Trans Retinoic Acid therapy (ATRA) has proved a very effective means of long-term therapy (*19*). APL though, only represents a small proportion of all AML cases. Consequently, long-term survival rates in AML are around 40% in the young and 5% in patients above 60 years of age (this disease is predominantly observed in the elderly) (10, 49).

In recent years, our knowledge of the underlying cancer biology in AML has greatly improved. The identification of genetic aberrations relevant to the tumour has made it possible to stratify patients into risk groups, which has helped to improve disease management (23) (Table 1.4). However, this has not managed to meet satisfactory levels with patients presenting with favourable cytogenetics correlating with a 5-year overall survival (OS) ~60%, intermediate 30-40% and adverse only 5-10% respectively.

Risk Category	Genetic abnormality
Favourable	t(8;21)(q22;q22.1); RUNX1-RUNX1T1 inv(16)(p13.1q22) or t(16;16)(p13.1;q22); CBFB-MYH11 Mutated NPM1 without FLT3-ITD or with FLT3-ITD^{low} Biallelic mutated CEBPA
Intermediate	Mutated NPM1 and FLT3-ITD^{high} Wild-type NPM1 without FLT3-ITD or with FLT3-ITD^{low} (without adverse-risk genetic lesions t(9;11)(p21.3;q23.3); MLLT3-KMT2A Cytogenetic abnormalities not classified as favourable or adverse
Adverse	t(6;9)(p23;q34.1); *DEK-NUP214* t(v;11q23.3); KMT2A rearranged t(9;22)(q34.1;q11.2); *BCR-ABL1* inv(3)(q21.3q26.2) or t(3;3)(q21.3;q26.2); *GATA2,MECOM(EVI1)* -5 or del(5q); -7; -17/abn(17p) Complex karyotype, monosomal karyotype Wild-type *NPM1* and *FLT3*-ITD^{high} Mutated *RUNX1#* Mutated *ASXL1#* Mutated *TP53*

Table 1.4: ELN defined AML risk groups. Current stratification of cytogenetic and molecular genetic alterations (as per ELN guidelines). Risk profile will help direct treatment with risk profile usually indicative of patient response (23). **#** Not adverse if occurs with favourable abnormalities.

Increased understanding of the disease has not yet translated into effective new therapies (42); however, that is not to say there has not been a plethora of new approaches devised. There is a growing focus on targeted treatments that aim to address underlying genomic aberrations. In the US as recent as April 2017, Midostaurin a multi-kinase inhibitor was approved by the FDA for patients that harbour mutations in the *FLT3* gene. The field of AML targeted therapies currently focuses on trying to target disease-initiating and co-operating mutations with the aim of eliminating those founding clones and sub-clones (20, 42), with popular targets including *FLT3* (50-54), CD33(55-57), CXCR4 (58-60), DNA methylation (18, 61-64) and tyrosine-protein kinase Kit (c-*KIT) (65-68)*.

Although some of these drugs look promising (Table 1.5), to date none of these targeted therapies have been more efficacious than current treatment regimens, including the recently approved use of Midostaurin in patients with *FLT3* mutations (69). Many of these targets are crucial to normal cell development and physiological processes, and as such targeting these pathways without inducing toxicity is a challenge (42). One reason for the lack of efficacy in the targeted therapies could be the stratification criteria of patient groups. A number of genetic studies to date have reported that aberrations in the *FLT3* gene lead to constituent activation or dysregulation of the protein, which in turn drives leukaemogenesis. The RATIFY trials (the data that led to Midostaurin approval in 2017) observed that patients with a *FLT3* mutation given Midostaurin had a 22% lower-risk of death than patients with a *FLT3* mutation not given

Midostaurin (70). This trial did not assess Midostaurin efficacy in *FLT3* wild-type (WT) patients, this is surprising as a previous phase 2 trial that used Midostaurin by Fischer T et al. did include *FLT3* WT patients and observed WT response (71). Therefore, there are patients that respond to Midostaurin, but it is not dependent on *FLT3* mutational status.

Class of agent	Agents	Refs
Protein kinase inhibitors	▪ **FLT3 inhibition** *(Midostaurin, Quizartinib, Gilteritinib, Crenolanib*) ▪ **KIT inhibitors** *(Dasatinib)* ▪ **PI3K/AKT/mTOR inhibitors** *(Everolimus, Sirolimus, API-2, GSK2141795)* ▪ **MEK inhibition** *(Trametinib, selumetinib)* ▪ **Aurora** *(Barasertib)* **and polo-like kinase** *(Volasertib)* **inhibitors, CDK4/6** *(Palbociclib)*, **CHK1** *(SCH900776)*, **WEE1** *(AZD1775) inhibitors* ▪ **SRC** *(Dasatinib)* **and HCK** *(RK-20449)* **inhibitors**	(70, 72-74) (75) (76-79) (80, 81) (82-87) (75, 87)
Epigenetic modulators	▪ **Hypomethylating agents** *(SGI-110)* ▪ **HDAC inhibitors** ▪ **IDH1 and IDH2 inhibitors** *(AG-221, AG-120)* ▪ **DOT1L inhibitors** *(EPZ-5676)* ▪ **BET-bromodomain inhibitors** *(OTX-015)*	(88) (89) (90-94) (95, 96) (97, 98)
Chemotherapeutic agents	▪ **CPX-351** ▪ **Vosaroxin** *(Topoisomerase II inhibitor*)	(99) (100)
Mitochondrial inhibitors	▪ **Bcl-2, Bcl-xL, and Mcl-1 inhibitors** ▪ **Caseinolytic protease inhibitors**	(101) (102)
Targeted inhibition of oncogenic proteins	▪ **EVI1 targeting** ▪ **NPM1 targeting** ▪ **Hedgehog inhibitors**	(103) (104) (105, 106)
Antibodies and immuno-therapies	▪ **Monoclonal antibodies** *(CD33, CD44, CD47, CD123, CLEC12A)* ▪ **Immunoconjugates** *(SGN33A)* ▪ **BiTEs** *(AMG 330)* **and DARTs** ▪ **CAR T cells** ▪ **Immune checkpoint inhibitors** *(PD-1/PD-L1, CTLA-4)* ▪ **Anti-KIR antibody** *(IPH-2101)* ▪ **Vaccines** *(WT1)*	(107) (108) (109, 110) (111-115) (116-118) (119) (120, 121)
Therapies to disrupt AML environmental interaction	▪ **CXCR4 and CXCL12 antagonists** *(AMD 3100, LY2510924, LY2624587)* ▪ **Antiangiogenic therapy**	(122-125) (126)

Table 1.5 – Emerging therapies in AML treatment. Summary of the most promising agents currently in clinical trials, as well as novel approaches in pre-clinical development.

These trials demonstrate that targeted compounds (such as Midostaurin) can be very effective, however, further research and understanding is required for better patient stratification. Instances of Midostaurin failure in *FLT3* mutant patients, suggest a *FLT3* mutation may not necessarily be sufficient for constitutive activation of the *FLT3* substrates, as epigenetic events coupled with interactions with the microenvironment could potentially result in a net

effect of *FLT3* mediated signalling not being crucial to disease propagation (127). In addition, the FLT3 protein may not be expressed in all the cases where a *FLT3* mutation is present (69, 128). These reasons collectively could explain why Midostaurin did not provide a response in all *FLT3* mutant patients during the RATIFY trials.

1.1.6 Treatment resistance and relapse

Treatment resistance (an inability to achieve complete remission [CR]) or relapse (CR initially achieved) is common in AML, with event free survival in patients remaining poor despite implementation of intensive myelosuppressive regimens and improvements to supportive care (129). Around 10-40% of newly diagnosed patients that undergo intense chemotherapy do not manage to achieve CR (<5% blast count following 2 cycles of intense induction chemotherapy) (130) and are considered treatment resistant (131). Patients can also develop early relapse (re-emergence of AML blasts < 6 months after initially achieving CR) (132) and late relapse (re-emergence of AML blasts > 6 months after initially achieving CR) and it has been shown that the time it takes for relapse can significantly alter which therapeutic intervention will be effective (133, 134).

Relapse occurs due to minimal residual disease (MRD), which is defined as subclinical levels of leukaemia, cells that persist following treatment but are not present at detectable numbers, or do not induce clinically overt disease (135, 136). Mechanisms that underpin clinical relapse are not as simple as the re-emergence of a dominant clone or evolution from the original dominant clone (19). Relapse can also arise from minor subclones, develop as a second leukaemia from the same pre-leukaemic clone that the treated disease arose from or be an entirely separate therapy-related leukaemia (13, 14, 137). These separate sources of treatment related relapse highlight the importance of selecting targets that are considered to be initiating events in leukaemogenesis therefore, clonal sensitivity to treatments will be broader, and stable remission more likely (136).

The leukaemic stem/initiator cell (LSC/LIC) was the first cancer stem cell to be described in 1994 by Lapidot et al. (11, 138, 139), and have capacities for self-renewal, proliferation and differentiation. Relapse is associated with the failure to eradicate this cell population as they are characterised by the ability to give rise to new leukemic blast populations (140-142). Whether these cells need to be rare stem cells is a polarising issue, as studies have shown that early progenitor cells possess the same colony forming traits (143). LICs are regularly chemo-resistant due to their infrequent cell divisions and the relationship they share with the microenvironment (144, 145), this behaviour enables survival in the presence of DNA damaging chemotherapy agents (11, 146, 147).

1.2 Tumour microenvironment

1.2.1 Cellular Composition

The concept of the bone marrow microenvironment (BMM) having a role in regulating haematopoietic cells is well established (148, 149). The BMM is composed of HSCs, endothelial cells, osteoblasts, osteoclasts, and mesenchymal stem cells (MSCs). The MSCs can differentiate into adipocytes, stromal cells, fibroblasts, and myocytes (150-155). These cells cluster to form defined niches that help in the development of haematopoietic cells (156).

1.2.2 Role of microenvironment in AML progression

The BMM has a key role in the haematological malignancies, and as discussed contributes to the survival and progression of leukaemic blasts (11, 157). Evidence is now emerging of the BMMs role in the initiation of myeloid malignancies including AML (158, 159). In these rare examples patients that have received BM transplants develop leukaemia as a pre-existing dysregulated niche initiates leukaemogenesis (160). This concept is based on the idea that a healthy BMM keeps any abnormal clones with the potential to transform in check. However, following introduction into the recipients dysregulated BMM, the clone now has a competitive advantage and undergoes clonal selection, thus developing leukaemia (160).

Relapse in AML occurs because of residual disease in the form of LSC that are unaffected by cytotoxic drugs, and evidence suggests that this resistance is facilitated through the LSCs ability to reside in BMM niches (13). It is thought that these niches promote chemo resistance, mediated through the promotion of LSCs quiescent hallmarks (remaining in G0), subsequently the LSCs are able to remain in such niches during regeneration (14, 161).

These normal BM niches are usually where HSCs reside, but instead these spaces are hijacked by LSCs and blasts – this occurs particularly in the endosteal (EN) and vascular niches (VN). Stromal cells and osteoblasts produce the complex ECM that facilitates LSC adhesion to BM niches; whilst in the EN, osteoblasts promote dormancy. Osteoclasts maintain a high calcium concentration and provide transforming growth factor beta (TGF-β) that also aids in LSC and blasts localisation. T-regulatory cells occupy the EN surface helping to circumvent immune surveillance. While the release of other cytokines, growth factors (GFs) and chemokines (e.g. CXCL12) by stromal, endothelial, mesenchymal and CXCL12-abundant cells helps to orchestrate LSC and blast migration to other niches (e.g. perivascular) (Figure 1.3).

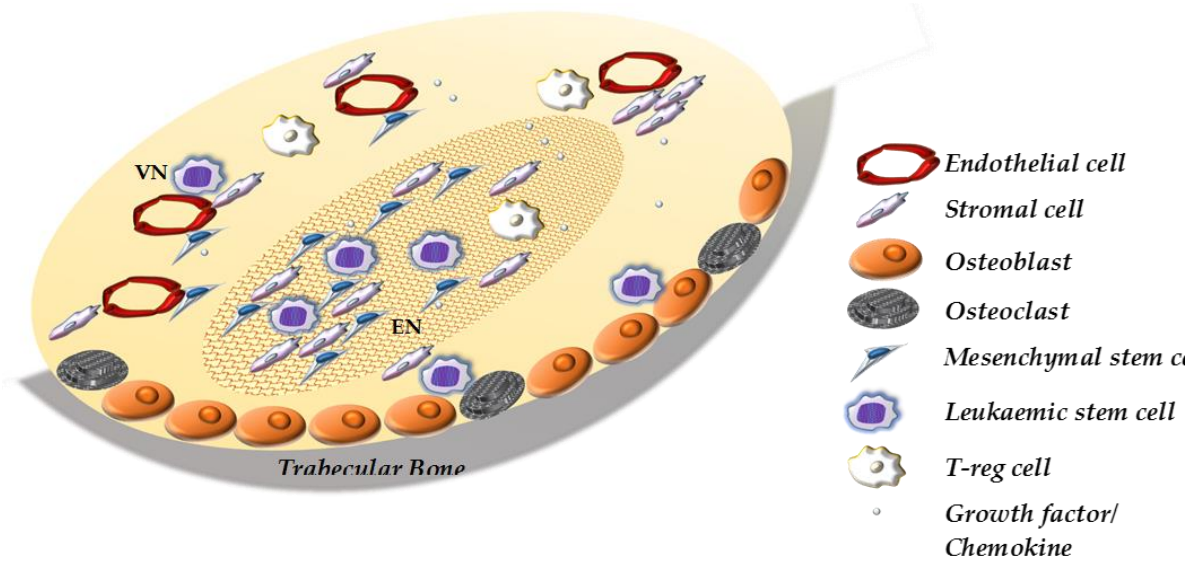

Figure 1.3: Bone marrow stromal microenvironment. Depicted are the different BM niches that LSCs and blasts can reside. These niches comprise multiple cell types including endothelial cells, MSCs, osteoclasts, osteoblasts, adipocytes, and stromal cells.

BM niches are stabilised through a number of factors as well as interactions between the cells of the BMM (13). The BMM is believed to coax the cells into niches where aspects of the LSC can be modulated further. Migration to these niches has been documented through chemotaxis via the interaction between CXCR4 and stromal derived factor 1 (SDF-1/CXCL12) (15). Retention of leukaemic cells is possible through cellular adhesion molecules such as VLA-4, fibronectin, integrins and hyaluronic acid (16, 18, 19). The LSC dormancy is maintained through osteopontin, N-cadherins and angiopoietin-1 conferring chemo-resistance (20).

1.2.3 Leukaemia induced remodelling of the microenvironment

During overt disease, evidence indicates that malignant cells reshape and modify the microenvironment to suit the needs of disease progression, and this is at the expense of normal haematopoiesis (162, 163) (Figure 1.4). To achieve this environment, leukaemic cells drive remodelling of mesenchymal, endothelial and nerve components (164). These include the dysregulated expression of CXCL12 in mesenchymal and endothelial cells, while essential HSC factors are reduced (165-167). Neuropathy characterised by a decrease in sympathetic nerve fibres and unsheathing of schwann cells is believed to exacerbate homing and engraftment of LCSs, while normal HSCs are forced to the periphery (168, 169).

Vascular remodelling within the BM is a unifying feature of the myeloid malignancies and increased micro vessel density is correlative with poor outcome in leukaemia (170, 171). The leukaemic cells have been shown to secrete pro-angiogenic factors such as Fibroblast growth factor (FGF), as well as pro-inflammatory cytokines; interleukin-6 (IL-6), IL-1β and tumour necrosis factor alpha (TNFα) which stimulate endothelial cell proliferation (172-174). In

turn, the expansion of endothelial cells that secrete granulocyte colony-stimulating factor (G-CSF) and granulocyte macrophage colony-stimulating factor (GM-CSF) raises the concentrations of these cytokines that have been linked with destabilising vascular integrity, thus inducing vascular leakiness (175). All of which helps to perpetuate a pro-leukaemic environment.

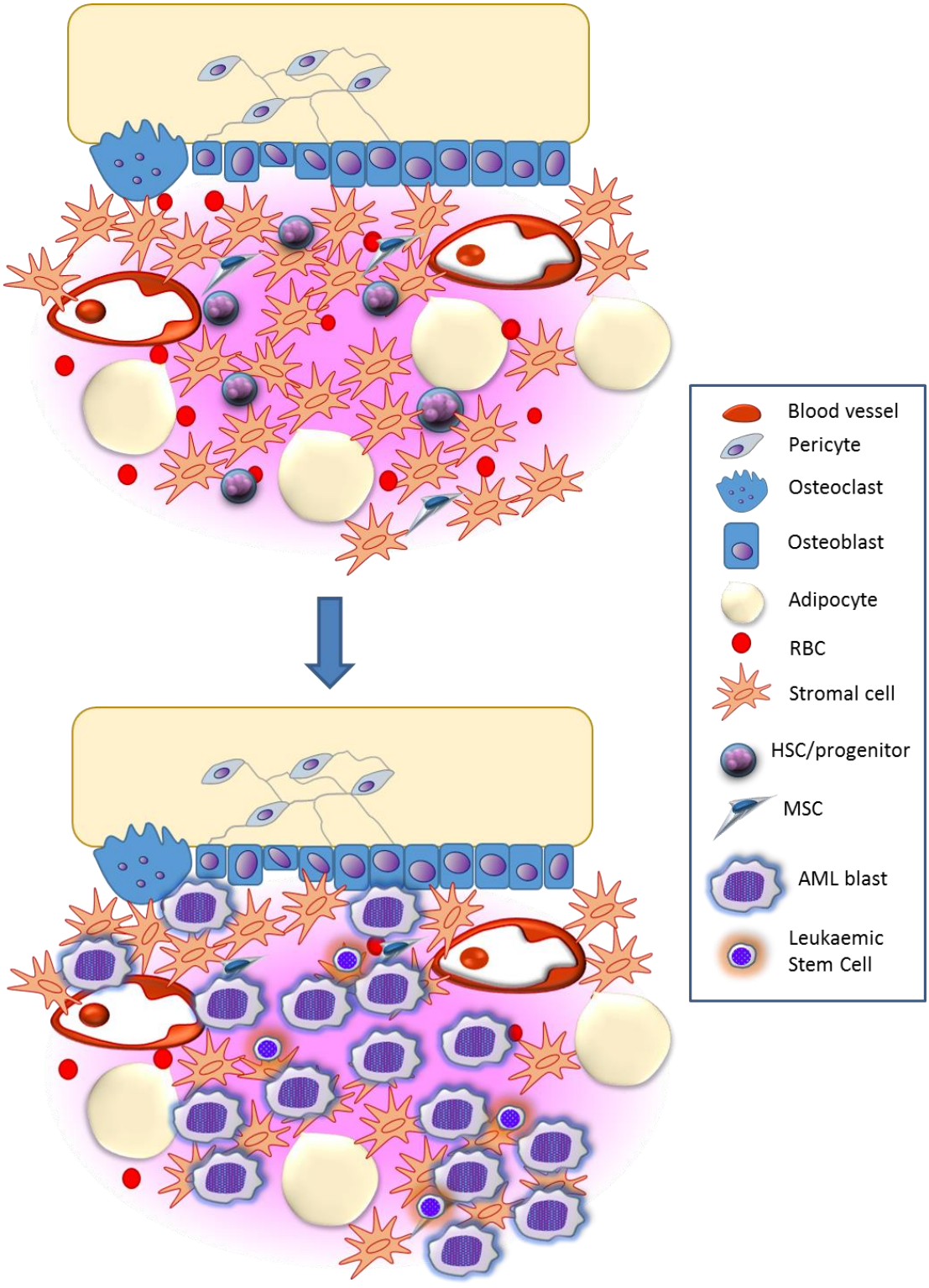

Figure 1.4: Model of the bone marrow microenvironment and the expansion of AML. The microenvironemnt is reshaped by maligncancy and undergoes remodelling that positively effects leukaemic expansion at the expense of normal haematopoiesis.

As a consequence of leukaemia directed mesenchymal remodelling various degrees of fibrosis can be observed in the BM, and the extent of BM fibrosis positively correlates with poor prognosis (176, 177). Under the influence of leukaemic cells, MSCs skew their differentiation in favour of osteoblastic generation and as a result their activity leads to fibrosis (178). Current evidence suggests that it is not necessarily the fibrosis that malignant cells require for disease propagation, but the support of disease-associated osteoblasts (179).

Finally, leukaemia cells were recently described as being able to subsist by hijacking lipolytic processes in adipose tissue to fuel metabolic needs while evading chemotherapy induced apoptosis (180). It is described that leukaemia can bypass apoptosis in this scenario, as the fatty acid oxidation pathway interferes with the oligomerisation of pro-apoptotic proteins BAX and BAK (175, 181).

1.3 Cell signalling and kinase networks

1.3.1 Cell communication and molecular cross-talk

A fundamental property of all organisms is their ability to adapt to their environment (182). This process is facilitated by the coordination of numerous proteins that receive, process and send signals with the environment. This communication mediates life and ranges from an organism interacting with the wider environment, to signals exchanged between two cells within an organism, down to intracellular interactions between regions of one cell – this is known as cell signalling.

Cell signalling is fundamental to all cellular function. Homeostasis, metabolism, migration, cell death and countless other processes are regulated by cell signalling. Signalling pathways represent collections of kinases and signalling proteins that coordinate together in distinct groups to mediate a cellular function. The significance of kinase signalling is underscored by the human genome encoding for over 500 protein kinases and collectively comprise one largest groups of evolutionarily related proteins (183).

Protein kinases regulate signalling networks through reversible protein phosphorylation of tyrosine, serine or threonine residues on target protein substrates (184) and lipid phosphorylation generates secondary messengers which in turn activate numerous downstream protein kinase cascades (185, 186). Protein phosphorylation is the most studied protein post-translation modification (PTM) and regulates the transduction of signals from cell surface receptors to the nucleus where these signals can induce changes in gene expression, and therefore mediate cell behaviour (187, 188). Phosphorylation is not the only means of regulating signal transduction, as other PTMs (e.g. ubiquitination, methylation, and acetylation) and co-regulators such as GTPases and secondary messengers are crucial for network activity (184, 185).

The role of kinases in AML is important as these proteins regularly harbour mutations in AML. These events have been described as leading to constituent activation of kinase regulated signalling pathways and their downstream targets.

As previously discussed leukaemic cells also rely upon the microenvironment for survival. To navigate, respond and shape the microenvironment, leukaemic cells utilise numerous means of cell signalling to drive these interactions. Principally, leukaemic cells will secrete factors (IL6, IL1β, TNFα) to mediate stromal behaviour (paracrine signalling), which in turn should result in the upregulation of pro-leukaemic secreted factors (G-CSF). This exchange is termed heterotypic signalling whereby one cell type activates another cell type to reciprocally induce signalling in the original cell. Leukaemic cells activate the FLT3 receptor and therefore, downstream pathways through secretion of FLT3 ligand (autocrine signalling) (189).

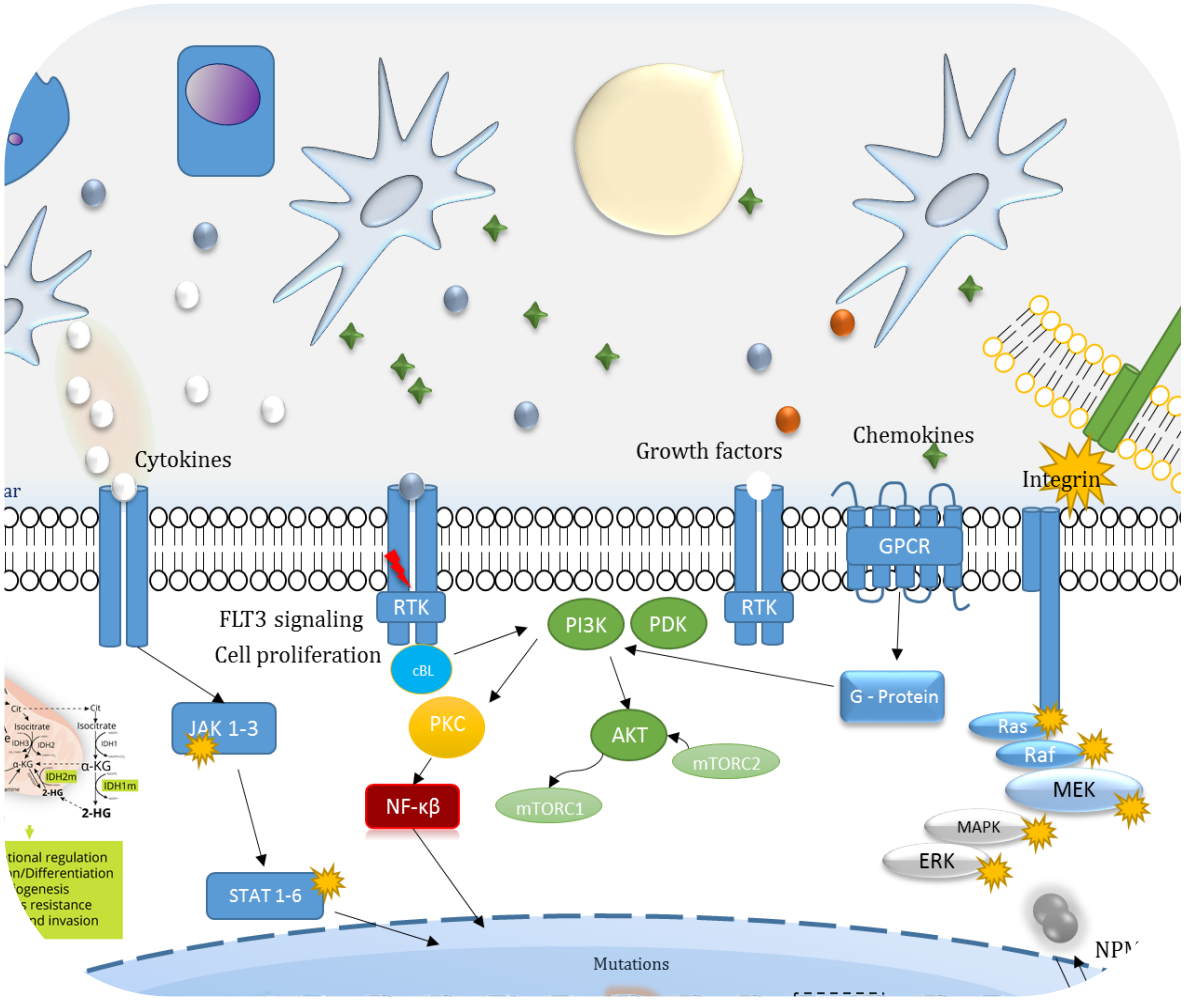

Figure 1.5: AML blast and stromal cell "crosstalk". A complex interplay that incorporates both the inherent cell biology and a heterogeneous cell population.

Stromal cells have been documented as being able to inhibit proliferation and apoptosis in leukaemia cells through gap junctions formed by connexins (190). Connexins are widely expressed on the cell surface of leukaemic cells and play a role in mediating leukaemic

chemoresistance (191). Although many of these connexins (i.e. cx32, cx43) have functional roles in regulating key signalling pathways such as MAPK and PI3K, connexins role in AML cell signalling has yet to be unravelled (192). Leukaemic cells also rely upon juxtacrine signalling through extra-cellular matrix (ECM) components, integrins and adhesion molecules that enable migration and niche homing within the BMM (193-195). These signalling mechanisms that mediate "crosstalk" with the BMM are summarised in Figure 1.5.

1.3.2 Canonical AML cell signalling

One set of therapeutic targets in AML are protein kinases (196). Many protein kinases are implicated in AML leukaemogenesis, as their activation plays critical roles in the regulation of many cellular functions (proliferation, survival, differentiation, and migration). Therefore, aberrant activation of these pathways is a key component of haematopoietic disease (197) (Figure 1.6).

Receptor Tyrosine Kinases (RTKs)

Several elements of signal transduction pathways are mutated in AML, with the most common occurring in the RTKs such as those in FLT3. Frequent over activation of RTKs through activating mutations or the binding of cytokines, GFs and chemokines leads to increased activation of downstream signalling kinases; phospho-inositide 3-kinase (PI3K), mitogen-activated protein kinases (MAPK) and the mechanistic target of rapamycin (mTOR) (197-202).

The PI3K/AKT/mTOR pathway regulates cell growth, cell survival, and apoptosis. The phospholipid products of PI3K activate downstream targets, including phosphoinositide-dependent kinase-1 (PDK1), AKT, and protein kinase c (PKC) (199, 203-205). The MAP-Kinase pathway can promote proliferation and malignant transformation in part due to the stimulation of cell growth (199). Ras is reported as being able to regulate both PI3K and MAPK (202). Raf activity is negatively regulated by AKT indicating a cross talk between the two pathways. Both PI3K and MAPK may result in the phosphorylation of many downstream targets and impose a role in the regulation of cell survival and proliferation (202). These pathways phosphorylate many key proteins involved in apoptosis (Bad, Bim, Bcl-1, caspases), which serve to potentiate AML cell survival.

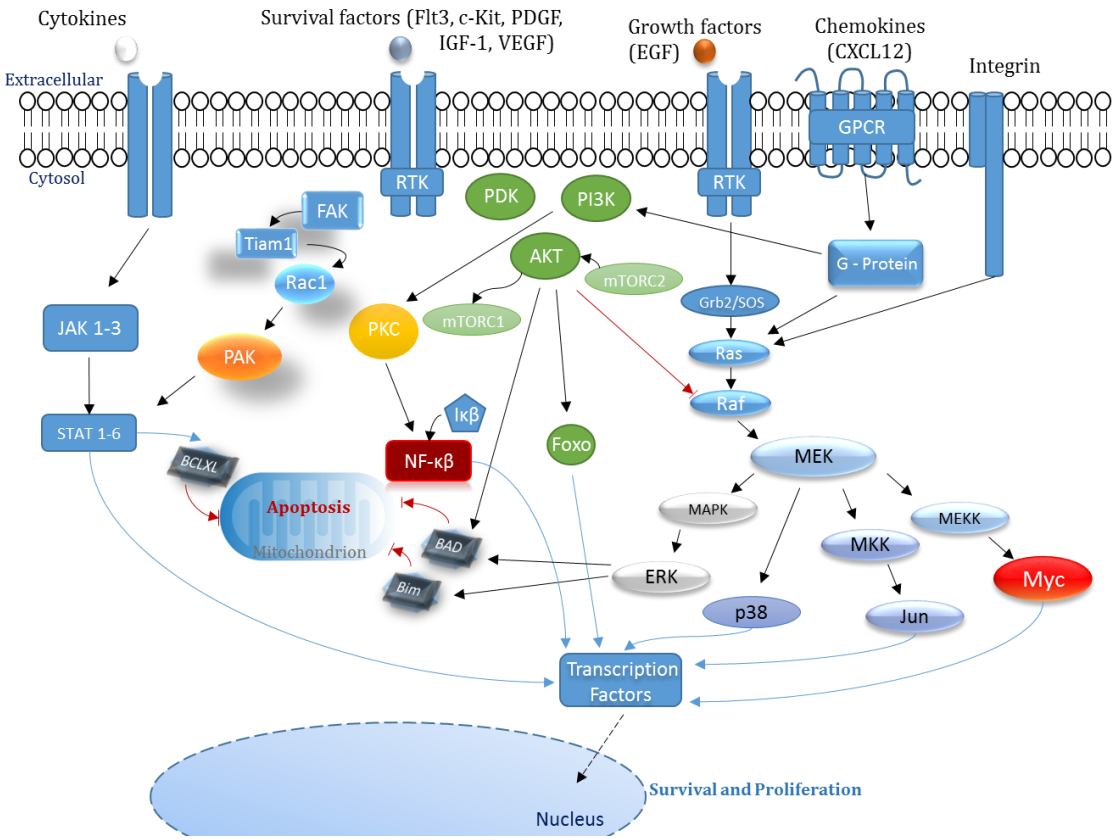

Figure 1.6: Signalling pathways of significance in AML. The main pathways thought to be potentiating AML are the JAK/STAT, Ras/Raf/MEK/ERK and PI3K/AKT signalling pathways (50). These are activated by a variety of cytokines, GFs and chemokines that function to potentiate or inhibit haematopoiesis, which include IL-3 and IL-7, SCF, VEGF, FLT3-ligand, G-CSF, type I interferons (IFN), TGF-β and CXCL12 (197). The JAK/STAT pathway is stimulated by activation of a cytokine receptor (IL-6, G-CSF), which results in STAT transcription factor activity (203).

Extracellular c-KIT mutations result in c-Kit receptor hyper-activation in response to stem cell factor (SCF) binding, this subsequently leads to strong activation of MAPK, PI3K and induces constitutive activation of signal transducers and activators of transcription 3 (STAT-3) (201). A result of which is the up regulation of Bcl-xL and c-MYC (197). AKT activates transcription of anti-apoptotic genes through the phosphorylation of IκB kinase (IKK) and regulation of nuclear factor-kappa B (NF-kB) (206). Oncogenic forms of FLT3 and KIT receptor activation are described as perpetuating a FAK/Tiam1/Rac1/PAK1 signalling axis, where by these signalling molecules play an essential role in regulating the nuclear translocation of STAT-5 in leukaemogenesis (207).

The Janus kinase/signal transducers and activators of transcription (JAK/STAT)

The JAK/STAT pathway allows for direct signalling from the cytokine receptor to the nucleus, which has been implicated in AML blast proliferation (50). Receptor associated JAK kinases (JAK1-3) are stimulated by ligand-mediated multimerisation of a receptor. The pathway can be activated through ligand binding of growth hormone receptors, interferon receptors, RTKs and GPCRs; however, in AML it is predominantly cytokine receptors (IL-6R and GCSFR) that

are responsible for pathway activity (208). Activated JAK-cytokine receptor complexes then phosphorylate one of the seven STAT family members, this phosphorylation results in STAT dimerisation and translocation to the nucleus, which leads to increased transcriptional activity and inhibition of apoptosis (209). IL-6, G-CSF and thrombopoietin (TPO) binding to their namesake receptors activates STAT3 downstream, whereas granulocyte macrophage (GM–CSF), TPO, and IL-3 binding primarily activate STAT5 downstream (178). AML patients have been described with truncated G-CSFR receptors that lack a binding site for regulatory protein SOCS-3, thus leading to increased pathway activity that favours proliferation (210). Increased STAT3 activity has been observed in 20-50% AML of patients and is associated with a poor prognosis, findings that led to STAT3 being considered as a candidate for targeted therapy in some patients (211).

The most frequently reported and therefore main pathways thought to potentiate AML are FLT3 driven PI3K/AKT, Ras/Raf/MEK/ERK and JAK/STAT signalling pathways (197). However, the particular kinase(s) that potentiate AML disease progression is not the same for all patients. With increased mechanistic understanding, targeting pathologically active protein kinases is a pharmacologically attractive approach, as manufacturing blockers to protein kinases is relatively simple due to the accessibility of kinase active sites (212, 213).

1.3.3 Network rewiring and plasticity

The proliferation of big data coupled with the integration of sophisticated computational bioinformatics has enabled the emergence of the systems biology paradigm, whereby network relationships are contextualised to account for crosstalk between nodes as opposed to the assumption of components acting in isolation. Consequently, the structure and topology of such networks are an expression of genomic information that can be modulated dynamically over time by both external (i.e. microenvironment) and internal perturbations (genomic aberrations). The consideration of these properties as a whole, is then what defines the phenotype of a given system.

Across time a number of factors can affect the activity and configuration of a network and these aspects will define how this system or network responds to internal and external elements. The plasticity of a kinase network and the potential for rewiring is broad and this is exemplified through the wirings of these networks being cell type specific that evolve during differentiation, ageing and in cancer (214-219) .

Malignant cells can respond to targeted inhibition of kinases by increasing the expression/activity of its effectors or the kinases downstream of the target, thus compensating for any reduced signalling output. For example, an acquired amplification of eIF4E or MYC in

response to the PI3K/mTOR inhibition can provide resistance to PI3K inhibitors (220). Kinase networks can also respond to inhibition by activating branches and parallel pathways that are independent of the targeted pathway. This is a common form of treatment resistance; as the activation of compensatory pathways facilitates the circumvention of the block in the network (221-224). Further studies have also shown the acquired activation of intracellular kinases in response to chronic inhibition of several kinases (225).

There are many mechanisms by which cancer cells can intrinsically circumvent, evolve resistance to, or engage the microenvironment to abrogate the pro-apoptotic effects or anti-proliferative effects of a particular treatment - much of which has rendered targeted therapies in AML ineffective. Even with the advancement of next generation platforms the prediction of patient response to different therapies is a serious challenge. These studies have also highlighted the significant role and frequency of cross-talk that exists between signalling pathways, traditionally such pathways have been conceptualised as linear axes that function in isolation (226-228) (Figure 1.7A). To fully understand the way in which kinases signal at a fundamental level and the shifts that occur during disease, cell signalling networks must be studied as a whole, without bias and in a high-content nature (229-231). Thus, enabling visualisation of the plasticity and cross talk between signalling proteins, which more accurately depicts global kinase signalling networks (Figure 1.7B).

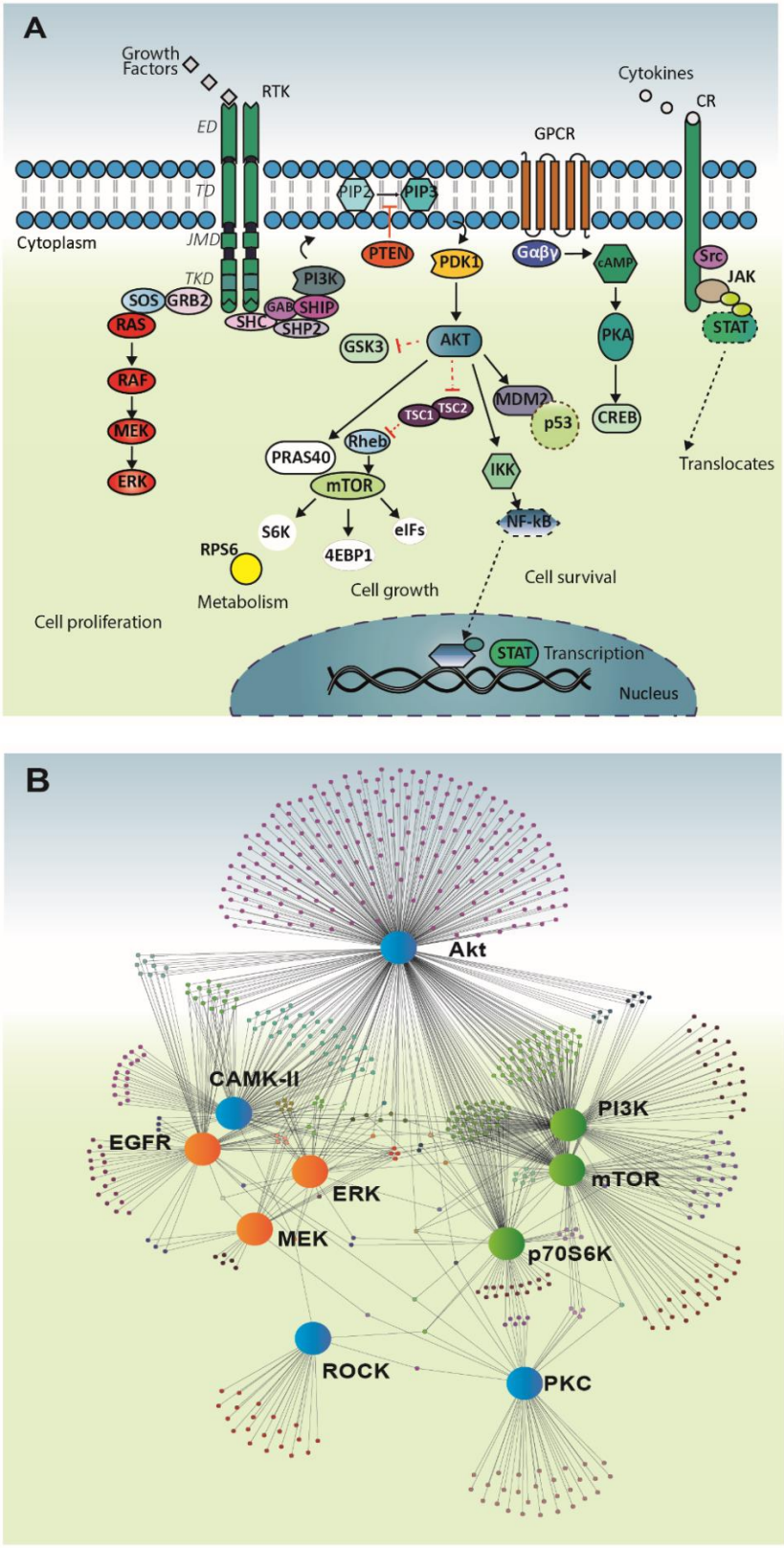

Figure 1.7: Models of cell signalling. (A) Example of a canonical signalling cascade, whereby linear distinct pathways transmit signalling to adaptor proteins and kinases, inducing functional outputs (i.e. cell proliferation, transcriptional activity, cell growth, metabolism, etc.). **(B)** Empirically defined kinase signalling network of MCF7 cells illustrating experimentally identified activity markers specific for this cell line. Each large node represents a kinase and the smaller nodes kinase substrates, edges linking nodes and substrates demonstrate the levels of cross talk between pathways. Figure from (232).

1.4 Proteomics

1.4.1 Mass spectrometry-based proteomics

Proteomics is the complete study of proteins of a biological system at a specific point in time. Numerous techniques have been employed to study proteins, but the technology that has contributed the most in recent years to define proteomics is mass spectrometry (MS). MS is an analytical technique that measures the mass to charge ratio (m/z) of ions after they have been converted to the gas-phase. All MS are built around the same three core components: an ion source, a mass analyser and a detector, however, there are variants of each of these components, and the selection of which depends on the application.

An MS experiment begins in the ion source, which converts the sample molecules from a liquid or solid phase into gas-phase ions. Upon entry into the MS ions are transported to the mass analyser via ion transfer optics at low pressure. Charged ions are then separated in the mass analyser according to their m/z, which allows discrimination between different molecular species. Ultimately, when each separated ion hits the detector, the relative ion abundance can be calculated by measuring the charge or current generated by the ion making contact with the detector. Plotting the relative ion intensity of ions against their m/z generates unique spectrums which can be used for compound identification.

Analysis of mass spectra generated by MS experiments can be used to determine both qualitative and quantification aspects of molecules contained in a sample. In recent years there has been increased areas of MS application and this follows the continual improvement in speed, sensitivity and resolution of the instruments. At present day, MS techniques are used in both industry and academia for specific and unbiased analyses of complex chemical and biochemical mixtures.

Electrospray ionisation (ESI) and matrix assisted laser desorption/ionisation (MALDI) are the two principal ionisation methods utilised in MS protein analysis, although ESI is more prevalent. ESI applies high voltage to a liquid-phase sample as it passes through an electrically conductive silica or capillary, to create a mist of charged ions that are in the gas phase (233). MALDI uses a laser to vaporise a crystallised solid phase sample which simultaneously ionises the sample before analysis (234). MALDI can capture spatial aspects of samples and accordingly is utilised for imaging applications (235). Although MALDI is used for peptide mass fingerprinting it is not as popular for high-throughput proteomic analysis, due to the lower time-efficiency of these instruments (236). ESI sources are more readily coupled to liquid-chromatography systems and reproducibility is far more reliable. Many laboratories now utilise an ESI variant termed “nano-ESI” for proteomic analysis, this variant of ESI is performed at lower flow rates

and increases the sensitivity of analysis due to higher ionisation efficiency, reduced ion suppression and higher analyte concentration by nanoflow LC (237, 238).

MS systems employ a range of mass analysers to identify peptides within a complex sample, which include quadrupoles, time of flight (TOF), 3D and linear ion traps, Fourier transform ion cyclotron resonance (FT-ICR) and Orbitraps. To identify peptides within complex samples, peptide masses are measured, these “precursor ions” are then selected and fragmented, before subsequent measurements. Many MS today will use a combination of more than one mass analyser to identify peptides.

A quadrupole ion trap consists of four rods which form a chamber where ions are trapped. Radio-frequency and electrical fields are applied to the rods to trap ions according to their m/z ratio while they move through the system at high speed. Quadrupoles are able to separate ions based on their unique m/z through manipulation of the radio-frequency voltages that are applied on the rods. The selection of specific voltage combinations allows for ions only of a particular m/z to maintain a stable trajectory when travelling through the quadrupole, prior to ion detection.

TOF analysers initially accelerate ions using an electrical field before allowing ions to drift free-field, wherein they then separate according to m/z, as it is this that dictates the speed by which they travel. Ion trap analysers, trap ions in an oscillating electrical field, which then depending on settings will eject ions from the trap according to m/z. FT-ICR based instruments, trap ions within a magnetic field, while an electrical field is applied to the chamber. This is a variation of the quadrupole ion traps. The m/z of each ion and the strength of the magnetic field determine the cyclotron frequency at which each ion rotates; rotating ions induce a charge on the detection electrodes, which can be converted into a mass spectrum using a Fourier transformation.

Orbitraps are similar to the FT-ICR instruments, as Obitrap instruments first trap ions using an electric field, before ejection into the Orbitrap. Ions then oscillate around the central electrode according to their m/z. The current induced by the oscillating ions on the detection electrodes can be transformed by a Fourier transformation into a mass spectrum.

The Linear Trap Quadrupole (LTQ)-Orbitrap, combines a linear quadrupole with an Orbitrap; here the intact masses are measured in the Orbitrap and precursor ions are fragmented in the quadrupole trap. Orbitraps have now become the benchmark analysers in the proteomics field, this is owing to their high mass resolution, high mass accuracy (1-2ppm), high sensitivity and relatively high dynamic range.

1.4.1.1 Sample preparation

For all MS experiments sample preparation is the critical step for successful proteomics analyses. Conceptually there are three principal approaches to preparing samples for proteomic analysis: bottom-up, middle-down and top-down (239). The bottom-up approach is the most commonly used in proteomics much like in genome sequencing; in this strategy proteins are proteolytically digested by a selected enzyme resulting in a complex mixture of variably sized peptides (depending the on protease). There are a number of different methods that include different proteases (trypsin, chymotrypsin, LysC, LysN, AspN, GluC and ArgC) to generate different peptide lengths which effect proteome coverage (240). The abundance and identity of the peptides can be extrapolated and inferences made after analysis, as to the quantitative and qualitative properties.

There are a number of factors that can affect method selection during bottom-up sample preparation (241). The first consideration regards protein extraction; if working with tissue then efficient steps need to be taken to ensure complete tissue disruption. If typically working with cells, then lysis is achieved with buffers that contain denaturing chaotropes (such as urea) to increase protein solubility or detergents. Following protein solubilisation, it is important to reduce chaotropes, detergents and contaminants as these can interfere with the efficiency of protein digestion, as chaotropes disrupt enzymatic activity. If proteins are immobilised on a solid support, removal of these elements can be achieved via two common strategies: polyacrylamide gel electrophoresis (PAGE) or filter-assisted sample preparation (FASP) (242)

In-solution protein digestions instead rely upon the dilution of disrupting substances to avoid a negative impact on the proteolytic yield. Solubilised and denatured proteins are subsequently reduced and alkylated with agents such as dithiothreitol (DTT) and iodoacetamide (IAM), respectively. Once sufficient IAM has bound to the thiol group of cysteines (inhibiting disulphide bond formation), consideration is required for the selection of enzyme used to digest protein mixtures. The most commonly used enzyme is trypsin, which cleaves proteins at the C-terminus of arginine (R) and lysine (K) residues (243). Other proteases, such as those mentioned previously, may be desired for certain proteomics experiments. Trypsin would not be ideal for the study of histone modifications given its cleavage of K residues or when the protein of interest has very few R/K residues (244). Some methods employ the utilisation of multiple proteases in parallel experiments thereby increasing coverage.

Both top-down and middle-down sample preparation differ to bottom-up preparation. Top down proteomic approaches aim is to characterise native proteins structures, and therefore

this technique requires no digestion (245). Middle-down methods do employ a digestion step; however, the peptides produced are usually much bigger than those in a bottom-up strategy (246). These strategies can be particularly useful in distinguishing isoform variants and for the study of multiple PTMs. However, despite the perspectives that middle-down and top-down provide, the complexity of whole-protein/large peptide fragmentation can make analysis problematic.

1.4.1.2 Liquid chromatography

The deep sequencing of complex proteomes (e.g. mammalian proteomes) requires the coupling of a separation step before the analytes enter into the MS. This is because the dynamic range and resolution of mass spectrometers are still limited and attempts to distinguish both low and high abundant species at the same time would be extremely difficult. To separate proteins, chemical properties such as their inherent hydrophobicity, charge and polarity can be exploited to fractionate complex mixtures in order to reduce ion suppression and increase peak resolution.

The most successful separation technique integrated with mass spectrometry, liquid chromatography (LC) is a widely used online (sample fractionation is directly coupled to the mass spectrometer) and offline method. LC-MS, separates molecular species based on the characteristics mention above - commonly hydrophobicity (as described here for reverse phase [RP] chromatography): a given sample when loaded on to a column containing a hydrophobic stationary phase, will bind with variable affinities under aqueous conditions. Elution will begin as a linearly increasing gradient of the organic mobile phase (acetonitrile [ACN] or methanol) is passed through the stationary phase. Peptides will elute as a function of their hydrophobicity. The time in which each species elutes from the column is termed the retention time (t_R) and is a distinctive characteristic of each peptide: hydrophilic peptides elute earlier from the column and hydrophobic peptides are retained longer in the column. Hence, the chromatographic separation expands the dynamic range and sensitivity of mass spectrometers. This is summarised in Figure 1.8A.

In addition, offline methods such as immunological/inorganic affinity purification (antibody and metal oxide) or 2D chromatography (such as strong cation exchange [SCX] and hydrophilic interaction chromatography [HILIC]) can also substantially reduce sample complexity. But the integration of these steps greatly increase sample preparation and MS run time.

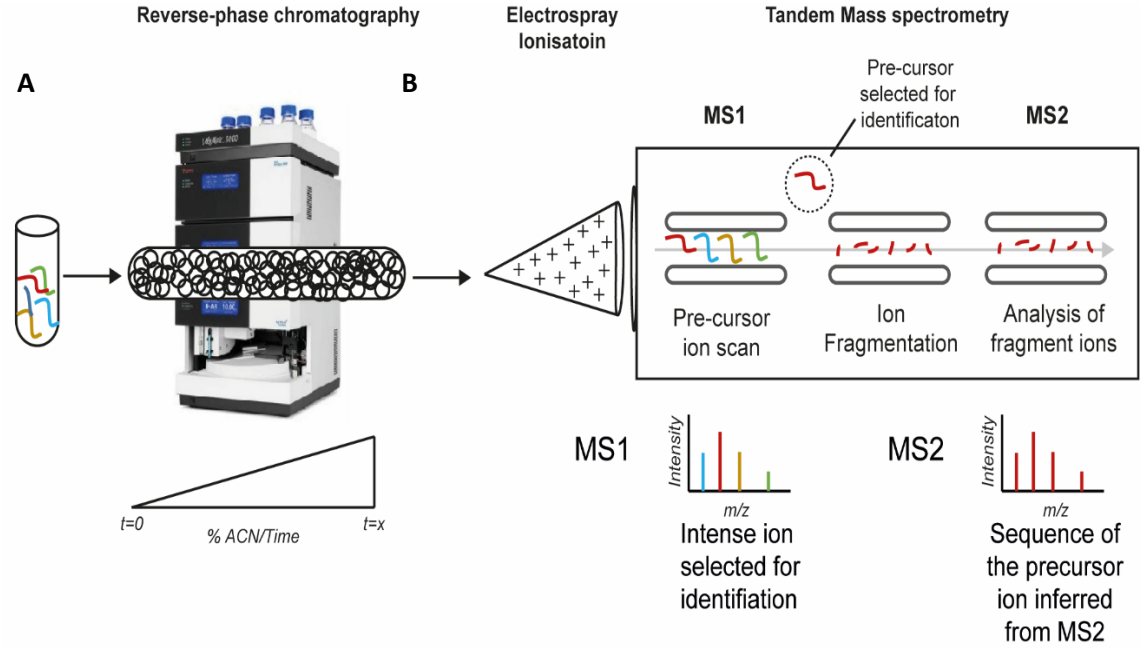

Figure 1.8: Principles of LC-MS/MS. (A) Each sample is separated by reverse-phase liquid chromatography prior to ionisation and introduction into the MS. Complex peptide samples are separated via LC using analytical columns, where peptides bind to the non-polar stationary phase under aqueous buffer and elute at a given retention time through the organic gradient depending on their hydrophobicity. These hydrophobic peptides are retained longer in the column. **(B)** Eluted peptides pass through the ESI emitter where the voltage charges droplets produce gas phase ions that then pass through the ion transfer capillary and are directed into the MS. Ions enter into the mass spectrometer where m/z intensities are measured in the first MS scan (MS1). A precursor is selected and isolated for fragmentation and intensities of fragmented ions are measured in the second MS scan (MS2). Inference of the MS2 data and subsequent comparison with a database enables peptide identification.

1.4.1.3 Qualitative MS proteomics

Qualitative proteomics for the identification of proteins and peptides can be carried out either in a targeted or untargeted manner. Experiments designed for targeted proteomics usually aim to measure with high precision the amount of known proteins within a sample. Untargeted proteomics, conversely, allows the unbiased identification of tens of thousands of proteins at once within a relatively short time.

Qualitative assignment of peptides and protein sequences is possible due to the existence of tandem mass spectrometry (MS/MS or MS2) analysis, which separates and fragments ions in a multiple-step process. In the first step, peptide ions are selected for their fragmentation. Fragmentation, can select peptides using two methods, data dependent acquisition (DDA) and data independent acquisition (DIA).

In DDA mode, the instrument is automated so that only a specific number of peptide ions, typically the “Top x” that generate a MS signal above a predefined intensity threshold are selected for fragmentation throughout the MS run. The DDA approach is limited by that fact

performance deteriorates as sample complexity increases, due to an inherent bias against less abundant ions; which subsequently will limit peptide identification and quantification of the sample. The increased sensitivity of newer instruments is due to shorter duty cycles (time it takes to acquire signals in a given setting) which has greatly increased the output of this approach.

In DIA strategies, all parent ions in an MS run are subjected to fragmentation. Peptides are identified by matching the transition ions to spectral repositories generated using previous DDA methods. The reported benefits of DIA are a broader dynamic range of signals, increased identification reproducibility and improved sensitivity and accuracy during quantification (247). The drawback is that this approach generates complex MS2 data that are difficult to interpret (248). An example of this approach is SWATH, which fragments and acquires all the ion spectra in sequential windows, through duration of the MS run (249)

Following selection, ions are subjected to fragmentation. This can occur in-source (although rarely applied in proteomic MS applications) or post-source in the collision zone. There are numerous means by which to transfer kinetic energy into ions, the two most commonly used in proteomics are electron transfer dissociation (ETD)/electron capture dissociation (ECD) and collision-induced dissociation (CID)/ higher-energy collision dissociation (HCD). Selection of the fragmentation method depends on both the instrument used for analysis and the sample, as different types of fragment ion are produced by each method. The most popular method for fragmentation is CID, whereby peptides are broken at the amide-backbone, generating *b*- and *y*-ions, whereas in ETD peptides are broken at the carboxyl-backbone, which generates c- and *z*-ions. HCD is similar to CID and specific to Orbitrap instruments, ions are transferred from the C-trap to a HCD cell where a higher voltage is applied to ions. The ions return to the C-trap, before fragments are injected into the Orbitrap for the generation of MS2 spectra. (Figure 1.8B)

MS2 spectra can be used to derive the sequence of amino acids that constitute the selected precursor ion without any prior knowledge (de novo sequencing). This is performed by calculating the difference in m/z between sequential peaks of the same ion type in a spectrum. This calculated difference in an ion series represents the loss of an amino acid, and therefore continuation through the series enables determination of a peptide sequence. This approach requires the identification of the ion series generated upon fragmentation, and is time consuming as until recently it was a manual operation. The pros of this approach are that novel peptides and peptide mutations can be revealed. The advent of recent software such as PEAKS (250) automates the process, making it a more user friendly approach.

The most common approach to undertake protein identification of large MS-based proteomics, is a database search approach, whereby the MS2 raw spectra are processed into peak lists. These lists are thereafter searched against a given database containing theoretical peptide spectra generated by *in silico* modelling of the experiment (251). This is highly automated and several software packages with different peptide identification scoring are available including Mascot (251), SEQUEST (252), X! Tandem(253), Andromeda (254). Until recently, Mascot was the most widely used of these software by the proteomics community (now Andromeda), and it scores a peak list using the MOWSE score. Initially, this search engine compares the experimentally produced peptide/proteome raw data with each entry in the database (± a given mass tolerance, defined by the user). The algorithm then calculates a probability score (*P*) that the peptide match is achieved by chance, and then converts *P* into a Mascot score as $-10 \times \log_{10}(P)$ (the Mascot score is inversely proportional the *P* value). This approach is popular as it is relatively fast and produces high throughput identification of peptides.

1.4.1.4 Quantitative MS proteomics

Qualitative proteomic analysis provides immense value to research. However, it has been the large-scale quantification of proteomes that has enabled researchers to address fundamental questions of biological systems and increase the collective understanding of biochemical processes (255, 256). There are two main methods applied in quantitative proteomics: label-based and labelled-free techniques.

Label-based approaches

Label-based approaches often involve the introduction of affinity tags that are of known, distinctive isotopic mass. These differentially labelled proteins or peptides from samples to be compared are then combined and analysed in the same LC-MS/MS run, and it is their relative intensities compared to heavy ion peptides (in isotopic labelling) or to a reporter ion (in isobaric labelling) which permits the calculation of peptide abundances.

Isotope-coded affinity tags (ICAT) (257) is an isotopic labelling method based on the covalent attachment at protein cysteine residues of heavy and light isotope tags (deuterium and hydrogen, respectively) which are attached to a biotin tag to enable purification. The mass difference between the heavy and light isotope-tagged samples can be resolved at the MS level. This processing at the MS level, leads to several technical limitations. These include the large tag interference that can occur during fragmentation and ICAT labelling is limited to cysteine-

containing proteins. Additionally, ICAT has a tendency to under-represent hydrophobic proteins, as these proteins are poorly recovered from avidin.

Isobaric labelling tandem mass tag (TMT) (258) and isobaric tags for relative and absolute quantitation (iTRAQ) (259) aim to address some of these limitations, by utilising reporter ions that are released during MS2. These reporter ions permit the identification and quantification of reporter groups (259). Despite popularity, TMT and iTRAQ present various drawbacks, primarily variability in labelling efficiency, limited identifications due to tag co-isolation and false positive fragmentation of precursors that have similar mass (260).

Stable isotope-labelled amino acids in cell culture (SILAC) (261), involves the incorporation of two differentially labelled amino acids into metabolically active cells during culture. One population of cells is cultured with media supplemented with unlabelled amino acids and the comparator population of cells is cultured with media supplemented with heavy amino acids (this mass shift is detectable by the mass spectrometer). Identical sample processing and equal protein mixing, enables the relative protein abundance to be calculated by comparing heavy labelled peptide ions to their unlabelled counterparts. In this approach, proteins are labelled as they are synthesised, which remedies purification and labelling kinetics issues (261). The major limitations of the SILAC approach are firstly, that its application to primary tissue samples is limited and a number of cells cannot tolerate these conditions. Secondly, there are a limited number of comparisons possible within an experiment. Additional drawbacks with SILAC, include the variable efficiency that isotopic amino acids are incorporated and the limited ability to apply this technique in the presence of serum (FBS) unless dialysed (the removal of small molecules such as amino acids, hormones and cytokines). This is because FBS contains unlabelled-light amino acids that would cause interference in heavy-labelled amino acid containing media. Despite these limitations, there are examples of the successful application of SILAC, remarkably mouse models raised on a SILAC-diet led to the protein labelling of various body organs without affecting their development (262).

Collectively, label-based approaches offer several options by which to perform quantitative proteomics analysis. Despite its feasibility and strength in particular experimental designs, there are crucial limitations. Namely, the increased complexity and time for sample preparation, limited experimental flexibility, labelling reagents that come at a relatively high cost and incompatibility with clinical samples. All of which collectively restrict the application of these approaches.

Label-free approaches

Label-free methods as the name suggests, require none of the pre-processing that labelled approaches entail, and also do not combine comparator samples within the same MS run. These approaches aim to either compare the abundance of peptides/proteins between samples or to perform absolute protein quantification at a global scale (263) and there are two different strategies that are currently used for the label-free quantification of proteomes.

The first approach, spectral counting, relies on the assumption that the abundance of a peptide selected for quantification is directly correlated with the number of MS2 scans triggered by that peptide (264). After counting the MS2 events for all peptides, the abundance of each particular protein is calculated by averaging the spectral counts of all peptides belonging to the given protein. This method is easy to implement. The limitation of the approach is that the quantitative capacity of spectral counting is often considered semi-quantitative, this is because the most abundant peptides are selected for MS2, thus neglecting low abundant peptides. Initiatives to improve and increase the usability of spectral counting for quantitation, include emPAI (exponentially modified PAI) (265) and APEX (Absolute Protein EXpression) (266). These methods try to correct the experimentally measured spectral counts with the expected peptides detection in silico.

The second label-free approach, constructs extracted ion chromatograms (XICs) of the precursor peptide ions. To construct an XIC, the *m/z* is integrated over the chromatographic time for each peptide, the peptide abundance is then determined by calculating either the area of peak or peak height for each eluted peptide. The accuracy and performance of this approach depends on the, *m/z* tolerance and size of the retention time windows used to generate XICs. These are modulated by the MS1 performance. The size of the retention time windows is crucial when generating XICs from complex samples, as they can have isobaric peptides within a given retention time window. Therefore, narrowing the *m/z* window can reduce the erroneous selection of peaks for quantification, but reduce the window too much and the XIC generated could miss the target peptide. This principle is described in the accurate mass and time (AMT) tagging data analysis of mass spectrometry data method for the accurate selection of LC-MS parameters for peptide/protein quantification (267).

A targeted label-free method that is conducted in triple quadrupoles instruments set in selection mode is called selective reaction monitoring (SRM), whereby sequential quadrupoles coordinate so that the first quadrupole specifically selects precursor ions to be fragmented, the second fragments the precursors and the third monitors to calculate abundance (268).

Subsequently, the abundance of a specific peptide is calculated by its product ion of a specific *m/z* derived from its particular precursor ion. Multiple reaction monitoring (MRM) is a similar concept to SRM but provides greater confidence in the quantification as it monitors multiple product ions from a precursor ion.

In the Cutillas lab, peptide quantification of label free LC-MS/MS data is facilitated by the computer program PESCAL (Peak Statistic Calculator), which quantifies peptides of complex samples in an untargeted manner and automates the generation of XICs comprised by *m/z* values centred at the peptide *tR* (269). Initially, a database is populated of peptides identified in the LC-MS/MS raw data file, with each peptide *m/z*, charge state (z), *tR* and name that were identified. The retention times of common peptides are calculated across samples in order to normalise for variability in the chromatography. The retention times are then used to calculate the XICs. To increase the accuracy of this method, peaks that are used to construct XICs must contain a minimum number of data points to pass QC. Furthermore, the ratios of the second and third isotopes of each peptide are correlated with the expected theoretical distribution. Incorporating this into the quantification improves the reliability and accuracy of peak-picking, helping to increase the correct assignation of isobaric peptides (269).

The strength of label free quantification is exemplified in this approach. Primarily, unlike labelled quantification methods, the number of possible samples that can be compared using PESCAL is theoretically limitless. Additionally, this strategy can compensate for missing values and performs peptide quantification and identification even if the peptide was not selected for MS/MS fragmentation, which can help with overlooked low abundant peptides. The other issue with a labelled approach is the compatible cell types and material, that is not an issue using label free approaches.

The limitations of large scale XIC quantification arise in the alignment of retention time shifts, this can be reduced by robust LC systems. Spurious peptide assignment to MS peaks can occur, although this will likely improve with the implementation of high mass-accuracy MS instruments. The caveat for all label-free methods, is that samples must be compared independently and controlling for intra-run discrepancies is a known issue with mass spectrometers. PESCAL by comparison is a highly reproducible, label-free quantification method that can report robust quantification and accurate quantitative readout (270), this has led to its successful implementation in addressing multiple biological questions (215, 271-273).

1.4.2 Mass spectrometry-based secretomics

The term secretome was coined by Tjalsma et al. (274), and was defined as the collective term for all the secreted proteins and secretory machinery of the bacteria cells being studied,

and has expanded to the repertoires of proteins that are secreted externally by cells (275). Secretomics is considered a branch of proteomics and publications in the area to date have focused predominantly on biomarker discovery, but secretomics can also be a powerful means to study disease progression and cell communication.

There are a number of techniques currently available to study the secretome and the choice of approach will primarily depend on whether the secretory protein sequence(s) of interest are known. If a known protein is being investigated then RNA sequencing, DNA microarrays and in silico methods have been demonstrated as means to track expression or model potentially secreted proteins. When the proteins being measured are unknown then approaches such as serial analysis of gene expression (SAGE), protein arrays, secretory traps and MS are more typically used (Figure 1.9).

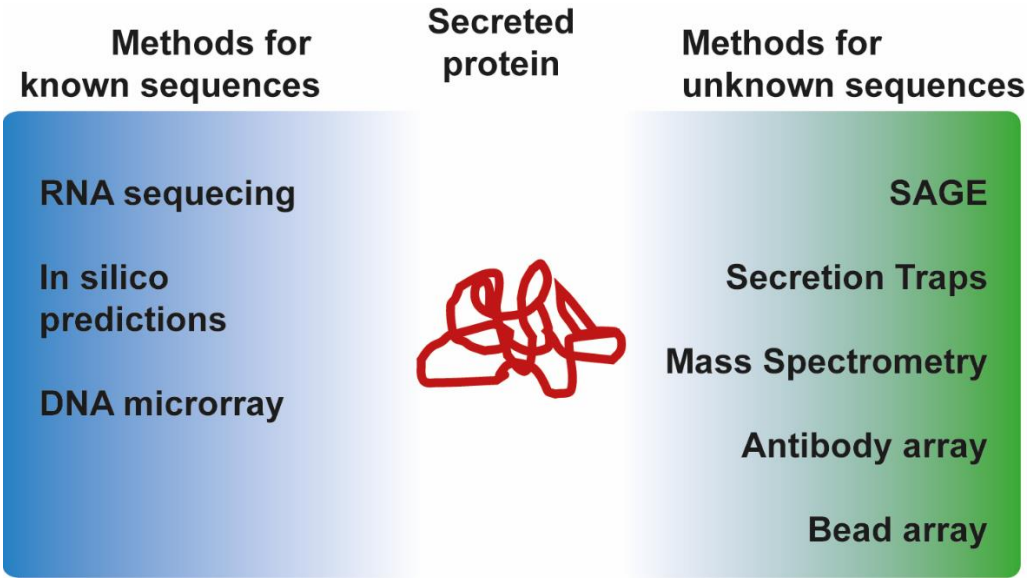

Figure 1.9: Approaches to study secretome composition. Schematic representative of the methodologies that can be used to investigate the secretome. Selection is usually directed on the type of study being undertaken.

Many secretomic studies begin with conditioned media (CM) and various enrichment strategies are employed (ultra-centrifugation, fractionation, ultra-filtration, protein precipitation, and lyophilisation) to concentrate secretory proteins and remove background material, as secreted proteins are present at very low concentration. Considerations (that will guide detection platform selection) need to be made regarding the system in which secreted proteins are collected, as the inclusion of serum introduces significant background that can mask proteins of interest during LC-MS detection. At the same time, serum starvation needs to be tolerable to cells, as excessive cell death leads to the release of proteins that will contaminate the secretome and confound results. Additionally, serum deprivation can induce differential responses in different cell types and alter the biology that is trying to be captured.

To enable the inclusion of serum in secretomic MS-based experiments, methods for serum protein removal have previously been devised. These protocols can involve metabolic labelling of cells, so that their secretome can be differentiated from serum proteins. Alternatively serum albumin binding to specially designed resins can used to remove background serum proteins (276). The drawbacks of metabolic labelling are that it is both time-consuming and not compatible with many cell types. Resins designed to remove serum proteins, also risk the unintentional removal of important non-serum proteins.

Although dependent on the nature of the study, an MS-based method offers unparalleled coverage when approaching secretome analysis in an unbiased manner. Protein arrays (antibody and bead) are very sensitive and robust; however, they are limited to measuring a defined set of proteins, of which need to be selected for analysis beforehand. RNA Sequencing and DNA microarrays have merit, but they are indirect read-outs of protein production/ secretion and secretomic relevance is inferred rather than directly measured. SAGE and secretion traps have historically been successful in identifying secretome components (277), but they are comparatively time-consuming methods that can be prone to error (259).

LC-MS/MS approaches to identify secretory proteins can be separated into two main methods, gel based and gel-independent techniques. Gel based methods include two-dimensional gel electrophoresis (2DE) and differential gel electrophoresis (DIGE), whereby secretomes are first separated to resolve discrete spots based on charge and mass, prior to gel extraction and identification using LC-MS/MS. This approach has proved successful in identifying secretory proteins in CM from numerous cells types including adipose stem cells, fibroblast feeder cells and leptin treated breast cancer cells (278-283). The advantages of this approach are that previously unknown proteins can be identified with high resolving power. Disadvantages include a low dynamic range that limits the identification of low abundant proteins, a relatively low-throughput, and reproducibility can be an issue.

Gel-independent LC-MS/MS techniques include the isotopic labelling of cells prior to conditioning media, this allows for the quantification of proteins synthesised by the cell type of interest in different conditions, which are then combined to be measured in one MS run (257, 284, 285). Common labelling strategies include the previously described SILAC, iTRAQ and ICAT. Examples of success using labelling approaches include the identification of secretory proteins from the microenvironment of glioma cells using ICAT (286), iTRAQ coupled LC-MS/MS which was used to decipher differences in the secretome of macrophages infected with influenza (287), and SILAC which was successfully used to study pancreatic and squamous cell carcinoma cancer secretomes (288, 289). Advantages to gel-independent methods include the ability to detect low abundance proteins coupled with high sequence coverage, and reproducibility is

increased by being able to include different biological conditions in the same MS run. The main disadvantage with label-based gel-independent techniques is that they are not always feasible in the cells of interest; SILAC media for example is not well tolerated by primary samples, ICAT is only appropriate for cysteine containing proteins (although ICAT is no longer popular).

Overall, LC-MS/MS based approaches to study secretomes have been proven to be the most powerful and unbiased means to directly identify and subsequently quantify secreted proteins. The current challenges involve optimising the sample processing and enrichment of secretomes prior to LC-MS/MS analysis.

1.5. Phosphoproteomics

Numerous studies have now demonstrated that the expression of individual genes at the mRNA level correlates poorly with the expression of the proteins they encode (290, 291). On a similar train of logic, it has become increasingly apparent that the abundance of particular enzymes, in most cases, does not correlate with their actual activities (292). In contrast, knowledge of their spatial distribution, post-translational regulation, and the abundance of the products of the reactions they govern are now appreciated as more representative readouts of their catalytic activity. As a result, the study of sub-proteomes – either in terms of sub-cellular distributions or specific populations of PTM proteins – has become a popular area of research, particularly with the increasing accessibility of MS technologies that are able to define these. Such studies often involve the specific enrichment of proteins possessing the PTM of interest (e.g. phosphorylation, acetylation, or glycosylation), isolation of a particular class of protein (e.g. kinases or histones), or purification of specific cellular organelles/compartments (e.g. mitochondria or Golgi apparatus).

Due to the long-known importance of protein phosphorylation in cellular signalling, its relatively simple and amenable chemistry, its relative abundance, and the development of ever more powerful MS and LC technologies, phosphoproteomics (the study of the entire complement of phosphorylated proteins in a biological system) has been perhaps the most studied sub-proteome in recent years.

1.5.1 The implications of phosphorylation events

The impact of phosphorylation on protein function is diverse in nature; (293) however, the main regulatory roles that have been demonstrated experimentally, are often tied to functional processes, demonstrating the importance of protein phosphorylation in cell function. Phosphorylation events play a key role in the propagation, amplification, and correct interpretation of signals from both intra- and extracellular sources.

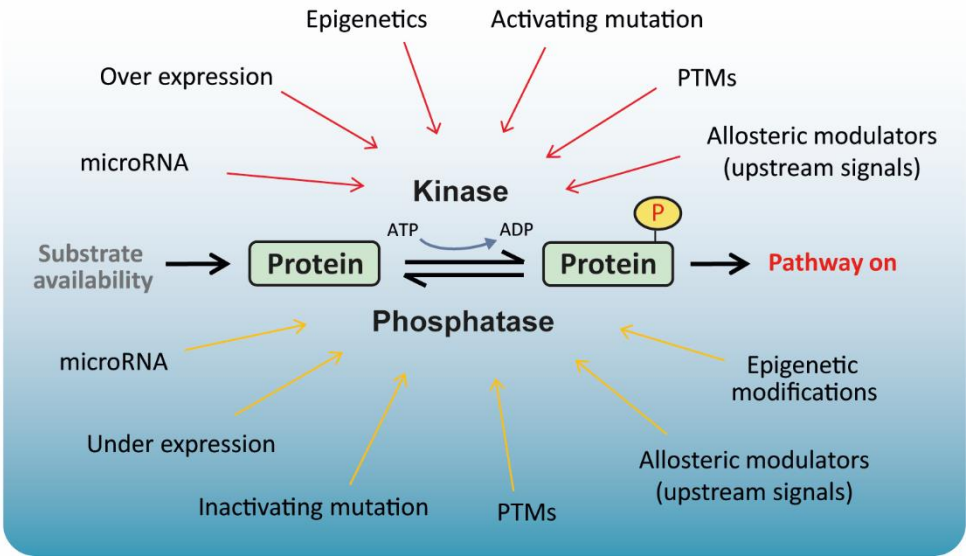

Figure 1.10: Molecular mechanisms that contribute to the activation of kinase signalling. Several molecular factors, in addition to expression, may affect kinase activity. Pathway activity may be influenced by somatic mutations, by upstream signals and by substrate availability. The action of protein phosphatases opposing the reaction may also be influenced by similar molecular events. Quantifying the phosphoprotein product of the kinase/phosphatase activity provides the most direct method of quantifying pathway activity.

The occupancy of individual phosphorylation sites is governed by both the kinases and phosphatases that phosphorylate and dephosphorylate their substrates. The expression of a phosphorylation event encompasses the rate at which both the respective kinases and phosphatases to this substrate catalyse their respective reactions. Therefore, the overall equilibrium between protein and phosphorylated protein encompasses the activity of these processes at one moment in time (Figure 1.10) (294). However, in addition to these regulators the balance is also determined by other aspects of the system, including: epigenetic and genetic regulation, allosteric modulation and mutations amongst others, that impact upon one phosphorylation event (182).

As the interaction between the kinases and phosphatases that regulate protein phosphorylation is complex, a proposed and now putative readout of their combined functions is through the quantification of the phosphorylated substrate (271, 295). MS has been instrumental in the unbiased assessment and global analysis of phosphorylation events, as tens of thousands of phosphorylation sites can be fully quantified in a single experiment, without the need of antibodies or arrays with preconceptions of targets.

1.5.2 Phosphopeptide enrichment strategies for MS analysis

When analysing phosphorylation events considerations need to be made regarding the fragile nature of the ATP gamma phosphate modification. This modification is unstable at both

high temperature and high pH due to β-elimination that is driven by OH^-. It is also crucial to inhibit phosphatases as they are still active following cell lysis and will act to remove phosphate groups from peptides (296). Therefore, to preserve and measure a representative phosphoproteome of the system being studied, it is essential to maintain a non-alkaline pH, inhibit phosphatase activity using inhibitors and keep samples below 4°C.

Against the backdrop of the proteome and complex peptide mixtures, phosphorylated peptides are at risk of being under sampled due to low stoichiometric abundance relative to other peptide species and MS technical issues. Principally ion suppression is what leads to less efficient phosphopeptide ionisation compared to unmodified species (297). Therefore, phosphopeptide-enrichment methods are required to increase the number of phosphopeptides that can be identified when undertaking phosphoproteomics. There are several approaches to enrich for phosphorylation events, namely chemical derivatisation, chromatography, immunological affinity purification and inorganic affinity purification (298). Approaches summarised in Figure 1.11.

Chemical derivatisation involves the removal and substitution of phosphate groups. The principle of this method is that substituting the phosphate group improves the peptide ionisation and MS2 fragmentation. The classical example involves β-elimination of phosphate mediated by providing OH- ions, followed by Michael addition of thiol-derived affinity tags (298). This technique has key deficiencies including sample loss, the addition of unwanted peptide modifications and a bias towards serine over threonine modifications.

Immunological-based affinity purification relies on the selective recognition of phosphorylated residues by specific antibodies that recognise pSer/pThr or pTyr residues (299). Antibody purification of pTyr containing protein and peptides has been successfully used for the study of pTyr residues, although there is a paucity of alternative pTyr enrichment approaches (300, 301). pSer/pThr antibodies have been demonstrated to be quite poor and not particularly specific.

Phosphopeptides can also be separated from unmodified species using different chromatography fractionation strategies, based on charge (SCX or strong anion exchange [SAX]), pKa or hydrophobicity (HILIC). Charge-based separation approaches exploit the differences in charge between phosphorylated and non-phosphorylated peptides. In SCX and SAX, peptide tR is proportional to the ionic strength of the mobile phase, and ions can be eluted using a pH or salt gradient. SCX chromatography selectively retains highly charged (+2 or higher) tryptic peptides, and as phosphopeptides have a net charge of 0 or +1 they will elute in the first fractions

while most unmodified species are retained (302). Whereas, SAX chromatography selectively retains phosphopeptides in the polar column to enrich for phosphopeptides (303). These fractionation approaches are effective when working with small amounts of phospho-material, or when coupled with other enrichment methods (304). The coupling of SCX and SAX with other methods (such as IMAC or TiO_2) to overcome their lack specificity for phosphopeptide enrichment alone result in good coverage of the phosphoproteome as recently demonstrated by some pre-fractionation strategies (305).

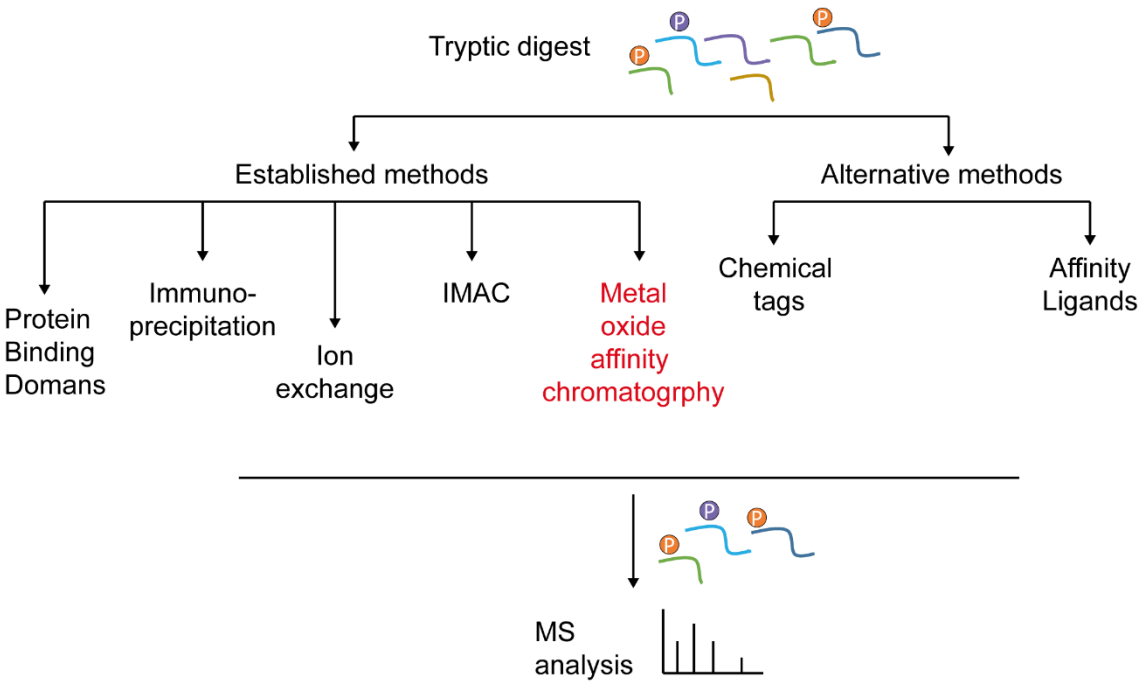

Figure 1.11: Established and alternative strategies for phosphopeptide enrichment. The selection of phospho-enrichment method depends on the sample and type of phosphopeptides. Established methods include purification based on protein binding domain affinity, antibody-based precipitation, immobilised metal ion affinity chromatography (IMAC), ion exchange and metal oxide affinity chromatography (MOAC). Alternative methods include chemical tags and affinity ligands.

The pH-dependent, negatively-charged phosphate groups can also be enriched by chelation with positively-charged metal ions contained in solid affinity matrices. The most commonly used methods based on this principle are immobilised metal ion affinity chromatography (IMAC), metal oxide affinity chromatography (MOAC) or combinations of both. IMAC resins chelate metal ions such as Fe^{3+}, Ni^{2+}, Cu^{2+}, and Ga^{2+} which in turn form ion-pair interactions with phosphate groups. Ti^{4+}-IMAC has proved highly reproducible (306). Metal-bound phosphopeptides can be recovered either by raising the pH or adding phosphatase ions (307). The specificity of IMAC to enrich for phosphopeptides can be limited due to the fact that some amino acids and acidic peptides bind to the transition metals.

MOAC, as mentioned above is based on the affinity of metal oxides, (such as TiO_2, ZrO_2 or AlO_3) to phosphate groups. TiO_2 remains the most widely used method given its high

enrichment efficiency (308). Similar to IMAC, specific and non-specific binding can occur in TiO_2-MOAC. The addition of TFA can reduce the binding of specific and non-specific acidic non-phosphorylated peptides, improving the selectivity for phosphate groups (309). Although multiply-phosphorylated peptides tend to tightly bind to TiO_2, efficient elution of phosphopeptides from TiO_2-MOAC is usually achieved using basic eluents, such as NH_4OH (310), and through the use of multiple round of elution steps (311). As a result, it is possible to achieve robust and sensitive label-free phosphoproteomic analysis using a single-shot TiO_2-MOAC based method. An approach that is adopted by many groups for MS-based phosphoproteomics (270, 312, 313).

Considerations need to be taken during MS and bioinformatic analysis of phosphoproteomics data. Phosphopeptides are not fragmented as well as non-phosphorylated peptides, owing to their lower positive charge (as the phosphate group is negatively charged). When CID fragmentation methods are implemented, a β-elimination reaction is induced, leading to a neutral loss of HPO_3, or H_3PO_4. This neutral loss results in an MS2 spectra with little sequence information and a very intense peptide peak (minus H_2PO_4). To compensate, fragmentation methods can be optimised for the sequencing of phosphopeptides, and such methods include neutral loss scanning or multistage activation.

Improved CID-based activation methods such as multistage activation contribute to reducing the prevalence of neutral loss ions in the MS2 spectra by fragmenting both a phosphopeptide and its theoretical m/z value following neutral loss, corresponding spectra are then combined. A HCD based fragmentation increases the accuracy of measured ions, as phosphopeptide sequences are measured in an Orbitrap mass analyser, generating more reproducible and site specific data (314). One drawback to the HCD fragmentation is its comparatively slow speed in most instruments compared to CID. This means in some systems a based CID approach can produce denser datasets.

Separate to CID based approaches for phosphopeptide identification are ETD based methods. ETD based fragmentation dissociates substrate peptides by electron transfer from a donor molecule (often from fluoranthene). The benefit of using ETD to trigger peptide amide backbone fragmentation, is that it preserves labile PTMs. ETD; however, has limited applicability to peptides of charge state 2^+ and 3^+, often encountered in tryptic peptides (315).

Collectively numerous ion fragmentation methods and computational approaches have been developed to improve the sequencing and accurate site localisation of phosphopeptides by MS, consideration of these strategies ensures the best possible coverage of the phosphoproteome can be achieved (316).

Computational methods to investigate cell signalling by phosphoproteomics have been developed in recent years (272), these approaches that can be used to estimate kinase activity directly from high-throughput MS data to understand the signalling response. These methods were recently tested as part of a benchmarking study by Hernandez-Armenta et al. (313). They compared the KSEA (kinase substrate enrichment analysis) method (developed in the Cutillas group) (271) with similar predictive algorithms (291) and reported a strong performance by all methods in correctly predicting kinase activity changes. The KSEA method assumes that the activity state of a given kinase can be inferred from the phosphorylation of its known substrates. As opposed to other techniques, this method does not directly measure kinases (317), but instead uses phosphoproteomic targets and kinase-substrate annotations (e.g. those included in PhosphoSitePlus, signor, or others (318)) to predict kinase activities. Hernandez-Armenta et al. also reported that the number known kinase substrates and the source of the evidence for interactions (*in vivo*, *in vitro,* or *in silico*) may influence the predictions (319).

1.6 Aims

The relationship between cells of the microenvironment and AML is complex, and studies discussed in this chapter have outlined the importance of this interaction and that successful future targeted therapeutic strategies will need to include means that can overcome the contribution of the BMM. In this PhD I undertook a multi-proteomic approach to understand the role of the microenvironment in AML, principally investigating how bone marrow stromal cells can modulate AML kinase networks and how this impacts leukaemic cell survival.

Chapter 2: Materials and Methods

2.1 Reagents

Name	Manufacturer	Product number	Supplementary info
CellTiter 96 AQueous non-radioactive cell proliferation assay	Promega	G5421	Cell viability assay reagent
RPMI-1640	Gibco	11875093	Culture medium for AML cell lines
DMEM	Gibco	11965092	Culture medium for HS-5 cells
IMDM	Gibco	12440061	Culture medium for MS-5 cells and primary AML
MEM α, no nucleosides	Gibco	12561056	Culture media for MS-5 cells
IMDM (no phenyl red)	Gibco	21056023	Culture medium for secretome analysis
Sodium Pyruvate (100 mM)	Gibco	11360070	Media supplement
L-Glutamine (200 mM)	Gibco	25030081	Media supplement
MEM Non-Essential Amino Acids Solution	Gibco	11140035	Media supplement
Heat-inactivated Foetal Bovine Serum (FBS), E.U approved	Gibco	10500-064	Serum used for maintenance and culturing of cells
EDTA-trypsin (0.05%/0.02%)	Sigma Aldrich	L11-004/T4299	Detach adherent cell lines during cell culture
Penicillin/streptomycin	Sigma Aldrich	P4333	Antibiotics for cell culture
Trypan Blue solution 0.4%, liquid, sterile-filtered, suitable for cell culture	Sigma Aldrich	T8154	Cell viability assay reagent

Table 2.1: A summary of cell culture reagents.

Name	Manufacturer	Product #	Primary Target	Concentration
Torin-1	Tocris	4247	mTORC1 / mTORC2	1 µM
Trametinib	Selleckchem	S2673	MEK1/MEK2	1 µM
Tofacitinib	Selleckchem	S5001	JAK 1-3	1 µM
Midostaurin	Selleckchem	2992	PKC, PDFR, VEGFR2, Syk, Flt3	1 µM
PF-3758309	Selleckchem	S7094	Pan PAK	1 µM
IPA-3	Tocris	3622	Pan PAK	2.5 µM
FRAX-597	Selleckchem	S7271	PAK1-4	20 nM

Table 2.2: A summary of kinase inhibitors.

Name	Manufacturer	Product number	Lot number	Source	Mol.weight (kDa)	Concentration
Recombinant Human S100-A4	Abcam	Ab191676	-	E.coli	12	10ng/ml
Recombinant Human S100-A4	R and D systems	4137-S4-050	QEG0315111	E. coli	12.4	10ng/ml
Recombinant Human S100-A11	Abcam	Ab90612	-	E.coli	11.7	10ng/ml
Recombinant Human Connective tissue growth factor (CTGF)	Abcam	Ab50044	-	E.coli	11	10-50ng/ml
Human recombinant Bone morphogenic protein-1 (BMP-1)	R and D systems	1927-ZN-010	MMH2016011	Mouse Myeloma cell line	70.5	10-20ng/ml
Recombinant Human Hepatocyte growth factor (HGF)	Peprotech	100-39	1114S201	Hi-5 insect cells	80	10-20ng/ml
Recombinant Human Macrophage-Colony stimulating factor-1 (CSF-1)	Millipore	GF053	2739425/ 2605445	E.coli	36.8	10ng/ml

Table 2.3: A summary of recombinant growth factors used in Chapter 4 experiments.

Primary Target	Code	Technique	Company	Dilution
Total CSF-1	ab9693	WB	Abcam	1:1000
Total S100-A4	ab41532	WB	Abcam	1:250
Phospho-ERK1/2 (Thr202; Tyr204)	4370	WB	CST	1:1000
Total p44/42 MAPK (Erk1/2)	9102	WB	CST	1:1000
Phospho-Akt (Ser473)	9271	WB	CST	1:1000
Total AKT	9272	WB	CST	1:1000
Total P70S6K	9202	WB	CST	1:1000
Phospho-p70/p85(Thr389;Thr412)	9206	WB	CST	1:1000
Phospho- 4EBP1 (Thr37; Thr46)	9459S	WB	CST	1:1000
Phospho-PAK4 (Ser474)	3241	WB	CST	1:1000
Total PAK 1	2602	WB/ Co-IP	CST	1:1000/1:50
Total PAK 2	2615	WB/ Co-IP	CST	1:1000/1:50
Total PAK 3	2609	Co-IP	CST	1:1000/1:50
Total PAK 4	3242s	WB/ Co-IP	CST	1:1000/1:50
Human/Mouse/Rat PAK4 (goat)	AF4178-SP	WB	R+D Systems	1:200
Histone H2B Antibody (N-20) polyclonal goat	sc-8650	WB	Santacruz	1:200
Total Vinculin	4650	Co-Ip	CST	1:50

phospho-PAK1/2 (ser199/204)/ (Ser192/197)	2605	WB	CST	1:1000
Phospho-PAK1(Thr423)/ PAK2(Thr402)	2601s	WB	CST	1:1000
GAPDH – Loading control	ab9485	WB	Abcam	1:2500
Lactate dehydrogenase – Loading control	ab85319	WB	Abcam	1:1000
α-Tubulin – Loading control	2144	WB	CST	1:1000
β-actin – Loading control	4967	WB	CST	1:2500
Amersham ECL Rabbit IgG, HRP-linked whole Ab (from donkey)	NA934	WB	GE Healthcare	1:5000
Amersham ECL Mouse IgG, HRP-linked whole Ab (from sheep)	NA931	WB	GE Healthcare	1:5000
EasyBlot anti Goat IgG, HRP	GTX628547-01-S	WB	Insight Biotech	1:5000

Table 2.4: A summary of antibodies used in western blots (WB) and co-immunoprecipitations (co-IP).

Antigen	Clone	Metal
CD19	HIB19	142Nd
CD117	104D2	143Nd
CD11b	ICRF44	144Nd
CD64	10.1	146Nd
CD123	6H6	151Eu
CD45	HI30	154Sm
CD33	WM53	158Gd
CD15	W6D3	164Dy
CD34	581	166Er
CD3	UCHT1	170Er
CD44	IM7	171Yb
CD38	HIT2	172Yb
HLA-DR	L243	174Yb
CD184	12G5	175Lu
CD14	M5E2	160Gd
CD16	3G8	148Nd
CD7	CD7-6B7	147Sm

Table 2.5: A summary of antibodies used in mass cytometry experiments.

Name	Manufacturer	Product #	Information
4% Paraformaldehyde	Santa cruz	30525-89-4	Fixing cells for CyTOF
4-12% mini-GEL	Invitrogen		Western blot
ACQUITY UPLC Peptide BEH C18 Column, 300Å, 1.7 µm, 2.1 mm X 50 mm	Waters	186003685	Analytical column used for LC separations during LC-MS/MS on XL instrument
nanoACQUITY UPLC Symmetry C18 Trap Column, 100Å, 5 µm, 180 µm x 20 mm	Waters	186006527	Trap column used for LC separations during LC-MS/MS on XL instrument
Acclaim™ PepMap™ 100 C18 analytical Column, 3µm, 100Å, 75 µm x 25 cm	Dionex	164261	Analytical column used for LC separations during LC-MS/MS on Q-Exactive plus instrument
Acclaim™ PepMap™ µ-Precolumns, 5µm, 100Å, 300 µm x 5 mm	Thermo Scientific	160454	Trap column used for LC separations during LC-MS/MS on Q-Exactive plus instrument
Bicinchoninic acid (BCA) assay	Thermo Scientific	23225	Protein concentration estimation
C18 micro-spin columns	Glygen	TT2C18.96	Offline peptide desalting spin column
C18/graphitic carbon TopTip micro-spin columns	Glygen	TT2MC18.96	Offline peptide desalting spin column
Deoxyribonuclease I from bovine pancreas, Type IV, lyophilized powder	Sigma Aldrich	D5025	To stop clumping of cells during the thawing of primary AML samples
Empty spin filter-tips TF2EMT	Glygen	TF2EMT	Spin tips used for compacting TiO_2 resin during phosphor-enrichment steps
Eppendorf Protein LoBind tubes (1.5/2ml)	Sigma Aldrich	0030 108.116/ 132	Low protein binding tubes for MS based proteomics to reduce protein loss
epT.I.P.S.® LoRetention tips, 50 – 1000 µL	Sigma Aldrich	0030072030	Low protein binding tips for MS based proteomics to reduce protein loss
epT.I.P.S.® LoRetention tips, 2 – 200 µL	Sigma Aldrich	0030072022	Low protein binding tips for MS based proteomics to reduce protein loss
FUJI Film X100 RX X-RAY Film (18x24cm)	Fisher	12715325	X-ray film for western blot analysis
Guava ViaCount Reagent for Flow Cytometry	Merck Millipore	4000-0040	Reagent for Guava viacount viability and proliferation assays
iBlot™ Transfer Stack, Nitrocellulose	Invitrogen	IB301001	PAGE reagent
Immobilised trypsin-tosyl lysine chloromethylketone (TLCK)	Thermo Scientific	20230	Immobilised trypsin beads used for protein digestion
mini-PROTEAN 12% PA-gels	Biorad	456-1044	PAGE reagent
Novex NuPAGE 4-12% Bis-Tris midi gel	Invitrogen	WG1402BX10	PAGE reagent
Novex NuPAGE 20X MOPS SDS running buffer	Invitrogen	NP0001	PAGE reagent
Novex NuPAGE 20X Transfer buffer	Invitrogen	NP0006	PAGE reagent
Novex NuPAGE Antioxidant	Invitrogen	NP0005	PAGE reagent
Oasis-HLB 1cc cartridges	Waters	WAT094225	Offline desalting method for peptide clean-up
Okadaic acid	Calbiochem	495604	Phosphatase inhibitor added to WB lysis buffer

Phenylmethylsulfonyl fluoride (PMSF)	Sigma Aldrich	93482	Serine protease inhibitor added during cell lysis for western blot and coIP
Phosphatase inhibitor cocktail I	Sigma Aldrich	P8340	Inhibitor added during cell lysis for western blot and coIP
Ponceau S Solution	Sigma Aldrich	93482	Reagent for checking transfer efficiency during western blot
Protein A/G PLUS-Agarose	Santa Cruz	sc-2003	Solid support for co-IP complex pull-down
PVDF membrane	Millipore	IPVH00010	Membrane used for western blot
SuperSignal West Pico ECL substrate	Thermo Scientifc	34080	Horseradish peroxidase (HRP) reagent for western blot visualisation
Titansphere TiO_2 beads (10 µm)	GL Science inc	5020-75010	Material used to bind phosphor-peptides during phosphor-enrichmnet
Trypsin from porcine pancreas	Sigma Aldrich	T6567	Soluble trypsin used for co-IP protein digestion and on-bead elution
Vivaspin 20 MWCO 1000	GE Healthcare Lifesciences	28932360	Columns used for secretome purification via ultra-filtration

Table 2.6: A summary of miscellaneous materials and reagents.

2.2 Cell lines and primary patient samples

Name	Species	Cell type	Morphology	Information	Ref
MS-5	Murine	BMSC	Adherent fibroblastic	Established by irradiation of the adherent cells, derived from the BM of C3H/HeN strain mice.	(320)
HS-5	Human	BMSC	Adherent, fibroblastic	HPV-16 E6/E7 transformed, derived from a healthy 30-year-old male.	(321)
P31/FUJ	Human	Peripheral blood derived myeloid blasts	Non-adherent, with monocytic characteristics	Established through long-term culture from the blast cells of a 7-year-old male, with AML (M5 subtype). Carries t(10;ll)(pl3;ql4) leading to CALM-AF10 fusion gene and is considered a complex karyotype.	(322)
MV4-11	Human	Peripheral blood derived myeloid blasts	Non-adherent, with monocytic features	Established through long-term culture from the blast cells of a 10-year-old male with biphenotypic B-myelomonocytic leukaemia, M5 substype. Possesses a t(4;11)(q21;q23), +8, +19 karyotype, leads to MLL-AF4 fusion gene.	(323)
HL-60	Human	Peripheral blood derived myeloid blasts	Non-adherent, promyelocytic features	Established through long-term culture from the blasts of a 35-year-old female with AML, considered M2 FAB subtype. Cells possess a number of cytogenetic abnormalities leading to complex karyotype.	(324)
CTS	Human	Peripheral blood derived myeloid blasts	Non-adherent, with monocytic features	Established from the blast cells of a 13-year-old female, with relapsed AML (M5 subtype). Cells possess a number of cytogenetic events including t(6;11)(q27;q23). Possesses deletions of the T-cell receptor δ1 gene.	(325)

Table 2.7: A summary of cell lines.

MV-411, HL-60, CTS and P31/FUJ cells were grown in RPMI 1640 media supplemented with 10% fetal bovine serum (FBS), penicillin and streptomycin (P/S) (each at 100 U/ml). Cells were maintained at a confluency of 0.5 - 2.0×10^6 cells/ml. Cell line incubated at 37°C in a humidified atmosphere at 5% CO_2.

MS-5 cells were grown in IMDM (clone 1) or α-MEM (clone 2) media supplemented with 10% FBS, P/S (each at 100 U/ml), 2mM L-Glutamine, with cells maintained at a confluency of 0.05 - 0.1x10^6 cells/ml. HS-5 cells were seeded in DMEM media supplemented with 10% FBS, P/S (each at 100 U/ml) and cell line were maintained at a confluency of 0.05 - 0.5x10^6 cells/ml. Cell line incubated at 37°C in a humidified atmosphere at 5% CO_2.

Primary cells were cultured in IMDM supplemented with 10% FBS, P/S (each at 100 U/ml) or with CM (production of which is outlined below). Cells when reanimated following LN_2 preservation, were thawed in the presence of DNase to reduce cell clumping and washed with PBS supplemented with 10% FBS. Once resuspended in appropriate media cells were normalised through incubation at 37°C in a humidified atmosphere of 5% CO_2 for 60 minutes, after this time cells were ready for experimentation.

2.2.1 Seeding for experimentation

For AML cell lines (MV4-11, HL-60, CTS, P31/FUJ) cells were harvested by transferring media to 50ml falcon tubes (no detachment required as suspension lines). Cells were centrifuged to pellets and old media aspirated before re-suspension in fresh media. The cells were then counted using a Beckman Coulter Vi-Cell cell viability analyser and seeded in fresh T75 flasks at a density of 0.5x10^6 cells/ml 24 hours prior to experimentation.

2.2.2 Clinical features of primary samples

Patients gave informed consent for the storage and use of their blood cells for research purposes. Experiments were performed in accordance with the Local Research Ethics Committee, as previous described (326). The clinical details of the 16 cases used in this study are shown below in Tables 2.7 and 2.8. Experiments were performed with primary samples in which mononuclear cells were extracted from the peripheral blood and BM of AML patients.

Patient ID (#)	FAB	Risk Group	Cytogenetics	Mutations
0	M5	Adverse	T(6;11) 11Q23	-
1	M4	Adverse	11Q23	No identified variants
2	M4	Intermediate	NORMAL	FLT3-ITD
3	M4	Favourable	INV (16)(P13Q22) ;CBFB/MYH11	-
4	M5	Adverse	T(11;17) MLL (11Q23)	-
5	M4	Favourable	INV (16)	-
6	M2	Adverse	COMPLEX (inc T(8;9))	TET2 (p.P133Qfs*12, VAF = 41.6%), NRAS (p.G13D, VAF = 43%)
7	2ND AML	Intermediate	11P-, + CLONAL T(2;3)	IDH2 (p.R140Q, VAF = 47%), NRAS (p.G13D, VAF = 48%)
8	2ND AML	Adverse	COMPLEX (inc -5,-7,-9,-10,-21)	ASXL1 (p.A809Cfs*13, VAF = 23%)
9	M5	Adverse	T(6;11)(Q27;Q23)	TET2 mutant, FLT3-WT
10	2ND AML	Adverse	5Q-, -7	No identified variants
11	M5	Adverse	11Q29	No identified variants
12	M0	Adverse	INV(3)(Q21Q26) AND T(8;13)(P21;Q14)	No identified variants
13	-	Adverse	T(6;11) MLL-MLLT4 REARRANGEMENT	-
14	M2	Adverse	T(6;9)	-
15	M5	Intermediate	ADD(21)(P11.2)	-

Table 2.8: Cytogenetic and molecular features of the primary AML samples used in studies. If cell coloured grey, then patient sample was screened for variants outlined in Table 2.9. 2ND AML denotes therapy related myeloid neoplasm.

Patient ID (#)	Risk Group	Sample Type	% PB blasts at Diagnosis	GENDER 1=M 2=F	Age at Diagnosis	Overall Survival (months)	Sample Status	Response to 1st treatment	EP
0	Adverse	PB	-	1	34	-	Pre-treatment	-	Yes
1	Adverse	BM	85	1	46	14	Pre-treatment	FAIL	-
2	Intermediate	PB	74	2	37	14	-	-	-
3	Favourable	PB	84	2	20	-	-	-	-
4	Adverse	PB	64	1	27	-	-	-	-
5	Favourable	PB	71	2	52	-	-	-	-
6	Adverse	PB	64	1	62	9	Relapse	CR	Yes
7	Intermediate	-	-	-	-	4.5	Relapse	-	Yes
8	Adverse	BM	10	1	56	5.5	Pre-treatment	CR	Yes
9	Adverse	PB	98	1	36	12.5	Relapse	-	Yes
10	Adverse	PB	25	2	66	4	Pre-treatment	FAIL	Yes
11	Adverse	BM	79	2	64	0.05	Pre-treatment	-	Yes
12	Adverse	PB	-	1	39	6.5	Pre-treatment	FAIL	Yes
13	Adverse	PB	94	2	32	-	-	-	-
14	Adverse	PB	16	1	29	-	-	CR	-
15	Intermediate	PB	93	1	75	-	-	FAIL	Yes

Table 2.9: Clinical features of the included primary AML samples. PB = Peripheral blood, BM = Bone marrow, CR = Complete response, EP = Engraftment potential, - = information unavailable.

2.2.2.1 Panel Sequencing

Targeted enrichment of a 25 gene myeloid panel was achieved using an in-house True SeqCustom Amplicon (TSCA) design (Illumina, San Diego, USA). Genes included in this panel are shown below.

Gene	Exons	Gene	Exons
ASXL1	12	***KRAS***	2 + 3
BCOR	all	***MPL***	10
CALR	9	***NPM1***	12
CBL	7 + 8 + 9	***NRAS***	2 + 3
CEBPA	all	***PDGFRA***	12, 14, 18
CSF3R	14 - 17	***PHF6***	all
DNMT3A	all	***PTPN11***	3 + 13
ETV6	all	***RUNX1***	all
EZH2	all	***SETBP1***	4
FLT3	14 + 15 + 20	***SF3B1***	12 - 16
GATA2	all	***SRSF2***	1
GNAS	8 + 9	***TET2***	all
IDH1	4	***TP53***	all
IDH2	4	***U2AF1***	2 + 6
IKZF1	all	***WT1***	7 + 9
JAK2	12 + 14	***ZRSR2***	all
KIT	2, 8-11, 13 + 17		

Table 2.10: Selected genes that were screened for variants in patients #1, 2, 6-12.

2.3 Stromal secretome production

For the preparation of the CM, MS-5 or HS-5 cells were cultured until 60% confluent in their respective media. The growth medium was then removed, and cells washed with PBS. Fresh IMDM containing either 0.5% (v/v) FBS for starved conditions, 10% FBS for serum containing assays and 0% FBS for MS experiments was added. Cells were cultured for a further 24-72 hours prior to CM collection. Supernatant were then centrifuged to pellet debris, media would then either proceed to secretome enrichment, be used as supportive CM immediately or it was stored at 80°C.

Ultrafiltration – Vivaspin 20 columns

The method for stromal secretome purification and filtration is described in Figure 2.1 below. Subsequent LC-MS/MS analysis of the stromal secretome, was only conducted on >5kDa fraction of secretome containing no serum. Production and acquisition of the AML/MS-5 co-culture secretomes and AML only secretomes is detailed in Figure 3.18. Following purification of co-culture secretomes all laboratory processing was the same as that described for experiments utilising the stromal secretome alone.

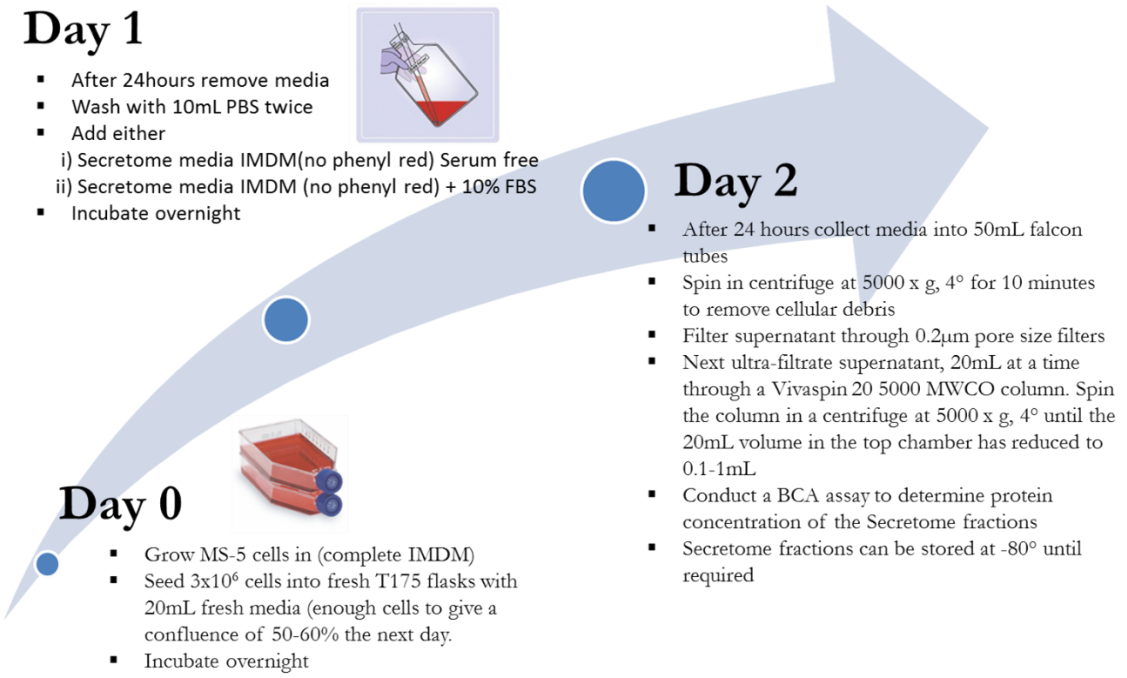

Figure 2.1: Protocol for producing MS-5 and HS-5 conditioned media and enrichment of secretome.

Methanol/chloroform precipitation

Following collection of CM, samples were mixed with methanol in a 1:4 ratio before undergoing vortex. Then 1 part chloroform was introduced prior to further vortex. Next 3 parts milliQ H_2O was added and vortexing continued (at this point samples should appear cloudy). Samples were then centrifuged for 2 minutes at x 12,000 g. Following centrifugation, the sample should have separated into phases, the top aqueous layer was removed being sure not to disrupt the thin wafer protein layer. Another 3 parts of methanol were added followed by vortexing and centrifugation for 2 minutes at x 24,000 g. As much methanol as possible was removed without disturbing the protein pellet prior to solubilising with lysis buffer.

2.4 Cell lysis

Suspension cells were transferred to 50ml falcon tubes before being gently centrifuged and washed 3 times with ice-cold PBS (supplemented with 1 mM Na_3VO_4 and 1 mM NaF). The cell pellet was then lysed with 500µl lysis buffer/1x10^7cells. Each pellet was then solubilised via pipetting and left on ice for 40 minutes. Lysates were then sonicated using a diagenode bioruptor (40 cycles of 40 seconds on and 30 seconds off) and centrifuged at 20,000 x g for 10 minutes (5°C), resulting supernatants were kept for further analysis. The protein concentration of each lysate was then determined via bicinchoninic acid (BCA) assay (Bovine serum albumin [BSA] was used to construct a standard curve (correlating absorbance at 595 nm with protein concentration).

Lysis Buffer	Composition	Application
Tris Triton/NP40 Buffer	50mM Tris-HCl (pH 7.4), 150mM NaCl, 1mM EDTA, 1% Triton/NP-40. Supplemented with phosphatase inhibitors (1mM Na_3VO_4, 1mM NaF, 10mM DTT, 200mM PMSF and 1mM Okadaic Acid) and protease inhibitors (protease inhibitor cocktail; Sigma Aldrich-Aldrich)	**Western Blot**
Tris - CHAPS lysis buffer	150mM NaCl, 50mM Tris-HCl(pH7.4), 0.3% CHAPS, 1mM EDTA. Supplemented with phosphatase inhibitors (1mM Na_3VO_4, 1mM NaF, 10mM DTT, 200mM PMSF and 1mM Okadaic Acid) and protease inhibitors (protease inhibitor cocktail; Sigma Aldrich-Aldrich)	**Co-immunoprecipitation, Western blot**
Hepes – CHAPS lysis buffer	0.3% CHAPS, 50mM Hepes (pH7.4), 150mM NaCl. Supplemented with phosphatase inhibitors (1mM Na_3VO_4, 1mM NaF, 10mM DTT, 200mM PMSF, 1mM -glycerol phosphate, and 2.5mM $Na_2H_2P_2O_7$ and 1mM Okadaic Acid) and protease inhibitors (protease inhibitor cocktail; Sigma Aldrich-Aldrich)	**Co-immunoprecipitation**
Urea lysis buffer	8M Urea in 20 mM HEPES pH 8.0. Supplemented with 1 mM Na_3VO_4, 1 mM NaF, 1mM -glycerol phosphate, and 2.5mM $Na_2H_2P_2O_7$)	**Secretome solubilisation, LC/MS-MS sample preparation**

Table 2.11: A summary of lysis buffers, buffer composition and the applications for which they were applied.

2.5 Western Blot

40μg of protein lysate was mixed with 4X Laemmli buffer and heated to 95°C before being loaded into a 4-15% gradient gel and resolved by SDS–polyacrylamide gel electrophoresis. Subsequent proteins were transferred to polyvinylidene difluoride membranes (PVDF). Once blocked, membranes were incubated with primary and secondary antibodies (*Table.2.2*) and developed with SuperSignal West Pico Chemiluminescent Substrate (Thermo Scientific) exposing x-ray films (FUJI film) or imaged using a ChemiDoc system.

2.6 Guava ViaCount

Ex-vivo testing of cell lines and AML primary cells treated with CM (from HS-5 or MS-5 cells), enriched secretomes (10μg/ml), recombinant GFs (10ng/ml) or kinase inhibitor (1μM) and cell proliferation, viability and apoptosis were measured with a Guava PCA cell analyser (Guava Technologies Inc.). Briefly assays were run in 96-well plates and cells seeded at a density of $2x10^4$ cells/well in 100ul. Results obtained using 75μl/well Guava ViaCount reagent (Millipore) according to the manufacturer's instructions. Seeding corrections made by normalising counts to Day 0 measurements of respective test condition.

2.7 Gene expression microarray

Survival plots are produced using the BloodSpot database. This database provides gene expression profiles of genes and gene signatures in both healthy and malignant haematopoiesis. Kaplan-Meier survival analysis is based on gene expression above or below median for the six given gene queries using an AML dataset from The Cancer Genome Atlas (TCGA) that contains 183 patients with AML. Input data produced on an Affymetrix U133 Plus 2 microarray platform used by the TCGA.

2.8 CyTOF

Primary cells were coated with metal conjugated antibodies, as indicated by the manufacturer. Mass cytometry was used to characterize CD markers in AML cells. Cells ($4x10^6$) were transferred to fresh tubes, washed twice with PBS and cells were then incubated with 1x Cell-ID™ Cisplatin6 solution (Fluidigm; Cat. 201064) for 5 minutes at room temperature (RT). Cells were washed with Maxpar Cell Staining buffer and pellets resuspended and incubated with 50 µL of 20 µg/mL HAG (human γ-Globulins, Sigma-Aldrich; Cat. G4386-1G) for 20 minutes at RT. After adding 50 µL of antibody mix (1/50 dilution of each antibody; Table 2.5), samples were incubated for 30 minutes at RT. The cells were then washed twice with Maxpar Cell Staining buffer, pellets were resuspended in Fix and Perm Buffer and left overnight at 4^{o}C. The following day, intercalator (Ir) was added to a final concentration of 1x and samples were incubated for 20 minutes at RT. Permeabilised cells were washed twice with Maxpar Cell Staining buffer and twice with Maxpar water. Samples were analysed on a CyTOF2 mass cytometer (Fluidigm) and data were normalized using the normalizer within the DVS Sciences CyTOF Instrument Control Software (v 6.0.626).

2.9 Co-immunoprecipitation (co-IP)

Following protein quantification 250µg of protein in each lysate was normalised to a final volume of 500µl with fresh lysis buffer. After normalisation each sample was incubated with 10µl of target protein antibody for 40 minutes to overnight at 4°C with constant agitation (in some instances a pre-clear step was included). Next 40µl/sample of protein A/G sepharose beads (Santa-cruz) [pre-conditioned in lysis buffer] were incorporated and incubated a further 20 mins at 4°C with constant agitation. The resultant complexes were captured and washed 3 times each with the following: lysis buffer, lysis buffer (without detergent) and 25mM NH_4HCO_3. Samples analysed by LC-MS/MS underwent on-bead tryptic digestion.

2.10 Liquid Chromatography – Tandem Mass Spectrometry Sample preparation

2.10.1 Secretome solubilisation

100µg of purified secretome proteins (>5kDa) were solubilised with 8M urea to a normalised volume or 500µg for phosphoproteomics. These proteins were then reduced through 30 minutes incubation at RT with 10mM DTT and alkylated with 17.5mM IAM under the same conditions. The samples were then diluted to bring urea concentration <2M.

2.10.2 Tryptic Digestion

For solubilised secretome samples, 80µg of TPCK-immobilised trypsin beads (Thermo Scientific)[preconditioned by washing beads 3 times with 20mM Hepes at 5°C] were added to each sample before incubating samples overnight with constant agitation at 37°C. Co-IP complexes for LC-MS/MS analysis after last 25mM NH_4HCO_3 wash and centrifugation at 5000 x g for 5 minutes 4°C were re-suspended in 150µl of NH_4HCO_3 that contained 170ng/sample of soluble trypsin (Sigma Aldrich) and incubated overnight with constant agitation at 37°C

2.10.3 Peptide desalting utilising solid phase extraction

Following tryptic digestion, samples underwent centrifugation to remove either immobilised trypsin beads or protein sepharose A/G beads (if soluble trypsin used then samples would be acidified with 1%TFA to inactivate trypsin). Samples were then desalted by means of reversed-phase solid-phase extraction, using either OASIS HLB cartridges for secretome samples (as larger volume) or carbon C18 spin-tips for co-IP lysates.

OASIS HLB cartridges were held in a vacuum manifold (P = 5.0 in Hg 0.5) and conditioned with LC-MS grade ACN before equilibration with 99% H_2O; 1% ACN; 0.1% TFA. Secretome, total proteomics or phospho-peptide samples were then loaded into individual cartridges and washed with 99% H_2O; 1% ACN; 0.1% TFA to remove residual salts. The bound peptides were then eluted with 70% ACN, 30% H_2O, 0.1% TFA. C18 spin tips underwent the same sequence of conditioning and equilibration before sample loading and elution, except the washes were achieved by centrifugation at 1500 x g for 2 minutes instead of a vacuum manifold. The eluted peptide solution was then snap-frozen on dry-ice for 15 minutes and lyophilised overnight with a speedvac. In the morning, peptide extracts were stored at -20°C.

For phosphoproteomics the bound peptides were then eluted with 500µl 1M glycolic acid (50% ACN; 5%TFA) instead of 70% ACN; 30% H2O for proteomics. Desalted peptide samples for phosphoproteomics analysis were then normalised up to 500 µl through the addition of 1M glycolic acid (80% ACN; 5% TFA), and subsequently stored on ice prior to phospho-enrichment.

2.10.4 Phosphopeptide enrichment

Following desalting each sample was incubated with 50µg TiO_2 resin/µg protein (1% TFA) at RT for 5 minutes, with constant agitation. The samples were centrifuged at 500 x g for 1 minute, 400µl of the supernatant transferred to a fresh lo-bind Eppendorf on ice, and the remaining 100µl was used to re-suspend the TiO_2. The 100µl resuspended sample (containing the resin) was then loaded into Glygen empty TF2EMT filter-tips (pre-washed with 100% ACN) and centrifuged at 1,500 x g for 3 minutes. Any residual TiO_2 was resuspended with 200µl 1M glycolic acid (80% ACN; 5% TFA) and loaded into the Glygen tips as before. The reserved 400µl of each sample was then washed over the resin (2x washes of 200µl), centrifuging at 1,500 x g for 3 minutes between loading of each aliquot. Each TiO_2 packed Glygen tip was then washed with 200µl 1M glycolic acid (80% ACN; 5% TFA) (this was to remove non-phosphorylated peptides). Then 200µl 100mM $NH_4CH_3CO_2$ (75% H2O; 25% ACN) (this was to remove acidic non-phosphorylated peptides). Then three 200 µl washes of (90% H_2O; 10% ACN) (this was to ensure complete removal of any salts and bound non-phosphorylated peptides from the TiO_2 layer prior to elution) – centrifuging at 1,500 x g for 2 minutes between each wash. The bound phosphopeptides were then eluted with four 50µl washes with 5% NH_4OH (90% H_2O; 10% ACN), 200µl eluent in total. Each sample was then snap-frozen on dry ice for 15 minutes and lyophilised in speedvac. Samples were then stored in -80°C.

2.11 Liquid Chromatography – Tandem Mass Spectrometry analysis

2.11.1 Liquid chromatography separation

Peptide extracts were re-suspended in 14-20µl of reconstitution buffer (97% H_20, 3% ACN, 0.1% TFA, 50 fmol/μl^{-1} enolase peptide digest) and sonicated for 5 minutes at RT. 4µl was loaded onto a LC-MS/MS system. This consisted of a nanoflow ultrahigh pressure liquid chromatography system (UPLC, nanoAcquity, Waters) system coupled online to an Orbitrap XL mass spectrometer (Thermo Fisher Scientific) or UltiMate 3000 RSLCnano (Dionex) coupled to an Q Exactive Plus (Thermo Fisher Scientific).

For Orbitrap XL experiments, the LC system delivered a flow of 2µL/min (loading) and 300 nL/min (gradient elution) with a backpressure of ~ 4,000 psi. Samples were separated across a BEH 75 µm x 100 mm analytical column (Waters) using a gradient between solvents A and B. Solvent A (98% HPLC-MS grade H_20, 2% ACN, 0.1% formic acid [FA]) and solvent B (80% ACN, 20% H_20, 0.1% FA). The gradient: 1% B for 5 min, 1% B to 35% B over 100 min, following elution the column was washed with 85% B for 5 min and equilibrated with 1% B for 7 min.

For Q-Exactive Plus experiments, the LC system delivered a flow of 2 µL/min (loading) and 300 nL/min (gradient elution) with a backpressure of 15 bar. Samples were loaded into a

PepMap µ-Precolumn (Acclaim) and separated across a PepMap 100 column analytical column (Acclaim) using a gradient between solvents A and B. The gradient: 1% B for 5 min, 1% B to 35% B over 120 min, following elution the column was washed with 85% B for 7 min and equilibrated with 3% B for 7 min.

2.11.2 Mass spectrometry analysis

Following LC separation peptide ions were analysed on one of two mass spectrometers, the Thermo LTQ-Orbitrap XL or the Q exactive Plus. These two mass spectrometers both utilise a Orbitrap mass analyser; however, they differ in the assembly of the ion optics that proceeds detection as well as the LTQ-XL instruments coupling of a linear trap quadrupole (LTQ) prior to the Orbitrap (Figure 2.2).

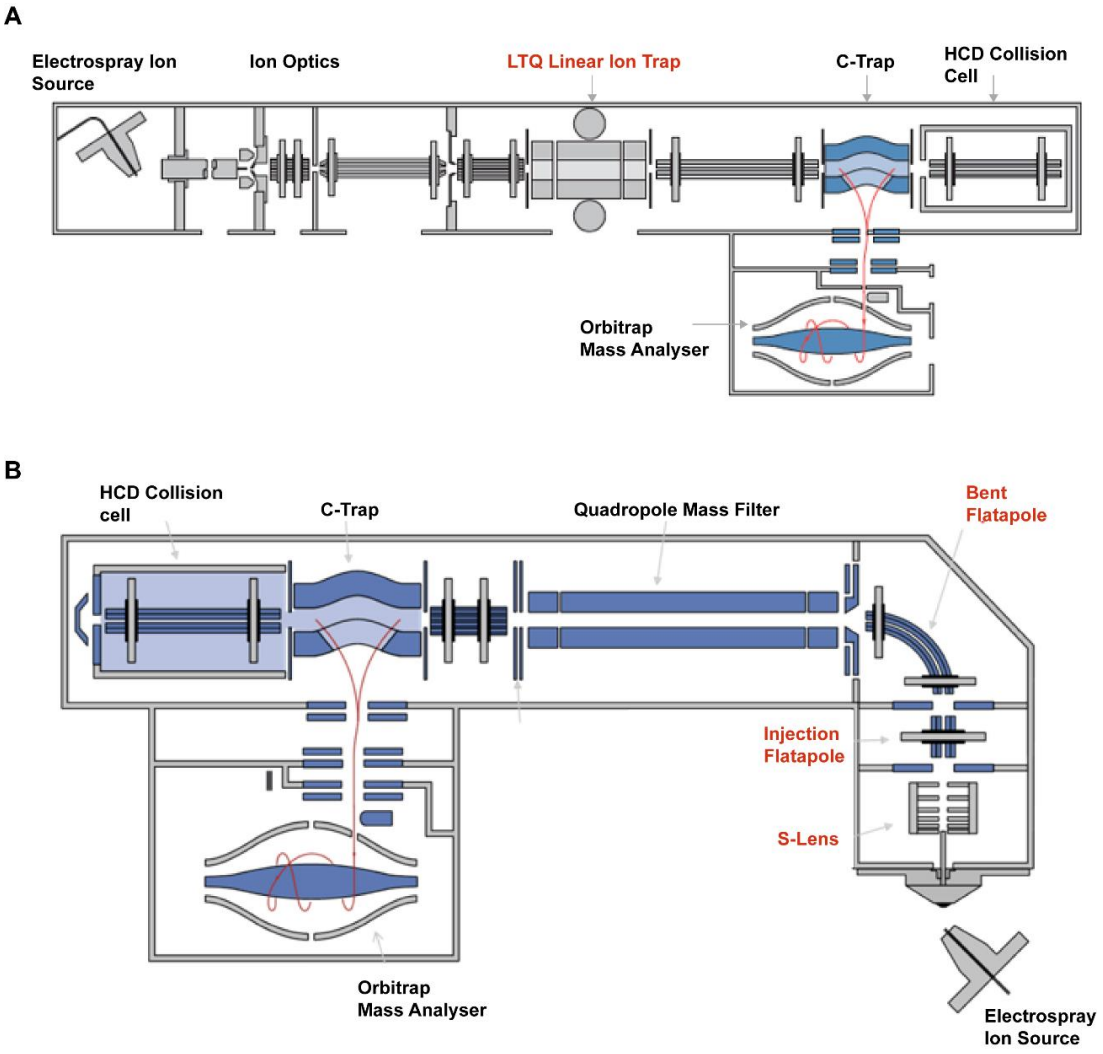

Figure 2.2: Schematics of the LTQ Orbitrap-XL and Q-Exactive Plus mass spectrometers. The major components of the LTQ -XL **(A)** and Q-Exactive plus **(B)** are displayed (not to scale). The features that distinguish these instruments from each other are in red text. Base diagrams sourced from thermofisher.com

An Orbitrap consists of two electrodes, one a barrel-like electrode and the other a spindle like electrode. An ion will orbit around the spindle like electrode at a frequency that is

determined by the ion's m/z ratio and the mass spectrum of the ions present within the Orbitrap is obtained by Fourier transformation of the current produced from the trapped ions. In the LTQ-XL ions enter the system through electrospray ionisation and are focused using the ion optics to the LTQ linear ion trap, whereby ions are directed into the LTQ (Figure 2.2A). The ion frequency given by their m/z determines ion motion within the trap. The principle of a LTQ is to accumulate ions before sending them to the Orbitrap for mass analysis. In the Q-Exactive the ion optics are more sophisticated with the implementation of a stacked-ring ion guide (S-lens), this approach greatly improves the efficiency of ion transfer into the system as the series of lenses are capable of focussing ions. The Q-Exactive also incorporates a bend flatapole that helps to remove neutral species before ion selection in the quadrupoles (Figure 2.2B). Once ions reach the ion trap they are confined and proceed to orbit at a frequency directly related to their m/z. Precursor selection (MS1) and fragmentation in the LTQ- XL those occurs in the linear ion trap (CID fragmentation). Whereas in the Q-Exactive Plus, both MS1 and MS2 are acquired in the Orbitrap. The Q-Exactive approach permits almost instantaneous mass selection and expands the C-trap's ability to store packets of ions derived from multiple precursor ions prior to injection into the Orbitrap mass analyser.

For DDA using the LTQ-Orbitrap system full scan survey spectra (m/z 375-1,800) were acquired with a 30,000 resolution. A maximum of the 5 most abundant multiple charged ions registered in each survey spectrum were selected in a data-dependent manner, fragmented by collision induced dissociation (multi-stage activation enabled) with a normalized collision energy of 35% and scanned in the LTQ (m/z 50-2,000). Neutral losses of 98, 49, 32.7, and 24.5 were accounted for and dynamic exclusion was enabled therefore reducing analysis of the same precursor ion within 60 second windows. The Q-Exactive Plus system acquired full scan survey spectra (m/z 375-1,500) with a 70,000 resolution. The 20 most intense ions for each MS1 scan were selected for HCD using an isolation width of 1.6 Da and MS/MS analysis (m/z 200-2,000) with a resolution of 17,500. A 30 second dynamic exclusion was enabled with an exclusion list of 10 ppm mass window. This produced duty cycles of 2.1 seconds.

When possible, experiments were conducted on the Q-Exactive plus platform due to its increased sensitivity and higher throughput. This is because its duty cycle is much shorter than that of the XL, thus enabling the identification of a greater number of peptides during the same chromatographic separation time.

2.12 Data analysis

2.12.1 Protein identification

Mascot Distiller 2.3.2 was used to fit an ideal isotopic distribution to the MS/MS data to maximise peptide identification and Mascot 2.5 search engine was used to match peaks to peptides in proteins present in the Uniprot/SwissProt Database (both human and mouse species for secretome distinction). The process was automated with Mascot Daemon 2.5.0, mass tolerance was set to ± 10 ppm, with variable modifications phospho (ST), phospho (Y) gln→pyro-glu (N-term Q) and oxidation (M) included in the search. Carbamidomethyl (C) as fixed modification. Trypsin was selected as digestion enzyme and 2 miss cleavages were allowed. Sites of modification are reported when they had delta scores >10.

2.12.2 Protein quantification

Peptide and subsequent protein quantification was achieved using in-house developed PESCAL (Peak statistics calculator) software (127). PESCAL constructs extracted ion chromatograms (XICs) for each peptide identified with the MASCOT search engine. With each constructed XIC, peak heights could be calculated. These peptide peak heights were then normalised to the sum of the intensities for each individual sample and the average fold change between conditions could be determined. Statistical significance between conditions was considered significant when the Student T-Tests produced $P < 0.05$. Further data processing and analysis was conducted within Microsoft Excel (2007/2010) or R (v3.3.2/v3.4.1 – reshape2, ggplot2, gplots, readXL, Hmisc and limma packages).

2.12.3 Kinase substrate enrichment analysis

Kinase substrate enrichment analysis (KSEA) algorithm was used to categorise phosphopeptides into groups that are recognised as substrate groups of a particular kinase. These substrate groups are defined by public repositories PhosphoSitePlus (318) (327), Phospho.ELM (328), and PhosphoPOINT (329), and through in-house experiments as defined by the CTAM database (215). The significance of each kinase enrichment were calculated using a *Z*-score formula as previously described (330). KSEA can infer kinase activity by taking the $\log_2$ mean intensities of phosphorylated peptides that are phosphorylated at sites exclusive to a particular kinase, these intensities are normalised to the SD of the phosphopeptide intensities in the whole dataset and by the number of known substrates of the given kinase. *Z*-scores were subsequently transformed to *P*-values using a function written in excel Visual Basic for Applications (VBA).

$$\text{Z- score} = \frac{(mS - mP) \times m^{1/2}}{d}$$

mS = the mean of each kinase group $\log_2$ fold-changes against control
mP = the mean of $\log_2$ of the entire data set mean changes
m = size of the substrate group
d = SD of the mean abundances of the whole data set

2.12.4 K-means clustering

The K-means clustering algorithm was used as an unsupervised approach to distribute the quantified phosphopeptides across a number of clusters. Phosphopeptides would be assigned to the centroid that was within the nearest mean to each phosphopeptide, the space distance is calculated through Euclidean distribution. After each round of assignment, the centroids are redistributed to represent the new mean of the cluster and phosphopeptide cluster assignment is corrected for the new means, this process repeats until phosphopeptides no longer change cluster assignment. The significance of the k-means enrichment for kinase substrates, ontologies and pathways was determined for each cluster using an in-house VBA script. This script utilises a hypergeometric test approach to calculate the extent of enrichment using the formula:

$$\text{Enrichment significance} = \text{Log}_2([a/b]/[c/d])$$

a = the number events of a particular ontology, pathway or group in a given cluster
b = the total number of events in a cluster
c = the number of events specific of the ontology, pathway or group
d = the total number of events

Chapter 3: Characterising the composition of AML supportive secretomes derived from stromal MS-5 and HS-5 cell lines

3.1 Introduction and aims of the study

The BMM is recognised as a crucial component in the progression and development of AML (144, 145, 331, 332). Previous studies have mainly examined the niche contribution to AML behaviour, be that mediating treatment resistance through chemotaxis of AML clones to protection (333, 334), induction to a quiescent state (335, 336) or by remodelling of the surrounding vasculature altering the supply of other factors for AML survival (175, 337). This has led to great interest in chemotaxis inducing factors such as CXCL12/SDF-1 and various chemokines, as well as matrix metalloproteases that are hypothesised to be crucial in the remodelling of the environment that AML cells reside (338-340). These studies are leading to new therapeutic directions that focus on disrupting these interactions. However, such approaches are primarily focussed on the CXCL12-CXCR4 axis and means by which to interfere with this gradient (124, 341-344).

Ex vivo observations of primary AML cells indicate that there is more to the stromal chemical mediated interactions with AML than just migration (345, 346). A large number of studies have described how bone marrow stromal cell (BMSC) CM is able to support the viability and proliferation of primary AML cells ex vivo (346-348). To this end a small number of cell lines have traditionally been utilised including MS-5, M2-10B4, HS-27, HESS-5, HS-27a and HS-5 in order to produce CM to support AML viability ex vivo (124, 321, 347, 349-351). Alternatively, a number of papers have supplemented AML cultures with exogenous GFs in an attempt to extend AML survival (352-354). These factors include Stem cell factor (SCF), IL-3, GM-CSF, G-CSF and IL-6 (355-359).

Previous publications have concluded that AML interactions with the stromal cytokine network and the release of other soluble mediators, are important for the proliferation of more primitive AML progenitors (164, 335, 360, 361). Therefore, in this chapter experiments first aimed to characterise the composition of the BMSC secretome (the totality of secreted proteins) using MS-based proteomics, which to date has not been undertaken.

Having established proteins of the stromal secretome without any of the preconceptions that are required when designing a cytokine array, we then sought to identify the proteins that are responsible for maintaining AML blast survival ex vivo. Although, there are known factors that help to extend AML cell lines in culture, the majority of primary AML cell

studies have demonstrated a need for either stromal CM or co-culture with stromal cells for primary material to be maintained for any length of time (346, 353, 354, 362, 363). Furthermore, as much of the currently described stromal secretome are signalling molecules, it was hypothesised that any novel proteins would likely activate signalling nodes. Therefore, knowing which precise nodes and the regularity that these nodes are activated could prove useful in future efforts to disrupt the AML support network.

3.2 Validating supportive qualities of the MS-5 and HS-5 cell lines

Following the acquisition of the BMSC lines MS-5 and HS-5 we needed to confirm that in our hands these support AML cells in culture. To ascertain supportive qualities, we first undertook viability assays with primary AML cells. These cells were maintained ex vivo for seven days with either HS-5 or MS-5 conditioned stromal media or unconditioned IMDM media (supplemented with 10% FBS). Figure 3.1 shows that there was a substantial increase in viable cell number at Day 7 when cells were maintained in HS-5 CM (p=0.0047) and MS-5 CM (p=0.0108) compared to seeding, whereas the unconditioned media was unable to sustain the initial viable cells incubated on Day 1 (p=0.0061). These results demonstrate the supportive capacity of BMSC CM in AML.

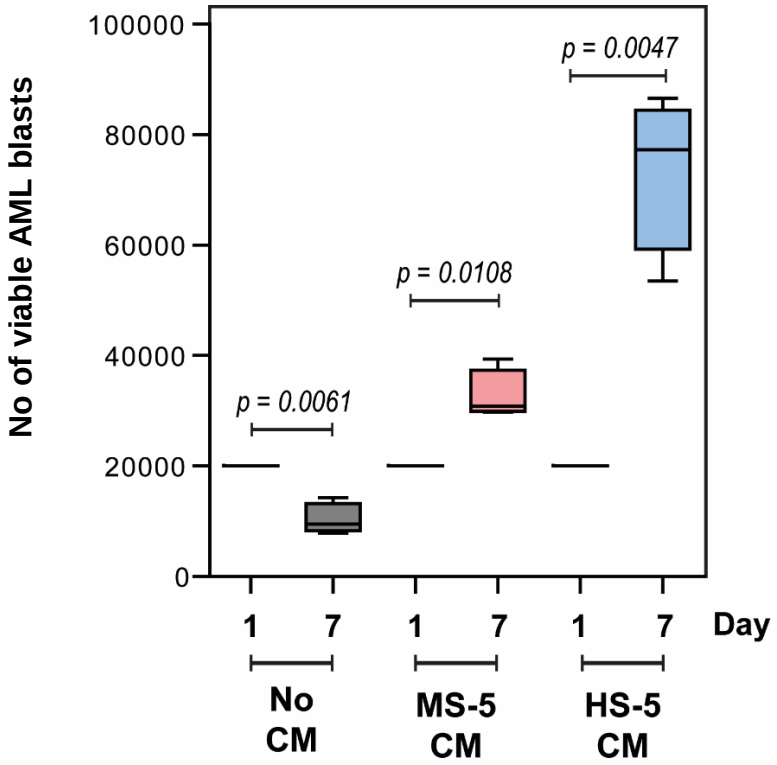

Figure 3.1: Stromal conditioned media extends primary AML cell survival ex vivo. HS-5 and MS-5 CM maintains primary AML cells in culture over 7 days. Viable cell numbers measured by Guava viacount assay on days 1 and 7. $2x10^4$/well were seeded in technical triplicates for each patient in indicated media (No CM contained IMDM media, all samples contained 10% FBS), each condition run in n=4 biological replicates.

To establish if these effects were mediated by the protein or metabolite component of the media we fractionated the CM produced by MS-5 cells using a centrifugal filter that

separates molecules by molecular weight. MV4-11 cells were then cultured in a serum starved environment containing the different secretome fractions. Figure 3.2 shows that, as expected, serum had a strong effect on AML cell growth. However, in the absence of serum (i.e. without the supportive role of GFs and cytokines), it was the >5kDa fraction of the CM (the protein component) that induced the greatest level of proliferation in the MV4-11 cells relative to the control. Incubation with the <5kDa fraction (metabolite component) led to a decrease in proliferation and the total unfractionated secretome had a moderate effect on proliferation. These results suggested that proteins, rather than small molecule metabolites, in the BMSC CM support AML viability and proliferation.

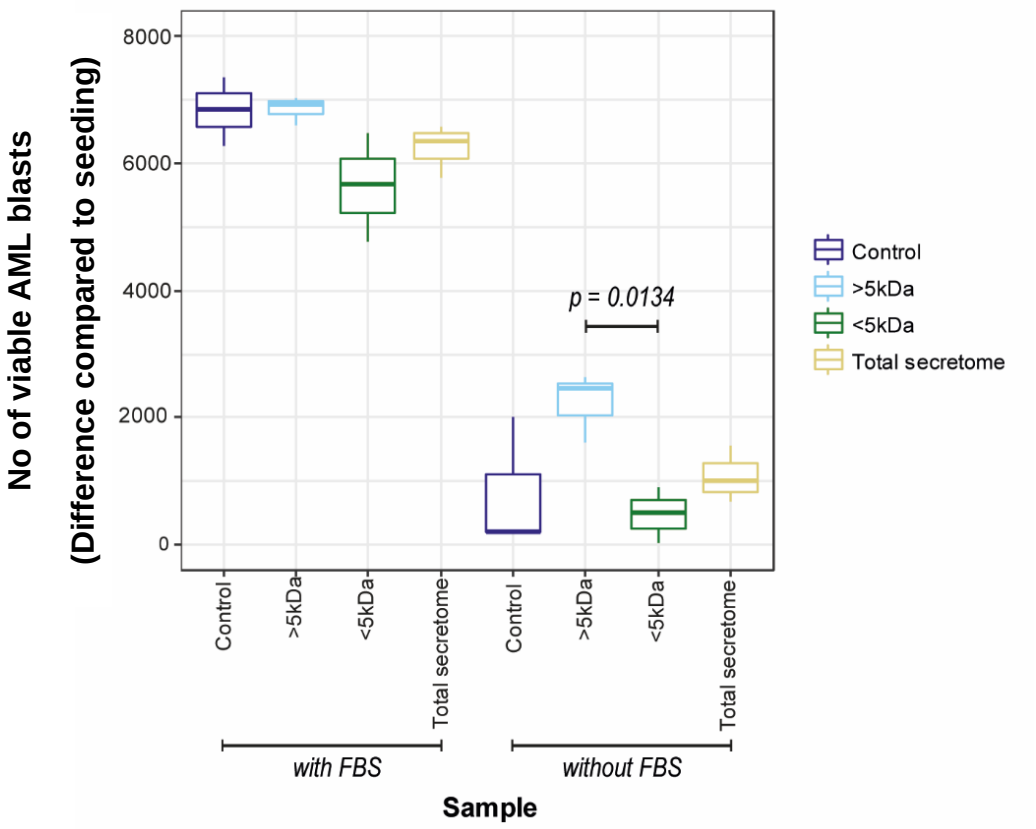

Figure 3.2: Dissection of the supportive role MS-5 secretome plays in AML cell survival. Effects of fractionated MS5 CM on the proliferation of MV4-11 cells (with/without 10% FBS). 100% 72hr MS-5 CM was fractionated with Vivaspin 20 columns to create >5kDa, <5kDa fractions. $2x10^4$ cells/well were seeded in n=4 technical replicates for each condition and supplemented with 10µg/ml of indicated fraction or unfractionated MS-5 CM (+/- 10% FBS). Viable cells numbers were measured 1 hour after plating and 24 hours later by Guava viacount assay, growth determined by calculating difference in viable count.

3.3 Optimisation of stromal conditioned media

Initial experiments had confirmed that the stromal cell lines we possessed support primary AML cells. However, to ensure we were realising optimal effects we set out to test a number of variables that may indeed affect the level of support the BMSCs can offer AML cells in an ex vivo environment. Aspects of CM production that were investigated during optimisation are detailed in the following sections.

Days of media conditioning in presence of stromal cells

In the literature the length of conditioning regimens can be quite variable with studies choosing to condition media in the presence of stromal cells for a range of 3-5 days (321). In choosing an appropriate range of time points to measure supportive capacity, it was postulated that too short a period of time would lead to insufficient secretion of the factors that support primary AML cells. However, conditioning the media excessively would likely lead to the media being depleted of key essential amino acids, carbohydrates, as well as the 10% serum supplementation. All of which would start to produce a less supportive medium. With these considerations, HS-5 cells were used to condition media for 2, 3, 4 and 5 days before assessing the ability of the CMs to maintain primary AML cells in ex vivo culture.

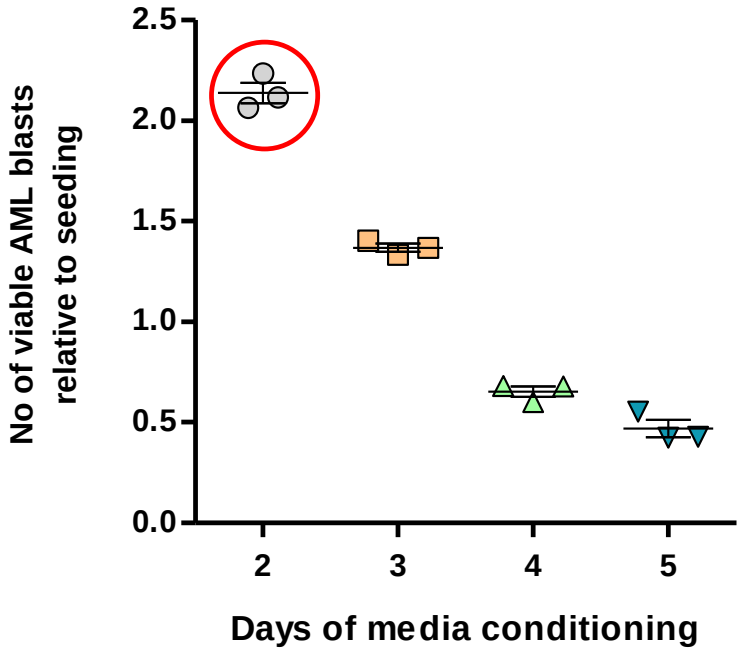

Figure 3.3: Optimising the duration of stromal media conditioning. IMDM media (+10% FBS) was conditioned with HS-5 cells for 2, 3, 4 and 5 days, subsequently these HS-5 CMs were used to maintain $2x10^4$ primary AML cells from patient #0 ex vivo for 10 days. Graph displays the relative number of viable AML blasts measured by Beckman Coulter Vi-Cell counter at Day 10 compared Day 1 when using the different HS-5 CMs. Each condition run in technical triplicates. Red circle indicates supportive CM.

Optimisation of the number of days required to sufficiently condition media with HS-5 cells revealed that 2 days of conditioning was optimal. Results showed that 3 days of conditioning was also appropriate with the viable number of AML blasts at Day 3 still higher than that compared to Day 1. However, after 4 days of conditioning the CM lost its supportive qualities. This is likely due to the HS-5 cells utilisation of key components in the media, as well as the increase in inhibitory elements released through cell death and increased confluency.

Flask size, media volume and cell confluency

A key consideration when conditioning media is the concentration of factors and how actively stromal cells are secreting supportive factors. Initially CM was prepared in T175 flasks and 20ml of IMDM media conditioned at a time. During optimisation steps, it was reasoned that this could be improved on. This volume (20ml) is quite a large volume of media, which introduces pros and cons: positively this will mean that the likelihood of key nutrients being depleted from the media is reduced, as well as any inhibitory secretions and metabolites being diluted. Adversely this also means that supportive factors will be diluted at these volumes. A large flask such as a T175 means that more cells can be seeded without the cells becoming too confluent, an important consideration also as both HS-5 and MS-5 cells have quite high proliferation rates and have been described as losing their supportive capacity following growth beyond a confluency of 85% (364). Therefore, making the system too small could compromise the supportive nature entirely. To assess whether the current method was optimal HS-5 cells were seeded in T175 flasks, as any smaller would quickly lead to confluent flasks at a range of densities from 0.3-1.0 x10^6 cells/flask. The cells were seeded with either 10, 15 or 20ml of media, lower volumes were not selected as there was concern as to whether such volumes would be sufficient to cover the area of the flask. Following 48 hours of conditioning, CM was collected used to maintain primary AML cells for 4 days in culture and the cells were then analysed for viability and cell number.

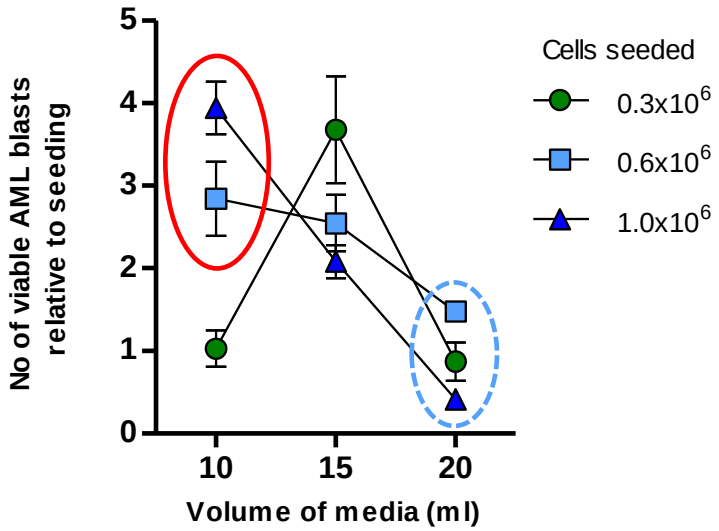

Figure 3.4: Optimising stromal cell confluency and conditioned media volume. CM was obtained from HS-5 cells cultured in IMDM media (+10% FBS) following incubation for 48 hours in T175 flasks using cell densities described in the legend. The volume of CM also varied from 10-20 ml across the flasks. The resultant CM were used to maintain primary AML cells in culture for 4 days, after which cell numbers were measured using a guava viacount assays on a Guava flow cytometer. Each condition run in technical triplicates. Red circle represents most supportive conditions and blue circle least.

Analysis comparing the ability of the different HS-5 CM to maintain primary AML blasts in culture revealed that after 4 days, the most supportive media was produced by seeding flasks

with $1.0x10^6$ HS-5 cells in 10ml of IMDM media (Figure 3.4). Additionally, similar results were observed when seeding $0.3x10^6$ cells in 15ml of medium, although, this CM produced much higher error bars when assessing its ability to maintain AML. Interestingly seeding $0.3x10^6$ HS-5 cells did not produce very supportive media when grown in 10 or 20ml of media. A likely explanation is that 20ml of media diluted the supportive factors, as each cell density used to produce CM was observed as the least supportive conditions (blue circle). It is notable that the combination of high HS-5 cell densities and low media volumes (red circle) did not lead to less supportive CM.

Inclusion of 0.22µM sterile filtration step

Following the incubation with either MS-5 or HS-5 cells, collected supernatant would be centrifuged at high speed to pellet any debris before filtration through a 0.22µM filter to both ensure sterility of the media that would be added to the AML cells, and to ensure no stromal cells were being taken forward. Despite these benefits, there were concerns that potentially important proteins could bind to the filter and thus compromise the supportive capacity of the media. Therefore, CM produced by MS-5 cells was split, half of the CM was sterile filtered and half not, following filtration the media was used to maintain primary AML cells in culture.

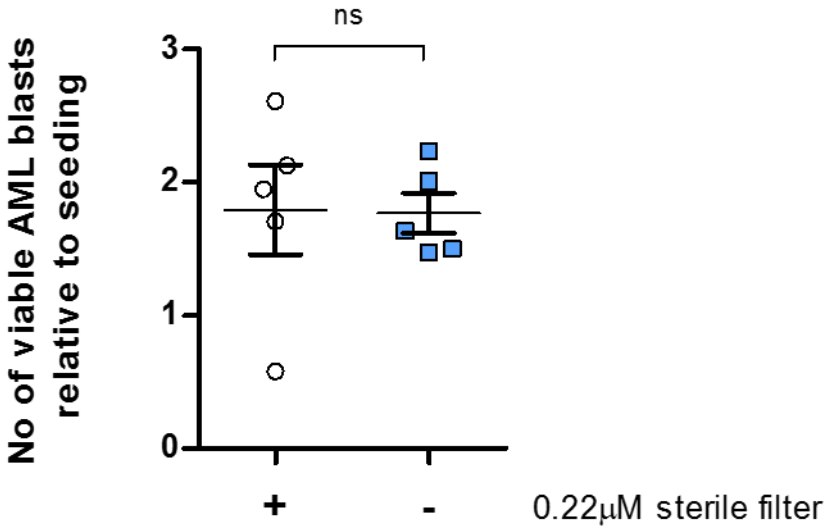

Figure 3.5: Determination of factor loss during filtration. MS-5 were used to condition IMDM media (+10% FBS) for 48 hours. CM was both sterile filtered and not filtered and in parallel used to maintain $1x10^5$ primary AML blasts in 2ml/well in culture. Cell numbers measured using Beckman Coulter Vi-Cell counter 48 hours later. Each condition run in n=5 technical replicates.

Comparing viable AML cell numbers after culturing with the two differently processed CM showed that sterile filtration had no impact on the supportive properties of the media (Figure 3.5). It could be argued that not sterile filtering the media leads to more reproducible results, as the sterile filtered CM led to one replicate where the viable AML cell number was less than the number of viable AML cells seeded. However, as the difference was not statistically

significant the HS-5 and MS-5 CM in future experiments would continue to be sterile filtered as it reduces the chances of cellular debris being incubated with the AML cells in subsequent experiments.

Fresh or frozen conditioned media

One aspect of these experiments to be established was the impact of snap freezing the media between the time of production and being used in experiments. If snap freezing did not impact the supportive capacity of the CM, then practically this would be advantageous, as well help to control for variances between CM batches. However, it is widely accepted that the freeze thaw process leads to protein degradation and therefore it is likely to affect the composition of the CM. However, if it did not affect the components that are responsible for maintaining AML survival then it would still be a feasible approach. As with the sterile filtration optimisation, an identical batch of MS-5 CM was used both fresh and following a freeze thaw to maintain primary AML blasts ex vivo.

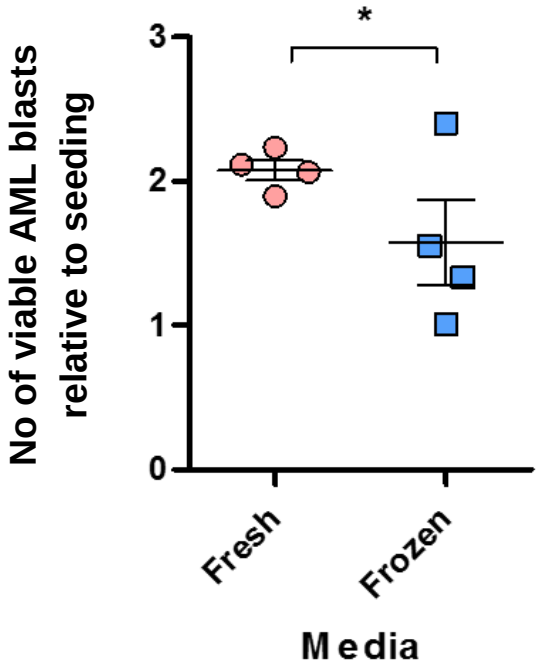

Figure 3.6: Effects of the freeze thaw process on the ability of CM to maintain AML ex vivo. MS-5 cells were used to condition IMDM media (+10% FBS) for 48 hours. CM was both freeze thawed and used fresh in parallel to maintain $1x10^5$ primary AML blasts in 2ml/well in culture. Graph displays the relative number of viable cells measured by Beckman Coulter Vi-Cell counter at Day 10 compared to seeding. Each condition run in n=4 technical replicates, * $p<0.05$.

Analysis of the number of viable AML blasts following 10 days in culture showed that fresh MS-5 CM was a more reliable means of maintaining AML blasts in culture (Figure 3.6). CM that had been frozen was able to maintain AML cells in culture, however, on average, it did not work as well as fresh CM and the range in AML viability between each replicate was likely down to the variable protein degradation that had occurred in the CM during the freeze thaw process.

These experiments showed that it was important to use fresh CM in experiments, but the CM retained some supportive capacity if frozen between experiments.

Cell lines, clones and AML co-culture

Experiments up to this point had individually assessed the effects of MS-5 or HS-5 CM on maintaining AML blasts ex vivo. The opportunity arose whereby a new MS-5 clone became available and it was desirable to establish which stromal cell line produced the most supportive media. Collectively the lab possessed two MS-5 clones that shall be referred to as clone #1 and clone #2, as well as HS-5. At the same time as establishing the support of different clones it was postulated that stromal and AML cell line co-cultures may produce the most supportive media. This idea was based on the fact that heterotypic signalling between the cells can lead to the secretion of supportive factors that otherwise would not be released under cell independent stromal conditions (365). To assess this primary AML cells from patient #0 were maintained in culture using CM from each of MS-5 clone #1, clone #2 and HS-5 cells, additionally CM was collected from these cell types whilst being co-cultured with P31/FUJ cells (AML cell line). Patient #0 cells were kept in culture for seven days being measured by guava viacount assay on days one and seven.

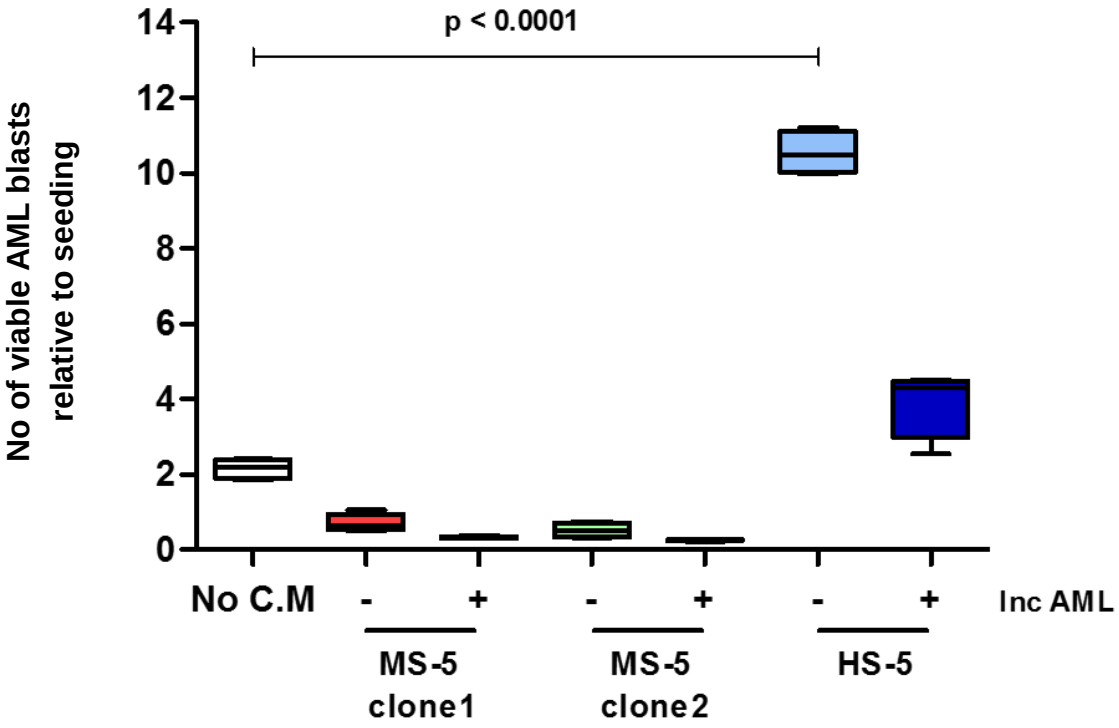

Figure 3.7: HS-5 stromal conditioned media is the optimum means of extending primary AML cell survival ex vivo. MS-5 (clones #1 and #2) and HS-5 cells ([+/-] P31/FUJ cells) were used to condition IMDM media (+10% FBS) for 48 hours. The resultant CM were used to culture patient #0 primary AML blasts over 7 days, viable cell numbers measured by Guava viacount assay and reported relative to viable AML blast counts recorded on Day 1. Each condition were run in n=4 technical replicates. P values calculated using a repeated measures ANOVA.

Assessment of AML cell growth revealed that on this occasion CM from either of the MS-5 clones was unsupportive, with even the AML cells grown in unconditioned media performing better (Figure 3.7). At the time of this experiment, the MS-5 clone #1 was at passage 20 and MS-5 cells were usually used in the range of passage 5-15, so it is possible that this clone has lost its supportive capabilities. The MS-5 clone #2 CM was also ineffective at maintaining primary AML cells over the course of seven days in culture, one key difference in this clone was that it required α-MEM media for maintenance, a departure from the previous IMDM media which primary AML cells are known to grow well in. HS-5 CM on the other hand was extremely successful at supporting AML growth with HS-5 CM leading to there being ~10.5 times more viable primary AML cells at day seven compared to day one. Finally, the inclusion of AML cells during stromal conditioning of the media was not a successful experiment; in all cases, this produced a less supportive CM. This was probably due to an increase in flask confluency, which would have inhibited the secretion of supportive components. Additionally, the P31/FUJ cell line has a high proliferation rate and likely stripped the media of crucial factors while releasing many acidic metabolites. Following utilisation of the key nutrients from the media, there would have been an increase in cell death, releasing inhibitory factors that could have had a negative effect on AML survival in later experiments.

These experiments combined with previous experiments demonstrated that HS-5 media and earlier passages of MS-5 clone #1 (in all subsequent experiments that utilise MS-5 CM, capacity to support AML cells was verified first) produced the most supportive CM for maintaining AML ex vivo. Future experiments did not use CM from AML co-cultures and only known AML supportive media were used such as IMDM. These experiments also raised questions regarding the balance of pro-survival and pro-apoptotic factors secreted/released into the media during conditioning.

Mixtures of conditioned media combined with fresh media

The previous optimisation experiments raised the issue of the impact that pro-apoptotic content, acidic metabolites, and the stripping of serum, glutamine and essential amino acids from media. Optimisation strategies had shown that less complex cell mixtures, with moderate confluency and relatively short conditioning times were most effective at producing an optimal concentrated supportive medium.

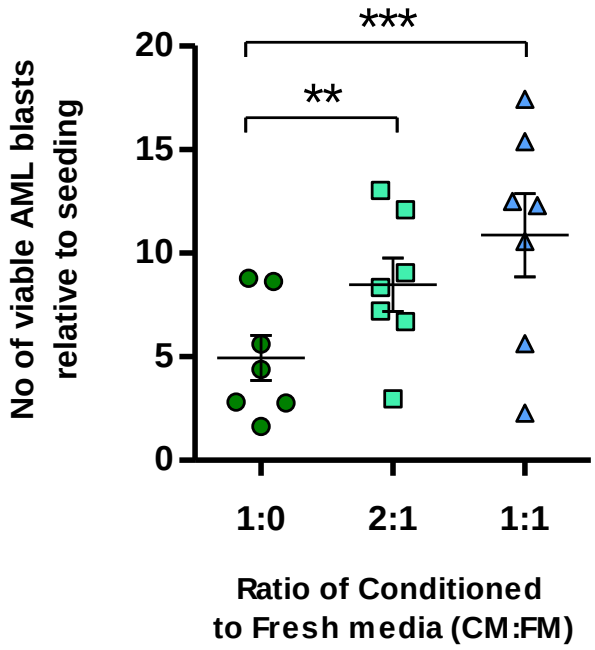

Figure 3.8: Controlling for serum utilisation and accumulation of non-supportive components. HS-5 cells were used to condition IMDM media (+10% FBS) for 48 hours. The HS-5 CM was mixed with fresh IMDM media (FM) in ratios of 2:1 and 1:1. Mixed CM and unmixed HS-5 CM were then used to maintain $1x10^5$ primary AML blasts in 2ml/well. Graph displays the relative number of viable AML blasts measured by Beckman Coulter Vi-Cell counter at Day 10 compared to seeding. Each condition run in n=7 technical replicates, P values calculated using a repeated measures ANOVA; * p<0.05 **p<0.01 ***p<0.001.

To counteract the negative components that are also part of CM, it was postulated that mixing CM with fresh complete media could replenish any key factors depleted from the media, while simultaneously diluting acidic metabolites. To investigate this HS-5 CM was mixed 2:1 and 1:1 with fresh IMDM media and run in parallel with 100% HS-5 CM.

Mixing conditioned and fresh media produced a range of results with each condition producing varying levels of support. Analysis of the data revealed that on average, AML survival in each condition increased as the proportion of fresh media increased during ten days in culture (Figure 3.8). Using HS-5 CM mixed with fresh media in 2:1 and 1:1 ratios resulted in a statistically significant increase in AML supportive capacity when compared to using 100% HS-5 CM only to maintain primary AML ex vivo. Notably the 1:1 ratio captured the dynamic nature of CM and the issue of batch effects, as there were instances where the supportive factors were either not present or present at lower abundances.

3.4 Optimisation of secretome purification

Once we established conditions that produced optimal BMSC CM (using both HS-5 and MS-5 cells), we next sought to purify the supportive component from the media for cell signalling experiments and LC-MS/MS analysis. Enrichment approaches included ultrafiltration of the CM using Vivaspin 20 columns that were used to concentrate the stromal secretome (Figure 2.1), and a methanol-chloroform based precipitation. Vivaspin columns (GE Healthcare) separate proteins through a membrane that discriminates based on a molecular weight cut off. We

decided to split the media into two fractions, molecules that are >5kDa (proteins) and those <5kDa (metabolites and small peptides), as most cytokines and GFs are between 5-30kDa (in the >5kDa fraction).

3.5 Western blot analysis of secretome effects on signalling nodes

Following confirmation of the BMSC secretomes ability to support primary AML survival we next sought to establish effects that the stromal secretome has on signalling nodes commonly upregulated in AML, such as PAK1 which has previously been reported as one of the most active kinases in AML (271).

Once ultra-filtration of the stromal secretome was optimised in my hands, experiments began investigating the effects of the stromal secretome on signalling in MV4-11 cells (chosen as were less profoundly affected by serum deprivation compared to P31/FUJ), with PAK phosphorylation chosen as a representative signalling readout. Figure 3.9 shows western blot analysis of phospho-PAK expression in MV4-11 cells following stimulation stromal secretome (containing proteins with a molecular weight >5kDa).

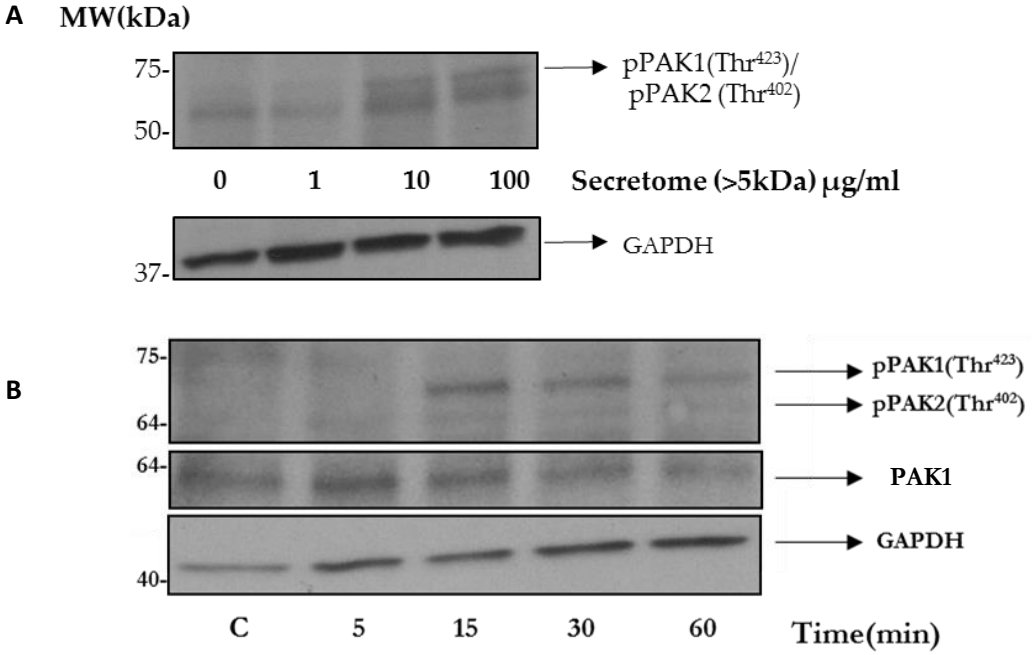

Figure 3.9: Increase in PAK phosphorylation in MV4-11 cells over secretome time-course. (A) MV4-11 cells serum starved for 4 hours and then treated for 30 minutes with a titration of (0-100µg/ml) >5kDa MS-5 secretome. Cells then analysed by western blot (30µg/lane) to observe effects on PAK1 and PAK2 phosphorylation. **(B)** Time course of >5kDa MS-5 secretome, measuring effects of 10µg/ml on PAK phosphorylation in MV4-11 cells across 60 minutes following 4 hours of serum starvation. Accordingly PAK1 and GAPDH included as loading controls.

MV4-11 cells were serum starved for 4 hours before being incubated for 30 minutes with a titration of MS-5 stromal secretome (>5kDa) [Range of 0-100µg/ml] before lysing and measuring PAK phosphorylation. These experiments determined that 10 µg/ml of secretome was sufficient to induce increased PAK phosphorylation (Figure 3.9A). After establishing that the

optimum secretome concentration a secretome time-course was devised. Again MV4-11 cells were serum starved for 4 hours before being incubated over a time course of 60 minutes with 10µg/mL of MS-5 stromal secretome (>5kDa) (Figure 3.9B). Western blot analysis using an antibody targeted against both pPAK1^{Thr423} and pPAK2^{Thr402} (phosphorylation sites that indicate kinase activation) showed that by 15 minutes levels of pPAK1^{Thr423} increase substantially compared to the control (time=0). Further pPAK2^{Thr402} levels increased over time suggesting that the secretome is a modulator of PAK activity and is either stimulating PAK or effects the regulation of PAK.

3.6 LC-MS/MS analysis of MS-5 secretome

Having demonstrated a method for secretome purification that modulates cell growth in guava assays, while simultaneously effecting cell signalling dynamics through western blot analysis, we next sought to establish specific factors that contribute to these biological observations in AML cells. To this end, MS-5 secretome was purified as described previously using Vivaspin 20 columns and 100µg of the MS-5 secretome was combined with 8M Urea. Proteins were then reduced, alkylated and digested overnight with immobilised trypsin. Secretome peptides were desalted offline using C18 spin columns as detailed in the methods (section 2.10) prior to LC-MS/MS separation and detection. Following a 180 minute gradient and selecting for the top 5 precursor ions to undergo fragmentation, the analysis yielded 11456 MS1 scans and 9768 MS2 scans (Figure 3.10).

The raw data was then searched using the MASCOT search engine and this protein identification data was combined with the quantification undertaken by PESCAL software, this generated a list of 2106 identified peptides with relative abundances. The peptides belonging to the same protein were concatenated and their relative abundance summed, proteins with a MASCOT score >50 (a confidence score for protein identification) and >2 unique peptides identified were selected for further analysis which resulted in 293 proteins.

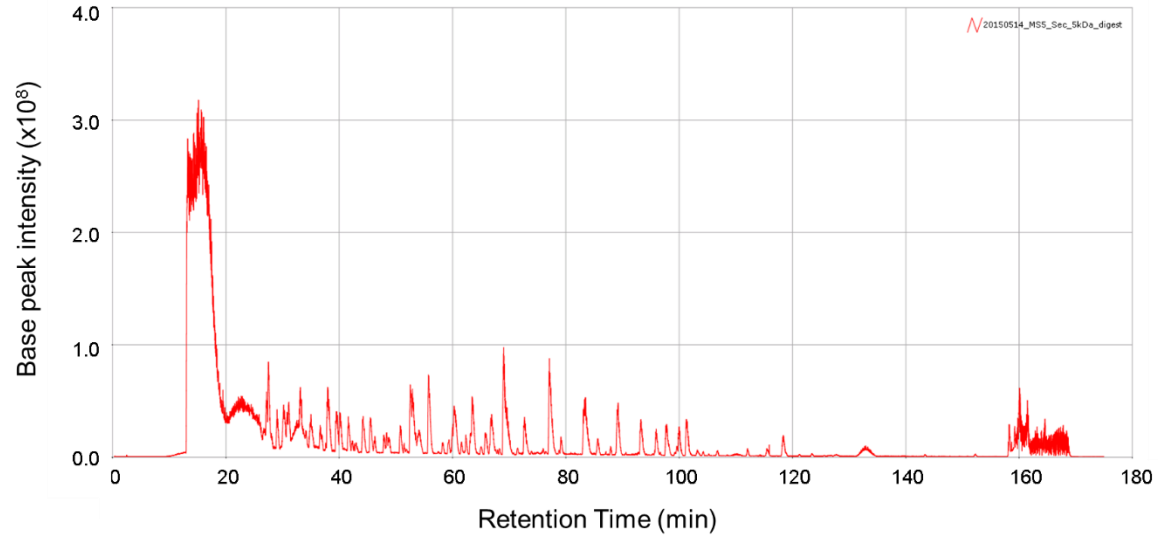

Figure 3.10: Base peak chromatogram produced during LC-MS/MS analysis of MS-5 secretome. Basepeak intensity displaying the most intense mass signal for a given mass spectrum, across a 180-minute gradient on an LTQ-XL MC-MS/MS, analysing 80µg of trypsin digested MS-5 secretome.

In order to extract biological significance from a list of 293 proteins, we performed an assessment of the most abundant proteins without normalising for protein size (Figure 3.11 and Table 3.1), this analysis showed that Fibronectin was the most abundant protein in the stromal secretome. Fibronectin is a very well established stromal secreted protein that forms a core component of the ECM and helps to keep blasts in niches (144). Other proteins identified in this analysis that have been implicated in cancer before were vimentin (366) and cathepsin B (367-369), among many others.

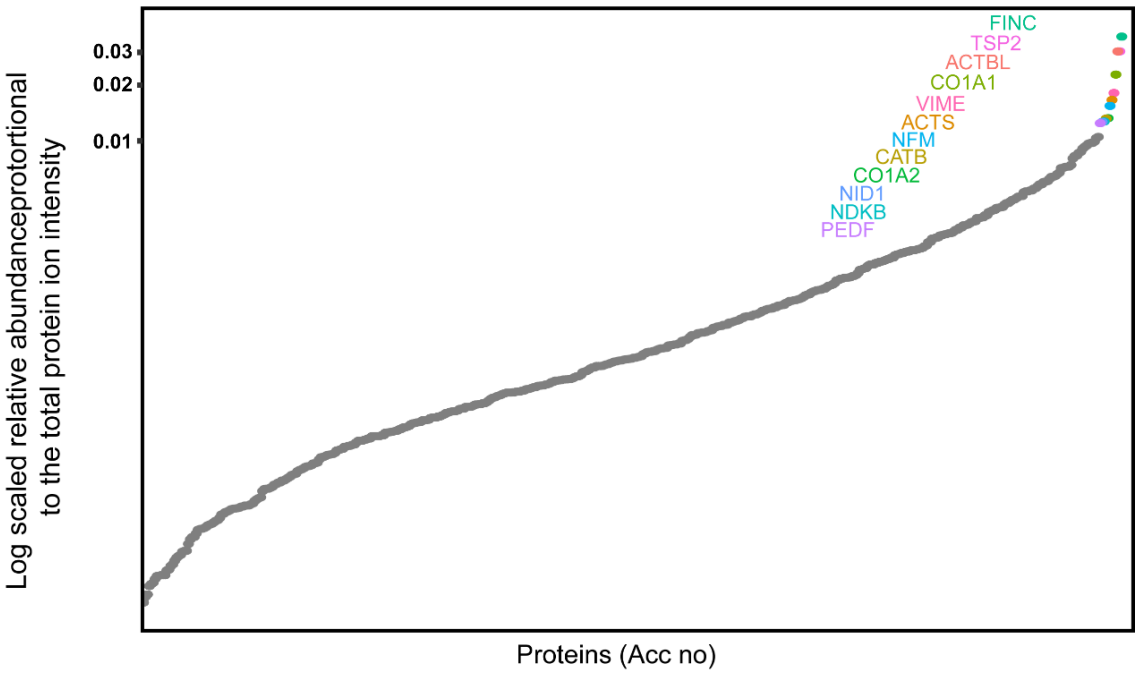

Figure 3.11: Relative abundance of secreted MS-5 proteins following LC-MS/MS analysis. Quantitative secretomic analysis of MS-5 secretome, quantifying MS ion intensity for all corresponding peptides of identified proteins. Scores normalised by the total ion chromatogram and ordered according to Log transformed relative abundance. Abundance averaged across n=3 technical replicates. The top 12 most abundant proteins are named.

The 12th most abundant protein identified in the analysis was Pigment epithelium derived factor (PEDF), which is a secreted glycoprotein, and unlike the other abundant proteins identified has previously been described as having anti-cancer activities (370).

Protein ID	Protein	Mol. weight (kDa)
FINC	Fibrinogen	263
TSP2	Thrombospondin-2	130
ACTBL	Beta-actin-like protein 2	42
CO1A1	Collagen alpha-1(I) chain	139
VIME	Vimentin	54
ACTS	Actin, alpha skeletal muscle	42
NFM	Neurofilament medium polypeptide	102
CATB	Cathepsin B	38
CO1A2	Collagen alpha-2(I) chain	129
NID1	Nidogen-1	137
NDKB	Nucleoside diphosphate kinase B	16
PEDF	Pigment epithelium-derived factor	50

Table 3.1: The most abundant proteins in secretome.

When summed protein intensities were normalised to their respective molecular weights in analysis, large proteins such as fibronectin were no longer in the top 20 most abundant proteins. This allowed for the identification of signalling proteins such as Protein S100-A4, which is a very well described secreted protein of tumour and stromal cells (Figure 3.12).

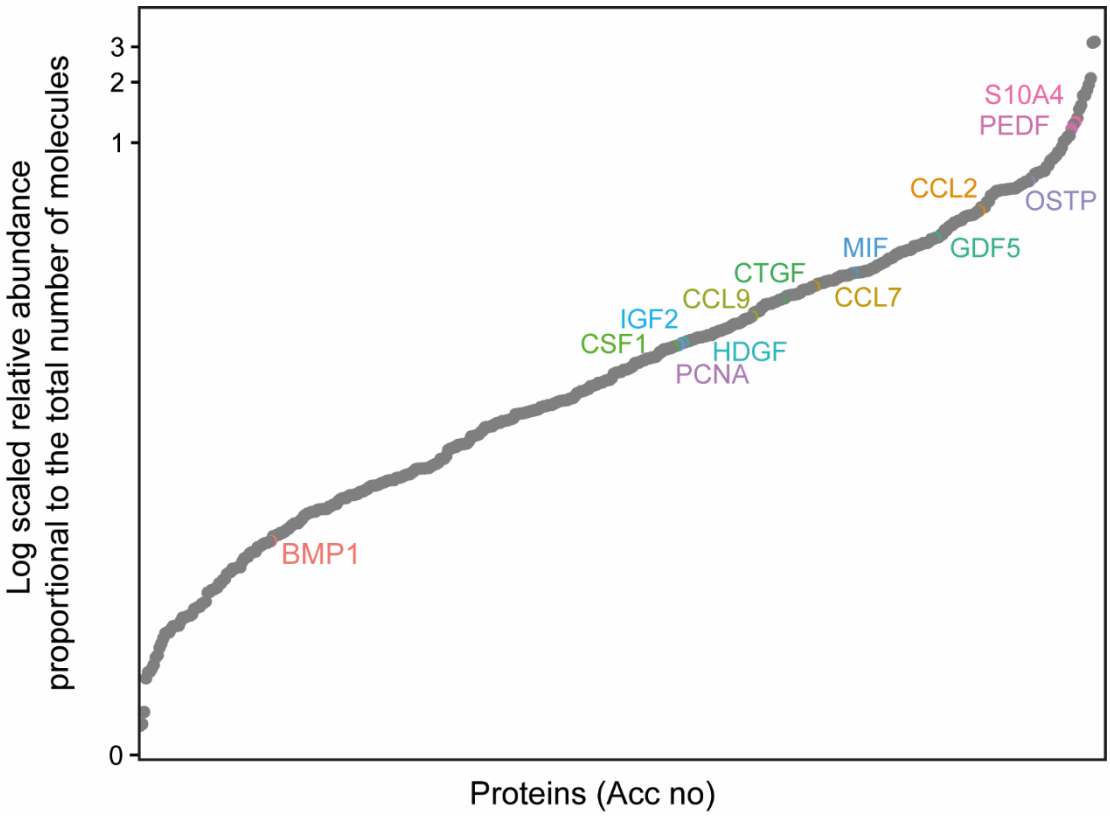

Figure 3.12: Relative abundance of secreted MS-5 proteins to total ion intensity. Quantitative secretomic analysis of MS-5 secretome, quantifying MS ion intensity for all corresponding peptides of identified proteins. Scores normalised by molecular weights and ordered according to Log transformed relative abundance. Abundance averaged across n=3 technical replicates. GFs of interest are coloured.

Filtering for GFs and chemokines identified 14 proteins of interest (Figure 3.13). The most abundant of which was protein S100-A4 followed by PEDF. Protein S100-A4 supports VEGF via the RAGE receptor, promoting endothelial cell migration (371). Osteopontin, the next most abundant GF, has a well-described role in the BMSM helping to keep LSCs in a dormant state (372). Growth/differentiation factor 5 (GDF5) has previously been implicated in regulating TGF-β dependant processes that influence LSC migration (373). Connective tissue growth factor is another signalling protein that is thought to enhance AML cell growth, via a mechanism that implicates pSmad1/5 signalling (374).

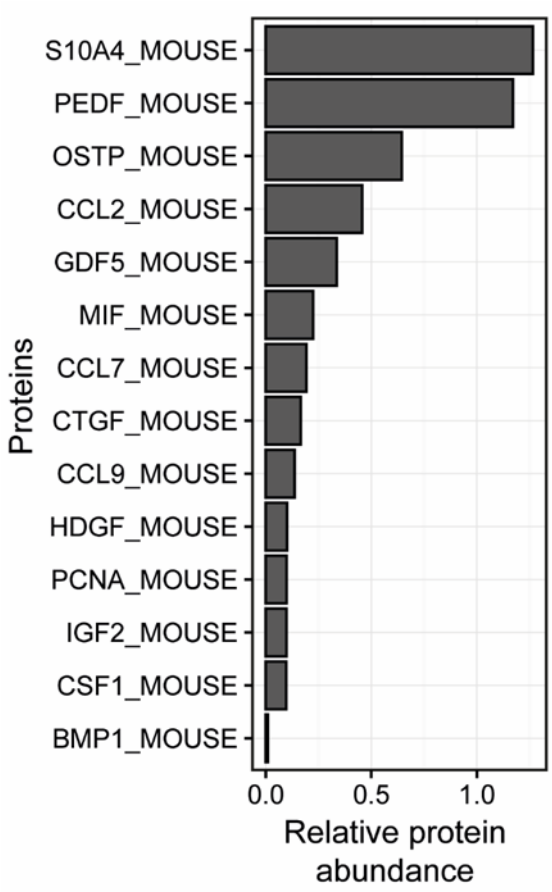

Figure 3.13: List of the most abundant secreted MS-5 growth factors. Calculated protein abundance normalised by molecular weight of GFs identified in the MS-5 secretome, proteins ordered according to Log transformed relative abundance. Abundance averaged across n=3 technical replicates.

To fully characterise the MS-5 stromal secretome, analysis that incorporated gene ontology (GO) searches were undertaken. By submitting the identified MS-5 secretomic components to the Panther GO search engine it was possible to classify functions and processes for 208 of the identified proteins. These proteins were then assigned to 23 different protein classes as shown in Figure 3.14A, we were interested in the signalling molecules protein class. This group that consisted of 16 proteins could be subdivided into 4 further groups; cytokines, GFs, membrane-bound signalling molecules and peptide hormones (Figure 3.14B). This analysis made it possible to visualise the proportions of protein classes by which the secretome was composed, with signalling molecules being one of the largest classes. The identified signalling molecules did not differ significantly from those detailed in Figure 3.13, with the notable exception of SPRC and PR23C. SPARC (Osteonectin), was recently described as having a role in leukaemia cell self-renewal, whereby SPARC activation of the integrin-linked kinase/AKT (ILK/AKT) pathway, this subsequently activates β-catenin signalling (375). Prolactin-2C3 is only expressed in mice, therefore it is unlikely to be a protein of interest in the context of the present works aims.

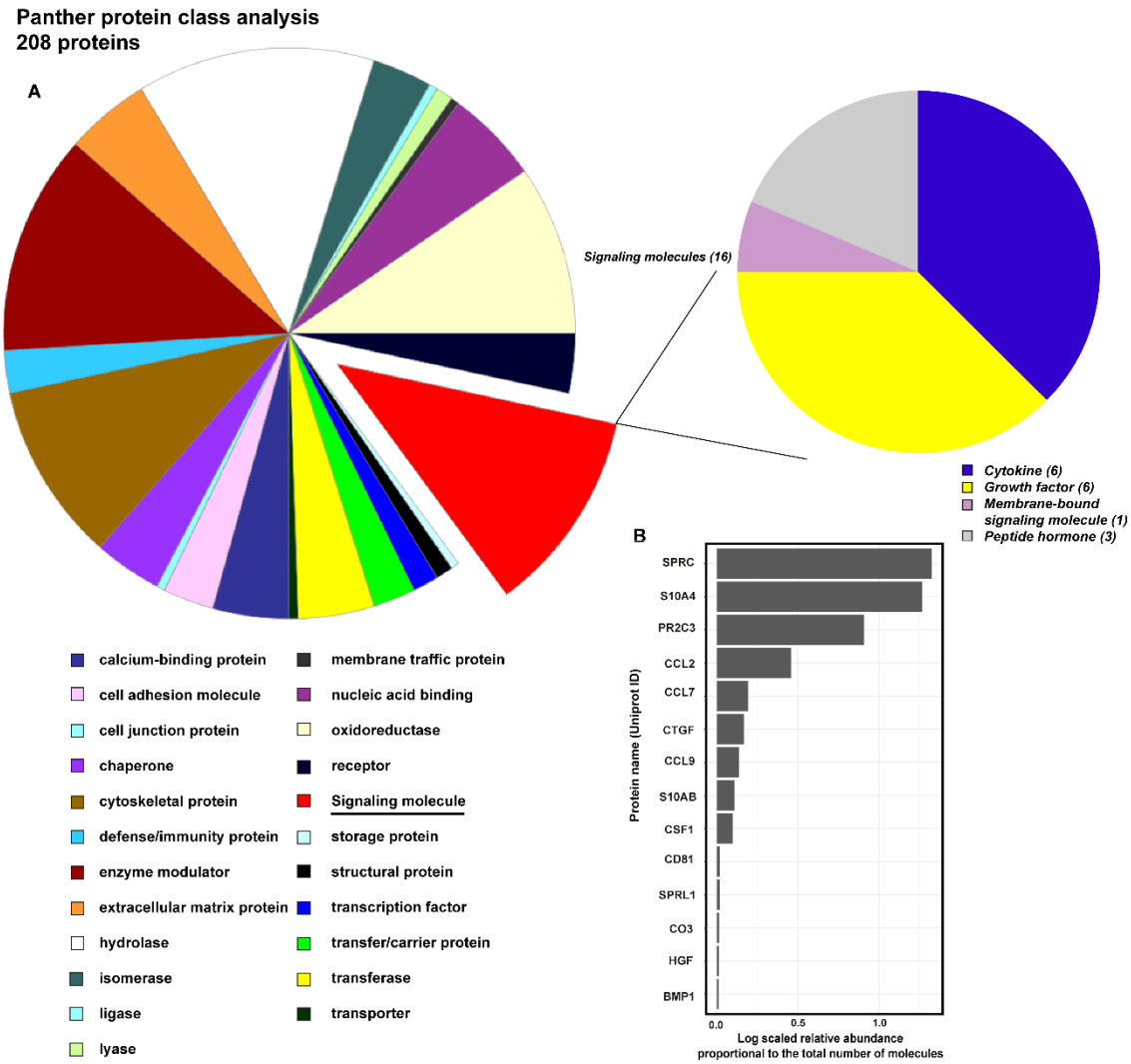

Figure 3.14: Panther gene ontology analysis of MS-5 secretome. Proteins of the MS-5 secretome identified by LC-MS/MS analysis were submitted to Panther gene ontology enrichment analysis. **(A)** Panther assigned 208 identified MS-5 proteins that met confidence criteria into protein class. **(B)** Enriched signalling molecules detected by panther analysis displayed with Log transformed relative abundance normalised by molecular weight. Abundance averaged across 3 technical replicates.

Enrichment and LC-MS/MS analysis of the MS-5 secretome provided potential candidate factors that could be important in maintaining primary AML cell survival as well as activating signalling in these cells. However, we decided that a more quantitative approach was necessary in order to select proteins to investigate for biological function in AML.

3.7 LC-MS/MS analysis of HS-5 secretome

LC-MS/MS analysis of the MS-5 secretome was undertaken first and subsequent HS-5 based experiments revealed that the CM produced by this cell line was superior for maintaining AML viability (Figure 3.7). This observation coupled with the successful use of both cell lines in the literature for sustaining AML ex vivo suggested that there were different factors being secreted by the two cell lines. To establish if this was true we also enriched the HS-5 secretome and conducted LC-MS/MS analysis.

The process of enriching proteins in the secretome from HS-5 or MS-5 CM can be achieved through a number of methods. Previous MS-5 secretome enrichment had been achieved using the Vivaspin 20 molecular weight cut off (MWCO) columns that separate proteins utilising size exclusion. During those experiments it was postulated that proteins may be lost through binding to the semi-permeable membrane that separates the >5kDa and <5kDa compartments. To investigate this, HS-5 secretome was processed both utilising the MWCO approach as well as the classical method of methanol chloroform (MC) precipitation to enrich for the protein component.

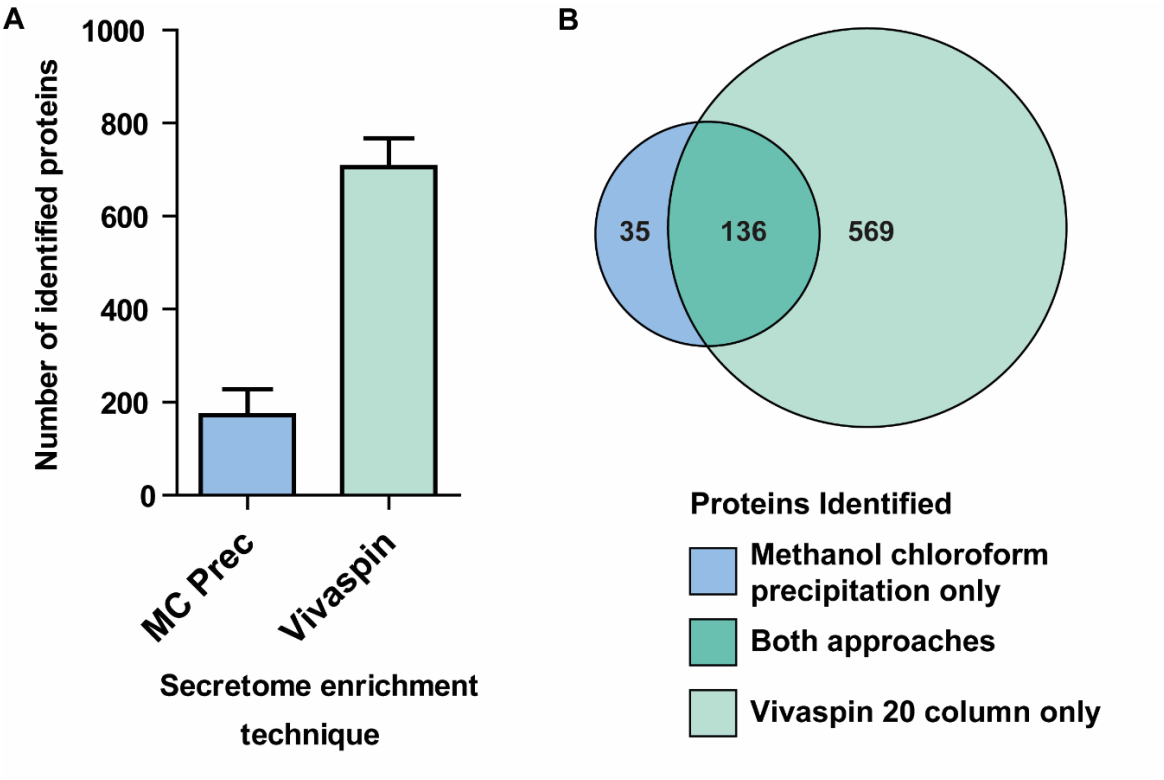

Figure 3.15: Optimisation of secretome enrichment finds Vivaspin columns best approach. Methanol chloroform precipitation and Vivaspin 20 columns used to enrich for secretomes from HS-5 CM. **(A)** Number of identified proteins determined by LC-MS/MS and MASCOT analysis. Proteins counted if they returned a MASCOT score >50 and >2 unique peptides identified. **(B)** Protein identification consensus between approaches. n=3 samples run in analytical triplicates per approach.

Utilising both approaches (although others were available, familiar protocols were undertaken) HS-5 CM was collected, proteins enriched, before proteins were processed for LC-MS/MS analysis (as detailed in methods section 2.10). Once samples were analysed, peptides identified, and proteins determined (using MASCOT and bioinformatic tools), coverage of each approach was assessed. On average secretome assessment using the Vivaspin approach identified 705 HS-5 proteins and the MC precipitation only identified 171 HS-5 proteins at the end of analysis (Figure 3.15A). The difference between the approaches was stark and strongly supported proceeding to analyse the stromal secretome using the Vivaspin 20 columns.

To find merit within the MC approach, the coverage of the proteome that both methods conferred was assessed, as it may have been that the chemistry involved in the MC precipitation could capture proteins that are not possible to identify when employing the Vivaspin method. Analysis revealed that the MC precipitation approach identified 35 proteins that were not found in the Vivaspin approach. These proteins however, were keratins, collagens and myosins – likely present due to the increased sample handling in the MC precipitation. 136 proteins were identified using both approaches and 569 proteins were identified using the Vivapspin method that could not be detected using the MC precipitation method (Figure 3.15B). The results from these experiments suggested that the Vivaspin approach was indeed the best method in our hands to examine the stromal secretome.

Analysis of the total HS-5 secretome using Vivaspin enrichment coupled to LC-MS/MS detection enabled the identification of 695 proteins, in which >2 unique peptides with a MASCOT score >50 were detected. Assessment of these proteins by abundance and normalisation for protein size produced a spread of data visualised in Figure 3.16A, with all potential signalling molecules coloured. In the HS-5 secretome there were substantially more signalling molecules identified compared to that identified in MS-5 based experiments.

Closer consideration of the identified signalling molecules showed that by far the most abundant signalling proteins in the secretome were transforming growth factor-beta-induced protein ig-h3 (BGH3) previously described as playing a role in cell adhesion (376), TSP1 and TSP2 commonly found in BM stromal media and Latent-transforming growth factor beta-binding proteins 1 and 2 (LTBP1, LTBP2) which were recently described as being crucial to invasion and proliferation in other cancer types (377) (Figure 3.16B). Other factors previously described as being important in leukaemia included IL6, IL8, NOV and OSTP (378-381). Further, there were signalling proteins identified that were also detected during MS-5 secretome analysis including, BMP-1, CTGF, S100 proteins, CSF-1, HGF related proteins and CCL proteins.

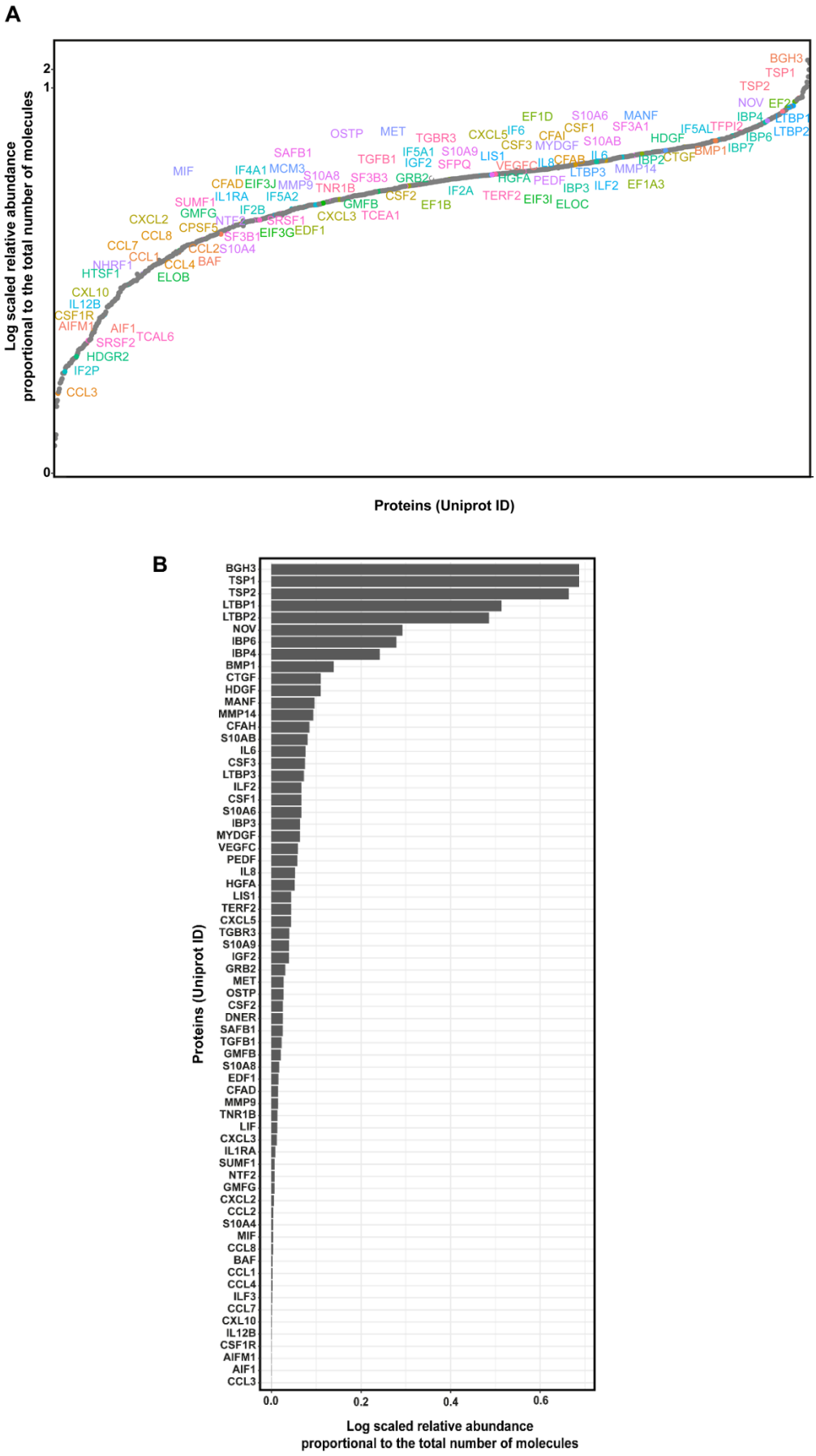

Figure 3.16: List of the most abundant secreted HS-5 growth factors. (A) All 695 identified HS-5 proteins that met confidence criteria. Signalling molecules coloured. **(B)** Potential signalling molecules, ordered according to Log transformed relative abundance scores, which are normalised by molecular weights. Abundance averaged across 3 independent samples run in analytical triplicates.

To extract more biological insights from the data, Panther GO enrichment analysis was undertaken, in which all 682 proteins that were identified across all runs were submitted for GO annotation. This analysis sorted the proteins into 23 different protein classes, these included cytoskeletal proteins, extracellular matrix proteins, cell adhesion molecules and signalling molecules (Figure 3.17A). A total of 35 proteins were considered signalling molecules (this does not include calcium binding proteins, receptors, cell junction proteins, or transcription factors that can act as signalling molecules). The 35 signalling molecules could be further subdivided into cytokines (16), GFs (12), membrane-bound signalling molecules (4) and peptide hormones (3). A detailed list of these 35 proteins is illustrated in (Figure 3.17B), with the 5 most abundant of these proteins being complement C3 (CO3), SPARC (SPRC), semaphorin-7A (SEM7A), inhibin beta A chain (INHBA) and NOV. CO3 and SEM7A have roles in inflammation and the immune response, proteins SPARC, NOV and INHBA have a myriad of roles in development being described as modulators of growth, differentiation, migration and survival (375, 382, 383).

To understand how these proteins may in concert direct cellular function, GO pathway analysis was implemented on the HS-5 secretome LC-MS/MS data. This showed that by fold enrichment the highest-ranking pathway was glycolysis, followed by the pentose phosphate pathway and the plasminogen-activating cascade (Figure 3.17C). From a signalling perspective the components of the HS-5 stromal secretome displayed enrichment towards integrin signalling pathways and cytoskeletal regulation by Rho GTPase. All of these had low p-values, however, there were processes involved (Parkinsons, Alzheimers, Huntington disease – although diseases with strong signalling elements) that suggested these BM stromal based experiments needed further stratification to limit associated processes more specifically to AML.

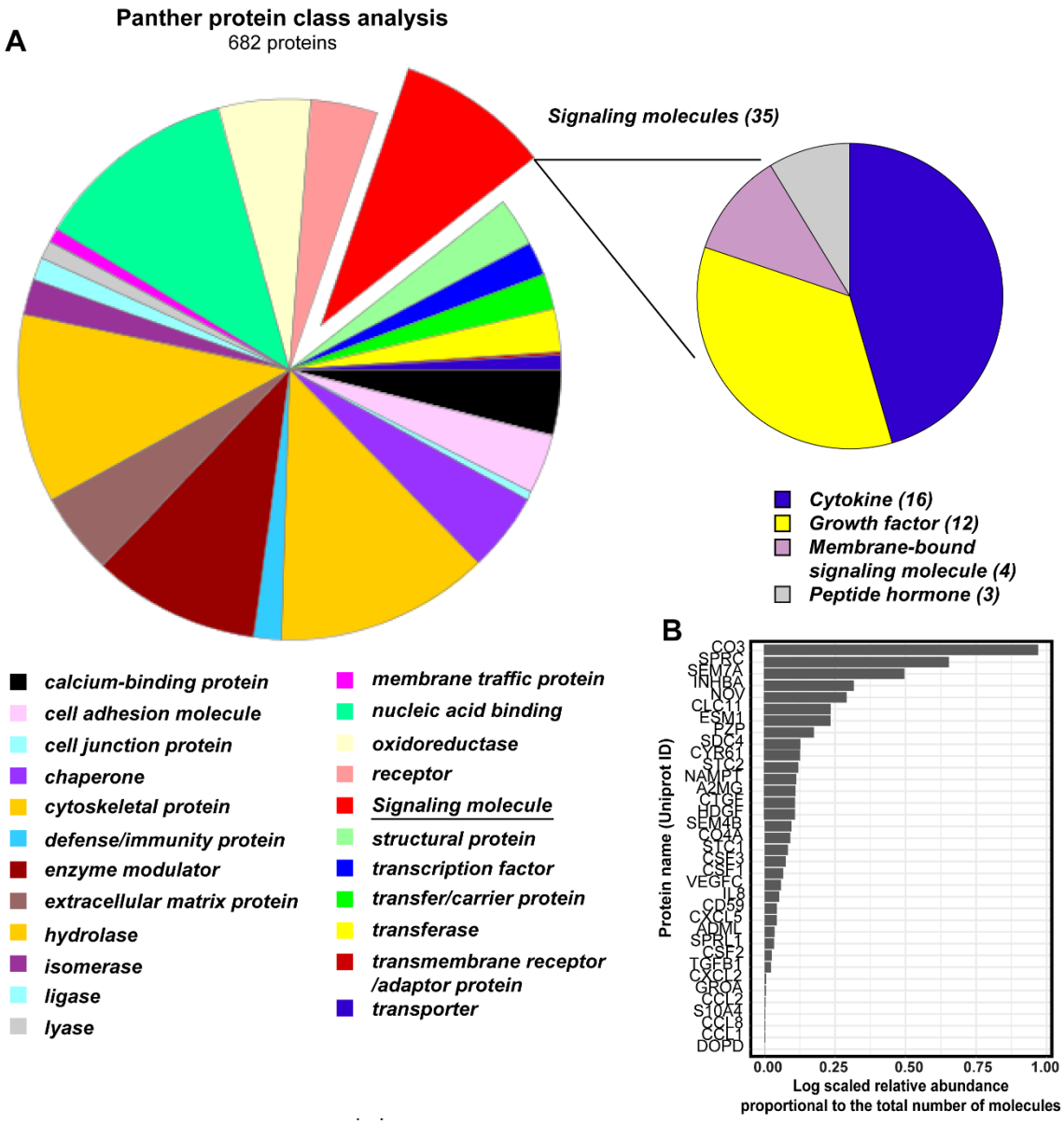

C

PANTHER Pathways	# Proteins	Expectancy Score	Fold Enrichment	P value
Glycolysis	20	0.66	16.79	1.96E-08
Pentose phosphate pathway	8	0.26	15.26	2.53E-02
Plasminogen activating cascade	18	0.59	13.57	3.32E-05
Parkinson disease	100	3.28	7.94	2.96E-13
Cytoskeletal regulation by Rho GTPase	82	2.69	7.45	1.59E-09
Blood coagulation	48	1.57	6.36	9.40E-04
Integrin signalling pathway	194	6.36	5.98	1.01E-15
Huntington disease	142	4.65	3.87	2.89E-04
Alzheimer disease-presenilin pathway	122	4	3.5	1.13E-02
CCKR signaling map	173	5.67	2.82	4.12E-02

Figure 3.17: Panther gene ontology analysis of HS-5 secretome. (A) Protein class assignment for 695 identified HS-5 proteins that met confidence criteria. **(B** Log transformed relative abundance normalised by molecular weights of all signalling molecules detected by panther analysis. Abundance averaged across 3 independent samples run in analytical triplicates. **(C)** Top 10 Panther GO results for total HS-5 secretome identifications with a MASCOT score >50 and >2 unique peptides identified..

3.8 Co-culture models to induce dynamic stromal protein expression

Experiments so far enabled us to determine components of the MS-5 stromal secretome whilst under basal conditions. While it was possible to speculate as to which proteins likely supported AML blast survival it was still unclear which of these 502 proteins were responsible for inducing intracellular signalling (Figure 3.9) and whether these same proteins were responsible for the changes in MV4-11 cell viability and proliferation (Figure 3.2).

To establish which proteins of the stromal secretome had relevance in AML, it was devised that we could produce secretomes of variable composition by culturing MS-5 mouse stromal cells with human AML cells both in the same environment and independently. It was postulated that any differences in secretome composition may give indications as to which proteins were more important to AML, with dynamic abundance between the secretomes acting as a surrogate marker for utilisation and/or positive feedback mechanisms for secretome production (Figure 3.18).

Protein mass spectrometry can differentiate peptide sequences originating from different organisms provided tryptic peptides differ by at least one amino acid that changes the mass of the peptide. This contrasts with immunochemical methods where antibodies often cross-react with proteins of closely related organisms. Therefore, conducting the co-culture experiments with cell lines derived from different species enabled identification of which cells were responsible for the secretion of specific components of the secretome. Discrimination between the protein origins was possible because on average 1 in every 10 amino acids is different between human and murine proteins. These differences are small enough that most proteins share sufficient homology to interact with antibodies, yet the difference is still detectable by mass spectrometry. Therefore, the species of the proteins within the co-culture secretomes revealed if a protein was secreted by a stromal cell (mouse) or an AML cell (human). Finally, we decided to co-culture MS-5 cells with a panel of AML cell lines: MV4-11, P31/FUJ, HL-60 and CTS.

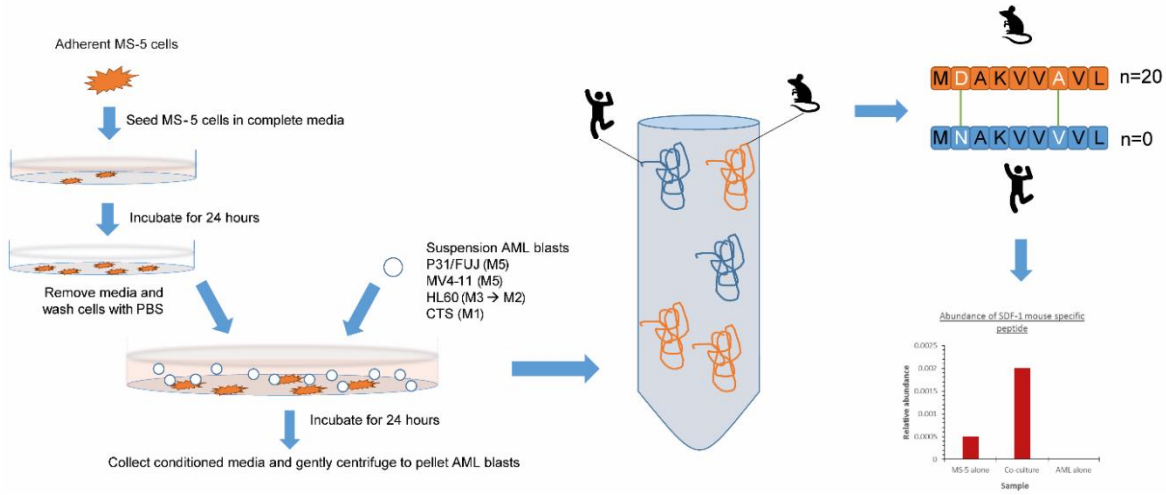

Figure 3.18: Schematic for AML – MS-5 co-culture model. To create the co-culture MS-5 cells were seeded in flasks in complete media and left to grow for 24 hours. After stromal cells were established, the growth medium was removed, and cells were washed twice with PBS. In parallel AML blasts (P31/FUJ, MV4-11, HL-60, and CTS) were grown in culture for 24 hours before being harvested and pelleted to remove media. The appropriate number of blasts/flask were then re-suspended in fresh serum-free media and the suspension was then gently introduced into the flask containing MS-5 stromal cells. These populations were then left a further 24 hours before the supernatant was carefully collected from the flasks. As the supernatant contains the AML blasts, suspensions are gently centrifuged as to not stress the cells. The resultant CM was then harvested and underwent secretome purification steps as detailed previously. The remaining MS-5 cells were then washed with pre-warmed PBS and trypsinised before viability assays or cell lysis. AML blast pellets were re-suspended in media or PBS before further experimentation.

3.9 Co-culture viability assays

In parallel to the secretome digestion, the cells following co-culture were collected and assays were run to assess the effects of co-culture on cell viability. As serum proteins generate a lot of background during mass spectrometry analysis, serum was omitted from the co-cultures when producing the secretomes. This also allowed for the investigation of the supportive qualities that MS-5 cells and secreted proteins could provide. We assessed the viability of the cells prior to the experiments at time = 0, as well as AML blast viability in a serum starved environment alone and in co-culture with MS-5 cells. MS-5 cells were also cultured alone to establish if cells were detrimentally affected by the presence of AML blasts. Additionally, we wanted to see if the viability of the different AML types was consequential to the starvation-stromal effect.

Although the initial changes in cell viability were not large, they were statistically significant and demonstrate that after just 24 hours incubation MS-5 co-culture did positively affect AML cell viability. The assay only measured viability at the 24 hour time-point (as time of secretome harvesting), but the viability of MV4-11, P31/FUJ and CTS cells was dropping in the unsupported environment. In the stromal cell supported environment viability was maintained if not increased, suggesting that that co-culture was preventing the drop in AML viability in these

models (Figure 3.19). In contrast, the viability of HL60 cells was unaffected by the stromal environment, suggesting an independence from the microenvironment.

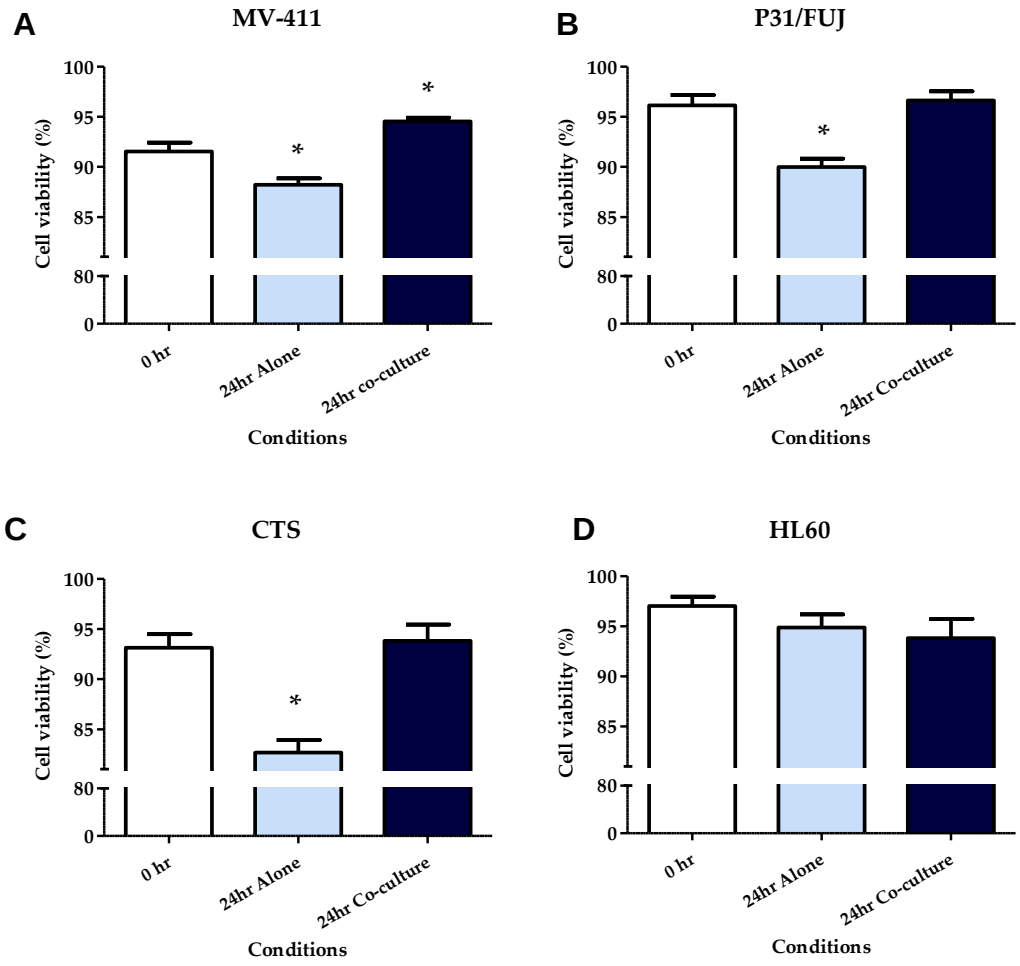

Figure 3.19: AML cell viability over 24 hours following serum starvation in culture alone or in co-culture with MS-5 stromal cells. $1x10^7$ cells seeded in T175 flasks with and without $1x10^6$ MS-5 cells in 20ml IMDM media (no serum as media collected for LC-MS/MS analysis). Following 24 hours **(A)** MV4-11 cell viability **(B)** P31/FUJ cell viability **(C)** CTS cell viability **(D)** HL60 cell viability, were measured with a Beckman Vi-cell counter. Each condition run in technical triplicates and cell counts run in analytical triplicates. * $p<0.05$

3.10 LC-MS/MS analysis of co-culture secretomes

LC-MS/MS analysis of MS-5 secretomes following co-culture with the AML cell lines identified 246 secreted proteins (with a MASCOT score >50 and >2 peptides identified) which were only detected exclusively from murine derived peptides (therefore secreted by stromal cells and not AML cells). Of these identifications 133 were found to be statistically significant changes in protein abundance across cultures following the co-culture experiment, these changes are represented as a heatmap in Figure 3.20.

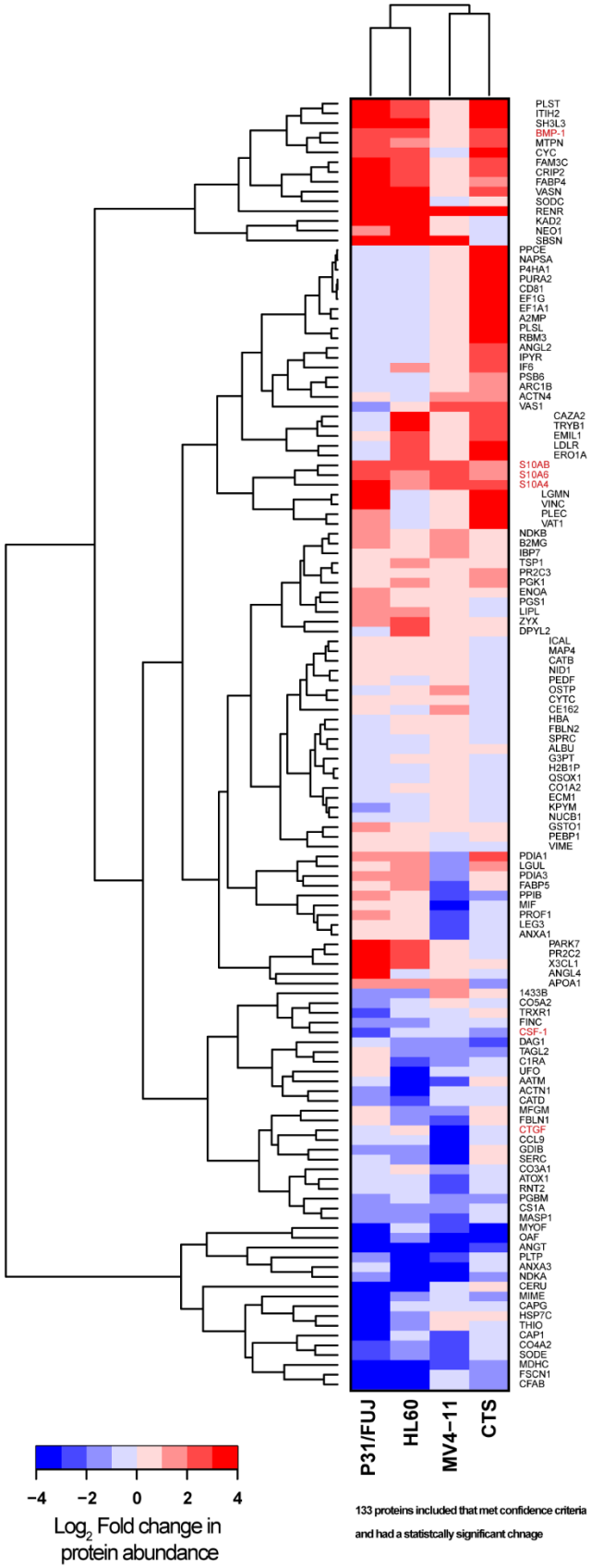

Figure 3.20: Hierarchical clustering analysis of the changes in protein expression in AML-MS5 co-cultures. Heatmap displays the 133 proteins secreted by MS-5 cells (murine specific peptides) that significantly changed in abundance following 24 hours co-culture with AML cell lines compared to CM from MS-5 grown independently. Each co-culture run in technical triplicates and each replicate analysed by LC-MS/MS in analytical triplicates. Heatmap and dendrograms produced in R environment using 'ggplots' package.

In the P31/FUJ cultures 6 stromal secreted proteins were significantly increased (at >2 Log_2 fold change and p<0.05) and 16 decreased (at <-2 Log_2 fold and p<0.05) compared to secreted protein abundance in MS-5 independent cultures. Of the 6 stromal proteins that increased in abundance following AML co-culture there were some notable proteins that were observed in the MS-5 secretome only experiments too; these included S100-A4, S100-A6, S100-A11 and BMP-1 (Figure 3.21A).

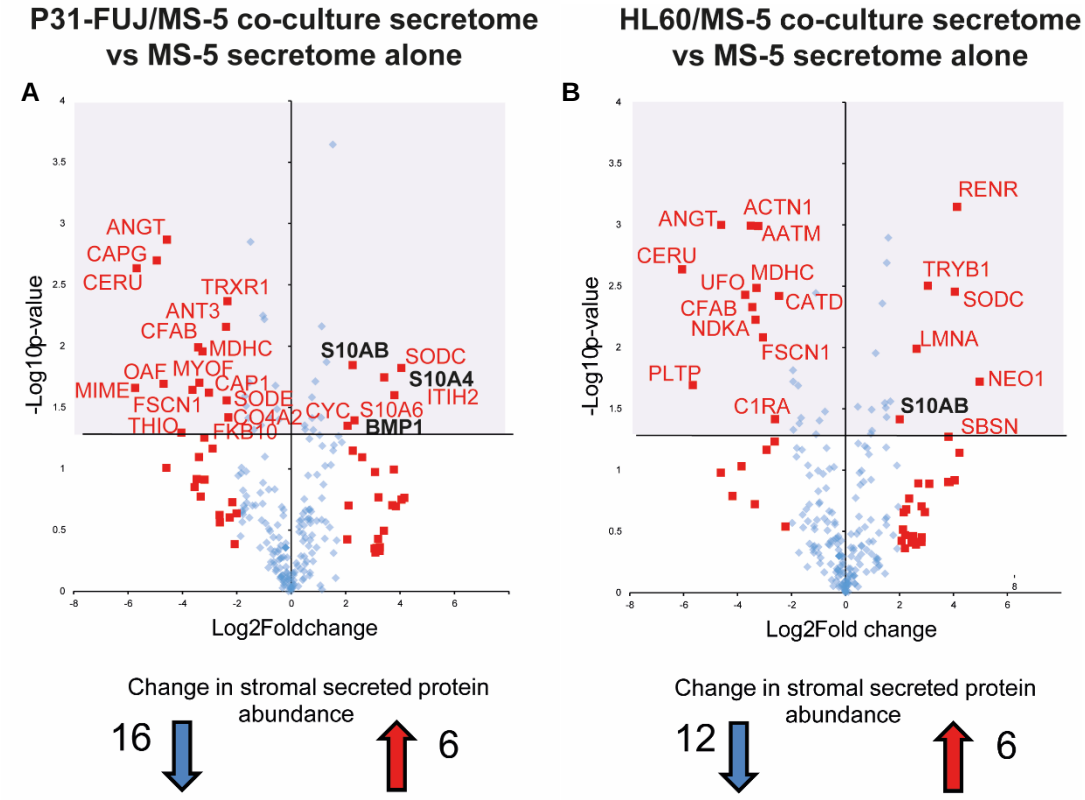

Figure 3.21: Volcano plots of stromal factors that significantly increase and decrease following co-culture with P31/FUJ and HL60 cells. Murine derived proteins in the CM from MS-5 cells incubated with **(A)** P31/FUJ **(B)** HL60 cell lines for 24 hours and compared to CM from MS-5 only cultures. Markers red if protein abundance <2> Log_2 fold change compared to control and above line if statistically significant. Each co-culture run in technical triplicates and each replicate analysed by LC-MS/MS in analytical triplicates.

In the HL60 cultures 6 stromal secreted proteins were also significantly increased (at >2 Log_2 fold change and p<0.05) and 12 decreased (at <-2 Log_2 fold and p<0.05) compared to secreted protein abundance in MS-5 independent cultures (Figure 3.21B). Notable proteins that increased in these cultures include renin receptor (RENR) a known component in BMSM that can become dysregulated in AML (384), and suprabasin (SBSN) previously described as a proto-oncogene in other cancers that can aid in metastasis and invasion (385-388), and S100-A11.

In the MV4-11 cultures 4 stromal secreted proteins were observed as significantly increased (at >2 Log_2 fold change and p<0.05) and 17 decreased (at <-2 Log_2 fold and p<0.05) compared to secreted protein abundance in MS-5 independent cultures (Figure 3.22A). Within

the subset of proteins that increased in expression following AML co-culture the proteins S100-A11, SBSN, and S100-A6 could potentially act as signalling proteins that augment AML survival and proliferation. Unlike the P31/FUJ and HL60 co-cultures, the abundance of a number of potential signalling molecules decreased in MV4-11 co-cultures. These included CTGF which in previous secretome analysis experiments was always one of the most abundant (Figure 3.16B), and CCL9 and Galectin-3 (LEG3) which are inflammatory chemokines that decreased in abundance.

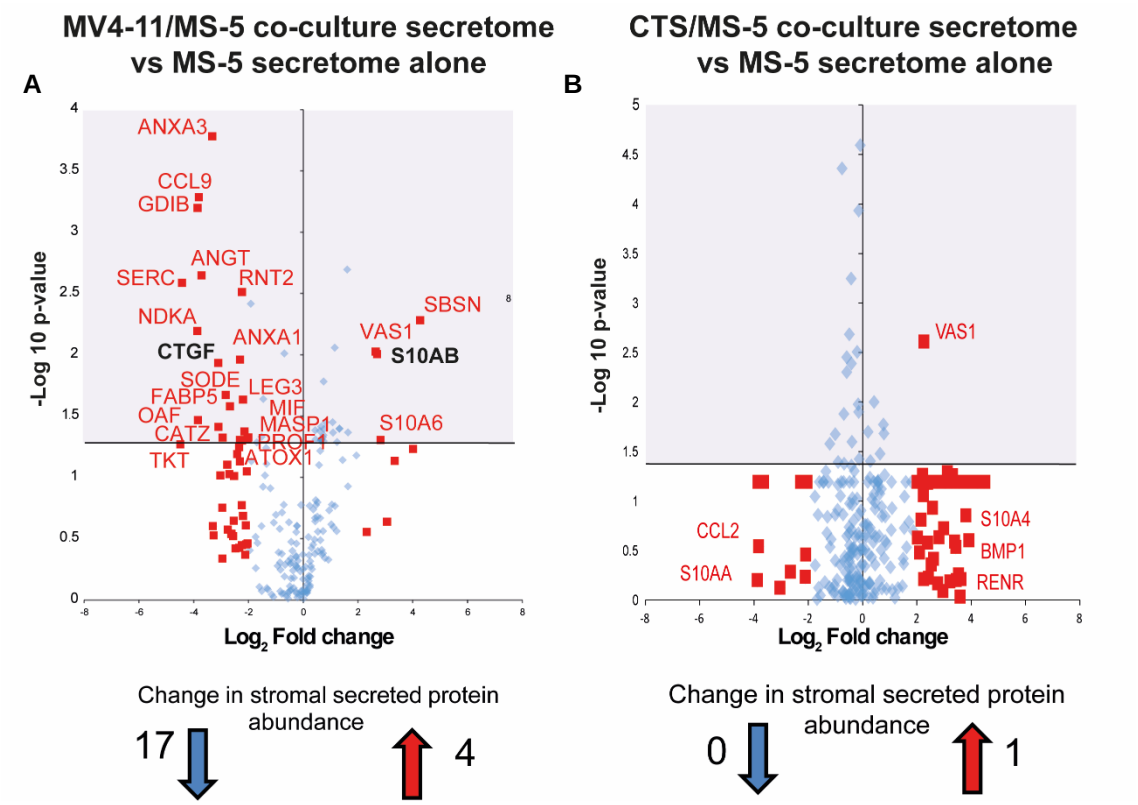

Figure 3.22: Volcano plots of stromal factors that significantly increase and decrease following co-culture with MV4-11 and CTS cells. Murine derived proteins in the CM from MS-5 cells incubated with **(A)** MV4-11 **(B)** CTS cell lines for 24 hours and compared to CM from MS-5 only cultures. Markers red if protein abundance <2> Log_2 fold change compared to control and above line if statistically significant. Each co-culture run in technical triplicates and each replicate analysed by LC-MS/MS in analytical triplicates.

Finally, in the CTS cultures only 1 stromal secreted protein significantly increased (at >2 Log_2 fold change and $p<0.05$) and 0 decreased (at <-2 Log_2 fold and $p<0.05$) compared to secreted protein abundance in MS-5 independent cultures (Figure 3.22B). The MS-5 secretomes following CTS co-culture did not contain as many significantly modulated proteins as observed with other cell lines, with only VAS1 is the only change that is statistically significant. Although of the identified proteins, candidates such as S100-A4, BMP-1 and RENR exhibited high fold change differences between independent and co-culture CTS models.

3.11 Panel of six stromal secretome proteins selected for further investigation

Several of the secreted proteins that changed in abundance during co-cultures have previously been described as being secreted in other systems (371, 389, 390) and possess the capacity to act as signalling molecules. Consideration of this data coupled with the MS-5 and HS-5 independent analysis (sections 3.6 and 3.7) six proteins were selected for further investigation including; S100-A4, S100-A11, connective tissue growth factor (CTGF), hepatocyte growth factor (HGF), bone morphogenic protein-1 (BMP-1), and colony stimulating factor-1 (CSF-1) (Figure 3.23).

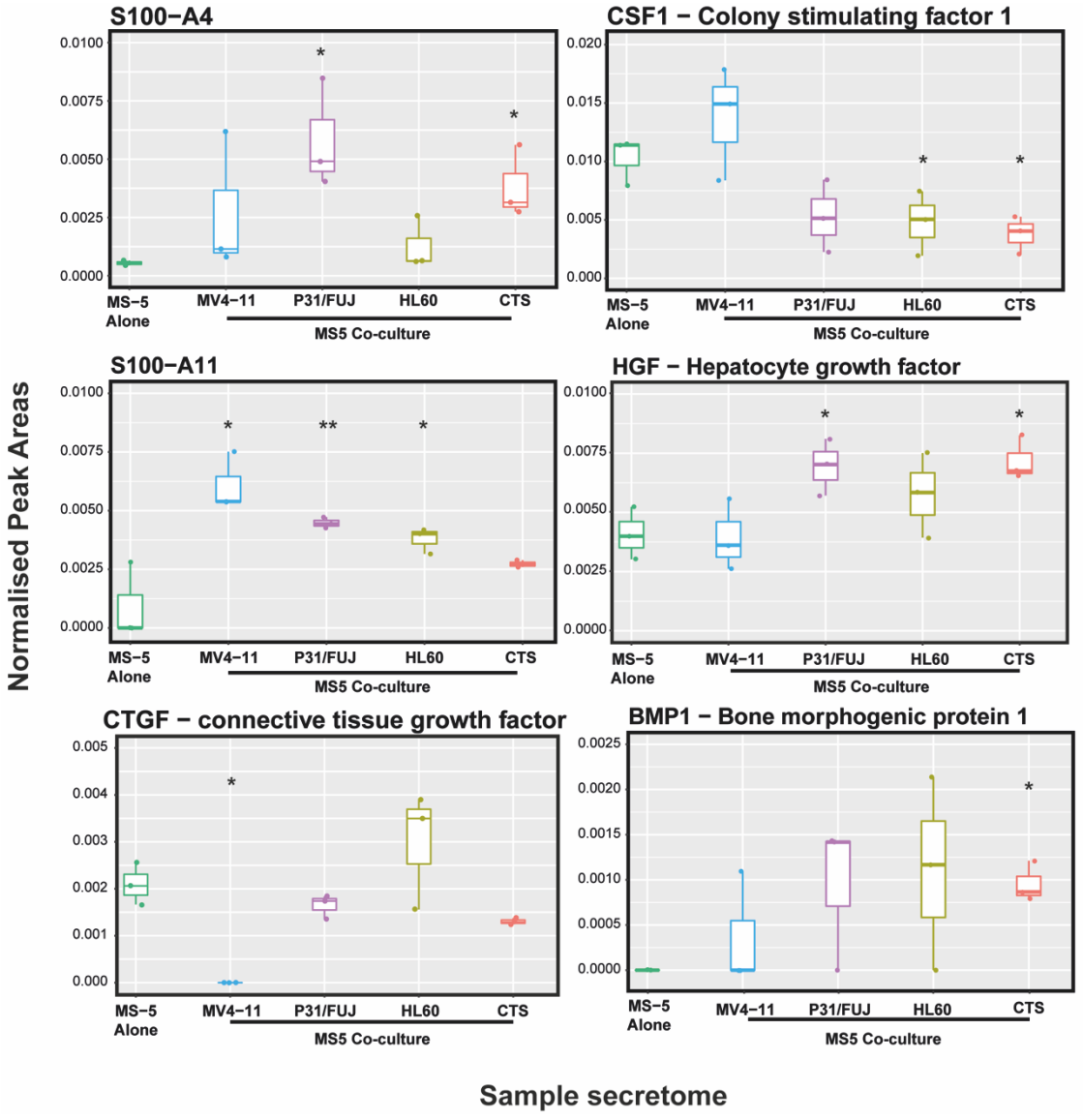

Figure 3.23: Box plots of six chosen stromal proteins that changed dynamically across the co-cultures. CTFG, S100-A11, BMP-1, CSF-1, HGF, S100-A4 were the chosen proteins, all were murine specific in origin and did not appear in AML cell line only cultures. Boxplot values represent normalised quantified abundance of specified proteins in MS-5 only cultures and in the AML co-cultures; n=3 independent technical replicates; P value calculated by unpaired two-sided t test comparing co-cultures to MS-5 only samples * p<0.05 ** p<0.01.

The first important characteristic that is common to these 6 growth proteins was that none of these were detected in the secretome of the AML cell lines that were grown in the

absence of MS-5 cells. This is a crucial property of these cells as this study is looking for means by which the microenvironment supports AML progression, therefore these proteins needed to be secreted by the stromal cells. Additionally, from a technical perspective if these candidates were being secreted by both cell types then any increases in abundance could just be due to having more cells present in culture, not necessarily because AML interaction induces increased secretion.

S100-A4 was selected as firstly it was the most abundant signalling molecule identified in the MS-5 and HS-5 secretome (Figure 3.13). Secondly during AML/MS-5 co-culture experiments S100-A4 abundance changed dynamically across the co-cultures. In each of the AML co-cultures murine S100-A4 was elevated compared to the MS-5 only cultures. In particular, murine S100-A4 levels were very high in P31/FUJ and CTS cultures, while being variable in MV4-11 cultures (Figure 3.23). This potentially suggests that in different AML types S100-A4 has varying impact, with P31/FUJ cells possessing the feedback mechanisms to potentiate S100-A4 secretion that HL60 cells do not. Alternatively, S100-A4 may have more relevance to HL60 cells and the lower abundance is indicative of the utilisation of S100-A4. This pattern of expression coupled with previous reports describing S100-A4 as a metastatic potentiating factor in solid tumours make S100-A4 a suitable candidate for further investigation.

CSF-1 became a candidate because, as with S100-A4, it was identified in all secretome experiments (Figure 3.14B) (Figure 3.16B). CSF-1 was unique as it had previously been implicated in haematopoietic precursor cell maintenance, and the receptor of which (CSF1R) has been suggested as a potential biomarker of disease outcome (391). Assessment of CSF-1 levels during co-culture revealed that MS-5 cells independently secrete relatively high levels of CSF-1 into the media. However, in the presence of AML cells (in particular P31/FUJ, CTS and HL60) CSF-1 levels decrease (Figure 3.23). This response could be due to utilisation of CSF-1 by these cell lines, with MV4-11 not experiencing the same reduction due to a lack of CSF1R expression. Alternatively, CSF-1 may elicit a regulatory function on AML growth and therefore, mechanisms may be activated to reduce its influence.

The third protein to be investigated further was S100-A11. Another of the S100 protein family that was consistently one of the most statistically significant proteins to be elevated following stromal co-culture (Figure 3.21). Looking at the pattern of expression displayed across the co-cultures, this protein had a similar pattern of expression to CSF-1, with S100-A11 being recorded highest in MV4-11 cultures compared to the other cultures (Figure 3.23). However, like S100-A4 it was detected at very low levels in MS-5 cells grown alone, this suggests S100-A11 expression was driven by AML and stromal cell interaction during co-culture.

HGF was selected as a protein for further investigation as the MET receptor (receptor to HGF) has previously been investigated in AML (392). In these studies, HGF and HGF co-binding proteins were identified in the HS-5 investigations. In co-culture experiments HGF was consistently abundant, which was also unique compared to other potential signalling molecules identified (Figure 3.23).

CTGF selection was guided by its relative abundance in MS-5 (Figure 3.14B) and HS-5 (Figure 3.16B) independent experiments. Functionally CTGF has been described previously as a signalling molecule and its oncogenic properties have been investigated, although not in the context of AML (393, 394). In the AML/MS-5 co-culture experiments, CTGF expression was unique to the other proteins. P31/FUJ and CTS co-cultures exhibited the same CTGF abundance as that recorded in MS-5 cells cultured alone (Figure 3.23). However, in the MV4-11 co-culture CTGF expression was not detected. CTGF expression was relatively high in the HL60 co-culture compared to the other cultures. HL60 is a representative model of APL, a form of AML that is distinct from other leukaemias. This observation made CTGF a protein of interest as its expression was potentially subtype specific expression.

Finally, BMP-1 was chosen as it was detected in the MS-5 secretome experiments at low levels, but it was also very strongly expressed in the HS-5 secretome experiments (Figure 3.16A). In the co-culture experiments it was consistently elevated across AML cell lines (Figure 3.20). Additionally, in the AML co-culture experiments it was barely observed in the MS-5 only secretome and was consistently high in CTS secretome samples (Figure 3.23). BMP-1 is an astacin metalloprotease and has not previously been reported as a receptor agonist however, it is capable of indirectly activating BMP signalling cascades (395, 396). Additionally, we observed shifts in expression during co-culture experiments suggesting that BMP-1 had a role to play in AML/stromal cell interactions.

It is important to state that other signalling molecules were identified in experiments conducted throughout this chapter, with a plethora of candidates raised in the HS-5 secretome following LC-MS/MS analysis. These proteins were not followed up as some candidates such as IL-6, SPARC and TSP1/2 had been previously investigated and to some degree characterised within the AML system (357, 375, 397, 398). For other candidates such as NOV, SBSN, S100-A6 and LTBP1/2 it was not possible to acquire either biologically suitable recombinant versions or antibodies (including neutralising) at the time.

3.12 Western blot analysis of S100-A4 and CSF-1 presence in primary co-culture secretomes

Following the identification and selection of six proteins from stromal secretomes, experiments were devised to establish if these factors are present in co-culture secretomes of primary AML and MS-5 cells. It was important to validate that these proteins are secreted in the presence of primary cells and not just when cultured in the presence of cell lines, thus providing evidence that these proteins were relevant in primary AML and that the dynamic behaviour of protein abundance was not unique to AML cell lines. CM was collected from primary AML co-cultures with MS-5 cells and the secretome enrichment executed as described previously with Vivaspin 20 columns (section 2.3). These experiments focussed on CSF-1 and S100-A4 proteins, as suitable antibodies directed to these secreted proteins were readily available.

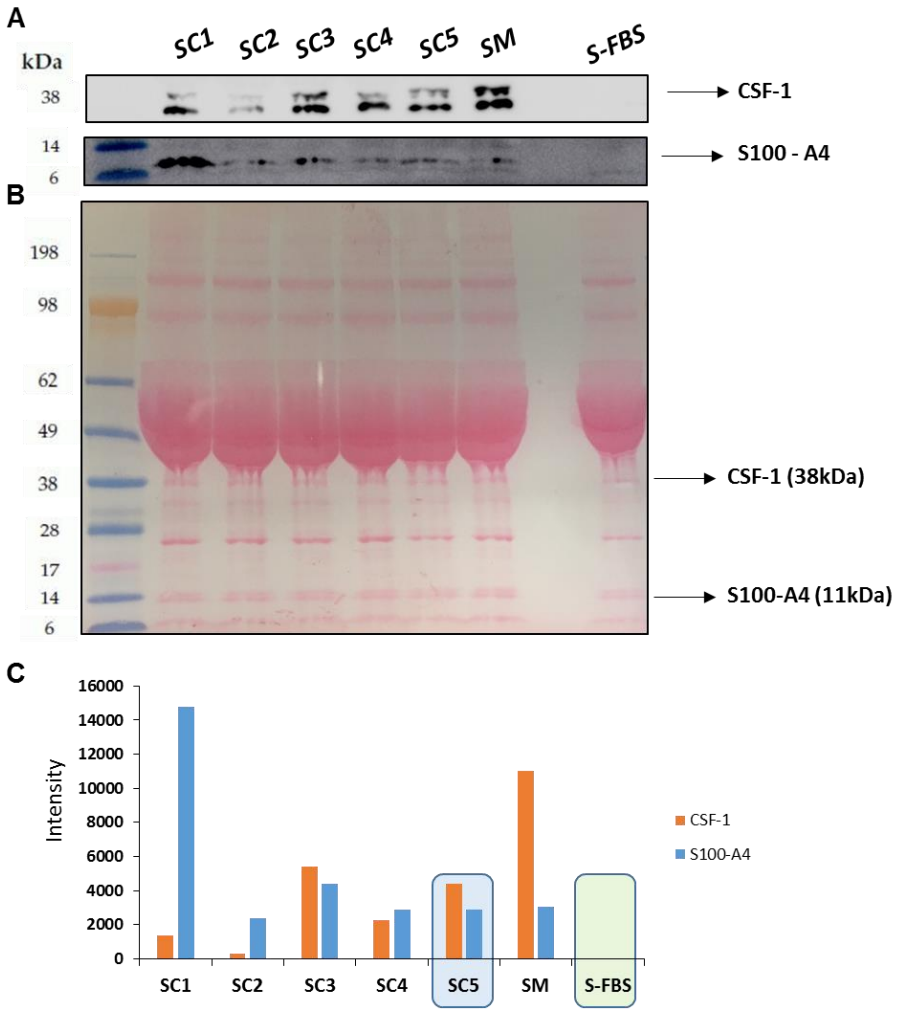

Figure 3.24: Co-culture secretomes derived from different AML patients induce variable CSF-1 and S100-A4 abundance. The CM from five primary samples kept in AML/MS-5 co-cultures for 24 hours were fractionated, and 30µg of each >5kDA secretome were analysed by western blot. **(A)** Western blots for total CSF-1 and total S100-A4 proteins **(B)** Ponceau stain of concentrated >5kDa secretomes produced by patient blast/MS5 cell co-cultures **(C)** Densitometry of the western blots above, intensities calculated using ImageJ software, normalised protein abundances for CSF-1 and S100-A4, intensities normalised to Ponceau stain intensities at the equivalent molecular weight. **SM**; MS-5 secretome only, **SC**; AML/MS-5 co-culture secretome.

Five primary AML patient samples were incubated with MS-5 cells for 24 hours and the >5kDa secretomes produced were separated and analysed by western blot. Primary AML cells as discussed earlier in the chapter are sensitive to ex vivo conditions and as a result for these experiments 10% FBS was included during primary cell co-culture. To control for FBS inclusion, additional FBS and IMDM media controls were included to be sure that neither CSF-1 nor S100-A4 were present in the FBS being used. Western blot assessment of CSF-1 expression via western blot revealed that CSF-1 was highly expressed in MS-5 cell only controls (SM) – as seen in Mass Spectrometry analysis – and variable expression was picked up in the co-culture samples (Figure 3.24A). The co-culture patient secretome from patient SC3 exhibited relatively high CSF-1 expression, whereas, the patient SC2 co-culture secretome had a very low abundance of CSF-1 in the co-culture secretome.

S100-A4 expression in the patient co-cultures was also variable, with the MS-5 only cells (SM) producing low levels of S100-A4 in secretomes, and this held true for most of the co-culture secretomes from patients (SC2-SC5). However, in patient SC1 there were extremely high levels of S100-A4 detected in the enriched co-culture secretome (Figure 3.24A). To quantify and compare conditions, densitometry was undertaken and protein bands were normalised. It was reasoned that due to the variable nature of secretome composition choosing a specific protein as a loading control could be misleading. Therefore, the complementary ponceau stain for the blot was used to normalise protein intensity (Figure 3.24B).

Densitometric analysis of the western blots confirmed that CSF-1 was most abundant in the independent MS-5 cells (SM) and was substantially reduced in all of the patient co-culture secretomes (Figure 3.24C). S100-A4 following normalisation was expressed at consistent levels across the secretomes, with the exception of SC1, in which S100-A4 abundance was almost 4-fold higher than any of the other patient secretomes. The green box in Figure 3.35C highlights the absence of any of the factors in the cell free media containing FBS. An oversight during analysis was that both the S100-A4 and CSF-1 antibodies lacked reactivity towards bovine species. Therefore, despite no band detection in the FBS only lane, the antibody used would not have detected bovine derived CSF-1 or S100-A4. The contribution of these factors from FBS was not possible to assess from this western blot.

The substantial increase in S100-A4 specific to the SC1 sample and none of the other AML patient secretomes raised the possibility that S100-A4 was either secreted by stimulated MS-5 cells or alternatively secreted by the AML cells within the SC1 sample. To ascertain if either hypothesis was correct, the experiment was repeated with the same five patient samples with the addition of cultures containing just the primary AML cells alone – to observe if these factors could be secreted by AML cells.

Western blot analysis of CSF-1 expression revealed that CSF-1 was not observed in any of the AML patient cell only cultures and was only observed in MS-5 containing cultures (Figure 3.25A). S100-A4 was lowly expressed in the MS-5 only sample and expression increased substantially in co-culture models. It became apparent that patient #1 AML cells were capable of secreting S100-A4, but this expression was not observed in the other AML cell only samples. These western blots highlight the heterogeneity of AML samples and perhaps their capacity to shape and interact within the environment they are presented with.

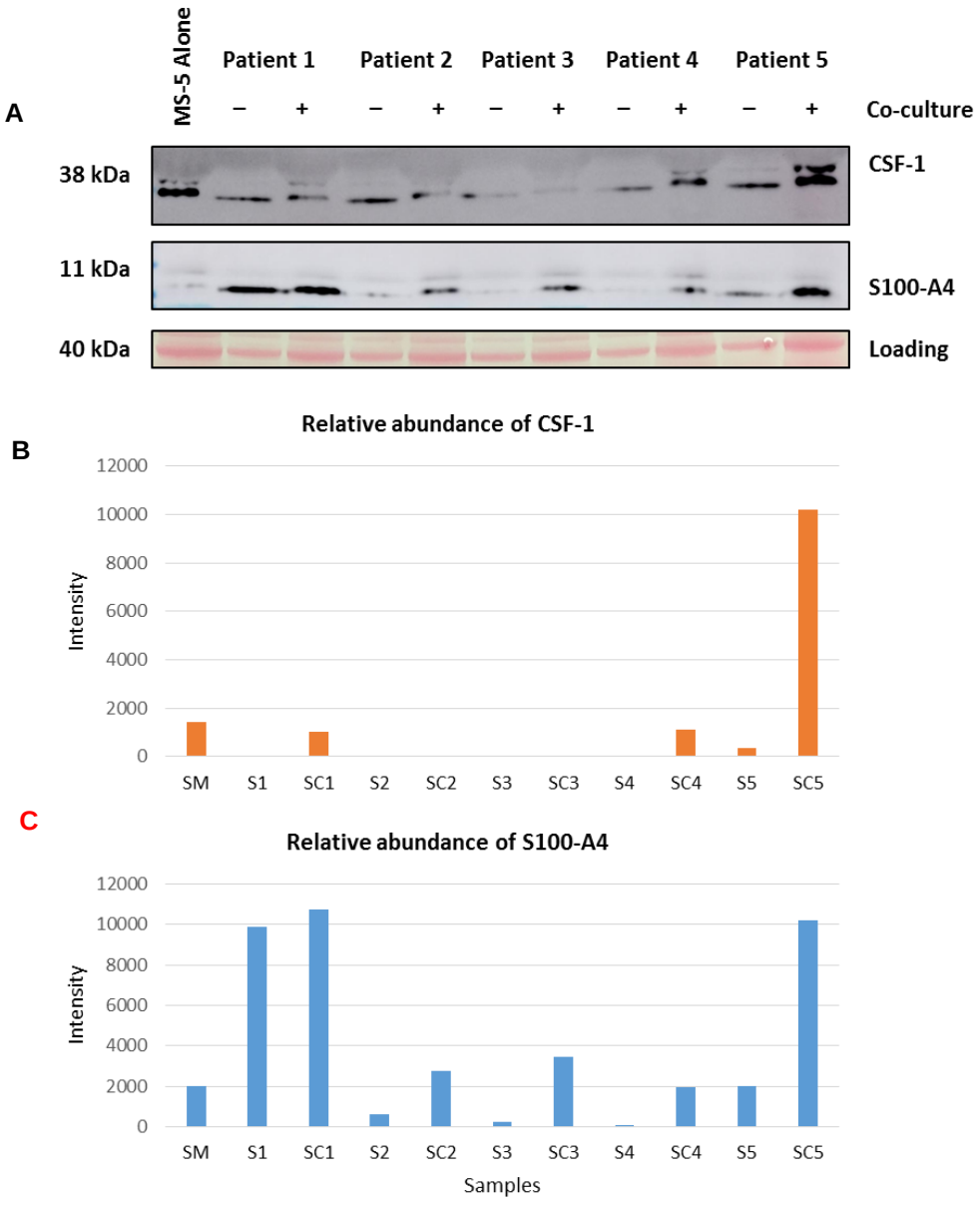

Figure 3.25: Individual and co-culture secretomes produced by 5 AML patients exhibit variable CSF-1 and S100-A4 abundance. The CM from five primary samples cultured in AML/MS-5 co-cultures for 24 hours and independently were fractionated, and 30µg of each >5kDA secretome were analysed by western blot. **(A)** Western blots for total CSF-1 and total S100-A4 proteins, Ponceau stain used as loading control. Densitometry of **(B)** CSF-1 **(C)** S100-A4 western blots, intensities calculated using ImageJ software and normalised to ponceau bands. **SM**; MS-5 secretome only, **SC**; AML/MS-5 co-culture secretome.

Normalisation of CSF-1 band intensities to the loading control revealed that the patient #5 (SC5) co-culture secretome contained substantially more CSF-1 than the other samples measured (Figure 3.25B). The MS-5 only sample (SM) displayed low levels of CSF-1, which were matched by the SC1 and SC4 co-cultures. The AML only secretomes (S1-S4) had no detectable CSF-1, but S5 had trace levels of CSF-1. SC5 co-culture revealed that patient #5 cells drive MS-5 cells expression of CSF-1 as there was 5-fold more CSF-1 in this secretome than what was produced by MS-5 cells alone. Co-culture secretomes SC2 and SC3 did exhibit detectable levels of CSF-1. These experiments mirror observations from the mass spectrometric analysis, such as comparatively low abundancy of CSF-1 and the variability in co-culture abundances between AML samples. One big difference however, was realised in SC5, in which co-culture induced high levels of CSF-1 – in cell lines, co-culture resulted in diminished CSF-1 compared to MS-5 only controls.

Analysis of S100-A4 secretome expression revealed that co-culture induced increased S100-A4 expression for every AML patient sample. S100-A4 was expressed in patients S1 and S5 to levels equivalent or higher than that which were observed in MS-5 cells alone (Figure 3.25C), and there were also trace levels detected in patients S2, S3 and S4. The co-culture secretomes SC1-SC4 had S100-A4 levels that were equivalent to the combination of SM and the appropriate patient sample. But when comparing the S100-A4 pattern of expression in SM, S5 and SC5, S100-A4 secretion was increased. The relative S100-A4 abundance and the dynamics in expression between cultures mirrored observations from the mass spectrometric analysis. However, these experiments suggested that S100-A4 can be secreted by some AML patient samples.

3.13 Summary

It was proposed that stromal secretomes derived from MS-5 and HS-5 cells which positively affect AML survival likely contain pathologically relevant proteins that have yet to be implicated in the progression, resistance and fate of the disease. Accordingly, experiments were designed to identify these factors from the milieu that is the AML tumour microenvironment and use the resolving power of LC-MS/MS platforms to identify these secreted proteins.

Firstly, it was reasoned that to stand the best chance of identifying such proteins we needed the CM by which stromal secretomes were going to be enriched, to be as supportive as possible. To ensure that conditions were optimal a number of elements in the production of stromal CM were assessed, such as cell line, days of conditioning, the effects of snap-freezing on supportive integrity and means to reduce the impact of acidic metabolites and nutrient exhaustion (Figures 3.3-3.8). Following adjustment of these parameters the supportive qualities of CM were enhanced.

Having confirmed the supportive qualities of the optimised HS-5 and MS-5 (clone #1) CM, it was important to assess the effects of the secretome on the activity of commonly upregulated signalling nodes in AML. To assess this, intracellular signalling in AML cells was measured by western blot following stimulation with MS-5 secretome (Figure 3.9). This data showed that the MS-5 stromal secretome did indeed lead to increased abundance of the known PAK phosphorylation sites, known markers of PAK activity. This suggested that the secretome was affecting the nature of cell signalling and therefore, could modulate the behaviour of AML cells.

It had been observed that these stromal secretomes were able to modulate AML cell fate in our hands, and as such it was desirable to know exactly which components of these complex protein mixtures were capable of directing AML behaviour. LC-MS/MS based secretomic analysis was undertaken of both MS-5 and HS-5 cell lines to decipher their constituents. Analysis of the MS-5 secretome identified 293 proteins (Figure 3.11), of which 16 were considered signalling molecules following GO protein class assignment (Figure 3.14). LC-MS/MS analysis of the HS-5 secretome identified substantially more proteins (569) (Figure 3.16A), however, this was probably due to a switch in mass spectrometer, as HS-5 secretomic analysis was conducted with the faster Q-Exactive plus, whereas the MS-5 secretome was analysed using an LTQ-XL. The HS-5 secretome comprised 68 signalling molecules according to uniprot GO assignment (Figure 3.16B), 35 of which were also recognised in Panther GO enrichment analysis (Figure 3.17). These experiments identified a number of stromal cell derived molecules with AML relevance that corroborated with the literature, but also provided a large number of potential signalling candidates.

Following thorough LC-MS/MS characterisation of the stromal secretomes it was not possible to validate the relevance of all the potential candidates in AML as the list was too long. Therefore, to try and elucidate which proteins were relevant a series of cell line based co-culture experiments were devised. It was postulated AML co-culture with MS-5 cells would result in secretomes of variable abundance that would reveal proteins relevant in AML survival. This method revealed that a number of secretomic proteins changed during co-culture experiments, but there were a panel of six proteins that consistently and significantly changed across co-culture experiments (Figure 3.23).

It was postulated that, these co-culture experiments had been conducted with AML cell lines and therefore, validation was required in primary AML cells to confirm that these findings translate in primary material. To assess factor expression in primary AML/MS-5 co-culture, western blot analysis was employed as these cells could not be maintained in a serum free environment – serum proteins would create too much background for LC-MS/MS analysis.

Analysis of S100-A4 and CSF-1 expression confirmed that these proteins do dynamically change in primary AML co-cultures (Figure 3.24). However, following repeats that included patient only secretomes, analysis revealed that some primary AML cells were able to secrete S100-A4 also (Figure 3.25). This was not anticipated, but it only served to highlight the heterogeneity of the disease and potentially the variable importance of different GFs in different patients. As the AML cells from patient #1 were able to produce S100-A4 independently and did so in relatively large quantities, whereas other patient samples required the microenvironment to provide or drive expression of those proteins (both S100-A4 and CSF-1). These preliminary findings hinted at the plasticity of the microenvironment and how it could be adapted to suit the needs of AML, be that in the supply of a GF, through helping to drive GF expression or a combination of both.

In summary, mass spectrometry-based detection of stromal secretomes relevant to the progression of AML and survival of ex vivo primary cells identified 293 MS-5 derived proteins and 569 HS-5 derived proteins. Analysis of these proteins revealed that the approach was able to identify well known supportive elements of AML survival as well as identify many novel stromal derived proteins. Western blot analysis was able to validate the approach as a means of identifying new secretomic factors. The following chapters describe experiments exploring the functional relevance and signalling properties of these set of newly discovered dynamic secretome components.

Chapter 4: Empirical determination of identified protein components from the BMSM and their role in AML survival

4.1 Introduction and aims of the study

The LC-MS/MS based approach reported in Chapter 3 revealed that a panel of six stromal secreted proteins may play a role in the supportive effects that CM confer to AML cell survival. These proteins were consistently observed in a series of co-culture models as well as in independent analysis of MS-5 and HS-5 secretomes. Proteins that were identified in both HS-5 and early MS-5 secretomes (used for western blots and MS analysis) were of interest as these secretomes were both capable of increasing the phosphorylation of relevant AML signalling proteins (Figure 3.9) and extend primary AML cells ex vivo survival (Figure 3.1). As both CM had been observed as supportive at the time of LC-MS/MS analysis, it was rationalised that the supportive proteins would be present in both CM. The identified proteins included S100-A4, S100-A11, CTGF, BMP-1, CSF-1 and HGF.

S100 proteins so called due to the solubility of these 10kDa proteins in 100% saturated ammonium sulphate are a group of proteins that share high sequence and structural similarity, yet each participate in a distinct function (399, 400). The structure and function of S100 proteins is controlled by calcium binding, and as a result S100 proteins are very sensitive to calcium levels and can translate intracellular calcium changes into biological action (401). S100 proteins have both intracellular and extracellular functions and regulate their targets by binding to them (402). S100 expression in the extracellular space and their subsequent role in cell communication through cell-surface receptor binding is well described (400, 403).

LC-MS/MS analysis of both the MS-5 and HS-5 stromal secretomes identified S100 proteins A4 and A11. These proteins have not previously been described as having a role in leukaemia, but they have both been previously implicated in solid tumours (371, 389, 404-410). Instances when S100 proteins become dysregulated, S100 expression is typically upregulated, however, S100 protein expression can vary depending on the cancer type (371). S100-A11 exhibits increased expression in non-small cell lung cancer, but is decreased in small-cell lung cancer (411). S100-A4 dysregulation has been previously heavily linked with cancer progression, in particular in breast, lung, prostate, colorectal, melanoma, renal and pancreatic. In each of these cases S100-A4 dysregulation correlates with poor prognosis and metastatic disease (412). Additionally, it is reported that S100-A4 both drives metastasis, and in the host stroma contributes to metastatic dissemination (413).

In many of these cases S100-A4 and S100-A11 have a described interaction with the receptor for advanced glycosylation end products (RAGE). It has previously been demonstrated that RAGE receptor activation is capable of downstream activation of RAS, ERK, PI3K-AKT, STAT3 and NF-kB pathways, consequently activated cells then exhibit enhanced proliferation, migration and maintain an inflammatory environment (414). S100-A4 proteins have also been described as being able to interact with surface receptors Epidermal Growth Factor Receptor (EGFR), ErbB2 receptor and G-Protein Coupled Receptors (GPCRs), shown below in Figure 4.1 (415, 416).

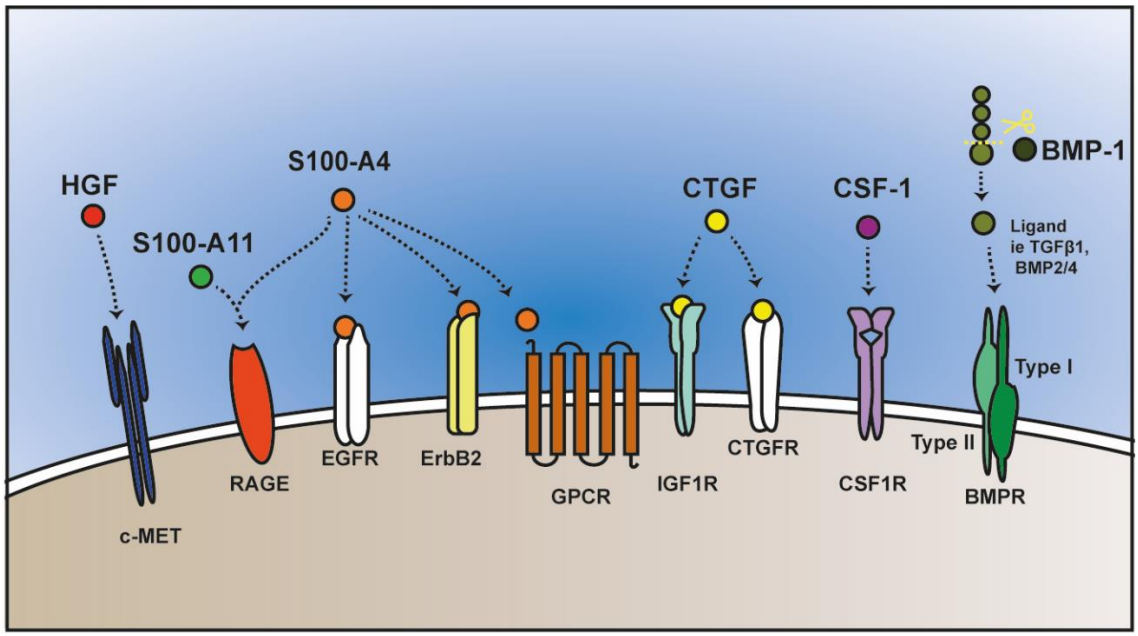

Figure 4.1: Known receptors with specificity to selected secretome derived factors. Depicted secretomic proteins bind with specificity as ligands to known receptors and induce cell signalling. Except BMP-1 which is an astacin metalloprotease, instead of effecting receptor mediated signalling through traditional GF routes, BMP-1 cleaves pro-proteins into signalling proteins (such TGFβ), which then activate signalling cascades.

CTGF the third selected secretome derived GF is a 38kDa mitogen known to be expressed and secreted in the BM (417). This GF promotes proliferation and differentiation of chondrocytes and mediates cell adhesion in many cell types including fibroblasts, endothelial and epithelial cells under physiological conditions (418). In the pathological setting CTGF is thought to also be crucial in facilitating desmoplasia, adhesion, migration, potentiating angiogenesis and metastasis (419). The gene that encodes CTGF, *CCN2* is considered both an oncogene and a tumour suppressor depending on the cancer in question, however, in the majority of cases its expression correlates with adverse outcome (418). Previous articles have noted that *CCN2* expression is observed in tumour cells and cells of the microenvironment, which suggests that CTGF mediated tumour progression may not be driven by tumour cell secretion of CTGF (393).These aspects of CTGF make it an interesting candidate, coupled with it not previously being described in AML. The signalling capabilities of this GF have previously been

reported as being supportive of JNK and ERK signalling (420), this is thought to be mediated by interactions with the cell-surface receptors CTGFR and Insulin-like Growth Factor 1 Receptors (IGF1R) (421).

HGF also known as scatter factor is a very well characterised GF. This mitogenic secreted factor has an extensively described interaction with the c-MET receptor and has been shown to be a potent mechanism in hepatic progenitor cell survival and migration (422, 423). In the pathological setting the HGF/c-MET axis has been also shown to be at the heart of certain drug resistant tumour phenotypes (224, 424). HGF has previously been shown to be a GF that facilitates aggressive invasive cancer phenotypes, helping to establish a permissive microenvironment, with experimental models demonstrating a dependence on the HGF/c-MET pathway in solid tumours (390, 425, 426). The role of HGF in AML has been investigated before, whereby it was described that some AML cell lines were able to produce HGF and activate c-MET in an autocrine manner (392).

CSF-1 is a very potent GF that is crucial in guiding haematopoietic cell fate (427). CSF-1 is produced by monocytes/macrophages, endothelial cells, fibroblasts, and BMSCs (428). CSF-1 only has one known receptor which is the CSF1R, and this receptor's expression is limited to that of mononuclear myeloid cells (monoblasts, promonocyte, monocyte, macrophage) and osteoclasts (429). CSF-1 is the most pleiotropic macrophage GF, capable of stimulating survival, proliferation, motility and differentiation of mononuclear cells (428, 430). However, the ability of CSF-1 to support survival and proliferation depends on the cell's differentiation status, in the case of early progenitor cells CSF-1 stimulation is described as not being sufficient for activation and synergy with co-receptors is necessary (431). However, following differentiation CSF-1 alone is sufficient (432). CSF-1 is important in the regulation of normal mononuclear myeloid cells, however, the precise role that this GF plays in AML is yet to be uncovered. CSF-1 has been discussed in the context of high risk AML, which are believed to be more resistant to therapy through the maintenance of an undifferentiated $CD34^{+}CD38^{-}$ leukaemic initiator population. If CSF-1 is important in these populations it suggests that the cells would need co-activation of another receptor, the ligand of which could be present within the stromal secretome.

BMP-1 is a unique protein in comparison to the other candidates, as it is an astacin metalloprotease and has not previously been described for any GF properties. However, this protein was first discovered due to the induction in bone formation that it was able to elicit (433). BMP-1 is capable of indirect activation of some TGFβ-like proteins which in turn bind to BMP receptors type 1 and type 2 activating BMP signalling cascades (395, 434, 435). BMP signalling can also be induced by a number of different BMPs that are members of the TGF-β superfamily, signal transduction through the BMP pathway activates SMAD substrates (436).

BMP receptor activation can lead to the activation of numerous canonical and non-canonical pathways (TGF-β, MAPK, PKC, PI3K/AKT, Wnt) (437), the specific destination to which the signal is transduced to is believed to be guided by the specific ligand that activates the BMP surface receptor (438, 439). BMP signalling is critical in embryogenesis, and in maintaining adult tissue homeostasis (440). BMPs have been implicated in cell proliferation, differentiation, and apoptosis, however, they have yet to be investigated in AML.

In this chapter, we sought to determine the effects of the individual identified secretome derived proteins and the bulk secretome on AML behaviour, and subsequently how these influence AML cell fate. In Chapter 3 we were able to identify proteins whose secretion or utilisation changed in response to AML cells. Following that work it was important to characterise the effects on AML survival and proliferation.

In the literature the AML/BMSM relationship is mainly described in the context of treatment resistance, in particular resistance to chemotherapy (156, 441, 442). Taking this into consideration we also monitored AML sensitivity to targeted kinase inhibitors in the presence of the stromal secretome, as these proteins were likely to affect AML signalling.

Finally, we examined how long primary AML cells could be maintained in culture with HS-5 CM alone, before examining these cells via CyTOF to study AML clonality and whether HS-5 conditioning selected for specific AML clones.

4.2 Optimisation of recombinant protein stimulation of primary AML cells

The co-culture experiments undertaken in Chapter 3 enabled the selection of six proteins. These six proteins had previously been described as being secreted proteins and had the capacity to behave as a signalling molecule. These conclusions were based on text mining, therefore to establish if these proteins were relevant in AML we needed to functionally assess how these factors alter primary AML cells capacity for survival.

To establish the relevance of each protein, we acquired pure (>99%), human, biologically active recombinant versions of the proteins, which were then used to maintain primary AML cells ex vivo; the cells came from a patient deemed high risk due to unfavourable cytogenetics (11Q23) (Patient #1). These cells were chosen as the sample contained a high blast count prior to enrichment for mononuclear cells using Ficoll (85%), following which blast percentage be close to if not 100%, this ensured that it was the AML population that was being measured. A high-risk patient was selected as it had previously been found by Pearce et al. that AML blasts from adverse-risk patients are faster and more successful at engrafting within the microenvironment (443), perhaps suggesting a greater dependency on crosstalk with the microenvironment.

The patient cells were plated in 18 conditions and grown in culture for 7 days, cell viability was assessed by Guava easyCyte flow cytometry on days 1, 2, 3, 5 and 7. Patient #1 cells began the experiment with a high viability of 96% (Day 0), which is unusual for primary cells following reanimation from LN_2 storage. The cells were seeded in both serum containing (10%) and serum starved (0.5% FBS) conditions in the presence of 10ng/ml concentration of each recombinant protein (RP) (except the >5kDa MS-5 secretome which was added at 10µg/ml, as optimised in Chapter 3). This concentration was chosen as it was the recommended dose for each of the six RPs from their respective manufacturers, additionally GF supplementation of AML cultures with factors such as IL-3, FLT3 ligand and IL-6 are frequently used at 10ng/ml (444).

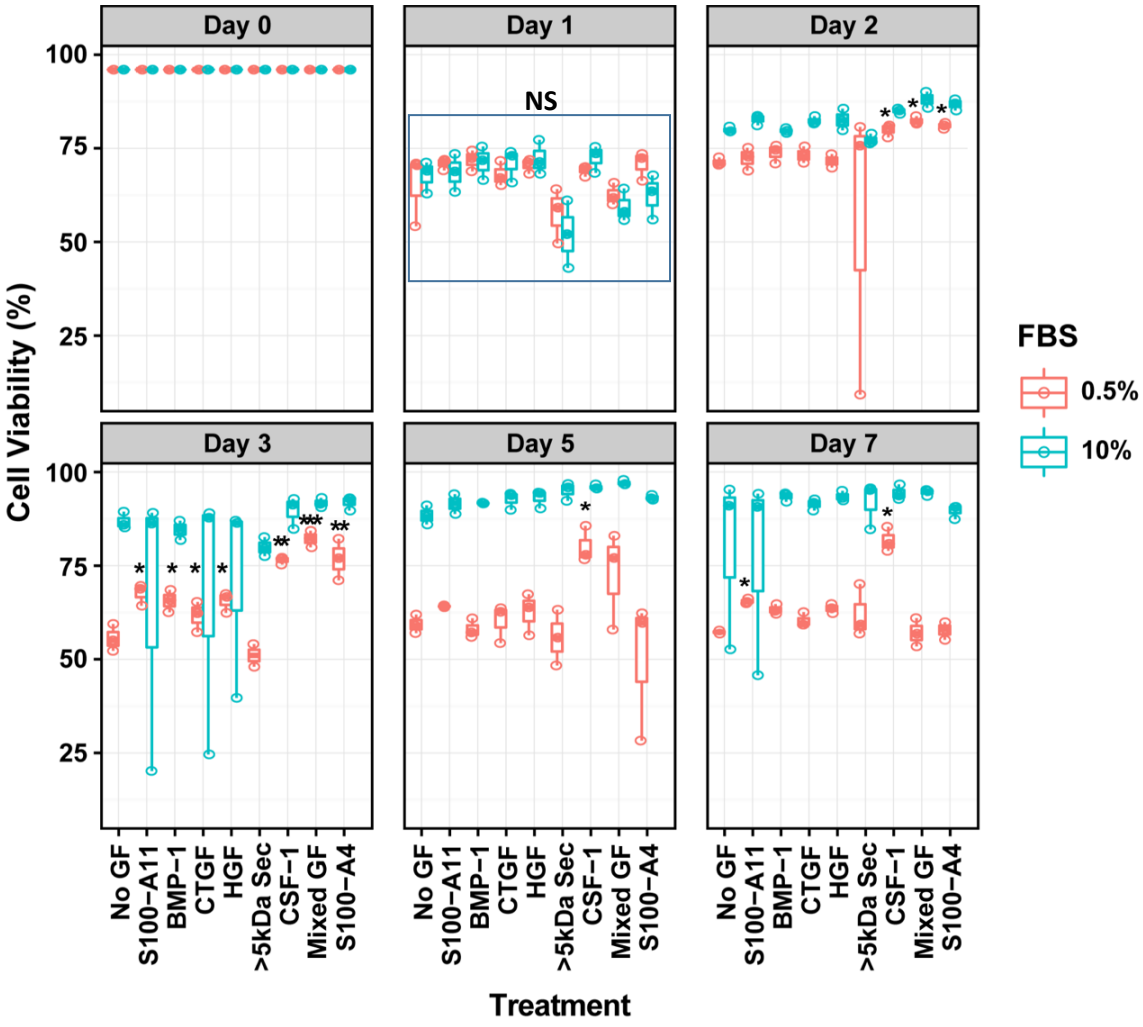

Figure 4.2: Cell viability assay of high risk primary AML patient cells grown for seven days with growth factors in serum starved or serum stimulated setting. On Day 0 $2x10^4$ cells/well seeded with 10ng/ml of indicated GF, 10µg/ml >5kDa MS-5 Sec or 10ng/ml each of the GFs in the Mixed GF sample (+0.5%/ 10% FBS). Viability measured on Days 1, 3, 5 and 7, using the Guava Viacount assay on a Guava flow cytometer. Boxplots produced using 'ggplots' package on R workspace, technical replicates n=3 per condition; P value calculated by unpaired two-sided t-test comparing no GF controls to GF stimulated samples *p<0.05 **p<0.01 ***p<0.001.

Comparing AML cell viability at Day 0 (measured on a Beckman Coulter vi-cell analyser) to Day 1 (measured on the Guava easyCyte flow cytometer) there was a significant drop in viability across all conditions regardless of treatment (Figure 4.2). This difference could be due to the accuracy of the analysers, with perhaps the Beckman Coulter overestimating cell viability at Day 0 (by including any cell like shape than has not taken up trypan blue). Alternatively, this could be demonstrating the selection of a particular AML clone, with all conditions displaying a decrease in cell viability after one day, which was followed by a recovery in FBS containing samples in subsequent time points. Analysis of cell viability at Day 1 revealed that the inclusion of 10% FBS did not have a significant effect on AML survival compared to starved conditions (Figure 4.2, blue box). There was also no significant difference in survival between cells stimulated with the secretome derived proteins compared to those with no GF treatments. However, AML cells in bulk factor conditions (>5kDa secretome and Mixed RP) were not as viable on the Day 1 time point ($p=0.002$ and $p=0.045$).

At Day 2 differences in cell viability began to significantly change between serum containing and serum starved conditions, with the 10% FBS containing samples displaying higher viability (Figure 4.2). Additionally, at Day 2; CSF-1 ($p=0.02$), S100-A4 ($p=0.015$) and the Mixed GF samples ($p=0.001$) began to exhibit increased AML viability compared to untreated samples, particularly in the serum starved setting. At Day 3 the AML cells maintained in 10% FBS were clearly maintaining a higher viability than those in starved conditions. The GF effects were also becoming more pronounced in the starved conditions with CSF-1, S100-A4 and the Mixed GF samples containing AML cells with higher viability. Comparisons between serum starved and serum containing experiments at Day 3 showed that the removal of serum allowed for better visualisation of the individual GF effects, and in the serum starved conditions, all of the GFs increased viability compared to no GF supplementation.

By Day 5 it was clear that including 10% FBS in samples had dramatic effects on AML cell survival, comparisons between the 10% and 0.5% FBS no GF treated samples (average across n=4, 88.4% [10%] and 59.3% [0.5%]) revealed there was a 29.1% difference in viability ($p=0.0075$). Analysis of GF treatments in 0.5% FBS samples showed that both CSF-1 ($p=0.037$) and Mixed GF ($p=0.267$) were very good at maintaining primary AML cells, with the viability significantly higher than no GF samples and almost reaching that conferred by 10% FBS. Finally, by Day 7 10% FBS containing samples were much healthier than serum starved samples. Serum starved, yet CSF-1 treated cells were almost as viable as AML cells grown with 10% FBS, which could suggest that CSF-1 has a role in anti-apoptotic signalling, as these cells did not exhibit markers of cell death like the other serum starved samples.

It is worth noting that in these experiments the MS-5 secretome was not particularly supportive, which is at odds with previous experiments as well as the literature. As the secretome was snap frozen following collection and concentration, it is possible crucial elements may have dropped below the supportive threshold. Finally, in some conditions there were outlier results, in these replicates big drops in viability were recorded (of note; Day 2 MS-5 secretome and Day 3 S100-A11, CTGF, HGF). These instances demonstrate the fragility of these cells and the capacity for primary AML cells to quickly perish in culture.

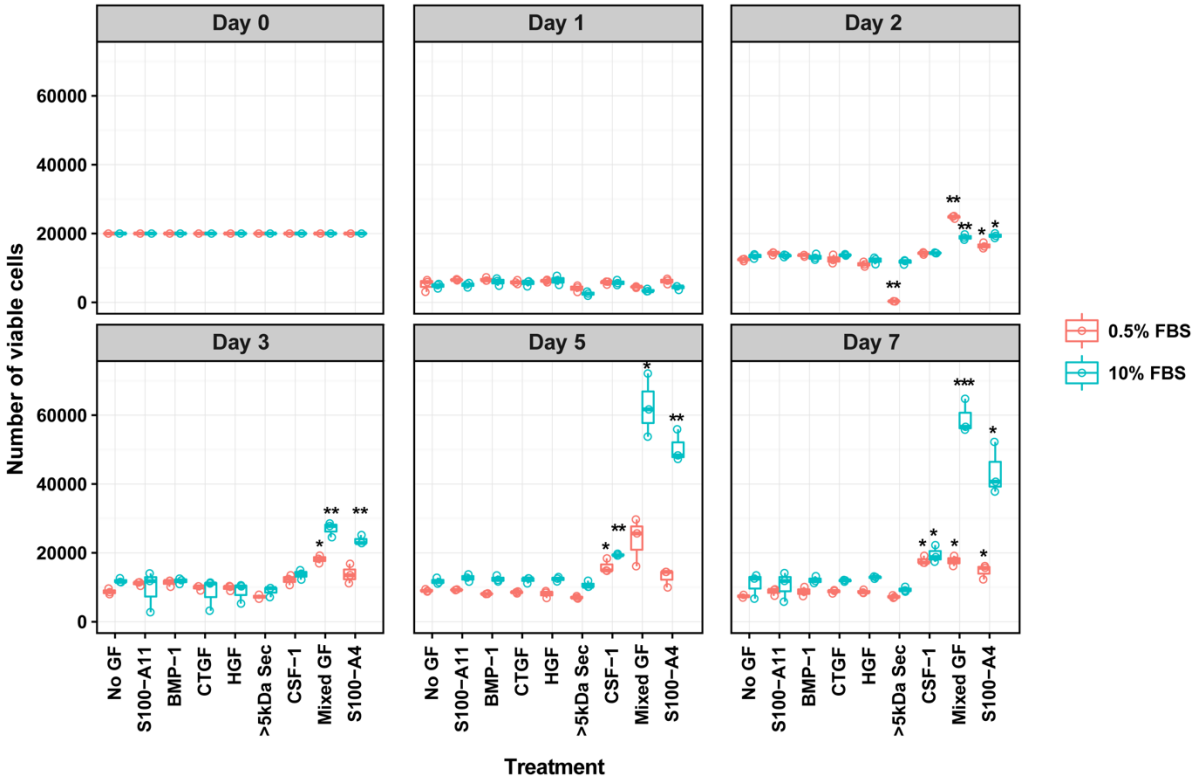

Figure 4.3: Cell growth assay of high risk primary AML patient cells grown for seven days with growth factors in serum starved or serum stimulated setting. On Day 0 $2x10^4$ cells/well seeded with 10ng/ml of indicated GF, 10µg/ml >5kDa MS-5 Sec or 10ng/ml each of the GFs in the Mixed GF sample (+0.5%/ 10% FBS). Viable cell numbers measured on Days 1, 3, 5 and 7, using the Guava Viacount assay on a Guava flow cytometer. Boxplots produced using 'ggplots' package on R workspace, technical replicates n=3 per condition; P value calculated by unpaired two-sided t-test comparing no GF controls to GF stimulated samples *p<0.05 **p<0.01 ***p<0.001.

Cell proliferation during the same time course was assessed by measuring the growth of viable cells across the seven days. Assessment of cell growth during the same time course revealed strong differences to the viability assays. Initially all samples behaved similarly with a substantial drop in viable cell number, which could suggest that the conditions were not supportive for all AML cells (Figure 4.3). However, by Day 2 viable cell numbers begin to recover across all conditions, as cells started proliferating, except for the MS-5 secretome treated cells in a serum starved environment.

At time point Day 3 the results indicated a significant increase in proliferation of viable cells when Mixed GFs (p=0.0049) and S100-A4 (p=0.001) were introduced to cultures. This increase continued and by Day 5 it was clear that the GFs in the Mixed GF sample, and in particular S100-A4 based on the individual GF condition were conferring a strong proliferative signal (Figure 4.3, panel Day 5). CSF-1 cell numbers were also elevated, but this was likely due to a lack of cell death than an increase in proliferation based on the viability assays (Figure 4.2, Day 5 panel). Finally, on Day 7 the most supportive condition as hypothesised was the Mixed GF condition with 10% FBS. There was no significant difference in cell growth when assessing S100-A11, BMP-1, CTGF, HGF and MS-5 secretome compared to no GF supplementation. CSF-1 (p=0.035), S100-A4 (p=0.014) and the Mixed GF (p=0.001) samples in serum starved conditions were all able to maintain viable AML cell numbers, close to that seeded on Day 0. CSF-1 achieved this irrespective of serum starvation. S100-A4 in the presence of serum however, was capable of inducing significant cell proliferation (p=0.014), cell numbers at Day 1 dwindled as low as $4.3x10^3$ cells, but by Day 5 expansion reached $5.6x10^4$ cells. The difference between Mixed GF and S100-A4 in serum containing conditions could have been due to a combination of the proliferative capacity conferred by S100-A4 with complementary serum activation, with the addition of the anti-apoptotic properties that CSF-1 possesses. Analysis of both Day 5 and Day 7 cell numbers revealed that FBS supplementation combined with 10ng/ml of S100-A4 stimulated patient#1 cells to grow 2.49 fold more than S100-A4 stimulation in serum starved conditions (p=0.012). Consequently, serum supplementation was included in subsequent assays as it enhanced the proliferative effects of S100-A4. We could be confident it was S100-A4 that conferred the proliferative phenotype as the no GF control with serum elicited substantially less cell growth (p=0.014).

4.3 Survival assays using purified recombinant forms of identified signalling molecules secreted by stromal cells

Optimisation experiments demonstrated that these proteins effect cell viability, with CSF-1 and S100-A4 in particular able to support AML cell growth. This growth was significantly enhanced when the GFs were combined in the Mixed GF condition. Due to the heterogeneity of AML we thought it important to expand the cohort as it was probable that different AML patients would respond to different factors.

To test this hypothesis four additional AML patient samples were acquired (clinical features described in Chapter 2.2) and seven day survival assays were conducted following the approach used in optimisation experiments. Patient samples comprised a mixed cohort of risk status, patients #1, #4 were high risk patients, patient #2 was intermediate risk and patients #3, #5 were favourable risk. This experiment did not contain the power to make conclusions on risk

group response to the potentially supportive factors, however, we believed by having a heterogeneous cohort we would increase the probability of identifying cells that would respond to all of the GFs. Common to all AML patient samples was FAB classification, M4 or M5, which means that morphologically these cells were considered monocytic leukaemias, expressing markers of differentiation. These markers of differentiation are regularly surface receptors, thus increasing the likelihood of these GFs being relevant to these cells survival in ex vivo conditions.

Analysis of primary AML cell viability following seven days of ex vivo culture with different GFs in a serum containing setting revealed that all patient samples were more viable when treated with GFs. However, in line with the nature of AML biology, the extent of each GFs support was heterogeneous across the patients. The first observation that could be garnered from the results was that after seven days of GF treatment, AML viability was higher than after one day. Whereas samples with no GF treatment either displayed comparable or lower viability than AML cells at Day 1 (Figure 4.4).

In the optimisation experiments it was speculated that the global decrease in cell number following the Day 1 time point was due to AML clones within the total population undergoing cell death, while the remaining clones persisted through utilisation of the available GFs, which lead to the subsequent proliferation of AML cells by Day 7. This pattern was reproduced in these assays too. At Day 1 each patient's cell viability was comparable across conditions and by Day 7, every condition with supportive GFs had increased in viability compared to the equivalent at Day 1 or compared to the no control at Day 7 (Figure 4.4). There were only two exceptions, patient #1 with no GF treatment which managed to maintain a very high viability regardless of GF treatment, although this increase in viability was not significant ($p=0.49$). The other exception was observed in Mixed GF treatment of patient #3 cells. Although these cells had ~ 25% higher viability than the no GF condition by Day 7, they presented with a lower viability than what was measured at Day 1 (Figure 4.4, Panel Patient 3).

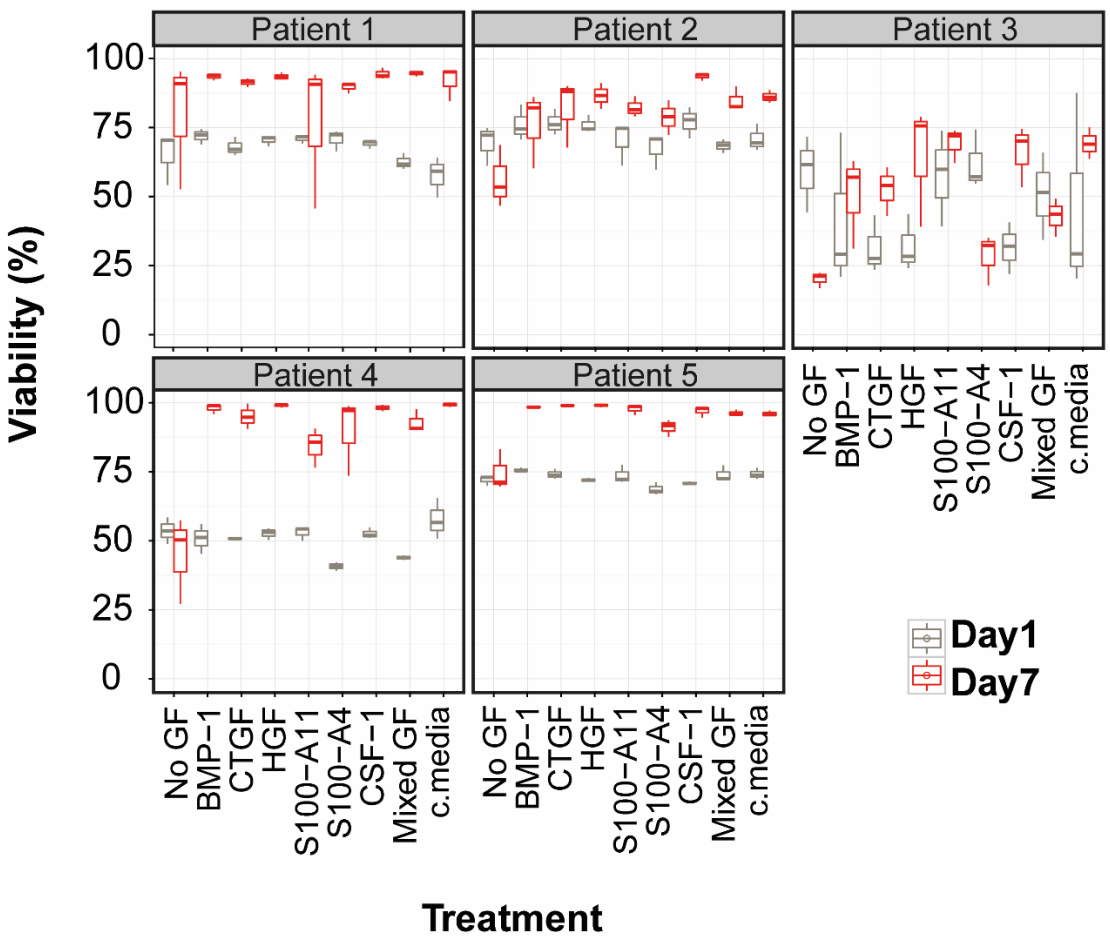

Figure 4.4: The effects of stromal derived growth factor panel on ex vivo survival of five primary AML patient samples. On Day 0, 2x10^4 cells/well seeded with 10ng/ml of indicated GF, 10ng/ml each of the GFs in the Mixed GF sample or MS-5 CM (+10% FBS). Viability measured on Days 1 and 7, using the Guava Viacount assay on a Guava flow cytometer. Patient samples n=5, technical replicates n=4 per condition; P value calculated by unpaired two-sided t-test comparing Day 7 no GF controls to GF stimulated samples *p<0.05 **p<0.01 ***p<0.001. Boxplots produced using 'ggplots' package on R workspace.

Comparisons between the GFs individual ability to maintain patient viability revealed that CSF-1 always maintained the highest viability in all patients, while the S100 proteins were consistently the least supportive individual GFs in the panel. This was particularly evident in patient #3, where S100-A4 supplementation by Day 7 only maintained viability at 28.4% (p=0.09), whereas HGF (64.5%)(p=0.05), CSF-1 (66%)(p=0.011) and MS-5 CM (69.2%)(p=0.004) were able to sustain patient#3 primary AML cell viability at much higher levels. The other GF that maintained patient #3 cell viability was S100-A11 (69.3%) (p=0.005), as S100-A11 only has one known receptor, the RAGE receptor that it shares with S100-A4, it is notable that they elicited such opposing effects. One explanation for this could be the fact that S100-A4 has a number of other known receptors (EGFR, erbB2, GPCR) and its interactions with these receptors, or another receptor that either S100 protein has affinity to that is yet to be described, that yields the functional discrepancy between the GFs. Finally, in each of the patients the effect of Mixed GF treatment on cell viability was the average of each of the viability in the individual GF samples.

4.4 Proliferation assays using purified recombinant forms of identified signalling molecules secreted by stromal cells

Cell survival is one metric for assessing the impact of these GFs on AML progression, but another aspect that characterises AML as a disease is the expansion and proliferation of these cells throughout a patient's BM. The five patient samples used in the survival assays were also measured for cell growth in the presence of the panel of GFs.

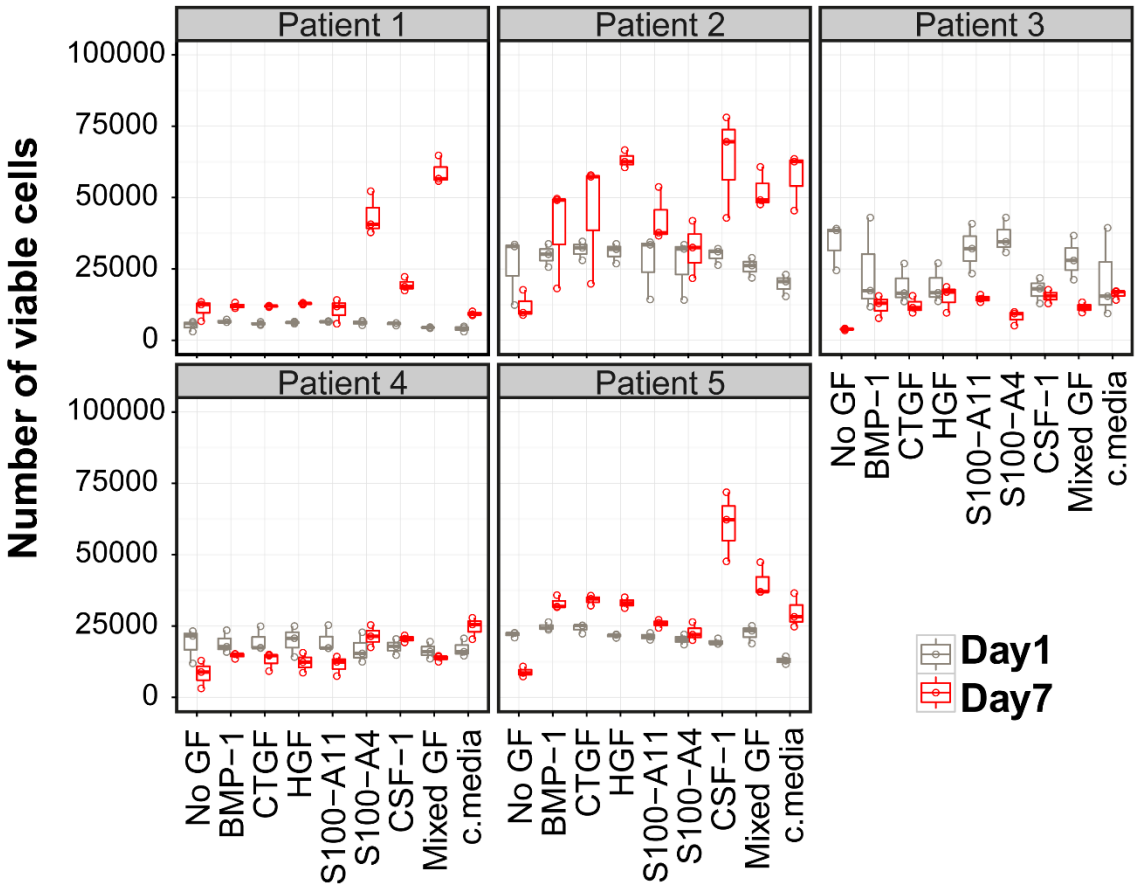

Figure 4.5: Cell growth assays reveal that factors induce increase cell growth across patients compared to no growth factor. On Day 0, 2x10^4 cells/well seeded with 10ng/ml of indicated GF, 10ng/ml each of the GFs in the Mixed GF sample or MS-5 CM (+10% FBS). Viable cell numbers measured on Days 0, 1 and 7, using the Guava viacount assay on a Guava flow cytometer (Day 1 and 7 counts normalised to respective Day 0 wells). Patient samples n=5, technical replicates n=4 per condition; P value calculated by unpaired two-sided t-test comparing Day 7 no GF controls to GF stimulated samples *p<0.05 **p<0.01 ***p<0.001. Boxplots produced using 'ggplots' package on R workspace.

As discussed in the optimisation experiments seven days of incubation with the GFs led patient #1 cells to expand substantially, with S100-A4 in particular eliciting a spike in cell growth. This effect was only enhanced following the addition of the rest of the panel of GFs, as the Mixed GF treatment led to substantial growth in patient #1 cells (p=0.002) (Figure 4.5). Cell growth in patient #4 which based on risk group is the closest matched sample to patient #1 cells, was very different. These cells did not exhibit the same profound expansion in the presence of any of the GFs, however, there was increased growth in GF treated samples and the most confluent

samples were those grown with CSF-1, S100-A4 or samples that would have contained both in the CM.

Patient #2 cells, showed some of the most profound and consistent cell growth in response to the panel of GFs (Figure 4.5, Panel Patient 2). Day 1 measurements of cell growth did not report the same drop in cell number that was observed in the optimisation experiments. Patient #2 derived cells instead proliferated by Day 1, although modestly from the $2x10^4$ cells seeded on Day 0 and this proliferation continued through to Day 7. At the end of the experiment patient #2 were most responsive to HGF ($p=0.001$), as the variation between replicates was minimal, although every GF induced proliferation that was not observed in the no GF conditions. The S100 proteins were not the most potent GFs to induce growth in patient #2 cells, as CSF-1 induced the most proliferation ($p=0.05$).

Patient #3 derived cells did not proliferate in response to GF treatment, with the differences between the conditions representative of the GFs ability to maintain cell viability in the samples. All conditions by Day 7 had less viable cells remaining than what were seeded at the beginning of the assay, although patient #3 cells with no GF treatment were nearly all dead by Day 7. GF treatment of patient #5 cells lead to dramatic growth compared to the no GF controls across the time course (Figure 4.5, Panel Patient 5). Initially there was little difference between control and GF treated conditions at Day 1 assessment, with only small increases in cell number observed. However, by Day 7 no GF controls plummeted in viable cell numbers, whereas GF treated samples were all measured at higher densities than what was seeded, suggesting that this was proliferation and not just maintenance of the cells originally seeded. Discrimination between the GFs revealed that the S100 proteins induced the least proliferative phenotype in patient #5 cells. It is worth noting that S100 proteins were most influential in samples derived from high risk patients. Samples from other risk groups were not as responsive to the S100 proteins, but these are just observations, conclusions cannot be drawn from such a low sample size. In patient #5 the factor that induced the most growth was CSF-1 ($p=0.016$) and the samples containing bulk GFs (which also include CSF-1), were the next most proliferative observations.

4.5 Gene expression analysis of secretome derived proteins within TCGA AML dataset

Ex vivo functional experiments using the panel of stromal derived GFs showed that primary AML cells viability and growth were positively affected by these GFs, although the extent of which was heterogeneous across patients. These experiments were focussed on identifying proteins of the stromal secretome that positively affect AML progression, however, as experiments in Chapter 3 showed (Figure 3.25), there are instances where these proteins (S100-A4) can be overexpressed and secreted by the AML cells too. To observe the expression of these factors across populations we examined gene expression data from AML and healthy populations. The data was sourced from the TCGA (The Cancer Genome Atlas), details of cohort in Table 4.1 (18).

Dataset	Organism	Source	No of samples	Characteristics
TCGA AML vs normal	Human AML	TCGA	183	Various genetic aberrations, including t(8;21), inv(16), t(15;17), t(11q23), complex karyotype, WBM

Table 4.1: Features of the dataset used to compare gene expression of growth factors in AML. WBM = Whole Bone Marrow

This cohort that contained 183 samples AML samples that were compared to the normal population and separated into groups based on whether they were above and below median expression of the genes that are translated into the potentially AML supportive proteins undergoing validation. Correlation of CSF-1 gene expression with patient survival showed that patients with higher expression of CSF-1 had a statistically significant (p=0.0175) worse prognosis than patients with lower expression of CSF-1 (Figure 4.6A). Following 2000 days (~5.5 years) CSF-1 expression had no bearing on outcome, therefore patients with higher CSF-1 expression harbour an AML that is able to progress faster.

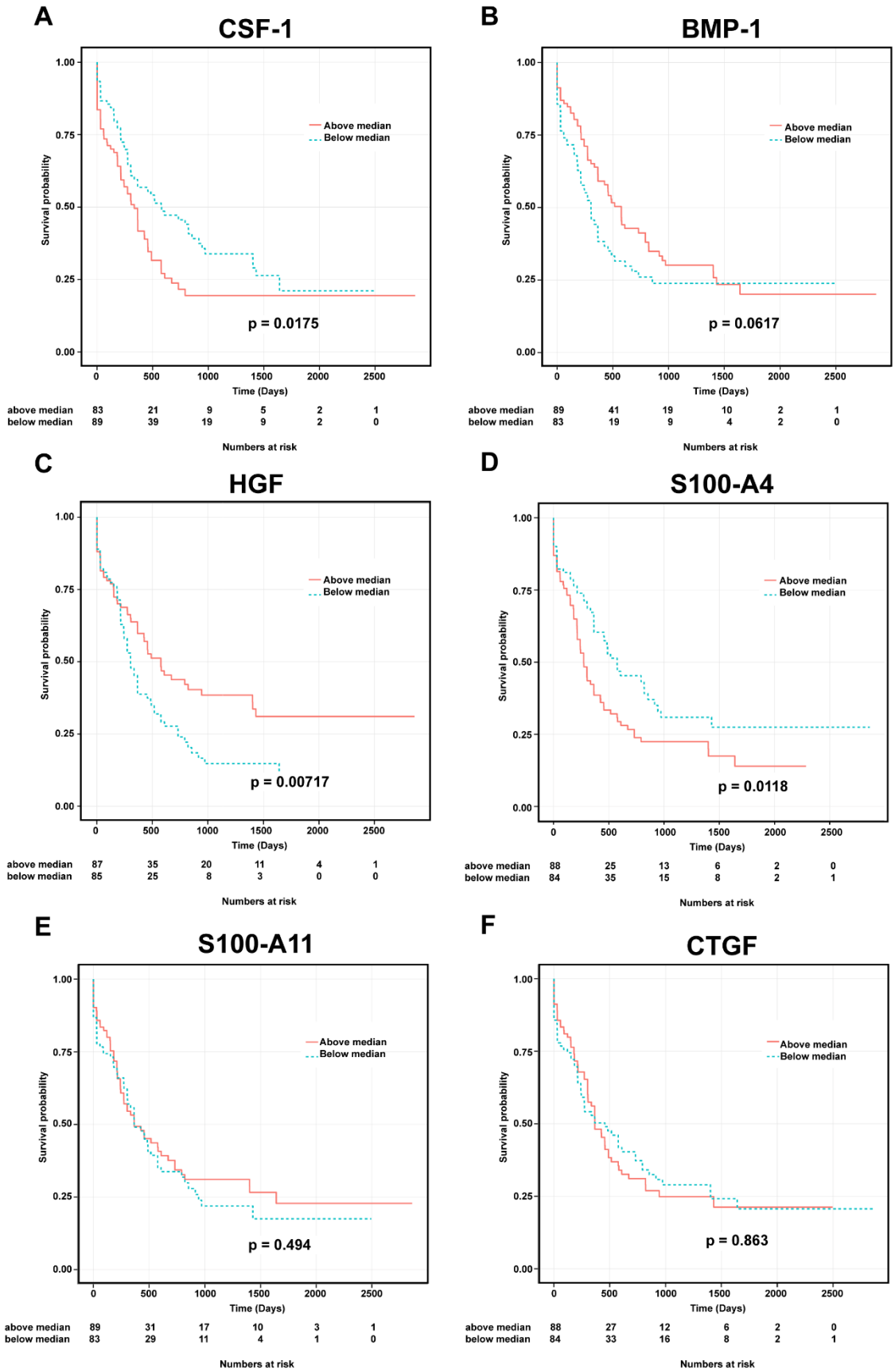

Figure 4.6: Kaplan Meier curves displaying the difference in AML patient survival with higher or lower expression of growth factor genes. The gene expression of a 172 AML sample cohort were compared to the normal population and separated into groups based on whether they were above and below median expression of **(A)** CSF-1 **(B)** BMP-1 **(C)** HGF **(D)** S100-A4 **(E)** S100-A11 **(F)** CTGF, patient numbers were assessed at six time points across 2000 days.

BMP-1 gene expression was not as indicative of patient outcome as CSF-1. Analysis of BMP-1 expression and survival rates suggested that increased BMP-1 expression could lead to a more favourable outcome, as patients with lower than the median BMP-1 expression actually exhibit poorer survival (p = 0.0617) (Figure 4.6B).

HGF gene expression data followed a similar pattern to that observed for BMP-1, although HGF expression leads to a statistically significant difference in survival (p=0.00717). In this analysis HGF expression positively correlated with greater survival (Figure 4.6C). This finding is paradoxical based on the known functional roles of HGF, including proliferation and invasion, traits that are commonly displayed by aggressive cancers.

S100-A4 gene expression data followed a trend in keeping with experiments conducted in Chapter 3 that identified it as a candidate for investigation, as well as the strong induction of proliferation in patient #1. Higher S100-A4 gene expression correlated with poor survival when assessing 172 AML samples of mixed subtypes (Figure 4.6D), the difference in survival between higher and lower expression of S100-A4 was statistically significant (p=0.0118).

The last two stromal proteins of interest S100-A11 (Figure 4.6E) and CTFG (Figure 4.6F) did not exhibit gene expression that correlated with survival, both S100-A11 and CTGF had non-significant separations in survival when comparing high and low gene expression. When analysing these findings, it is important to consider how heterogeneous AML is and how the cohort that was assessed in the gene expression analysis consisted of very different AML. It is possible that if favourable risk AML patients were analysed separately to high risk AML patients, then correlations between expression of these genes and survival could have been very different. Unfortunately, these types of analysis are not possible to request of the TCGA repository. This analysis collectively reinforces the hypothesis that it is the stromal cells that are responsible for the panel of six identified proteins, with S100-A4 the only protein that this analysis correlates with AML gene expression.

4.6 Kinase inhibition of common AML signalling nodes are altered following culture with stromal conditioned media

Following the confirmation that the panel of stromal derived GFs were relevant to AML cell function and considering that these proteins were chosen based on potential capacity to behave as signalling proteins, we considered whether these proteins would alter AML response to targeted inhibition of the main AML effector signalling pathways. To investigate if stromal proteins effect AML sensitivity to kinase inhibition, a panel of kinase inhibitors were selected

that specifically targeted traditional AML mediators. Inhibition of mTOR, MAPK, JAK, PAK and FLT3/cKIT was achieved using selected compounds that are listed in Table 4.2.

Inhibitor	Intended Target	Other targets	Structure	**Reason for inclusion**
Torin-1	mTORC1 mTORC2	No known	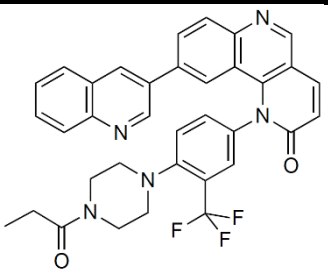	Specific inhibitor of mTOR. Abnormalities of mTOR signaling are strongly associated with leukaemic cell proliferation, as a result it is a regular candidate for combination strategies. (445-447)
Trametinib	MEK1 MEK2	No known	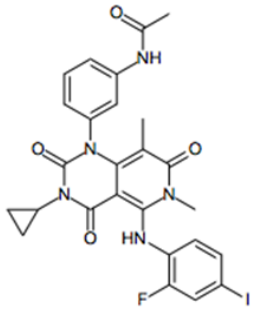	Extremely specific inhibitor of MEK1 and MEK2, components of the MAPK pathway. MAPK is a downstream effector of the FLT3 and RAS proteins. (80, 448)
Tofacitinib	JAK3 JAK2 JAK1	No known	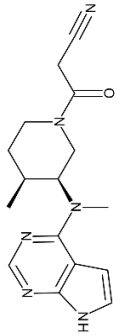	Highly selective inhibitor of JAK isoforms. Aberrant JAK-STAT signalling has been associated with the proliferative leukaemic phenotype, at least partly due to over activation of the cytokine receptors that activate JAK. (449)
PF-3758039	PAK6 PAK5 PAK4	PAK1 PAK3 PAK2	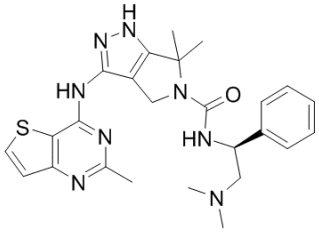	A potent inhibitor of PAK1 previously been described as one of the most active kinases in AML, and the functions it mediates are commonly associated with microenvironment interactions (adhesion, migration, survival). (206, 271)
Midostaurin	FLT3	PKCα/β/γ, Syk Flk-1 Akt PKA c-Kit c-Fgr c-Src PDFRβ VEGFR1/2	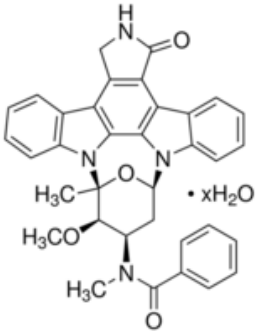	Currently the only FDA approved kinase inhibitor for treatment of *FLT3* mutant AML patients. (70)

Table 4.2: Panel of targeted kinase inhibitors used in kinase inhibition studies.

MAPK inhibition with Trametinib

Trametinib was selected as an agent as it is highly specific in targeting MEK1 and MEK2. We wished to target the MAPK pathway in these AML cells as it is one of the most frequently documented as being a downstream effector of aberrant upstream signalling (198). Targeting MEK1 and MEK2 with selective inhibitor Trametinib led to a substantial drop in AML cell viability when introduced to cells growing in IMDM (+10%FBS) media only (no HS-5 CM), with some patient samples almost completely succumbing to MEK inhibition. However, when the same AML patient cells were treated with Trametinib, but in the presence of HS-5 CM, they were not as compromised as cells in non-CM. In HS-5 CM some patient cells (2/11) exhibited no drop in viability when treated with the inhibitor (Figure 4.7A).

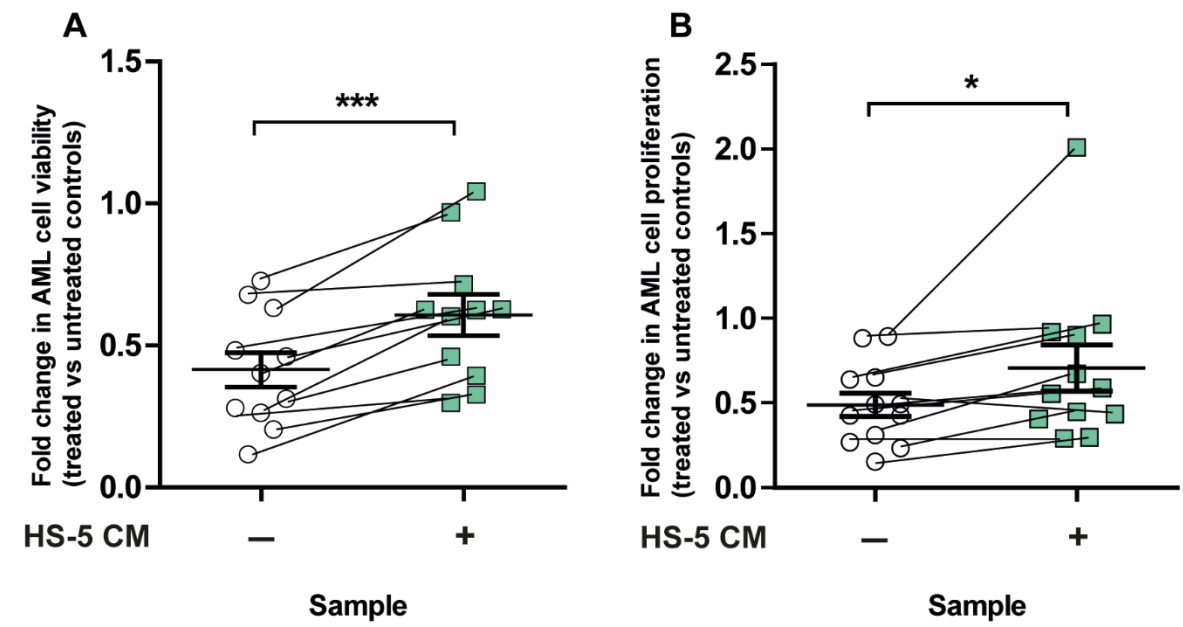

Figure 4.7: Primary AML targeted MEK inhibition with/without HS5 conditioned media. Guava easycyte flow cytometry implemented to measure cell viability and proliferation of 12 primary AML samples. Measured fold change in **(A)** viability and **(B)** proliferation following 72 hours treatment with 1µM Trametinib compared to vehicle controls (+/-) HS-5 CM (+10% FBS)**.** Patients n=11 for viability and n=12 for proliferation, each data point represents the average of four technical replicates, significance determined by paired T-Test matching patient samples *p<0.05, ***p<0.001.

Analysis of AML cell proliferation following Trametinib treatments revealed cells were profoundly affected by MEK inhibition, with proliferation on average reducing by half across patients when Trametinib was introduced without HS-5 CM (Figure 4.7B). The introduction of Trametinib in the presence of HS-5 CM, however, did not lead to the same reduction in proliferation, as proliferation was only reduced by 25% following Trametinib treatment compared to the untreated controls following 72 hours of culture. It is notable that the response to MEK inhibition was variable across the patients, in some cases MEK inhibition did not affect AML proliferation in the absence of HS-5 CM, while in the presence of HS-5 CM there were some patient's samples where proliferation reduced by 75%.

Inhibition of mTOR with Torin-1 compound

Canonically described being the downstream component of the PI3K/AKT/mTOR pathway, mTOR forms part of a signalling axis frequently mutated in cancer. Although the pathway does not accumulate the level of genetic aberrations in AML that are witnessed in other cancers, it is directly downstream of frequently mutated receptors such as FLT3 and c-KIT. The pathway mediates proliferation, differentiation and survival in haematopoietic cells, the activation of which is controlled by the extracellular binding of ligands to the insulin receptor (IR), FLT3R, c-KITR, EGFR, insulin-like growth factor receptor (IGF-1R) and CSF1R (446, 450-452). Importantly a number of these receptors recognise the identified secretome candidate proteins. Previous studies have investigated intrinsic routes of pathway activation and dysregulation, namely through mutation as well as potential autocrine activation of the pathway through IGF-1 secretion (453). The role of the microenvironment pathologically modulating this axis in the AML setting has not yet been investigated, however.

To establish if the microenvironment is able to modulate AML cell signalling through the identified GFs, and possibly factors that we have failed to identify, the primary AML patient cells used to investigate MEK inhibition were maintained ex vivo, in both conditioned and non-conditioned media. Simultaneously cells were treated with the mTOR inhibitor Torin-1, which is a potent, highly selective ATP-competitive inhibitor of both mTORC1 and mTORC2 (454). This approach should have revealed if the HS-5 stromal secretome effects AML signalling networks to the extent of fundamentally modulating cell sensitivity to the inhibition of mTOR or the downstream effects of PI3K and AKT activity (assuming that there is significant canonical activity of the pathway).

72 hours of 1μM Torin-1 treatment [concentration as used in Pan et al. (455)] on primary AML cells maintained in the absence of HS-5 CM decreased AML viability compared to that of the matched DMSO control cells. This was not surprising, due to the reported role of the mTOR pathway in haematopoietic precursor cells (445, 456, 457), the average viability in these cells dropped to 0.72 of that recorded for the DMSO control cells, both cultured in the absence of HS-5 CM (Figure 4.8A). Torin-1 treatment of primary AML cells cultured in the presence of HS-5 CM revealed that primary AML cells were more sensitive to mTOR inhibition in these conditions compared to when in non-conditioned media, with viability decreasing on average by a further 20%.

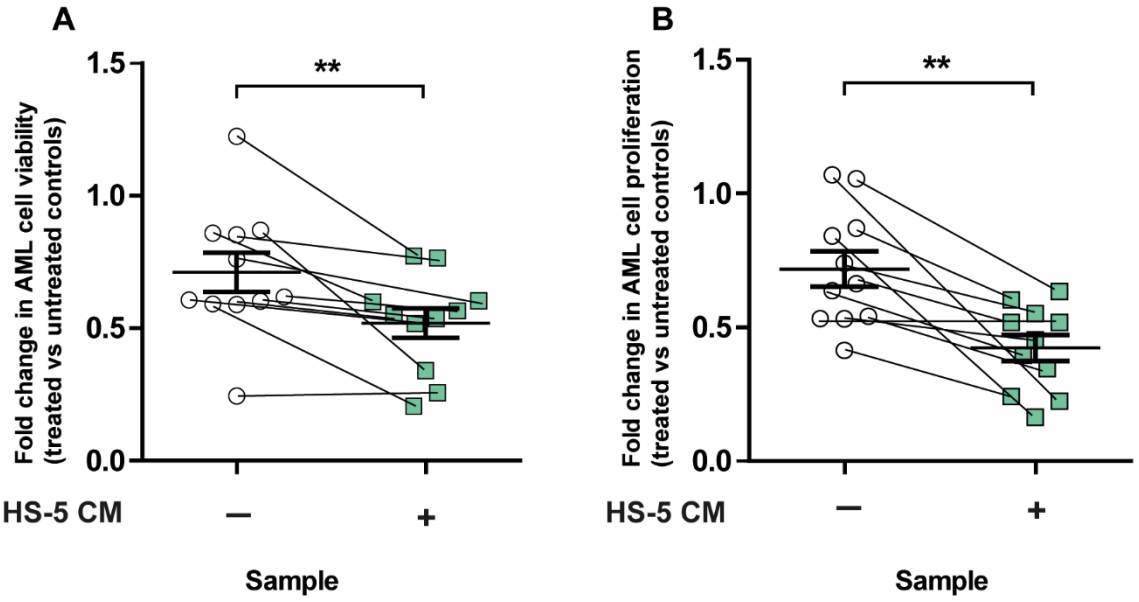

Figure 4.8: Primary AML targeted mTOR inhibition with/without HS5 conditioned media. Guava easycyte flow cytometry implemented to measure cell viability and proliferation of 11 primary AML samples. Measured fold change in **(A)** viability and **(B)** proliferation following 72 hours treatment with 1µM Torin-1 compared to DMSO vehicle controls (+/-) HS-5 CM (+10%FBS)**.** Patients n=11, each data point represents the average of four technical replicates, significance determined by paired T-Test matching patient samples *p<0.05, **p<0.01, ***p<0.001.

In the same patients, assessment of cell proliferation following Torin-1 treatment in the absence of HS-5 CM observed patient cells respond in a heterogeneous manner (Figure 4.8B). Approximately four of the eleven patient samples exhibited no change in proliferation compared to the matched DMSO control cells, while others decreased by half compared to the untreated controls. On average mTOR inhibition with Torin-1 in the absence of HS-5 CM reduced proliferation to 0.66 of that recorded in the same AML patient cells that were not treated with Torin-1. When proliferation was measured in the same patient cells treated with Torin-1, but this time in the presence HS-5 CM, proliferation very potently and consistently decreased. Combining Torin-1 treatment with HS-5 CM led proliferation to drop to 0.39 of that recorded in the same AML patient cells which were not treated with Torin-1.

Collectively these results suggest that either mTOR or pathways associated with mTOR are being activated by components of the HS-5 CM. Thus, increasing the AML cells sensitivity to Torin-1 treatment, as these cells now had increased activation of substrates whose activity is regulated by mTOR. Additionally, Torin-1 had profound effects on functions such as proliferation – a function that mTOR regulates. This kinase is documented as being a nutrient and GF sensing kinase, which would rationalise the mTOR response to changes in media composition.

Multi-kinase inhibition with Midostaurin

In Chapter 1 the significance of the FLT3 tyrosine kinase was discussed, in particular the *FLT3* gene which is the most frequently mutated gene in AML and as a result has been the focus

of targeted kinase inhibitor therapies in AML. To this end, Midostaurin is currently the only FDA approved kinase inhibitor for the treatment of AML. Although Midostaurin is licensed as a FLT3 inhibitor, it is a very promiscuous compound as demonstrated in Table 4.2. For clinical relevance this compound was included in the panel of inhibitors.

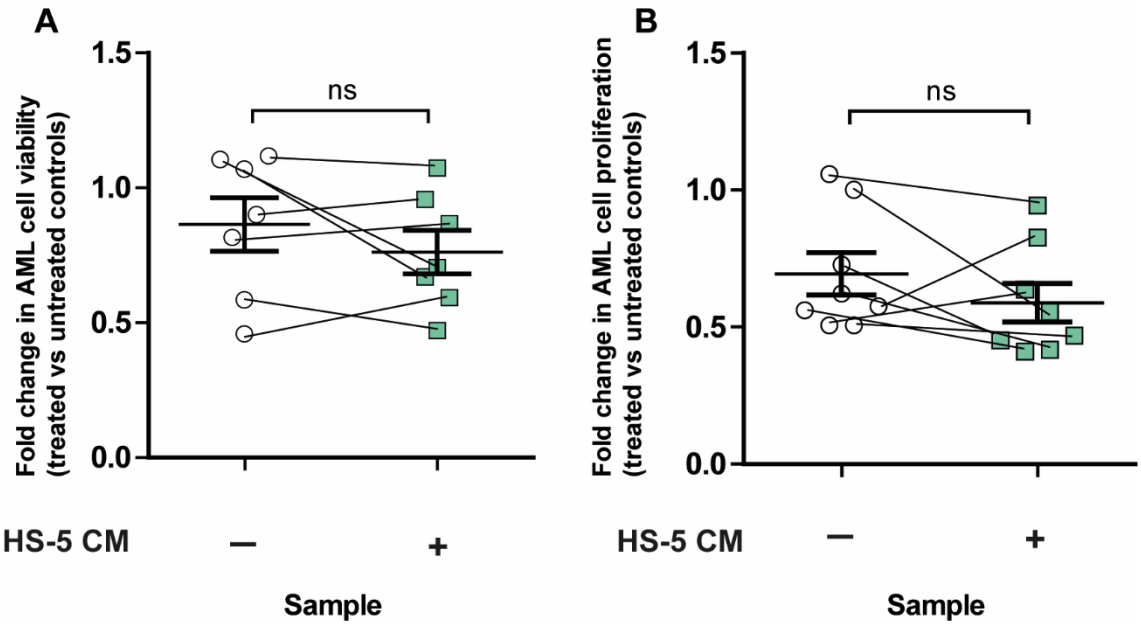

Figure 4.9: Primary AML pan kinase inhibition with/without HS5 conditioned media. Guava easycyte flow cytometry implemented to measure cell viability and proliferation of 8 primary AML samples. Measured fold change in **(A)** viability and **(B)** proliferation following 72 hours treatment with 1µM Midostaurin compared to DMSO vehicle controls (+/-) HS-5 CM (+10%FBS)**.** Patients n=8, each data point represents the average of four technical replicates, significance determined by paired T-Test matching patient samples *p<0.05, **p<0.01, ***p<0.001.

72 hours of 1µM Midostaurin treatment on primary AML cells maintained in an absence of HS-5 CM led to a decrease in AML viability to 0.86 on average, compared to matched DMSO control cells (Figure 4.9A). In the presence of HS-5 CM, treatment with Midostaurin reduced AML viability to 0.76 compared to matched DMSO controls whilst in the presence of HS-5 CM. Coupled with the spread of data these differences were not statistically significant. Analysis of specific data points revealed that Midostaurin effected some patient cells profoundly with viability in these patient cells reducing to levels 0.5 of that recorded in the untreated patient samples. These changes however, were not dependent on HS-5 secreted proteins.

Assessment of cell proliferation revealed that Midostaurin was potent at lowering the abundance of primary AML cells in both the presence (0.58) and absence (0.69) of HS-5 CM after 72 hours of incubation (Figure 4.9B). As observed when assessing viability, the variance in the results were non-statistically significant changes between conditions. It is notable that some of the primary AML samples were unperturbed by the presence of Midostaurin with relative proliferation levels registering on par with the untreated viability.

These experiments showed that Midostaurin can effect AML proliferation, which is reasonable considering that FLT3 is upstream of numerous proliferative pathways (458-460). It was also observed that in some cases the stromal proteins contributed by HS-5 cells were unable to modulate the primary AML response to Midostaurin. This finding suggested that for some patients the HS-5 proteins were not strong mediators of pathways that are targeted by Midostaurin or that the response to inhibition with Midostaurin is dominant over such agonists. The heterogeneity within the subset demonstrates the unpredictability of non-specific kinase inhibitors. As one may expect a compound that inhibits many kinases to consistently reduce AML viability due to its indiscriminative approach. However, in the viability assays there were primary samples that exhibited no change in viability compared to their untreated controls (Figure 4.9A).

JAK1-3 inhibition with Tofacitinib

The JAK-STAT pathway is a critical signalling cascade in the transduction of extracellular signals to the nucleus. It has been documented that many GFs and cytokines regulate cellular functions such as haematopoiesis, growth and immunity through this pathway (208, 461, 462). Pathologically increased activity of STAT3 has been reported in 20-50% of AML patients, as well as there being reported instances of STAT5 and STAT1 activation which are mediated by JAK activity (209-211, 463). These observations made the JAK-STAT pathway a likely mediator of the AML response to the presence of stromal proteins. Tofacitinib as detailed in Table 4.2 is a very selective compound for just the JAK isoforms 1-3, and therefore was a suitable agent for inhibiting this pathway.

Treating primary AML cells with Tofacitinib for 72 hours in non-HS-5 CM on average barely reduced AML viability (0.89) compared to that of match DMSO control cells (Figure 4.10A). In the presence of HS-5 CM, JAK inhibition with Tofacitinib led to no discernible change in AML viability (0.89) compared to the matched DMSO treated primary AML in similar conditions. This suggested that either the concentration of Tofacitinib was too low or the activity of this pathway in these patient samples was not high.

Assessment of cell proliferation following treatment revealed that Tofacitinib was capable of lowering the abundance of primary AML cells in the presence of HS-5 CM (0.69), however, in the absence of HS-5 CM, Tofacitinib barely effected proliferation (0.96) (Figure 4.10B). This difference was statistically significant, but as observed in inhibition experiments with other agents, there was heterogeneity within the response. Paradoxically a number of the primary AML samples exhibited higher rates of proliferation following treatment compared to

matched DMSO controls when HS-5 CM was absent. Experiments and cell response were more consistent when performed in HS-5 CM.

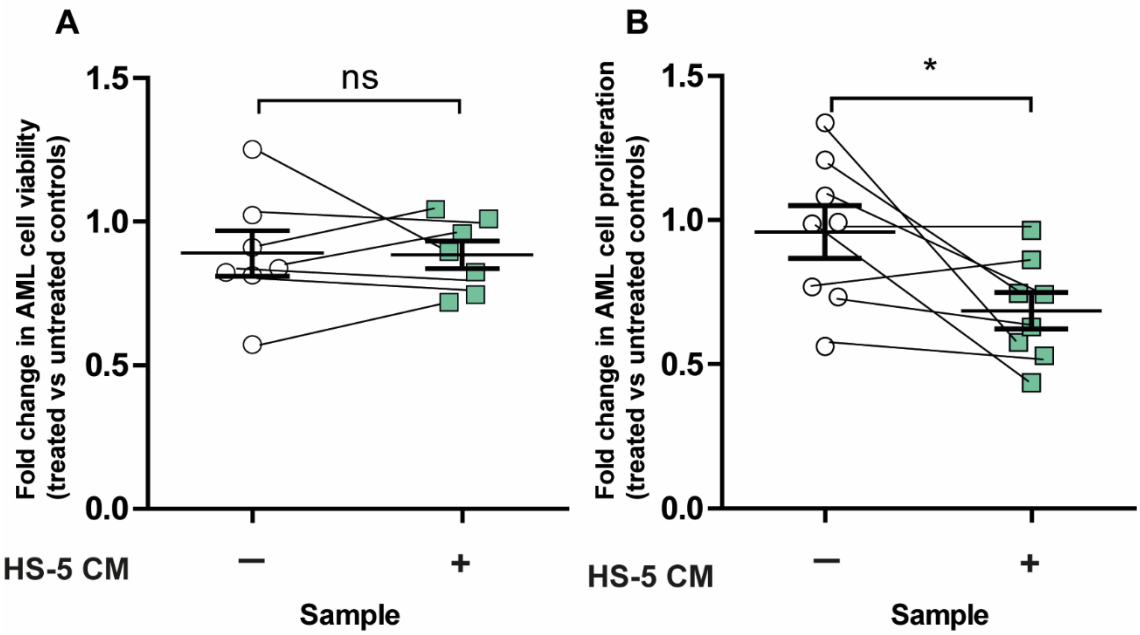

Figure 4.10: Primary AML targeted JAK inhibition with/without HS5 conditioned media. Guava easycyte flow cytometry implemented to measure cell viability and proliferation of 8 primary AML samples. Measured fold change in **(A)** viability and **(B)** proliferation following 72 hours treatment with 1µM Tofacitinib compared to DMSO vehicle controls (+/-) HS-5 CM (+10%FBS)**.** Patients n=8, each data point represents the average of four technical replicates, significance determined by paired T-Test matching patient samples *p<0.05, **p<0.01, ***p<0.001.

The observed proliferation drop that occurred in the presence of stromal proteins suggested that within the stromal complement there were proteins that activated JAK and therefore, the cells predominantly started utilising the JAK-STAT pathway for proliferative signal relay, hence the drop in proliferation following administration of Tofacitinib. This was not observed in the viability experiments and could have been due to a number of other GFs (perhaps mitogenic) within the stromal secretome that activated other survival pathways, leading to a net effect of unaffected viability following JAK inhibition.

PAK inhibition with PF-3758309

The final inhibitor incorporated into the inhibition studies was PF-3758309 which is a potent inhibitor with specificity towards PAKs, in particular group 2 PAKs as detailed in Table 4.2. PAK was selected as a target due to its previously reported status as one of the most active kinases in AML (271). The PAKs are also known effector proteins of the Rho GTPases (464), this makes them potential mediators of key AML cell functions that can be influenced by the microenvironment, such as migration and survival.

Incubating primary AML cells with PF-3758309 for 72 hours in the absence of HS-5 CM decreased AML viability substantially (0.28) compared to that of the matched DMSO control cells (Figure 4.11A). This compound was highly potent in primary AML cells, with three patient

samples exhibiting less than 25% viability compared to the matched untreated cells after a relatively small interval. The same AML patient cells treated in the presence of HS-5 CM did experience improvements in cell viability, however, this improvement was marginal (0.4). As all of the patients demonstrated modest increases in viability, these differences were in fact statistically significant.

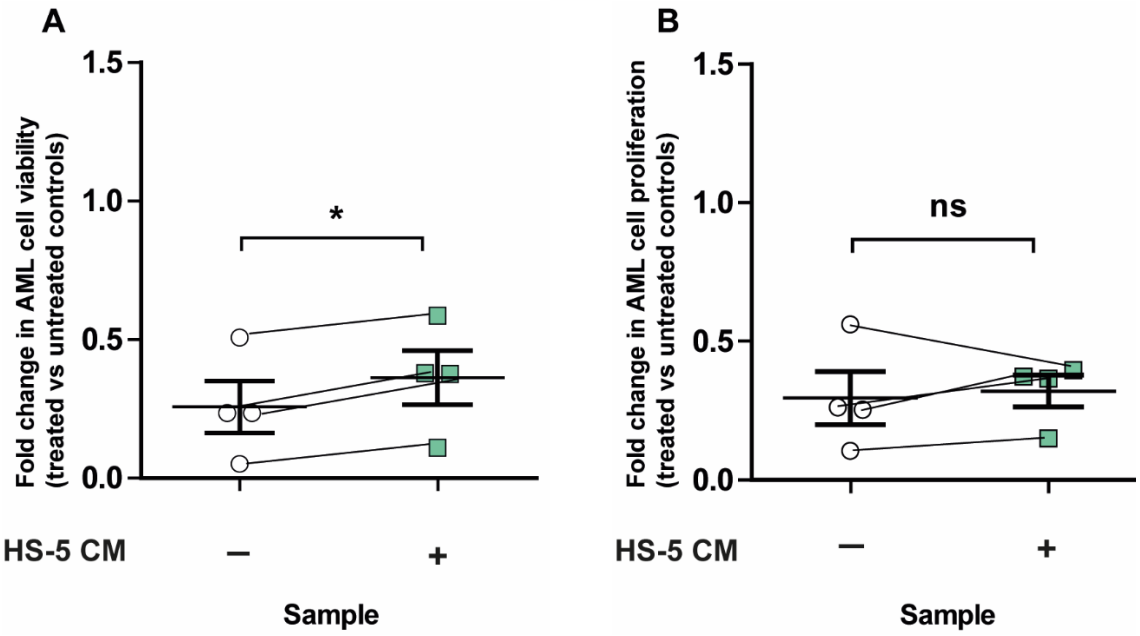

Figure 4.11: Primary AML targeted PAK inhibition with/without HS5 conditioned media. Guava easycyte flow cytometry implemented to measure cell viability and proliferation of 4 primary AML samples. Measured fold change in **(A)** viability and **(B)** proliferation following 72 hours treatment with 1μM PF-3758309 compared to DMSO vehicle controls (+/-) HS-5 CM (+10%FBS)**.** Patients n= 4, each data point represents the average of four technical replicates, significance determined by paired T-Test matching patient samples *p<0.05, **p<0.01, ***p<0.001.

The effects of PF-3758309 treatment on AML cell proliferation were consistent between HS-5 CM absent and HS-5 present conditions, suggesting that PAK inhibition significantly compromised AML cell proliferation. Regardless of the HS-5 CM, AML proliferation relative to matched untreated cells was profoundly compromised (Figure 4.11B). The observed effects of PAK inhibition could be explained by a few options, firstly the PAKs as previously described could be so pivotal to AML function that inhibition was not tolerable. Secondly, it could have been that the concentrations used were excessive or that PF-3758309 is in fact more promiscuous than first thought.

Considering the response of AML patient samples to kinase inhibitors collectively, there was a trend for the HS-5 secreted stromal proteins present in the CM to effect AML cell signalling and importantly cellular fate. This is a consequence of HS-5 CM induced cell signalling as 75% patients were more sensitive to mTOR inhibition following in the presence of HS-5 CM, simultaneously the same patient cohort were less sensitive (89% of the patients) to MEK inhibition in the presence of HS-5 CM (Table 4.3A). Patient samples #0, #10, #14 and #15

received Torin-1, Trametinib and PF-3758309 treatment and although these represent a small cohort, MEK and PAK inhibition were more effective at reducing cell viability in non-conditioned media. Whereas Torin-1 inhibition was more effective at lowering patient cell viability in the presence of HS-5 CM. Tofacitinib and Midostaurin were more heterogeneous in response and did not share a relationship with any of the responses to the other inhibitors.

A

Relative Viability compared to untreated pateint cells

Control	C.Media	Effect	Control	C.Media	Effect	Control	C.Media	Effect	Control	C.Media	Effect	Control	C.Media	Effect	Px ID
Torin			Trametinib			Midostaurin			Tofacitinib			PF-3758309			
0.22	0.00	↓	0.40	0.63	↑							0.51	0.59	↑	0
0.87	0.34	↓	0.26	0.60	↑							0.23	0.38	↑	14
0.61	0.54	↓	0.48	0.63	↑							0.23	0.38	↑	10
0.59	0.21	↓	0.12	0.39	↑							0.05	0.11	↑	15
0.59	0.55	-	0.28	0.30	-	1.07	0.67	↓	0.81	0.75	↓				6
0.76	0.60	↓	0.63	1.04	↑	1.12	1.07	-	0.84	0.96	↑				7
0.62	0.57	-	0.46	0.62	↑	0.58	0.47	↓	0.57	0.72	↑				8
1.22	0.77	↓	0.73	0.97	↑	1.10	0.70	↓	1.25	0.90	↓				9
0.60	0.52	↓	0.68	0.71	-	0.82	0.87	-	1.02	1.01	-				1
0.24	0.26	-	0.31	0.46	↑	0.46	0.59	↑	0.82	0.82	-				13
0.86	0.60	↓	0.20	0.33	↑	0.90	0.96	-	0.91	1.04	↑				11
0.85	0.77	↓	0.95	2.12	↑	0.81	1.45	↑	1.63	0.47	↓				12
FDR	0.0031			0.0096			0.9352			0.3669			0.0164		

B

Relative Proliferation compared to untreated pateint cells

Control	C.Media	Effect	Control	C.Media	Effect	Control	C.Media	Effect	Control	C.Media	Effect	Control	C.Media	Effect	Px ID
Torin			Trametinib			Midostaurin			Tofacitinib			PF-3758309			
0.84	0.16	↓	0.23	0.45	↓							0.10	0.15	-	0
0.64	0.40	↓	0.43	0.59	↑							0.25	0.37	↑	14
1.07	0.00	↓	0.31	0.67	↑							0.26	0.37	↑	10
0.00	0.22	↑	0.49	0.43	↓							0.56	0.40	↓	15
0.53	0.52	-	0.27	0.30	-	1.00	0.56	↓	0.73	0.63	↓				6
0.74	0.55	↓	0.64	0.97	↑	1.06	0.94	↓	0.77	0.86	↑				7
0.66	0.52	↓	0.49	0.55	↑	0.56	0.41	↓	0.56	0.53	-				8
1.06	0.63	↓	0.65	0.90	↑	0.73	0.45	↓	1.08	0.75	↓				9
0.54	0.35	↓	0.88	0.92	-	0.62	0.42	↓	1.21	0.74	↓				1
0.41	0.24	↓	0.43	0.41	-	0.51	0.47	-	1.34	0.58	↓				13
0.53	0.45	↓	0.15	0.29	↑	0.51	0.64	↑	0.99	0.96	-				11
0.87	0.60	↓	0.89	2.01	↑	0.58	0.83	↑	0.99	0.44	↓				12
FDR	0.0165			0.0342			0.2184			0.0375			0.7204		

Table 4.3: Overview of primary AML response to kinase inhibitors across patients. Tables reflect the relative changes in **(A)** viability and **(B)** proliferation observed in primary AML cells treated with kinase inhibitors compared to untreated cells +/- HS-5 stromal factors. Each relative value is averaged across 4 replicates and FDRs represent the p-values generated using paired T-Tests. If a patient sample in CM demonstrated a >0.05< relative change in viability/proliferation after inhibition compared to the same cells in non-conditioned media, then effect is marked with ↑ or ↓.

The effects of targeted kinase inhibition on proliferation whilst under the influence of stromal factors generated trends similar to that observed in changes to viability (Table 4.3B). As with viability Torin-1 treatment had more profound effects on proliferation in the presence of HS-5 stromal factors than in non-conditioned media. Trametinib induced a more heterogeneous proliferative response, with 7/12 patients experiencing positively altered proliferation in the presence of stromal proteins compared to without. Midostaurin and Tofacitinib were both more effective at inhibiting proliferation in the presence of stromal proteins than without, although Tofacitinib was the only condition to do so with statistical significance (p=0.037). PAK inhibition was not significantly modulated by the presence or absence of stromal proteins, as it was potent regardless.

4.7 Investigating the influence of stromal derived factors on phenotypic heterogeneity and selection in AML

Having established that individual proteins present within both the HS-5 and MS-5 stromal secretomes had the capacity to alter AML cell fate and that targeted kinase inhibition was altered in the presence of the full stromal secretome produced by HS-5 cells. I then sought to establish if the microenvironment derived proteins were selecting for specific AML clones or if AML clones were adapting to their microenvironment. It was hypothesised that sub-populations within a particular sample may be more responsive to the microenvironment; samples that can be maintained in culture contained populations that were responsive to elements that comprise the stromal secretome or they adapted to these elements. These responsive cells would likely activate particular signalling nodes, hence the changes in response to compounds such as Torin-1 in the presence of stromal factors. Therefore, CyTOF analysis was undertaken to see if responsive AML populations that displayed extended life in culture could be characterised.

4.7.1 AML cells survive 36 days in culture due to HS-5 conditioned media

Optimisation experiments testing CM from MS-5 and HS-5 cells determined that HS-5 secretome was ultimately superior to MS-5 CM in sustaining primary AML cells from patient 0. During these experiments it was observed that cell counts could initially drop before stabilising and eventually increase. It was speculated that the HS-5 stromal secretome was inducing the selection and expansion of specific AML populations.

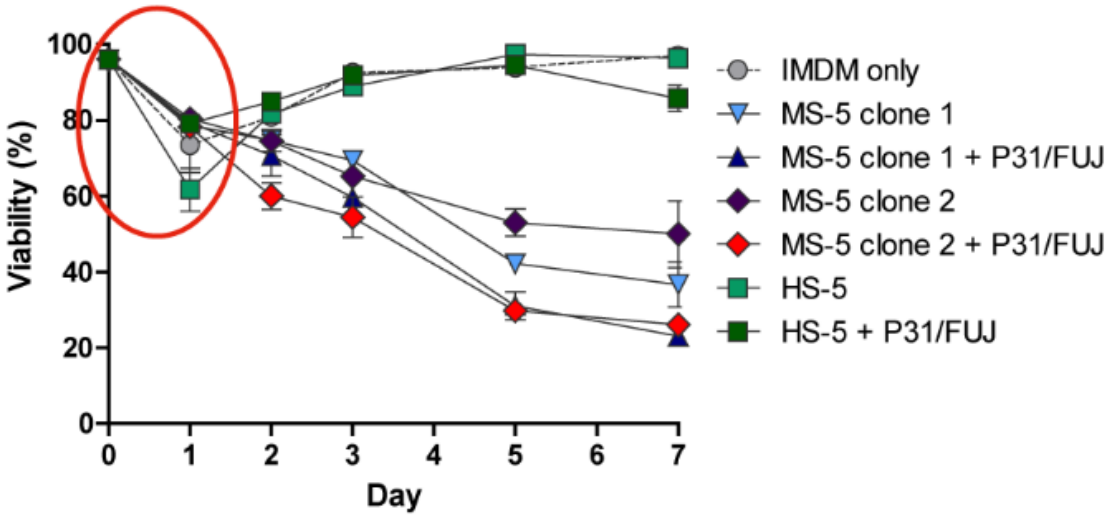

Figure.4.12: HS-5 conditioned media is the most successful at maintaining Patient #0 cell viability across seven days. On Day 0, $1x10^5$ cells/well with 2ml indicated CM (+10% FBS) in a 6-well plate. Viability was measured across seven days, using the Guava viacount assay on a Guava flow cytometer. Patient #0 cells run in n=6 technical replicates per condition. Red circle indicates the initial drop in viability at Day 1.

To test this an extension of previous experiments was devised with patient #0 cells, instead of ceasing experiments at Day 7 we sought to see how long we could maintain these

cells, as well as establish if independent AML cells could be rescued following incubation with HS-5 CM. Across seven days, primary AML cell viability was significantly affected by the medium in which they were grown (Figure 4.12). Monitoring the effect of HS-5 CM, AML viability was maintained close to 90% across the seven days. Utilisation of CM produced through HS-5/AML (P31/FUJ) co-culture offered no benefit compared to what is achieved by HS-5 CM alone. Unexpectedly, MS-5 clones were poor at sustaining primary AML cells in culture. It was reasoned that this was likely due to MS-5 clone #1 being past supportive passage age, hence the introduction of clone #2. Clone #2 was probably not ideal for producing AML supportive media as guidelines for this new cell line recommended α-mem media supplemented with serum, essential amino acids, L-glutamine and sodium pyruvate. It is likely that this medium was not suitable for AML growth and it would have probably been more supportive if IMDM medium was utilised for conditioning.

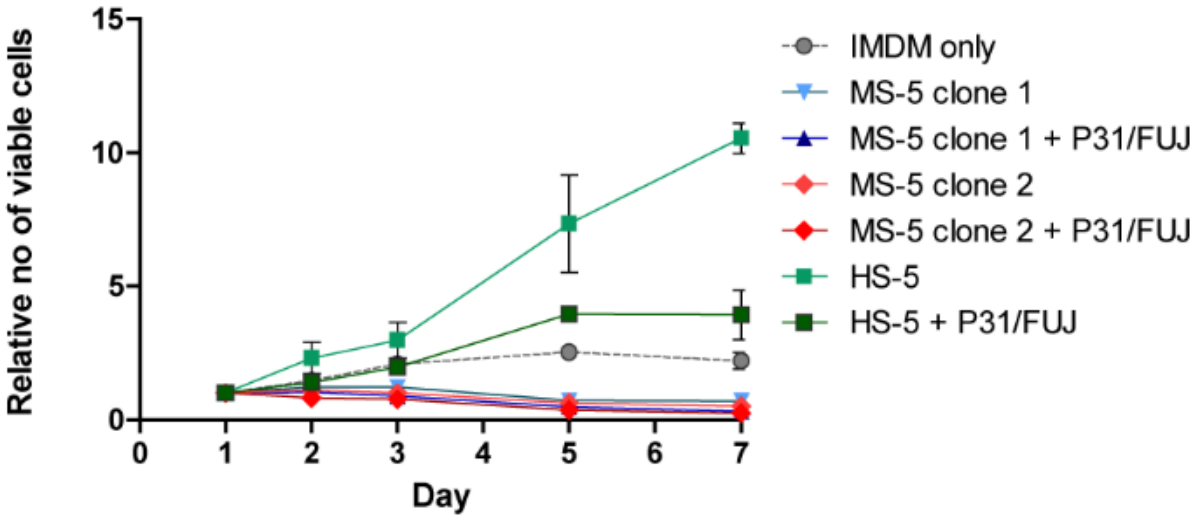

Figure 4.13: Relative primary AML cell proliferation. On Day 0, 1x10^5 cells/well with 2ml indicated CM (+10% FBS) in a 6-well plate. Viable cell numbers were measured across seven days, using the Guava viacount assay on a Guava flow cytometer and the count at each time point was normalised to the matched well recording on Day 1 to correct for any seeding differences. Patient #0 cells run in n=6 technical replicates per condition. Red circle indicates the initial drop in viability at Day 1.

Assessment of cell growth over seven days (with seeding correction) revealed that compared to the growth after Day 1, HS-5 only media was sufficient to generate a ten-fold increase in cell number (Figure 4.13), this is substantially higher than that recorded for the IMDM only control in which maximum cell number was recorded at Day 5 around four-fold higher than Day 1. The HS-5/AML co-culture medium was slightly more supportive than the IMDM only conditions, however, the presence of P31/FUJ cells in the media depleted the media of supportive components conferred by HS-5 cells (as seen in Chapter 3). The primary AML cells from patient #0 were still growing and dividing in the HS-5 media by the Day 7 timepoint, other conditions reached a growth plateau at Day 5.

The patient #0 cells grown in HS-5 media were collected, reseeded and maintained in culture. During this period each time cells were replated and media replenished cell viability was measured (Figure 4.14A). Over the course of the culture the AML cells maintained a very high viablilty from Day 5 onwards. There was a drop in viability between days 20 and 30, this was due to a low cell density replating which took the cells a while to recover from. However, after 30 days the cells were climbing in viability again – reaching >95%.

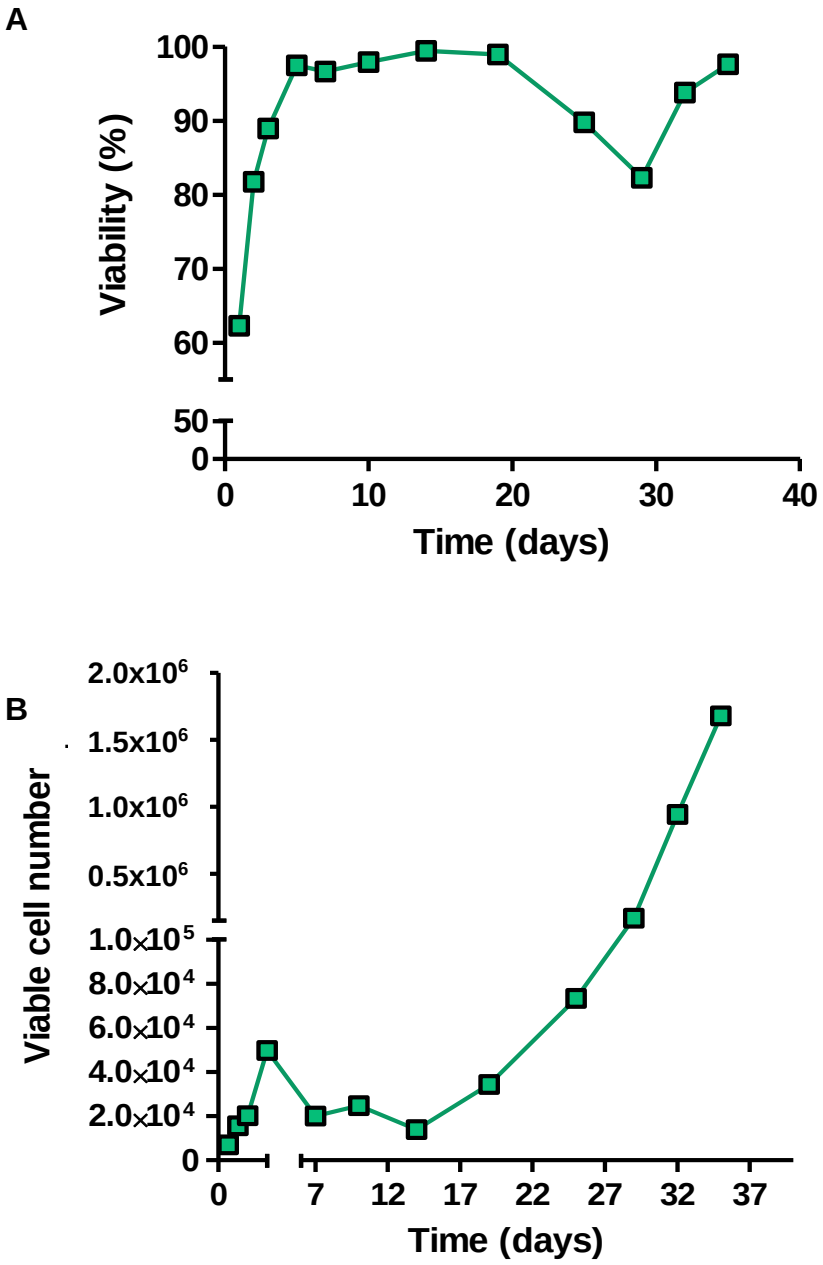

Figure 4.14: Patient #0 cells during 36 day time-course in culture. Viable Patient #0 cells from figure 4.13 grown in HS-5 CM pooled and reseeded in 2ml fresh HS-5 CM (+10% FBS) in 6 well plates. From Day 7 to Day 36 cell **(A)** viablilty and **(B)** viable cell counts measured using Luna 2 cell counter, measurements averaged across 3 counts.

In parralel to AML viability assessment of the viable AML cell count indicates that over the time-course as long as the supportive media was maintained and that cells were not reseeded at too lower number, patient #0 cells continued growing in the log phase (Figure

4.14B). It is not documented in the literature that primary AML cells can survive this long ex vivo without stromal co-culture. Therefore, this population of 'Day 36' ex vivo primary cells that were acquired from patient #0 (clinical features in Chapter 2) were selected for characterisation.

4.7.2 Mass cytometry (CyTOF) principles

Mass cytometry or (**Cy**tometry – **T**ime **O**f **F**light) is a technique that couples the inductively coupled plasma MS (ICP-MS) with time of flight MS to measure metal-conjugated antibodies, whose binding enables the distinction of single cell expression of target proteins (Figure 4.15). Currently this technique serves as the best means by which to undertake single cell proteomics.

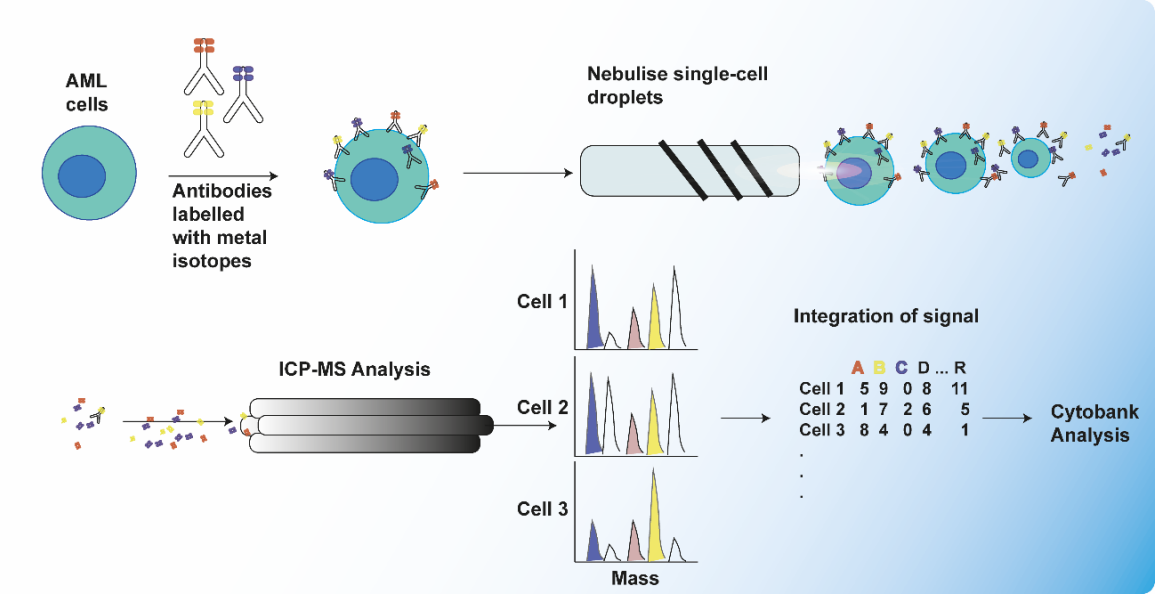

Figure 4.15 CyTOF principle.

The principles of CyTOF are based around the conjugation of heavy metal isotopes to antibodies raised to specific target proteins. Following blocking and binding of the antibodies to the target cell population, cells are fixed and inducted into the instrument. Upon induction into the machine cells are separated to single cell droplets and nebulised. This removes most of the biological matter and water leaving a predominantly heavy metal aerosol to be carried to the inductively coupled plasma (ICP) torch. The aerosol droplets are then vaporised, atomised and ionised at the ICP source for MS analysis. Ionisation occurs as a result of collisions with free electrons that are released by the collision induced ionisation of argon gas within the plasma torch. The ion beam that leaves the plasma torch enters the ion optical chamber before high mass ions are guided by the quadrupole to the TOF chamber. This stage is important as quadrupole selection removes any endogenous cellular or low molecular weight argon ions. Heavy mass ions are then pushed into the TOF chamber where electrostatic force orthogonally accelerates the ions to the detector and ions are separated by m/z. The mass cytometric data is

then integrated to give single cell read outs of heavy metal abundance. This heavy metal corresponds to protein expression, combining and grouping cells by these signatures allows clonality to be elucidated.

4.7.3 Understanding the AML response to stromal conditioned media using AML phenotype antibody panel

Lapidot et al. were the first to describe that only AML cells, which display a $CD34^{+}CD38^{-}$ phenotype, are capable of engraftment and generating leukaemia (138). Since this paper, it was generally accepted that selecting for a $CD34^{+}CD38^{-}$ population enriches for the leukaemia initiating LSCs (138). This is not a hard and fast rule though, as this phenotype can actually encompass a heterogeneous cell population consisting of both normal and leukemic cells. Identifying leukaemic initiating cells is harder still as there have been a number of publications since that contradict the doctrine of a $CD34^{+}CD38^{-}$ exclusive phenotype in AML. These publications stated that it is possible for $CD38^{+}$ $CD34^{-}$ AML cells to engraft and induce leukaemia in immuno-deficient mice (143, 465-467). Despite this evidence, $CD34^{+}CD38^{-}$ are still widely considered necessary for LSC identification (11, 138). Considering the lack of consensus in identifying AML sub-populations and importantly those clones that can initiate leukaemia - which historically are believed to be most treatment resistant and interactive with the BMM - it was difficult to select just a few markers to measure the effects of stromal factors on AML clonality. Therefore, to monitor how particular AML populations within a patient sample responded to the complement of HS-5 stromal secretome, an already characterised panel of antibodies optimised for AML phenotyping was utilised to monitor any changes in the phenotype of patient #0 cells over 36 days in culture. The antibody panel is comprised of 17 antibodies (Table 4.4).

Target	Clinical significance	Function	Refs
CD7	Immature AML cells, poor response to standard therapy	T cell antigen	(468)
CD34	High expression correlative with poor outcome	Cell adhesion factor indicative of a haematopoietic precursor cells	(469, 470)
HLA-DR	Expressed in most AML, generally absent in APL	MHC class 2 surface receptor Immature precursor	(471, 472)
CD38	Heterogeneous expression, but most patients have CD38+ blasts – believed to be absent in LSCs	Type II transmembrane glycoprotein	(138, 473)
CD33	Detected on 85-90% AML patient blasts	Myeloid cell marker indicative of monocytic differentiation	(474)
CD184	High relapse rates and poor outcome	CXCR4 the receptor of SDF-1/CXCL12	(475)
CD123	Observed as being present in AML blasts and LSCs	IL-3 receptor	(476)
CD64	Strong expression distinguishes monocytic disease, especially if co-expressed with CD15	Fc gamma receptor – indicative of monocytic differentiation	(477)
CD14	CD14 positivity associated with lower complete remission rates	Myeloid Cell-Specific Leucine-Rich Glycoprotein, indicative of monocytic differentiation	(478)
CD45	Located on all haematopoietic cells except erythrocytes and platelets	Marker for a protein tyrosine phosphatase (PTP). CD45 is also called the common leukocyte antigen	(479)
CD44	Marker of LSC	Directs HSCs to the bone marrow. Expression crucial to leukaemogenesis	(193, 475)
CD11b	Indicator of adverse disease	NK cell marker	(480)
CD3	T cell marker	Part of the T-cell receptor complex and defining feature of T cell lineage	(481)
CD19	B cell marker, although aberrant expression has been described in AML	Antigen receptor of B-lymphocytes	(482)
CD117	Stem cell marker	Immature precursor, c-KIT	(483)
CD16	Potential therapeutic target	Fcγ receptor III is a marker of NK cells, neutrophils, leukocytes, monocytes and macrophages	(484)
CD15	Expressed on AML blasts and correlates with a favourable prognosis	Myeloid cells, adhesion molecule normally expressed on neutrophils that mediates phagocytosis and chemiotaxis	(485)

Table 4.4: Panel of CyTOF antibodies used to characterise potential AML clones within patient samples.

To monitor the changes that may have occurred within patient #0 cells across the 36 days, three conditions/time points were selected; patient #0 cells at Day 0, Day 1 following 24 hours of maintenance in HS-5 CM and Day 36 – all the cells maintained from Figure 4.14. All of these samples were processed at the same time; this was possible as there was access to multiple vials of patient #0's cells (stored in liquid nitrogen). Therefore, at Day 35 one vial was

thawed and maintained in HS-5 media for 24 hours, the following day the 'Day 0' sample was prepared by thawing another vial. Once all samples were ready on day 36, cells were fixed and stained with the heavy-metal conjugated antibodies and analysed by CyTOF.

To analyse the effect of HS-5 CM on the primary AML cells from patient #0, single cell expression of each of the markers were interpreted by performing viSNE analysis. viSNE allows visualization of multi-dimensional single-cell data by finding a two dimensional representation of single-cell data that best preserves local and global geometry of the population (486). viSNE maps are similar to a biaxial plot, but the positions of cells reflect their proximity in a multi-dimensional space rather than two-dimensional space. Colour, the third dimension, is integrated into the plot to represent the single-cell expression of a particular feature (i.e. CD34).

Analysis of the generated viSNE plots revealed that 36 days of HS-5 influence caused the cells which comprised the patient #0 AML population to spatially change (Figure 4.16, red arrows). The gating employed in pre-processing meant that only live cells were measured in the viSNE analysis. Analysis of the spread of data at each of the time-points revealed that Day 0 cells did not cluster as tightly suggesting the starting population of cells were quite heterogeneous. Following 24 hours of HS-5 conditioning, the geometry of the data indicated that there was a selective shift developing, and by Day 36, cell populations clustered into a more defined shape.

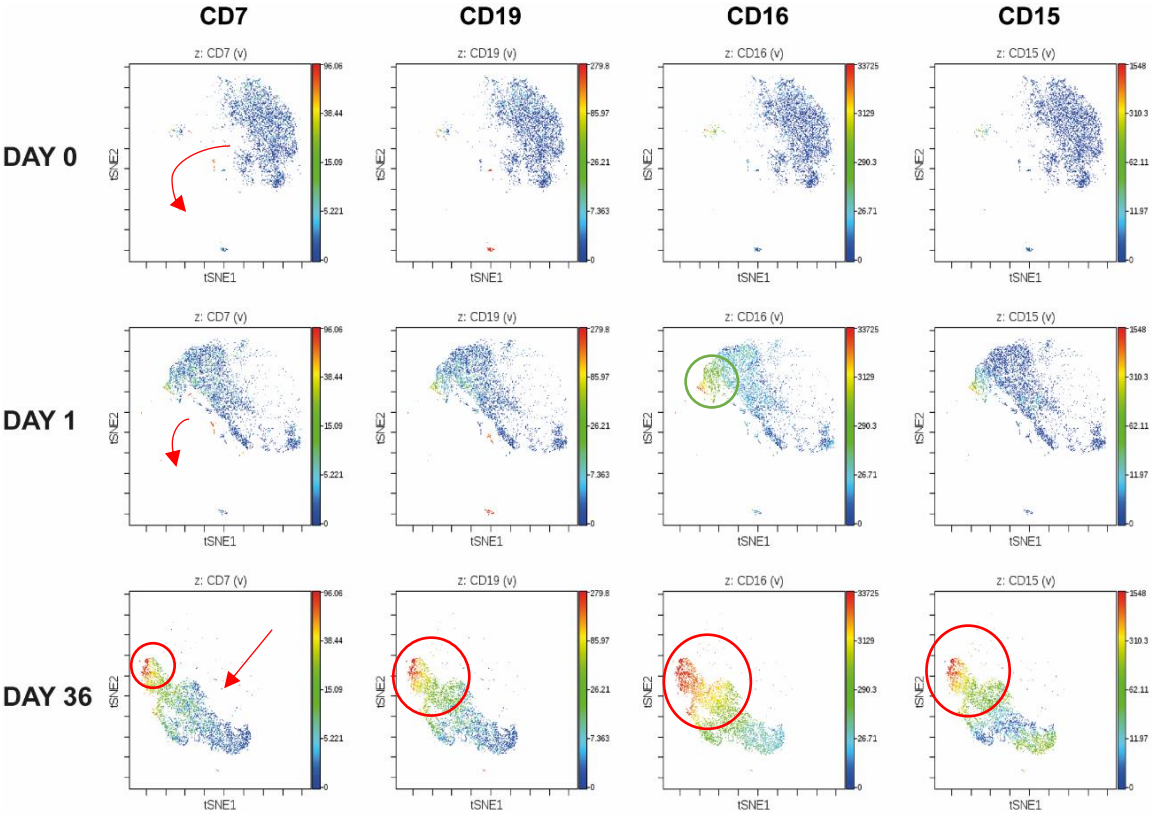

Figure 4.16: ViSNE analysis of markers CD7, CD19, CD16 and CD15 during 36 days in culture. Application of viSNE to patient #0 samples at Day 0, 1 and 36, cells stained with 17 markers and measured with mass cytometry. Cells separated into spatially distinct subsets based on the combination of markers that they express. Each point in the biaxial plots represents an individual cell, colour represents expression of indicated marker on a particular cell (see colour scale for expression levels). The axes are in arbitrary units.

This first set of markers were grouped based on a shared absence of expression at Day 0, followed by the gradual emergence of expression of sub populations that highly expressed these markers by Day 36 (Figure 4.16). The strongest marker of this set, CD16 (Fcγ receptor) was expressed in a particular population of cells that arose following 24 hours of HS-5 conditioning (green circle), and as detailed in Table 4.4, CD16 is considered a potential therapeutic target. By Day 36 this population expanded considerably, and within this population of cells, there were varying degrees of CD7, CD19 and CD15 co-expression (red circles). These markers are all considered lymphoid markers, suggesting the emergence of biphenotypic subpopulations or lymphoid cells. These markers could aid in microenvironment interactions, CD15 is an adhesion molecule that helps to facilitate cell interactions and niche localisation.

The second set of markers were grouped together as cells that began at Day 0 with modest expression and were consistently expressed after 24 hours of HS-5 conditioning. However, following 36 days in culture under the influence of HS-5 secreted proteins, there was the emergence of high CD14, CD45, CD44 and CD11b expression (Figure 4.17). All of these markers have previously been described as indicators of adverse risk and poor outcome (Table 4.4) – patient #0 had been classified adverse risk based on cytogenetics. CD11b is regarded as a surrogate for poor performing leukaemias, commonly found in patients that are non-responsive

to standard treatments. During the time course, cells harbouring this marker expanded, to the extent where nearly all cells exhibited expression. Additionally, there was marked increase in monocytic markers (CD14 and CD45), these are usually more differentiated expressing proteins that aid in microenvironment interactions. Finally, CD45 which has low expression in haematopoietic cells, except in erythrocytes and platelets, was consistently expressed throughout the duration of the experiment.

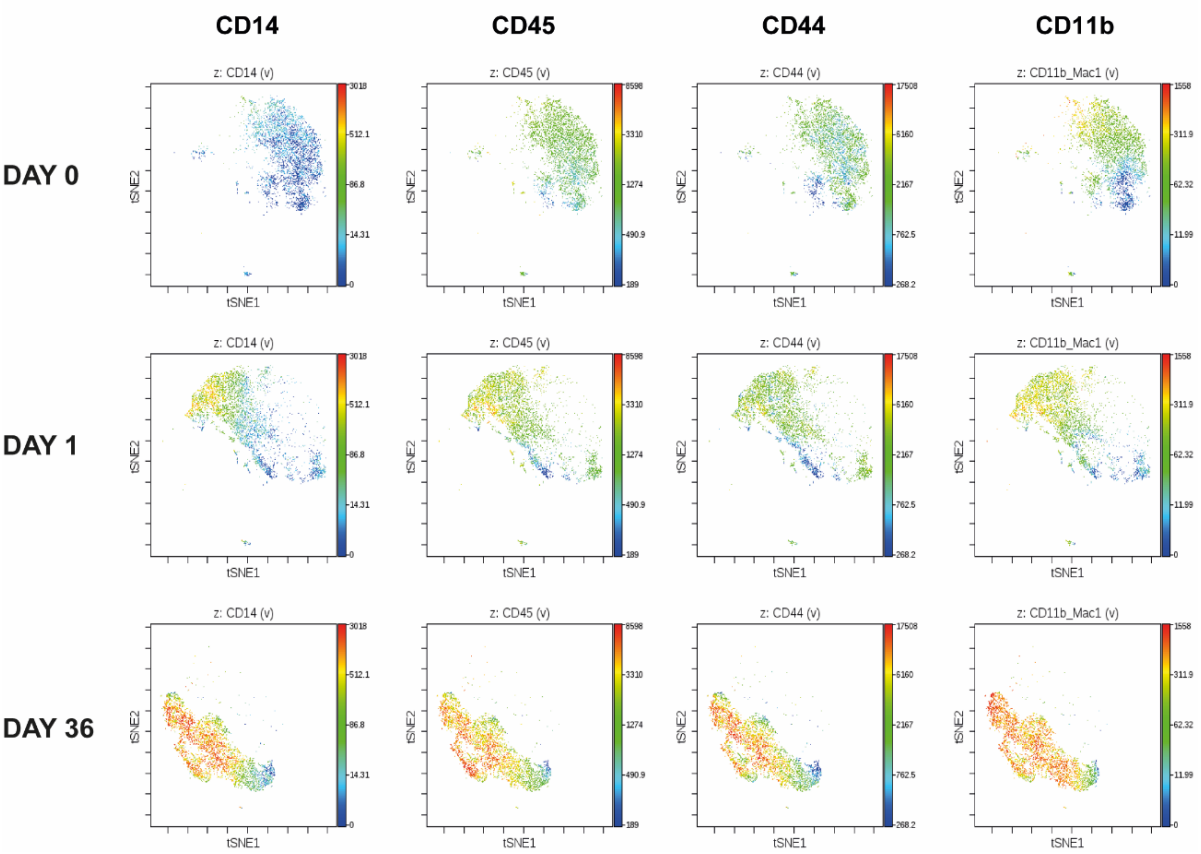

Figure 4.17: ViSNE analysis of markers CD14, CD45, CD144 and CD11b during 36 days in culture. Application of viSNE to patient #0 samples at Day 0, 1 and 36, cells stained with 17 markers and measured with mass cytometry. Cells separated into spatially distinct subsets based on the combination of markers that they express. Each point in the biaxial plots represents an individual cell, colour represents expression of indicated marker on a particular cell (see colour scale for expression levels). The axes are in arbitrary units.

The third selected group of markers comprise known AML cell surface receptors. CD184 (CXCR4) expression was minimal at Day 0, however, 24 hours after HS-5 conditioning a small population of cells emerged that had very strong CD184 expression (Figure 4.18, red circle). This population of cells was not sustained, as CyTOF measurements at Day 36 shows that most cells are $CD186^{-}$, with only a small subset exhibiting modest expression. CD123 (IL-3 receptor) was moderately expressed at Day 0 (Figure 4.18), following CD184, cells that harboured CD123 expression increased in the presence of HS-5 CM, although expression was not as focussed and more global. Nevertheless, by Day 36 there were no cells remaining that were $CD123^{+}$. CD64 (Fc gamma R1 receptor), unlike the previous two receptors was not strongly expressed at either Day

0 or Day 1 time points. However, by Day 36 a small population of cells that strongly expressed the receptor emerged (Figure 4.18, blue circle). This particular cluster of cells also co-expressed the marker CD15 (Figure 4.16, red circle) and the combined expression is an indicator of monocytic AML cells.

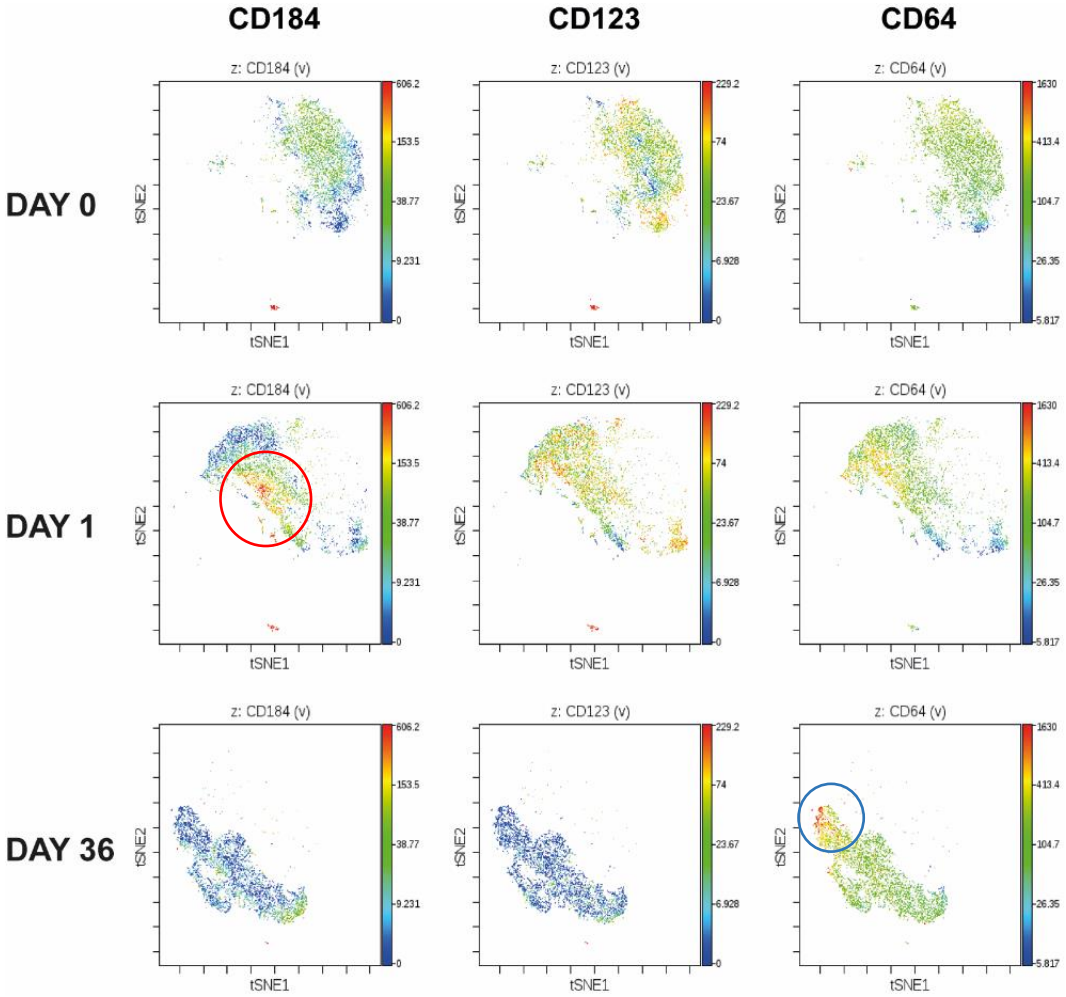

Figure 4.18: ViSNE analysis of markers CD184, CD123 and CD64 during 36 days in culture. Application of viSNE to patient #0 samples at Day 0, 1 and 36, cells stained with 17 markers and measured with mass cytometry. Cells separated into spatially distinct subsets based on the combination of markers that they express. Each point in the biaxial plots represents an individual cell, colour represents expression of indicated marker on a particular cell (see colour scale for expression levels). The axes are in arbitrary units.

The last panel of markers represent common AML markers. CD3 (T cell co-receptor) is an aberrantly expressed T cell marker in AML (487), this marker was not strongly expressed over the time-course, although there was consistent and moderate expression (Figure 4.19). CD117 (c-kit receptor) is a marker that is described as an early stem cell marker (456). This marker was sporadically expressed at the beginning of the time course and did not increase in expression following 24 hours of HS-5 conditioning. By the last time point there was strong expression observed in a small cell population (Figure 4.19, red circle). CD33 is a myeloid cell marker that is widely expressed in AML and its expression was present throughout the duration of this experiment, with very pronounced expression recorded on Day 1. HLA-DR is a major

histocompatibility complex (MHC) 2 cell surface receptor that is used to distinguish APL, as APL cells do not usually express HLA-DR. In these experiments, HLA-DR was strongly expressed at Day 0, with a notable cluster of very high expressing cells. HLA-DR was moderate after 24 hours. By Day 36 however, a localised population of cells emerged that were positive for other AML markers such as CD33, but now have low or absent HLA-DR expression (Figure 4.19, blue circles). HLA-DR is usually expressed on immature cells; therefore, this may represent a population of more mature cells that have arisen following 36 days of culture.

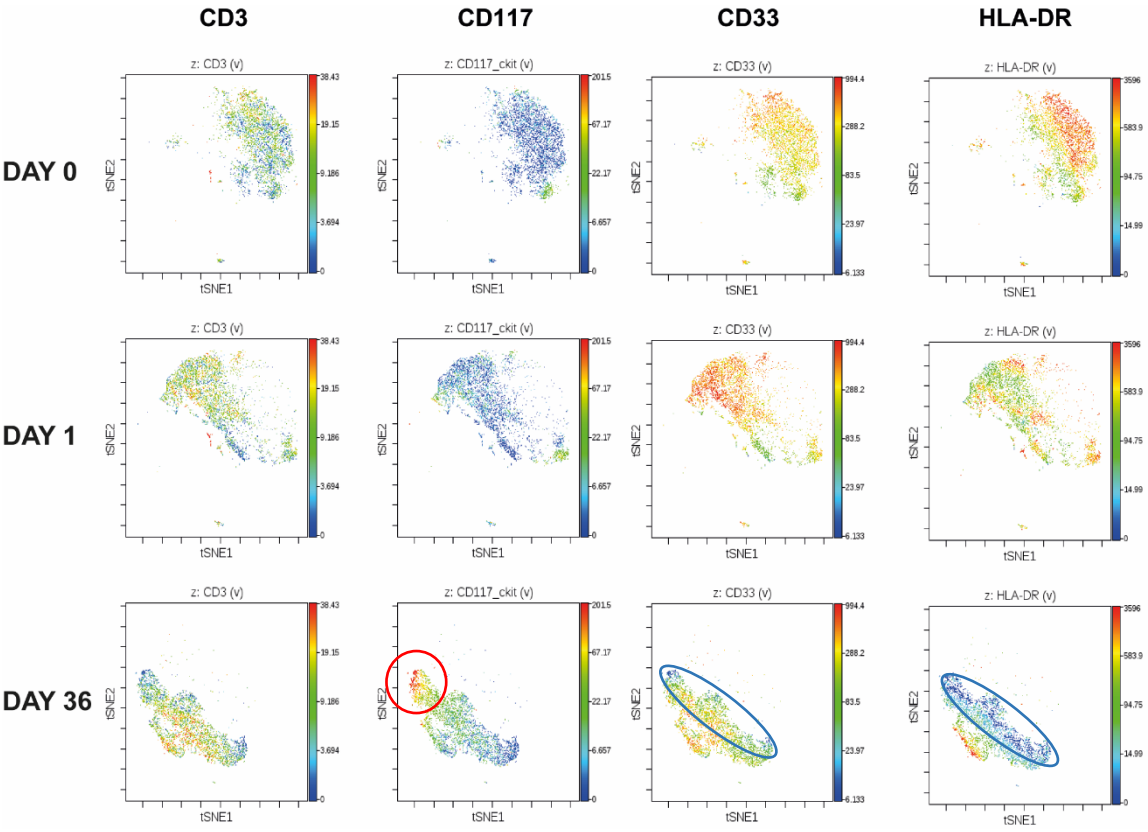

Figure 4.19: ViSNE analysis of markers CD3, CD117, CD33 and HLA-DR during 36 days in culture. Application of viSNE to patient #0 samples at Day 0, 1 and 36, cells stained with 17 markers and measured with mass cytometry. Cells separated into spatially distinct subsets based on the combination of markers that they express. Each point in the biaxial plots represents an individual cell, colour represents expression of indicated marker on a particular cell (see colour scale for expression levels). The axes are in arbitrary units.

The final two markers to be assessed CD34 and CD38 are the traditional markers that are used for characterising LSCs (as discussed at the beginning of this section). Assessment of these markers expression at Day 0 observed that all cells in the sample expressed moderate to high levels of both CD34 and CD38 – the markers of AML initiating cells (Figure 4.20). This expression was varied with pockets of $CD34^{high}CD38^{high}$ cells, but also a small cluster of $CD34^{high}CD38^{low}$ cells (red circles). At Day 1, there was still consistent expression of both markers, with an increase in $CD38^{high}$ cells, as well as the persistence of the $CD34^{high}CD38^{low}$ cells. The last condition measured at Day 36 showed that all cells were $CD34^{-}$; this could have been because

all CD34^{+} cells had all undergone cell death or possibly cell differentiation and now expressed CD33 instead. There was persistent expression of CD38^{+} cells, initially these finding would suggest that these HS-5 CM was not optimal for maintaining the leukaemia initiating population. However, there are a number of papers that report the capacity of CD34^{-}CD38^{+} cells to behave as leukaemia initiators and induce engraftment (75-78); this population was abundant by Day 36 (Figure 4.20, blue circles).

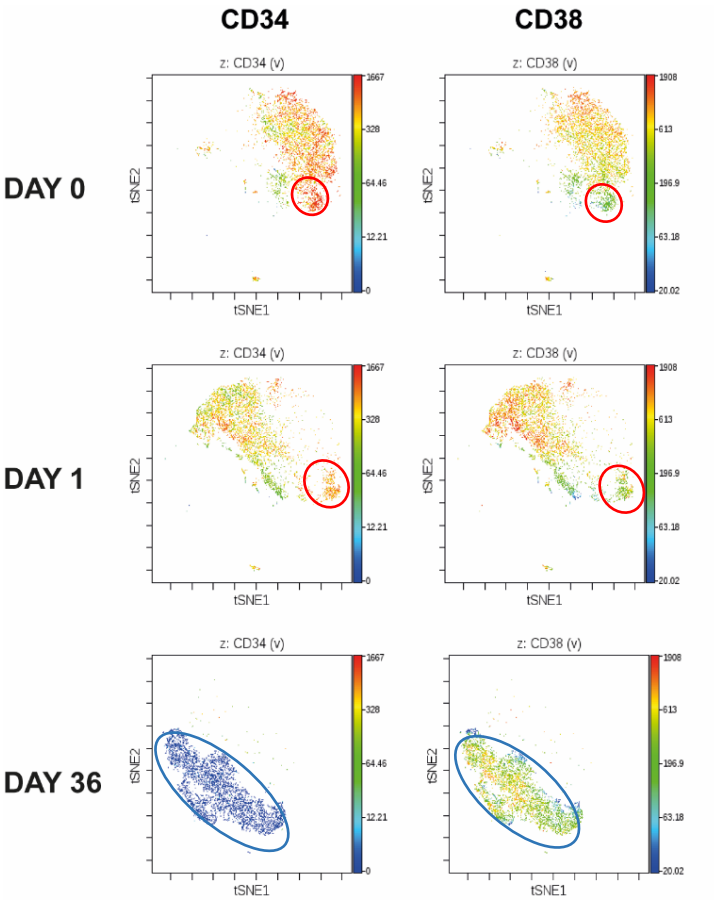

Figure 4.20: ViSNE analysis of key LIC markers CD34 and CD38 during 36 days in culture. Application of viSNE to patient #0 samples at Day 0, 1 and 36, cells stained with 17 markers and measured with mass cytometry. Cells separated into spatially distinct subsets based on the combination of markers that they express. Each point in the biaxial plots represents an individual cell, colour represents expression of indicated marker on a particular cell (see colour scale for expression levels). The axes are in arbitrary units.

By interpreting the CyTOF results collectively, it was clear that the AML cells adapted to their environment, as the global population changed considerably over the 36 days, the changes in global marker expression are summarised in Figure 4.21. The total AML population showed an increase in differentiation over time through the loss of naïve markers such as CD34, CD123 and HLA-DR, while at the same time acquiring strong expression of CD14 which is a marker of monocytic differentiation. Notably, the expression of markers that are reported to facilitate microenvironment interactions increased in expression (CD44, CD15, CD16), as well as the transient expression of CXCR4 (CD184) which would have been initially important in niche localisation if in vivo. Many of the markers that increased in expression over 36 days are also

indicators of poor outcome (CD117, CD7, CD44, CD45, CD14, CD11b), demonstrating the support that the microenvironment can provide AML cells.

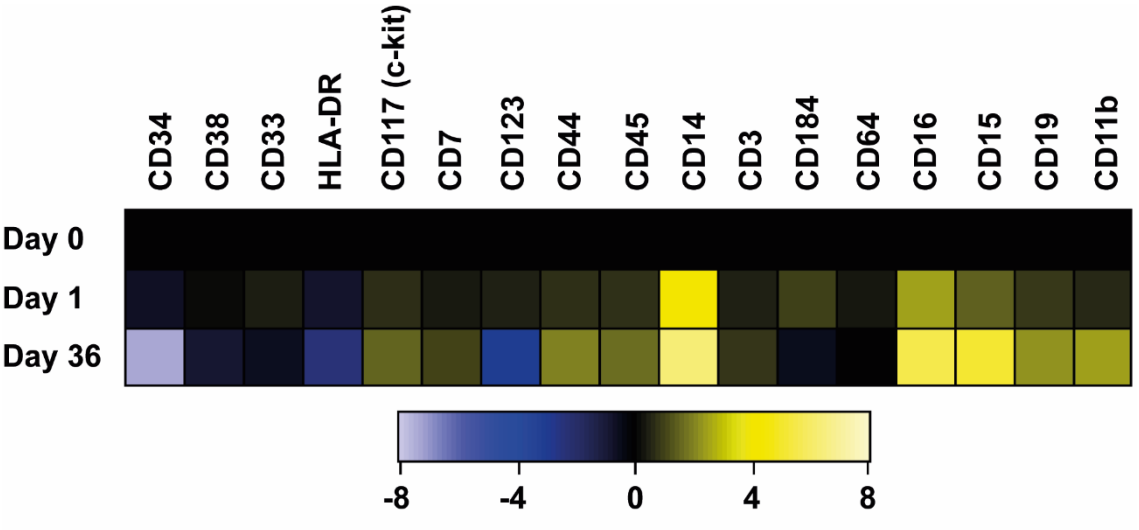

Figure 4.21: Heatmap of surface marker expression during 36 days of ex vivo cell culture. Calculated Log_2 fold change of Day 1 and Day 36 mean surface marker expression on live-gated cells relative to marker expression on Day 0.

The unexpected finding in the analysis was the ability of HS-5 media to induce the expression of markers or select for clones that were not present at Day 0, but by Day 36 clones that highly expressed these markers could be identified in the sample. A marker that followed this pattern was CD16 (Figure 4.16 and 4.21), this is interesting as the marker has recently been described as a novel therapeutic target (488). Thus, HS-5 CM may be able to induce the expression of subpopulations that confer poor patient outcome, but at the same time could be inducing the expression of potential therapeutic targets such as CD16.

4.8 Summary

The initial objective of the experiments presented in this chapter was to functionally validate the selected panel of stromal derived proteins in primary AML cells and characterise how these proteins and the secretome as a whole could potentiate AML progression. This was achieved by utilising purified human RPs in addition to the described stromal secretomes in Chapter 3 to maintain primary AML cells in long term ex vivo cultures. Simultaneously, survival and proliferation assays were conducted to examine primary AML response, and when exogenous proteins potentiated survival, CyTOF analysis captured how this shaped AML clonality.

Initially, recombinant versions of the six identified proteins (S100-A4, S100-A11, BMP-1, CTGF, HGF, CSF-1) were acquired and adverse risk primary AML cells were treated with 10ng/ml of each RP in both serum starved and serum containing (10% FBS) environments and maintained in culture for seven days. Assessment across the time-course observed that S100-A4, CSF-1 and a combination of all the RPs induced significant proliferation in the primary cells (Figure 4.3), while at the end of the time-course each of the proteins were more supportive than the No GF controls (Figure 4.2). Although not all proteins affected proliferation, all modulated viability to some degree, and it was concluded that the concentrations were sufficient to induce a functional response. Serum inclusion was maintained to reduce cellular stress, additionally it was postulated that serum may have been necessary for a full response to the stromal derived proteins. This reasoning was based on the response of patient #1 cells to stimulation with S100-A4.

Following the validation that these proteins effected patient #1 cells, both survival and proliferation assays were conducted on a larger cohort of five primary AML samples. Survival assays determined that despite heterogeneity in the degree of response to each GF, 4/5 patients exhibited substantially higher viability after seven days in culture compared to the No GF controls (Figure 4.4) An interesting but underpowered observation in these studies was that the AML response to GFs correlated with age in the albeit small sample set, with AML cells that responded to the proteins being from older patients that have poorer outcome and the least responsive being from younger patients that usually respond better to treatment (Table 2.8).

The heterogeneous response of different primary samples to the secretome derived proteins suggested that these proteins were indeed important in AML, but which GF(s) and the degree of impact will vary from patient to patient. To estimate the impact of these GFs in a wider cohort gene expression analysis of the proteins was undertaken using the TCGA AML dataset which compared the gene expression of the proteins of 183 patient samples to the normal population. Although this did not measure stromal cell expression, this revealed that patients

with above median gene expression of CSF-1 (p=0.0175) and S100-A4 (p=0.0118) had a statistically significant worse survival than those below the median (Figure 4.6). Patients with above median gene expression of HGF on the other hand, demonstrated better survival (p=0.00717). The gene expression of the other proteins did not significantly correlate with outcome. Although these observations substantiated CSF-1 and S100-A4, the gene expression analysis did not rule out the other proteins as there are aspects of protein function and behaviour that cannot be captured using this approach.

To further characterise how the HS-5 secretome supports primary AML, kinase inhibition studies were undertaken targeting key signalling nodes in AML (MAPK, mTOR, FLT3, JAK and PAK) (Figure 4.2). It was hypothesised that signalling molecules that comprise the HS-5 stromal secretome would engage these pathways to mediate survival and proliferation. Experiments revealed that instead of the inhibitors abrogating the effects of the supportive effects of the secretome, the secretome modulated AML sensitivity to the kinase inhibitors. Patient cohorts in the presence of the stromal secretome would become less sensitive to MAPK inhibition (Figure 4.7), and more sensitive to mTOR inhibition (Figure 4.8). FLT3 and JAK inhibition were not significantly altered and regardless of secretome PAK inhibition profoundly affected cells (Figure 4.11). This suggested that stromal cells can influence AML cell signalling, thus demonstrating a means by which AML could withstand kinase inhibitor therapies – in accordance with the poor clinical response observed to FLT3 inhibition (54, 489).

In parallel to kinase inhibition experiments, a sample of primary AML cells had been maintained in culture for 36 days and with peaks and troughs in viable cell numbers observed during the 36 days (Figure 4.12 and Figure 4.14), it was hypothesised to be indicative of clonal selection. In order to assess the clonality of the sample and changes that may have occurred in the population CyTOF was performed on the cells that had been maintained in culture for 36 days using an AML phenotyping panel (Table 4.4), in addition to samples from the same patient at Day 0 and following 24 hours in culture exposed to the same factors. This study identified that the clonality of the patient populations did indeed change over the course long-term culture (Figure 4.16), and assessment of the phenotypic markers changed considerably (Figure 4.21). Cells that expressed the traditional LIC marker combination $CD34^{high}CD38^{low}$ were not maintained, instead it was the $CD34^{-}CD38^{+}$ cell population that persisted, which have also been shown to behave as leukaemia initiators and induce engraftment (143, 465-467). Collectively, the long-term maintenance of primary AML cells in HS-5 CM induced the selection of clones that confer poor patient outcome, but at the same time arose the expression of potential therapeutic targets.

In summary, primary AML functional studies validated that these secretome derived proteins (S100-A4, S100-A11, BMP-1, CTGF, HGF and CSF01) are a group of proteins that can extend and maintain primary AML cells ex vivo and as these are proteins that are secreted by mesenchymal cells of the BM (as well some AML cells), these proteins are also likely to be important in vivo. Particularly, as short-term exposure to bulk HS-5 factors was sufficient to modulate the sensitivity of primary AML cells to targeted kinase inhibitors. Thus, implying that proteins endogenous to the BMSM can modulate signalling activity in AML cells away from inherent signalling node dependencies. CyTOF analysis revealed the AML cells maintained long term developed expression of microenvironment sensing molecules and markers symptomatic of aggressive disease, which respond poorly to treatment. It remained to be proven, however, the means by which the stromal secretome and cells of the microenvironment modulate AML behaviour. This was the aim of the work described in the following chapter.

Chapter 5: Determining the heterogeneity of AML cell signalling and the response of the phosphoproteome to BMSM stimulation

5.1 Introduction and aims of the study

Results described in Chapter 3 and 4 identified that MS-5 and HS-5 derived secretomes along with selected components S100-A4, S100-A11, CTGF, BMP-1, CSF-1 and HGF support AML cell survival. Chapter 4 also revealed the heterogeneity in response to these proteins as well as the effects that stromal GFs can have on the viability and growth of primary AML.

Building on these findings we sought to map the signalling that underpinned the functional data produced so far. As we observed that the patient response varied during both bulk stromal secretomes and individual GF treatments, it was speculated that these conditions likely activated different signalling nodes and that each patient AML's dependency on those nodes, was responsible for the heterogeneity observed in the previous chapter.

Once the topology of single GF stimulation on cell signalling pathways was established in these AML patient cells, signalling experiments could be expanded to characterise patient response to bulk HS-5 secretome. In Chapter 3 we observed that HS-5 CM was the most supportive media. This biologically relevant and complex stimulant was utilised to stimulate a number of patient samples and map the effected signalling nodes. Following the literature and previous genomic studies (23, 32) it was unlikely that there would be considerable consensus for activated signalling nodes in these experiments. AML is a group of diseases which possess distinct clinicopathologic and genomic signatures that present with the classical expansion of myeloblasts in the BM (490). Therefore, AML is profoundly heterogeneous due to various routes of leukaemogenesis. In each patient sample the formation of kinase networks will be somewhat distinct from patient to patient, thus it was hypothesised that HS-5 CM would possess a broad range of agonists to adequately monitor stromal derived factors effects on kinase network activity.

Secretomic stimulation of AML signalling pathways is one mechanism for stromal cells to influence AML cell signalling which is a form of chemical signalling as discussed in Chapter 1. It is a well described means of communication that facilitates heterotypic signalling (491) (Figure 5.1A). This however, does not adequately encompass the communication that occurs between leukaemic blasts and the BMSM, as cell-cell adhesion is a well described phenomenon in this scenario that can serve to promote malignant haematopoietic cell survival (60, 492-496) (Figure 5.1B). In addition to these studies there is a strong body of research investigating integrins role in leukaemic blast interaction with cells of the BMSM in the context of both AML and acute

lymphoblastic leukaemia (ALL) (495). Integrins which are surface glycoproteins enable leukaemic cell adhesion to the extracellular matrix, as well as crucially, integrin receptors of BMSM cells (497, 498). Examples of this type of interaction include integrin β3 signalling and very late antigen 4 (VLA-4) binding to stromal adhesion molecules vascular cell adhesion molecule 1 (VCAM-1), OPN and fibronectin (492, 499-502). All of these interactions have been shown to activate critical pro-survival and proliferative nodes in leukaemic blasts and BMSM cells. The best described example includes the interaction of ALL blasts with BMSM cells, which led to the subsequent activation of NF-κβ signalling in surrounding stromal cells (503).

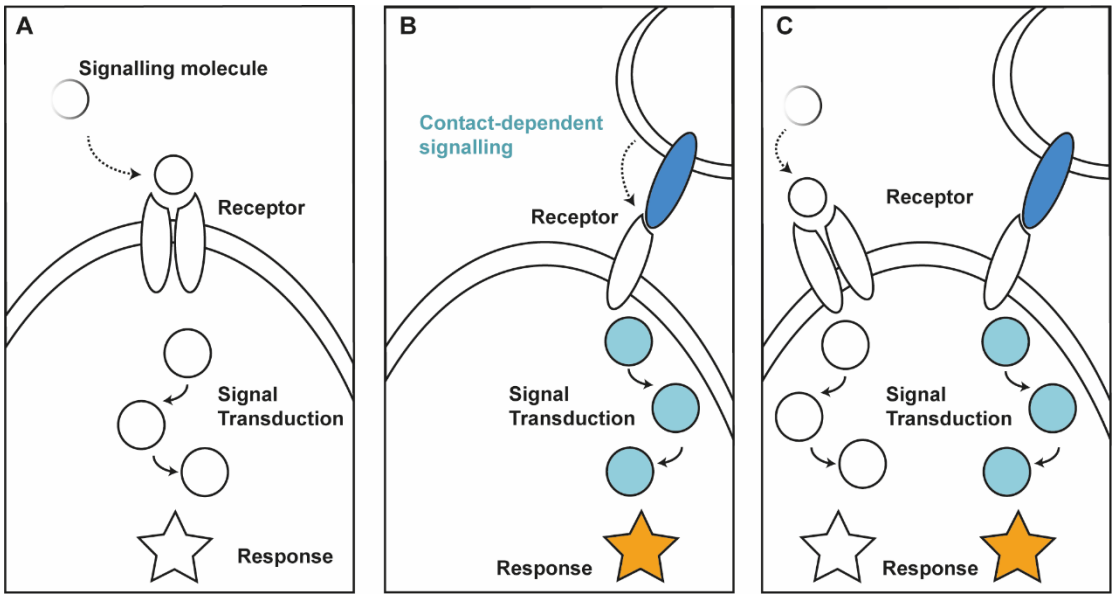

Figure 5.1: Concept of cell signalling and the means of signal transduction. (A) Chemical signalling, signalling molecule binds to complimentary receptor leading to a series of molecular events - commonly phosphorylation mediated by protein or lipid kinases, culminating in a cellular response. **(B)** Contact-dependent signalling, membrane bound-ligands (notch), integrins, ECM proteins (fibronectin) or surface glycoproteins on one cell interact with the appropriate receptor on an adjacent cell, initiating signal transduction. **(C)** Complex communication networks enable non-cell autonomous responses.

We proposed that a primary co-culture between AML blasts and the MS-5 cell line (represents the BMSM), would expand upon previous models that have been used to study the intricate cross talk between these populations and mediate leukaemia progression (144, 504, 505). The aim was that this model coupled with MS based phosphoproteomics would enable characterisation of the AML-BMSM signalling as represented in Figure 5.1C.

In this chapter we aimed to:

(i) Dissect the signalling nodes that are activated in AML cells following RP panel stimulation.

(ii) Characterise kinase activity heterogeneity in patients to bulk HS-5 CM.

(iii) Establish the heterotypic signalling that exists between BMSCs and AML cells, utilising AML-BMSM cell co-culture.

5.2 Analysis of AML signalling response to network perturbation following GF stimulation

5.2.1 GF response of major signalling nodes

Having established a panel of RPs that are secreted by both MS-5 and HS-5 cells that possess the capacity to extend primary AML ex vivo survival, as well as positively regulate cell proliferation, it was sought to understand how these proteins activated signalling pathways within an AML network. It was hypothesised that, the signalling axis MAPK and PI3K/AKT/mTOR would likely be perturbed by these signalling molecules due to the effects of HS-5 conditioned medium on AML sensitivity to targeted inhibitors of these pathways in Chapter 4.

The RPs were first used to treat the AML cell line P31/FUJ. This cell line is very resistant to chemotherapy agents and is an M5 FAB classification, therefore it displays a higher level of differentiation and should express more surface receptors than some of the less differentiated cell lines such as CTS.

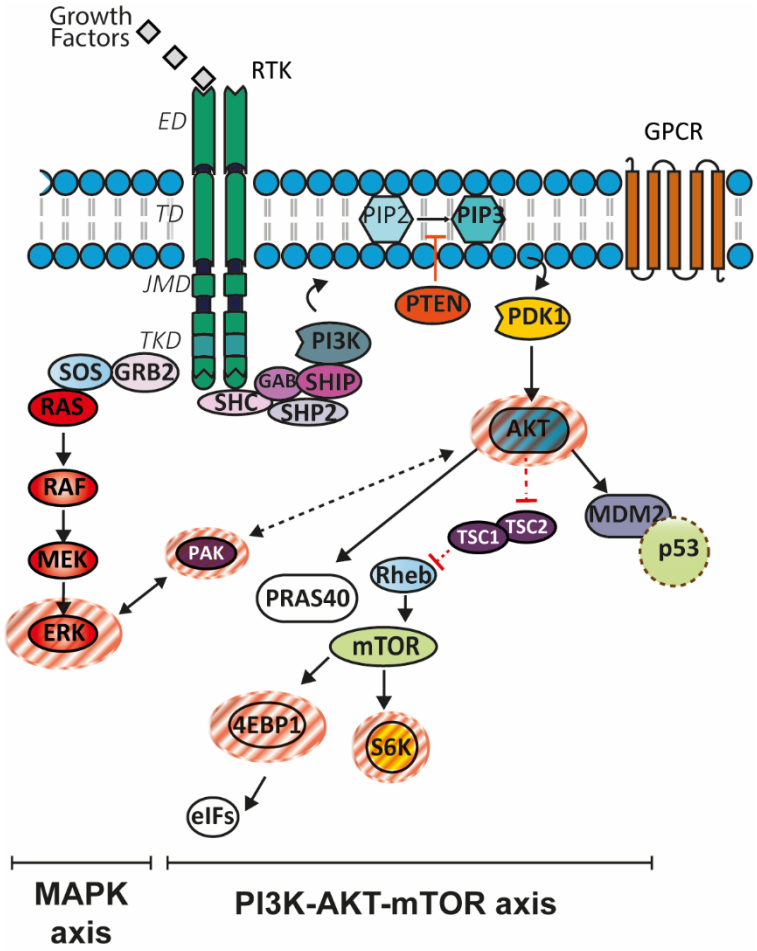

Figure 5.2: MAPK and PI3K-AKT-mTOR signalling axis. Red circles denote targets assessed by western blot.

P31/FUJ cells were serum starved for 4 hours to bring basal signalling levels in P31/FUJ cells to a basal state. Subsequently cells were stimulated for 15 minutes with 10ng/ml of each

of the recombinant GFs, as well as all the GFs combined and the MS-5 secretome (10ug/ml). We observed that CSF-1 and the MS-5 secretome induced downstream activity in MAPK signalling axis, with a modest increase represented by phosphorylation of ERK1$^{T185/Y187}$/ERK2$^{T202/Y204}$ (Figure 5.3). More significant was the phosphorylation of ERK1$^{T185/Y187}$ in the mixed GF sample, which was substantially increased compared to that of the starved sample and the phosphorylation observed in the CSF-1 and secretome samples. Stimulation with the remaining GFs was insufficient to activate the MAPK signalling axis in P31 cells.

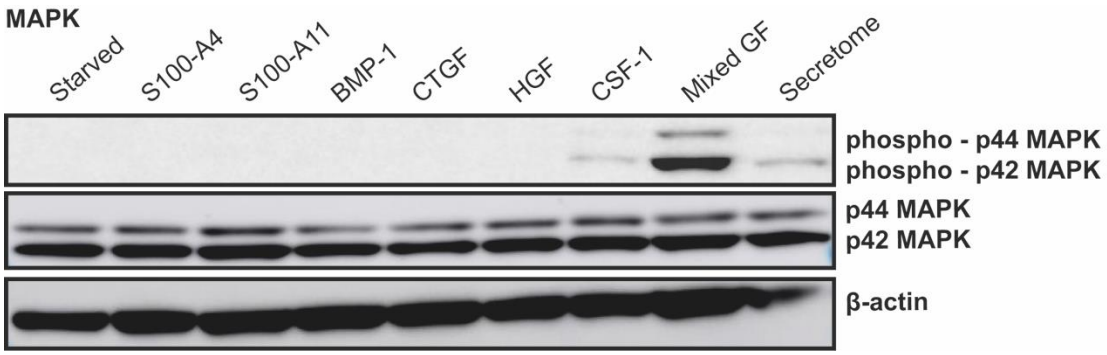

Figure 5.3: Western blot analysis of MAPK signalling in P31/FUJ cells. Cells starved 4hr prior to 15 minutes stimulation with 10ng/ml of recombinant factor. Western blots for the activatory phosphorylation sites on ERK1/2. Loading controls for the total p44 and p42 MAPK proteins and B-actin are shown in each case.

Assessment of the PI3K-AKT-mTOR signalling axis was more complex than that of the MAPK pathway. First observing AKT status in P31/FUJ cells stimulated with the GFs revealed the preference P31/FUJ cells have on the pathway, with AKT^{S473} phosphorylation elevated in serum starved cells (Figure 5.3A). Each of the GFs maintained AKT phosphorylation, with the complex mixtures (Mixed GF and secretome) resulting in the stongest bands, HGF was the only GF to decrease AKT phosphorylation.

Downstream of AKT in the signalling axis is mTOR (506, 507). To assess the recombinant factors effects on mTOR activity, known mTOR substrate p70 S6K was measured at p70^{T389} and p85$^{T412\ (508,\ 509)}$, mTOR has been described as positively responding to the environment through activation of p70 S6K and these phosphorylation sites are critical for the activation of p70 S6K (510). Analysis revealed that again there was activity in the pathway following 4 hours of starvation, however, there was also strong phosphorylation of the pathway in the Mixed GF and secretome samples (Figure 5.3B). These findings correlated with the observations from Chapter 4 where increased sensitivity of primary AML cells to Torin-1 was observed in the presence of HS-5 stromal factors (Figure 4.8). This suggested that the combination of these factors that are represented in both the Mixed GF and stromal secretome samples are capable of activating mTOR and therefore increase AML cell sensitivity to Torin-1 treatment. It is worth noting the

CTGF and HGF treatment alone reduced the phosphorylation of p70 S6K compared to that expressed in the serum starved control.

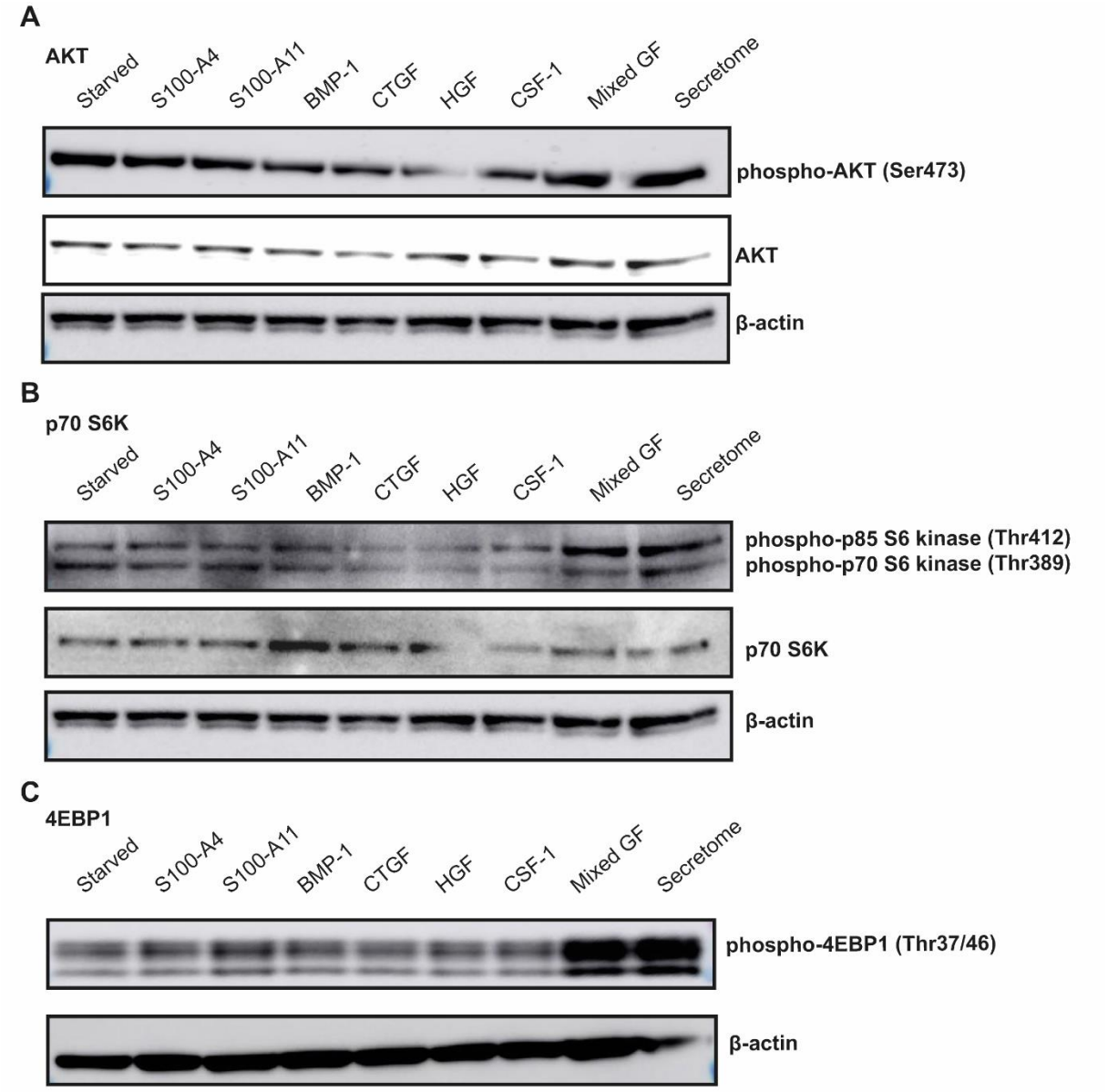

Figure 5.4: Western blot analysis of AKT/mTOR signalling in P31/FUJ cells. Cells starved 4hr prior to 15 minutes stimulation with 10ng/ml of recombinant factor. **(A)** Western blots for the activatory phosphorylation sites on AKT, mTOR activation markers **(B)** p70 S6K and **(C)** 4EBP1. Loading controls for the total proteins and B-actin are shown in each case.

4EBP1 is another substrate that is regulated by mTOR (511). 4EBP1 is a translation inhibitor protein due to its binding of translation initiation factor eIF4E (512). This action is abrogated though by phosphorylation of Ser65 and Thr70 (513), and mTOR primes 4EBP1 for this phosphorylation by phosphorylating residues Thr37 and Thr46 (514). Assessment of 4EBP1 status following stimulation with the GFs revealed that the s100 proteins A4 and A11 slightly increased phosphorylation of the Thr37 and Thr46 residues, with little change observed in these markers between starved and the rest of the single GFs (Figure 5.4C). Stimulating P31/FUJ cells with more complex mixtures however, profoundly impacted phosphorylation of 4EBP1 at these

sites, with both Mixed GF and MS-5 secretome stimulation driving expression markers associated with cell growth and translation initiation. These finding suggest that the individual GFs alone were not enough to stimulate upstream pathways sufficiently to impact on downstream targets like 4EBP1. However, the binding of upstream receptors (multiple or the same) with numerous molecules was potent enough to modulate 4EBP1.

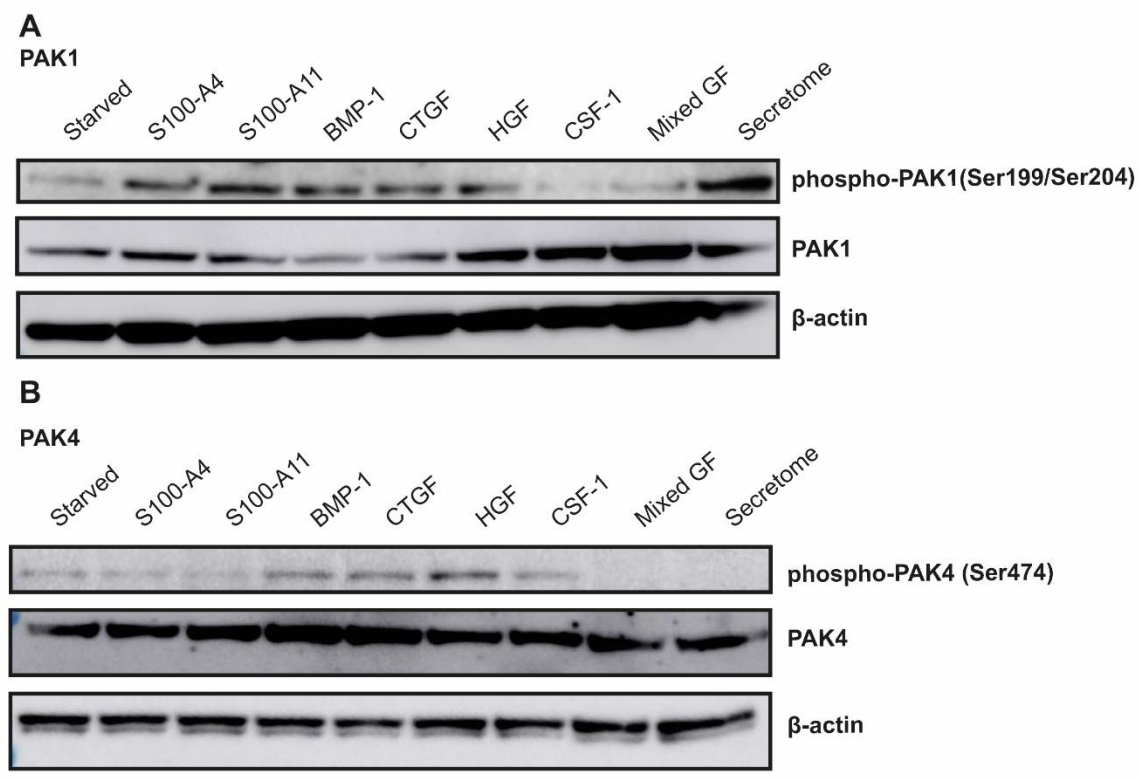

Figure 5.5: Western blot analysis of PAK signalling in P31/FUJ cells. Cells starved 1hr prior to 15 minutes stimulation with 10ng/ml of recombinant factor. **(A)** Western blots for the activatory phosphorylation sites of group 1 PAK1 (Ser199; Ser204) and group 2 **(B)** PAK4 (Ser474). Loading controls for the total proteins and B-actin are shown in each case.

The PAKs are a group of kinases that were hypothesised to be important due to PAKs potential to facilitate AML-stromal crosstalk. PAK is a kinase observed as being frequently overactive in AML (206, 207, 271) and PAKs functions range from cell migration, survival, proliferation and actin cytoskeleton remodelling (515). In Chapter 3 it was observed that the MS-5 stromal secretome was able to induce PAK1 phosphorylation, and kinase inhibition studies in Chapter 4 revealed that the PAK specific inhibitor PF-3758309, which has more selectivity towards group 2 PAKs (such as PAK4), was very effective at inducing cell death in primary AML cells. In accordance with results from Chapter 3, secretome stimulation of P31/FUJ cells leads to strong PAK1^{S199} phosphorylation, a surrogate marker of induced kinase activity (516, 517). Treatment with HGF also phosphorylated PAK1^{S199} which has previously been observed as being able to activate PAK via Rac (518). Most of the GFs individually activated PAK1 except CSF-1 which inhibited PAK1^{S199} phosphorylation (Figure 5.5A). Unlike the secretome treatment, Mixed

GF treatment of P31/FUJ cells was insufficient to phosphorylate PAK1^{S199}. As each of the GFs were individually capable of inducing PAK1 phosphorylation except CSF-1, it may be that CSF-1's inhibitory effect was dominant over the other GFs.

The phosphorylation of PAK4, marketed as the primary target of PF-3758309, was examined following recombinant GF treatment (Figure 5.5B). PAK4 has not previously been linked with AML, but all primary AML samples were very sensitive to its chemical inhibition. Western blot analysis showed that BMP-1, CTGF and HGF induce phosphorylation of PAK4^{S474} (marker of activity), as with PAK1, the combined mixture of GFs did not induce phosphorylation. Unlike PAK1, the secretome was unable to induce phosphorylation in PAK4^{S474}.

5.2.2 Phosphoproteomic analysis of GF stimulated primary AML cells

Western blot analysis of P31/FUJ individually treated with the stromal GFs confirmed that these proteins at a concentration of 10ng/ml were capable of inducing changes in key signalling nodes that are important in cell function and thought to be important in AML progression. These studies however, only observed changes to an AML cell line and AML cell lines are not truly representative of AML biology – principally as cell lines are able to survive independently, a characteristic that primary AML cells do not possess. Resultantly we felt it appropriate to study these GF effects in primary AML cells, as it was likely that the P31/FUJ cells were not responding to the GFs in a manner that cells dependent on the microenvironment and the stromal secretome would. This raised the possibility that in cell lines we could be observing changes that would not occur in primary AML cells, as well as minimising the potential impact these GFs could have on AML cell signalling and cell survival.

In Chapter 4 primary patient samples had a very strong albeit heterogeneous response to the panel of recombinant GFs. Due to the number of proteins in the panel, it was reasoned that selecting one patient that displayed a strong functional response to the proteins would be a good approach to establish pathways that mediate AML survival, as well as mechanistically determine how these proteins support AML. Therefore, patient #1 was selected for experimentation as these patient cells responded in a very pronounced manner to S100-A4 and Mixed GF stimulation during proliferation assays (Figure 5.6), additionally CSF-1 was very effective at maintaining viability in these cells.

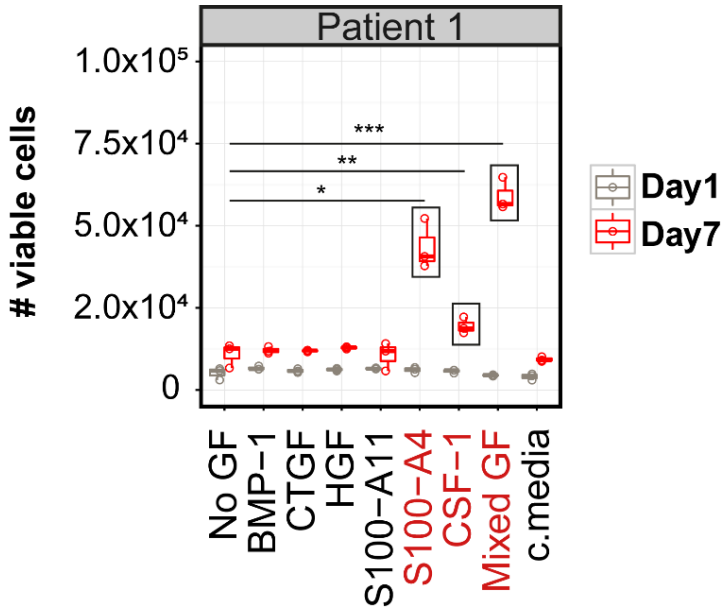

Figure 5.6: Patient #1 selected to for phosphoproteomic analysis based on functional response to GF stimulation. Results from Chapter 4 that demonstrate treatment with S100-A4, CSF-1 and Mixed GF conditions elicit statistically significant changes in patient #1 AML cell growth. * denotes p-value <0.05 **<0.01 ***<0.001, n=4 technical replicates per condition.

For phosphoproteomic analysis of patient #1 AML cell response to the stromal secretome derived proteins, cells were first serum starved for 60 minutes prior to stimulation with the GFs. Serum starvation was employed as it was reasoned that the serum GFs and cytokines could activate many pathways that otherwise would be inactive, possibly masking the effects of the stromal derived proteins. To control for the serum starvation a 'No GF' condition was included in which cells were starved and then processed, with no GF treatment. Secondly a 'basal' condition was included where for the duration of the starvation and stimulation patient #1 cells were kept in serum complete IMDM media prior to processing with the rest of the samples. In GF stimulated samples, once patient #1 cells had been starved for 60 minutes, 10ng/ml of the chosen GF or 10µg/ml of bulk secretome were spiked into the media. Cells were then stimulated for 15 minutes to capture early phosphorylation events that were induced by the receptor binding of these GFs. The full experimental design is outlined below in Figure 5.7.

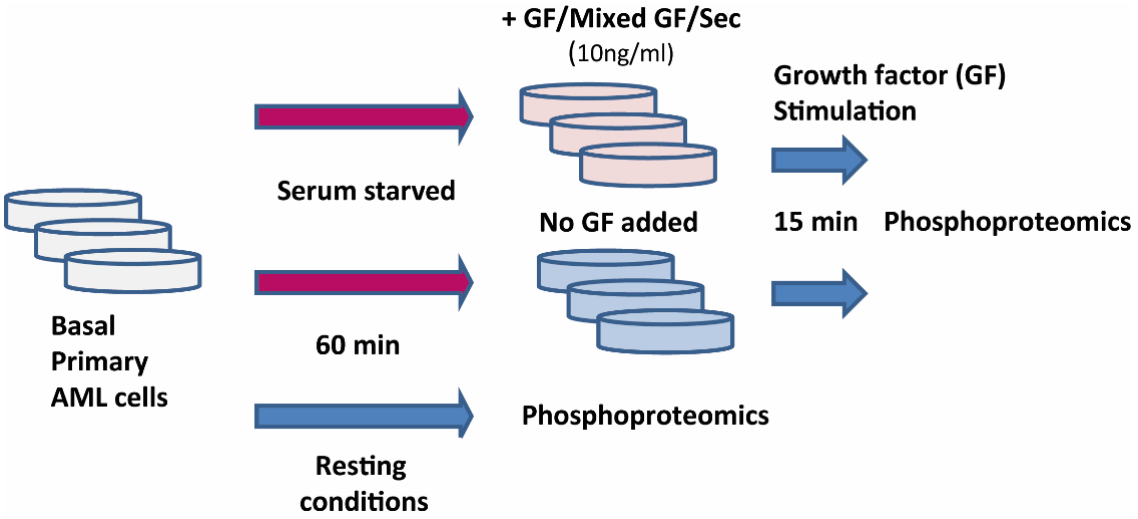

Figure 5.7: Experimental design used to define the activity of kinase signalling following growth factor stimulation. Primary AML cells from patient #1 were reanimated and starved 1hr prior to 15 minutes stimulation with 10ng/ml of single GF or Mixed GFs, 10µg/ml MS-5 secretome or starved only. In parallel resting cells that were not starved were also processed (basal). The cells were then lysed, proteins digested, and phosphopeptides enriched using TiO_2. Each sample was then analysed by LC-MS/MS in triplicate. This MS data was searched against the Swissprot database using MASCOT and the subsequent output of peptide identifications were combined to make a unique database. Each phosphopeptide within the database was then quantified using in house software PESCAL and the quantitative data analysed using a combination of Excel and R environments.

5.2.2.1 Mass spectrometry data quality control

To assess the quality of the data derived through mass spectrometry experiments, quality control steps were undertaken regarding the datasets which included quantification of the area under the total ions chromatogram (TIC) (Figure 5.8A); assessment of the identity assignment to each phosphopeptide (Figure 5.8B); assessment of the chromatography linearity by calculating the linear relation in retention times across all samples (Figure 5.8C); evaluation of the distribution of phosphopeptide intensities; and determination of intensity normalisation efficiency that is employed to remove technical noise (Figure 5.8D).

The performance of an LC-MS/MS run can be estimated by calculating the sum of the area under the chromatographic peaks per scan before totalling. Xcalibur software was used to visualise TIC intensities and quantification of the sum of chromatographic areas determined the mean intensity was in the E^{12} range (Fig 5.8A). Following protein identification using the MASCOT database, the number of peptide ions whose identity was assigned with high confidence (FDR<0.05) for each of the total 30 LC-MS/MS runs that were used to generate the database were determined. A total of 3,857 unique phosphopeptide ions were identified with FDR<0.05, which is less than previous experiments generated in the same laboratory (Fig 5.8B) (215), however, those experiments utilised cell lines and not primary tissue so it is possible that the lower than expected number of identifications was down to the fragile nature of the source material. The accuracy of the peptide quantitation that is performed by the PESCAL algorithm relies upon accurate retention time alignment (tR). This was assessed by tracing the tR which

are populated in a database for each peptide ion for all the samples. The linearity of the pairwise alignments between peptide retention times of two samples illustrates the consistency in of tR alignments (Figure 5.8C). Finally, after label-free quantification by the PESCAL algorithm, the data were log_2 transformed. Normal distribution of the data was deduced by visual inspection of the peptide intensities, which enabled following parametric statistical analyses (Figure 5.8D). Normalisation of the Log_2-transformed data and inspection of these data proved the capacity of normalisation to make distributions across the samples homogenous in statistical properties.

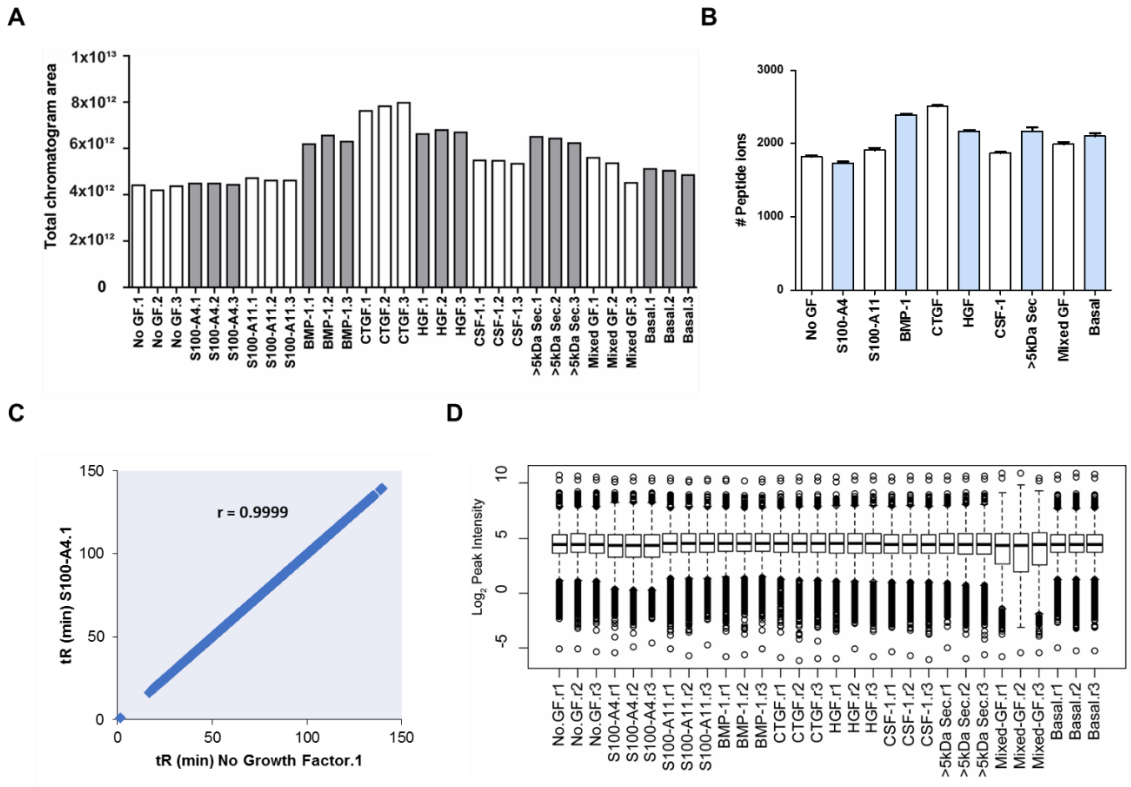

Figure 5.8: Quality control of MS data used to analyse the phosphoproteomes of GF stimulated AML cells. (A) Quantification of total area under the chromatographic peaks contained in 30 LC-MS/MS runs. **(B)** The average number of identified peptide ions (FDR<0.05) per condition across 30 LC-MS/MS to generate the phosphopeptide database. **(C)** Representative alignment between retention times of two experimental. **(D)** Box plots demonstrating the distribution of log2-transformed peptide peak intensities post-quantile normalisation.

The steps undertaken to assess the quality of these experiments advocate the quality of the dataset and demonstrate that the pre-processing applied is capable of removing confounding variables. It was therefore appropriate to conduct downstream analysis of this dataset to draw conclusions on the effects of the stromal secretome derived proteins on the AML phosphoproteome.

5.2.2.2 Differential abundance induced by GF stimulation

The data shown in Figure 5.9 served as preliminary indication of the differential modulation of the phosphoproteomes of patient #1 following 15 minutes stimulation with the recombinant factors in comparison to the phosphoproteome patient #1 cells that had not been stimulated with a single GF or combination of factors.

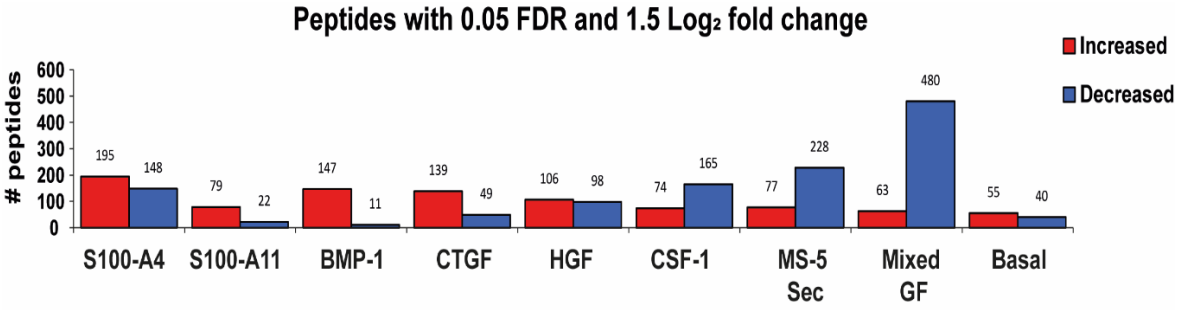

Figure 5.9: Differential abundance analysis of the patient #1 phosphoproteomics data following GF stimulation. Differential abundance analysis of the phosphoproteomics data. The number of phosphopeptides either significantly increased (red) or decreased (blue) in abundance are shown when compared to starved patient #1 that were not subjected to GF stimulation. Fold change, log_2 fold-change vs No GF control; adjusted P, is the corrected P-value for multiple testing by the Benjamini-Hochberg method.

The experimental condition that generated the greatest global increase in phosphopeptide expression was from S100-A4 treatment (195 phosphopeptides), which was also the GF that generated the most proliferation in previous functional experiments, and the condition that yielded the least change when compared to starved cells was generated by the basal conditions.

The notable trend in this dataset was the decrease in phosphopeptide expression following GF stimulation that occurs in CSF-1, Mixed GF and MS-5 secretome conditions. In particular the Mixed GF condition induced a significant decrease in phosphopeptide expression with 480 peptides decreasing by 1.5 Log_2 fold that were significant compared to unstimulated cells.

5.2.2.3 Associations between patient #1 AML phosphoproteomes following stimulation with GFs

To compare the phosphoproteomes of patient #1 cells following treatment, hierarchical clustering of the phosphopeptide fold changes between GF stimulated and unstimulated samples was performed as presented in Figure 5.10. This analysis demonstrated that the two phosphoproteomes that were globally remarkably different to the unstimulated and basal samples were that of the Mixed GF and S100-A4 stimulated cells. The basal phosphoproteome

was not too dissimilar to the unstimulated sample, which was reassuring as it suggested that the starvation did not significantly compromise the cells.

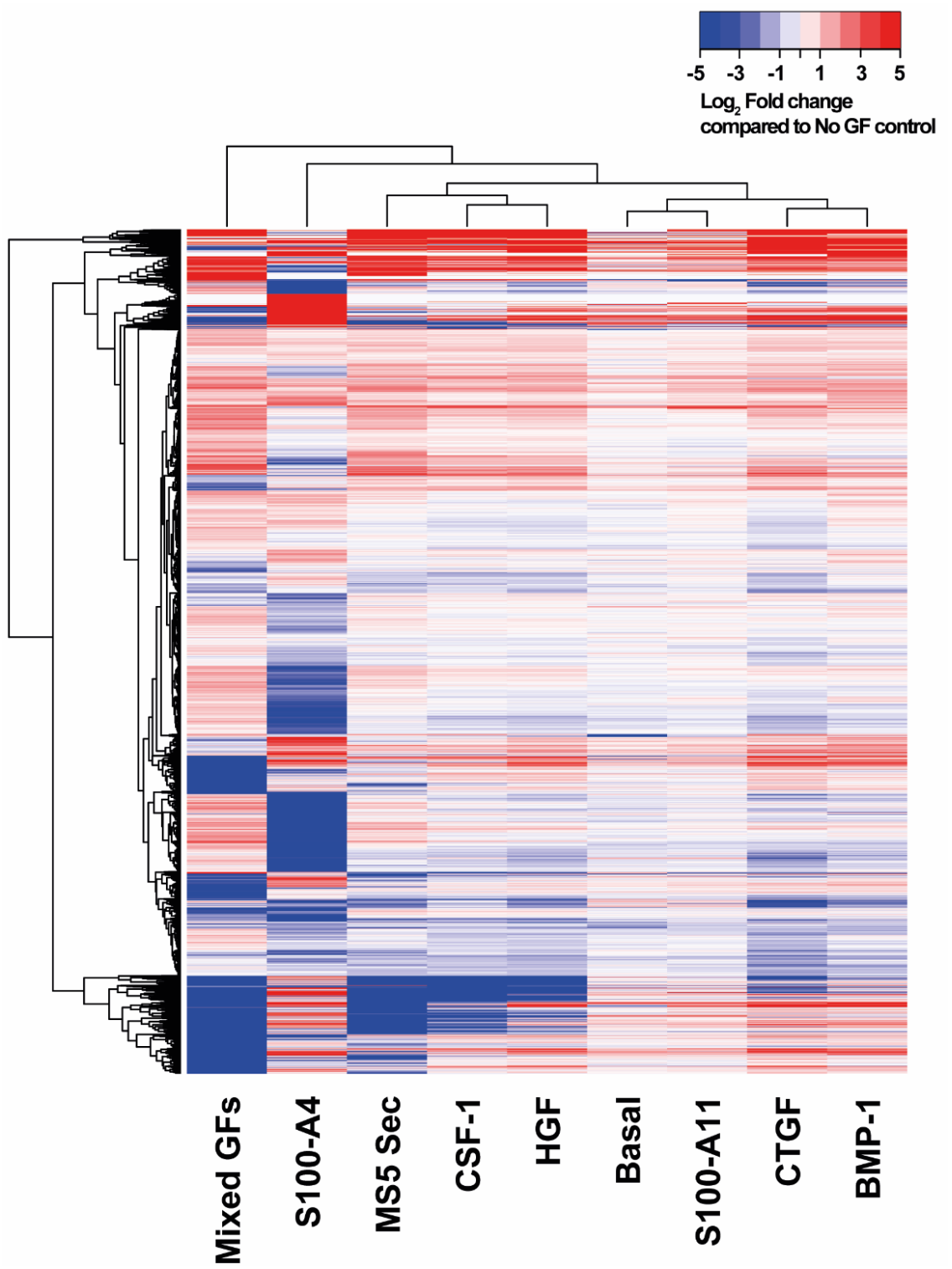

Figure 5.10: Hierarchical clustering analysis of recombinant factor stimulated phosphopeptide expression in patient #1 cells. Heatmap represents the Log2 Fold change phosphopeptide expression of patients #1 cells following (10ng/ml) GF stimulation compared to unstimulated patient #1 cells. Expression averaged across 3 analytical replicates, heatmap and dendrograms produced using ggplots package in R workspace.

This pattern of clustering suggested that S100-A4 was the GF contributing to the proliferative phenotype observed in patient #1 following Mixed GF treatment, as this sample

group closest to the Mixed GF sample. CSF-1 and HGF clustered together with the MS5 secretome treated cells, and had a similar expression profile to that of the Mixed GF sample. CTGF and BMP-1 on the other hand, did not cluster with the Mixed GF sample.

5.2.2.4 KSEA analysis of phosphoproteomes to examine differences in kinase activity

Kinase substrate enrichment analysis as described in the methods (section 2.12), is an approach to infer kinase activity from the phosphoproteomics data. The method groups substrates into sets that are known to be phosphorylated by a particular kinase and global differences in the abundance of these substrate groups across samples enables the inference of kinase activity. In this analysis, KSEA can indicate kinases in patient #1 cells that putatively increased or decreased following GF stimulation by comparing the expression of substrate groups to that recorded in the No GF stimulation samples (Figure 5.11).

Systematic assessment of putative kinase activity changes in patient #1 cells following GF stimulation showed that S100-A4 treatment lead to potent increases in casein kinase 2 subunit alpha (CK2A2), Lck kinase, InsR and ATR. Secondary to these increases were putative increases in AKT, Src and glycogen synthase kinase-3 beta (GSK3B) activities. All of these kinases that increased in activity are implicated in cell growth and proliferation. The kinases that significantly decreased in activity following S100-A4 treatment were casein kinase 1 alpha isoform (CK1A), casein kinase 2 alpha subunit (CK2A1) and homeodomain-interacting protein kinase 2 (HIPK2). These kinases have defined roles in p53 mediated apoptosis.

S100-A11 treatment in this experiment led to strong putative increases in mTOR activity, with activity also detected in the Fes tyrosine kinase and cyclin dependent kinase 1 (CDK1). Protein kinase C alpha (PKCA), Calcium/calmodulin-dependent protein kinase type 1 (CAMK1A), PAK1, Rho-associated protein kinase 1 (ROCK1), citron rho-interacting kinase (CRIK), MRCKA, myosin light chain kinase (smMLCK) all decreased in activity compared to the untreated cells.

BMP-1 treatment strongly activated mTOR, ERK1, ERK2, CDK1 and S6K kinases in primary AML cells compared to untreated cells. To a lesser extent Fes and CK2A1 were also more active compared to untreated cells. BMP-1 treatment led to a significant drop in Rho kinases including ROCK1, MRCKA, CRIK and smMLCK.

CTGF treatment in patient #1 cells putatively activated mTOR signalling as well as its upstream binding partner AKT1, the only other kinases to significantly increase in activity were ERK1 and ERK2. Putative kinase activities that relatively decreased to that of the untreated samples were CK1A, ATR, p70S6K, CK2A1 and the Rho kinases (ROCK1, MRCKA, CRIK and smMLCK).

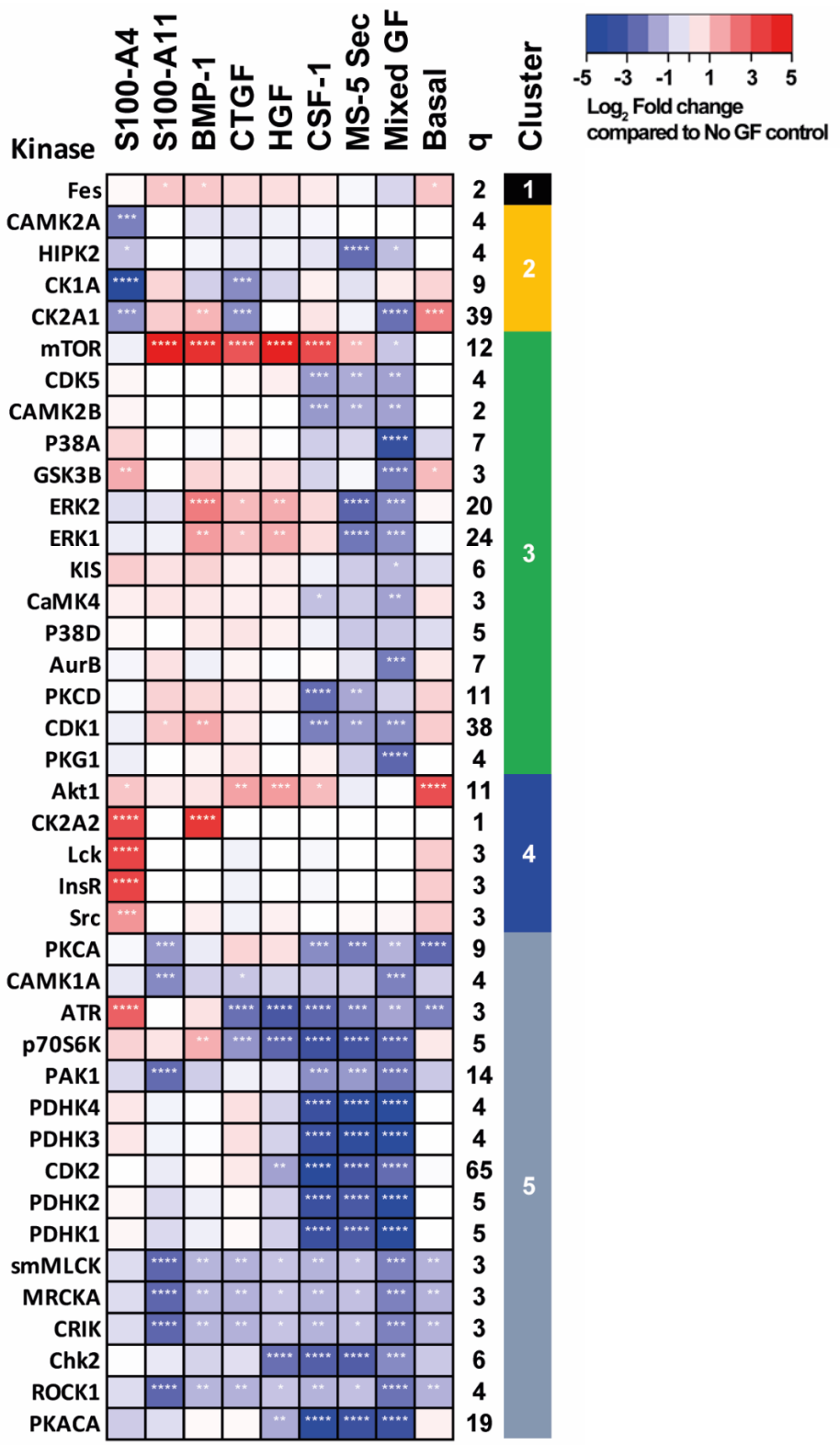

Figure 5.11: Heatmap of kinase substrate enrichment analysis (KSEA). The phosphorylation status of known kinase substrates are quantified and compared between (10ng/ml) GF treatments to determine relative kinase activities in Patient #1 cells. Growth factor (GF), Mixed recombinant growth factors (Mixed GF), q – no of substrates. *p<0.05, ** p<0.01, *** p<0.001, **** p<0.0001

HGF treatment like CTGF treatment activated AKT1 and mTOR as well as the MAPK kinases ERK1 and ERK2. HGF however, also led to a decrease in p70S6K, DNA damage kinases ATR and checkpoint kinase 2 (chk2), and the Rho kinases ROCK1, MRCKA, CRIK and smMLCK.

CSF-1 treatment induced putative increases in AKT1 and mTOR activity and non-significantly increased ERK1 and ERK2 kinase activities. CSF-1 treatment led to a profound reduction in the putative kinase activity of the Rho kinases (ROCK1, PAK1, MRCKA, CRIK and smMLCKs), DNA damage kinases (ATR and Chk2), metabolic kinases pyruvate dehydrogenase kinases 1,2,3,4 (PDHK), cell cycle regulators (CDK1, CDK2, CDK5) and protein kinase c alpha and delta isoforms (PKCD and PKCA).

The complex secretome of MS-5 cells effected patient #1 kinase activity identically to CSF-1 treatment typified by the global putative reduction in activity except for three kinases. In addition, MS-5 secretome led to a decrease in ERK1, ERK2 and AKT1 activity. The Mixed GF sample profoundly reduced kinase activity relative to that of unstimulated patient #1 AML cells, further than that observed for the MS-5 secretome. No kinases were recorded as increasing in activity following treatment.

Comparing kinase activity in the resting basal sample to unstimulated (but starved) samples revealed a decrease in the activity of the Rho kinases, therefore starvation possibly increases the activity of these kinases in patient #1 cells. Additional kinases that were observed as less active following starvation were ATR and PKCA. Kinases that increased in activity following starvation included AKT1, CK2A1, GSK3B and Fes.

The PCA presented in Figure 5.12A demonstrates how the phosphoproteome/network of the patient #1 cells was most different following S100-A4 and Mixed GF (a greater distance from these points in PC space) compared to the no GF control sample. This was a robust response as it was observed in each of the replicates and reassuringly the phosphorylome of basal cells also occupied the same position in the PC-space as the no GF control. Equally, this showed that the patient #1 phosphoproteome following stimulation with CSF-1, HGF and BMP-1 did not significantly separate.

The data shown in Figure 5.10 also suggested that, as seen in Figure 5.12A, that patient #1 cells responded minimally to many of the single GF treatments. However, when taking into account another principal component, analysis reveals subtler changes in the signalling responses, and the routes through which the secretome derived GFs induced signals in patient #1 cells (Figure 5.12B). The PC space segregates into composites of s100 proteins (bottom left), complex mixtures (bottom right), metalloprotease (top left), GFs (top right) and the unstimulated and basal samples cluster together centrally. These observations support findings in Figures 4.4 and 4.5 and corroborate the hypothesis that these stromal derived proteins can have profound effects on AML signalling networks.

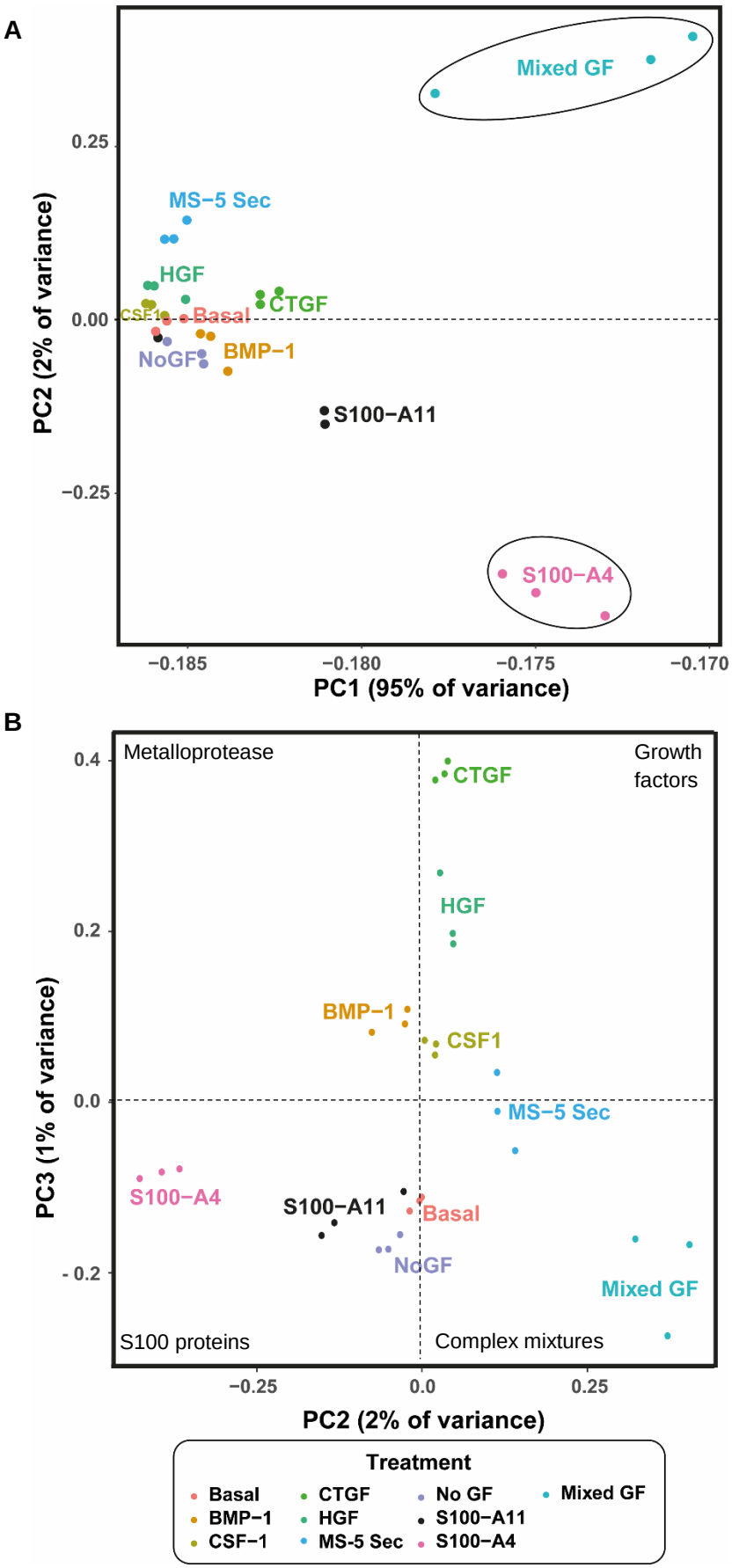

Figure 5.12: Multivariate analysis of GF stimulated patient #1 datasets highlights the distinct effect S100-A4 and Mixed GF conditions can have on the AML phosphorylome. PCA of the log2 fold-ratios for the 2,915 phosphopeptides that significantly changed in **(A)** PC1 vs PC2 and **(B)** PC2 vs PC3 (as shown in figure 5.10).

5.3 Characterise kinase activity heterogeneity in patients to bulk HS-5 conditioned media

The observations gathered in the last experiment confirmed that the panel of stromal derived GFs do in fact alter signalling networks in primary AML samples. However, the experiment only compared the effect of the GFs on AML signalling in one patient sample. Those experiments revealed particular aspects of AML signalling networks that are perturbed by single GF treatment, however, in reality the cells would not experience these proteins in isolation. Additionally, multi-variate analysis showed that secretome stimulation of AML cells lead to similar effects on the phosphoproteome to that observed for the Mixed GF condition. Therefore, it was hypothesised that bulk HS-5 CM could be used to understand the effects these signalling molecules have on a larger cohort of AML patient samples, while simultaneously assessing the heterogeneity of AML kinase network activity.

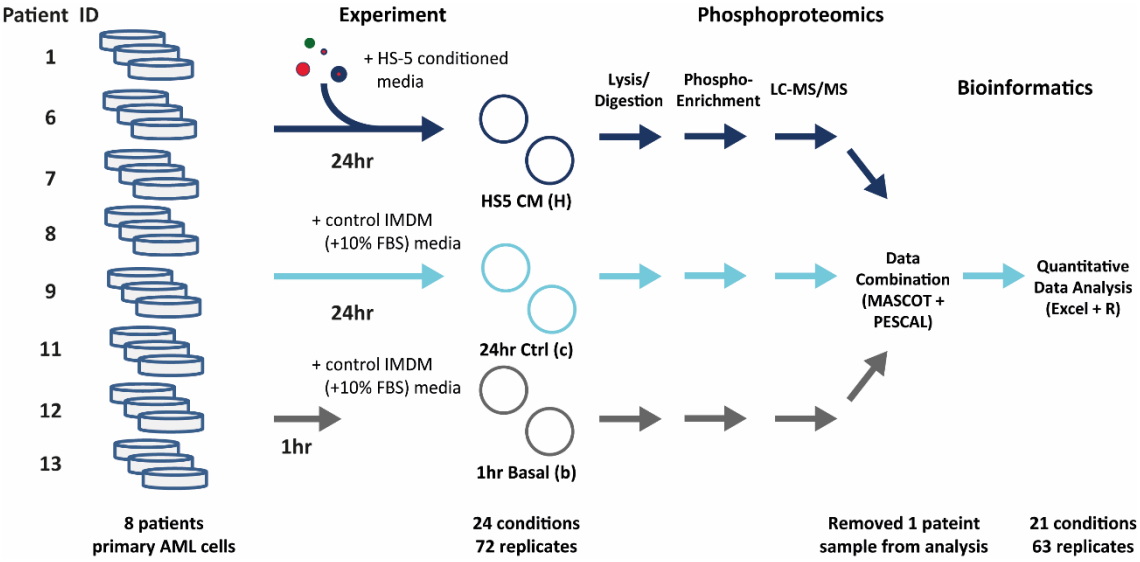

Figure 5.13: Experimental design to determine the heterogeneity in AML signalling network response to growth with HS-5 conditioned media.

Eight patient samples were obtained, and cells were reanimated before being seeded in one of three conditions. Each patient sample was seeded for 1 hour in control IMDM media (supplemented with 10% FBS), this condition was included to measure the endogenous baseline signalling that these cells employ. Patient samples were also kept for 24 hours in the IMDM control media, this was used to be able to control for the effects of culture, as well as the inevitable levels of hypothesised apoptosis – AML cells do not like being maintained ex vivo. The final test condition was to maintain cells in the supportive HS-5 CM for 24 hours to be able to visualise the heterogenic patient responses to the complex mixture of stromal proteins that make up HS-5 CM (full schematic detailed in Figure 5.13).

5.3.1 Differential abundance

Analysis of this experiment retrieved 19,484 peptides, of which 17,360 were phosphorylated (89.1% phospho-enrichment). The data shown in Figure 5.14 served as preliminary indication of the differential modulation of the phosphoproteomes of primary AML grown in HS-5 CM for 24 hours in comparison to the phosphoproteome of either basal or HS-5 independent primary AML cells.

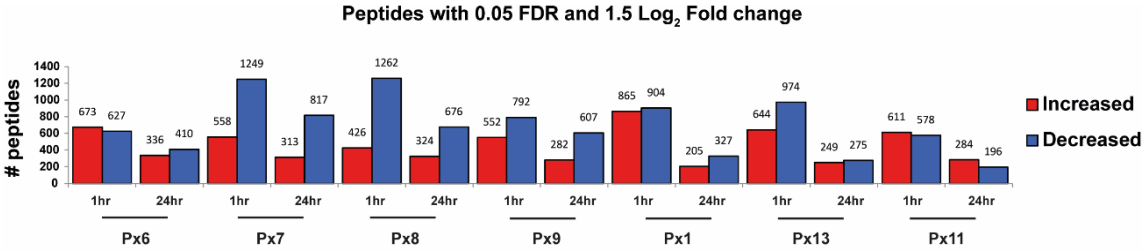

Figure 5.14: Differential abundance analysis of the primary AML phosphoproteomics data. Differential abundance analysis of the phosphoproteomics data. The number of phosphopeptides either significantly increased (red) or decreased (blue) in abundance compared to HS5 CM independent cells are shown. Fold change, log_2 fold-change vs 1hr Basal or 24hr HS5 independent control; adjusted *P*, is the corrected *P*-value for multiple testing by the Benjamini-Hochberg method.

5.3.2 Heterogeneous phosphoproteomic signature

In order to systematically analyse the biochemical modulations after maintaining primary AML cells with HS-5 CM or stromal independent media and establish how an expanded patient cohort behaves in response to stromal derived proteins, the phosphoproteomics dataset was filtered and clustered using k-means. This analysis included only those peptides that were significantly modulated in at least one condition compared to the 1 hour IMDM control and peptides were grouped into 9 clusters using the method described in Section 2.12.4.

The data shown in Figure 5.15 indicated that there were high levels of heterogeneity in phosphorylation kinetics upon culture with and without HS-5 CM between patient samples. For all clusters differences in the HS-5 maintained patient phosphoproteomes were more pronounced with the 1 hour control conditions, compared to the 24 hour control conditions (Figure 5.15A). Assessment of the nine k-means assigned clusters revealed that clusters 1, 2, 3, and 9 contained peptides that increased following HS-5 conditioning and clusters 4 and 5 went down respectively. Cluster 1 represented phosphopeptides that increased in expression for patients #1, #9, #11 and #13 following 24 hours of HS-5 conditioning, these peptides strongly enriched for many ontologies, of note was the alternative NF-kappa B pathway (Figure 5.15B).

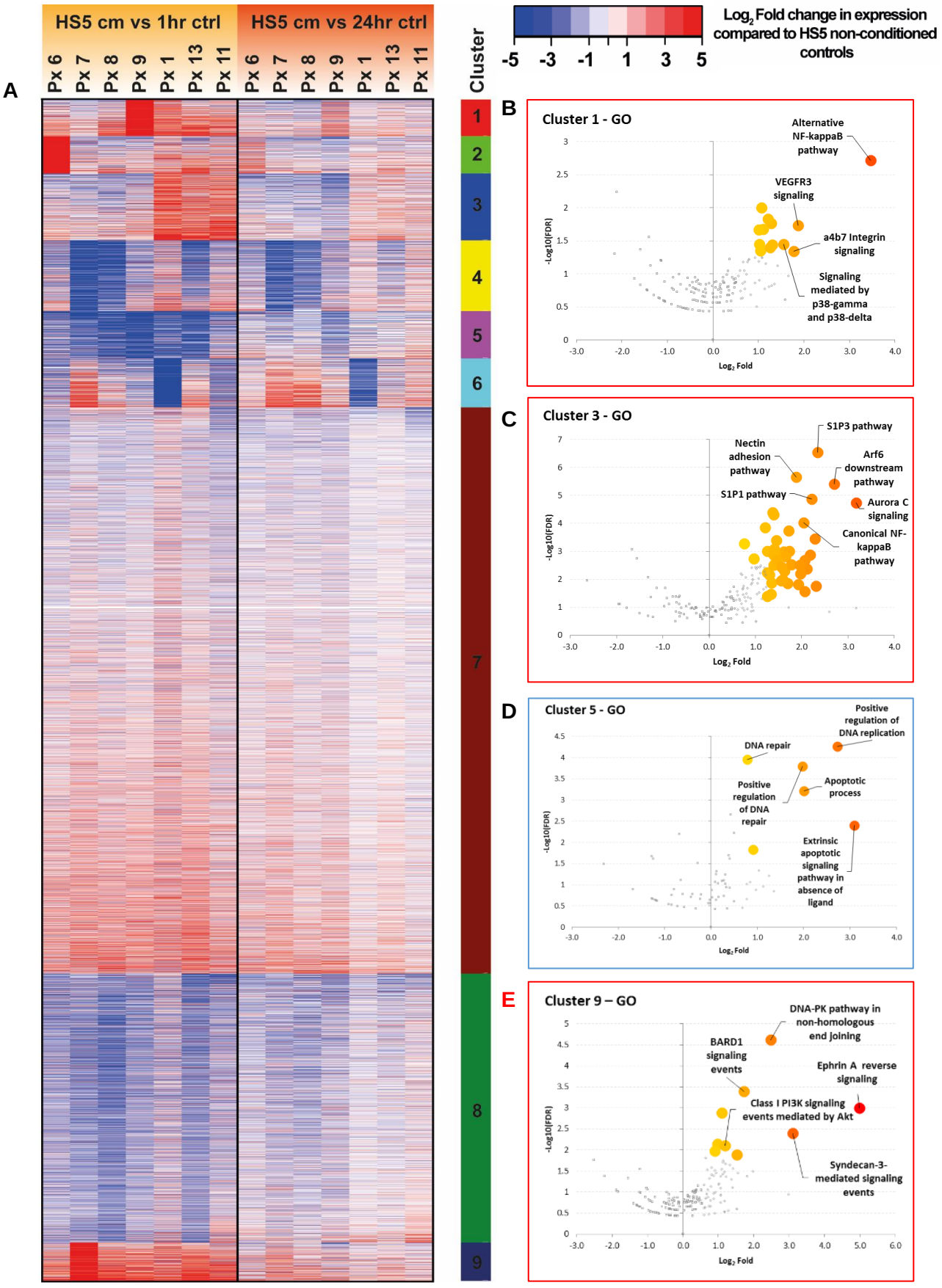

Figure 5.15: Heterogeneous response of primary AML to HS-5 conditioning. (A) Heatmap of the Log_2 fold-ratios for each of the phosphopeptides grown in HS-5 CM compared to no conditioning control. K-means clustering assigns phosphopeptides into 9 clusters each comparison n=3 technical replicates, GO analysis of clusters **(B)** 1, **(C)** 3, **(D)** 5 and **(E)** 9 displays enriched processes in respective cluster.

Cluster 3 contained phosphopeptides that increase following HS-5 conditioning (Figure 5.15C), with significant enrichment of the S1P3 pathway, NF-kB pathway and pathways associated with signal transduction that results in activation of MAPK and AKT. Cluster 9 represents phosphopeptides that were highly abundant after 24 hours, compared to 1 hour conditions and these phosphopeptides enriched for GOs associated with DNA-PK activity, BARD1 signalling events and PI3K signalling mediated by AKT (Figure 5.15E).

Clusters 4, 5, 6 and 8 demonstrate phosphopeptides that decreased in HS-5 conditioned cells compared to non-conditioned cells. Clusters 4 and 6 contain peptides that strongly decreased in patients #1, #7 and #8, however, cluster 5 contains phosphopeptides that decreased in all patients. GO analysis of these phosphopeptides revealed a consensus for DNA repair, and apoptotic signalling, suggesting that there was less DNA damage and cell death occurring in HS-5 conditioned samples than in the non-conditioned samples (Figure 5.15D).

5.3.3 Implementation of KSEA reveals temporal effects of HS-5 factors on kinase activity

KSEA analysis of this data echoed findings revealed by k-means analysis, principally that there was profound heterogeneity in both basal and HS-5 induced kinase activity between patient samples. The KSEA output was processed using a multivariate approach, hierarchical clustering demonstrated that samples separated by time with HS-5 conditioned samples compared to 1-hour and 24-hour controls segregating (Figure 5.16). One patient sample (patient #8) did not group with the other samples by time and instead both time points involving this sample clustered together. An observation that suggested this patient sample was not significantly modulated by the experimental conditions.

Assessment of kinase behaviour between the conditions revealed that kinase activity on average was higher in patient cells following 24 hours of cell culture than what was observed at 1 hour. Global kinase activity was substantially increased in HS-5 conditions compared to the kinase activity in the 1-hour controls, this difference was not as pronounced during comparison to the 24-hour controls. Notable kinases that putatively increase in activity over time included, the AKT-mTOR pathway (AKT1, mTOR, p70S6K, RSK2, p90RSK), substrates of the tyrosine kinases (Brk, Syk, Lck), Src, mitogen activated protein kinases (JNK1, JNK2, JNK3, MEK2), JAKs (JAK2, JAK3) and PAK1.

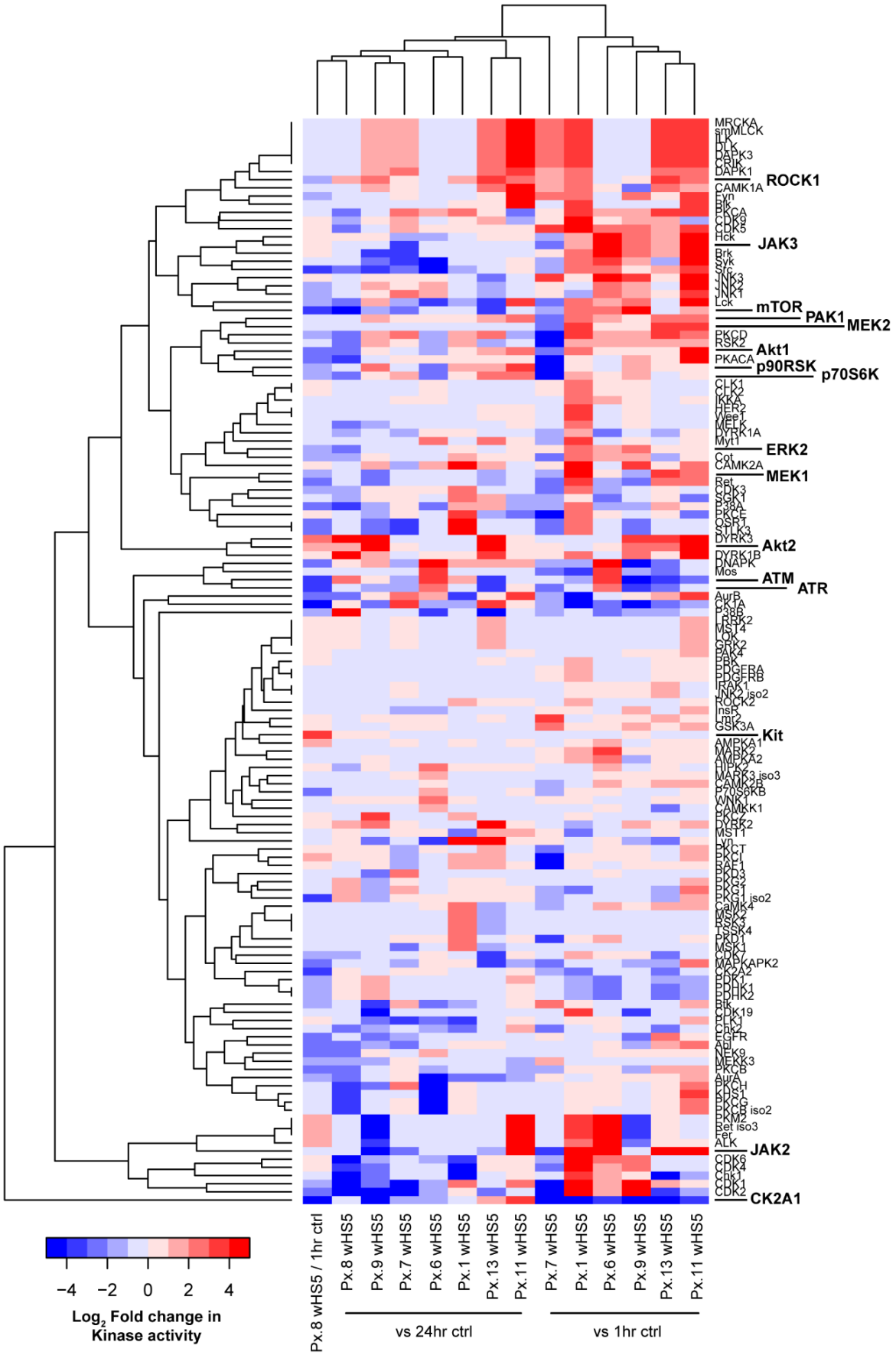

Figure 5.16: KSEA heatmap of temporal effects of HS-5 derived factors on AML kinase activity. The phosphorylation status of known kinase substrates were quantified and compared between HS-5 conditioning treatments to determine relative kinase activities, each comparison contains n=3 technical replicates. Heatmap and dendrograms produced using ggplots package in R workspace.

There were few kinases that demonstrated consistent HS-5 induced activity across the patient samples, however, there were kinases whose putative activity decreased in most patient samples following HS-5 conditioning, and these included CK2A1 and CK1A. Patient specific HS-5 induced kinase activities were observed in patient #6, in which DNA damage kinases DNAPK, ATM and ATR were all highly activated. Patient #8 was observed as having HS-5 induced putative activity of c-Kit, AKT2 and Dual specificity tyrosine-phosphorylation-regulated kinase 3 (DYRK3). Patient #1 had HS-5 induced high activity of JAK2 and patients #7, #11 and #13 all exhibited a consistent increase in kinase activity in a set of 9 kinases (MRCKA, smMLCK, ILK, DLK, DAPK1, DAPK3, CRIK, CamK1A and ROCK1).

5.3.4 Condensing the global and heterogeneous effects HS-5 conditioning has on seven primary AML phosphoproteomes

Having established that the effect of HS-5 CM had quite substantial effects on the phosphoproteome of these seven AML patient samples, thus causing sizable shift in kinase behaviour. PCA analysis of the phosphoproteomics data was undertaken in an effort to visualise if these very different AML proteomes globally responded in a similar manner to the influence of HS-5 cells. Analysis of PCA scores demonstrated the heterogeneity within this data set, with three PCs being required to reach a cumulative proportion of 0.9 and twenty PCs being required to fully comprise the variances within the data (Table 5.1).

Importance of components:	PC1	PC2	PC3	PC4	PC5	PC6	PC7
Standard deviation	4.013	1.02481	0.8875	0.71022	0.64069	0.5441	0.48071
Proportion of Variance	0.8052	0.05251	0.03938	0.02522	0.02052	0.0148	0.01155
Cumulative Proportion	0.8052	0.85772	0.8971	0.92232	0.94285	0.9577	0.9692
	PC8	PC9	PC10	PC11	PC12	PC13	PC14
Standard deviation	0.37307	0.32925	0.2849	0.24826	0.22384	0.20123	0.17032
Proportion of Variance	0.00696	0.00542	0.00406	0.00308	0.00251	0.00202	0.00145
Cumulative Proportion	0.97616	0.98158	0.98564	0.98872	0.99123	0.99325	0.9947
	PC15	PC16	PC17	PC18	PC19	PC20	
Standard deviation	0.16207	0.16059	0.13881	0.12497	0.1017	0.09325	
Proportion of Variance	0.00131	0.00129	0.00096	0.00078	0.00052	0.00043	
Cumulative Proportion	0.99601	0.9973	0.99827	0.99905	0.99957	1	

Table 5.1: Summary table of the PCA scores for the HS-5 phosphoproteomics analysis.

To capture the variance within the dataset a PCA was employed to represent the experiment (Figure 5.17). The heterogeneity of these samples was apparent by the lack of shared PC space occupied by any of the 1 hour basal control samples, all of these samples were positioned in distant locations, samples 6b, 7b, 8b and 13b do not cluster together. Interestingly HS-5 conditioning for five of the patient samples (6H, 7H, 8H, 9H, 11H and 13H) led these conditions to converge and cluster together centrally within the PC plot. Although 1H does not cluster with the other HS-5 treated samples. Next to 1H is also the respective 24-hour control of

this condition, suggesting that this sample did not respond to HS-5 conditioning, but responded to the stresses and influence of cell culture.

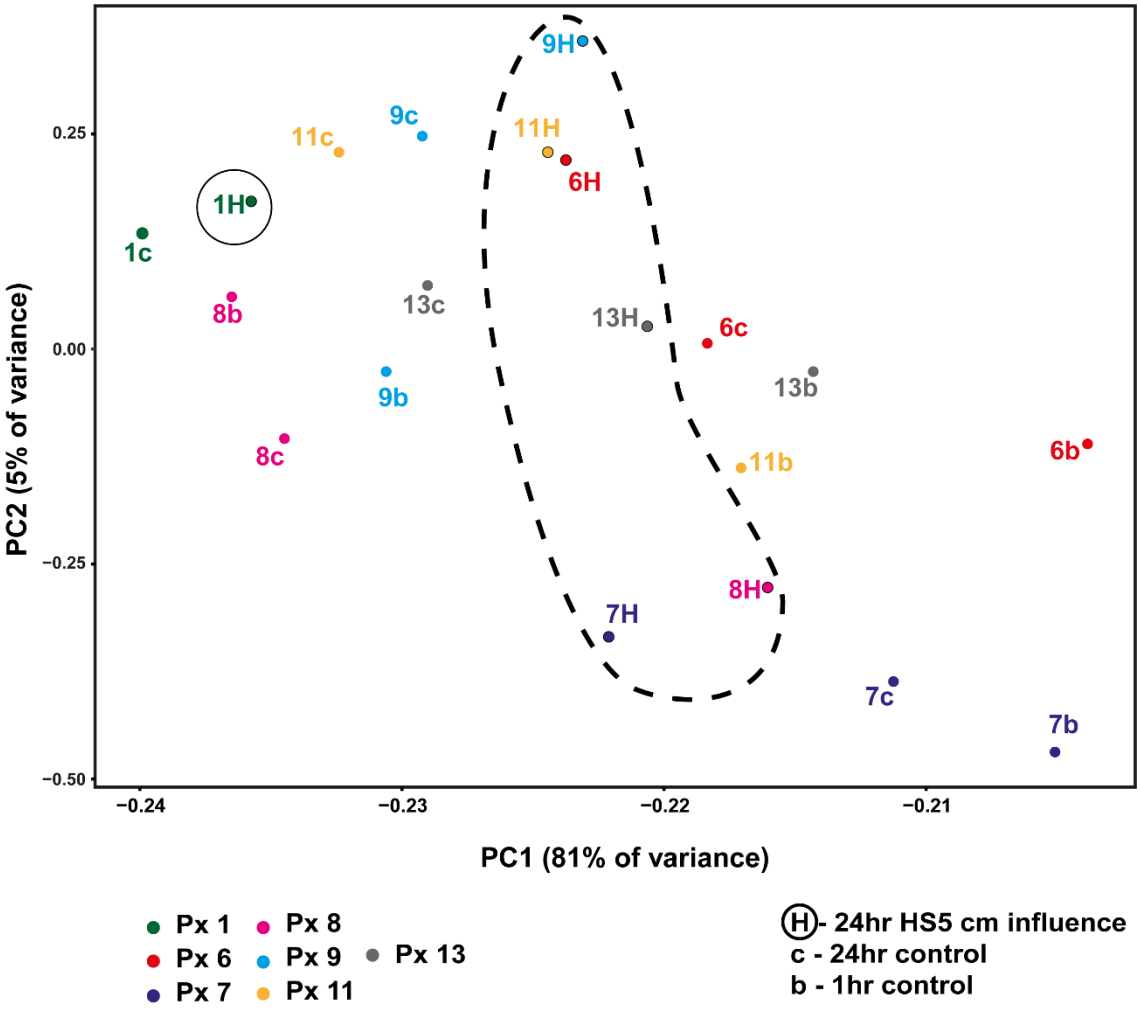

Figure 5.17: Principal component analysis of primary AML cells grown in HS-5 CM. For each sample an average was taken across 3 technical replicates. The subsequent variance in the average phosphopeptide expression per sample could be explained through 20 principle components. Principle component (PC) 1 and PC2 have been selected to visually display the data, collectively they explain 86% of the variance in the data.

Collectively these results were in line with the literature highlighting that in AML the clonal and genetic heterogeneity that characterises the disease (519, 520) extends through to the formation of AML kinase networks. This defines the response of primary AML cells to bulk factors that comprise forms of the stromal secretome. In trying to characterise the heterogeneity of AML kinase activity in response to bulk secretome, it is clear that the common dysregulated kinases in cancer are implicated in AML (MAPK, PI3K-AKT-mTOR, and JAK) and mediate the AML response to the microenvironment. However, there are a number of other factors contributing to AML behaviour, that include but not limited to receptor expression, ECM protein expression, nutrient sensors, feedback mechanisms and the precise wiring of kinase networks for a given cell type.

5.4 AML/Stromal cell co-culture: how MS-5 cells modulate AML signalling networks

Experiments investigating the influence of stromal cells using CM and GFs explain means by which these cells could communicate. However, using a preconditioned media or fixed concentration of reagent does not capture many of the dynamic elements of cell communication. Therefore, to investigate the heterotypic signalling that exists between BMSCs and AML cells in more detail, we used a similar approach to the one used to identify dynamically expressed proteins of the secretome, AML/MS-5 cell co-culture. For this set of investigations experimental models sought to exploit two technical considerations of these cell types; species and adherent/non-adherent nature of cell types.

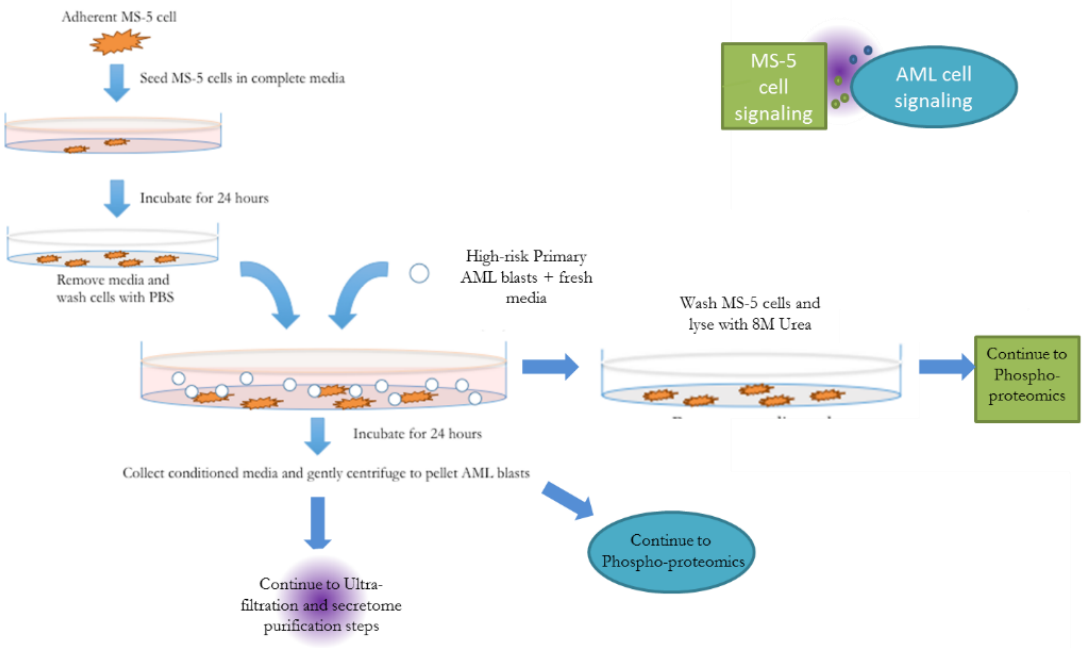

Figure 5.18: Experimental design for MS-5/AML cell co-culture. Experimental design is similar to that employed in secretome co-culture experiments. On this occasion cells were separated by taking advantage of distinct characteristics of adherent MS-5 cell features and non-adherent features of the primary AML cell populations prior to phospho-enrichment and LC-MS/MS analysis.

Adherent MS-5 cells were seeded 24 hours prior to co-culture to provide an unperturbed stromal cell layer. Following which seeding media was removed, MS-5 cells were washed with PBS and fresh media containing non-adherent primary AML patient cells were introduced. In parallel the same primary AML cells were incubated independently and cultures incubated for 24 hours. Following incubation, non-adherent primary AML cells were gently extracted and processed for phosphoproteomics. After which MS-5 cells were gently washed with ice cold PBS to remove any residual AML cells and then lysed with urea on plate (Figure 5.18). Finally, to control for any cross-over stromal MS-5 cells were of murine origin and therefore protein identification was conducted against murine proteomes and primary AML cell

protein identification was against the human proteome, this approach takes advantage of the specificity of mass spectrometers.

5.4.1 Examination of co-culture induced relationships

In order to globally assess the effects stromal cell co-culture has on primary AML cells both hierarchical clustering and PCA were undertaken to identify global trends induced by co-culture on primary AML cell phosphoproteomes. Hierarchical clustering analysis of the experiment revealed that samples clustered primarily by patient, which is in accordance with results produced in section 5.3. Samples then segregated according to co-culture status, the order by which patient samples separated did not clearly correlate with any of the clinical features of the patient samples (Table 2.7). Qualitatively, it is good that the most closely matched samples were those of the experimental replicates.

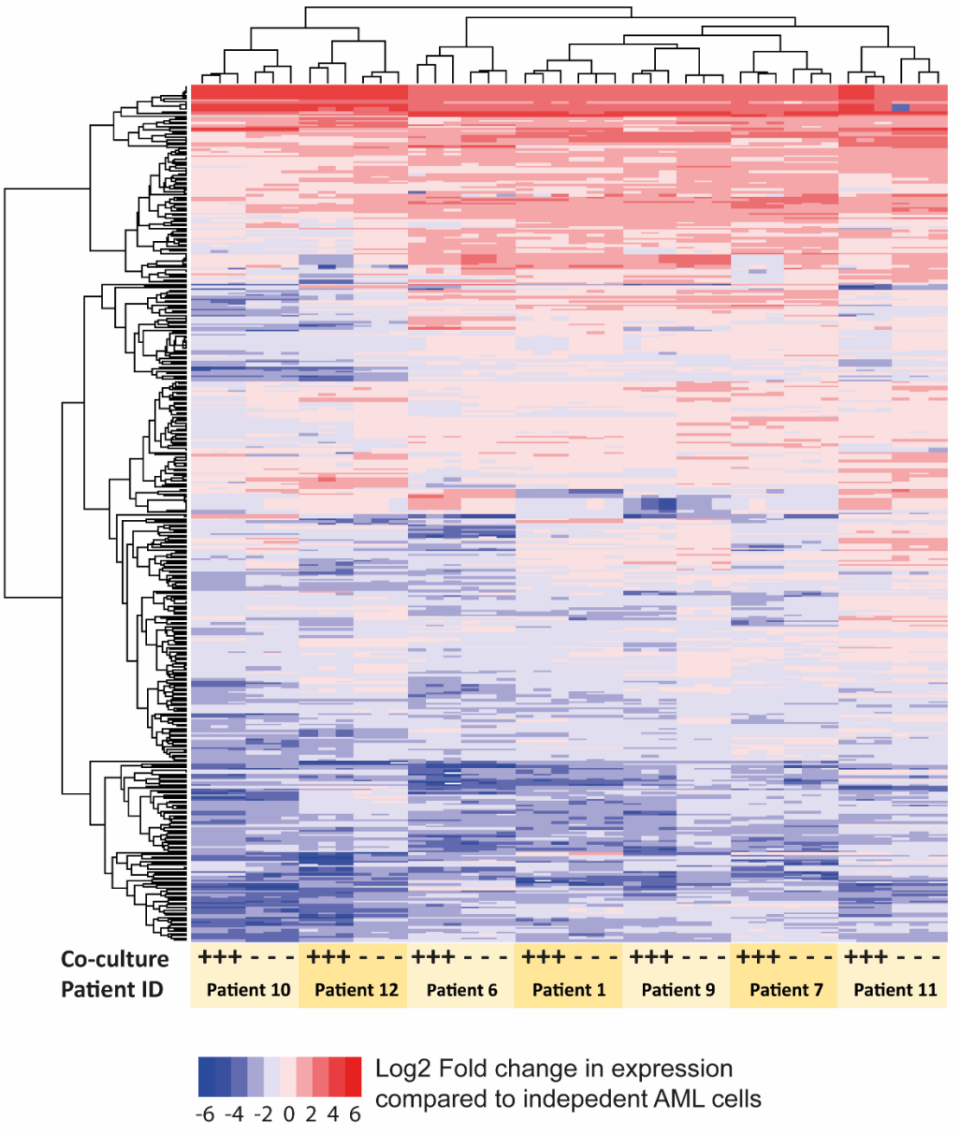

Figure 5.19: Hierarchical clustering analysis of AML phosphoproteomes following MS-5 cell co-culture. Heatmap produced by comparing phosphopeptides expression in an individual sample to the average expression of the phosphopeptide across all samples, each condition n=3 analytical replicates and dendrograms produced using ggplots package in R workspace.

PCA inspection of the phosphoproteomic data mirrored the findings of the hierarchical clustering analysis. Each patient sample occupied a distinct region within the PC environment particularly patient samples #10-12, although samples #1, #6, #7, #9 clustered quite tightly (Figure 5.20). Some samples such as patient #6 did not change substantially following MS-5 co-culture with these conditions clustering very tightly, however, co-culture and independent conditions of patient #12 samples did separate substantially in the PC space.

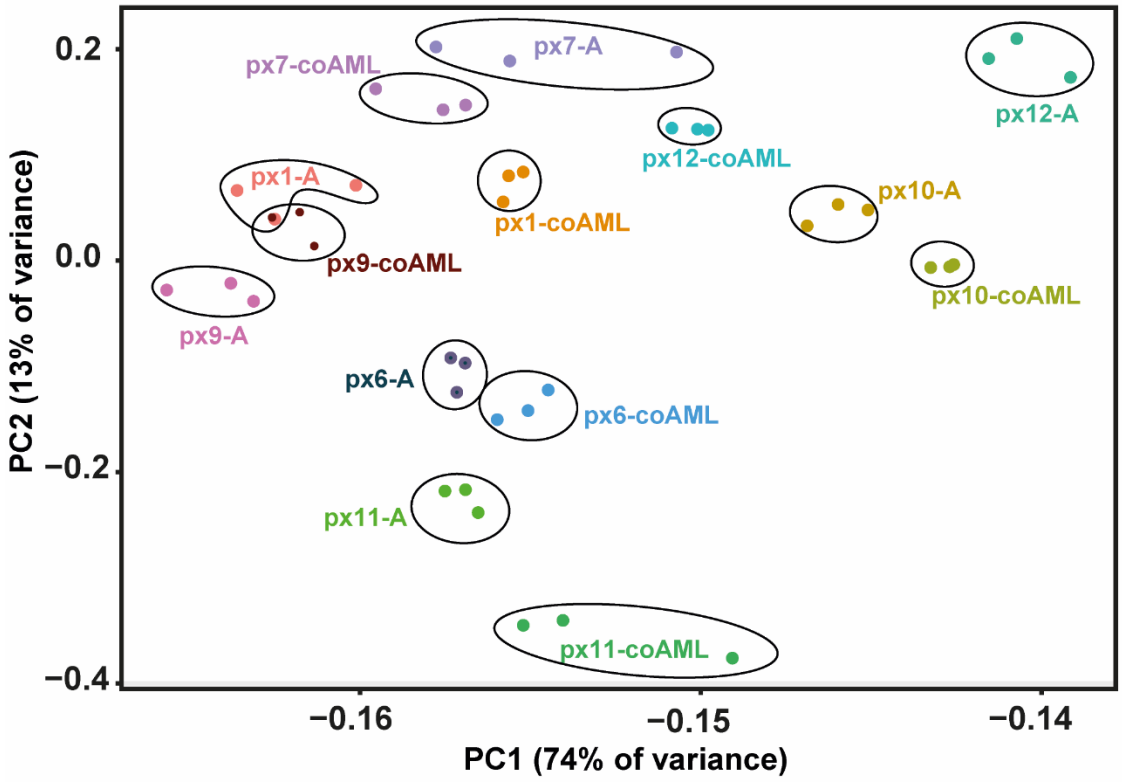

Figure 5.20: PCA of 7 primary AML samples representing the changes in phosphoproteomic expression that co-culture with MS-5 cells induces in these AML cells. PCA of the Log_2 fold-ratios for the 8,045 peptides that significantly changed, presenting PC1 and PC2. Each dot represents an analytical replicate; each condition is coloured denoting sample.

There were examples of unexpected correlations such as that observed between the patient #1 independently cultured and patient #9 co-cultured samples, these both cluster together, suggesting that the influence of MS-5 cells induced one AML population to behave similarly to another independent AML subpopulation.

5.4.2 KSEA analysis of phosphoproteomes identifies three groups of responders

Following the patient specific relationships of the multivariate analysis, it was hypothesised that interrogation of kinase specific responses within patient samples maybe more informative of MS-5 cell induced activity in primary AML cells. Therefore, KSEA was undertaken

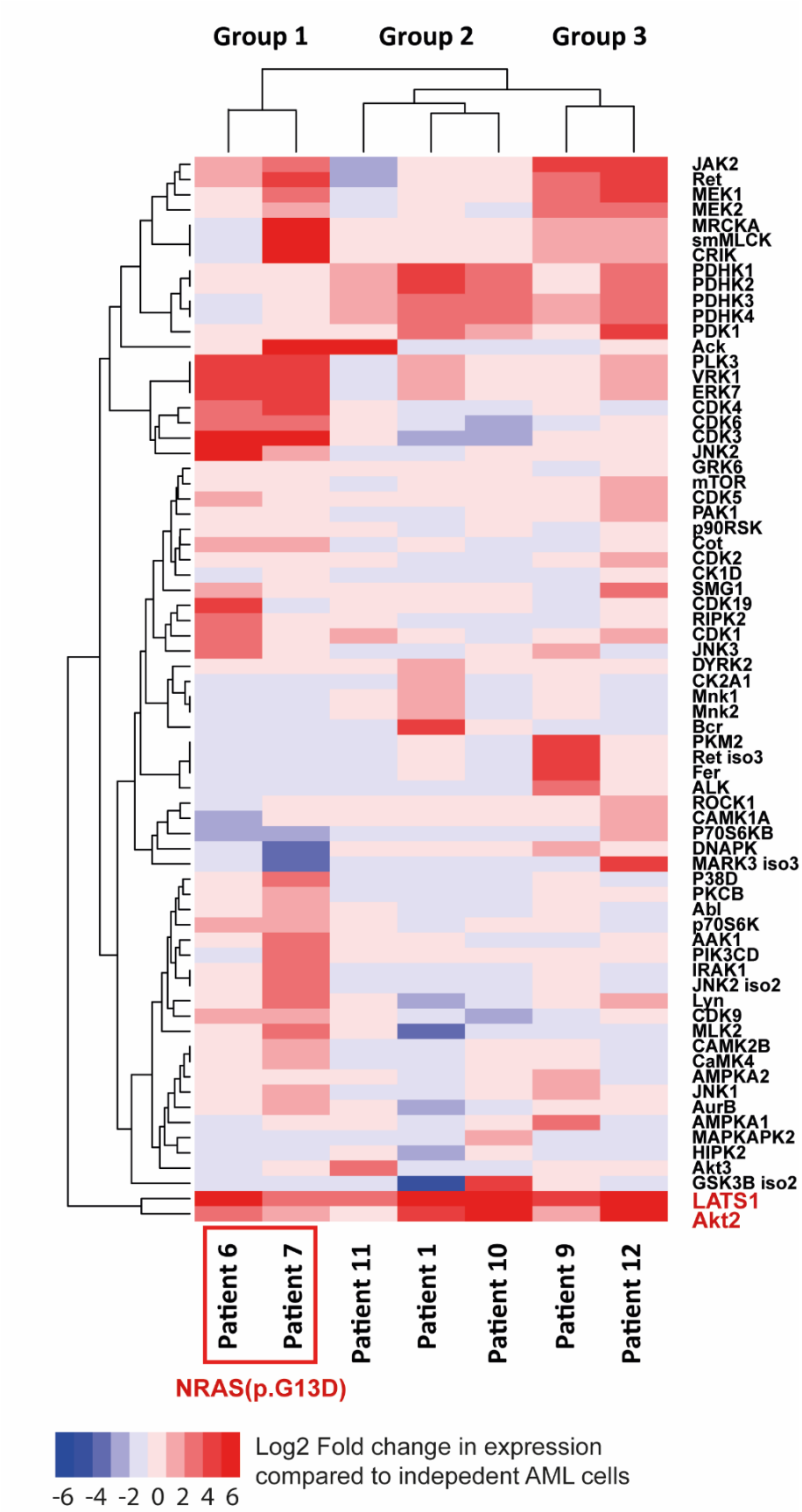

Figure 5.21: KSEA of significantly modulated kinases in primary AML cells following MS-5 co-culture. The phosphorylation status of known kinase substrates were quantified and compared between co-cultured and independently grown primary AML cells to determine relative kinase activities. Heatmap and dendrograms produced using ggplots package in R workspace. Analytical replicates n = 3. Red box signifies that these samples both harbour an NRAS(p.G13D) mutation.

comparing the relative kinase activity of MS-5 co-cultured primary AML cells to the same primary AML cells grown independent of MS-5 cells. Hierarchical clustering of significant changes to kinase activity between samples identified three groups of kinase response to stromal co-culture (Figure 5.21).

Two patient samples clustered separately to the other samples, by relative putative kinase activity change to MS-5 co-culture and formed group 1. Group 1 was distinguished by the strong increase in Polo-like kinase 3 (PLK3), VRK1, ERK7, CDK3, CDK4, CDK6, and JNK2. These patients also had an increase in JAK2 and Ret activity that was also observed in group 3. These patient samples also did not exhibit increased activity of the pyruvate dehydrogenase kinases 1-4 (PDHK1-4) which occurred in both groups 2 and 3. A notable feature that was shared by patients #6 and #7, was that these two patients that segregated most from the other patient samples (Group 1), possessed a significant NRAS mutation (p.G13D) detailed in Table 2.7. This mutation is believed to render NRAS constituently active. What is notable about the clustering of these samples is that it suggested this mutation could influence the way an AML cell population interprets and interacts with other cell types; however, this observation is from a sample size n=2 and therefore, it is not possible to make any conclusions.

The group 2 response comprised patients #1, #10 and #11. These patient samples all were characterised by a strong increase in PDHK1-4 activity but lacked the putative MEK and CDK activity that was present in other response groups. PDHK1-4 activity can lead to a decrease in glucose metabolism and altered glucose metabolism has been described as a means of reducing apoptosis and inducing chemo-resistance (521).

Group 3 was made up of patients #9 and #12. These patients clustered as they had high PDHK1-4 activity, however, unlike group 2, group 3 also displayed increased MEK1 and MEK2 activity following MS-5 co-culture. Additionally, as observed in group 1 there was also increased putative activity in JAK2 and Ret kinases. Patient #9 in this group did have a mutation on TET2 and exhibited a relatively modest increase in PDHK1-4 activity compared to other samples. This was notable, as both patients in group 1 had mutations in epigenetic modulators (patient #6 TET2, patient #7 IDH2 mutant), and these are commonly mutated epigenetic genes that also have complex roles in metabolism (522).

Finally, there were three kinases that displayed increased activity in all patient samples following MS-5 co-culture, PDK1, AKT2, and LATS1. The AKT2 and LATS1 kinases have previously been implicated in regulating cell growth and proliferation. LATS1 is most commonly reported as a tumour suppressor, helping to regulate cell growth and size. However, with previous theories on AML treatment resistance including microenvironment mediated quiescence of AML

cells, the increase in cell growth regulator (LATS1) following MS-5 interactions would fit this theory (523).

5.4.3 K-means clustering analysis of primary AML phosphoproteomics to study the influence of MS-5 stromal co-culture on 'ex vivo' leukaemic behaviour

Similar to the systematic analysis employed in section 5.3.2, k-means clustering was used to study the biochemical modulations in primary AML cells following 24 hours of MS-5 co-culture. The phosphoproteomics dataset was filtered and clustered using k-means to include only those peptides that were significantly modulated in at least one co-culture compared to the respective primary sample maintained in culture independently. Of the 9,065 peptides quantified in this experiment, 7,794 were phosphorylated (86% enrichment efficiency). Peptides were grouped into 8 clusters using the method described in Section 2.12.4.

The data in Figure 5.20 revealed the heterogeneity in patient cell response to the presence of MS-5 cells during 24 hours of ex vivo culture. The k-means analysis of this data further showed how distinct each AML sample can be, exemplified by the varying significance of each clusters per sample (Figure 5.22A). One big difference between this analysis of co-culture induced signalling changes and that of single GF stimulation (Figure 5.10) and HS-5 secretome experiments (Figure 5.15), was the trend for increased phosphopeptide expression, whereas in other experiments there was a quite substantial drop in the expression of many phosphopeptides.

Analysis of the eight identified clusters and the expression of the phosphopeptides that comprise them suggested each primary sample had a different relationship with the MS-5 cells. All of the clusters except cluster 6, contained phosphopeptides that did not significantly change in expression for most of the primary samples. However, in each of clusters 2, 3, 4 and 7 there was one primary sample that would exhibit a strong increase in expression for the phosphopeptides that comprised that particular cluster following co-culture.

The peptides (n=424) that comprised cluster 2 were highly expressed in patient #6 co-cultured cells relative to independently cultured AML cells, with expression increasing 8.4 Log_2 fold on average. GO analysis using approaches previously outlined (section 5.3.2) revealed enrichment of Ras protein signal transduction, small GTPase mediated signal transduction, cell surface receptor signalling and VEGF production (Figure 5.22Bi). These ontologies would be consistent with the means by which MS-5 cells could activate AML cells and VEGF production is suggestive the production of a secreted proteins to positively regulate stromal assistance.

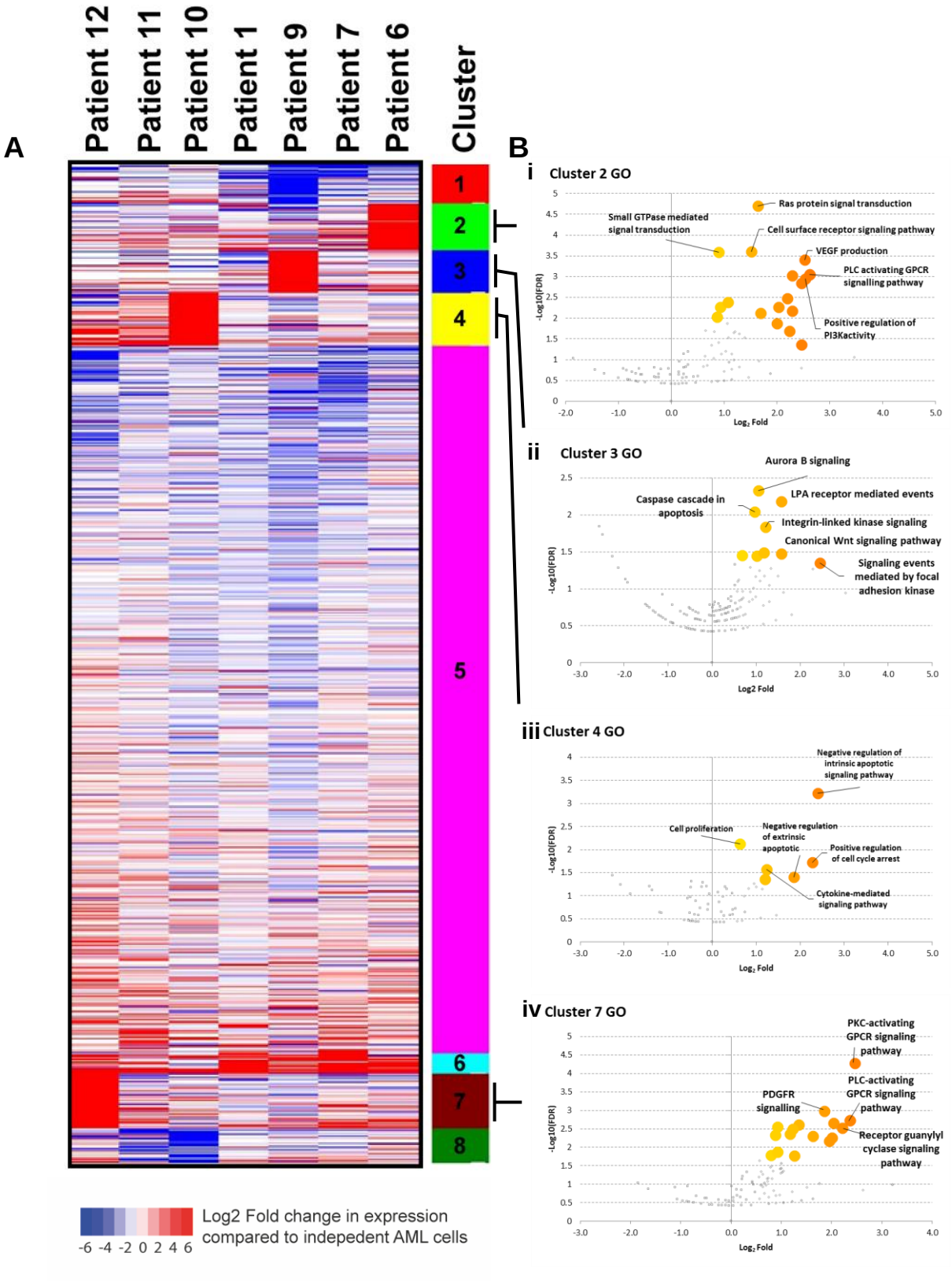

Figure 5.22: K-means clustering analysis comparing AML cells grown in MS-5 co-culture compared to those independently grown. (A) Heatmap of the Log_2 fold-ratios for each of the phosphopeptides grown in MS-5 co-culture compared to no co-culture, each comparison includes n=3 analytical replicates. K-means clustering assigns phosphopeptides into 8 clusters **(B)** GO analysis of phosphopeptides that comprise clusters (i) 2 (ii) 3 (iii) 4 (iv) 7.

Cluster 3 was relevant for patient #9 cells as these phosphopeptides (n=381) increased on average by a Log_2 fold change of 9.4. Subsequent GO analysis revealed that these enriched

phosphopeptides are associated with Aurora B signalling, caspase cascade in apoptosis, LPA receptor events, canonical Wnt signalling, ILK signalling and FAK mediated signalling events (Figure 5.22Bii). Cluster 4 contains phosphopeptides (n=484) that were on average 8.9 Log_2 fold higher in patient #10, 3.0 Log_2 fold in patient #11 and 2 Log_2 fold in patient #12 following co-culture (Figure 5.22A). GO enrichment analysis of these phosphopeptides reported processes including negative regulation of both intrinsic and extrinsic apoptotic signalling, cell proliferation, cytokine mediated signalling pathway activity and positive regulation of cell cycle arrest (Figure 5.22Biii).

The last cluster to represent a group of phosphopeptides relevant to one primary AML sample's response to MS-5 co-culture was cluster 7. This cluster represented 504 phosphopeptides and on average the expression of these peptides increased 7.4 Log_2 fold in patient #12 cells following MS-5 co-culture. GO enrichment of these phosphopeptides revealed that these enriched for both PKC and PLC activated GPCR signalling, PDGFR signalling and receptor guanylyl cyclase signalling (Figure 5.22Biv). The enrichment of these ontologies suggested that MS-5 co-culture interactions with patient #12 cells were mediated through GPCR pathways, pathways that were not as significant in the other primary AML co-cultures.

5.4.4 Phosphopeptides that are increased in all AML primary samples following MS-5 cell co-cultures

Having established and analysed the k-means in which one primary AML sample exhibited a strong increase in expression, cluster 6 contained phosphopeptides (n=176) that were enriched for in all patient samples following co-culture (Figure 5.23A). This was also the only cluster in which phosphopeptide expression increased following co-culture for patients #1, #7 and #11.

KSEA analysis of these 176 phosphopeptides revealed that there were four kinases that significantly increased in activity; AKT, CDK5, Dual-specificity tyrosine-regulated kinase 2 (DYRK2) and LATS1 (Figure 5.23B). AKT as discussed previously is a key mediator of cell growth, proliferation and survival. CDK5 is a pleiotropic kinase with defined roles in a myriad of cellular processes (524). CDK5 notably has previously been described as an inhibitor of apoptosis through phosphorylation of AKT at Ser^{473} (525), which supports the increased AKT activity. CDK5 has also previously been implicated in regulating actin cytoskeleton and mediating cell adhesion and migration in the microenvironment, an action executed through PAK1 phosphorylation (frequently seen as one of the most active kinases in AML) (526, 527). Finally, CDK5 has recently been described as being able to exert control on the expression of HIF1α target genes, vascular endothelial growth factor (VEGF)-A and VEGF receptor 1 (528) to drive tumour angiogenesis and induce secretion of pro-angiogenic molecules (529). DYRK2 has previously been described as a

regulator of cancer cell metastasis (530) and a determinant of epithelial mesenchymal transition (EMT) in solid tumours (531), however, DYRK2 inhibits an invasive phenotype. The last kinase that was identified as more active was LATS1, as discussed in section 5.4.2 LATS1 is a regulatory kinase that typically controls cell size and proliferation. GO analysis of cluster 6 determined that these peptides that were increased in all patients enriched for the biological processes: negative regulation of extrinsic apoptotic signalling, negative regulation of apoptotic signalling and the cellular component disassembly involved in the execution of apoptosis (Figure 5.23C). These findings suggest that MS-5 co-culture induced increased survival in each of the primary samples, through the activation of anti-apoptotic pathways.

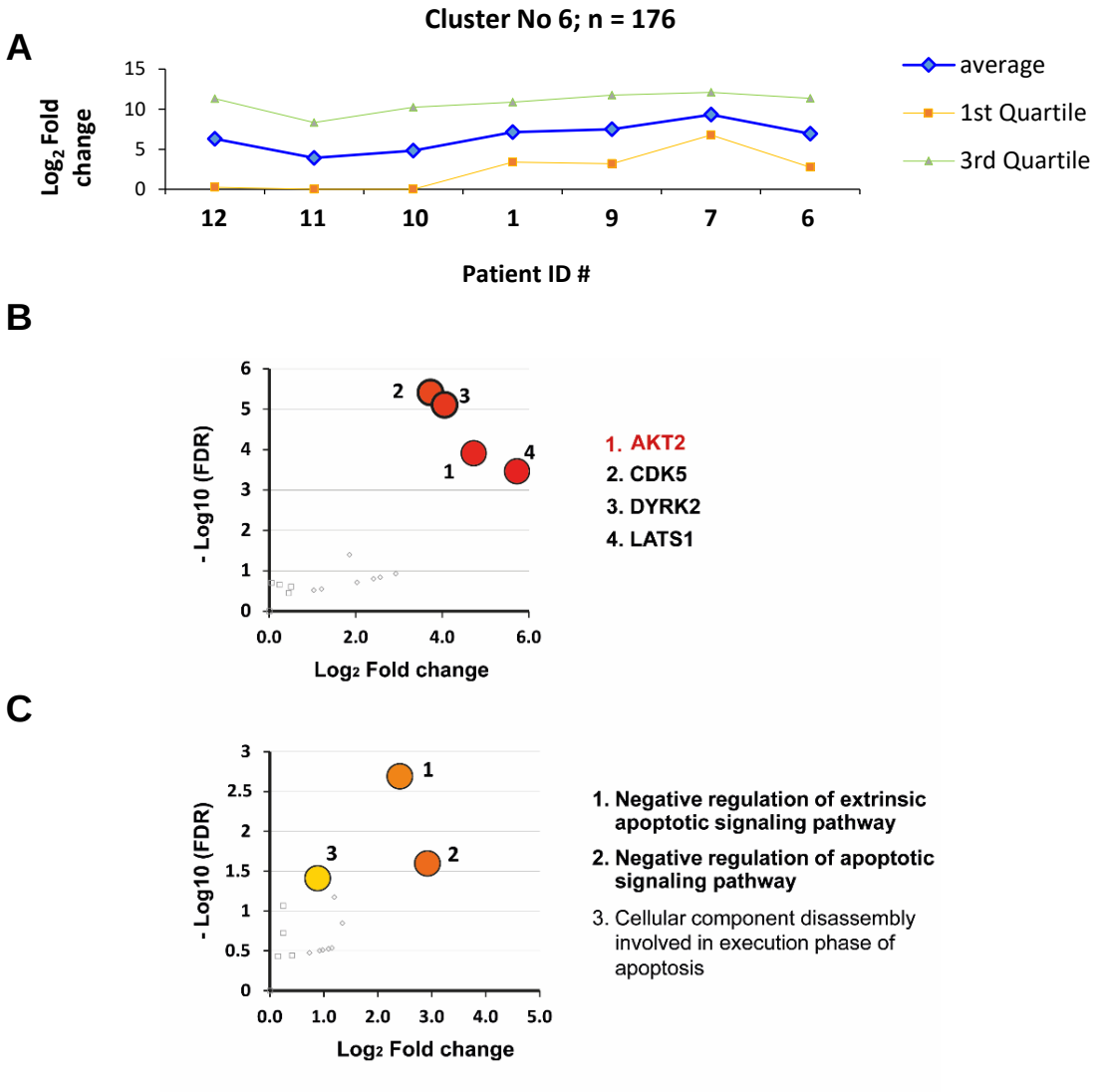

Figure 5.23: K-means analysis reveals that there is enrichment for phosphopeptides that are indicative of AKT2 activity and an increase in anti-apoptotic signalling. (A) Average Log_2 Fold change in phosphopeptide expression for patient sample following co-culture with MS-5 cells, n=176 phosphopeptides, run in analytical triplicate. **(B)** KSEA determined changes in kinase activity following co-culture with MS-5 cells. **(C)** Enriched gene ontologies in all patient samples following MS-5 co-culture.

5.5 AML/Stromal cell co-culture: identifying patterns of MS-5 response to different primary AML disease

Phosphoproteomic analysis of the primary AML cells following MS-5 co-culture confirmed our predictions that the secretome was not the only means by which BMSCs can influence AML cell signalling, with the observation of additional signalling events in a co-culture system to that elicited by CM alone. Simultaneously to the analysis of the primary AML patient phosphoproteomes, we additionally collected the MS-5 cells that had been used to provide the supportive network for these AML cells. These cells while supporting the AML cells were in turn being influenced and therefore we predicted that it may be possible to identify activated positive feedback mechanisms induced by AML cells in the MS-5 cells by once again employing a global LC-MS/MS based phosphoproteomic approach. Upon completion of lysis, the eight MS-5 populations underwent the same phosphoproteomic workflow as the primary AML cells to determine the heterotypic signalling in this co-culture model.

5.5.1 Differential abundance

Analysis of this experiment retrieved 8,961 peptides, of which 8029 were phosphorylated (90% phospho-enrichment efficiency). The data shown in Figure 5.24 served as preliminary indication of the effect that each primary AML sample had on respective MS-5 phosphoproteomes. Superficially, these results indicated that AML samples from patent #7 and patient #12 had quite profound effects on the MS-5 cells, with patient #7 cells inducing 235 phosphopeptides to significantly increase >1.5 Log_2 fold and 726 phosphopeptides to significantly decrease <1.5 Log_2 fold – collectively nearly $1x10^3$ phosphopeptides significantly changed as a result of 24 hours of co-culture with patient #7 cells.

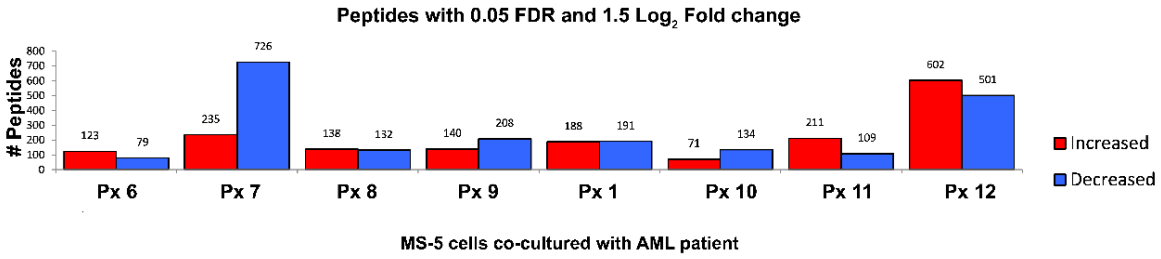

Figure 5.24: Differential abundance analysis of MS-5 phosphoproteomes following co-culture. Differential abundance analysis of the phosphoproteomics data. The number of phosphopeptides either significantly increased (red) or decreased (blue) in abundance compared to independent MS-5 cells are shown. Fold change, log_2 fold-change vs MS-5 independent control; adjusted *P*, is the corrected *P*-value for multiple testing by the Benjamini-Hochberg method.

Patient #12 cells substantially altered phosphopeptide expression of the MS-5 cells that they were cultured with, 602 phosphopeptides increased >1.5 Log2 fold and 501 phosphopeptides decreased <1.5 Log_2 fold. Those two MS-5 populations were outliers, with all

other AML co-cultures only inducing 100-200 significant changes in the MS-5 global LC-MS/MS phosphopeptides analysis.

5.5.2 Global phosphoproteomic analysis of MS-5 cells following AML co-culture

To compare the phosphoproteomes of the MS-5 cells following primary AML co-culture, hierarchical clustering of the phosphopeptide fold changes between co-cultured MS-5 cells and independent MS-5 culutres was performed as presented in Figure 5.25. This analysis revealed that for many of the MS-5 populations the effects of different primary AML cells in culture were homogeneous, as MS-5 cells cultured with cells from patients #1, #6, #8 and #9 all clustered together following mutlivariate analysis. MS-5 cells cultured with patient samples #10 and #11 did not produce remarkably different expression profiles to that of the MS-5 cells described as closely clustering (MS-5 cells with patients cells #1, #6, #8 and #9), as there were only a few clusters of proteins in which MS-5 cells cultured with patients cells #10 and #11 differed from the other MS-5 populations. These differences though distinguished the phosphoproteome of MS-5 cells cultured with patients cells #10 and #11 as distinct from other MS-5 cells.

MS-5 cells incubated with patient #7 cells clustered separatly to the left of the clustering plot, this was likely due to the clusters of decreased phosphopetide expression, which were apparent in the differential analysis in Figure 5.24. The other MS-5 sample identified as being different compared to the other samples was that cultured with patient #12 cells. In the clustering analysis this sample distinctly segregated by itself, with a number phosphopeptides that were unchanged in the other samples clearly highly increased or decreased in these cells.

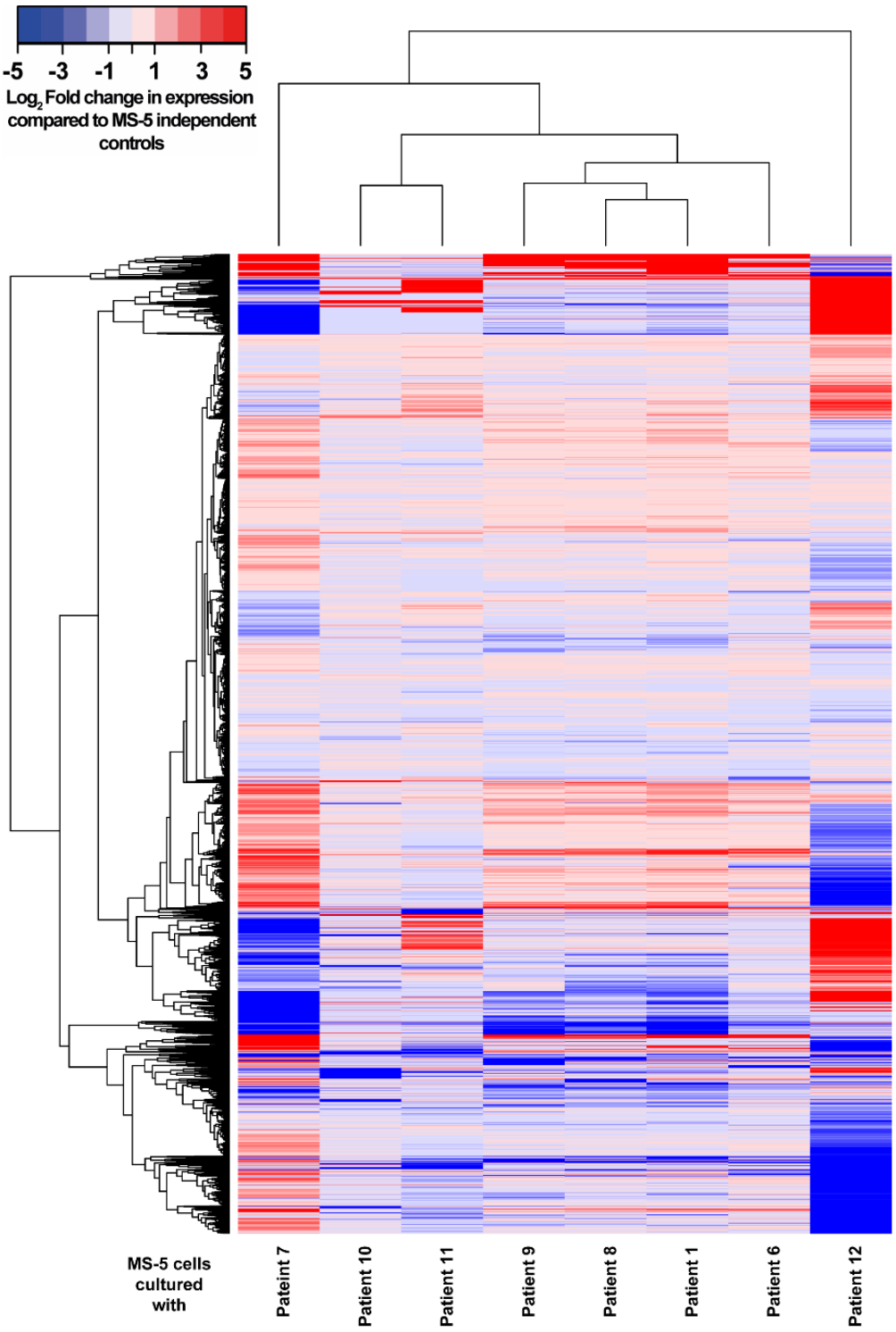

Figure 5.25: Hierarchical clustering of MS-5 phosphopeptide expression fold changes in response to co-culture with patient AML cells. Fold change is relative to phosphopeptide expression of MS-5 cells grown in presence of AML to those grown in the absence, averaged across 3 analytical replicates, heatmap and dendrograms produced using ggplots package in R workspace.

To understand how these changes in phosphopeptide expression functionally effected the MS-5 populations, GO enrichment analysis was conducted as outlined in the methods and displayed in Figure 5.26. Ontologies are ranked by the number of samples that the ontology was

enriched in following AML co-culture (highest to lowest) and ontologies were only included if the process was enriched ($p<0.05$) in 2 or more samples.

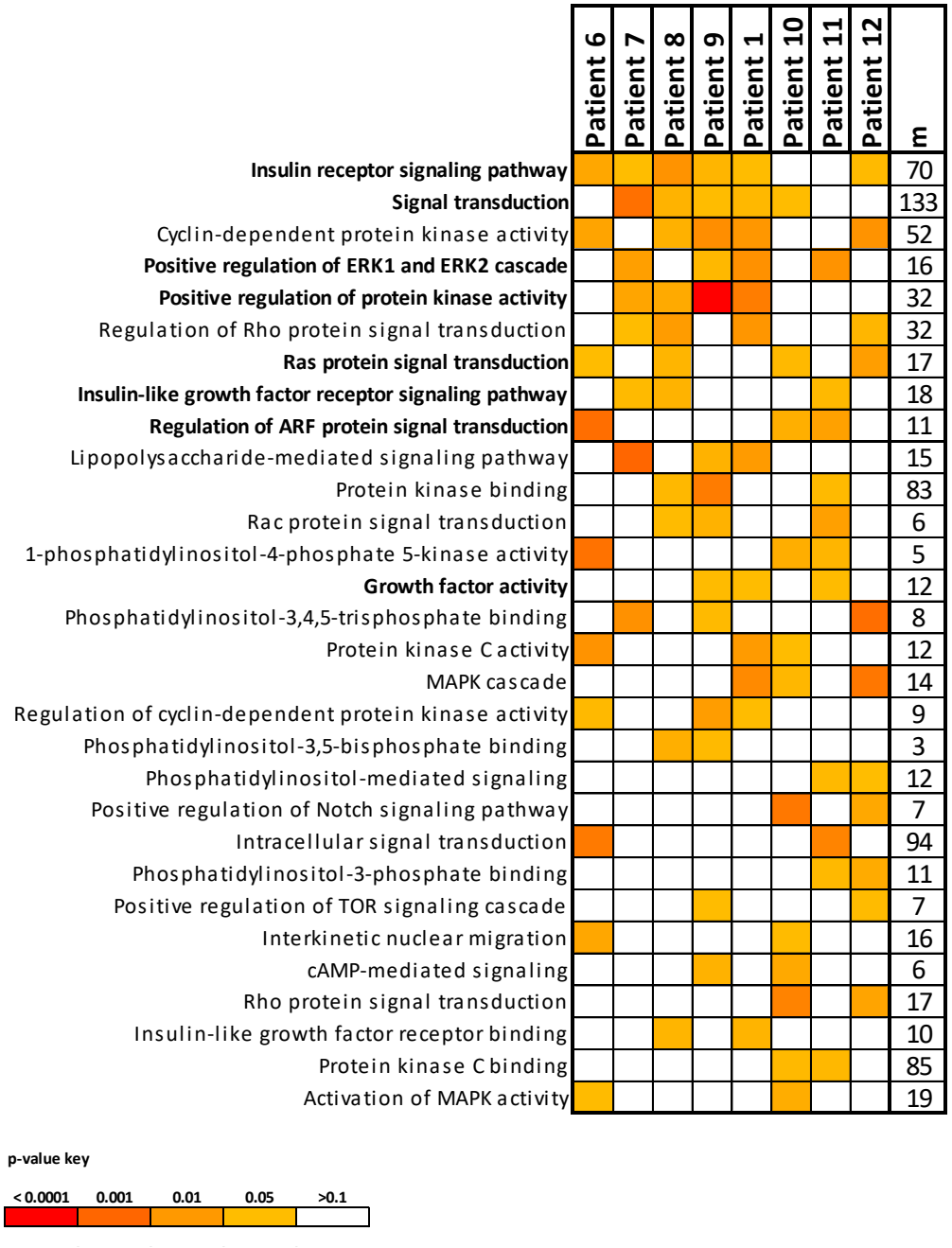

Figure 5.26: Heatmap of enriched GO processes in MS-5 cells following AML co-culture. Enrichment measures change phosphopeptide expression of MS-5 cells grown in presence of AML to those grown in the absence, averaged across 3 analytical replicates. m; no of substrates.

The most frequently enriched process is that of activity in the insulin receptor signalling pathway (n=6), followed by signal transduction and CDK1 activity (both n=5). Other notable processes included the positive regulation of protein kinase activity, Ras protein signal transduction and GF activity. These ontologies are collectively indicative of increased RTK activity and receptor mediated signalling. Thus, strongly suggesting that the primary AML cells were regulating and stimulating MS-5 cell signalling pathways.

5.5.3 KSEA analysis of MS-5 following AML co-cultures reveals two patterns of kinase activity

To establish the effect that these primary AML cells were having on MS-5 kinase networks, KSEA was implemented as described in the methods section 2.12. Hierarchical clustering of the KSEA output showed that the kinase response to the primary AML cells was in agreement with Figure 5.25 showing that there were two signatures of response (Figure 5.27). The first sample group included MS-5 populations that were cultured with samples from patient's #7, #10, #11 and #12, although the dendrogram did indicate a segregation between patient sample #12 and the rest of group 1. The remaining MS-5 populations cultured with patient samples #1, #6, #8 and #9 clustered together to form group 2.

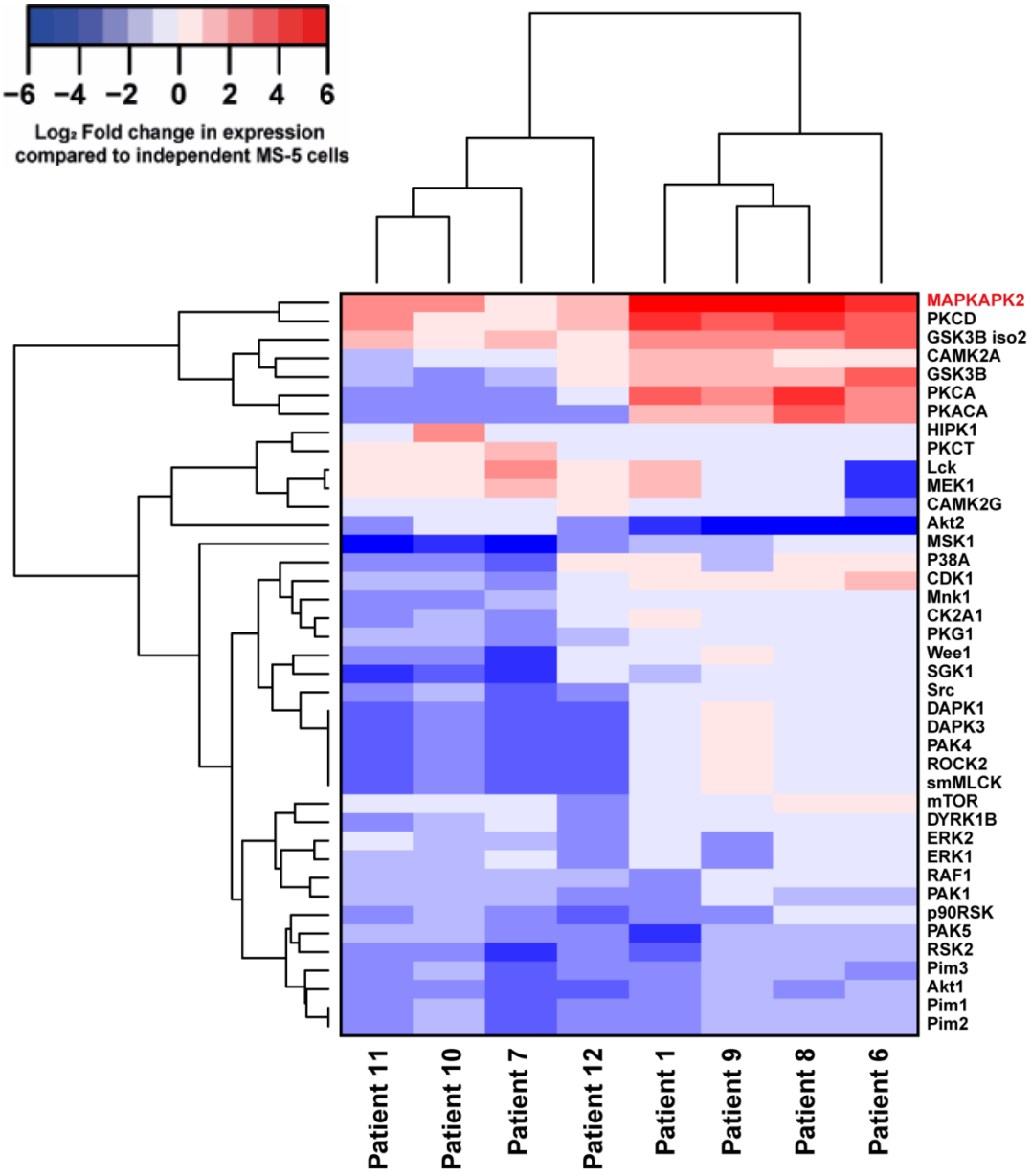

Figure 5.27: KSEA of significantly modulated kinases in MS-5 cells following co-culture. The phosphorylation status of known kinase substrates were quantified and compared between co-cultured and independently grown MS-5 cells to determine relative kinase activities. Each comparison calculated using 3 analytical replicates. Heatmap and dendrograms produced using ggplots package in R workspace.

Assessment of specific kinase expression patterns showed that the kinase to be putatively upregulated across all MS-5 cell populations following AML co-culture was MAP kinase-activated protein kinase 2 (MAPKAPK2). In addition there was also consistent putative upregulation in the phosphorylation of PKCδ and GSK-3β isoform 2 substrates. Group 2 MS-5 populations consistantly demonstrated increased putative activity in CAMK2A, GSK-3β, PKCα and cAMP-dependent protein kinase catalytic subunit alpha (PKACA). Whereas, MS-5 populations in group 1 exhibited putative decreases in these three kinases following co-culture. CDK1 was moderately increased in group 2 MS-5 populations, and strongly decreased in group 1 populations, this observation was in accordance with GO findings in Figure 5.26. In general many kinases assessed by KSEA decreased in activity following AML co-culture, in particular kinases mediated by Rho family GTPases, the AKT-mTOR pathway, and the RAF-MEK-ERK signalling axis.

5.5.4 AML blast independence and embedding in MS-5 stromal cells could correlate with PCA observations

The hierarchical clustering analysis suggested that, as seen in Figure 5.27, MS-5 cells separated into patterns of response. MS-5 cells incubated with patient #1, #6, #8 and #9 cells responded similarly, whereas other MS-5 phosphoproteomic signatures were not as predictable. PCA analysis of the phosphoproteomics data was undertaken to further visualise spatially how different MS-5 populations were responding to the AML patient cells. (Figure 5.28).

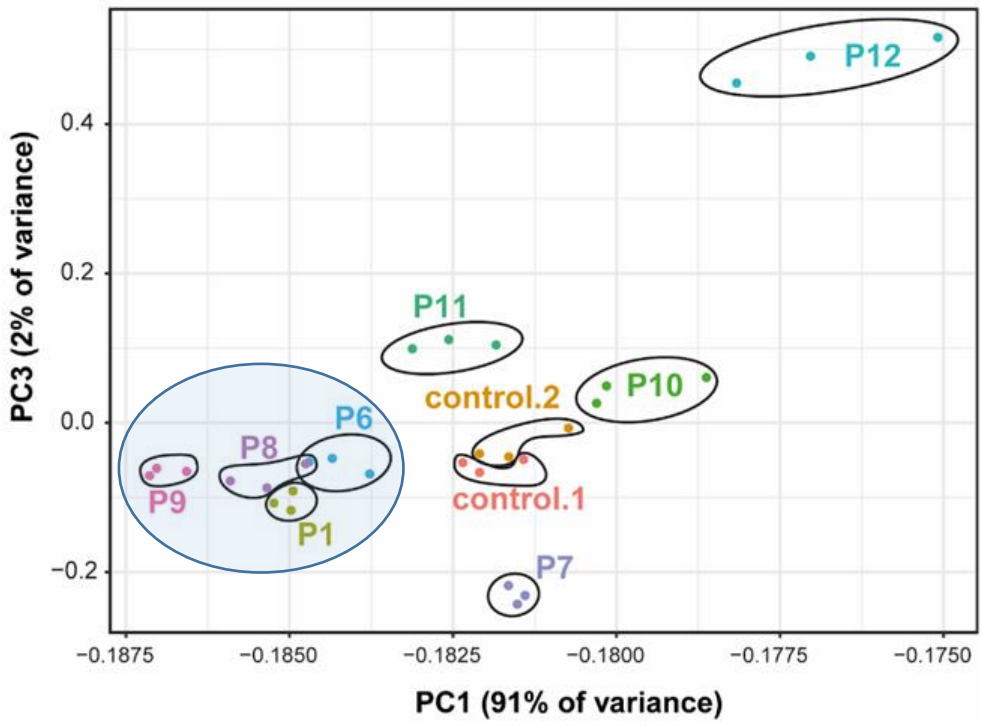

Figure 5.28: Multivariate analysis of MS-5 cells following co-culture demonstrates AML influence. PCA of the Log_2 fold-ratios for the 8029 phosphopeptides that significantly changed in PC1 vs PC3.

The MS-5 populations that all responded in a similar manner to AML co-culture with patient #1, #6, #8 and #9 cells shared the same PC space (blue circle), and these cells were derived from the same parent MS-5 cells as controls 1 and 2. GO analysis suggested that all these cell populations had increased RTK activity and were being regulated by the AML cells, whether this is responsible for the supportive behaviour MS-5 cells exhibit towards AML cells is to be confirmed.

MS-5 populations cultured with patient #10 and #11 cells shared PC space with the two-separate control MS-5 conditions (MS-5 cells maintained in culture 24 hours independently) that had no exposure to AML cells. These samples also displayed no insulin receptor pathway enrichment in MS-5 populations following co-culture, additionally there was no enrichment for protein kinase activity or CDK1 activity. As these ontologies were suggestive of increased RTK activity in MS-5 cells as a consequence of AML influence and that these cells share PC space with the control MS-5 cells, collectively this data suggests that the AML cells did not significantly integrate or impact on MS-5 cell behaviour in these samples.

The MS-5 cells co-cultured with patient #12 and patient #7 cells did not display either of these two phenotypes and in PC space were isolated, and this was not due to irreproducible replicates not clustering together. As MS-5 cells cultured with patient #12 cells separated so profoundly from the other MS-5 populations it was hypothesised that perhaps there was something clinically different about these AML cells that would explain the polarity in MS-5 phosphoproteomic expression to the other samples. This analysis revealed that that patient #12 was distinct in that this patient's AML was classified as M0 – denoting minimal differentiation. If these cells did not possess the receptors or machinery to manipulate the MS-5 cells as the other AML cells did, then this would go some way to explaining these observations. Additionally, these patients tend to have a higher percentage of $CD34^{+}$ cells, and it is these cells that are documented as having a preference for niche engraftment (11) – meaning that the MS-5 population being analysed may have contained some patient #12 AML blasts.

Assessment of patient #7's clinical features identified that these cells were the only non-adverse risk sample included in the experiment. Patient #7 cells were of intermediate risk, when analysing PC1 these MS-5 cells cultured with this AML do align with the control cells and it is only after considering PC3 that MS-5 cultured with patient #7 cells deviate from other cultures. These results suggest that AML of different risk groups, likely have different relationships and impact on the microenvironment, a recent paper has already suggested that de novo AML induces greater dysregulation in the microenvironment (532).

Phosphoproteomic analysis of MS-5 cells co-cultured with primary AML cells suggested that there were signatures being identified that were indicative of environmental dependence and independence. To try and functionally validate these observations, images were taken of primary AML cells from the same patients in co-culture to assess interactions. Analysis of cultures by microscopy showed that patient #10 cells in co-culture morphologically appeared to cluster into defined round groups, almost appearing to be resting on top of the MS-5 cells (Figure 5.29). Similarly, cultures containing patient #11 cells looked to have more of these clusters that rest above MS-5 cells. Patient #8 cells on the other hand, were not as abundant and nor did there appear to be any clusters of AML cells. Instead the AML cells were integrated within the stromal cells, possibly suggestive of a more microenvironment-interactive cell. Patient #9 cells in this assessment were definitely more abundant than the patient #8 AML cells and had the signs of some clusters. But they too, were not very rounded and had the morphology of a spread cell that was interacting. Additionally, patient #9 cells did not look like they were resting atop the MS-5 cells like patient's #10 and #11.

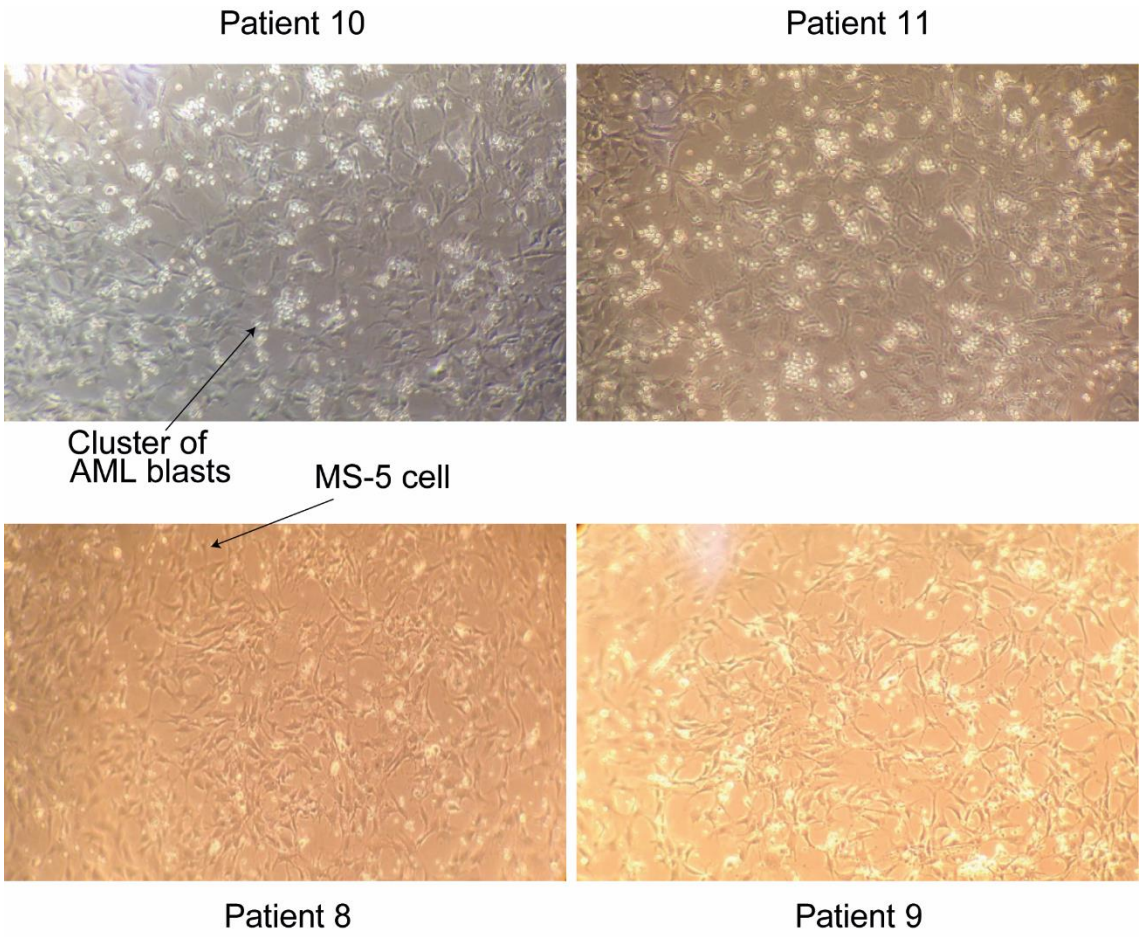

Figure 5.29: Bright field images of primary AML/MS-5 co-cultures prior to phosphoproteomic analysis. Arrows indicate the clusters of AML blasts and MS-5 cells in co-culture. Patient samples #10 and #11 in co-culture do not integrate with the MS-5 cells (microenvironment independent), with the presence of AML clusters. Patient samples #8 and #9 in co-culture do integrate with the MS-5 cells (microenvironment interactive).

Relating these morphological observations to the phosphoproteomics data, MS-5 cells that had been cultured with patients #10 and #11 clustered with the AML independent MS-5 cells in Figure 5.28. Under the microscope these cells looked to favour clustering with other AML cells as opposed to integrating with the MS-5 stromal layer. This would correlate with the less divergent phosphoproteome of MS-5 cells that were cultured with these AML cells. Whereas, patients #8 and #9 did not share PC space with independent control MS-5 cells, they instead clustered with MS-5 cells that had been cultured with other primary AML cells. Thus, suggesting that these could be representative phosphoproteomes of AML influenced MS-5 cells.

5.6 Summary

The experiments described in this chapter aimed to decipher the role of BMSCs in AML kinase signalling. The initial objective was to define the signalling pathways activated in AML cells following stimulation with both the identified secretomic components from Chapter 3, as well as the complete secretome. Due to the heterogeneity of the disease, experiments were expanded to identify frequently activated signalling nodes in AML by treating primary samples with bulk HS-5 secretome. Subsequently, to establish the heterotypic signalling that exists between BMSCs and AML cells co-culture models were designed and label-free phosphoproteomics used to assess signalling dynamics.

P31/FUJ cells were serum starved and treated with 10ng/ml of the six secretome derived proteins, the proteins mixed and 10μg/ml of the bulk secretome. Western blot analysis was employed to investigate the influence of these proteins on the targets of the kinase inhibition studies detailed in Chapter 4 - principally components of the MAPK and PI3K-AKT-mTOR axis (Figure 5.2). The experiments revealed that CSF-1 and the complex mixtures activated MAPK in these cells (Figure 5.3). Assessment of AKT showed that these cells in all conditions, AKT was highly active (Figure 5.4), this is likely due the constituent activation of AKT observed in P31/FUJ cells. Western blot analysis of the mTOR substrates S6K and 4EBP1 suggested that the individual GFs alone were not enough to stimulate upstream pathways sufficiently to impact on downstream targets like S6K and 4EBP1. However, binding of upstream receptors (multiple or the same) with numerous molecules was potent enough for activation of mTOR substrates. PAK activity was also positively regulated by the S100 proteins, conversely the Mixed GF condition inhibited PAK phosphorylation (Figure 5.5), whereas the stromal secretome activated PAK1 suggesting there are other molecules in the secretome capable of activating PAK1. These data confirmed the differential effects that kinase inhibitors had on AML cells in the presence of the complete stromal secretome (Table 4.3).

Following this validation that the RPs were capable of activating key AML signalling nodes in P31/FUJ cells, the phosphoproteome of patient # 1 cells was chosen to assess pathway

activity in primary AML, as these cells displayed dynamic responses to the secretome derived protein treatments (Figure 5.6). This was achieved through the use of mass spectrometry-based phosphoproteomic profiling of patient #1 cells under treatment with the panel of stromal derived proteins individually and in combination (Figure 5.7). Prior to any biological interpretation, a thorough quality control analysis of the dataset determined that the data were of high qualitative and quantitative quality, both in terms of the identification of phosphopeptides and the retention time alignment for accurate label-free quantification across samples (Figure 5.8). Previous papers (533, 534) have reported the strength of fitting linear models to quantitative data to then assess differential abundance of phosphopeptides against the control sample (No GF). This assessment revealed that S100-A4 caused the most phosphopeptides to significantly ($P<0.05$) increase in abundance by >1.5 Log_2 fold and mixed secretomes, in particular the Mixed GF condition induced the largest significant ($P<0.05$) decrease in phosphopeptide expression with 480 peptides decreasing by >1.5 Log_2 fold relative to unstimulated cells (Figure 5.9).

To assess relationships between the effects of the secretome derived proteins on the patient #1 phosphoproteome, the similarity between the log_2 fold-ratios of all the phosphopeptides across the treatments were assessed using hierarchical clustering and PCA (Figure 5.10 and Figure 5.12). This analysis demonstrated that the two phosphoproteomes that were remarkably different to the unstimulated and basal samples were that of the Mixed GF and S100-A4 stimulated cells, which was in agreement with the proliferative response observed when patient #1 cells were treated with the secretome derived proteins in Chapter 4 (Figure 4.5). Relative changes in kinase activity across patient #1 phosphoproteomes was achieved using in house KSEA software, systematic assessment determined that the single protein treatments induced increased activity in AKT, mTOR, ERK1 and ERK2, with S100-A4 also increasing ATR, CK2A2 and InsR activity which was not observed in the other treatments (Figure 5.11). Complex protein mixtures induced global decreases in kinase activity, which was unexpected. If this was not a technical issue or anomaly, it could be that as these mixtures were supportive, and stress induced activation of signalling pathways had subsided. Alternatively, it could have been due to a lack of signal perpetuation, as a result of receptor internalisation from high GF concentrations. This needed to be repeated and investigated in a larger cohort, to determine if the stromal secretome mediates survival through the activation/inactivation of particular signalling nodes.

To investigate the global effects of the stromal secretome on AML kinase networks, a cohort of primary AML samples were maintained for 24 hours both with and without HS-5 stromal derived proteins prior to label-free phosphoproteomics (Figure 5.13). Previous studies had shown that basal levels of kinase activity in primary AML cells can be extremely

heterogeneous (535, 536), however, as HS-5 CM had proved effective at maintaining AML viability (Chapter 3) and modulating kinase inhibitor efficacy (Chapter 4). Differential abundance demonstrated that patient phosphoproteomes were profoundly modulated by HS-5 CM compared to the same patient cells maintained in independent cultures for both 1 and 24 hours (Figure 5.14).

Following this, k-means clustering analysis was undertaken to determine relationships patient phosphoproteomes following 24 hours of HS-5 secretome treatment. This analysis grouped phosphopeptides into 9 clusters based on significant ($P<0.05$) $\log_2$ fold changes in expression relative to the 1 hour and 24 hour independent patient phosphoproteomes (Figure 5.15). Primary AML phosphoproteomes displayed heterogeneous expression signatures across the clusters, however there was a broad consensus for increased phosphopeptide expression in clusters (1, 3 and 9), and decreased expression in cluster 5. GO enrichment analysis of phosphopeptides assigned to these clusters identified enrichment for increased NF-κB mediated signalling, DNA-PK pathway activity and AKT mediated PI3K signalling, while cluster 5 (decreased expression) phosphopeptides enriched for apoptosis processes (Figure 5.15D). This demonstrated that despite huge heterogeneity in phosphoproteomes there is consensus for anti-apoptotic signalling. In addition, hierarchical clustering of KSEA data demonstrated the breadth of kinases that are temporally activated and deactivated in response to the HS-5 CM (Figure 5.16). To compare patient phosphoproteome similarity across conditions, the data was analysed using PC analysis (Figure 5.17). This analysis demonstrated that the basal phosphoproteomes at 1 hour were distinct and did not cluster to share the same PC space; following 24 hours of HS-5 conditioning 6/7 samples had migrated centrally to occupy a similar region. This indicated that despite their different basal phosphoproteomes, stimulation with the HS-5 secretome effected the phosphoproteomes similarly, suggesting that signals may have been transmitted via different routes in the network that ultimately induce the same cellular response.

To investigate the effects of the BMSM on AML cell signalling, whilst accounting for contribution of juxtacrine signalling and the ability of cells to respond to each other dynamically (heterotypic signalling), a label-free phosphoproteomic study was conceived to analyse primary AML cells and MS-5 cells following 24 hours co-culture (Figure 5.18). Seven primary AML samples were seeded in MS-5 co-culture and to assess the effects of co-culture on patient phosphoproteomes, hierarchical clustering and PC analysis were undertaken (5.19 and Figure 5.20). These results showed that individual phosphoproteomes clustered by biological replicates and then by co-culture, suggesting the analysed populations were pure and that as observed previously each patient phosphoproteome was quite distinct. KSEA measuring the influence of

MS-5 co-culture on kinase activity was more defined than what was observed during secretome stimulation (Figure 5.21). Changes in kinase activity were now consistent, with activity signatures clustering into three groups. These groups were defined by increases in kinase activity, as opposed to decreases in kinase activity as observed in both single GF and HS-5 secretome treated AML phosphoproteomic experiments. Group 1 patients were distinguished by the strong putative increases in PLK3, VRK1, ERK7, CDK3, CDK4, CDK6, and JNK2 kinas activity. The group 2 response was characterised by a strong putative increase in PDHK1-4 activity, but lacked both the MEK and CDK activity that was present in other response groups. Finally, group 3 patients displayed increased MEK1 and MEK2 activity following MS-5 co-culture, in addition to increased activity in JAK2 and Ret. Group 1 responders also harboured an NRAS mutation (p.G13D) detailed in Table 2.7, and this suggested that the NRAS mutations could influence patient cells ability to respond to MS-5 cells, although this requires further investigation.

To attribute biological significance to these changes in kinase activity K-means clustering analysis was undertaken to assign phosphopeptides to similar clusters prior to GO analysis. (Figure 5.22). This exercise demonstrates the heterogeneity in how MS-5 cells can modulate AML phosphoproteomes, as clusters 2, 3, 4 and 7 each contained phosphopeptides that were exclusively upregulated in one patient sample. Each of these clusters comprised substrates that enriched for specific pathways; Ras signalling and VEGF production (in cluster 2); aurora B, ILK and Wnt signalling (in cluster 3), anti-apoptotic signalling (in cluster 4); PKC and PLC mediated GPCR signalling (in cluster 7). The patient specific expression in these clusters suggests that these are examples of the heterogeneous signalling network dependencies that can arise in AML cells, which then shape how AML cells interact with other cells. Phosphopeptides that comprised cluster 6 were more abundant in all patient samples following MS-5 co-culture. GO analysis of these peptides suggested that MS-5 cells are able to support these primary AML cells in culture by upregulating anti-apoptotic pathways, while KSEA analysis implicated these phosphopeptides as substrates of AKT2, LATS1, CDK5 and DYRK2 signalling pathways (Figure 5.23).

Finally, recent studies had demonstrated that other tumour types can engage and instigate reciprocal signalling with surrounding stromal cells (491) to regulate cancer cell growth and survival. Following experiments that demonstrated how MS-5 cells could potentiate both anti-apoptotic signalling and modulate the activity of proliferative kinases AKT and LATS1 in primary AML, phosphoproteomic experiments were undertaken to characterise how AML co-culture affected MS-5 cell phosphoproteomes. To determine if such reciprocal mechanisms could be identified within the devised co-culture system, the phosphoproteomes of co-cultured MS-5 cells were compared those of AML naïve MS-5 cells. These experiments showed that the phosphoproteome of MS-5 cells across co-cultures were modulated by the presence of AML

cells (Figure 5.24) and hierarchical clustering of the log_2 fold changes in phosphopeptide expression demonstrated that MS-5 cell populations clustered into two groups, with one MS-5 population that did not cluster with either group (Figure 5.25). GO enrichment analysis of all significantly modulated peptides ($P<0.05$) revealed that 6/8 of MS-5 populations exhibited increased insulin receptor signalling and signal transduction following AML co-culture (Figure 5.26). This suggested that different AML cell populations were capable of modulating MS-5 cell signalling and KSEA revealed all MS-5 cells that had been cultured with AML cells exhibited increased activity of MAPKAPK2, PKCD and GSK3β pathways (Figure 5.27). Previous studies have demonstrated that cytokine production is suppressed during loss of MAPKAPK2 function (537), thus representing a potential means of AML mediated heterotypic signalling to regulate cell survival. It remains to be mechanistically proven however, whether this finding is biologically relevant.

To integrate signalling and biological observations, KSEA and PC analysis were conducted on the significantly ($p<0.05$) modulated log_2 phosphopeptide fold changes (Figure 5.28). Analysis determined that there were two kinase signatures, an AML/MS-5 interacting group that separated in PC space from AML naïve MS-5 cells (Figure 5.28, blue circle) and a AML/MS-5 independent group that did not separate. Further, these findings matched phenotypic microscopy observations of the cultures (Figure 5.29), “interactive” co-cultures exhibited increased AML single cell embedding in the stromal layer, whereas the “independent” co-cultures were typified by clusters of AML cells separate from the stromal layer.

Taken together, these experiments showed that AML kinase signalling network underwent significant and heterogeneous shifts in activity following stimulation with stromal secreted proteins. Most strikingly, different primary AML samples were able to respond to stromal cells through both homogeneous and heterogeneous network routes, while simultaneously stimulating signalling nodes implicated in cytokine production.

Chapter 6: Functional and biochemical characterisation of PAK signalling in AML

6.1 Introduction and aims of the study

Our group using a kinase substrate enrichment approach (KSEA) had previously analysed a panel of primary AML samples comparing the relative activity of the protein kinases, this work revealed that the substrates of PAK were frequently overexpressed in the samples compared to healthy controls (Figure 6.1) (271). Experiments in Chapter 3 showed that PAK is modulated by the stromal secretome (Figure 3.9) and subsequent work demonstrated that in culture primary AML cells were profoundly sensitive to PAK inhibitors compared to that of other kinase inhibitors (Chapter 4). Other studies have also shown PAK to be a key mediator of leukaemogenesis in FLT3 and KIT driven leukaemia and these neoplasms also exhibited sensitivity to current PAK inhibitors (IPA-3 and PF-3758309) (207, 538, 539).

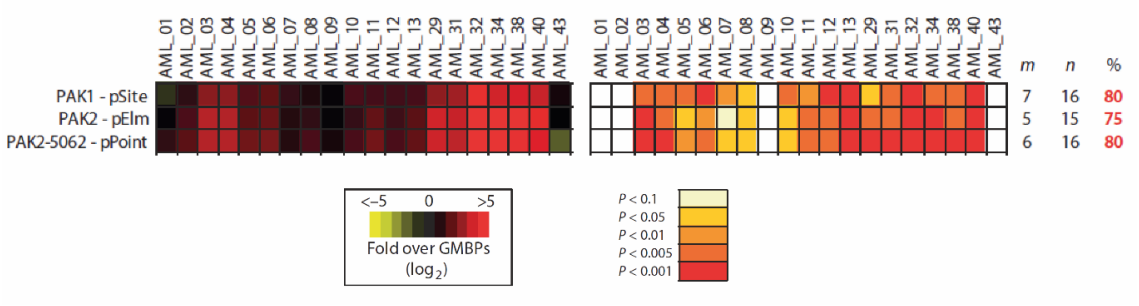

Figure 6.1: Global kinase substrate enrichment analysis (KSEA) reveals substrates of PAK are one the most frequently enriched groups in primary AML cells. Phospho-peptide enrichment followed by liquid chromatography-mass spec/mass spec (LC-MS/MS) quantification was conducted on primary cells from 20 AML patients and granulocyte colony-stimulating factor-mobilised peripheral blood (GMPB) cells from 5 healthy donors. The heatmap on the left shows enrichment of the PAK substrate groups in AML patients compared to the healthy donors, of which there is quite a large increase in expression. The right heatmap shows the statistical significance of the changes/patient. Definitions m, no of substrates in the substrate group for that particular PAK; n, no of cases significant change in the PAK substrate group; %, proportion of AML patients with significant enrichment of PAK. Figure adapted from (271).

PAKs are a group of highly conserved serine/threonine protein kinases that sit directly downstream of the Rho GTPases, most notably CDC42 and Rac (540, 541). The PAKs have been shown to function as effectors of GTPases as well as with PDK1 (542), PKA (543) , PI3K (544) and AKT (545). Through their kinase activity they mediate the downstream signalling that induces the physiological effects of GTPase signalling (Figure 6.2). PAKs regulate apoptotic pathways through interactions with the apoptotic effectors like BAD, BimL and DLC1. Hormone independence through phosphorylation of the oestrogen receptor (ER) and cell cycle progression can be regulated through PAK interactions with Histone 3 (H3), Aurora A kinases and polo-like kinase (PLK1). PAK can also modulate cell growth through its influence of

transcription factors and co-regulators SNAI1, SHARP, FKHR and CtBP1. These same substrates also enable PAK to influence the epithelial-mesenchymal (EMT).

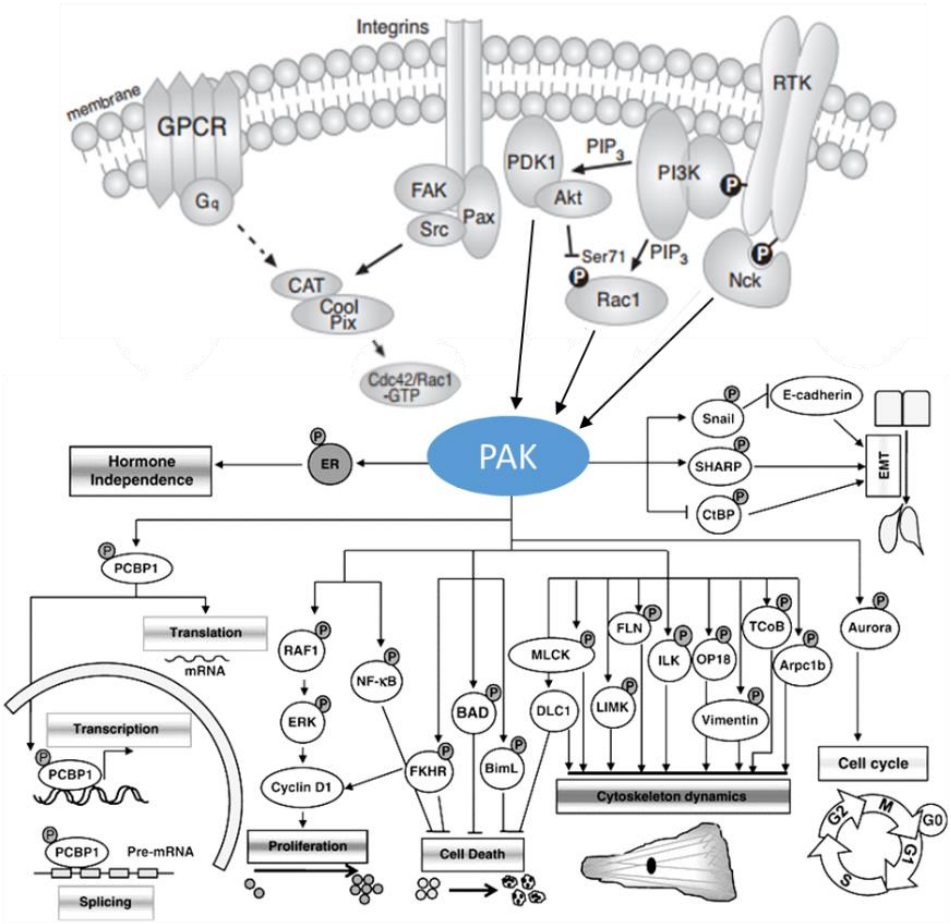

Figure 6.2: PAK signalling cascade in a physiological context. Upstream of PAK lie many signalling pathways. Signals can be initiated through signalling molecules binding to G-protein coupled receptors (GPRC), receptor tyrosine kinases (RTK) or integrin's. Downstream effectors of these membrane proteins eventually activate PAK through Rho GTPases such as Cdc42 and Rac. Once activated PAK can influence a myriad of functions; cell proliferation through the MAPK pathway by phosphorylating Raf1, cytoskeletal dynamics by phosphorylating regulators such as myosin light chain kinase (MILCK), Lim domain kinase(LIMK), and filamin A. Figure adapted from (546).

There are six isoforms described in mammalian cells, and based on structural and functional characteristics these isoforms can be further sub-divided into two groups (546).The group I PAKs comprise of the isoforms PAK1, PAK2 and PAK3; group II is comprised of PAK4, PAK5/7 and PAK6 (547). Both groups of PAKs have distinct and shared functions and are recognised as key positive regulators of AKT, ERK and Wnt signalling in most cell types (539).

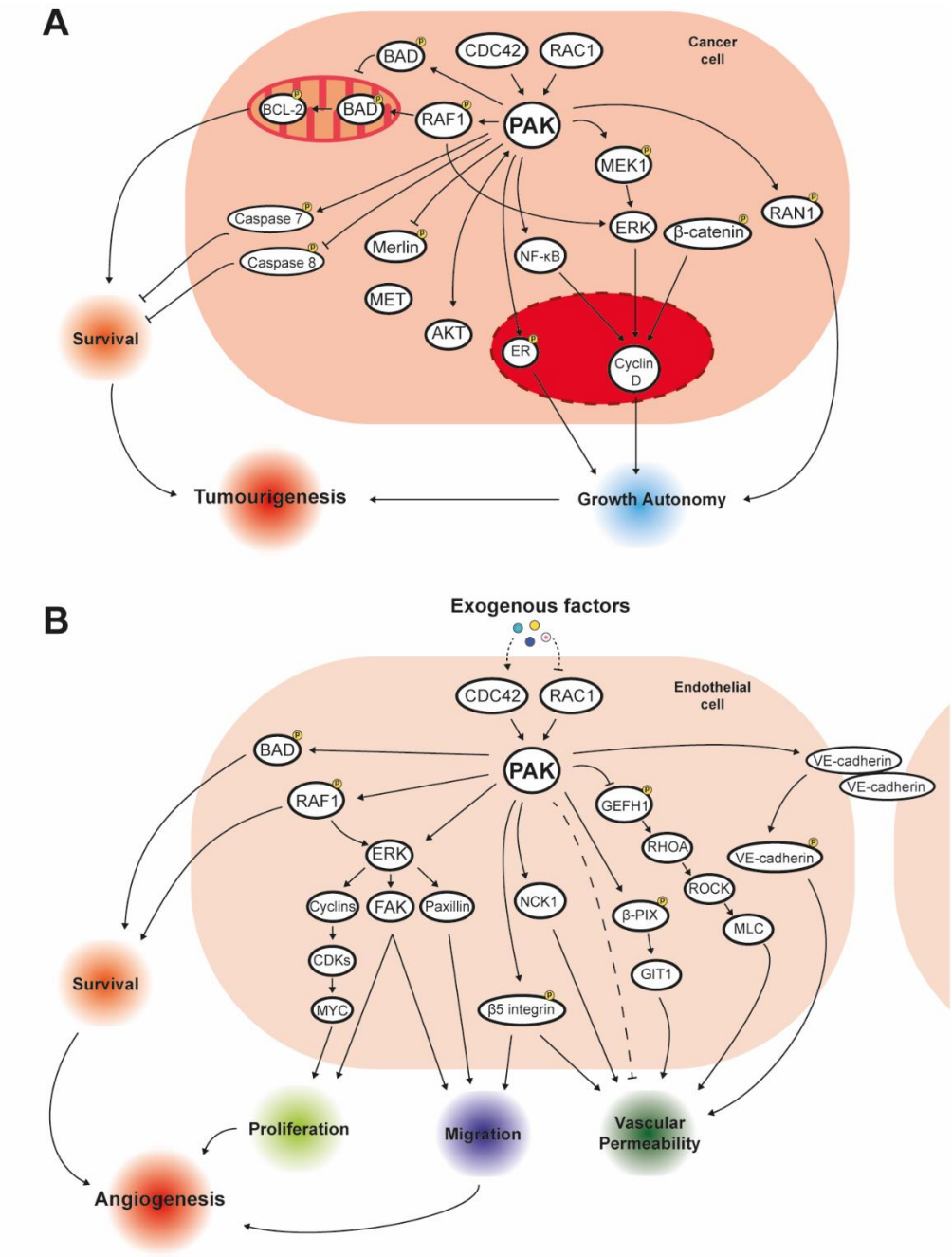

Figure 6.3: Oncogenic PAK signalling characterised in solid tumours. (A) Describes PAKs implications in signalling pathways effecting cell survival and growth signal autonomy. PAK has been implicated in the activation of AKT and NF-κB however, the exact mechanism of action is currently unknown. It is known to interact with apoptotic proteins such as BAD and caspases 7 and 8 to influence cell survival. Interactions with MEK1 and β-catenin are known to effect cell cycle progression and therefore growth and proliferation. **(B)** Over activity of PAK in an oncogenic context is essential for angiogenesis, cell proliferation, survival, attachment and migration. The phosphorylation of BAD and C-RAF by PAK protects against apoptotic stimuli. The ERK pathway is exploited for cellular proliferation and migration by the RAC–PAK pathway. Vascular permeability is mediated by PAK through modulation of cell–cell adhesion molecules. MLCK phosphorylation by PAK generates increased contractility and permeability.

Oncogenic overexpression of PAK has been described in a number of solid tumours including breast, colorectal, pancreatic and ovarian, with expression positively correlating with advanced disease and poor outcome (515, 547-549). In these tumours PAK promotes cell growth, helps evade apoptosis and mediates invasion and metastasis (Figure 6.3) (515, 548-551).

It has been shown that PAK is overexpressed in AML (271) and due to the position of PAK in the signalling cascade it is postulated that PAK either helps drive or facilitate disease progression. We hypothesised that for some patients PAK is a key contributor to the AML pathophysiology. If this is the case then targeting PAK could be a viable means of treatment for these patients, results in Chapter 4 demonstrate how sensitive AML cells can be to PAK inhibition. But to effectively target PAK it is important to understand the mechanisms that underpin and regulate PAK activity in AML. Work presented in this chapter sought to functionally and biochemically characterise PAK signalling in AML utilising proteomic approaches.

The aims of this chapter were to:

(i) Determine factors that lead to PAK activation in AML.

(ii) Optimise a co-immunoprecipitation coupled mass spectrometry approach.

(iii) Identify PAK binding partners in AML using co-immunoprecipitation.

(iv) Validate identified interactions and the contribution to AML.

6.2 Meta-analysis of genetic mutations in AML

To account for the increased PAK activity in AML (271), we investigated the mutational status of PAK in AML with a meta-analysis of published large-scale genomics data. Using this approach, we aimed to establish if the increased activation of PAK had foundations in mutations that could induce constitutive activation, loss of substrate specificity or overexpression of the protein. To evaluate an appropriate cohort we conducted a search of the catalogue of somatic mutations in cancer (COSMIC) generated by the Sanger institute. This is the largest repository of whole genome sequenced AML patient samples (n=390). In total there were 8178 separate genes identified as carrying a mutation in at least one individual across 390 AML patients. The frequency of these mutations was as previously described in the literature with *NPM1, FLT3, DNMT3A* and *GATA2* the most prevalent across the samples (Figure 6.4).

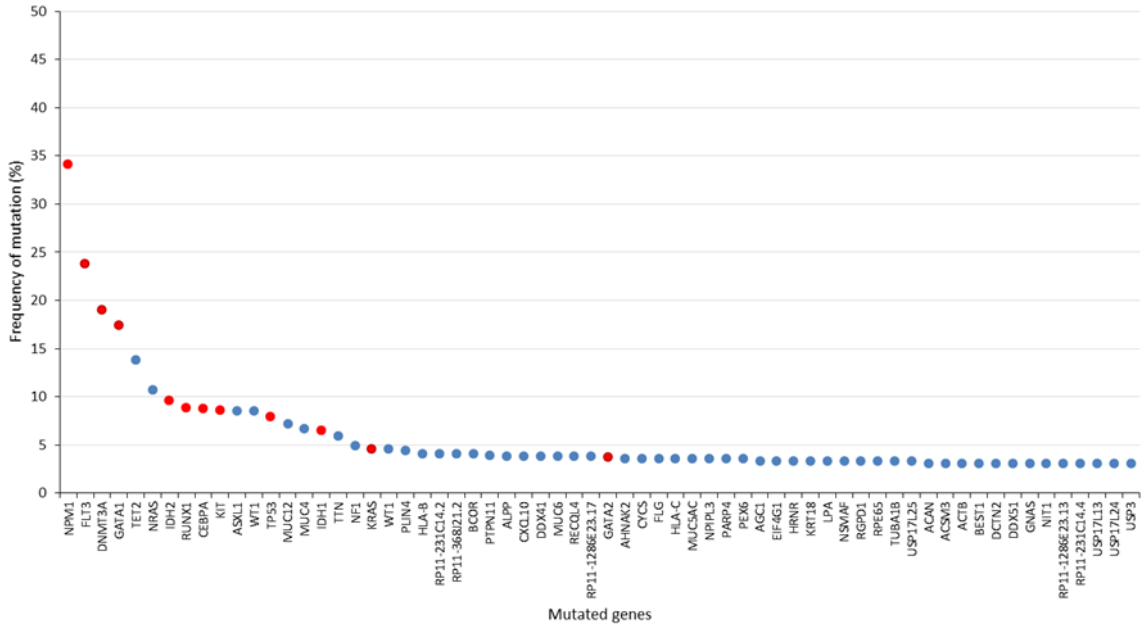

Figure 6.4: Meta-analysis of genetic mutations from COSMIC repository of 390 whole genome sequenced AML patients. The graph shows genes that were mutated in at least 3% of patients, 8178 mutated genes identified across a screen of 390 AML patients. Genes that are well annotated in the literature as being implicated in AML are highlighted red. None of the PAK genes were mutated in this dataset.

This repository contained many of the characteristics that the literature has previously described in AML, such as *NPM1, FLT*3 and epigenetic regulators frequently harbouring the most mutations, thus we believed it to be representative of AML. Within this dataset there were no mutations in PAK, with the independent Sanger annotated resources also listing PAK as a gene that harbours no mutations in these 390 AML genomes. This finding suggests that there are mechanisms other than genetic, in AML that contribute to disease progression.

In the instances where PAK exhibits a high level of activity there are many routes by which this activity could be facilitated. Protein expression can be affected by epigenetic regulation; ligand binding and cell-cell interactions can activate cell-signalling pathways, as demonstrated by work in Chapter 5. Despite an absence of PAK mutations in these screens, that is not to say there is no genetic contribution as these screens were only in coding regions of the genome and deregulation of a particular target protein can arise through the acquisition of mutations in non-coding DNA elements.

6.3 Western blot analysis of PAK expression in AML cell lines

Following the revelation that AML frequently lacks PAK mutations it was deemed pertinent to establish PAK activity in cell models MV4-11 and P31/FUJ. Previously Chapters 3 and 5 have demonstrated that PAK activity can be altered by elements of the microenvironment (Figure 3.9 and Figure 5.5). For these experiments it was important to establish that between

the cell lines we possessed models that displayed both good protein expression of all PAK isoforms and displayed strong basal levels of activity.

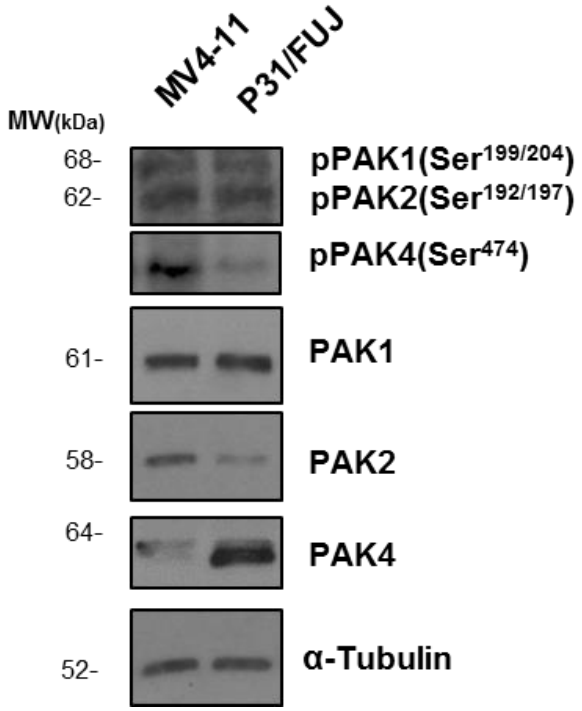

Figure 6.5: Western blot showing the activity and basal expression of the PAK isoforms AML cell line. Equal numbers of MV4-11 and P31/FUJ cells were lysed in 500µl of Tris-Triton lysis buffer. 30µg of samples analysed by western blot for PAK isoforms, and α-tubulin loading control.

Western blot analysis of MV4-11 showed that the cell line strongly expressed the group 1 PAKs (PAK1 and PAK2) and had mild expression of PAK4 (Figure 6.5). MV4-11 also exhibited high expression of the activatory phosphorylation sites of PAK1$^{S199/204}$, PAK2$^{S192/197}$ and PAK4^{S474}. P31/FUJ had very strong expression of PAK1 and PAK4 isoforms, however, PAK2 was only moderately expressed. Assessment of the PAK activity markers revealed that P31/FUJ had high basal levels of PAK1 and PAK2 activity, but very low basal levels of PAK4 activity. Collectively these results suggested that both MV4-11 and P31/FUJ were good models for studying the importance of PAK1 and PAK2 activity in AML, however, MV4-11 was a better candidate to study PAK4.

6.4 Co-immunoprecipitation optimisation

Having identified a suitable model of AML that expressed high levels of phosphorylated PAK, the aim of this section was to optimise an approach that would enable the study of dynamic PAK binding partners (i.e. proteins that bind PAK as a function of its activation status), as these could provide a read out of activity and downstream could even serve as additional drug targets for patients with overactive PAK signalling.

6.4.1 Principle of approach

Co-immunoprecipitation (co-IP) is a common technique used to identify protein-protein interactions. The technique relies on the ability to identify a good antibody and requires the optimisation of multiple aspects to ensure that the user is able to capture an accurate representation of the protein interactions that occur in cells.

In a bid to identify the proteins that regulate PAK activity in AML and thus map the functional mechanisms involved in executing PAK function, it was decided that an optimised co-IP represented the most powerful and practical means of investigation. Initial optimisation experiments investigated the efficiency of isolating PAK complexes using different lysis buffers, wash buffers, varying antibody incubation times and employing different protein elution steps (Table 6.1). The optimised approach is described in Figure 6.6.

Experimental aspect	Optimisation
Antibody	• Antibodies were used at different concentrations to achieve optimal ratio of antibody to target protein • Investigated PAK antibody incubation times (15min – 12 hours) to try and maximise the resolution of different interaction types (transient-constituent binders)
Lysis Buffer	• Tested different detergents (Triton X-100, NP-40 and **CHAPS**) • Tested HEPES based and Tris based lysis buffers
Wash buffer	• Varied ionic stringency and pH of buffers that washed non-specific proteins away from complexes – too strong and weak interactors are lost
Non-specific protein control	• The inclusion of a pre-clear step – incubation with solid support before antibody, which allowed for the removal of non-specific proteins from the lysate • In some samples a pre-clear step was not included in case it was removing actual binding partners
Bead elution	• Optimised a faster and cleaner elution technique of direct trypsin digestion of proteins from protein A/G sepharose beads. This reduced contaminants.
Protein Detection	• The western blot detection required a lot of optimisation. In particular with detection antibodies and overcoming the light/heavy chain interference from the co-IP antibody when probing with detection antibody (many antibodies are raised in rabbit, leading to cross reactivity).

Table 6.1: Co-Immunoprecipitation optimisation. Aspects of the technique that were optimised in an effort to preserve PAK protein-complexes for analysis and effectively reduce identification of non-specific interactions.

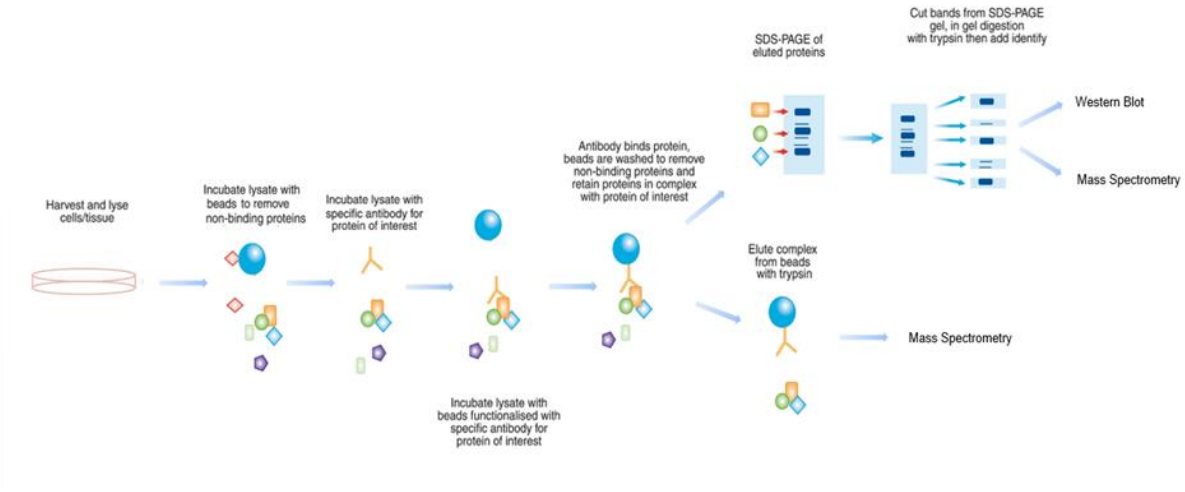

Figure 6.6: Optimised co-immunoprecipitation workflow: First cells are prepared in culture under desired experimental conditions. After treatment cells are washed in PBS and protease inhibitors before harvesting and lysis using a CHAPS HEPES based buffer. Cellular debris is spun down and removed, resultant supernatant is normalised for each sample so that they each contain the same amount of protein. Protein A/G beads are pre-conditioned in lysis buffer before pre-clearing sample lysate with the beads (10 min). Beads are then removed with the non-specific proteins bound, ready to incubate the sample lysate with the PAK specific antibody. After allowing enough time for immune complexes to form (40min – overnight), freshly conditioned protein A/G beads are introduced so antibody complexes can be captured (20 min – 4 hours). It is important to get the timing right otherwise associated proteins could disassociate. After capture protein complexes are eluted and washed to remove any non-specific binders or non-constituent binders (3x washes lysis buffer, 3x washes Tris-buffer, 3x washes NH_4HCO_3). At this point it is possible to directly digest elute from the beads and analyse the sample using mass spectrometry or the sample can be mixed with Laemmli buffer and interactions probed for by western blot. Figure adapted from (552).

6.4.2 Effects of detergent type on PAK protein yield

To effectively capture protein interactions, it is important to try and preserve protein complex formation during the immunoprecipitation process. One element that has previously been shown to have a large effect on complex preservation is the composition of the lysis buffer used to extract proteins (552). Therefore, to increase PAK yield and preserve potential interactions a series of detergents and buffer combinations were tested.

Three detergents Triton-X100 (1%), NP-40 (1%) and CHAPS (0.3%) were tested as part of a Tris based buffer, Triton X-100 was also tested as part of the typically strong RIPA buffer and a Hepes based CHAPS buffer was included. These investigations sought to establish which buffers/detergents led to good PAK recovery across isoforms. Equal numbers of P31/FUJ cells ($1x10^7$) were harvested and lysed with 500µl of each lysis buffer according to methods section 2.4. 30µg of each lysate was then subjected to SDS-PAGE and protein recovery assessed via western blot (Figure 6.7)

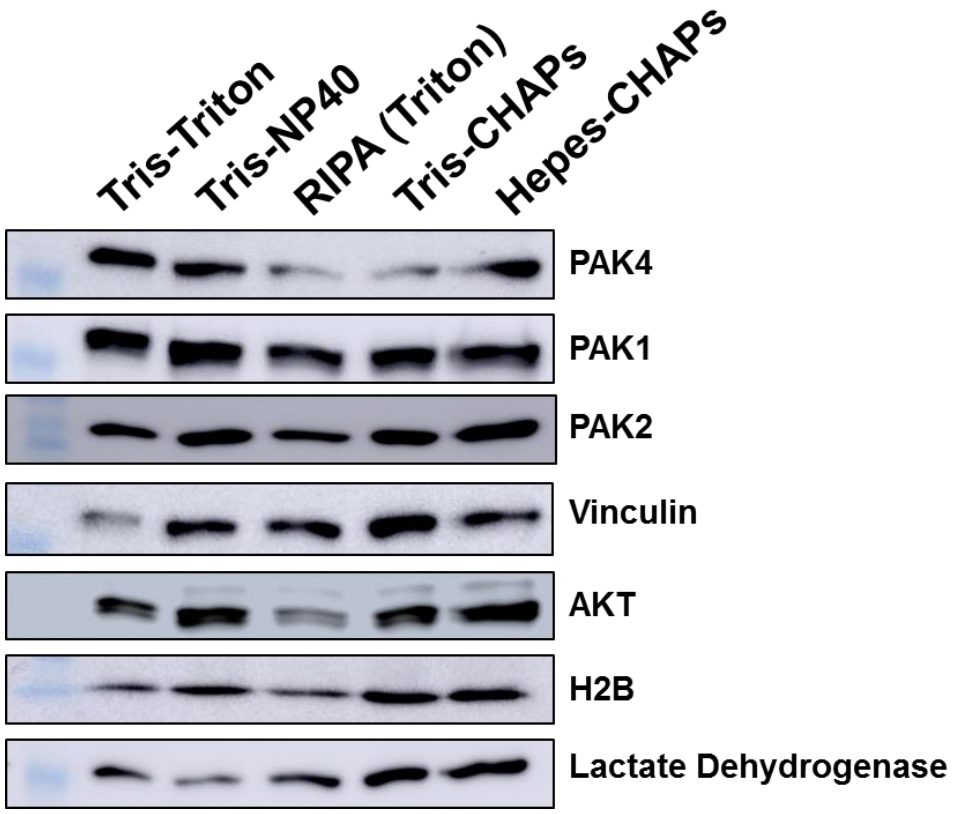

Figure 6.7: Hepes based CHAPS lysis buffer is optimal for PAK analysis. Equal numbers of P31/FUJ cells were lysed in 500µl of Tris or Hepes buffers containing Triton X-100, CHAPS or NP40 detergent. 30µg of samples analysed by western blot for PAK isoforms, vinculin, AKT, Histone 2B and lactate dehydrogenase.

The results of the experiment revealed that all lysis buffers performed well in recovering the group 1 PAKs, however, PAK 4 was not recovered well in RIPA and Tris-CHAPs based buffers. PAK4 was well recovered in Tris-Triton, Tris-NP40 and Hepes-CHAPs buffers. Analysis of the other cytosolic proteins such as AKT and vinculin demonstrated that CHAPs was the best detergent for the recovery of these proteins. Finally, H2B recovery was assessed to measure the recovery of nuclear proteins and analysis showed that the CHAPs based buffers yielded the highest recovery. Collectively these results indicated that the Hepes based CHAPs buffer was the most efficient buffer for both the recovery of PAK proteins, and also the preservation of proteins from both cytosolic and nuclear fractions. If PAK does localise to other compartments during certain conditions, it is important to be able to capture these events or potential binding partners would be lost.

6.4.3 On-bead protein digestion

As previously discussed, efforts were made to optimise PAK recovery prior to co-IP through lysis buffer optimisation, in these same experiments PAK antibody specificity was also optimal as the antibodies used were also co-IP compatible. Utilising the approach as detailed in Figure 6.6, PAK complexes were pull down, washed and subjected to SDS PAGE. The Subsequent gel was stained with Coomassie blue and proteins visualised (Figure 6.8A). Samples 1 (PAK1 Ab) and 2 (PAK2 Ab) had no detectable protein bands, samples 3 (PAK3 Ab) and 4 (PAK4 Ab) had

bands around the region of PAK and the total lysate (TL) and empty bead (EB) controls both displayed that large amounts of protein were still present in lysates. The TL sample had undergone no form of immunoprecipitation and the EB sample was that of the lysate following incubation with the sepharose beads, this control was desirable as protein loss in this sample represents non-specific proteins that have affinity to the solid support used to elute co-IP complexes.

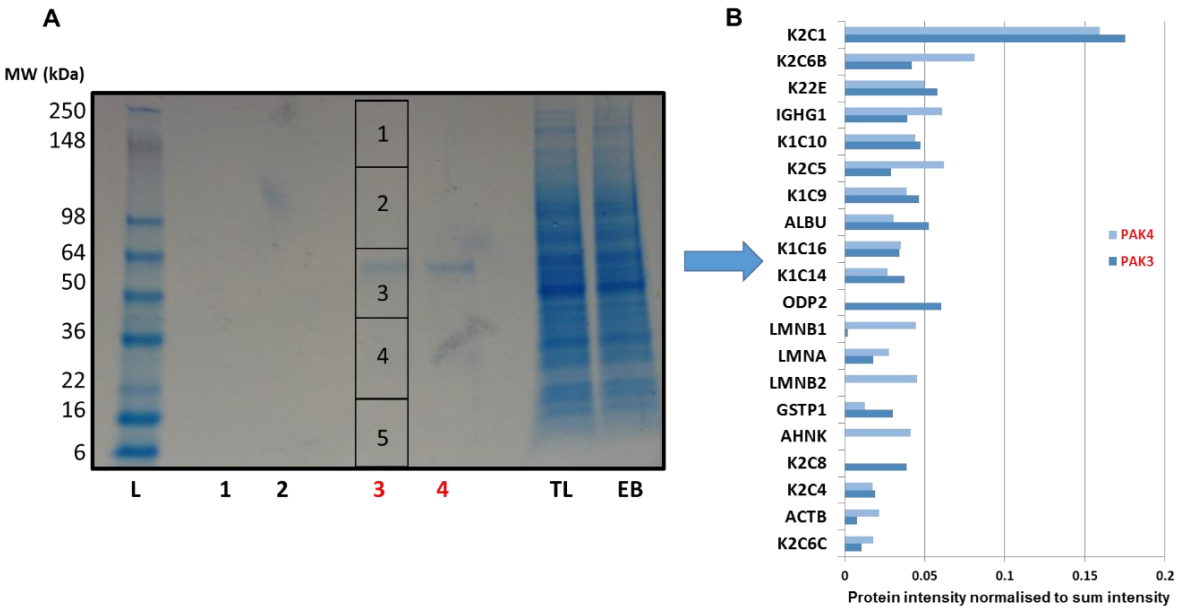

Figure 6.8: In-gel digestion of PAK co-IP complexes leads to no PAK detected in mass spectrometer. (A) Coomassie stain of PAK pulldown experiments following SDS PAGE. Sample lanes 3 and 4 cut into five bands (marked 1-5) for protein extraction and sample clean-up. **(B)** Pooled fractions run analysed by LC-MS/MS, 20 most abundant identified proteins displayed, PAK not identified. L; ladder, TL; total lysate, EC; Empty bead control.

The Coomassie stain suggested that no protein had been enriched in samples 1 and 2. Therefore, as samples 3 and 4 did have bands in the appropriate regions, bands were excised, proteins extracted from gel pieces and processed for LC-MS/MS detection. This approach failed to identify any peptides derived from PAK proteins in the mass spectrometer, with the most common peptides being that of the contaminant keratin (Figure 6.8B).

In order to remove the contaminants and streamline the protocol, as lengthy processing only increases the chances for immuno-complexes to dissociate, the experiment was repeated. However, following wash steps, tryptic digestion was undertaken whilst the protein complexes were still immobilised on-bead. Proteins identified in these experiments (Figure 6.9, red markers) that met the selection criteria (MASCOT score > 50, >2 peptides counted, protein absent in antibody free negative control, >2 Log_2 fold enrichment in targeted pull-down over control) supported using co-immunoprecipitation as a means to identify PAK binding partners. The pull-down experiments in Figure 6.8 were successful when targeting PAK1, PAK2 and PAK4 with identification of these target proteins consistently the most abundant proteins. The PAK3

targeted pull-down, however, was not successful, as the target protein was not identified in the experiment (Figure 6.9C). This could have been either due to the quality of the antibody, or more likely, because PAK3 expression occurs nearly exclusively in the brain.

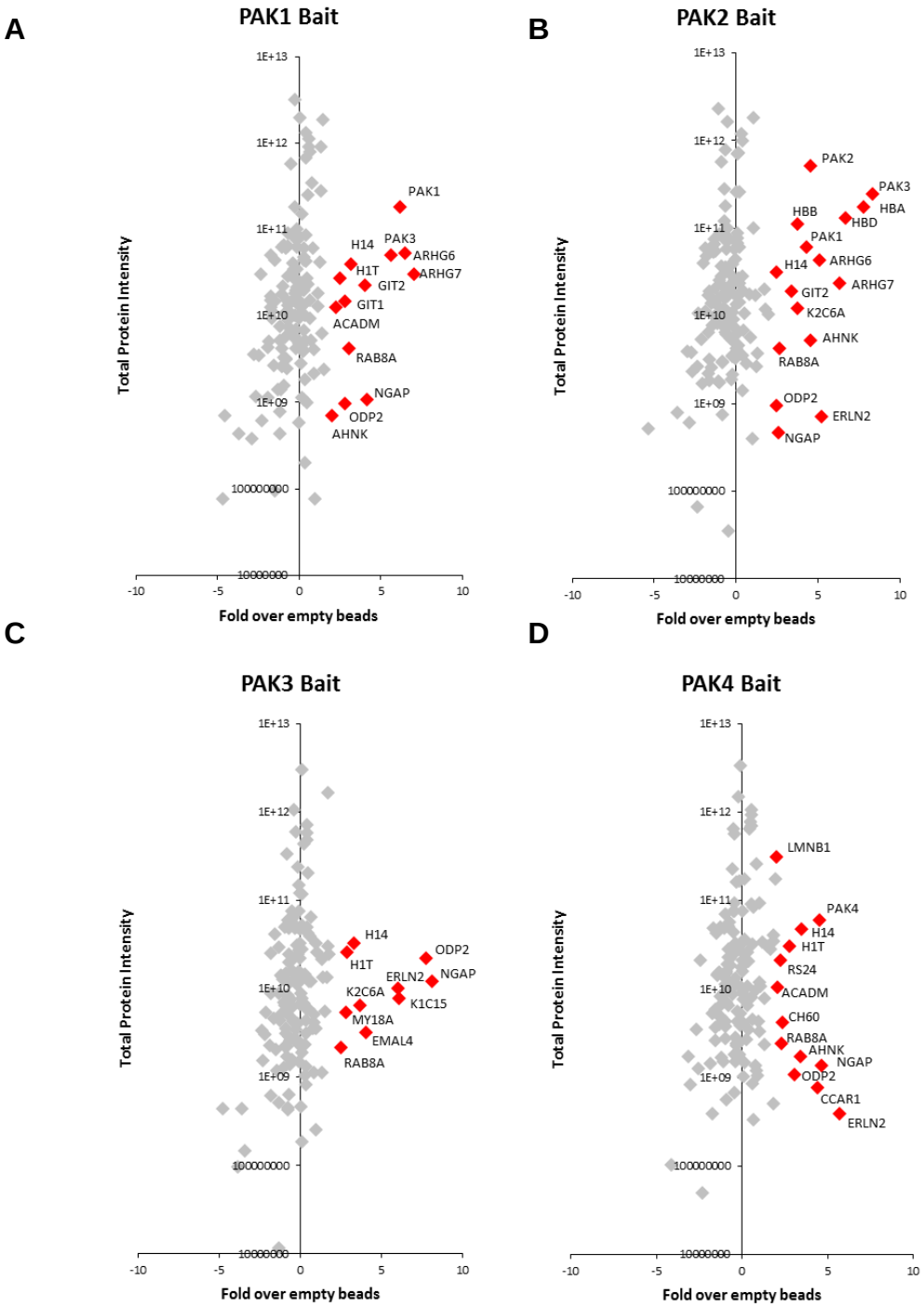

Figure 6.9: Co-Immunoprecipitation optimised pull-down results. Co-immunoprecipitation of PAK proteins led to the identification of proteins highlighted in red, which following analysis were deemed to be enriched for in target protein pull down experiments. **(A)** Pull-down of PAK1 and proteins in complex. **(B)** Pull-down of PAK2 and proteins in complex. **(C)** Pull-down of PAK3 and proteins in complex, PAK3 not identified so experiment considered unsuccessful. **(D)** Pull-down of PAK4 and proteins in complex.

An assessment of proteins identified in each of the successful pull-down experiments (Figure 6.10) revealed some distinctions between the group I PAKs (PAK1, PAK2) and group II

PAKs (PAK4) pull-downs. In the PAK1 and PAK2 pull-downs known binders of PAKs were present (PAK1, PAK2, GIT1, GIT2, ARHGEF6, ARHGEF7) providing a positive control (553), although PAK3 was identified this was likely due to identical peptide sequences shared between PAK1 and PAK3. The PAK4 pull-down did not identify any known protein interactions, but this probably reflects the lack of known interactions. Other proteins that were shared across the conditions were Ras-related protein Rab-8A (RAB8A) Ras GTPase-activating protein nGAP (RASAL2), Histone H1t (HIST1H1T), Histone H1.4 (HIST1H1E), Medium-chain specific acyl-CoA dehydrogenase, mitochondria (ACADM), Erlin-2 (ERLIN2), Neuroblast differentiation-associated protein AHNAK (AHNK) and Dihydrolipoyllysine-residue acetyltransferase component of pyruvate dehydrogenase complex, mitochondrial (DLAT).

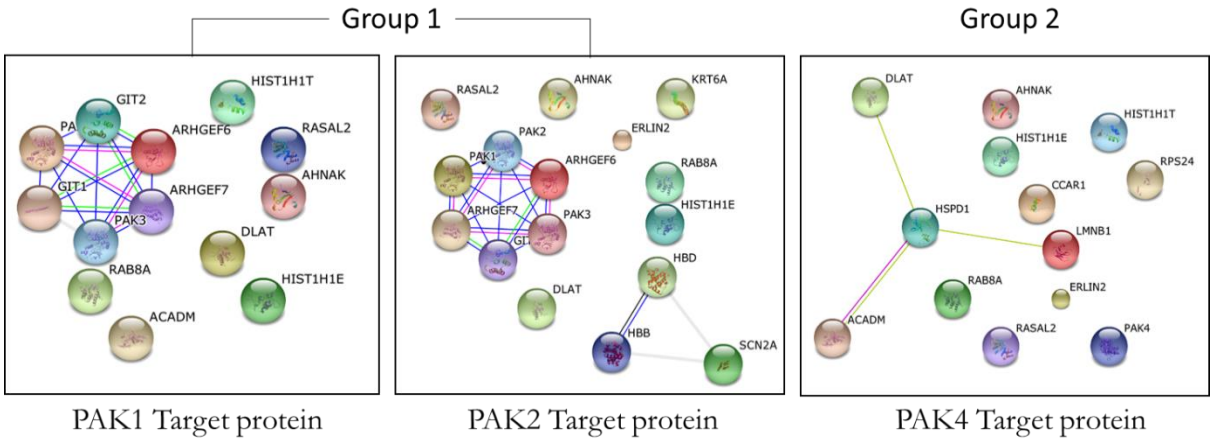

Figure 6.10: Proteins identified in pull-down experiments of PAK1, PAK2 and PAK4. Protein string analysis confirms the pull-down of known binding partners of PAK1 and PAK2. Although no known binders of PAK4 were pulled down, this is probably more of a reflection of the lack of knowledge to date.

6.5 Optimisation of conditions for dynamic complex formation

Having established a co-immunoprecipitation protocol that showed specificity to PAK and its known binding partners, investigations focussed on conditions that may promote dynamic PAK complex formation. Work presented in Chapter 3 and Chapter 5 demonstrated that the secretome can stimulate PAK1 and PAK2 phosphorylation (Figure 3.9 and Figure 5.5A), however, it was also observed that secretome treatment led to a reduction in PAK4 phosphorylation (Figure 5.5B). Accordingly, a number of preliminary PAK pulldown experiments were conducted investigating the effects of secretome stimulation on the composition of PAK pull-down complexes. As serum modulation had been a successful approach in revealing regulatory binding partners of PI3K by Beltran et al. (552), this too was employed to modulate PAK interactions (Figure 6.11). The final set of studies performed to modulate PAK interactions employed the use of PAK inhibitors IPA-3 and PF-3758309.

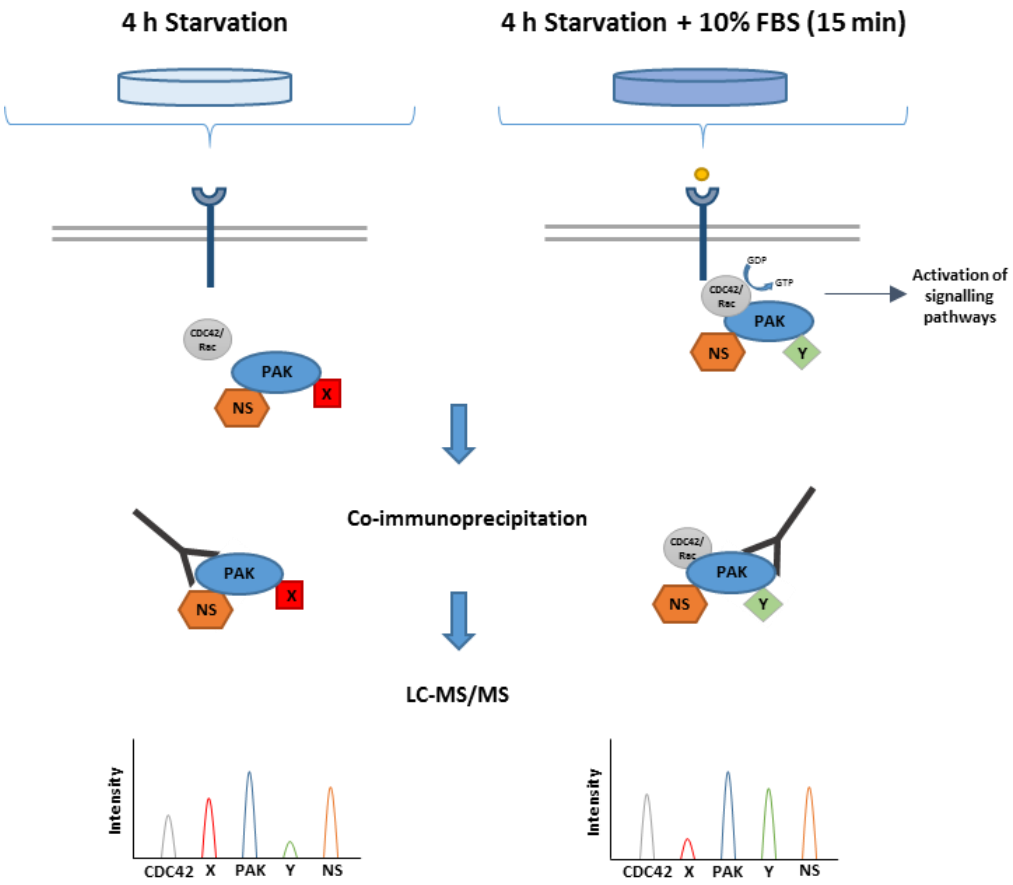

Figure 6.11: PAK co-immunoprecipitation strategy. For each treatment MV4-11 or P31/FUJ cells were serum starved for 4 hours first to bring signalling to a baseline so that dynamic binders of an active pathway would bind after 15 minutes of 10% serum stimulation. Subsequent co-immunoprecipitation of PAK followed by LC-MS/MS analysis should reveal dynamic PAK binding partners (X and Y) between the conditions, whereas the abundance of non-specific binders (NS) should not change across the conditions.

6.5.1 Serum deprivation followed by secretome stimulation

To investigate the impact of the secretome on PAK activity and therefore, PAK behaviour and interactions, the optimal conditions for secretome induced or inhibited PAK phosphorylation needed to be determined. Western blot experiments were devised to understand PAK response during serum starvation and following stimulation with either MS-5 fractionated secretomes (both >5kDa and <5kDa) or unfractionated MS-5 CM.

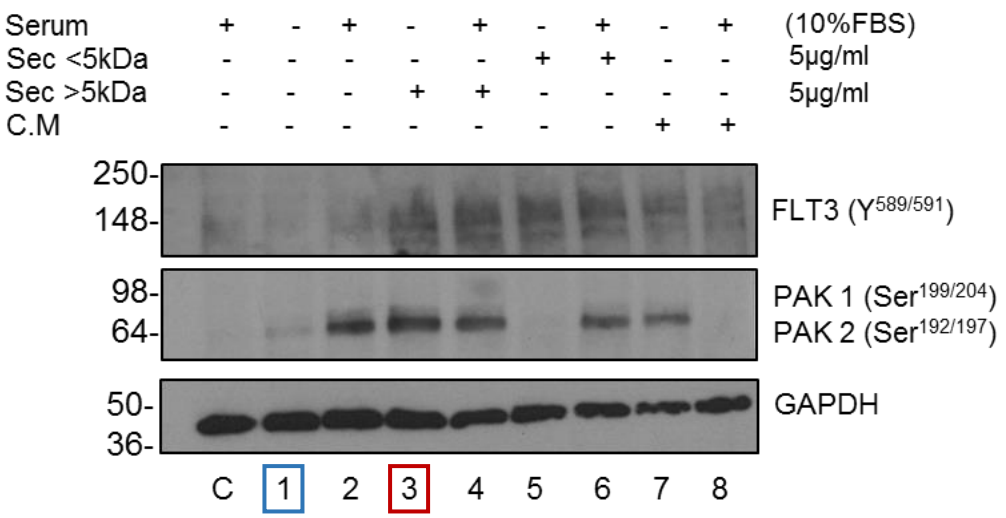

Figure 6.12: Western blot analysis of PAK1 and PAK2 status during secretome and serum stimulation. AML cells starved for 4 hours (except basal condition [C]) prior to 15 minutes stimulation with 10% serum, 5µg/ml >5kDa/<5kDa secretome or MS-5 CM as indicated above. Western blots for the activatory phosphorylation sites on PAK1, PAK2 and FLT3. Loading controls for GAPDH are shown in each case. C; basal conditions.

Western blot analysis revealed that both the basal condition (C) and serum starvation (1, blue square) did not induce phosphorylation of PAK1, while minimal phosphorylation of PAK2 was recorded in the starved sample (Figure 6.12). Stimulation with the >5kDa secretome fraction after starvation induced large amounts of PAK phosphorylation (3, red square), the <5kDa was able to induce PAK phosphorylation in the presence of serum and conversely CM alone could induce PAK phosphorylation, but in the presence of serum it could not. It was concluded from these results that PAKs (1, 2, 4) would be pulled down following MV4-11 cells undergoing the treatments highlighted with the blue and red squares (Figure 6.12) alongside an empty antibody pull down control.

Co-IP of PAK proteins from MV4-11 cells stimulated with MS-5 secretome identified 41 proteins in these experiments (Figure 6.13A, red zone) that met the selection criteria (MASCOT score > 50, >2 peptides counted, protein absent in antibody free negative control, >2 Log_2 fold enrichment in targeted pull-down over control). The 41 proteins identified are listed in Figure 6.13B and as in early controls PAK proteins (coloured red) were the most enriched proteins (except PAK4) and known binders such as ARHG7, GIT1, ARGH6, GIT2 and ARHG8 (coloured orange) were also identified (Figure 6.13C), suggesting the co-IP had worked.

A

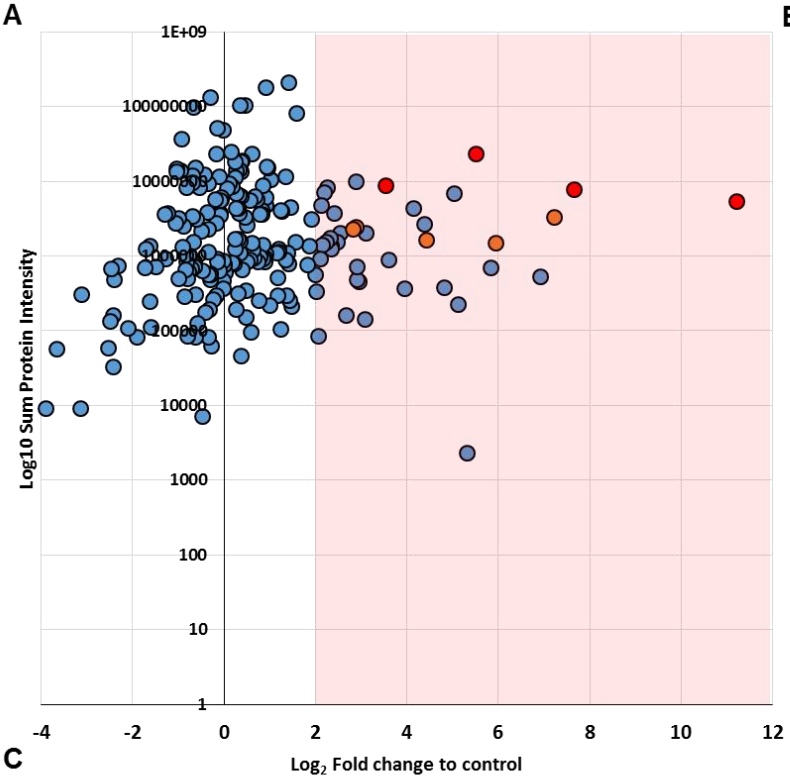

B

Protein	Log_2 FC	Mascot score	No of peptides
PAK3	11.21	240.1	6
PAK1	7.65	266.6	8
ARHG7	7.24	248.0	7
APOBR	6.92	61.5	2
GIT1	5.95	92.0	5
RL6	5.83	58.6	3
PAK2	5.52	549.8	19
TITIN	5.31	149.7	2
FMNL	5.11	84.3	2
NPM	5.03	195.1	11
COQ7	4.82	84.1	2
ARHG6	4.43	312.0	6
FCERG	4.38	111.8	4
TCPD	4.14	426.3	12
RL34	3.95	96.3	4
RL28	3.59	123.4	5
PAK4	3.54	312.0	13
RS19	3.11	179.1	7
LPP	3.08	62.0	2
RL19	2.95	94.9	3
GNAI2	2.91	72.9	2
RL7	2.91	131.7	2
GIT2	2.89	394.5	16
ARHG2	2.88	218.8	10
RL13	2.83	171.1	5
UMPS	2.67	82.1	2
BAG6	2.54	164.3	2
RS9	2.46	146.3	8
RL3	2.40	85.4	7
DDX17	2.34	99.9	4
SFI1	2.34	57.1	2
RL10L	2.32	149.2	2
RL10	2.26	106.9	6
RL18	2.23	55.4	3
RS5	2.19	105.3	10
RL35	2.14	55.0	4
IGHG3	2.13	151.6	4
RS10	2.10	70.9	3
SYFA	2.06	130.0	2
RL26	2.01	104.2	2
RS13	2.00	75.3	4

C

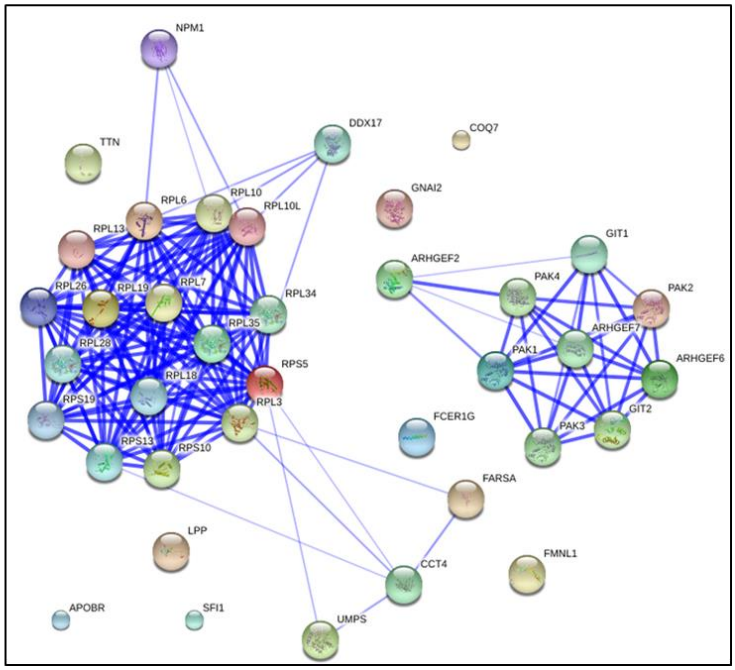

Figure 6.13: Co-Immunoprecipitation of PAK in MV4-11 cells following secretome stimulation. Co-immunoprecipitation of PAKs led to the identification of proteins which following analysis were enriched in target protein pull down experiments. **(A)** Eluents of **p**ull-down using PAK1, 2 and 4 antibodies combined compared to no antibody control **(B)** Table listing fold change enrichment, mascot score and number of peptides detected. **(C)** STRING protein analysis of pull down proteins that had a fold enrichment of >2 Log2 fold, >2 proteins identified, >50 mascot score between conditions. Independent technical replicates n=2. Red = Bait proteins, orange = known interactors.

Comparisons between the PAK co-IPs however, were not as revelatory. When protein enrichment was compared between conditions (secretome stimulated vs serum starved) there were no significant enrichments, with only Ig lambda chain V-I region (LV105) being enriched and this had a borderline mascot score of 51.29 and only 2 peptides identified (Figure 6.14). The

proteins that were more abundant in the starved conditions are represented in the blue region and mainly comprised of keratins. These findings suggested that secretome stimulation would not be the best means to elicit dynamic PAK binding.

A

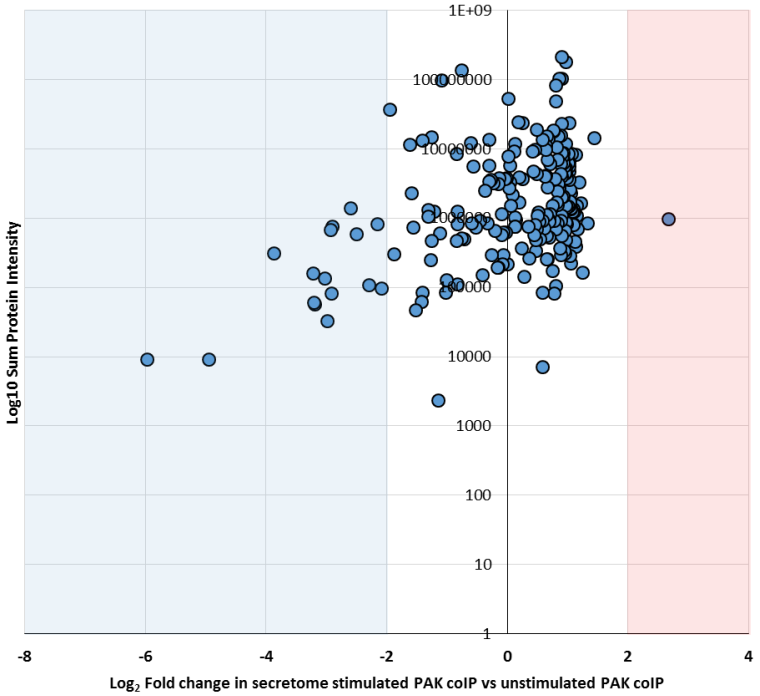

B

Protein	Log_2FR	Mascot score	No of peptides
LV105	2.66	51.29	2
DCD	-2.09	154.77	3
K2C6A	-2.16	317.38	8
DESP	-2.30	152.12	6
HORN	-2.51	428.41	12
K2C1B	-2.60	214.24	3
K1C13	-2.91	275.88	5
K2C3	-2.91	364.75	2
K1C26	-2.94	58.18	2
KSYK	-2.98	63.32	3
K1C16	-3.03	265.47	3
PLAK	-3.20	230.19	7
FILA2	-3.21	129.88	3
K2C74	-3.22	118.36	3
K1C12	-3.87	92.45	2
K2C79	-4.95	241.31	3
KRT84	-5.98	216.15	3
CD79B	-13.17	70.69	2

Figure 6.14: Comparison between secretome stimulation PAK pulldown and unstimulated reveals no substantial enrichment. Co-immunoprecipitation of PAKs led to the identification of proteins which following analysis were enriched in target protein pull down experiments. **(A)** Eluents of **p**ull-down using PAK1, 2 and 4 antibodies combined compared to no antibody control **(B)** Table listing fold change enrichment, mascot score and number of peptides detected. Independent technical replicates n=2. Red = Bait proteins, orange = known interactors.

6.5.2 PAK pulldown following PAK inhibition treatment

Earlier experiments had shown that PAK is active during basal conditions and this was also observed in the Casado et al. study, where all patient samples were measured following no stimulation (271). Thus, it was proposed that PAK pulldown of all isoforms in an AML model would include known interactors and unknown interactors that were important in the disease context. To reveal the unknown interactors, one could also treat AML cells with PAK inhibitors and observe across the experiments which proteins consistently followed the stoichiometry of known interactors.

MV4-11 cells were treated for 2 hours with the PAK inhibitors IPA-3 (20µM) and PF-3758309 (1µM), subsequently PAK1, PAK2 and PAK4 were separately pulled down in each of the untreated and treated conditions. Co-IPs were processed as described in previous optimisation experiments (section 6.4.1 and 6.5.1) and the findings are summarised in Figure 6.15.

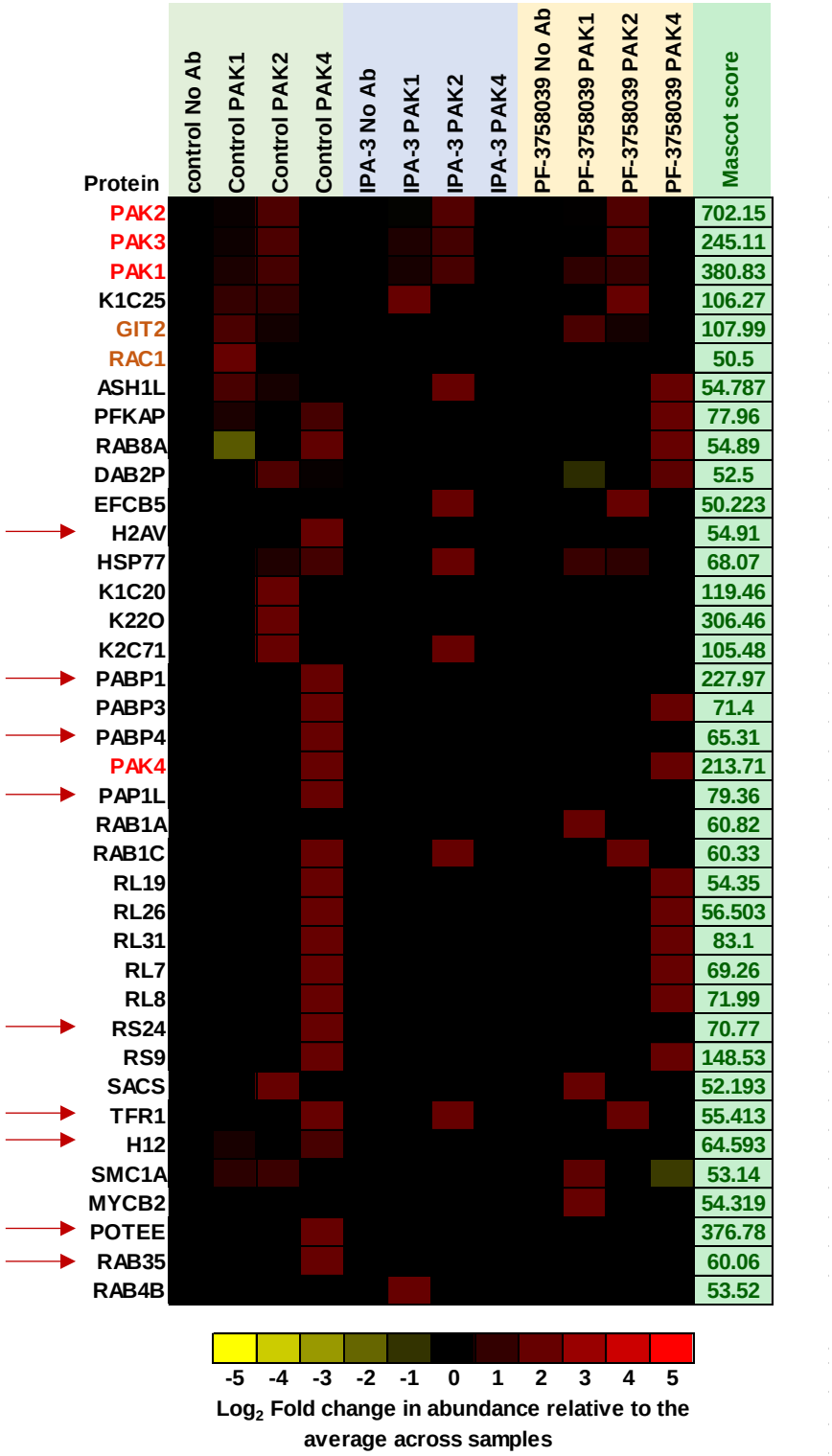

Figure 6.15: Heatmap of PAK pull-down in MV4-11 following PAK inhibitor treatment. AML cells treated with 20µM IPA-3 or 1µM PF-3758309 for 2 hours, then lysed with 0.1% CHAPS buffer. Co-IP baits targeted PAK1, PAK2 and PAK4. Heatmap made using sum normalised peptide ion intensities average across 2 independent technical replicates. Relative abundance determined by comparing Log_2 fold change of individual samples to the average across all samples. Proteins labelled in orange are known PAK interactors.

Assessment of each of the proteins identified in the pull-down experiments showed that none of the presented proteins were detected in the antibody free controls and that the PAK2 antibody was the best performing antibody, with this antibody managing to strongly and

consistently pull down the group 1 PAK isoforms. The PAK 1 antibody was good at pulling down PAK1, but not PAK2. The PAK4 antibody was very good at pulling down PAK4 in the untreated and PF-3758309 conditions, but PAK4 was absent in the IPA-3 condition, suggesting the pull down didn't work (Figure 6.15).

Known PAK interactors identified in this experiment included GIT2 and RAC1 (Figure 6.15, orange text), these proteins were abundant in the PAK1 pulldown of untreated AML cells and GIT2 was detected in the PAK2 pulldown of untreated cells, this was probably due to the antibodies ability to enrich PAK1. IPA-3 treatment led to the loss of these known interactors in PAK co-IPs. PF-3758309 treatment also inhibited RAC1 binding across co-IPs, however, there was still detectable GIT2 in the PAK 1 pulldown. The only enriched proteins that followed this trend were the keratins K1C20 and K22O which are unlikely to be key regulators of PAK activity in AML.

No known PAK4 interactors were identified in the co-IP experiments, however, there were a number of proteins that only appeared strongly in the PAK4 co-IP of untreated cells, which were completely absent in all other conditions. These included histones H2AV, H12, Transferrin receptor protein 1 (TFR1), the small Rab GTPase (RAB35), Polyadenylate-binding proteins 1 and 3 (PABP1, PABP3), ribosomal protein (RS24) and Polyadenylate-binding protein 1-like protein (PAP1L). These proteins represented an encouraging list of candidates, particularly RAB35 as it is similar to known PAK4 binders which are predominantly small GTPases like CDC42. To have more confidence in these candidates, it would have been desirable to have had a known PAK4 interactor to compare pulldown affinity behaviour. Due to the amount of further optimisation that would have been required regarding inhibitor concentrations, other means of inducing variable PAK complex formation were pursued.

6.5.3 Serum deprivation followed by serum stimulation

Despite the lack of enrichment for PAK pulldown proteins following secretome stimulation, the western blot experiments during secretome optimisation (Figure 6.12) indicated serum manipulation significantly affected PAK phosphorylation. Considering further, that there were more enriched proteins in the serum starved pull down previously undertaken (Figure 6.14) and that previous studies had been successful using this approach (552), a strategy was employed that would starve MV4-11 cells, before stimulation with serum.

Co-IP of PAK proteins from MV4-11 cells stimulated with serum identified 20 proteins in these experiments (Figure 6.16A) that met the selection criteria (MASCOT score > 50, >2 peptides counted, protein absent in antibody free negative control, >2 Log_2 fold enrichment in targeted pull-down over control). Figure 6.16 demonstrates that PAK was successfully pulldown

and compared to the non-targeting control PAK was significantly enriched (red proteins), along with known binders (orange proteins).

A

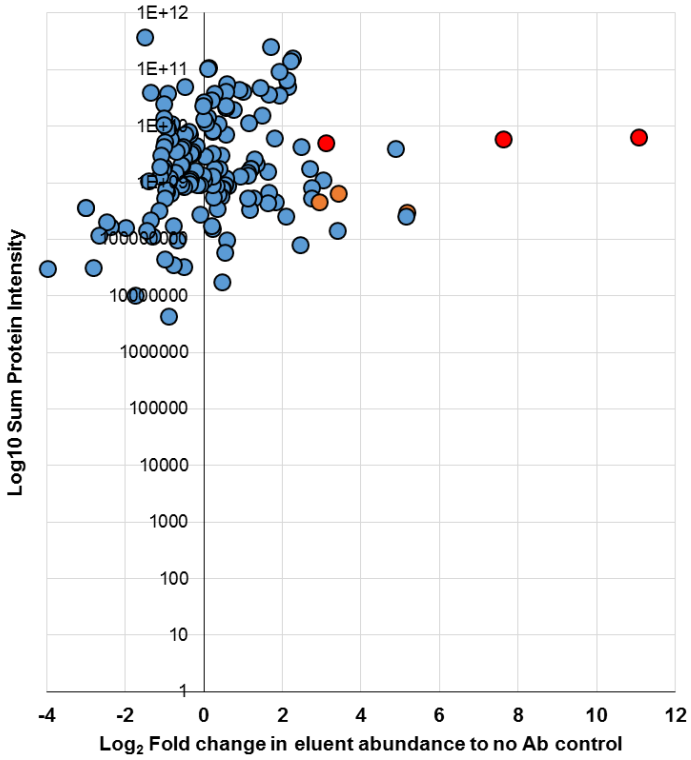

B

Protein	Log_2FC	Mascot score	No of peptides
PAK3	11.1	222.5	66.0
PAK2	7.6	310.3	21.0
ARHG7	5.2	140.9	11.0
ARHG6	5.1	98.9	10.0
H2A2B	4.9	195.6	40.0
MYH9	3.4	127.9	2.0
MCM4	3.4	128.4	6.0
PAK1	3.1	370.1	45.0
H2A3	3.0	326.1	15.0
GIT2	3.0	158.3	7.0
RUVB2	2.8	132.8	12.0
ATPB	2.7	55.3	3.0
TCPA	2.7	149.0	22.0
H2BFS	2.5	459.1	36.0
KSYK	2.4	66.4	5.0
ACTBL	2.3	420.8	600.0
ACTG	2.2	1244.4	122.0
POTEJ	2.1	327.2	290.0
ACTH	2.1	885.6	522.0
1A74	2.1	54.9	123.0

Figure 6.16: Co-Immunoprecipitation of PAK in MV4-11 cells following both serum starvation and stimulation. Co-immunoprecipitation of PAKs led to the identification of proteins which following analysis were deemed to be enriched, in target protein pull down experiments. **(A)** Eluents of pull down using PAK1, 2 and 4 antibodies combined **(B)** Table listing fold change enrichment, mascot score and number of peptides detected. Independent technical replicates n=2. Red = Bait proteins, orange = known interactors.

Analysis comparing the serum stimulated AML cell PAK co-IPs to the serum starved AML cell co-IPs revealed 29 proteins enriched with >2 Log_2 fold enrichment in the serum stimulated pull-down and 13 proteins showed >2 Log_2 fold enrichment in the serum starved pull-down (Figure 6.17A). Proteins that increased in abundance following stimulation included known PAK interactor MYH9 (coloured blue) as well as numerous histones (coloured red). Fewer proteins were enriched in the starved sample but this should display a preference for proteins that are not dependant on PAK phosphorylation. Proteins such as Leupaxin (LPXN) which is a negative regulator of known PAK interactor paxillin and B cell receptor signalling was an interesting protein to be enriched in PAK pull downs following serum starvation (554, 555), as well as Ikaros (IKZF1) a transcription regulator of haematopoietic cell differentiation and Thyroid receptor-interacting protein 6 (TRIP6) (Figure 6.17B).

Proteins that were enriched following serum modulation are presented in interaction complexes that display previously described interactions (Figure 6.17C). Proteins identified as enriched in the PAK pulldown following serum stimulation were very well interlinked even

though none had previously been implicated with any of the PAK isoforms (except MYH). This could explain the presence of these proteins, if one member bound PAK it is possible the whole complex was pulled down too, this may explain why so many histones were identified. The serum starved enrichment interactors are not as well interlinked, however, LPXN did have one known interactor also identified. These finding were encouraging, but required more biological replicates, as to date only two had been performed.

A

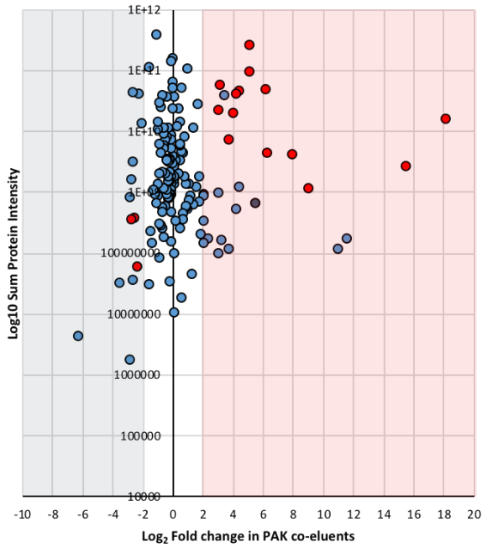

B

Enriched in Serum Stimulated

Protein	Log_2Fold	Mascot score	No of Peptides
H3C	18.14217	299	160
H33	15.52142	402	15
K2C79	11.62918	184	32
RL13	11.03758	72	3
H2A3	8.994325	326	15
H2A2B	7.927733	196	40
H2BFS	6.308552	459	36
H2B3B	6.159067	395	308
MYH9	5.540747	128	2
H2B1A	5.097373	228	957
H2AZ	5.092251	216	293
ADT3	4.451116	93	39
H2A2C	4.432922	343	209
H31T	4.243069	349	99
ATPB	4.181885	55	3
H15	4.060095	510	34
H2B1K	3.765416	493	63
HS90B	3.732618	86	4
H12	3.466379	532	108
HS90A	3.234623	95	4
H4	3.176722	523	94
RL13A	3.073157	71	2
H1T	3.048202	141	95
K2C6A	3.002178	637	20
PHB2	2.362329	178	5
RL3	2.105865	146	14
RS9	2.09297	116	8
HNRPC	2.061454	60	2
HNRPU	2.026308	101	5

Enriched in Serum Starved

Protein	Log_2Fold	Mascot score	No of Peptides
K2C1B	-2.05981	91.2	131
GSTP1	-2.20909	749	101
IKZF1	-2.32192	113	4
LPXN	-2.51282	199	11
K1C9	-2.605	1511	207
TBB2B	-2.61034	620	115
ILK	-2.66128	97.1	8
K2C8	-2.73958	179	90
TRIP6	-2.77499	59.9	6
HORN	-2.79904	379	30
RL19	-2.80315	58	1
FHL1	-3.53329	75.4	4
SUCB1	-6.23605	125	2

Serum stimulated AML cells show an enrichment for histones in PAK pull-down

C

Enriched for in stimulated

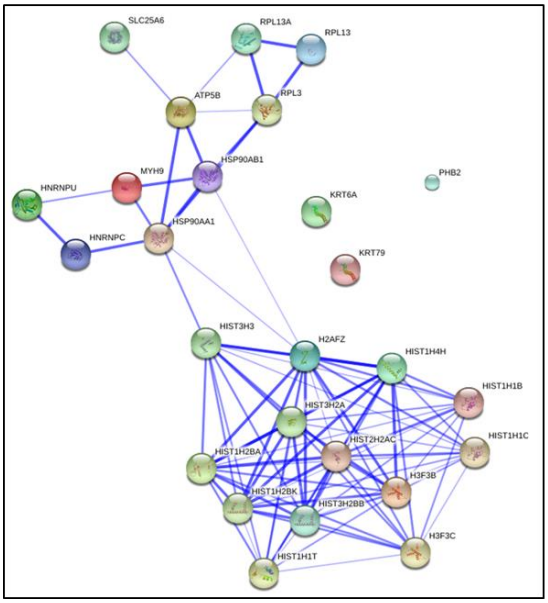

Enriched for in starved

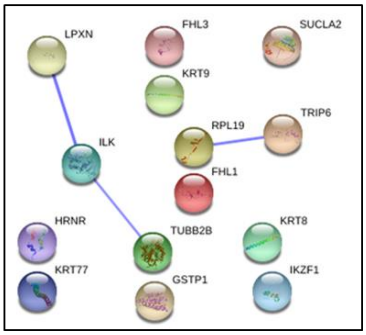

Figure 6.17 Comparison of PAK complex co-eluents between serum stimulated and starved cells reveals enrichment for histones. (A) Analysis comparing dynamic co-IP proteins following PAK pulldown in serum stimulated and serum starved conditions. **(B)** Table listing fold change enrichment, mascot score and number of peptides detected. **(C)** STRING protein analysis of pull down proteins that had a fold enrichment of >2 Log2 fold, >2 proteins identified, >50 mascot score between conditions. Independent technical replicates n=2. Red = Bait proteins, orange = known interactors.

6.6 Investigation of PAK signalling dynamics across isoforms

Following the optimisation results it was decided that to determine PAK regulatory binding proteins, serum starvation followed by stimulation would be employed as preliminary experiments suggested a novel PAK interaction with histones. Experiments were devised to investigate basal, serum starved, and serum stimulated interactors of PAK1, PAK2, and PAK4 in biological and technical triplicates. It was postulated that starving the cells for 4 hours would lower the activation status of signalling pathways and subsequent stimulation with serum for 15 minutes would then mobilise PAK interactions. Subsequent comparisons between the serum starved and serum-stimulated conditions should then reveal the dynamic binders of PAK isoforms (Figure 6.11). Experiments to date extended antibody incubation overnight in the hope of maximal PAK binding, however, trouble shooting previous co-IPs postulated that due to the transient nature of kinases, and the susceptibility of protein complexes to dissociation, identification of binders may be enhanced by shorter PAK antibody incubations. Accordingly, this step was shortened to 1 hour.

Co-IP of PAK1 and PAK2 proteins from cells grown under basal conditions identified known PAK binders (including Filamin A and Filamin C), in addition to PAK1 and PAK2, to be more abundant in the relevant IP experiment (containing a specific anti-PAK antibody) than in the non-specific binding controls (no anti-PAK antibody present, Figure 6.18a, part i) (556). The co-IP was repeated using cells that had been starved of serum for 4 hours; under these conditions, FLNA, FLNC and Serine/threonine-protein kinase PLK4 were identified as being significantly enriched for across 3 biological replicates compared to the non-specific binding controls (Figure 6.18a, part ii). Finally, in the cells that were starved for 4 hours before serum stimulated for 15 minutes only PAK1 and FLNA were consistently enriched for across the replicates relative to the non-specific binding controls (Figure 6.18a, part iii).

Co-IP of PAK4 grown under basal conditions enriched for known PAK binder FLNA, PLK4 which was observed in the group I PAKs under basal conditions, as well as Four and a half LIM domains protein 1 (FHL1) compared to the non-specific binding control (Figure 6.18b, part i). Co-IP of PAK4 in cells that had been serum starved for 4 hours enriched for FLNA and Toll like receptor 5 (TLR5) compared to the non-specific binding controls after serum starvation (Figure 6.18b, part ii). Finally, cells that were serum stimulated for 15 minutes following serum starvation led to the enrichment of FLNA, FLNC, FHL1, as well as E3 ubiquitin-protein ligase TRIM21 (RO52) and 40S ribosomal protein S18 (RS18) compared to the non-specific binding control under the same conditions (Figure 6.18b, part iii).

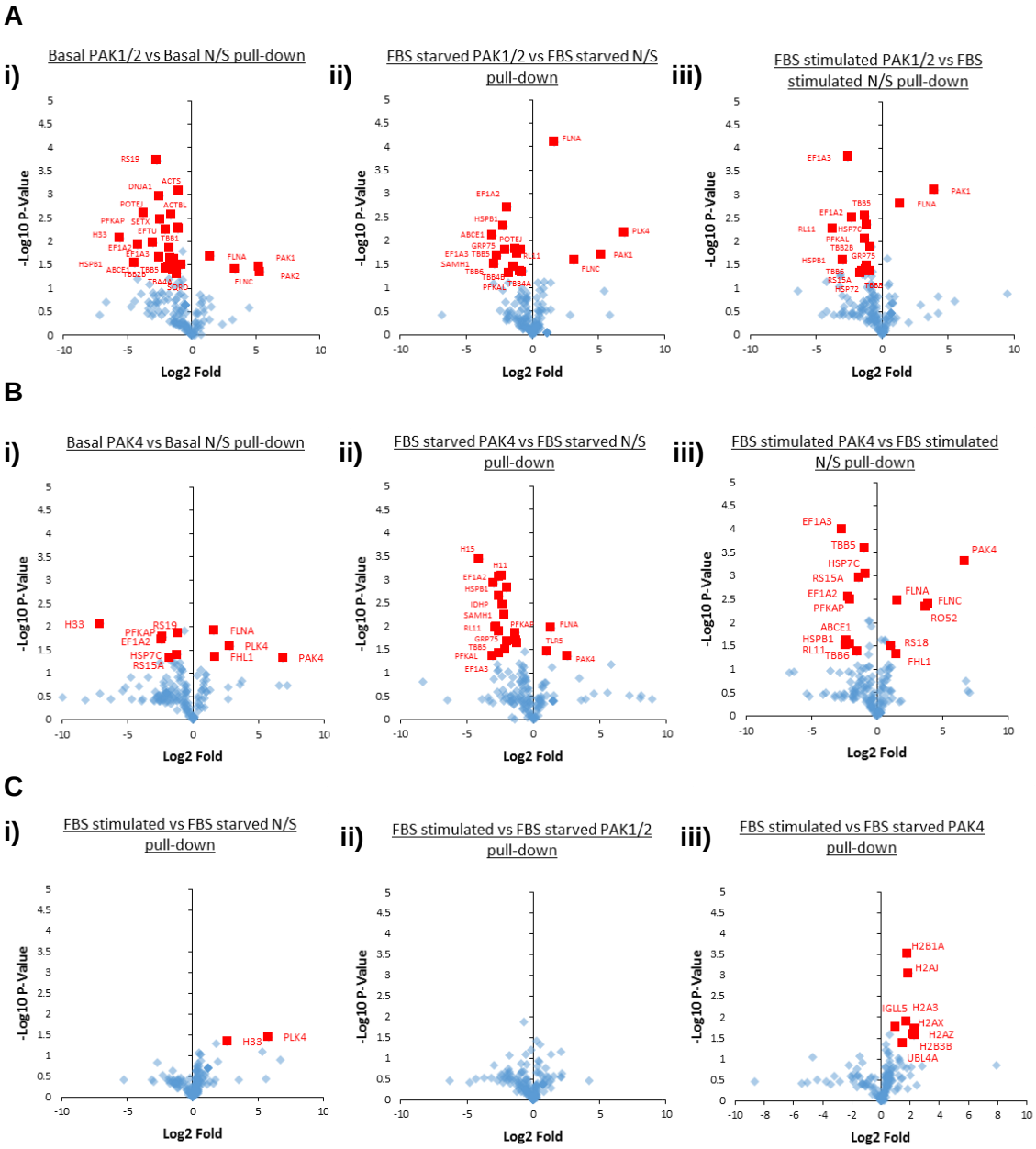

Figure 6.18: Volcano plots of proteins identified in targeted PAK1, 2, 4 pull-downs coupled with LC-MS/MS detection. (A) Shows enriched proteins in PAK1 and PAK2 pull-downs compared to non-specific binding control [i] under basal conditions [ii] following 4 hours serum starvation [iii] after 15 minutes serum stimulation with 10% FBS following 4 hours serum starvation. **(B)** Shows enriched proteins in PAK4 pull-downs compared to non-specific binding control [i] under basal conditions [ii] following 4 hours serum starvation [iii] after 15 minutes serum stimulation with 10% FBS following 4 hours serum starvation. Red markers indicate statistically significant changes that are greater than 2 Log2 fold changes between the samples. **(C)** Displays enriched proteins when comparing serum stimulated and serum starved co-IP complexes in [i] non-specific protein controls [ii] between PAK1/2 co-IPs [iii] between PAK4 co-IPs. Proteins on the right are enriched for in serum stimulated pull-downs and left are enriched for in serum-starved pull-downs.

Comparisons between non-specific binding control complexes immunoprecipitated from serum starved cells and serum stimulated cells following starvation revealed histone H33 and PLK4 as being consistently more abundant in the serum stimulated conditions, with no proteins consistently more abundant in the serum starved pull-downs (Figure 6.18c, part i). In

the PAK1 and PAK2 co-IP's no proteins were significantly more abundant in serum stimulated cells compared to the serum starved cells, or vice versa (Figure 6.18c, part ii). However, PAK4 co-IP complexes exhibited significant enrichment for histones H2B1A, H2AJ, H2A3, H2AZ, H2B3B, H2AX, Immunoglobulin lambda-like polypeptide 5 (IGLL5) and Ubiquitin-like protein 4A (UBL4A) in the P31/FUJ cells that were stimulated with serum for 15 minutes compared to the PAK4 co-IP of P31/FUJ cells that were only serum starved (Figure 6.18c, part iii). This suggested that these proteins bind to PAK4 dynamically upon cell stimulation. No proteins were significantly more abundant in the PAK4 co-IP following serum starvation of P31/FUJ cells compared to the PAK4 co-IP serum stimulated P31/FUJ cells.

The proteins identified as putative dynamic binders of PAK4 (Figure 6.18c, part iii) were searched against the literature and Figure 6.19 shows the current knowledge of these proteins interactions. PAK4 is not described as interacting with histones but they show a specific enrichment across 3 biological replicates and showed a significant enrichment over the non-specific controls. The observation of a dynamic histone interaction that appears upon PAK4 activation is very interesting, as this would be suggestive of PAK4 migration to the nucleus where it could influence many cellular functions in AML progression.

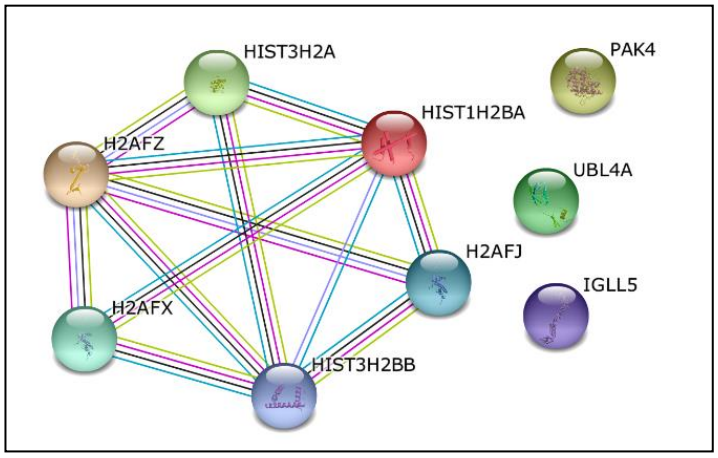

Figure 6.19: Protein string of PAK4 pull-down proteins that are significantly enriched for in serum stimulated P31/FUJ. PAK4 complexed with histones - H2B1A, H2AJ, H2A3, H2AZ, H2B3B, H2AX, Immunoglobulin lambda-like polypeptide 5 (IGLL5) and Ubiquitin-like protein 4A (UBL4A).

6.7 Summary

It had been proposed in previous studies that in cancer and in particular treatment resistant neoplasms that kinase networks undergo network rewiring and establish interactions that would not necessarily occur under physiologically conditions (215, 216). Having observed that the underlying kinase networks that help govern AML response to the microenvironment were extremely heterogeneous, it had been a quandary that PAK inhibition was always so potent in undermining AML cell survival (Figure 4.11). This observation coupled with previous studies (206, 271) that documented PAK as one the most active kinases in AML (Figure 6.1), led to experiments that studied the nature of PAK activation in AML and protein interaction studies to try and establish mechanistically the relevance of high PAK activity.

Firstly, to determine the source of PAK activity and the underlying source of this constituent binding interactions, a meta-analysis was conducted of 390 AML exomes. In this cohort it was observed that there were no mutations on PAK reported. This finding was unexpected as AML is a disease which is characterised by high levels of genetic instability that aids in the acquisition of further genetic aberrations to help perpetuate disease progression. Therefore, for a kinase that is so frequently overactive in patients to not harbour any genetic aberrations suggests that there must be either epigenetic elements, exogenous factors (i.e. microenvironment) or dysregulated upstream signals and/or binding partners that help drive this signalling.

Experiments conducted as part of Chapters 3 and 5 had already revealed that the exogenous factors from the microenvironment had the ability to modulate PAK signalling in the AML cell lines; MV4-11 and P31/FUJ – especially in the isoforms PAK1 and PAK2. Therefore, these were believed to be appropriate models to study PAK interactions in AML. Further to these findings, it was deemed important to establish PAK isoform expression in these lines. Subsequent western blots demonstrated that both cell lines highly expressed PAK1, MV4-11 expressed higher levels of PAK2 and P31/FUJ expressed higher levels of PAK4. These findings were important as they suggested that MV4-11 would be a better model for studying PAK2 and P31/FUJ with PAK4. However, the relative levels of phosphorylation to expression highlight that the cell lines that expressed less protein also displayed relatively more active protein, as seen with PAK4 expression in MV-411 and PAK2 expression in P31/FUJ (Figure 6.5).

Having validated appropriate models that collectively had high expression of all PAK isoforms present in haematopoietic cells (PAK1, PAK2 and PAK4), the focus shifted to optimisation of protein interaction studies. Following the success of co-IP in identifying novel kinase regulatory proteins (552), studies began to implement a co-IP protocol that effectively immunoprecipitated PAK isoforms and known PAK binding partners. Following optimisation of

a number of elements that effected the enrichment of PAK protein complexes (summarised in Table 6.1) an MS based protocol that displayed both specificity and sensitivity to all PAK isoforms (except PAK3 as not expressed in haematopoietic cells), while being able to detect the known interactors (GIT1, GIT2, ARHGEF6 and ARHGEF7) was established (Figure 6.9 and 6.10).

Once a suitable protocol had been established a number of conditions were experimented with to reveal dynamic PAK binding partners, including secretome stimulation, PAK inhibition and serum modulation. PAK co-IP of secretome stimulated MV4-11 cells was able to identify PAK and known PAK interactors (Figure 6.12), however, this treatment was not capable of revealing any secretome induced PAK binding partners (Figure 6.13). This finding was surprising as western blot analysis had demonstrated potent effects on the expression of phosphorylation sites PAK1 ($Ser^{199/204}$) and PAK2 ($Ser^{192/197}$) (Figure 6.11). Retrospectively this line of enquiry should have been pursued further, only owing to MS issues were experiments not repeated.

Co-IP experiments using PAK Inhibitors served as a demonstration of these inhibitors ability to disrupt PAK complexes. IPA-3 was more efficient at disrupting group 1 PAKs, as known PAK binders (GIT2 and RAC1) were lost completely following treatment which PF-3758309 only partially achieved. One caveat to this is that IPA-3 was used at higher concentrations. Unfortunately, there were no proteins in the PAK1 or PAK2 co-IPs that followed the pattern of expression that known binders exhibited (Figure 6.18). Conversely PAK4 co-IPs, did uncover a number of dynamically expressed nuclear proteins that included histones and PABPs, however, these could not be corroborated as no known PAK4 binders were identified.

Despite the promising findings that PAK4 pulldowns revealed following inhibitor treatments, experiments focussed again on the effects serum modulation had on PAK behaviour. This shift away from PAK inhibition studies was fuelled by suspicions that inhibitor treatments may create artefacts or drastically change the behaviour of potential binders independent of the inhibitors PAK specific effects. Experiments investigating the effects of serum starvation followed by stimulation on PAK complex formation revealed a number of dynamic binders that met confidence thresholds (Figure 6.15). Notable candidates included LPXN which PAK enriched for during serum starved conditions, previous studies have demonstrated LPXN as negatively regulating known PAK binder paxillin (557, 558), this appeared as strong evidence for LPXN as an interactor of group 1 PAKs. Numerous proteins were enriched in the serum stimulated PAK co-IPs compared to serum starved and these were mostly histones (6.15C). Histones had also been prominent proteins in the inhibitor based co-IPs that were lost following PAK inhibition, as these candidates had now been identified in two different

experiments it was concluded that a co-IP with sufficient statistical power should be undertaken to validate these findings.

Having established optimal conditions for both the co-IP technique and conditions by which to elicit dynamic PAK protein complexes, these aspects were brought together to identify PAK binding partners. These experiments revealed that only PAK4 with statistical significance enriched for H2B1A, H2AJ, H2A3, H2AZ, H2B3B, H2AX, IGLL5 and UBL4A (Figure 6.19). This supported previous observations of histone enrichment in PAK4 co-IPs, as this had been observed in 5 independent biological replicates. The group 1 PAK serum modulated co-IPs did not reveal any enriched PAK binding partners (Figure 6.18Cii), despite LPXN being observed in the first serum modulated experiment. This was probably a symptom of the shorter 1hour incubation.

Taken together, these experiments showed that PAK activity and expression in AML is variable, and this heterogeneity cannot directly be explained through accumulation of genetic aberrations. Following the optimisation of a co-IP coupled MS approach it was possible to investigate dynamic binding partners of PAK principally focussing on PAK response following compound inhibition or starvation and rapid stimulation. Most strikingly, PAK4 – the least described of the PAK isoforms – consistently demonstrated binding of H2 histones during serum modulation that was not observed under other conditions, indicating an interaction not previously reported in PAK4.

Chapter 7: Discussion

AML is a complex disorder encompassing a collection of distinct sub-types that present with excessive proliferation of undifferentiated progenitor cells in the BM (23). Consequently, this disease is characterised by its profound molecular heterogeneity, sustained by clonal populations that continually acquire new genetic aberrations, thus creating a repertoire of resistors to therapeutic intervention (18).

Kinases are commonly dysregulated to help promote leukaemogenesis, typified by frequent activating mutations in FLT3 and RAS proteins, these are believed to help induce a proliferative phenotype (31, 32). Kinases and the networks they signal within, manage cellular responses to both external and internal stimuli. The response to and shaping of the microenvironment has been demonstrated to be a key feature in leukaemic progression and resistance to therapeutic strategies (559-561). Cross-talk with surrounding niche cells is thought to be important in mechanisms relating to survival, proliferation, self-renewal and immune evasion (122, 124, 145, 154, 343).

The work presented in this thesis focused on investigating how components of the microenvironment impact cell signalling networks in leukaemic cells and in turn how these leukaemic cells modulate stromal cell signalling. In order to examine this, three approaches were taken: (i) the secretome of known AML supportive stromal cells were assessed by MS to elucidate novel proteins; (ii) functional characterisation of secretome derived proteins assessed any supportive qualities in primary AML; and (iii) how these proteins and the BMSM as a whole impact cell signalling in leukaemia.

Understanding the mechanisms by which the microenvironment can facilitate leukaemic cell survival and propagation are increasingly becoming more important in the pursuit of effective therapeutic strategies that can achieve complete clearance of leukaemia (46, 145). Despite the previous identification of stromal GFs that can mediate leukaemia behaviour (such as niche localisation), and agreement of extensive cross-talk between cell populations, there has been a lack of unbiased global proteomic strategies to identify novel proteins of the microenvironment that could support and aid in the propagation of AML (47, 125, 562-564). Therefore, protocols for generating CM of known AML supportive BMSC lines were optimised and the resultant secretomes enriched and analysed by LC-MS/MS based proteomics (Chapter 3). BMSC secreted proteins that exhibited modulated abundance in the presence of leukaemic cells, suggested relevance in cellular processes. In an effort to establish roles for such proteins, the purified recombinant forms relevance in survival, proliferation and treatment resistance were functionally assessed (Chapter 4). Kinases that regulate cell signalling pathways are

frequently dysregulated in cancer and leukaemia (70, 565, 566). The phosphoproteomes of heterogeneous primary AML cells were exposed to both single/bulk stromal proteins and BMSC co-culture, these investigations sought to define basal kinase network activities of both AML and BMSCs, then subsequently infer how they are regulated by one another (Chapter 5).

PAK has previously been described as one of the most active kinases in AML (271). We observed that (unlike other kinase inhibitors) secretomic components were unable to modulate AML's profound sensitivity to PAK inhibition, this suggested a fundamental dependency on PAK signalling. To investigate this activity, interaction studies were developed to identify novel binding partners that facilitate PAK function in AML (Chapter 6).

7.1 Characterising the composition of AML supportive secretomes derived from stromal MS-5 and HS-5 cell lines

7.1.1 Context and motivation for stromal secretome dissection

As discussed in Chapter 1, the propagation of AML and the treatment resistance it commonly displays is at least in part mediated through cross-talk and interactions with the BMM (122, 567-570). Aspects of this interaction have been previously utilised in culture to extend ex vivo survival of primary AML material (355-359). It has been reported in previous studies that the supportive nature of the microenvironment can be harnessed using stromal cell lines (MS-5, HS-5), which are capable of retaining expression of the naïve $CD34^{+}CD38^{-}$ cell populations (353, 571-573).

In this group of studies, it was hypothesized that the full complement of stromal derived proteins – where previous works have shown are imperative for leukaemic cell progression - are yet to be defined (122, 568, 569). The importance of identifying these proteins is multi-faceted: firstly knowing the precise proteins that drive aspects of the disorder can serve as important biomarkers to characterise a patient's disease - which has been proven to be crucial in disease maintenance to date (574). This motivation is a long-term outcome, but the immediate benefit of understanding the proteins at play, is their utilisation in studying AML biology. Identification of these molecules enables avenues of investigation which are not possible if cells cannot be maintained in culture for any extended periods of time. Further, to induce such viable phenotypes through secreted proteins means that the AML cells would be responding to these signalling molecules through receptor mediator signalling. Thus, secretomic studies offered an opportunity to identify novel signalling molecules by which to investigate AML kinase networks.

Due to the unsupervised nature by which secretomic components were to be identified, the supportive elements of the stromal secretome needed to be as abundant and preserved as possible before LC-MS/MS analysis (Figure 3.9). Additionally, at the time of the experiments an untargeted label-free LC-MS/MS method for the study of secretomic changes was not readily available. Therefore, prior to identifying components of the stromal secretome, aspects of the workflow had to be optimised to ensure sufficient coverage of the secretome could be achieved (Figure 3.18).

7.1.2 Variables that characterise conditioned media and secretomes

The extensive testing of BMSC conditioning regimens and the aspects that contribute to the production of a substrate for primary AML maintenance, culminated in the optimisation of a media that can extend primary AML cell culture longer than previously documented without physical co-culture (575, 576). What became apparent early during experimentation was the

lack of effect BMSC models were having on AML cell lines (Figure 3.2). Many historical studies have documented CM being important for the growth of cell lines (such as HL60) however, it was FBS that was more of a determinant in cell line growth (346). Serum starved conditions did not record notable effects until the HS-5 secretome was enriched and fractionated. This is pertinent as it questions the suitability of cell lines as a model for AML, clinically, AML cells (or at least the disease propagating cells) are extensively documented as being dependent on the microenvironment for progression, if a cell line does not exhibit this feature, it questions the suitability of such a model when investigating AML survival.

The process of optimisation also highlighted the extensive variability that can be observed in CM. A multitude of proteins effected the supportive capacity of the media (Figures 3.3-3.8). The literature does not go to any great lengths in detailing how CM were produced (364, 427, 577, 578). Consequently, this makes results from such research hard to standardise and reproduce.

Following extensive investigation, it was possible to deduce a set of parameters that, if adhered to, produced supportive media that could maintain primary AML cells longer than routinely observed. Due to availability it was not possible to assess or compare how CM from primary BMSCs differed to that which was used in these studies.

7.1.3 Label free LC-MS/MS based secretomics

Previous studies of the leukaemia microenvironment have focussed on preconceived protein arrays that can limit both the scope of investigations and inherently introduce selection bias (579-581). In the work presented here, an unbiased approach identified a plethora of candidate proteins that could be relevant to particular AML cells, or indirectly, cells of the microenvironment that can support AML (Figure 3.12 and Figure 3.16). The co-culture experiments revealed 133 statistically significant changing proteins (Figure 3.20) which is competitive with most approaches (275, 289, 386, 582, 583). Analysis of secretomic changes in abundance across the co-cultures culminated in the selection of 6 identified stromal proteins that had also been identified previously in MS-5 and HS-5 independent secretome analysis. These candidates would be substantiated as modulators of AML behaviour following validation experiments in Chapter 4.

7.1.4 Technical considerations and limitations of the study

When drawing conclusions from this study it is always important to consider the source of these data. Although MS-5 and HS-5 are appreciated as reliable models of the BMSM that support primary AML in culture (573, 584, 585), these are not primary BMSCs and therefore, identified GFs need to be substantiated in primary tissue. Preferably primary cells would have

been used to investigate the secretome, but this material was unavailable. An advantage of cell lines is that they are homogeneous populations, primary BMSCs on the other hand are not and would have observed even higher levels of heterogeneity between experiments due to the nature of these cells, which would have impacted reproducibility. Having primary cells in culture (especially non-tumour) does not mean they would respond in a manner reminiscent to what is observed in vivo, which would have also served to make meaningful results difficult to obtain. Therefore, a more robust model, would follow that employed in these studies with subsequent histological assessment of BM trephines to compare expression in healthy and leukaemic cohorts to validate findings (586).

The inherent limitations of the LC-MS/MS based secretomic approach used in these investigations include: CM needed to be produced in a serum free environment, this could have had an impact on cell behaviour and secretome production; utilisation of AML cell lines that are not dependent on the microenvironment for survival; lost coverage of the proteome in co-culture. Distinguishing cell specific synthesised proteins based on species specific protein sequences meant that there were a number of peptides that were excluded from analysis due to species sequence homology, thus reducing coverage.

LC-MS/MS analysis of the HS-5 secretome identified substantially more proteins than those identified when analysing the MS-5 secretome. This is primarily down to the HS-5 secretome being analysed on a Q-Exactive plus compared to the LTQ-XL which was used for the MS-5 secretome. The Q-Exactive as described in Chapter 1 allows for much greater sensitivity and throughput, with better spacing. In the western validation experiments only S100-A4 and CSF-1 were validated. This was due to the unavailability of suitable antibodies raised against the other 4 proteins at the time.

7.1.5 Implications and future work

This study, whilst highlighting the utility of discovery-based MS methods for investigating the BMSC secretome and the efficacy of label-free methods in this context, it serves to expand our knowledge regarding the complexity and variability that occurs in secretome composition. Efforts to increase coverage of the secretome, culminated in a method that can reliably quantify approximately 700 extracellular proteins per sample which is competitive with other labelled MS methods (288, 289, 587). The most important advantage of this approach is that it is compatible with any cell origin, unlike SILAC approaches for example (261, 284). In addition, this approach enables the examination of the secretome in an unbiased manner, given the variability of secretome composition this is an extremely desirable feature when searching for novel players that mediate disease phenotypes.

Building on the foundations presented in this chapter it would be useful to compare directly label free approaches to those of labelled approaches. A plausible primary cell model could be achieved through the transduction of an enzyme-based tagging system in a stromal cell line, which could be utilised in co-culture with primary cells (583). A caveat to this approach is that the efficiency of labelling can be variable, while it is debatable whether the transduction produces cells with altered protein behaviour. Otherwise this may be another effective method to investigate the supportive contribution of such cells, in a human system.

Both MS-5 and HS-5 cell lines are used by numerous labs to facilitate leukaemia research and knowing the precise proteins that constitute the supportive complement produced by these cells has merit. As described in Chapter 4 the understanding of such proteins can help to identify cleaner and more reproducible means of sustaining leukaemic cells in culture that do not involve introducing other cell populations (346, 364, 584, 585, 588, 589). Western blot experiments (Figure 3.25) showed the heterogeneity in cross-talk that occurs in leukaemia. S100-A4 expression was shown to be present in some AML, with patient #1 cells secreting an abundance of the protein. Conversely, patient #2-4 cultures did not secrete S100-A4 and relied upon MS-5 cells for production. Patient #5 co-cultures on the other hand, displayed a synergistic process as neither cell type could secrete high levels of S100-A4 independently, but in co-culture high S100-A4 levels were detected. Due to cross-species reactivity it was not possible to conclude which cells were responsible for the elevated secretion.

CXCL12 was not observed in experiments, this is unsurprising as CXCL12 is known to be secreted specifically by cells defined by their secretion of the protein (333, 590, 591). This highlights subsequent experiments that should be conducted. Determination of the secretome from other cell types that compose the BMM are all avenues of investigation that need to be explored to fully understand the cross-talk of the BMM. Ideally the model would comprise multiple cell types, as a multicellular model would induce differential secretome production to that produced in independent cell assessments, due to the influence of other cell types (592, 593).

7.2 Empirical determination of identified protein components from the BMSM and their role in AML survival

7.2.1 Introduction and context of investigations

The microenvironment is critical for AML survival, influencing cell behaviour and ultimately being a determinant of cell fate (164, 165, 559). Having established six stromal cell derived proteins whose expression dynamically changed in the presence of AML cell lines – S100-A4, S100-A11, BMP-1, CTGF, HGF, CSF-1 – it was important to functionally validate the role of these proteins in primary AML cells, if any. AML is extremely heterogeneous and as a result, each patient's disease is unique (594). Consequently, to establish if these proteins were relevant in AML, survival and proliferation were investigated as a metric of response in a mixed cohort of primary AML cells.

An extension of this work looked to characterise the bulk HS-5 secretomes ability to recapitulate other observed aspects of the in vivo microenvironment, namely does it sculpt the phenotype of primary AML cells across extended conditioning, and/or aid in tolerating targeted kinase inhibition. Previous studies had investigated stromal cell co-culture and shown that these models could help AML cells resist chemotherapy (346, 354, 595). If the aforementioned hypothesis were true, then these studies would support that these proteins are important in AML progression, while providing the appropriate conditions by which to measure the signalling network response to these proteins.

7.2.2 Validation of secretomic protein function in AML

To test the strength of the label free MS approach to identify secretomic proteins that positively affect AML cells, purified human recombinant forms were used individually and in combination to maintain primary AML cells in culture for seven days. Guava easycyte flow cytometry was used to assess both the viability and proliferation of these cells.

Initial analysis of the guava flow cytometric data revealed that the different RPs were able to maintain viability in AML cells to varying degrees across the patients. However, in all patient samples the inclusion of a GF was more supportive than no GF control (Figure 4.4). The CM and Mixed GF treatments elicited similar responses in each patient tested, suggesting that components responsible for MS-5 CM support in primary AML culture were present in the Mixed GF sample. Thus, providing evidence that the label-free MS approach undertaken was able to identify supportive components of the MS-5 secretome.

The GFs influence on cell proliferation differed to their effects on viability. Cells in some patient samples underwent substantial growth in response to GFs. In particular patient #1 to S100-A4 and the Mixed GF; patient #2 cells responded to all GFs except to the S100 proteins;

patient #3 and #4 cells increased in growth when compared to no GF, but this change was not profound; and patient #5 cells were responsive to most GFs, in particular CSF-1 (Figure 4.5). S100 proteins are known to stimulate proliferation and invasion in other cancers (371, 389, 400), therefore the profound response that patient #1 cells had to the GFs supported this role. CSF-1 is known to only have one receptor, CSF1R (450, 596). CSF1R possesses tyrosine kinase activity, which upon binding to CSF-1 can activate PI3K mediated proliferation in myeloid cells (597). Proliferation studies demonstrate that CSF-1 is capable of stimulating proliferation in primary AML patients. The heterogeneous response of different primary samples to the secretome derived proteins suggested that these proteins were indeed important in AML, but which protein(s) and the degree of impact will vary from patient to patient. Taken together these functional data provide strong support for the validity of the secretome derived proteins being key constituents of the CM that potentiates primary AML survival ex vivo.

7.2.3 Analysis of kinase inhibition to abrogate stromal secretome response

To further characterise how the HS-5 secretome supports primary AML, kinase inhibition studies were undertaken targeting key signalling nodes in AML (MAPK, mTOR, FLT3, JAK and PAK) (Table 4.2) (197, 206, 271, 447, 460, 598). It was hypothesised that signalling molecules that comprise the HS-5 stromal secretome would engage these pathways to mediate survival and proliferation. The caveat to this approach was that it was not possible to define protein specific responses to kinase inhibition. A switch to the HS-5 bulk secretome was employed for both practical and economic reasons, as the heterogeneous nature of primary AML cells meant it was important to test these studies in a larger cohort. To test these GFs individually in a larger cohort with multiple kinase inhibitors conceivably would have resulted in, (12 [patients] x 4 [replicates] x 6 [inhibitors conditions] x 9 [GF conditions] = 2592 samples). Therefore, treatment with the complex mixture that contained all the GFs meant that supportive mechanisms should have been engaged. If there was a consensus for downstream pathway activation to mediate response to supportive elements, then kinase inhibition of AML implicated pathways would have abrogated such support.

Patient cohorts in the presence of the stromal secretome were able to tolerate MAPK inhibition (Figure 4.7) but became sensitive to mTOR inhibition (Figure 4.8). FLT3 and JAK inhibition were not significantly altered and, regardless of secretome, PAK inhibition profoundly affected cells (Figure 4.11). Retrospectively Midostaurin treatment was too high in concentration, studies (599) have reported nM range for FLT3 selectivity. Therefore, during treatment there were probably multiple kinases inhibited, hence no discrimination between +/- stromal proteins was observed.

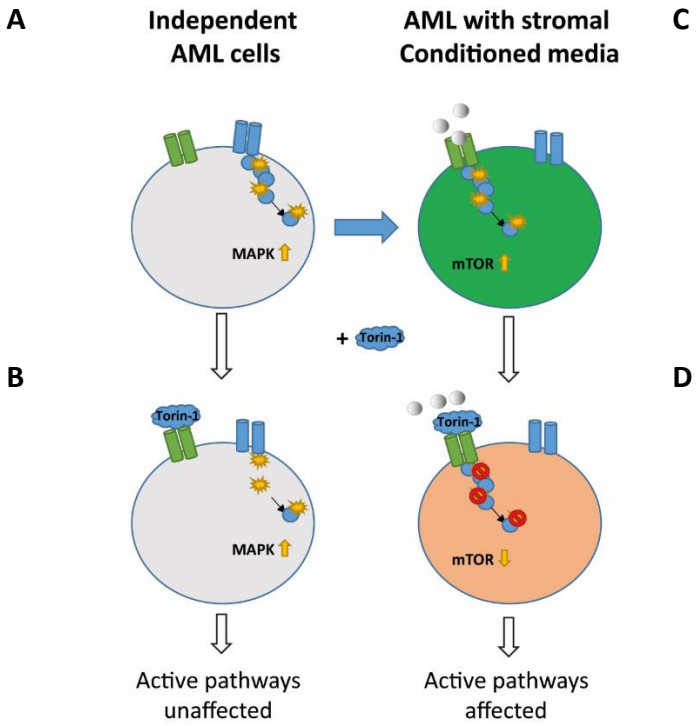

Figure 7.1: Theory for bone marrow stromal cell-initiated activation of AML cell signalling nodes. (A) AML cells that are grown independent of a BMSCs or CM, inherently rely upon particular signalling (such as MAPK). **(B)** If these cells are then treated with a specific kinase inhibitor (Torin-1) to a kinase that is not dependent, then the cells are unaffected by the inhibitor. **(C)** When the same AMLs are grown in the presence of BMSCs or CM, other signalling nodes may now become activated by factors or cell contact (such as mTOR). **(D)** Treatment with the same Torin-1 inhibitor now will effect cell behaviour, as active nodes are now being inhibited, while previous inherent dependencies may not be as crucial.

These data revealed aspects of AML cell signalling not previously explored, with the stromal proteins potentially able to switch signalling node dependencies within samples. These experiments suggested that these AML cells had a predisposition for MAPK mediated signalling, which had previously been investigated in AML (198). The simultaneous increase in sensitivity to Torin-1 in patients that decrease in sensitivity to MAPK inhibition following the introduction of HS-5 stromal proteins, suggested that signalling node dependencies were being altered (Figure 7.1). Unpublished studies by Dr Hijazi in the Cutillas lab have shown that Trametinib and Torin-1 are extremely specific in vivo inhibitors of MEK and mTOR kinase activity. Knowledge of these observations had an influence on the interpretation of the described findings and the relevance of the HS-5 secretome in the context of MAPK and mTOR activity.

For kinases that would have previously been active/inactive, the binding of a stromal GF stimulated pathway activity of otherwise relatively inactive pathways, altering the overall state of kinase networks and response to inhibition. As a whole, these analyses confirm the plasticity of signalling in AML. The dual targeting of pathways such as MAPK and mTOR is a recently proposed means of therapy (600, 601) in AML, which could prove effective in achieving a complete response if the treatment is not toxic. Collectively, the AML response to four targeted inhibitors and Midostaurin suggests that the MAPK and mTOR pathways are responsive to the

environment elements and were more plastic as a result. PAK and JAK inhibition revealed a uniform response to inhibition irrespective of the presence of signalling molecules used in the study, AML were either unaffected by the HS-5 conditioning or these pathways are not as plastic.

7.2.4 Analysis of AML adaption to stromal conditioned medium

To test how HS-5 secretome shapes the clonality of AML cell populations, primary cells were grown ex vivo with HS-5 CM and assessed at three time points. The phenotype of these cells was monitored by CyTOF using a panel of antibodies raised against validated markers of AML phenotypes (485, 574, 602, 603). The resulting data were extracted and analysed computationally using established cytobank software and ViSNE algorithms to visualise changes in the AML cellular populations (486).

Initial analysis of the CyTOF data revealed that the AML population changed considerably in culture. This was posited based on the change in cluster shape and position of the cell populations as represented in the VISNE analysis (Figure 4.16). Positioning in the ViSNE plot follows much the same principles of a PC plot in that the position occupied in the PC space is indicative of the expression of all markers being assessed (486). The Day 36 sample was the only sample of Figure 4.12 to survive in culture and what distinguished this sample was the presence of HS-5 CM.

CyTOF analysis revealed that long-term maintenance of these AML cells developed clones possessing microenvironment sensing molecules and markers symptomatic of aggressive disease that responds poorly to treatment (Figure 4.21). Based on the literature, it was unexpected that $CD34^{+}CD38^{-}$ populations decreased, a population normally maintained under influence of the microenvironment (138, 604). However, there are now a number of papers that report the capacity of $CD34^{-}CD38^{+}$ cells to behave as leukaemia initiators and induce engraftment (143, 465-467); this population was abundant by Day 36 (Figure 4.20, blue circles).

7.2.5 Technical considerations

It is important to note that all experiments with the recombinant GFs were conducted at the concentrations recommended by manufacturers, as being within the biologically active range. These concentrations are equivalent to those used by other studies, when adding GFs to support primary AML (352-354). Expansion of the patient cohort would have given the necessary power to extract clinical feature related observations (such as risk group associated responses to the secretome derived proteins).

To fully validate the patient response to secretome derived proteins, it would have been desirable to execute primary AML maintenance experiments using BMSC CM with the inclusion of individual neutralising antibodies. These experiments were not possible due to the

unavailability of neutralising antibodies to the secretome derived proteins. If these became available, then full validation would be possible.

Kinase inhibition studies used concentrations previously used in the laboratory for AML based kinase inhibition experiments (536). Although IC50 experiments were not conducted on each inhibitor in the primary AML samples, experiments were deemed appropriate as the investigation was assessing the ability of CM to alter response, for these purposes the experiments were controlled. Following these observations, it would have been desirable to continue to expand the inhibitor panel and patient numbers. These investigations will be continued in the future. In addition, kinase inhibition will be repeated with the panel of secretome derived GFs, patient selection shall be guided by the results of Chapter 5.

The results of the CyTOF experiment although informative, need to be expanded. The nature of the experiment dictated that there were only enough cells by Day 36 to run the experiment once. Therefore, these experiments need to be repeated in multiple patient samples. At the same time it would be useful to include antibodies that target other relevant receptors, those important in AML and known receptors to components of the secretome (such as FLT3, CSF1R, c-MET) (Figure 4.1) (392, 450, 458, 605, 606). These were not included as the delicate nature of the cells dictated the implementation of an already optimised AML phenotyping panel.

7.2.6 Implications and future work

Despite heterogeneity in patient response, the six proteins identified in Chapter 3 induced increased cell survival compared to no GF conditions. Validation of these proteins being secreted in AML were observed in western experiments (Section 3.12) and these are proteins known to be present in the BM (607). However, histological staining of BM trephines from both healthy and leukaemic bone samples would give clinical confirmation.

The immediate scientific benefit from identifying a panel of purified proteins that extend ex vivo culture, is the increased capacity for experimentation of primary AML tissue. The study of primary cells is traditionally difficult, before the characterisation of any new disease elements can be undertaken, researchers need to first take necessary steps to stop leukaemic cells from succumbing to an ex vivo environment. This can then confound and limit studies, as cells in culture are already initiating apoptotic machinery, this is not true in the BM (346, 608). When studying means of effectively treating relevant AML cells, it is necessary to work with cells that are going to respond in a manner that is akin to in vivo, otherwise findings are unlikely to translate or be very informative. Increasing stromal cell independent survival in culture opens the opportunity to study these cells in previously difficult platforms, as experiments with

primary cells that need to embed in a stromal feeder layer to survive can make investigations of the primary cells difficult. As removal of the feeder cells for analysis of the target cells can alter the behaviour of the primary cells being investigated.

Kinase inhibition studies highlighted the impact that stromal secretomes can have on kinase signalling in AML, and therefore, the secretome has implications on kinase inhibitor efficacy. These experiments showed the context in which kinase inhibitors are deemed appropriate changes with the environment. Inherently certain AML clones may utilise particular signaling nodes, but in the microenvironment the dependence on such nodes may shift, as observed with MAPK and mTOR signalling in the presence and absence of HS-5 stromal proteins (Figure 4.7 and Figure 4.8). The extent of this phenomena could be further tested to identify other pathways that respond accordingly, as well as include more inhibitors in the analysis. It would be desirable to address whether this pertains specifically to inhibitors with limited off-targets, or if this behavior is specific to particular pathways.

The CyTOF study has profiled cells in a condition not previously documented. This experiment tracked the effects of the HS-5 CM on the clonality of primary AML cells that without such adaption would have succumbed in culture, as observed in parallel conditions. Although there was the loss of the $CD34^{+}CD38^{-}$ population which has previously been documented as maintained by MSCs (for up to 6 weeks) by other studies (576, 609), this investigation revealed the expansion of an aggressive, pro-microenvironment population with previously defined initiator properties (143). These findings reinforce the concept of the microenvironment crosstalk perpetuating leukaemia and driving aggressive phenotypes (560, 610, 611).

7.3 Determining the heterogeneity of AML cell signalling and the response of the phosphoproteome to BMSM stimulation

7.3.1 Context

The pathophysiology that underpins AML cannot be fully explained for most patients, with only those that present with APL having a defined driving event (t[15;17]) – which makes this the only AML subtype to be successfully treated with a targeted therapy (612). For other patients the disease is profoundly heterogeneous, as demonstrated by many of the large-scale genome studies undertaken (18, 31, 32). The findings of these studies have been used to help guide targeted therapies over the past 20-30 years, which as discussed in Chapter 1 has not lead to any significant innovation in AML (23). As many of the most frequently mutated genes encode signalling proteins, tyrosine kinase inhibitors (TKI) have become the focus of many targeted strategies (613, 614).

It was hypothesised that many patients could be non-responsive to TKI-based therapies due to inaccurate stratification. When patients are selected for treatment on the assumption of aberrant kinase activity driving a phenotype (i.e. FLT3) due to genetic aberrations, then treatment selection is assuming that mRNA expression and protein expression, and neglects a host of other biological factors (epigenetic regulation, protein-protein interactions, phosphatase activity, amongst others) that effect network composition and activity (290, 291). Kinase mutations are unlikely to be the sole driver of disease, however. A recent paper by Creixell et al. (216) demonstrated some of the means by which the accumulation of minor genetic events can lead to the rewiring of signalling networks. Considering these factors, it was posited that these types of alterations could influence the kind of relationship that AML cells have with the microenvironment, and by extension the response to the secretome derived proteins.

In Chapter 1, the study of phosphoproteomics was discussed, in particular how the measurement of phosphopeptide abundance using unbiased MS-based techniques is the most comprehensive readout of putative protein function, as it considers the biological contribution of numerous factors (Figure 1.10). Thus, to study the heterogeneity of kinase networks in AML and the impact of the microenvironment on kinase network activity, primary AML cells were stimulated with the identified proteins from Chapter 4 (Figure 5.7), the bulk secretome (Figure 5.13) and by direct co-culture with MS-5 cells (Figure 5.18). These experiments set out to understand if there were inherent features that determine how AML cells interact with the microenvironment or if cell signalling networks do respond in a homogenous manner (360, 560). Additionally, were cells wired to respond in a homogenous manner to certain stimuli (contact dependent), and a heterogeneous manner to other stimuli (chemical).

Finally, Tape et al. (491) recently demonstrated that cancer cells can utilise the signalling networks of stromal cells in a non-cell autonomous manner, to regulate cancer signalling and function in a reciprocal manner – heterotypic signalling. Considering this concept, it was investigated whether primary AML cells in culture were able to direct the behaviour of MS-5 cells to propagate their own progression.

7.3.2 Analysis of single GF stimulated pathways in AML

In order to examine how the panel of secretome derived GFs stimulated proliferation and supported cell survival it was important to characterise how these molecules modulate signalling networks (611). To assess this, GF treatments were first optimised for signalling experiments by examining the status of well described signalling nodes in AML by assessing activity markers following stimulation with 10ng/ml of each GF in P31/FUJ cells (Figure 5.2)(207, 600). These concentrations were selected as these were effective in maintaining viability and inducing proliferation in previous experiments (Figure 4.4 and Figure 4.5). Assessment of key signalling nodes (MAPK, AKT, mTOR substrates, PAK) (207, 600, 601, 615, 616) revealed that GF combination conditions had profound effects on MAPK activity (Figure 5.3), and phosphorylation of the mTOR substrates 4EBP1 and p70S6K (Figure 5.4). The PAK kinases were more phosphorylated following single GF treatments or secretome treatment in PAK1 respectively (Figure 5.5). Collectively these results suggested that the tested concentrations were sufficient to activate signalling nodes of AML cells.

Following validation that the GFs were capable of activating key AML signalling nodes in P31/FUJ cells, the phosphoproteome of patient # 1 cells was chosen to assess pathway activity in primary AML, as these cells displayed dynamic responses to the secretome derived protein treatments (Figure 5.6).

To assess relationships between the effects of the secretome derived proteins on the patient #1 phosphoproteome, the similarity between the $\log_2$ fold-ratios of all the phosphopeptides across the treatments were assessed using hierarchical clustering and PCA (Figure 5.10 and Figure 5.12). This analysis demonstrated that phosphoproteomes of the samples were in agreement with the proliferative response observed when patient #1 cells were treated in Chapter 4. Both S100-A4 and Mixed GF phosphoproteomes clustered independently to the other samples, all of which did not show substantial proliferative difference in patient #1 cells. KSEA analysis of the experiment revealed that changes in kinase activity as a result of tratment were very heterogeneous (Figure 5.11). Systematic assessment determined that the single protein treatments induced increased activity in AKT, mTOR, ERK1 and ERK2, with S100-A4 also increasing ATR, CK2A2 and InsR activity which was not observed in the other treatments (Figure 5.11). The multivariate analysis captured the proliferative phenotypes of these cells,

whereas the KSEA analysis was correlative with the maintained viability observed in survival assays, with single GF treatments leading to consistent enrichment for AKT and mTOR. Excluding S100 proteins ERK signalling was also enriched in these scenarios of high viability. S100-A4 treatment induced signalling in ATR, Src and InsR pathways, which were not observed in the other single GF treatments. As these are the only kinases whose activity did not decrease in Mixed GF conditions, results indicate that these are the pathways that S100-A4 and Mixed GF conditions stimulate to induce proliferation.

It is important to note that the discrepancy between kinase activities in individual GF treatments and the complex mixtures could be due to time of analysis. Fifteen minutes post stimulation was optimal for capturing the activated pathways of single GF treatment at a concentration of 10ng/ml. Whereas, the complex mixtures that contained 10ng/ml each of the six GFs (Mixed GF) or 10µg/ml of >5kDa MS-5 secretome led to an onset of signal transduction that was not captured and not sustained. Previous studies of receptor regulation and signal transduction maintenance have reported that when receptors such as EGFR are exposed to low levels of ligand, they are endocytosed via clathrin-mediated endocytosis and recycled to the surface to help sustain and prolong signalling (617). However, when EGFR is exposed to high ligand levels the receptor it is internalised and committed to lysosomal degradation through clathrin-independent endocytosis, thus ceasing signalling (618). Expanding on EGFR, clathrin-independent endocytosis has been reported to regulate adaptor proteins, HGFR, IFN, TGF and GPCRs (619, 620). It is therefore possible, that the reduced kinase activity in the complex samples (Mixed GF and >5kDa MS-5 sec) was due to ligand concentration being saturated, inducing receptor internalisation and degradation. Whereas, the lower ligand concentrations may have induced sustained receptor signalling, producing the higher activities observed in Figure 5.11. To clarify if this was indeed the case the experiment could be repeated at different time points to ascertain optimal pathway activation because of complex ligand mixtures. Varying GF concentration combinations could be investigated; however, altering GF concentration would then create a discrepancy between the conditions that increased primary AML survival (Figure 5.6) and those being used to investigate the pathways responsible for such phenotypes.

7.3.3 Analysis of kinase network heterogeneity in response to secretome

In order to examine the similarities and differences between the effects of the secretomic proteins on the AML phosphoproteome of numerous patients, a panel of seven primary AML patients were grown with HS-5 CM prior to phosphoproteomic analysis. Initial analysis of the data revealed that both phosphoproteome expression and kinase activity levels were extremely heterogeneous (Figure 5.15 and Figure 5.16).

The relationship between the effects of the HS-5 secretome on the seven patient samples were assessed by means of several multivariate analyses. To compare patient phosphoproteome similarity across patients, the data was analysed using 3-dimensional PC analysis (Figure 5.17). This analysis demonstrated that the basal phosphoproteomes at 1 hour were all distinct and did not share the same PC space. Following 24 hours of HS-5 conditioning 5/7 samples had migrated centrally to occupy a similar region. This indicates that, despite substantially different basal phosphoproteomes, stimulation with the HS-5 secretome affected the phosphoproteomes similarly, suggesting that although signals may have been transmitted via different routes within the network, ultimately the same cellular response can be achieved (216, 621).

7.3.4 Analysis of co-culture on AML signalling networks

To investigate the effects of the BMSM on AML cell signalling fully, it was essential to incorporate the contribution of juxtacrine signalling and the ability of cells to respond to each other dynamically (heterotypic signalling) (491, 622). To establish how these cells regulate each other's signalling networks a label-free phosphoproteomic study was conceived to analyse primary AML cells and MS-5 cells following 24 hours co-culture (Figure 5.18). Careful enrichment and the utilisation of human and mouse genomes made it possible to distinguish co-culture phosphopeptide origin by MS (237).

Comparing the K-means cluster analysis of primary AML cells in MS-5 co-culture to that of the primary AML following HS-5 conditioning, suggests that for consistent and stable AML survival, the secretome alone is insufficient. Principally, this could be due to the lack of bidirectional signalling, which has been demonstrated in other cancer models to be necessary to positively regulate pro-tumorigenic effects (491). Some patient cells can survive in CM (as seen in Chapter 4), which as observed in the CyTOF experiments is owing to the endogenous expression of the necessary complimentary receptors to proteins that comprise the stromal secretome (450, 623). Other features such as low metabolic rate, network topology and a good anti-apoptotic predisposition would also facilitate and contribute to extended survival (624-627). These findings capture the inherent heterogeneity observed between patients visualised by the ability to survive alone (594). In co-culture, however, the environment is dynamic and responsive, therefore, AML cells can also potentially shape the environment in which they find themselves, if independent survival is not possible (560). This is probably why the primary AML response was more consistent during MS-5 co-culture, encapsulated by the uniform increase in phosphorylation of anti-apoptotic substrates (Figure 5.23, cluster 6).

The consensus for increased expression of the phosphopeptides contained within k-means cluster 6 is interesting, as functions for each of the four kinases (AKT, DYRK2, CDK5 and

LATS1) that's activity increased (determined by KSEA) following MS-5 co-culture form aspects of the microenvironment mediated hypothesis that encapsulates AML persistence, treatment resistance and relapse. Increased AKT activity is known to promote cell survival through anti-apoptotic signalling (545, 628, 629), CDK5 activity can maintain the pro-angiogenic environment, which is crucial to sustain AML cells (529). DYRK2 and LATS1 are regulatory kinases that are capable of regulating AML and drive the features that have led the field to believe the microenvironment induces a quiescent phenotype in AML (630, 631). DYRK2 and LATS1 could be the mediators that lead to the drop in AML growth and proliferation, while promoting nestling in small niches, thus making them chemo-resistant (568, 624, 625, 632). These are hypotheses, however, and require further investigation. But these are reported functions of these kinases that were consistently enriched as activated kinases in AML following co-culture with MS-5 cells.

7.3.5 Analysis of co-culture on MS-5 signalling networks

Recent studies had demonstrated that other tumour types can engage and instigate reciprocal signalling with surrounding stromal cells (633) that could regulate cancer cell growth and survival. MS-5 co-culture enabled primary cells from patient samples that exhibited profound phosphoproteomic heterogeneity in HS-5 conditioning experiments (Figure 5.16), to respond in a homogeneous manner while facilitating survival. This included potentiating both anti-apoptotic signalling and modulating the activity of proliferative kinases AKT and LATS1. To establish the phosphoproteomic landscape in MS-5 cells and identify pathways modulated by AML during co-culture, label-free LC-MS/MS based phosphoproteomics were undertaken (Figure 5.18).

Differential abundance analysis demonstrated that there was not profound modulation across the whole proteome, with approximately 300 phosphopeptides significantly changed per co-culture (Figure 5.24). GO enrichment analysis of all significantly modulated peptides ($P<0.05$) revealed that 6/8 of MS-5 populations exhibited increased insulin receptor signalling and signal transduction following AML co-culture (Figure 5.26). This suggested that different AML cell populations were activating signalling pathways in the MS-5 cells (634). KSEA identified three kinases that increased in activity in all eight AML co-culture experiments, which are MAPKAPK2, PKCδ and GSK3β. These are all candidates with roles in reciprocal signalling as these kinases were ubiquitously upregulated in AML co-culture compared to independent MS-5 cells. It may be argued that kinases such as PKCδ are traditionally associated with tumour suppressive effects, in these circumstances however, there are well established hypothesises that the BMM induces quiescence in AML cells, which is a regulative behaviour that increases survival (635-637).

The nature of cross-talk and cell-cell interactions is more nuanced than the single mechanism described above (456). KSEA analysis identified two signalling signatures, that in PC space separate, one away from the control cells and one that cluster with them (Figure 5.28). These two groups also exhibited different morphology and behaviour that are being referred to as BM independent and BM interactive (Figure 5.29).

7.3.6 Implications and future work

Using an untargeted approach, the results of Chapter 5 provide insight to the nature of kinase networks in AML cells and MS-5 cells, and the means by which these cells are able to respond to each other. Experiments revealed that, in spite of the increased understanding the field has garnered in AML biology and the heterogeneity that underpins it (456, 565, 566, 638, 639), knowledge of AML signalling networks, pathway plasticity and adaptations are still greatly limited. Thus, these investigations serve to highlight the heterogeneity of such kinase networks and how they are activated or inactivated by the stromal cells of the BM (615).

Single GF treatments displayed how P31/FUJ cells can be used as an appropriate model to study aspects of AML biology (535), although this cell line did not respond in a manner consistent with the patient#1 primary AML cells tested in single GF studies. Results in section 5.3 showed that primary cells grown in independent culture do not respond to stromal secretomes in a consistent manner either. Single GF treatment experiments in primary AML cells revealed that there were increases in pathway activity relative to untreated cells during single GF treatments (typically mTOR or ATR activity), however, complex mixtures induced relative decreases in global kinase signalling compared to unstimulated cells. These experiments need to be explored in further patients, as the explanation to these observations could relate to a number of factors (patient specific, saturated ligand concentration leading to receptor internalisation, reduction in stress signals, and means of quiescence).

Co-culture signalling experiments notably observed a clustering of patients based on response to the MS-5 cells, these cells also harboured the same NRAS mutation (p.G13D)(448). These signatures did not cluster on inherent basal kinase activity, but on changes in kinase activity following co-culture, this is suggestive of a mutation that influences the way an AML cell population interprets and interacts with other cell types (640). As mentioned previously, this needs to be assessed in further patients that harbour this genotype.

Analysis of MS-5 cells kinase activity following co-culture revealed that RTK signalling was increased in many samples (Figure 5.26). Multivariate analysis of KSEA data revealed two MS-5 phosphoproteomic signatures, one for a group of MS-5 cells seeded with cells that integrated within the stromal network and one for a group MS-5 cells that were seeded with

AML cells that clustered separately. These signatures combined with phenotypic observations are suggestive of stromal interactive AML cells and stromal independent AML cells (641).

Taken together, these experiments showed that AML kinase signalling networks underwent significant and heterogeneous shifts in activity following stimulation with stromal secreted proteins. Most strikingly, different primary AML samples were able to respond to stromal cells through both homogeneous (contact dependent AKT, LATS1 activations) and heterogeneous network routes (response to BMSC secretome), while simultaneously stimulating signalling nodes implicated in cytokine production (such as MAPKAPK2). Experiments to substantiate this potential heterotypic mechanism are of great interest and potentially a future target of therapeutic intervention, if key to AML shaping its niche.

7.4 Functional and biochemical characterisation of PAK signalling in AML

7.4.1 Context

It had been proposed in previous studies that in cancer and in particular treatment resistant neoplasms, kinase networks undergo network rewiring and establish interactions that would not necessarily occur under physiologically conditions (215, 216). Having observed that the underlying kinase networks that help to govern the AML response to the microenvironment are extremely heterogeneous, it had been a quandary that PAK inhibition was always so potent in undermining AML cell survival (Figure 4.11). This observation coupled with the study from Casado et al. (271) that documents that PAK is one the most active kinases in AML (Figure 6.1), lead to experiments that studied the nature of PAK activation in AML and protein interaction studies to try and establish mechanistically the relevance of high PAK activity.

7.4.2 Findings

Collectively, these experiments showed that PAK activity and expression in AML is variable, and this heterogeneity cannot directly be explained through accumulation of genetic aberrations. In agreement with previous works, analysis of AML models tested showed high PAK phosphorylation (Figure 6.5) (206, 207, 271, 551, 642).

Co-IP techniques were optimised so that PAK could be consistently immunoprecipitated. Following the establishment of a robust technique that was able to pulldown known PAK binders in complex to be identified by MS detection (Figure 6.9), PAK complex formation was tested to identify dynamic PAK binders in AML. To elicit such complexes, cells were serum starved before stimulation as used in previous works (552). In addition, preliminary experiments assessed secretomic stimulation and PAK inhibition, all of which revealed preliminary interaction candidates. Further investigations revealed that PAK4 – the least described of the PAK isoforms (540, 541, 550)– consistently demonstrated binding of H2 histones during serum modulation that was not observed under other conditions, indicating either a nuclear function or localisation that PAK4 has previously not been implicated in (539).

7.4.3 Technical considerations

Limitations of the co-IP experiments were the low number of biological replicates (n=2) in Figure 6.13 and Figure 6.14. These experiments may have identified a viable PAK interacting candidate for the group 1 isoforms if enough replicates were conducted, such as LPXN (554, 643, 644). This is an antibody-based approach and therefore, the technique was at the mercy of antibody quality (645). It was notable that serum starved optimisation experiments were able to identify known PAK interactors GIT1, GIT2, ARHGEF6 and ARHGEF7 (539, 646-648), although these were not identified in the large serum-based co-IP experiments. Other known PAK

interactors Filamin A and Filamin C were identified in the larger studies, these binding dynamics can be explained by the antibody incubation step, which was reduced from overnight to 1 hour. It was reasoned that excessive incubation would only lead to the accumulation of non-specific binders and dissociation of transient and important interactors, a type of interaction that would be common for PAK, given that it is a kinase (649, 650). This suggests that the Filamins are more transient PAK interactors and that the ARHGEFs and GITs interactors are more constitutive PAK interactors.

Unexplored means of optimisation included chemical preservation with cross linking agents (such as glutaraldehyde) as previously shown to be an effective means to identify weak interactions, although this requires extensive optimisation to ensure artefacts are not produced (651). Pulldown with magnetic beads was posited as an alternative solid support, potentially offering better bead retention and therefore, complex retention – this should be explored further (652). Approaches not selected due to their potential effects on protein structure, binding and behaviour, were techniques that involved the ectopic expression of protein GFP/FLAG-/HA-tags or BioID/APEX approaches (653-655).

The final aspect of consideration for this chapter, was the lack of primary tissue used in these experiments. Cell lines were used exclusively as it was deemed inappropriate to use primary cells in such experiments. However, this is probably necessary to reveal AML specific interactions for PAK. The previous chapters have discussed the impact of disease heterogeneity on AML kinase networks formation and kinetics, an overactive sample compared to a sample with relatively low PAK activity may have helped reveal the aberrant PAK interactors. Additionally, the inclusion of a non-AML sample would also have helped identify AML specific interactions.

7.4.4 Implications and future work

Studies conducted as part of this project help to substantiate PAKs importance in AML, augmenting previous research (206, 207, 271). Collectively, experiments showed that PAK activity and expression in AML is variable, and this heterogeneity cannot directly be explained through accumulation of genetic aberrations. Following the optimisation of a co-IP coupled MS approach it was possible to investigate dynamic binding partners of PAK principally focussing on PAK response following starvation and rapid stimulation. Experiments to date have identified PAK4 and a consistent dynamic binding of H2 histones during serum modulation that was not observed under other conditions, indicating either a nuclear function or localisation that PAK4 has previously not been implicated in.

Future work will look to validate the PAK4-H2 histone interaction further. The novel association of PAK4 with histones, coupled with AML's well described epigenetic component, represents an exciting mechanism to be explored (4, 18, 69, 656-660). PAK pulldown following treatment with epigenetic modulators (such as voronistat or Azacitidine) could reveal other important interactors. A dynamic relationship between a kinase and histones could offer insight to the mutual regulation of gene expression and kinase signalling (661).

The inclusion of primary AML based experiments; in particular, the comparison of the PAK interactome in a sample that exhibits high PAK activity to one that exhibits normal to low PAK activity could uncover aspects of the upregulated PAK signalling network. Abrogating PAK activity in culture is extremely lethal to AML (Figure 4.11) (536). However, PAK inhibition is not a viable means of therapy in the clinic, due to related toxicities (540). Therefore, more sophisticated means of targeting are required. Understanding of the adaptor proteins that mediate and regulate PAK activity in these AML might uncover new therapeutic opportunities.

7.5 Concluding remarks

Due to the combinatorial complexity of the number of variables involved in leukaemogenesis and resistance of a single clone (genomic aberrations, epigenetic factors, kinase signalling dynamics, metabolic abnormalities and environmental factors) AML has remained largely incurable (19, 442, 532, 567, 625, 662). The combination of factors also explains why targeted therapy has yet to really establish itself in this disease (excluding APL) and why chemotherapy-based regimens followed by SCT have been the only means of cure (23).

The increased understanding of disease biology is important in the pursuit of therapeutic innovation and the discovery of new targets (40, 569, 570). Therefore, the more that is understood about the contributing factors of disease heterogeneity the greater the likelihood of identifying new therapeutic strategies. Studies performed as part of this thesis highlight the power of MS-based proteomics in understanding the role of the microenvironment in AML. This represents the first time that an MS based approach was used to identify components of the AML supportive secretome and results have shown that these proteins alone can maintain primary cells for an extended period of weeks. It remains to be established what determines response to these proteins in leukaemic cells, and whether these proteins are transiently important in disease pathology or if they are a constant feature that define AML. These questions extend to other exogenous factors, touching on the role of the microenvironment in disease initiation and whether it has a larger role to play in the definition of inherent leukaemic features (164).

This work has posed pertinent questions in the pursuit and implementation of targeted therapies in AML, in particular the suitability of FLT3 kinase inhibitors. The selection of kinase inhibition based on mutational status assumes that profound molecular heterogeneity does not affect the topology and plasticity of kinase networks (39, 47, 446, 663-665). It has been hard to identify kinase mutations that have penetrance in the activity of global kinase networks in these studies. In addition, divergent network configurations also highlighted the difficulty in deciphering the precise configuration and activity of kinase networks across both cell types and patients (271, 456).

Finally, an unexpected and potentially significant observation was the switch in cell sensitivity to kinase inhibition – in both directions – whilst in the presence of proteins from the microenvironment. In the burgeoning field of kinase inhibitor therapeutics, the biological context in which kinase activity is measured in patient samples could result in significant variance from the in vivo situation. Inherently certain AML clones may utilise particular signalling

nodes, but in the microenvironment the dependence on such nodes may shift. These are important considerations as we proceed to towards personalised medicine.

Chapter 8: References

1. Dohner, H., D.J. Weisdorf, and C.D. Bloomfield, *Acute Myeloid Leukemia.* N Engl J Med, 2015. **373**(12): p. 1136-52.
2. Dores, G.M., S.S. Devesa, R.E. Curtis, M.S. Linet, and L.M. Morton, *Acute leukemia incidence and patient survival among children and adults in the United States, 2001-2007.* Blood, 2012. **119**(1): p. 34-43.
3. Deschler, B. and M. Lubbert, *Acute myeloid leukemia: epidemiology and etiology.* Cancer, 2006. **107**(9): p. 2099-107.
4. DiNardo, C.D. and J.E. Cortes, *Mutations in AML: prognostic and therapeutic implications.* Hematology Am Soc Hematol Educ Program, 2016. **2016**(1): p. 348-355.
5. Siegel, R.L., K.D. Miller, and A. Jemal, *Cancer statistics, 2016.* CA Cancer J Clin, 2016. **66**(1): p. 7-30.
6. Meyers, J., Y. Yu, J.A. Kaye, and K.L. Davis, *Medicare fee-for-service enrollees with primary acute myeloid leukemia: an analysis of treatment patterns, survival, and healthcare resource utilization and costs.* Appl Health Econ Health Policy, 2013. **11**(3): p. 275-86.
7. Sabattini, E., F. Bacci, C. Sagramoso, and S.A. Pileri, *WHO classification of tumours of haematopoietic and lymphoid tissues in 2008: an overview.* Pathologica, 2010. **102**(3): p. 83-7.
8. Bennett, J.M., et al., *Proposals for the classification of the acute leukaemias. French-American-British (FAB) co-operative group.* Br J Haematol, 1976. **33**(4): p. 451-8.
9. Vardiman, J.W., et al., *The 2008 revision of the World Health Organization (WHO) classification of myeloid neoplasms and acute leukemia: rationale and important changes.* Blood, 2009. **114**(5): p. 937-51.
10. Estey, E.H., *Acute myeloid leukemia: 2014 update on risk-stratification and management.* Am J Hematol, 2014. **89**(11): p. 1063-81.
11. Bonnet, D. and J.E. Dick, *Human acute myeloid leukemia is organized as a hierarchy that originates from a primitive hematopoietic cell.* Nat Med, 1997. **3**(7): p. 730-7.
12. Kronke, J., et al., *Monitoring of minimal residual disease in NPM1-mutated acute myeloid leukemia: a study from the German-Austrian acute myeloid leukemia study group.* J Clin Oncol, 2011. **29**(19): p. 2709-16.
13. Shlush, L.I., et al., *Identification of pre-leukaemic haematopoietic stem cells in acute leukaemia.* Nature, 2014. **506**(7488): p. 328-33.
14. Corces-Zimmerman, M.R., W.J. Hong, I.L. Weissman, B.C. Medeiros, and R. Majeti, *Preleukemic mutations in human acute myeloid leukemia affect epigenetic regulators and persist in remission.* Proc Natl Acad Sci U S A, 2014. **111**(7): p. 2548-53.
15. Kelly, L.M. and D.G. Gilliland, *Genetics of myeloid leukemias.* Annu Rev Genomics Hum Genet, 2002. **3**: p. 179-98.
16. Shih, A.H., O. Abdel-Wahab, J.P. Patel, and R.L. Levine, *The role of mutations in epigenetic regulators in myeloid malignancies.* Nat Rev Cancer, 2012. **12**(9): p. 599-612.
17. Woods, B.A. and R.L. Levine, *The role of mutations in epigenetic regulators in myeloid malignancies.* Immunol Rev, 2015. **263**(1): p. 22-35.
18. Cancer Genome Atlas Research, N., et al., *Genomic and epigenomic landscapes of adult de novo acute myeloid leukemia.* N Engl J Med, 2013. **368**(22): p. 2059-74.
19. Ding, L., et al., *Clonal evolution in relapsed acute myeloid leukaemia revealed by whole-genome sequencing.* Nature, 2012. **481**(7382): p. 506-10.
20. Welch, J.S., et al., *The origin and evolution of mutations in acute myeloid leukemia.* Cell, 2012. **150**(2): p. 264-78.
21. Arber, D.A., et al., *The 2016 revision to the World Health Organization classification of myeloid neoplasms and acute leukemia.* Blood, 2016. **127**(20): p. 2391-405.

22. Degos, L. and Z.Y. Wang, *All trans retinoic acid in acute promyelocytic leukemia.* Oncogene, 2001. **20**(49): p. 7140-5.
23. Dohner, H., et al., *Diagnosis and management of AML in adults: 2017 ELN recommendations from an international expert panel.* Blood, 2017. **129**(4): p. 424-447.
24. Walter, M.J., et al., *Clonal architecture of secondary acute myeloid leukemia.* N Engl J Med, 2012. **366**(12): p. 1090-8.
25. Byrd, J.C., et al., *Pretreatment cytogenetic abnormalities are predictive of induction success, cumulative incidence of relapse, and overall survival in adult patients with de novo acute myeloid leukemia: results from Cancer and Leukemia Group B (CALGB 8461).* Blood, 2002. **100**(13): p. 4325-36.
26. Dohner, K., P. Paschka, and H. Dohner, *[Acute myeloid leukemia].* Internist (Berl), 2015. **56**(4): p. 354-63.
27. Mrozek, K., M.D. Radmacher, C.D. Bloomfield, and G. Marcucci, *Molecular signatures in acute myeloid leukemia.* Curr Opin Hematol, 2009. **16**(2): p. 64-9.
28. Gaidzik, V. and K. Dohner, *Prognostic implications of gene mutations in acute myeloid leukemia with normal cytogenetics.* Semin Oncol, 2008. **35**(4): p. 346-55.
29. Marcucci, G., T. Haferlach, and H. Dohner, *Molecular genetics of adult acute myeloid leukemia: prognostic and therapeutic implications.* J Clin Oncol, 2011. **29**(5): p. 475-86.
30. Lindsley, R.C., et al., *Acute myeloid leukemia ontogeny is defined by distinct somatic mutations.* Blood, 2015. **125**(9): p. 1367-76.
31. Papaemmanuil, E., et al., *Genomic Classification and Prognosis in Acute Myeloid Leukemia.* N Engl J Med, 2016. **374**(23): p. 2209-2221.
32. Papaemmanuil, E., H. Dohner, and P.J. Campbell, *Genomic Classification in Acute Myeloid Leukemia.* N Engl J Med, 2016. **375**(9): p. 900-1.
33. Saultz, J.N. and R. Garzon, *Acute Myeloid Leukemia: A Concise Review.* J Clin Med, 2016. **5**(3).
34. Kelly, L.M., et al., *FLT3 internal tandem duplication mutations associated with human acute myeloid leukemias induce myeloproliferative disease in a murine bone marrow transplant model.* Blood, 2002. **99**(1): p. 310-8.
35. Badar, T., et al., *Detectable FLT3-ITD or RAS mutation at the time of transformation from MDS to AML predicts for very poor outcomes.* Leuk Res, 2015. **39**(12): p. 1367-74.
36. Pollard, J.A., et al., *Prevalence and prognostic significance of KIT mutations in pediatric patients with core binding factor AML enrolled on serial pediatric cooperative trials for de novo AML.* Blood, 2010. **115**(12): p. 2372-9.
37. Kavanagh, S., et al., *Emerging therapies for acute myeloid leukemia: translating biology into the clinic.* JCI Insight, 2017. **2**(18).
38. McCurdy, S.R. and M.J. Levis, *Emerging molecular predictive and prognostic factors in acute myeloid leukemia.* Leuk Lymphoma, 2017: p. 1-19.
39. Medinger, M. and J.R. Passweg, *Acute myeloid leukaemia genomics.* Br J Haematol, 2017. **179**(4): p. 530-542.
40. Chung, C. and H. Ma, *Driving Toward Precision Medicine for Acute Leukemias: Are We There Yet?* Pharmacotherapy, 2017. **37**(9): p. 1052-1072.
41. Lowenberg, B., et al., *High-dose daunorubicin in older patients with acute myeloid leukemia.* N Engl J Med, 2009. **361**(13): p. 1235-48.
42. Konig, H. and M. Levis, *Is targeted therapy feasible in acute myelogenous leukemia?* Curr Hematol Malig Rep, 2014. **9**(2): p. 118-27.
43. Cornelissen, J.J. and D. Blaise, *Hematopoietic stem cell transplantation for patients with AML in first complete remission.* Blood, 2016. **127**(1): p. 62-70.
44. Kantarjian, H.M., et al., *Multicenter, randomized, open-label, phase III trial of decitabine versus patient choice, with physician advice, of either supportive care or low-dose cytarabine for the treatment of older patients with newly diagnosed acute myeloid leukemia.* J Clin Oncol, 2012. **30**(21): p. 2670-7.

45. Fenaux, P., et al., *Azacitidine prolongs overall survival compared with conventional care regimens in elderly patients with low bone marrow blast count acute myeloid leukemia.* J Clin Oncol, 2010. **28**(4): p. 562-9.
46. Konopleva, M., Y. Tabe, Z. Zeng, and M. Andreeff, *Therapeutic targeting of microenvironmental interactions in leukemia: mechanisms and approaches.* Drug Resist Updat, 2009. **12**(4-5): p. 103-13.
47. Stein, E.M. and M.S. Tallman, *Emerging therapeutic drugs for AML.* Blood, 2016. **127**(1): p. 71-8.
48. Hanahan, D. and L.M. Coussens, *Accessories to the crime: functions of cells recruited to the tumor microenvironment.* Cancer Cell, 2012. **21**(3): p. 309-22.
49. Shah, A., T.M. Andersson, B. Rachet, M. Bjorkholm, and P.C. Lambert, *Survival and cure of acute myeloid leukaemia in England, 1971-2006: a population-based study.* Br J Haematol, 2013. **162**(4): p. 509-16.
50. Thiede, C., et al., *Analysis of FLT3-activating mutations in 979 patients with acute myelogenous leukemia: association with FAB subtypes and identification of subgroups with poor prognosis.* Blood, 2002. **99**(12): p. 4326-35.
51. Kottaridis, P.D., et al., *The presence of a FLT3 internal tandem duplication in patients with acute myeloid leukemia (AML) adds important prognostic information to cytogenetic risk group and response to the first cycle of chemotherapy: analysis of 854 patients from the United Kingdom Medical Research Council AML 10 and 12 trials.* Blood, 2001. **98**(6): p. 1752-9.
52. Schneider, F., et al., *Age-dependent frequencies of NPM1 mutations and FLT3-ITD in patients with normal karyotype AML (NK-AML).* Ann Hematol, 2012. **91**(1): p. 9-18.
53. Cortes, J.E., et al., *Phase I study of quizartinib administered daily to patients with relapsed or refractory acute myeloid leukemia irrespective of FMS-like tyrosine kinase 3-internal tandem duplication status.* J Clin Oncol, 2013. **31**(29): p. 3681-7.
54. Wander, S.A., M.J. Levis, and A.T. Fathi, *The evolving role of FLT3 inhibitors in acute myeloid leukemia: quizartinib and beyond.* Ther Adv Hematol, 2014. **5**(3): p. 65-77.
55. De Propris, M.S., et al., *High CD33 expression levels in acute myeloid leukemia cells carrying the nucleophosmin (NPM1) mutation.* Haematologica, 2011. **96**(10): p. 1548-51.
56. Laszlo, G.S., E.H. Estey, and R.B. Walter, *The past and future of CD33 as therapeutic target in acute myeloid leukemia.* Blood Rev, 2014. **28**(4): p. 143-53.
57. Jurcic, J.G., *What happened to anti-CD33 therapy for acute myeloid leukemia?* Curr Hematol Malig Rep, 2012. **7**(1): p. 65-73.
58. Peled, A. and S. Tavor, *Role of CXCR4 in the pathogenesis of acute myeloid leukemia.* Theranostics, 2013. **3**(1): p. 34-9.
59. Burger, J.A. and A. Peled, *CXCR4 antagonists: targeting the microenvironment in leukemia and other cancers.* Leukemia, 2009. **23**(1): p. 43-52.
60. Zeng, Z., et al., *Targeting the leukemia microenvironment by CXCR4 inhibition overcomes resistance to kinase inhibitors and chemotherapy in AML.* Blood, 2009. **113**(24): p. 6215-24.
61. Baylin, S.B., J.G. Herman, J.R. Graff, P.M. Vertino, and J.P. Issa, *Alterations in DNA methylation: a fundamental aspect of neoplasia.* Adv Cancer Res, 1998. **72**: p. 141-96.
62. Claus, R., C. Plass, S.A. Armstrong, and L. Bullinger, *DNA methylation profiling in acute myeloid leukemia: from recent technological advances to biological and clinical insights.* Future Oncol, 2010. **6**(9): p. 1415-31.
63. Chim, C.S., A.S. Wong, and Y.L. Kwong, *Infrequent hypermethylation of CEBPA promotor in acute myeloid leukaemia.* Br J Haematol, 2002. **119**(4): p. 988-90.
64. Chim, C.S., R. Liang, and Y.L. Kwong, *Hypermethylation of gene promoters in hematological neoplasia.* Hematol Oncol, 2002. **20**(4): p. 167-76.
65. Care, R.S., et al., *Incidence and prognosis of c-KIT and FLT3 mutations in core binding factor (CBF) acute myeloid leukaemias.* Br J Haematol, 2003. **121**(5): p. 775-7.

66. Paschka, P., et al., *Adverse prognostic significance of KIT mutations in adult acute myeloid leukemia with inv(16) and t(8;21): a Cancer and Leukemia Group B Study.* J Clin Oncol, 2006. **24**(24): p. 3904-11.
67. Park, S.H., et al., *Prognostic impact of c-KIT mutations in core binding factor acute myeloid leukemia.* Leuk Res, 2011. **35**(10): p. 1376-83.
68. Dos Santos, C., et al., *The Src and c-Kit kinase inhibitor dasatinib enhances p53-mediated targeting of human acute myeloid leukemia stem cells by chemotherapeutic agents.* Blood, 2013. **122**(11): p. 1900-13.
69. Wouters, B.J. and R. Delwel, *Epigenetics and approaches to targeted epigenetic therapy in acute myeloid leukemia.* Blood, 2016. **127**(1): p. 42-52.
70. Stone, R.M., et al., *Midostaurin plus Chemotherapy for Acute Myeloid Leukemia with a FLT3 Mutation.* N Engl J Med, 2017. **377**(5): p. 454-464.
71. Fischer, T., et al., *Phase IIB trial of oral Midostaurin (PKC412), the FMS-like tyrosine kinase 3 receptor (FLT3) and multi-targeted kinase inhibitor, in patients with acute myeloid leukemia and high-risk myelodysplastic syndrome with either wild-type or mutated FLT3.* J Clin Oncol, 2010. **28**(28): p. 4339-45.
72. Levis, M., et al., *Results from a randomized trial of salvage chemotherapy followed by lestaurtinib for patients with FLT3 mutant AML in first relapse.* Blood, 2011. **117**(12): p. 3294-301.
73. Knapper, S., et al., *A randomized assessment of adding the kinase inhibitor lestaurtinib to first-line chemotherapy for FLT3-mutated AML.* Blood, 2017. **129**(9): p. 1143-1154.
74. Rollig, C., et al., *Addition of sorafenib versus placebo to standard therapy in patients aged 60 years or younger with newly diagnosed acute myeloid leukaemia (SORAML): a multicentre, phase 2, randomised controlled trial.* Lancet Oncol, 2015. **16**(16): p. 1691-9.
75. Boissel, N., et al., *Dasatinib in high-risk core binding factor acute myeloid leukemia in first complete remission: a French Acute Myeloid Leukemia Intergroup trial.* Haematologica, 2015. **100**(6): p. 780-5.
76. Park, S., et al., *A phase Ib GOELAMS study of the mTOR inhibitor RAD001 in association with chemotherapy for AML patients in first relapse.* Leukemia, 2013. **27**(7): p. 1479-86.
77. Recher, C., et al., *Antileukemic activity of rapamycin in acute myeloid leukemia.* Blood, 2005. **105**(6): p. 2527-34.
78. Recher, C., C. Dos Santos, C. Demur, and B. Payrastre, *mTOR, a new therapeutic target in acute myeloid leukemia.* Cell Cycle, 2005. **4**(11): p. 1540-9.
79. Sampath, D., et al., *Phase I clinical, pharmacokinetic, and pharmacodynamic study of the Akt-inhibitor triciribine phosphate monohydrate in patients with advanced hematologic malignancies.* Leuk Res, 2013. **37**(11): p. 1461-7.
80. Borthakur, G., et al., *Activity of the oral mitogen-activated protein kinase kinase inhibitor trametinib in RAS-mutant relapsed or refractory myeloid malignancies.* Cancer, 2016. **122**(12): p. 1871-9.
81. Jain, N., et al., *Phase II study of the oral MEK inhibitor selumetinib in advanced acute myelogenous leukemia: a University of Chicago phase II consortium trial.* Clin Cancer Res, 2014. **20**(2): p. 490-8.
82. Kantarjian, H.M., et al., *Phase I study assessing the safety and tolerability of barasertib (AZD1152) with low-dose cytosine arabinoside in elderly patients with AML.* Clin Lymphoma Myeloma Leuk, 2013. **13**(5): p. 559-67.
83. Dohner, H., et al., *Randomized, phase 2 trial of low-dose cytarabine with or without volasertib in AML patients not suitable for induction therapy.* Blood, 2014. **124**(9): p. 1426-33.
84. Uras, I.Z., et al., *Palbociclib treatment of FLT3-ITD+ AML cells uncovers a kinase-dependent transcriptional regulation of FLT3 and PIM1 by CDK6.* Blood, 2016. **127**(23): p. 2890-902.

85. Karp, J.E., et al., *Phase I and pharmacologic trial of cytosine arabinoside with the selective checkpoint 1 inhibitor Sch 900776 in refractory acute leukemias.* Clin Cancer Res, 2012. **18**(24): p. 6723-31.
86. Zhou, L., et al., *A regimen combining the Wee1 inhibitor AZD1775 with HDAC inhibitors targets human acute myeloid leukemia cells harboring various genetic mutations.* Leukemia, 2015. **29**(4): p. 807-18.
87. Saito, Y., et al., *A pyrrolo-pyrimidine derivative targets human primary AML stem cells in vivo.* Sci Transl Med, 2013. **5**(181): p. 181ra52.
88. Issa, J.J., et al., *Safety and tolerability of guadecitabine (SGI-110) in patients with myelodysplastic syndrome and acute myeloid leukaemia: a multicentre, randomised, dose-escalation phase 1 study.* Lancet Oncol, 2015. **16**(9): p. 1099-1110.
89. Burianova, I., et al., *Histone deacetylase inhibitors in plasma cell leukemia treatment: effect of bone marrow microenvironment.* Neoplasma, 2017. **64**(2): p. 228-237.
90. Birendra, K.C. and C.D. DiNardo, *Evidence for Clinical Differentiation and Differentiation Syndrome in Patients With Acute Myeloid Leukemia and IDH1 Mutations Treated With the Targeted Mutant IDH1 Inhibitor, AG-120.* Clin Lymphoma Myeloma Leuk, 2016. **16**(8): p. 460-5.
91. Kats, L.M., et al., *A pharmacogenomic approach validates AG-221 as an effective and on-target therapy in IDH2 mutant AML.* Leukemia, 2017. **31**(6): p. 1466-1470.
92. Stein, E.M., *IDH2 inhibition in AML: Finally progress?* Best Pract Res Clin Haematol, 2015. **28**(2-3): p. 112-5.
93. Stein, E.M., et al., *Enasidenib in mutant-IDH2 relapsed or refractory acute myeloid leukemia.* Blood, 2017.
94. Yen, K., et al., *AG-221, a First-in-Class Therapy Targeting Acute Myeloid Leukemia Harboring Oncogenic IDH2 Mutations.* Cancer Discov, 2017. **7**(5): p. 478-493.
95. Klaus, C.R., et al., *DOT1L inhibitor EPZ-5676 displays synergistic antiproliferative activity in combination with standard of care drugs and hypomethylating agents in MLL-rearranged leukemia cells.* J Pharmacol Exp Ther, 2014. **350**(3): p. 646-56.
96. Waters, N.J., *Preclinical Pharmacokinetics and Pharmacodynamics of Pinometostat (EPZ-5676), a First-in-Class, Small Molecule S-Adenosyl Methionine Competitive Inhibitor of DOT1L.* Eur J Drug Metab Pharmacokinet, 2017.
97. Braun, T. and C. Gardin, *Investigational BET bromodomain protein inhibitors in early stage clinical trials for acute myelogenous leukemia (AML).* Expert Opin Investig Drugs, 2017. **26**(7): p. 803-811.
98. Berthon, C., et al., *Bromodomain inhibitor OTX015 in patients with acute leukaemia: a dose-escalation, phase 1 study.* Lancet Haematol, 2016. **3**(4): p. e186-95.
99. Cortes, J.E., et al., *Phase II, multicenter, randomized trial of CPX-351 (cytarabine:daunorubicin) liposome injection versus intensive salvage therapy in adults with first relapse AML.* Cancer, 2015. **121**(2): p. 234-42.
100. Daver, N., et al., *Vosaroxin in combination with decitabine in newly diagnosed older patients with acute myeloid leukemia or high-risk myelodysplastic syndrome.* Haematologica, 2017. **102**(10): p. 1709-1717.
101. Konopleva, M., et al., *Efficacy and Biological Correlates of Response in a Phase II Study of Venetoclax Monotherapy in Patients with Acute Myelogenous Leukemia.* Cancer Discov, 2016. **6**(10): p. 1106-1117.
102. Cole, A., et al., *Inhibition of the Mitochondrial Protease ClpP as a Therapeutic Strategy for Human Acute Myeloid Leukemia.* Cancer Cell, 2015. **27**(6): p. 864-76.
103. *CKMT1 May Be a Therapeutic Target in EVI1-Driven Acute Myeloid Leukemia.* Cancer Discov, 2017. **7**(4): p. 349.
104. Hourigan, C.S. and P.D. Aplan, *Accurate Medicine: Indirect Targeting of NPM1-Mutated AML.* Cancer Discov, 2016. **6**(10): p. 1087-1089.
105. Minami, Y., et al., *Phase I study of glasdegib (PF-04449913), an oral smoothened inhibitor, in Japanese patients with select hematologic malignancies.* Cancer Sci, 2017. **108**(8): p. 1628-1633.

106. Chaudhry, P., M. Singh, T.J. Triche, M. Guzman, and A.A. Merchant, *GLI3 repressor determines Hedgehog pathway activation and is required for response to SMO antagonist glasdegib in AML.* Blood, 2017. **129**(26): p. 3465-3475.
107. Lichtenegger, F.S., C. Krupka, S. Haubner, T. Kohnke, and M. Subklewe, *Recent developments in immunotherapy of acute myeloid leukemia.* J Hematol Oncol, 2017. **10**(1): p. 142.
108. Kung Sutherland, M.S., et al., *SGN-CD33A: a novel CD33-targeting antibody-drug conjugate using a pyrrolobenzodiazepine dimer is active in models of drug-resistant AML.* Blood, 2013. **122**(8): p. 1455-63.
109. Barrett, A.J., *Antibody darts on target for acute myelogenous leukemia.* Ann Transl Med, 2017. **5**(4): p. 80.
110. Aigner, M., et al., *T lymphocytes can be effectively recruited for ex vivo and in vivo lysis of AML blasts by a novel CD33/CD3-bispecific BiTE antibody construct.* Leukemia, 2013. **27**(5): p. 1107-15.
111. Kenderian, S.S., et al., *CD33-specific chimeric antigen receptor T cells exhibit potent preclinical activity against human acute myeloid leukemia.* Leukemia, 2015. **29**(8): p. 1637-47.
112. Mardiros, A., et al., *T cells expressing CD123-specific chimeric antigen receptors exhibit specific cytolytic effector functions and antitumor effects against human acute myeloid leukemia.* Blood, 2013. **122**(18): p. 3138-48.
113. Pizzitola, I., et al., *Chimeric antigen receptors against CD33/CD123 antigens efficiently target primary acute myeloid leukemia cells in vivo.* Leukemia, 2014. **28**(8): p. 1596-605.
114. Lynn, R.C., et al., *High-affinity FRbeta-specific CAR T cells eradicate AML and normal myeloid lineage without HSC toxicity.* Leukemia, 2016. **30**(6): p. 1355-64.
115. Wang, Q.S., et al., *Treatment of CD33-directed chimeric antigen receptor-modified T cells in one patient with relapsed and refractory acute myeloid leukemia.* Mol Ther, 2015. **23**(1): p. 184-91.
116. Yang, H., et al., *Expression of PD-L1, PD-L2, PD-1 and CTLA4 in myelodysplastic syndromes is enhanced by treatment with hypomethylating agents.* Leukemia, 2014. **28**(6): p. 1280-8.
117. Berger, R., et al., *Phase I safety and pharmacokinetic study of CT-011, a humanized antibody interacting with PD-1, in patients with advanced hematologic malignancies.* Clin Cancer Res, 2008. **14**(10): p. 3044-51.
118. Alatrash, G., N. Daver, and E.A. Mittendorf, *Targeting Immune Checkpoints in Hematologic Malignancies.* Pharmacol Rev, 2016. **68**(4): p. 1014-1025.
119. Vey, N., et al., *A phase 1 trial of the anti-inhibitory KIR mAb IPH2101 for AML in complete remission.* Blood, 2012. **120**(22): p. 4317-23.
120. Di Stasi, A., A.M. Jimenez, K. Minagawa, M. Al-Obaidi, and K. Rezvani, *Review of the Results of WT1 Peptide Vaccination Strategies for Myelodysplastic Syndromes and Acute Myeloid Leukemia from Nine Different Studies.* Front Immunol, 2015. **6**: p. 36.
121. Van den Bergh, J., et al., *Transpresentation of interleukin-15 by IL-15/IL-15Ralpha mRNA-engineered human dendritic cells boosts antitumoral natural killer cell activity.* Oncotarget, 2015. **6**(42): p. 44123-33.
122. Cho, B.S., H.J. Kim, and M. Konopleva, *Targeting the CXCL12/CXCR4 axis in acute myeloid leukemia: from bench to bedside.* Korean J Intern Med, 2017. **32**(2): p. 248-257.
123. Cho, B.S., et al., *Antileukemia activity of the novel peptidic CXCR4 antagonist LY2510924 as monotherapy and in combination with chemotherapy.* Blood, 2015. **126**(2): p. 222-32.
124. Nervi, B., et al., *Chemosensitization of acute myeloid leukemia (AML) following mobilization by the CXCR4 antagonist AMD3100.* Blood, 2009. **113**(24): p. 6206-14.
125. Peng, S.B., et al., *Inhibition of CXCR4 by LY2624587, a Fully Humanized Anti-CXCR4 Antibody Induces Apoptosis of Hematologic Malignancies.* PLoS One, 2016. **11**(3): p. e0150585.
126. Trujillo, A., C. McGee, and C.R. Cogle, *Angiogenesis in acute myeloid leukemia and opportunities for novel therapies.* J Oncol, 2012. **2012**: p. 128608.

127. Dombret, H. and C. Gardin, *An update of current treatments for adult acute myeloid leukemia.* Blood, 2016. **127**(1): p. 53-61.
128. Chalandon, Y. and J. Schwaller, *Targeting mutated protein tyrosine kinases and their signaling pathways in hematologic malignancies.* Haematologica, 2005. **90**(7): p. 949-68.
129. Walter, R.B., et al., *Resistance prediction in AML: analysis of 4601 patients from MRC/NCRI, HOVON/SAKK, SWOG and MD Anderson Cancer Center.* Leukemia, 2015. **29**(2): p. 312-20.
130. Cheson, B.D., et al., *Revised recommendations of the International Working Group for Diagnosis, Standardization of Response Criteria, Treatment Outcomes, and Reporting Standards for Therapeutic Trials in Acute Myeloid Leukemia.* J Clin Oncol, 2003. **21**(24): p. 4642-9.
131. Thol, F., R.F. Schlenk, M. Heuser, and A. Ganser, *How I treat refractory and early relapsed acute myeloid leukemia.* Blood, 2015. **126**(3): p. 319-27.
132. Dohner, H., et al., *Diagnosis and management of acute myeloid leukemia in adults: recommendations from an international expert panel, on behalf of the European LeukemiaNet.* Blood, 2010. **115**(3): p. 453-74.
133. Weltermann, A., et al., *Impact of cytogenetics on the prognosis of adults with de novo AML in first relapse.* Leukemia, 2004. **18**(2): p. 293-302.
134. Estey, E.H., *Treatment of relapsed and refractory acute myelogenous leukemia.* Leukemia, 2000. **14**(3): p. 476-9.
135. Cassinat, B., et al., *Quantitation of minimal residual disease in acute promyelocytic leukemia patients with t(15;17) translocation using real-time RT-PCR.* Leukemia, 2000. **14**(2): p. 324-8.
136. Grimwade, D. and S.D. Freeman, *Defining minimal residual disease in acute myeloid leukemia: which platforms are ready for "prime time"?* Blood, 2014. **124**(23): p. 3345-55.
137. Klco, J.M., et al., *Functional heterogeneity of genetically defined subclones in acute myeloid leukemia.* Cancer Cell, 2014. **25**(3): p. 379-92.
138. Lapidot, T., et al., *A cell initiating human acute myeloid leukaemia after transplantation into SCID mice.* Nature, 1994. **367**(6464): p. 645-8.
139. Bhatia, M., J.C. Wang, U. Kapp, D. Bonnet, and J.E. Dick, *Purification of primitive human hematopoietic cells capable of repopulating immune-deficient mice.* Proc Natl Acad Sci U S A, 1997. **94**(10): p. 5320-5.
140. Ishikawa, F., et al., *Chemotherapy-resistant human AML stem cells home to and engraft within the bone-marrow endosteal region.* Nat Biotechnol, 2007. **25**(11): p. 1315-21.
141. Costello, R.T., et al., *Human acute myeloid leukemia CD34+/CD38- progenitor cells have decreased sensitivity to chemotherapy and Fas-induced apoptosis, reduced immunogenicity, and impaired dendritic cell transformation capacities.* Cancer Res, 2000. **60**(16): p. 4403-11.
142. Terpstra, W., et al., *Fluorouracil selectively spares acute myeloid leukemia cells with long-term growth abilities in immunodeficient mice and in culture.* Blood, 1996. **88**(6): p. 1944-50.
143. Taussig, D.C., et al., *Leukemia-initiating cells from some acute myeloid leukemia patients with mutated nucleophosmin reside in the CD34(-) fraction.* Blood, 2010. **115**(10): p. 1976-1984.
144. Colmone, A., et al., *Leukemic cells create bone marrow niches that disrupt the behavior of normal hematopoietic progenitor cells.* Science, 2008. **322**(5909): p. 1861-5.
145. Konopleva, M.Y. and C.T. Jordan, *Leukemia stem cells and microenvironment: biology and therapeutic targeting.* J Clin Oncol, 2011. **29**(5): p. 591-9.
146. Dick, J.E., *Stem cell concepts renew cancer research.* Blood, 2008. **112**(13): p. 4793-807.
147. Saito, Y., et al., *Induction of cell cycle entry eliminates human leukemia stem cells in a mouse model of AML.* Nat Biotechnol, 2010. **28**(3): p. 275-80.

148. Doan, P.L. and J.P. Chute, *The vascular niche: home for normal and malignant hematopoietic stem cells.* Leukemia, 2012. **26**(1): p. 54-62.
149. McClugage, S.G., Jr., R.S. McCuskey, and H.A. Meineke, *Microscopy of living bone marrow in Situ. II. Influence of the microenvironment on hemopoiesis.* Blood, 1971. **38**(1): p. 96-107.
150. Fliedner, T.M., V.P. Bond, and E.P. Cronkite, *Structural, cytologic and autoradiographic (H3-thymidine) changes in the bone marrow following total body irradiation.* Am J Pathol, 1961. **38**: p. 599-623.
151. Lord, B.I., N.G. Testa, and J.H. Hendry, *The relative spatial distributions of CFUs and CFUc in the normal mouse femur.* Blood, 1975. **46**(1): p. 65-72.
152. Gong, J.K., *Endosteal marrow: a rich source of hematopoietic stem cells.* Science, 1978. **199**(4336): p. 1443-5.
153. Nilsson, S.K., H.M. Johnston, and J.A. Coverdale, *Spatial localization of transplanted hemopoietic stem cells: inferences for the localization of stem cell niches.* Blood, 2001. **97**(8): p. 2293-9.
154. Oh, I.H. and K.R. Kwon, *Concise review: multiple niches for hematopoietic stem cell regulations.* Stem Cells, 2010. **28**(7): p. 1243-9.
155. Knospe, W.H., S.A. Gregory, S.G. Husseini, W. Fried, and F.E. Trobaugh, Jr., *Origin and recovery of colony-forming units in locally curetted bone marrow of mice.* Blood, 1972. **39**(3): p. 331-40.
156. Tabe, Y. and M. Konopleva, *Role of Microenvironment in Resistance to Therapy in AML.* Curr Hematol Malig Rep, 2015. **10**(2): p. 96-103.
157. Kronke, J., et al., *Clonal evolution in relapsed NPM1-mutated acute myeloid leukemia.* Blood, 2013. **122**(1): p. 100-8.
158. Kode, A., et al., *Leukaemogenesis induced by an activating beta-catenin mutation in osteoblasts.* Nature, 2014. **506**(7487): p. 240-4.
159. Kode, A., et al., *FoxO1-dependent induction of acute myeloid leukemia by osteoblasts in mice.* Leukemia, 2016. **30**(1): p. 1-13.
160. Wiseman, D.H., *Donor cell leukemia: a review.* Biol Blood Marrow Transplant, 2011. **17**(6): p. 771-89.
161. Corces-Zimmerman, M.R. and R. Majeti, *Pre-leukemic evolution of hematopoietic stem cells: the importance of early mutations in leukemogenesis.* Leukemia, 2014. **28**(12): p. 2276-82.
162. Hoggatt, J., Y. Kfoury, and D.T. Scadden, *Hematopoietic Stem Cell Niche in Health and Disease.* Annu Rev Pathol, 2016. **11**: p. 555-81.
163. Schepers, K., T.B. Campbell, and E. Passegue, *Normal and leukemic stem cell niches: insights and therapeutic opportunities.* Cell Stem Cell, 2015. **16**(3): p. 254-67.
164. Medyouf, H., *The microenvironment in human myeloid malignancies: emerging concepts and therapeutic implications.* Blood, 2017. **129**(12): p. 1617-1626.
165. Agarwal, P. and R. Bhatia, *Influence of Bone Marrow Microenvironment on Leukemic Stem Cells: Breaking Up an Intimate Relationship.* Adv Cancer Res, 2015. **127**: p. 227-52.
166. Chen, S., et al., *Massive parallel RNA sequencing of highly purified mesenchymal elements in low-risk MDS reveals tissue-context-dependent activation of inflammatory programs.* Leukemia, 2016. **30**(9): p. 1938-42.
167. Zambetti, N.A., et al., *Mesenchymal Inflammation Drives Genotoxic Stress in Hematopoietic Stem Cells and Predicts Disease Evolution in Human Pre-leukemia.* Cell Stem Cell, 2016. **19**(5): p. 613-627.
168. Arranz, L., et al., *Neuropathy of haematopoietic stem cell niche is essential for myeloproliferative neoplasms.* Nature, 2014. **512**(7512): p. 78-81.
169. Hanoun, M., et al., *Acute myelogenous leukemia-induced sympathetic neuropathy promotes malignancy in an altered hematopoietic stem cell niche.* Cell Stem Cell, 2014. **15**(3): p. 365-375.

170. Shih, T.T.F., et al., *Bone marrow angiogenesis magnetic resonance imaging in patients with acute myeloid leukemia: peak enhancement ratio is an independent predictor for overall survival.* Blood, 2009. **113**(14): p. 3161-3167.
171. Hussong, J.W., G.M. Rodgers, and P.J. Shami, *Evidence of increased angiogenesis in patients with acute myeloid leukemia.* Blood, 2000. **95**(1): p. 309-13.
172. Itkin, T., et al., *Distinct bone marrow blood vessels differentially regulate haematopoiesis.* Nature, 2016. **532**(7599): p. 323-8.
173. Sainson, R.C., et al., *TNF primes endothelial cells for angiogenic sprouting by inducing a tip cell phenotype.* Blood, 2008. **111**(10): p. 4997-5007.
174. Aguayo, A., et al., *Angiogenesis in acute and chronic leukemias and myelodysplastic syndromes.* Blood, 2000. **96**(6): p. 2240-5.
175. Passaro, D., et al., *Increased Vascular Permeability in the Bone Marrow Microenvironment Contributes to Disease Progression and Drug Response in Acute Myeloid Leukemia.* Cancer Cell, 2017. **32**(3): p. 324-341 e6.
176. Wu, Z., et al., *Bone marrow fibrosis at diagnosis predicts survival for primary acute myeloid leukemia.* Clin Transl Oncol, 2017. **19**(12): p. 1462-1468.
177. Buesche, G., et al., *Marrow fibrosis predicts early fatal marrow failure in patients with myelodysplastic syndromes.* Leukemia, 2008. **22**(2): p. 313-22.
178. Mori, A., et al., *Acute promyelocytic leukemia with marrow fibrosis at initial presentation: possible involvement of transforming growth factor-beta(1).* Acta Haematol, 2000. **103**(4): p. 220-3.
179. Medyouf, H., et al., *Myelodysplastic cells in patients reprogram mesenchymal stromal cells to establish a transplantable stem cell niche disease unit.* Cell Stem Cell, 2014. **14**(6): p. 824-37.
180. Ye, H., et al., *Leukemic Stem Cells Evade Chemotherapy by Metabolic Adaptation to an Adipose Tissue Niche.* Cell Stem Cell, 2016. **19**(1): p. 23-37.
181. Samudio, I., et al., *Pharmacologic inhibition of fatty acid oxidation sensitizes human leukemia cells to apoptosis induction.* J Clin Invest, 2010. **120**(1): p. 142-56.
182. Cutillas, P.R. and C. Jorgensen, *Biological signalling activity measurements using mass spectrometry.* Biochem J, 2011. **434**(2): p. 189-99.
183. Manning, G., D.B. Whyte, R. Martinez, T. Hunter, and S. Sudarsanam, *The protein kinase complement of the human genome.* Science, 2002. **298**(5600): p. 1912-34.
184. Manning, G., G.D. Plowman, T. Hunter, and S. Sudarsanam, *Evolution of protein kinase signaling from yeast to man.* Trends Biochem Sci, 2002. **27**(10): p. 514-20.
185. Vanhaesebroeck, B., et al., *Synthesis and function of 3-phosphorylated inositol lipids.* Annu Rev Biochem, 2001. **70**: p. 535-602.
186. Katso, R., et al., *Cellular function of phosphoinositide 3-kinases: implications for development, homeostasis, and cancer.* Annu Rev Cell Dev Biol, 2001. **17**: p. 615-75.
187. Schlessinger, J., *New roles for Src kinases in control of cell survival and angiogenesis.* Cell, 2000. **100**(3): p. 293-6.
188. Hunter, T., *Signaling--2000 and beyond.* Cell, 2000. **100**(1): p. 113-27.
189. Zheng, R., et al., *FLT3 ligand causes autocrine signaling in acute myeloid leukemia cells.* Blood, 2004. **103**(1): p. 267-74.
190. Paraguassu-Braga, F.H., R. Borojevic, L.F. Bouzas, M.A. Barcinski, and A. Bonomo, *Bone marrow stroma inhibits proliferation and apoptosis in leukemic cells through gap junction-mediated cell communication.* Cell Death Differ, 2003. **10**(9): p. 1101-8.
191. Reikvam, H., et al., *Connexin expression in human acute myeloid leukemia cells: identification of patient subsets based on protein and global gene expression profiles.* Int J Mol Med, 2015. **35**(3): p. 645-52.
192. Foss, B., K.J. Tronstad, and O. Bruserud, *Connexin-based signaling in acute myelogenous leukemia (AML).* Biochim Biophys Acta, 2010. **1798**(1): p. 1-8.
193. Jin, L., K.J. Hope, Q. Zhai, F. Smadja-Joffe, and J.E. Dick, *Targeting of CD44 eradicates human acute myeloid leukemic stem cells.* Nat Med, 2006. **12**(10): p. 1167-74.

194. Maeda, T., M. Towatari, H. Kosugi, and H. Saito, *Up-regulation of costimulatory/adhesion molecules by histone deacetylase inhibitors in acute myeloid leukemia cells.* Blood, 2000. **96**(12): p. 3847-56.
195. Paietta, E., et al., *Acute myeloid leukaemia expressing the leucocyte integrin CD11b-a new leukaemic syndrome with poor prognosis: result of an ECOG database analysis. Eastern Cooperative Oncology Group.* Br J Haematol, 1998. **100**(2): p. 265-72.
196. Pearson, M.A. and D. Fabbro, *Targeting protein kinases in cancer therapy: a success?* Expert Rev Anticancer Ther, 2004. **4**(6): p. 1113-24.
197. Steelman, L.S., et al., *JAK/STAT, Raf/MEK/ERK, PI3K/Akt and BCR-ABL in cell cycle progression and leukemogenesis.* Leukemia, 2004. **18**(2): p. 189-218.
198. Milella, M., et al., *Therapeutic targeting of the MEK/MAPK signal transduction module in acute myeloid leukemia.* J Clin Invest, 2001. **108**(6): p. 851-9.
199. Boissel, N., et al., *Incidence and prognostic impact of c-Kit, FLT3, and Ras gene mutations in core binding factor acute myeloid leukemia (CBF-AML).* Leukemia, 2006. **20**(6): p. 965-70.
200. Cairoli, R., et al., *Prognostic impact of c-KIT mutations in core binding factor leukemias: an Italian retrospective study.* Blood, 2006. **107**(9): p. 3463-8.
201. Park, S., et al., *Role of the PI3K/AKT and mTOR signaling pathways in acute myeloid leukemia.* Haematologica, 2010. **95**(5): p. 819-28.
202. Lee, H.J., N. Daver, H.M. Kantarjian, S. Verstovsek, and F. Ravandi, *The role of JAK pathway dysregulation in the pathogenesis and treatment of acute myeloid leukemia.* Clin Cancer Res, 2013. **19**(2): p. 327-35.
203. Liu, H., Y. Qiu, L. Xiao, and F. Dong, *Involvement of protein kinase Cepsilon in the negative regulation of Akt activation stimulated by granulocyte colony-stimulating factor.* J Immunol, 2006. **176**(4): p. 2407-13.
204. Zabkiewicz, J., et al., *The PDK1 master kinase is over-expressed in acute myeloid leukemia and promotes PKC-mediated survival of leukemic blasts.* Haematologica, 2014. **99**(5): p. 858-64.
205. Guzman, M.L., et al., *Nuclear factor-kappaB is constitutively activated in primitive human acute myelogenous leukemia cells.* Blood, 2001. **98**(8): p. 2301-7.
206. Pandolfi, A., et al., *PAK1 is a therapeutic target in acute myeloid leukemia and myelodysplastic syndrome.* Blood, 2015. **126**(9): p. 1118-27.
207. Chatterjee, A., et al., *Regulation of Stat5 by FAK and PAK1 in Oncogenic FLT3- and KIT-Driven Leukemogenesis.* Cell Rep, 2014. **9**(4): p. 1333-48.
208. Ferrajoli, A., S. Faderl, F. Ravandi, and Z. Estrov, *The JAK-STAT pathway: a therapeutic target in hematological malignancies.* Curr Cancer Drug Targets, 2006. **6**(8): p. 671-9.
209. Furqan, M., N. Mukhi, B. Lee, and D. Liu, *Dysregulation of JAK-STAT pathway in hematological malignancies and JAK inhibitors for clinical application.* Biomark Res, 2013. **1**(1): p. 5.
210. Constantinescu, S.N., M. Girardot, and C. Pecquet, *Mining for JAK-STAT mutations in cancer.* Trends Biochem Sci, 2008. **33**(3): p. 122-31.
211. Ghoshal Gupta, S., H. Baumann, and M. Wetzler, *Epigenetic regulation of signal transducer and activator of transcription 3 in acute myeloid leukemia.* Leuk Res, 2008. **32**(7): p. 1005-14.
212. Noble, M.E., J.A. Endicott, and L.N. Johnson, *Protein kinase inhibitors: insights into drug design from structure.* Science, 2004. **303**(5665): p. 1800-5.
213. Zhang, J., P.L. Yang, and N.S. Gray, *Targeting cancer with small molecule kinase inhibitors.* Nat Rev Cancer, 2009. **9**(1): p. 28-39.
214. Miller-Jensen, K., K.A. Janes, J.S. Brugge, and D.A. Lauffenburger, *Common effector processing mediates cell-specific responses to stimuli.* Nature, 2007. **448**(7153): p. 604-8.
215. Wilkes, E.H., C. Terfve, J.G. Gribben, J. Saez-Rodriguez, and P.R. Cutillas, *Empirical inference of circuitry and plasticity in a kinase signaling network.* Proc Natl Acad Sci U S A, 2015. **112**(25): p. 7719-24.

216. Creixell, P., et al., *Kinome-wide decoding of network-attacking mutations rewiring cancer signaling.* Cell, 2015. **163**(1): p. 202-17.
217. Adlung, L., et al., *Protein abundance of AKT and ERK pathway components governs cell type-specific regulation of proliferation.* Mol Syst Biol, 2017. **13**(1): p. 904.
218. Iwamoto, N., et al., *Context-specific flow through the MEK/ERK module produces cell- and ligand-specific patterns of ERK single and double phosphorylation.* Sci Signal, 2016. **9**(413): p. ra13.
219. Casado, P., et al., *Proteomic and genomic integration identifies kinase and differentiation determinants of kinase inhibitor sensitivity in leukemia cells.* Leukemia, 2017.
220. Ilic, N., T. Utermark, H.R. Widlund, and T.M. Roberts, *PI3K-targeted therapy can be evaded by gene amplification along the MYC-eukaryotic translation initiation factor 4E (eIF4E) axis.* Proc Natl Acad Sci U S A, 2011. **108**(37): p. E699-708.
221. Jahangiri, A., et al., *Gene expression profile identifies tyrosine kinase c-Met as a targetable mediator of antiangiogenic therapy resistance.* Clin Cancer Res, 2013. **19**(7): p. 1773-83.
222. Girotti, M.R., et al., *Inhibiting EGF receptor or SRC family kinase signaling overcomes BRAF inhibitor resistance in melanoma.* Cancer Discov, 2013. **3**(2): p. 158-67.
223. Yonesaka, K., et al., *Activation of ERBB2 signaling causes resistance to the EGFR-directed therapeutic antibody cetuximab.* Sci Transl Med, 2011. **3**(99): p. 99ra86.
224. Engelman, J.A., et al., *MET amplification leads to gefitinib resistance in lung cancer by activating ERBB3 signaling.* Science, 2007. **316**(5827): p. 1039-43.
225. Engelman, J.A., et al., *Effective use of PI3K and MEK inhibitors to treat mutant Kras G12D and PIK3CA H1047R murine lung cancers.* Nat Med, 2008. **14**(12): p. 1351-6.
226. Wang, C., et al., *Functional crosstalk between AKT/mTOR and Ras/MAPK pathways in hepatocarcinogenesis: implications for the treatment of human liver cancer.* Cell Cycle, 2013. **12**(13): p. 1999-2010.
227. Bensimon, A., A.J. Heck, and R. Aebersold, *Mass spectrometry-based proteomics and network biology.* Annu Rev Biochem, 2012. **81**: p. 379-405.
228. Cazier, J.B. and I. Tomlinson, *General lessons from large-scale studies to identify human cancer predisposition genes.* J Pathol, 2010. **220**(2): p. 255-62.
229. Graves, L.M., J.S. Duncan, M.C. Whittle, and G.L. Johnson, *The dynamic nature of the kinome.* Biochem J, 2013. **450**(1): p. 1-8.
230. Logue, J.S. and D.K. Morrison, *Complexity in the signaling network: insights from the use of targeted inhibitors in cancer therapy.* Genes Dev, 2012. **26**(7): p. 641-50.
231. Kreeger, P.K. and D.A. Lauffenburger, *Cancer systems biology: a network modeling perspective.* Carcinogenesis, 2010. **31**(1): p. 2-8.
232. Dermit, M., A. Dokal, and P.R. Cutillas, *Approaches to identify kinase dependencies in cancer signalling networks.* FEBS Lett, 2017.
233. Alcolea, M.P., P. Casado, J.C. Rodriguez-Prados, B. Vanhaesebroeck, and P.R. Cutillas, *Phosphoproteomic analysis of leukemia cells under basal and drug-treated conditions identifies markers of kinase pathway activation and mechanisms of resistance.* Mol Cell Proteomics, 2012. **11**(8): p. 453-66.
234. Rajeeve, V., W. Pearce, M. Cascante, B. Vanhaesebroeck, and P.R. Cutillas, *Polyamine production is downstream and upstream of oncogenic PI3K signalling and contributes to tumour cell growth.* Biochem J, 2013. **450**(3): p. 619-28.
235. Nadler, W.M., et al., *MALDI versus ESI: The Impact of the Ion Source on Peptide Identification.* J Proteome Res, 2017. **16**(3): p. 1207-1215.
236. Walch, A., S. Rauser, S.O. Deininger, and H. Hofler, *MALDI imaging mass spectrometry for direct tissue analysis: a new frontier for molecular histology.* Histochem Cell Biol, 2008. **130**(3): p. 421-34.
237. Rajeeve, V., I. Vendrell, E. Wilkes, N. Torbett, and P.R. Cutillas, *Cross-species Proteomics Reveals Specific Modulation of Signaling in Cancer and Stromal Cells by Phosphoinositide 3-kinase (PI3K) Inhibitors.* Molecular & Cellular Proteomics, 2014. **13**(6): p. 1457-1470.

238. Han, C.L., et al., *An informatics-assisted label-free approach for personalized tissue membrane proteomics: case study on colorectal cancer.* Mol Cell Proteomics, 2011. **10**(4): p. M110 003087.
239. Moradian, A., A. Kalli, M.J. Sweredoski, and S. Hess, *The top-down, middle-down, and bottom-up mass spectrometry approaches for characterization of histone variants and their post-translational modifications.* Proteomics, 2014. **14**(4-5): p. 489-97.
240. Giansanti, P., L. Tsiatsiani, T.Y. Low, and A.J. Heck, *Six alternative proteases for mass spectrometry-based proteomics beyond trypsin.* Nat Protoc, 2016. **11**(5): p. 993-1006.
241. Canas, B., C. Pineiro, E. Calvo, D. Lopez-Ferrer, and J.M. Gallardo, *Trends in sample preparation for classical and second generation proteomics.* J Chromatogr A, 2007. **1153**(1-2): p. 235-58.
242. Wisniewski, J.R., A. Zougman, and M. Mann, *Combination of FASP and StageTip-based fractionation allows in-depth analysis of the hippocampal membrane proteome.* J Proteome Res, 2009. **8**(12): p. 5674-8.
243. Rodriguez, J., N. Gupta, R.D. Smith, and P.A. Pevzner, *Does trypsin cut before proline?* J Proteome Res, 2008. **7**(1): p. 300-5.
244. Garcia, B.A., et al., *Chemical derivatization of histones for facilitated analysis by mass spectrometry.* Nat Protoc, 2007. **2**(4): p. 933-8.
245. Hyung, S.J. and B.T. Ruotolo, *Integrating mass spectrometry of intact protein complexes into structural proteomics.* Proteomics, 2012. **12**(10): p. 1547-64.
246. Wu, C., et al., *A protease for 'middle-down' proteomics.* Nat Methods, 2012. **9**(8): p. 822-4.
247. Bilbao, A., et al., *Processing strategies and software solutions for data-independent acquisition in mass spectrometry.* Proteomics, 2015. **15**(5-6): p. 964-80.
248. Rost, H.L., et al., *OpenSWATH enables automated, targeted analysis of data-independent acquisition MS data.* Nat Biotechnol, 2014. **32**(3): p. 219-23.
249. Gillet, L.C., et al., *Targeted data extraction of the MS/MS spectra generated by data-independent acquisition: a new concept for consistent and accurate proteome analysis.* Mol Cell Proteomics, 2012. **11**(6): p. O111 016717.
250. Zhang, J., et al., *PEAKS DB: de novo sequencing assisted database search for sensitive and accurate peptide identification.* Mol Cell Proteomics, 2012. **11**(4): p. M111 010587.
251. Perkins, D.N., D.J. Pappin, D.M. Creasy, and J.S. Cottrell, *Probability-based protein identification by searching sequence databases using mass spectrometry data.* Electrophoresis, 1999. **20**(18): p. 3551-67.
252. Eng, J.K., A.L. McCormack, and J.R. Yates, *An approach to correlate tandem mass spectral data of peptides with amino acid sequences in a protein database.* J Am Soc Mass Spectrom, 1994. **5**(11): p. 976-89.
253. Craig, R. and R.C. Beavis, *TANDEM: matching proteins with tandem mass spectra.* Bioinformatics, 2004. **20**(9): p. 1466-7.
254. Cox, J., et al., *Andromeda: a peptide search engine integrated into the MaxQuant environment.* J Proteome Res, 2011. **10**(4): p. 1794-805.
255. Kim, M.S., et al., *A draft map of the human proteome.* Nature, 2014. **509**(7502): p. 575-81.
256. Wilhelm, M., et al., *Mass-spectrometry-based draft of the human proteome.* Nature, 2014. **509**(7502): p. 582-7.
257. Gygi, S.P., et al., *Quantitative analysis of complex protein mixtures using isotope-coded affinity tags.* Nat Biotechnol, 1999. **17**(10): p. 994-9.
258. Thompson, A., et al., *Tandem mass tags: a novel quantification strategy for comparative analysis of complex protein mixtures by MS/MS.* Anal Chem, 2003. **75**(8): p. 1895-904.
259. Ross, P.L., et al., *Multiplexed protein quantitation in Saccharomyces cerevisiae using amine-reactive isobaric tagging reagents.* Mol Cell Proteomics, 2004. **3**(12): p. 1154-69.
260. Sandberg, A., R.M. Branca, J. Lehtio, and J. Forshed, *Quantitative accuracy in mass spectrometry based proteomics of complex samples: the impact of labeling and precursor interference.* J Proteomics, 2014. **96**: p. 133-44.

261. Ong, S.E., et al., *Stable isotope labeling by amino acids in cell culture, SILAC, as a simple and accurate approach to expression proteomics.* Mol Cell Proteomics, 2002. **1**(5): p. 376-86.
262. Kruger, M., et al., *SILAC mouse for quantitative proteomics uncovers kindlin-3 as an essential factor for red blood cell function.* Cell, 2008. **134**(2): p. 353-64.
263. Bantscheff, M., S. Lemeer, M.M. Savitski, and B. Kuster, *Quantitative mass spectrometry in proteomics: critical review update from 2007 to the present.* Anal Bioanal Chem, 2012. **404**(4): p. 939-65.
264. Strassberger, V., T. Fugmann, D. Neri, and C. Roesli, *Chemical proteomic and bioinformatic strategies for the identification and quantification of vascular antigens in cancer.* J Proteomics, 2010. **73**(10): p. 1954-73.
265. Ishihama, Y., et al., *Exponentially modified protein abundance index (emPAI) for estimation of absolute protein amount in proteomics by the number of sequenced peptides per protein.* Mol Cell Proteomics, 2005. **4**(9): p. 1265-72.
266. Lu, P., C. Vogel, R. Wang, X. Yao, and E.M. Marcotte, *Absolute protein expression profiling estimates the relative contributions of transcriptional and translational regulation.* Nat Biotechnol, 2007. **25**(1): p. 117-24.
267. Yang, F., et al., *Applying a targeted label-free approach using LC-MS AMT tags to evaluate changes in protein phosphorylation following phosphatase inhibition.* J Proteome Res, 2007. **6**(11): p. 4489-97.
268. Picotti, P. and R. Aebersold, *Selected reaction monitoring-based proteomics: workflows, potential, pitfalls and future directions.* Nat Methods, 2012. **9**(6): p. 555-66.
269. Cutillas, P.R. and B. Vanhaesebroeck, *Quantitative profile of five murine core proteomes using label-free functional proteomics.* Mol Cell Proteomics, 2007. **6**(9): p. 1560-73.
270. Montoya, A., L. Beltran, P. Casado, J.C. Rodriguez-Prados, and P.R. Cutillas, *Characterization of a TiO(2) enrichment method for label-free quantitative phosphoproteomics.* Methods, 2011. **54**(4): p. 370-8.
271. Casado, P., et al., *Kinase-substrate enrichment analysis provides insights into the heterogeneity of signaling pathway activation in leukemia cells.* Sci Signal, 2013. **6**(268): p. rs6.
272. Terfve, C.D., E.H. Wilkes, P. Casado, P.R. Cutillas, and J. Saez-Rodriguez, *Large-scale models of signal propagation in human cells derived from discovery phosphoproteomic data.* Nat Commun, 2015. **6**: p. 8033.
273. Sciacovelli, M., et al., *Fumarate is an epigenetic modifier that elicits epithelial-to-mesenchymal transition.* Nature, 2016. **537**(7621): p. 544-547.
274. Tjalsma, H., A. Bolhuis, J.D. Jongbloed, S. Bron, and J.M. van Dijl, *Signal peptide-dependent protein transport in Bacillus subtilis: a genome-based survey of the secretome.* Microbiol Mol Biol Rev, 2000. **64**(3): p. 515-47.
275. Mukherjee, P. and S. Mani, *Methodologies to decipher the cell secretome.* Biochim Biophys Acta, 2013. **1834**(11): p. 2226-32.
276. Zwickl, H., et al., *A novel technique to specifically analyze the secretome of cells and tissues.* Electrophoresis, 2005. **26**(14): p. 2779-85.
277. Lee, S.J., B.D. Kim, and J.K. Rose, *Identification of eukaryotic secreted and cell surface proteins using the yeast secretion trap screen.* Nat Protoc, 2006. **1**(5): p. 2439-47.
278. Palka, G., et al., *[Cytogenetics in bone marrow transplantations. I. Bone marrow aplasia].* Boll Soc Ital Biol Sper, 1981. **57**(1): p. 20-6.
279. Perera, C.N., H.S. Spalding, S.I. Mohammed, and I.G. Camarillo, *Identification of proteins secreted from leptin stimulated MCF-7 breast cancer cells: a dual proteomic approach.* Exp Biol Med (Maywood), 2008. **233**(6): p. 708-20.
280. Buhr, N., et al., *Proteome analysis of the culture environment supporting undifferentiated mouse embryonic stem and germ cell growth.* Electrophoresis, 2007. **28**(10): p. 1615-23.

281. Volmer, M.W., et al., *Differential proteome analysis of conditioned media to detect Smad4 regulated secreted biomarkers in colon cancer.* Proteomics, 2005. **5**(10): p. 2587-601.
282. Prowse, A.B., et al., *A proteome analysis of conditioned media from human neonatal fibroblasts used in the maintenance of human embryonic stem cells.* Proteomics, 2005. **5**(4): p. 978-89.
283. Lim, J.W. and A. Bodnar, *Proteome analysis of conditioned medium from mouse embryonic fibroblast feeder layers which support the growth of human embryonic stem cells.* Proteomics, 2002. **2**(9): p. 1187-203.
284. Mann, M., *Functional and quantitative proteomics using SILAC.* Nat Rev Mol Cell Biol, 2006. **7**(12): p. 952-8.
285. Wiese, S., K.A. Reidegeld, H.E. Meyer, and B. Warscheid, *Protein labeling by iTRAQ: a new tool for quantitative mass spectrometry in proteome research.* Proteomics, 2007. **7**(3): p. 340-50.
286. Khwaja, F.W., et al., *Proteomic identification of the wt-p53-regulated tumor cell secretome.* Oncogene, 2006. **25**(58): p. 7650-61.
287. Lietzen, N., et al., *Quantitative subcellular proteome and secretome profiling of influenza A virus-infected human primary macrophages.* PLoS Pathog, 2011. **7**(5): p. e1001340.
288. Gronborg, M., et al., *Biomarker discovery from pancreatic cancer secretome using a differential proteomic approach.* Mol Cell Proteomics, 2006. **5**(1): p. 157-71.
289. Kashyap, M.K., et al., *SILAC-based quantitative proteomic approach to identify potential biomarkers from the esophageal squamous cell carcinoma secretome.* Cancer Biol Ther, 2010. **10**(8): p. 796-810.
290. Maier, T., M. Guell, and L. Serrano, *Correlation of mRNA and protein in complex biological samples.* FEBS Lett, 2009. **583**(24): p. 3966-73.
291. Greenbaum, D., C. Colangelo, K. Williams, and M. Gerstein, *Comparing protein abundance and mRNA expression levels on a genomic scale.* Genome Biol, 2003. **4**(9): p. 117.
292. Speers, A.E. and B.F. Cravatt, *Profiling enzyme activities in vivo using click chemistry methods.* Chem Biol, 2004. **11**(4): p. 535-46.
293. Long, X., Y. Lin, S. Ortiz-Vega, K. Yonezawa, and J. Avruch, *Rheb binds and regulates the mTOR kinase.* Curr Biol, 2005. **15**(8): p. 702-13.
294. Olsen, J.V., et al., *Global, in vivo, and site-specific phosphorylation dynamics in signaling networks.* Cell, 2006. **127**(3): p. 635-48.
295. Mischnik, M., et al., *IKAP: A heuristic framework for inference of kinase activities from Phosphoproteomics data.* Bioinformatics, 2016. **32**(3): p. 424-31.
296. Rowland, M.A., B. Harrison, and E.J. Deeds, *Phosphatase specificity and pathway insulation in signaling networks.* Biophys J, 2015. **108**(4): p. 986-96.
297. Lin, J., Z. Xie, H. Zhu, and J. Qian, *Understanding protein phosphorylation on a systems level.* Brief Funct Genomics, 2010. **9**(1): p. 32-42.
298. Thingholm, T.E., O.N. Jensen, and M.R. Larsen, *Analytical strategies for phosphoproteomics.* Proteomics, 2009. **9**(6): p. 1451-68.
299. Gronborg, M., et al., *A mass spectrometry-based proteomic approach for identification of serine/threonine-phosphorylated proteins by enrichment with phospho-specific antibodies: identification of a novel protein, Frigg, as a protein kinase A substrate.* Mol Cell Proteomics, 2002. **1**(7): p. 517-27.
300. Blagoev, B., S.E. Ong, I. Kratchmarova, and M. Mann, *Temporal analysis of phosphotyrosine-dependent signaling networks by quantitative proteomics.* Nat Biotechnol, 2004. **22**(9): p. 1139-45.
301. Rush, J., et al., *Immunoaffinity profiling of tyrosine phosphorylation in cancer cells.* Nat Biotechnol, 2005. **23**(1): p. 94-101.
302. Beausoleil, S.A., et al., *Large-scale characterization of HeLa cell nuclear phosphoproteins.* Proc Natl Acad Sci U S A, 2004. **101**(33): p. 12130-5.

303. Han, G., et al., *Large-scale phosphoproteome analysis of human liver tissue by enrichment and fractionation of phosphopeptides with strong anion exchange chromatography.* Proteomics, 2008. **8**(7): p. 1346-61.
304. Nie, S., et al., *Comprehensive profiling of phosphopeptides based on anion exchange followed by flow-through enrichment with titanium dioxide (AFET).* J Proteome Res, 2010. **9**(9): p. 4585-94.
305. Zarei, M., A. Sprenger, M. Rackiewicz, and J. Dengjel, *Fast and easy phosphopeptide fractionation by combinatorial ERLIC-SCX solid-phase extraction for in-depth phosphoproteome analysis.* Nat Protoc, 2016. **11**(1): p. 37-45.
306. Lai, A.C., C.F. Tsai, C.C. Hsu, Y.N. Sun, and Y.J. Chen, *Complementary Fe(3+)- and Ti(4+)-immobilized metal ion affinity chromatography for purification of acidic and basic phosphopeptides.* Rapid Commun Mass Spectrom, 2012. **26**(18): p. 2186-94.
307. Villen, J. and S.P. Gygi, *The SCX/IMAC enrichment approach for global phosphorylation analysis by mass spectrometry.* Nat Protoc, 2008. **3**(10): p. 1630-8.
308. Pinkse, M.W., P.M. Uitto, M.J. Hilhorst, B. Ooms, and A.J. Heck, *Selective isolation at the femtomole level of phosphopeptides from proteolytic digests using 2D-NanoLC-ESI-MS/MS and titanium oxide precolumns.* Anal Chem, 2004. **76**(14): p. 3935-43.
309. Larsen, M.R., T.E. Thingholm, O.N. Jensen, P. Roepstorff, and T.J. Jorgensen, *Highly selective enrichment of phosphorylated peptides from peptide mixtures using titanium dioxide microcolumns.* Mol Cell Proteomics, 2005. **4**(7): p. 873-86.
310. Aryal, U.K. and A.R. Ross, *Enrichment and analysis of phosphopeptides under different experimental conditions using titanium dioxide affinity chromatography and mass spectrometry.* Rapid Commun Mass Spectrom, 2010. **24**(2): p. 219-31.
311. Zarei, M., A. Sprenger, F. Metzger, C. Gretzmeier, and J. Dengjel, *Comparison of ERLIC-TiO2, HILIC-TiO2, and SCX-TiO2 for global phosphoproteomics approaches.* J Proteome Res, 2011. **10**(8): p. 3474-83.
312. Gedik, N., et al., *Proteomics/phosphoproteomics of left ventricular biopsies from patients with surgical coronary revascularization and pigs with coronary occlusion/reperfusion: remote ischemic preconditioning.* Sci Rep, 2017. **7**(1): p. 7629.
313. Herranz, N., et al., *mTOR regulates MAPKAPK2 translation to control the senescence-associated secretory phenotype.* Nat Cell Biol, 2015. **17**(9): p. 1205-17.
314. Olsen, J.V., et al., *Higher-energy C-trap dissociation for peptide modification analysis.* Nat Methods, 2007. **4**(9): p. 709-12.
315. Hart-Smith, G., *A review of electron-capture and electron-transfer dissociation tandem mass spectrometry in polymer chemistry.* Anal Chim Acta, 2014. **808**: p. 44-55.
316. Delom, F. and E. Chevet, *Phosphoprotein analysis: from proteins to proteomes.* Proteome Sci, 2006. **4**: p. 15.
317. McAllister, F.E., et al., *Mass spectrometry based method to increase throughput for kinome analyses using ATP probes.* Anal Chem, 2013. **85**(9): p. 4666-74.
318. Hornbeck, P.V., et al., *PhosphoSitePlus, 2014: mutations, PTMs and recalibrations.* Nucleic Acids Res, 2015. **43**(Database issue): p. D512-20.
319. Hernandez-Armenta, C., D. Ochoa, E. Goncalves, J. Saez-Rodriguez, and P. Beltrao, *Benchmarking substrate-based kinase activity inference using phosphoproteomic data.* Bioinformatics, 2017. **33**(12): p. 6.
320. Itoh, K., et al., *Reproducible establishment of hemopoietic supportive stromal cell lines from murine bone marrow.* Exp Hematol, 1989. **17**(2): p. 145-53.
321. Roecklein, B.A. and B. Torok-Storb, *Functionally distinct human marrow stromal cell lines immortalized by transduction with the human papilloma virus E6/E7 genes.* Blood, 1995. **85**(4): p. 997-1005.
322. Hirose, M., et al., *A novel monocytoid cultured cell line, P31/Fujioka, derived from acute monoblastic leukemia.* Gan, 1982. **73**(5): p. 735-41.
323. Lange, B., et al., *Growth factor requirements of childhood acute leukemia: establishment of GM-CSF-dependent cell lines.* Blood, 1987. **70**(1): p. 192-9.

324. Collins, S.J., *The HL-60 promyelocytic leukemia cell line: proliferation, differentiation, and cellular oncogene expression.* Blood, 1987. **70**(5): p. 1233-44.
325. Kakuda, H., et al., *A novel human leukaemic cell line, CTS, has a t(6;11) chromosomal translocation and characteristics of pluripotent stem cells.* Br J Haematol, 1996. **95**(2): p. 306-18.
326. Stevens, J., et al., *Serum selenium concentration at diagnosis and outcome in patients with haematological malignancies.* Br J Haematol, 2011. **154**(4): p. 448-56.
327. Hornbeck, P.V., I. Chabra, J.M. Kornhauser, E. Skrzypek, and B. Zhang, *PhosphoSite: A bioinformatics resource dedicated to physiological protein phosphorylation.* Proteomics, 2004. **4**(6): p. 1551-61.
328. Dinkel, H., et al., *Phospho.ELM: a database of phosphorylation sites--update 2011.* Nucleic Acids Res, 2011. **39**(Database issue): p. D261-7.
329. Yang, C.Y., et al., *PhosphoPOINT: a comprehensive human kinase interactome and phospho-protein database.* Bioinformatics, 2008. **24**(16): p. i14-20.
330. Kim, S.Y. and D.J. Volsky, *PAGE: parametric analysis of gene set enrichment.* BMC Bioinformatics, 2005. **6**: p. 144.
331. Payne, C.M., B. Greenberg, D. Cromey, and L. Woo, *Morphological evidence of an altered bone marrow microenvironment in patients with acute nonlymphoblastic leukemia and myelodysplastic disorders.* Exp Hematol, 1987. **15**(2): p. 143-53.
332. Barcellos-de-Souza, P., V. Gori, F. Bambi, and P. Chiarugi, *Tumor microenvironment: bone marrow-mesenchymal stem cells as key players.* Biochim Biophys Acta, 2013. **1836**(2): p. 321-35.
333. Gotou, A., *[Role of cytokines and SDF-1 in the regulation of hematopoietic cell localization in microenvironment].* Rinsho Ketsueki, 1999. **40**(4): p. 272-4.
334. Wei, L., et al., *[Effects of anti-CXCR4 monoclonal antibody on adhesion and proliferation of human acute myelocytic leukemia cell line HL-60].* Ai Zheng, 2004. **23**(11): p. 1273-7.
335. Jordan, C.T. and M.L. Guzman, *Mechanisms controlling pathogenesis and survival of leukemic stem cells.* Oncogene, 2004. **23**(43): p. 7178-87.
336. Zhang, M. and J.M. Rosen, *Stem cells in the etiology and treatment of cancer.* Curr Opin Genet Dev, 2006. **16**(1): p. 60-4.
337. Colmone, A. and D.A. Sipkins, *Beyond angiogenesis: the role of endothelium in the bone marrow vascular niche.* Transl Res, 2008. **151**(1): p. 1-9.
338. Ries, C., F. Loher, C. Zang, M.G. Ismair, and P.E. Petrides, *Matrix metalloproteinase production by bone marrow mononuclear cells from normal individuals and patients with acute and chronic myeloid leukemia or myelodysplastic syndromes.* Clin Cancer Res, 1999. **5**(5): p. 1115-24.
339. Hatfield, K.J., H. Reikvam, and O. Bruserud, *The crosstalk between the matrix metalloprotease system and the chemokine network in acute myeloid leukemia.* Curr Med Chem, 2010. **17**(36): p. 4448-61.
340. Chaudhary, A.K., S. Chaudhary, K. Ghosh, C. Shanmukaiah, and A.H. Nadkarni, *Secretion and Expression of Matrix Metalloproteinase-2 and 9 from Bone Marrow Mononuclear Cells in Myelodysplastic Syndrome and Acute Myeloid Leukemia.* Asian Pac J Cancer Prev, 2016. **17**(3): p. 1519-29.
341. Zeng, Z., et al., *Inhibition of CXCR4 with the novel RCP168 peptide overcomes stroma-mediated chemoresistance in chronic and acute leukemias.* Mol Cancer Ther, 2006. **5**(12): p. 3113-21.
342. Beider, K., et al., *CXCR4 antagonist 4F-benzoyl-TN14003 inhibits leukemia and multiple myeloma tumor growth.* Exp Hematol, 2011. **39**(3): p. 282-92.
343. Sison, E.A. and P. Brown, *The bone marrow microenvironment and leukemia: biology and therapeutic targeting.* Expert Rev Hematol, 2011. **4**(3): p. 271-83.
344. Zaitseva, L., et al., *Ibrutinib inhibits SDF1/CXCR4 mediated migration in AML.* Oncotarget, 2014. **5**(20): p. 9930-8.
345. Litwin, C., et al., *Role of the microenvironment in promoting angiogenesis in acute myeloid leukemia.* Am J Hematol, 2002. **70**(1): p. 22-30.

346. Konopleva, M., et al., *Stromal cells prevent apoptosis of AML cells by up-regulation of anti-apoptotic proteins.* Leukemia, 2002. **16**(9): p. 1713-24.
347. Shimakura, Y., et al., *Murine stromal cell line HESS-5 maintains reconstituting ability of Ex vivo-generated hematopoietic stem cells from human bone marrow and cytokine-mobilized peripheral blood.* Stem Cells, 2000. **18**(3): p. 183-9.
348. Spooncer, E., C.M. Heyworth, A. Dunn, and T.M. Dexter, *Self-renewal and differentiation of interleukin-3-dependent multipotent stem cells are modulated by stromal cells and serum factors.* Differentiation, 1986. **31**(2): p. 111-8.
349. Nishi, N., et al., *Granulocyte-colony stimulating factor and stem cell factor are the crucial factors in long-term culture of human primitive hematopoietic cells supported by a murine stromal cell line.* Exp Hematol, 1996. **24**(11): p. 1312-21.
350. Nishi, N., et al., *In vitro long-term culture of human primitive hematopoietic cells supported by murine stromal cell line MS-5.* Leukemia, 1997. **11 Suppl 3**: p. 468-73.
351. Garrido, S.M., F.R. Appelbaum, C.L. Willman, and D.E. Banker, *Acute myeloid leukemia cells are protected from spontaneous and drug-induced apoptosis by direct contact with a human bone marrow stromal cell line (HS-5).* Exp Hematol, 2001. **29**(4): p. 448-57.
352. Sontakke, P., M. Carretta, M. Capala, H. Schepers, and J.J. Schuringa, *Ex vivo assays to study self-renewal, long-term expansion, and leukemic transformation of genetically modified human hematopoietic and patient-derived leukemic stem cells.* Methods Mol Biol, 2014. **1185**: p. 195-210.
353. Schuringa, J.J. and H. Schepers, *Ex vivo assays to study self-renewal and long-term expansion of genetically modified primary human acute myeloid leukemia stem cells.* Methods Mol Biol, 2009. **538**: p. 287-300.
354. Griessinger, E., et al., *A niche-like culture system allowing the maintenance of primary human acute myeloid leukemia-initiating cells: a new tool to decipher their chemoresistance and self-renewal mechanisms.* Stem Cells Transl Med, 2014. **3**(4): p. 520-9.
355. Vellenga, E., et al., *The effects of GM-CSF and G-CSF in promoting growth of clonogenic cells in acute myeloblastic leukemia.* Blood, 1987. **69**(6): p. 1771-6.
356. Zhang, C.C. and H.F. Lodish, *Cytokines regulating hematopoietic stem cell function.* Curr Opin Hematol, 2008. **15**(4): p. 307-11.
357. Berthier, R., et al., *The MS-5 murine stromal cell line and hematopoietic growth factors synergize to support the megakaryocytic differentiation of embryonic stem cells.* Exp Hematol, 1997. **25**(6): p. 481-90.
358. Nishihara, M., et al., *A combination of stem cell factor and granulocyte colony-stimulating factor enhances the growth of human progenitor B cells supported by murine stromal cell line MS-5.* Eur J Immunol, 1998. **28**(3): p. 855-64.
359. Hattersley, G. and T.J. Chambers, *Effects of interleukin 3 and of granulocyte-macrophage and macrophage colony stimulating factors on osteoclast differentiation from mouse hemopoietic tissue.* J Cell Physiol, 1990. **142**(1): p. 201-9.
360. Kim, J.A., et al., *Microenvironmental remodeling as a parameter and prognostic factor of heterogeneous leukemogenesis in acute myelogenous leukemia.* Cancer Res, 2015. **75**(11): p. 2222-31.
361. Boyd, A.L., et al., *Niche displacement of human leukemic stem cells uniquely allows their competitive replacement with healthy HSPCs.* J Exp Med, 2014. **211**(10): p. 1925-35.
362. Koller, M.R., M. Oxender, T.C. Jensen, K.L. Goltry, and A.K. Smith, *Direct contact between CD34+lin- cells and stroma induces a soluble activity that specifically increases primitive hematopoietic cell production.* Exp Hematol, 1999. **27**(4): p. 734-41.
363. Bendall, L.J., A. Daniel, K. Kortlepel, and D.J. Gottlieb, *Bone marrow adherent layers inhibit apoptosis of acute myeloid leukemia cells.* Exp Hematol, 1994. **22**(13): p. 1252-60.
364. Zhou, B., et al., *A novel function for the haemopoietic supportive murine bone marrow MS-5 mesenchymal stromal cell line in promoting human vasculogenesis and angiogenesis.* Br J Haematol, 2012. **157**(3): p. 299-311.

365. Quail, D.F. and J.A. Joyce, *Microenvironmental regulation of tumor progression and metastasis.* Nat Med, 2013. **19**(11): p. 1423-37.
366. Pranjol, M.Z., N. Gutowski, M. Hannemann, and J. Whatmore, *The Potential Role of the Proteases Cathepsin D and Cathepsin L in the Progression and Metastasis of Epithelial Ovarian Cancer.* Biomolecules, 2015. **5**(4): p. 3260-79.
367. Podgorski, I. and B.F. Sloane, *Cathepsin B and its role(s) in cancer progression.* Biochem Soc Symp, 2003(70): p. 263-76.
368. Sloane, B.F., *Cathepsin B and cystatins: evidence for a role in cancer progression.* Semin Cancer Biol, 1990. **1**(2): p. 137-52.
369. Riether, C., C.M. Schurch, and A.F. Ochsenbein, *Regulation of hematopoietic and leukemic stem cells by the immune system.* Cell Death Differ, 2015. **22**(2): p. 187-98.
370. Belkacemi, L. and S.X. Zhang, *Anti-tumor effects of pigment epithelium-derived factor (PEDF): implication for cancer therapy. A mini-review.* J Exp Clin Cancer Res, 2016. **35**: p. 4.
371. Bresnick, A.R., D.J. Weber, and D.B. Zimmer, *S100 proteins in cancer.* Nat Rev Cancer, 2015. **15**(2): p. 96-109.
372. Sipkins, D.A., *Rendering the leukemia cell susceptible to attack.* N Engl J Med, 2009. **361**(13): p. 1307-9.
373. Maeda, Y., et al., *Myeloid Differentiation Factor 88 Signaling in Bone Marrow-Derived Cells Promotes Gastric Tumorigenesis by Generation of Inflammatory Microenvironment.* Cancer Prev Res (Phila), 2016. **9**(3): p. 253-63.
374. Pardali, K., M. Kowanetz, C.H. Heldin, and A. Moustakas, *Smad pathway-specific transcriptional regulation of the cell cycle inhibitor p21(WAF1/Cip1).* J Cell Physiol, 2005. **204**(1): p. 260-72.
375. Alachkar, H., et al., *SPARC promotes leukemic cell growth and predicts acute myeloid leukemia outcome.* J Clin Invest, 2014. **124**(4): p. 1512-24.
376. Skonier, J., et al., *beta ig-h3: a transforming growth factor-beta-responsive gene encoding a secreted protein that inhibits cell attachment in vitro and suppresses the growth of CHO cells in nude mice.* DNA Cell Biol, 1994. **13**(6): p. 571-84.
377. Wan, F., et al., *Knockdown of Latent Transforming Growth Factor-beta (TGF-beta)-Binding Protein 2 (LTBP2) Inhibits Invasion and Tumorigenesis in Thyroid Carcinoma Cells.* Oncol Res, 2017. **25**(4): p. 503-510.
378. Sanchez-Correa, B., et al., *Cytokine profiles in acute myeloid leukemia patients at diagnosis: survival is inversely correlated with IL-6 and directly correlated with IL-10 levels.* Cytokine, 2013. **61**(3): p. 885-91.
379. Liersch, R., et al., *Osteopontin is a prognostic factor for survival of acute myeloid leukemia patients.* Blood, 2012. **119**(22): p. 5215-20.
380. McCallum, L., et al., *A novel mechanism for BCR-ABL action: stimulated secretion of CCN3 is involved in growth and differentiation regulation.* Blood, 2006. **108**(5): p. 1716-23.
381. Suresh, S., et al., *The matricellular protein CCN3 regulates NOTCH1 signalling in chronic myeloid leukaemia.* J Pathol, 2013. **231**(3): p. 378-87.
382. Gupta, R., D. Hong, F. Iborra, S. Sarno, and T. Enver, *NOV (CCN3) functions as a regulator of human hematopoietic stem or progenitor cells.* Science, 2007. **316**(5824): p. 590-3.
383. Si, T., et al., *High expression of INHBA is an adverse prognostic factor for de novo acute myeloid leukemia.* Leuk Lymphoma, 2018. **59**(1): p. 114-120.
384. Beyazit, Y., et al., *Overexpression of the local bone marrow renin-angiotensin system in acute myeloid leukemia.* J Natl Med Assoc, 2007. **99**(1): p. 57-63.
385. Alam, M.T., et al., *Suprabasin as a novel tumor endothelial cell marker.* Cancer Sci, 2014. **105**(12): p. 1533-40.
386. Formolo, C.A., et al., *Secretome signature of invasive glioblastoma multiforme.* J Proteome Res, 2011. **10**(7): p. 3149-59.
387. Shao, C., et al., *Suprabasin is hypomethylated and associated with metastasis in salivary adenoid cystic carcinoma.* PLoS One, 2012. **7**(11): p. e48582.

388. Zhu, J., et al., *Overexpression of Suprabasin is Associated with Proliferation and Tumorigenicity of Esophageal Squamous Cell Carcinoma.* Sci Rep, 2016. **6**: p. 21549.
389. Boye, K. and G.M. Maelandsmo, *S100A4 and metastasis: a small actor playing many roles.* Am J Pathol, 2010. **176**(2): p. 528-35.
390. Sakai, K., S. Aoki, and K. Matsumoto, *Hepatocyte growth factor and Met in drug discovery.* J Biochem, 2015. **157**(5): p. 271-84.
391. Chase, A., et al., *Imatinib sensitivity as a consequence of a CSF1R-Y571D mutation and CSF1/CSF1R signaling abnormalities in the cell line GDM1.* Leukemia, 2009. **23**(2): p. 358-64.
392. Kentsis, A., et al., *Autocrine activation of the MET receptor tyrosine kinase in acute myeloid leukemia.* Nat Med, 2012. **18**(7): p. 1118-22.
393. Bennewith, K.L., et al., *The role of tumor cell-derived connective tissue growth factor (CTGF/CCN2) in pancreatic tumor growth.* Cancer Res, 2009. **69**(3): p. 775-84.
394. Lu, H., et al., *Targeting connective tissue growth factor (CTGF) in acute lymphoblastic leukemia preclinical models: anti-CTGF monoclonal antibody attenuates leukemia growth.* Ann Hematol, 2014. **93**(3): p. 485-492.
395. Ge, G. and D.S. Greenspan, *BMP1 controls TGFbeta1 activation via cleavage of latent TGFbeta-binding protein.* J Cell Biol, 2006. **175**(1): p. 111-20.
396. Malecaze, F., et al., *Upregulation of bone morphogenetic protein-1/mammalian tolloid and procollagen C-proteinase enhancer-1 in corneal scarring.* Invest Ophthalmol Vis Sci, 2014. **55**(10): p. 6712-21.
397. Bruno, E., S.D. Luikart, M.W. Long, and R. Hoffman, *Marrow-derived heparan sulfate proteoglycan mediates the adhesion of hematopoietic progenitor cells to cytokines.* Exp Hematol, 1995. **23**(11): p. 1212-7.
398. Salem, D., S. Abd El-Aziz, and M. Salah-Eldin, *Clinical Relevance of Thrombospondin Receptor (Cd36) Expression in Egyptian De Novo Adult Acute Myeloid Leukemia.* Cytometry Part B-Clinical Cytometry, 2012. **82b**(5): p. 338-339.
399. Moore, B.W., *A soluble protein characteristic of the nervous system.* Biochem Biophys Res Commun, 1965. **19**(6): p. 739-44.
400. Donato, R., et al., *Functions of S100 proteins.* Curr Mol Med, 2013. **13**(1): p. 24-57.
401. Yap, K.L., J.B. Ames, M.B. Swindells, and M. Ikura, *Diversity of conformational states and changes within the EF-hand protein superfamily.* Proteins, 1999. **37**(3): p. 499-507.
402. Leclerc, E. and C.W. Heizmann, *The importance of Ca2+/Zn2+ signaling S100 proteins and RAGE in translational medicine.* Front Biosci (Schol Ed), 2011. **3**: p. 1232-62.
403. Donato, R., *RAGE: a single receptor for several ligands and different cellular responses: the case of certain S100 proteins.* Curr Mol Med, 2007. **7**(8): p. 711-24.
404. Rehman, I., et al., *Dysregulated expression of S100A11 (calgizzarin) in prostate cancer and precursor lesions.* Hum Pathol, 2004. **35**(11): p. 1385-91.
405. Heizmann, C.W., G.E. Ackermann, and A. Galichet, *Pathologies involving the S100 proteins and RAGE.* Subcell Biochem, 2007. **45**: p. 93-138.
406. Salama, I., P.S. Malone, F. Mihaimeed, and J.L. Jones, *A review of the S100 proteins in cancer.* Eur J Surg Oncol, 2008. **34**(4): p. 357-64.
407. Leclerc, E. and S.W. Vetter, *The role of S100 proteins and their receptor RAGE in pancreatic cancer.* Biochim Biophys Acta, 2015. **1852**(12): p. 2706-11.
408. Woo, T., et al., *Up-Regulation of S100A11 in Lung Adenocarcinoma - Its Potential Relationship with Cancer Progression.* PLoS One, 2015. **10**(11): p. e0142642.
409. Saho, S., et al., *Active Secretion of Dimerized S100A11 Induced by the Peroxisome in Mesothelioma Cells.* Cancer Microenviron, 2016. **9**(2-3): p. 93-105.
410. Gabril, M., et al., *S100A11 is a potential prognostic marker for clear cell renal cell carcinoma.* Clin Exp Metastasis, 2016. **33**(1): p. 63-71.
411. Hao, J., et al., *Selective expression of S100A11 in lung cancer and its role in regulating proliferation of adenocarcinomas cells.* Mol Cell Biochem, 2012. **359**(1-2): p. 323-32.
412. Rudland, P.S., et al., *Prognostic significance of the metastasis-inducing protein S100A4 (p9Ka) in human breast cancer.* Cancer Res, 2000. **60**(6): p. 1595-603.

413. O'Connell, J.T., et al., *VEGF-A and Tenascin-C produced by S100A4+ stromal cells are important for metastatic colonization.* Proc Natl Acad Sci U S A, 2011. **108**(38): p. 16002-7.
414. Schmidt, A.M. and D.M. Stern, *Receptor for age (RAGE) is a gene within the major histocompatibility class III region: implications for host response mechanisms in homeostasis and chronic disease.* Front Biosci, 2001. **6**: p. D1151-60.
415. Klingelhofer, J., et al., *Epidermal growth factor receptor ligands as new extracellular targets for the metastasis-promoting S100A4 protein.* FEBS J, 2009. **276**(20): p. 5936-48.
416. Lorenz, S., G. Aust, and K. Krohn, *Ca(2+)-binding protein expression in primary human thyrocytes.* Biochim Biophys Acta, 2013. **1833**(12): p. 2703-2713.
417. Perbal, B., *CCN proteins: multifunctional signalling regulators.* Lancet, 2004. **363**(9402): p. 62-4.
418. Nakanishi, T., et al., *Effects of CTGF/Hcs24, a product of a hypertrophic chondrocyte-specific gene, on the proliferation and differentiation of chondrocytes in culture.* Endocrinology, 2000. **141**(1): p. 264-73.
419. Leask, A. and D.J. Abraham, *All in the CCN family: essential matricellular signaling modulators emerge from the bunker.* J Cell Sci, 2006. **119**(Pt 23): p. 4803-10.
420. Hu, X., et al., *The role of ERK and JNK signaling in connective tissue growth factor induced extracellular matrix protein production and scar formation.* Arch Dermatol Res, 2013. **305**(5): p. 433-45.
421. Kidd, M., S. Schimmack, B. Lawrence, D. Alaimo, and I.M. Modlin, *EGFR/TGFalpha and TGFbeta/CTGF Signaling in Neuroendocrine Neoplasia: Theoretical Therapeutic Targets.* Neuroendocrinology, 2013. **97**(1): p. 35-44.
422. Bladt, F., D. Riethmacher, S. Isenmann, A. Aguzzi, and C. Birchmeier, *Essential role for the c-met receptor in the migration of myogenic precursor cells into the limb bud.* Nature, 1995. **376**(6543): p. 768-71.
423. Bottaro, D.P., et al., *Identification of the hepatocyte growth factor receptor as the c-met proto-oncogene product.* Science, 1991. **251**(4995): p. 802-4.
424. Yano, S., et al., *Hepatocyte growth factor induces gefitinib resistance of lung adenocarcinoma with epidermal growth factor receptor-activating mutations.* Cancer Res, 2008. **68**(22): p. 9479-87.
425. *Correction: Response to MET Inhibitors in Patients with Stage IV Lung Adenocarcinomas Harboring MET Mutations Causing Exon 14 Skipping.* Cancer Discov, 2016. **6**(3): p. 330.
426. Cirri, P. and P. Chiarugi, *Cancer-associated-fibroblasts and tumour cells: a diabolic liaison driving cancer progression.* Cancer Metastasis Rev, 2012. **31**(1-2): p. 195-208.
427. Stanley, E.R. and P.M. Heard, *Factors regulating macrophage production and growth. Purification and some properties of the colony stimulating factor from medium conditioned by mouse L cells.* J Biol Chem, 1977. **252**(12): p. 4305-12.
428. Pixley, F.J. and E.R. Stanley, *CSF-1 regulation of the wandering macrophage: complexity in action.* Trends Cell Biol, 2004. **14**(11): p. 628-38.
429. Sherr, C.J., et al., *The c-fms proto-oncogene product is related to the receptor for the mononuclear phagocyte growth factor, CSF-1.* Cell, 1985. **41**(3): p. 665-76.
430. Metcalf, D., et al., *Synergistic suppression: anomalous inhibition of the proliferation of factor-dependent hemopoietic cells by combination of two colony-stimulating factors.* Proc Natl Acad Sci U S A, 1992. **89**(7): p. 2819-23.
431. Bartelmez, S.H., et al., *Interleukin 1 plus interleukin 3 plus colony-stimulating factor 1 are essential for clonal proliferation of primitive myeloid bone marrow cells.* Exp Hematol, 1989. **17**(3): p. 240-5.
432. Cecchini, M.G., et al., *Role of colony stimulating factor-1 in the establishment and regulation of tissue macrophages during postnatal development of the mouse.* Development, 1994. **120**(6): p. 1357-72.
433. Urist, M.R., *Bone: formation by autoinduction.* Science, 1965. **150**(3698): p. 893-9.
434. Sterchi, E.E., W. Stocker, and J.S. Bond, *Meprins, membrane-bound and secreted astacin metalloproteinases.* Mol Aspects Med, 2008. **29**(5): p. 309-28.

435. Kessler, E., K. Takahara, L. Biniaminov, M. Brusel, and D.S. Greenspan, *Bone morphogenetic protein-1: the type I procollagen C-proteinase.* Science, 1996. **271**(5247): p. 360-2.
436. de Caestecker, M., *The transforming growth factor-beta superfamily of receptors.* Cytokine Growth Factor Rev, 2004. **15**(1): p. 1-11.
437. Zhang, Y.E., *Non-Smad pathways in TGF-beta signaling.* Cell Res, 2009. **19**(1): p. 128-39.
438. Wang, R.N., et al., *Bone Morphogenetic Protein (BMP) signaling in development and human diseases.* Genes Dis, 2014. **1**(1): p. 87-105.
439. Broege, A., et al., *Bone morphogenetic proteins signal via SMAD and mitogen-activated protein (MAP) kinase pathways at distinct times during osteoclastogenesis.* J Biol Chem, 2013. **288**(52): p. 37230-40.
440. Rajagopal, R., et al., *Functions of the type 1 BMP receptor Acvr1 (Alk2) in lens development: cell proliferation, terminal differentiation, and survival.* Invest Ophthalmol Vis Sci, 2008. **49**(11): p. 4953-60.
441. Rashidi, A. and G.L. Uy, *Targeting the microenvironment in acute myeloid leukemia.* Curr Hematol Malig Rep, 2015. **10**(2): p. 126-31.
442. Bakker, E., M. Qattan, L. Mutti, C. Demonacos, and M. Krstic-Demonacos, *The role of microenvironment and immunity in drug response in leukemia.* Biochim Biophys Acta, 2016. **1863**(3): p. 414-426.
443. Pearce, D.J., et al., *AML engraftment in the NOD/SCID assay reflects the outcome of AML: implications for our understanding of the heterogeneity of AML.* Blood, 2006. **107**(3): p. 1166-73.
444. Bruserud, O., B.T. Gjertsen, B. Foss, and T.S. Huang, *New strategies in the treatment of acute myelogenous leukemia (AML): in vitro culture of aml cells--the present use in experimental studies and the possible importance for future therapeutic approaches.* Stem Cells, 2001. **19**(1): p. 1-11.
445. Gao, Y., C.Y. Yuan, and W. Yuan, *Will targeting PI3K/Akt/mTOR signaling work in hematopoietic malignancies?* Stem Cell Investig, 2016. **3**: p. 31.
446. Fransecky, L., L.H. Mochmann, and C.D. Baldus, *Outlook on PI3K/AKT/mTOR inhibition in acute leukemia.* Mol Cell Ther, 2015. **3**: p. 2.
447. Sandhofer, N., et al., *Dual PI3K/mTOR inhibition shows antileukemic activity in MLL-rearranged acute myeloid leukemia.* Leukemia, 2015. **29**(4): p. 828-38.
448. Burgess, M.R., et al., *Preclinical efficacy of MEK inhibition in Nras-mutant AML.* Blood, 2014. **124**(26): p. 3947-55.
449. van de Geijn, G.J., J. Gits, L.H. Aarts, C. Heijmans-Antonissen, and I.P. Touw, *G-CSF receptor truncations found in SCN/AML relieve SOCS3-controlled inhibition of STAT5 but leave suppression of STAT3 intact.* Blood, 2004. **104**(3): p. 667-74.
450. Stanley, E.R. and V. Chitu, *CSF-1 receptor signaling in myeloid cells.* Cold Spring Harb Perspect Biol, 2014. **6**(6).
451. Lindblad, O., et al., *Aberrant activation of the PI3K/mTOR pathway promotes resistance to sorafenib in AML.* Oncogene, 2016. **35**(39): p. 5119-31.
452. Huang, J., M. Nguyen-McCarty, E.O. Hexner, G. Danet-Desnoyers, and P.S. Klein, *Maintenance of hematopoietic stem cells through regulation of Wnt and mTOR pathways.* Nat Med, 2012. **18**(12): p. 1778-85.
453. Chapuis, N., et al., *Autocrine IGF-1/IGF-1R signaling is responsible for constitutive PI3K/Akt activation in acute myeloid leukemia: therapeutic value of neutralizing anti-IGF-1R antibody.* Haematologica, 2010. **95**(3): p. 415-23.
454. Liu, Q., et al., *Discovery of 1-(4-(4-propionylpiperazin-1-yl)-3-(trifluoromethyl)phenyl)-9-(quinolin-3-yl)benz o[h][1,6]naphthyridin-2(1H)-one as a highly potent, selective mammalian target of rapamycin (mTOR) inhibitor for the treatment of cancer.* J Med Chem, 2010. **53**(19): p. 7146-55.
455. Pan, X.N., et al., *Inhibition of c-Myc overcomes cytotoxic drug resistance in acute myeloid leukemia cells by promoting differentiation.* PLoS One, 2014. **9**(8): p. e105381.

456. Brenner, A.K., T.H. Andersson Tvedt, and O. Bruserud, *The Complexity of Targeting PI3K-Akt-mTOR Signalling in Human Acute Myeloid Leukaemia: The Importance of Leukemic Cell Heterogeneity, Neighbouring Mesenchymal Stem Cells and Immunocompetent Cells.* Molecules, 2016. **21**(11).
457. Hoshii, T., et al., *mTORC1 is essential for leukemia propagation but not stem cell self-renewal.* J Clin Invest, 2012. **122**(6): p. 2114-29.
458. Lyman, S.D., et al., *Molecular cloning of a ligand for the flt3/flk-2 tyrosine kinase receptor: a proliferative factor for primitive hematopoietic cells.* Cell, 1993. **75**(6): p. 1157-67.
459. Matthews, W., C.T. Jordan, G.W. Wiegand, D. Pardoll, and I.R. Lemischka, *A receptor tyrosine kinase specific to hematopoietic stem and progenitor cell-enriched populations.* Cell, 1991. **65**(7): p. 1143-52.
460. Gilliland, D.G. and J.D. Griffin, *The roles of FLT3 in hematopoiesis and leukemia.* Blood, 2002. **100**(5): p. 1532-42.
461. Friedrich, K., et al., *Activation of STAT5 by IL-4 relies on Janus kinase function but not on receptor tyrosine phosphorylation, and can contribute to both cell proliferation and gene regulation.* Int Immunol, 1999. **11**(8): p. 1283-94.
462. Bradley, H.L., T.S. Hawley, and K.D. Bunting, *Cell intrinsic defects in cytokine responsiveness of STAT5-deficient hematopoietic stem cells.* Blood, 2002. **100**(12): p. 3983-9.
463. Steensma, D.P., et al., *JAK2 V617F is a rare finding in de novo acute myeloid leukemia, but STAT3 activation is common and remains unexplained.* Leukemia, 2006. **20**(6): p. 971-8.
464. Rane, C.K. and A. Minden, *P21 activated kinases: structure, regulation, and functions.* Small GTPases, 2014. **5**.
465. Eppert, K., et al., *Stem cell gene expression programs influence clinical outcome in human leukemia.* Nature Medicine, 2011. **17**(9): p. 1086-U91.
466. Taussig, D.C., et al., *Anti-CD38 antibody-mediated clearance of human repopulating cells masks the heterogeneity of leukemia-initiating cells.* Blood, 2008. **112**(3): p. 568-75.
467. Sarry, J.E., et al., *Human acute myelogenous leukemia stem cells are rare and heterogeneous when assayed in NOD/SCID/IL2R gamma c-deficient mice.* Journal of Clinical Investigation, 2011. **121**(1): p. 384-395.
468. Kita, K., et al., *Clinical importance of CD7 expression in acute myelocytic leukemia. The Japan Cooperative Group of Leukemia/Lymphoma.* Blood, 1993. **81**(9): p. 2399-405.
469. Kanda, Y., et al., *The clinical significance of CD34 expression in response to therapy of patients with acute myeloid leukemia: an overview of 2483 patients from 22 studies.* Cancer, 2000. **88**(11): p. 2529-33.
470. van Stijn, A., et al., *Differences between the CD34+ and CD34- blast compartments in apoptosis resistance in acute myeloid leukemia.* Haematologica, 2003. **88**(5): p. 497-508.
471. Hanson, C.A., K.J. Gajl-Peczalska, J.L. Parkin, and R.D. Brunning, *Immunophenotyping of acute myeloid leukemia using monoclonal antibodies and the alkaline phosphatase-antialkaline phosphatase technique.* Blood, 1987. **70**(1): p. 83-9.
472. De Rossi, G., et al., *Immunological definition of acute promyelocytic leukemia (FAB M3): a study of 39 cases.* Eur J Haematol, 1990. **45**(3): p. 168-71.
473. Gerber, J.M., et al., *A clinically relevant population of leukemic CD34(+)CD38(-) cells in acute myeloid leukemia.* Blood, 2012. **119**(15): p. 3571-7.
474. Griffin, J.D., D. Linch, K. Sabbath, P. Larcom, and S.F. Schlossman, *A monoclonal antibody reactive with normal and leukemic human myeloid progenitor cells.* Leuk Res, 1984. **8**(4): p. 521-34.
475. Hwang, K., et al., *Flow cytometric quantification and immunophenotyping of leukemic stem cells in acute myeloid leukemia.* Ann Hematol, 2012. **91**(10): p. 1541-6.
476. Munoz, L., et al., *Interleukin-3 receptor alpha chain (CD123) is widely expressed in hematologic malignancies.* Haematologica, 2001. **86**(12): p. 1261-9.

477. Dunphy, C.H. and W. Tang, *The value of CD64 expression in distinguishing acute myeloid leukemia with monocytic differentiation from other subtypes of acute myeloid leukemia: a flow cytometric analysis of 64 cases.* Arch Pathol Lab Med, 2007. **131**(5): p. 748-54.
478. Choi, Y., et al., *Prognostic implications of CD14 positivity in acute myeloid leukemia arising from myelodysplastic syndrome.* Int J Hematol, 2013. **97**(2): p. 246-55.
479. Lacombe, F., et al., *Flow cytometry CD45 gating for immunophenotyping of acute myeloid leukemia.* Leukemia, 1997. **11**(11): p. 1878-86.
480. Graf, M., et al., *Expression of MAC-1 (CD11b) in acute myeloid leukemia (AML) is associated with an unfavorable prognosis.* Am J Hematol, 2006. **81**(4): p. 227-35.
481. Chetty, R. and K. Gatter, *CD3: structure, function, and role of immunostaining in clinical practice.* J Pathol, 1994. **173**(4): p. 303-7.
482. Walter, K., et al., *Aberrant expression of CD19 in AML with t(8;21) involves a poised chromatin structure and PAX5.* Oncogene, 2010. **29**(20): p. 2927-37.
483. Sperling, C., S. Schwartz, T. Buchner, E. Thiel, and W.D. Ludwig, *Expression of the stem cell factor receptor C-KIT (CD117) in acute leukemias.* Haematologica, 1997. **82**(5): p. 617-21.
484. Mandelboim, O., et al., *Human CD16 as a lysis receptor mediating direct natural killer cell cytotoxicity.* Proc Natl Acad Sci U S A, 1999. **96**(10): p. 5640-4.
485. Chisini, M., et al., *Independent prognostic impact of CD15 on complete remission achievement in patients with acute myeloid leukemia.* Hematol Oncol, 2016.
486. Amir el, A.D., et al., *viSNE enables visualization of high dimensional single-cell data and reveals phenotypic heterogeneity of leukemia.* Nat Biotechnol, 2013. **31**(6): p. 545-52.
487. Lewis, R.E., J.M. Cruse, C.M. Sanders, R.N. Webb, and J.L. Suggs, *Aberrant expression of T-cell markers in acute myeloid leukemia.* Exp Mol Pathol, 2007. **83**(3): p. 462-3.
488. Wiernik, A., et al., *Targeting natural killer cells to acute myeloid leukemia in vitro with a CD16 x 33 bispecific killer cell engager and ADAM17 inhibition.* Clin Cancer Res, 2013. **19**(14): p. 3844-55.
489. Larrosa-Garcia, M. and M.R. Baer, *FLT3 Inhibitors in Acute Myeloid Leukemia: Current Status and Future Directions.* Mol Cancer Ther, 2017. **16**(6): p. 991-1001.
490. Estey, E., R.L. Levine, and B. Lowenberg, *Current challenges in clinical development of "targeted therapies": the case of acute myeloid leukemia.* Blood, 2015. **125**(16): p. 2461-6.
491. Tape, C.J., et al., *Oncogenic KRAS Regulates Tumor Cell Signaling via Stromal Reciprocation.* Cell, 2016. **165**(7): p. 1818.
492. Matsunaga, T., et al., *Interaction between leukemic-cell VLA-4 and stromal fibronectin is a decisive factor for minimal residual disease of acute myelogenous leukemia.* Nat Med, 2003. **9**(9): p. 1158-65.
493. Gaundar, S.S., K.F. Bradstock, and L.J. Bendall, *p38MAPK inhibitors attenuate cytokine production by bone marrow stromal cells and reduce stroma-mediated proliferation of acute lymphoblastic leukemia cells.* Cell Cycle, 2009. **8**(18): p. 2975-83.
494. Bendall, L.J., K. Kortlepel, and D.J. Gottlieb, *Human acute myeloid leukemia cells bind to bone marrow stroma via a combination of beta-1 and beta-2 integrin mechanisms.* Blood, 1993. **82**(10): p. 3125-32.
495. Csanaky, G., E. Matutes, J.A. Vass, R. Morilla, and D. Catovsky, *Adhesion receptors on peripheral blood leukemic B cells. A comparative study on B cell chronic lymphocytic leukemia and related lymphoma/leukemias.* Leukemia, 1997. **11**(3): p. 408-15.
496. Seguin, L., J.S. Desgrosellier, S.M. Weis, and D.A. Cheresh, *Integrins and cancer: regulators of cancer stemness, metastasis, and drug resistance.* Trends Cell Biol, 2015. **25**(4): p. 234-40.
497. Hynes, R.O., *Integrins: bidirectional, allosteric signaling machines.* Cell, 2002. **110**(6): p. 673-87.
498. Guo, W. and F.G. Giancotti, *Integrin signalling during tumour progression.* Nat Rev Mol Cell Biol, 2004. **5**(10): p. 816-26.

499. Denkers, I.A., T.J. de Jong-de Boer, R.H. Beelen, G.J. Ossenkoppele, and M.M. Langenhuijsen, *VLA molecule expression may be involved in the release of acute myeloid leukaemic cells from the bone marrow.* Leuk Res, 1992. **16**(5): p. 469-74.
500. Reuss-Borst, M.A., H.J. Buhring, G. Klein, and C.A. Muller, *Adhesion molecules on CD34+ hematopoietic cells in normal human bone marrow and leukemia.* Ann Hematol, 1992. **65**(4): p. 169-74.
501. Reuss-Borst, M.A., Y. Ning, G. Klein, and C.A. Muller, *The vascular cell adhesion molecule (VCAM-1) is expressed on a subset of lymphoid and myeloid leukaemias.* Br J Haematol, 1995. **89**(2): p. 299-305.
502. Liesveld, J.L., J.M. Winslow, K.E. Frediani, D.H. Ryan, and C.N. Abboud, *Expression of integrins and examination of their adhesive function in normal and leukemic hematopoietic cells.* Blood, 1993. **81**(1): p. 112-21.
503. Jacamo, R., et al., *Reciprocal leukemia-stroma VCAM-1/VLA-4-dependent activation of NF-kappaB mediates chemoresistance.* Blood, 2014. **123**(17): p. 2691-702.
504. Wu, S., et al., *Interaction of bone marrow stromal cells with lymphoblasts and effects of predinsolone on cytokine expression.* Leuk Res, 2005. **29**(1): p. 63-72.
505. Juarez, J., R. Baraz, S. Gaundar, K. Bradstock, and L. Bendall, *Interaction of interleukin-7 and interleukin-3 with the CXCL12-induced proliferation of B-cell progenitor acute lymphoblastic leukemia.* Haematologica, 2007. **92**(4): p. 450-9.
506. Peterson, R.T., P.A. Beal, M.J. Comb, and S.L. Schreiber, *FKBP12-rapamycin-associated protein (FRAP) autophosphorylates at serine 2481 under translationally repressive conditions.* J Biol Chem, 2000. **275**(10): p. 7416-23.
507. Nave, B.T., M. Ouwens, D.J. Withers, D.R. Alessi, and P.R. Shepherd, *Mammalian target of rapamycin is a direct target for protein kinase B: identification of a convergence point for opposing effects of insulin and amino-acid deficiency on protein translation.* Biochem J, 1999. **344 Pt 2**: p. 427-31.
508. Weng, Q.P., et al., *Regulation of the p70 S6 kinase by phosphorylation in vivo. Analysis using site-specific anti-phosphopeptide antibodies.* J Biol Chem, 1998. **273**(26): p. 16621-9.
509. Pullen, N. and G. Thomas, *The modular phosphorylation and activation of p70s6k.* FEBS Lett, 1997. **410**(1): p. 78-82.
510. Fang, Y., M. Vilella-Bach, R. Bachmann, A. Flanigan, and J. Chen, *Phosphatidic acid-mediated mitogenic activation of mTOR signaling.* Science, 2001. **294**(5548): p. 1942-5.
511. Brunn, G.J., et al., *Phosphorylation of the translational repressor PHAS-I by the mammalian target of rapamycin.* Science, 1997. **277**(5322): p. 99-101.
512. Pause, A., et al., *Insulin-dependent stimulation of protein synthesis by phosphorylation of a regulator of 5'-cap function.* Nature, 1994. **371**(6500): p. 762-7.
513. Gingras, A.C., S.G. Kennedy, M.A. O'Leary, N. Sonenberg, and N. Hay, *4E-BP1, a repressor of mRNA translation, is phosphorylated and inactivated by the Akt(PKB) signaling pathway.* Genes Dev, 1998. **12**(4): p. 502-13.
514. Gingras, A.C., et al., *Regulation of 4E-BP1 phosphorylation: a novel two-step mechanism.* Genes Dev, 1999. **13**(11): p. 1422-37.
515. Radu, M., G. Semenova, R. Kosoff, and J. Chernoff, *PAK signalling during the development and progression of cancer.* Nat Rev Cancer, 2014. **14**(1): p. 13-25.
516. Gatti, A., Z. Huang, P.T. Tuazon, and J.A. Traugh, *Multisite autophosphorylation of p21-activated protein kinase gamma-PAK as a function of activation.* J Biol Chem, 1999. **274**(12): p. 8022-8.
517. Manser, E., et al., *Expression of constitutively active alpha-PAK reveals effects of the kinase on actin and focal complexes.* Mol Cell Biol, 1997. **17**(3): p. 1129-43.
518. Royal, I., N. Lamarche-Vane, L. Lamorte, K. Kaibuchi, and M. Park, *Activation of cdc42, rac, PAK, and rho-kinase in response to hepatocyte growth factor differentially regulates epithelial cell colony spreading and dissociation.* Mol Biol Cell, 2000. **11**(5): p. 1709-25.
519. Li, S., C.E. Mason, and A. Melnick, *Genetic and epigenetic heterogeneity in acute myeloid leukemia.* Curr Opin Genet Dev, 2016. **36**: p. 100-6.

520. Li, S., et al., *Distinct evolution and dynamics of epigenetic and genetic heterogeneity in acute myeloid leukemia.* Nat Med, 2016. **22**(7): p. 792-9.
521. Song, K., et al., *Resistance to chemotherapy is associated with altered glucose metabolism in acute myeloid leukemia.* Oncol Lett, 2016. **12**(1): p. 334-342.
522. Figueroa, M.E., et al., *Leukemic IDH1 and IDH2 mutations result in a hypermethylation phenotype, disrupt TET2 function, and impair hematopoietic differentiation.* Cancer Cell, 2010. **18**(6): p. 553-67.
523. Gal, H., et al., *Gene expression profiles of AML derived stem cells; similarity to hematopoietic stem cells.* Leukemia, 2006. **20**(12): p. 2147-54.
524. Dhavan, R. and L.H. Tsai, *A decade of CDK5.* Nat Rev Mol Cell Biol, 2001. **2**(10): p. 749-59.
525. Daval, M., T. Gurlo, S. Costes, C.J. Huang, and P.C. Butler, *Cyclin-dependent kinase 5 promotes pancreatic beta-cell survival via Fak-Akt signaling pathways.* Diabetes, 2011. **60**(4): p. 1186-97.
526. Nikolic, M., H. Dudek, Y.T. Kwon, Y.F. Ramos, and L.H. Tsai, *The cdk5/p35 kinase is essential for neurite outgrowth during neuronal differentiation.* Genes Dev, 1996. **10**(7): p. 816-25.
527. Nikolic, M., M.M. Chou, W. Lu, B.J. Mayer, and L.H. Tsai, *The p35/Cdk5 kinase is a neuron-specific Rac effector that inhibits Pak1 activity.* Nature, 1998. **395**(6698): p. 194-8.
528. Herzog, J., et al., *Cyclin-dependent kinase 5 stabilizes hypoxia-inducible factor-1alpha: a novel approach for inhibiting angiogenesis in hepatocellular carcinoma.* Oncotarget, 2016. **7**(19): p. 27108-21.
529. Pozo, K. and J.A. Bibb, *The Emerging Role of Cdk5 in Cancer.* Trends Cancer, 2016. **2**(10): p. 606-618.
530. Ito, D., et al., *Dual-specificity tyrosine-regulated kinase 2 is a suppressor and potential prognostic marker for liver metastasis of colorectal cancer.* Cancer Sci, 2017. **108**(8): p. 1565-1573.
531. Yamaguchi, N., et al., *DYRK2 regulates epithelial-mesenchymal-transition and chemosensitivity through Snail degradation in ovarian serous adenocarcinoma.* Tumour Biol, 2015. **36**(8): p. 5913-23.
532. Lopes, M.R., et al., *De novo AML exhibits greater microenvironment dysregulation compared to AML with myelodysplasia-related changes.* Sci Rep, 2017. **7**: p. 40707.
533. Jeanmougin, M., et al., *Should we abandon the t-test in the analysis of gene expression microarray data: a comparison of variance modeling strategies.* PLoS One, 2010. **5**(9): p. e12336.
534. Ting, L., et al., *Normalization and statistical analysis of quantitative proteomics data generated by metabolic labeling.* Mol Cell Proteomics, 2009. **8**(10): p. 2227-42.
535. Casado, P., et al., *Phosphoproteomics data classify hematological cancer cell lines according to tumor type and sensitivity to kinase inhibitors.* Genome Biol, 2013. **14**(4): p. R37.
536. Wilkes, E.H., P. Casado, V. Rajeeve, and P.R. Cutillas, *Kinase activity ranking using phosphoproteomics data (KARP) quantifies the contribution of protein kinases to the regulation of cell viability.* Mol Cell Proteomics, 2017. **16**(9): p. 1694-1704.
537. Rousseau, S., et al., *Inhibition of SAPK2a/p38 prevents hnRNP A0 phosphorylation by MAPKAP-K2 and its interaction with cytokine mRNAs.* EMBO J, 2002. **21**(23): p. 6505-14.
538. Martin, H., et al., *Pak and Rac GTPases promote oncogenic KIT-induced neoplasms.* J Clin Invest, 2013. **123**(10): p. 4449-63.
539. Arias-Romero, L.E. and J. Chernoff, *A tale of two Paks.* Biol Cell, 2008. **100**(2): p. 97-108.
540. Rudolph, J., J.J. Crawford, K.P. Hoeflich, and W. Wang, *Inhibitors of p21-activated kinases (PAKs).* J Med Chem, 2015. **58**(1): p. 111-29.
541. Eswaran, J., M. Soundararajan, and S. Knapp, *Targeting group II PAKs in cancer and metastasis.* Cancer Metastasis Rev, 2009. **28**(1-2): p. 209-17.

542. King, C.C., et al., *p21-activated kinase (PAK1) is phosphorylated and activated by 3-phosphoinositide-dependent kinase-1 (PDK1).* J Biol Chem, 2000. **275**(52): p. 41201-9.
543. Howe, A.K. and R.L. Juliano, *Regulation of anchorage-dependent signal transduction by protein kinase A and p21-activated kinase.* Nat Cell Biol, 2000. **2**(9): p. 593-600.
544. Tsakiridis, T., C. Taha, S. Grinstein, and A. Klip, *Insulin activates a p21-activated kinase in muscle cells via phosphatidylinositol 3-kinase.* J Biol Chem, 1996. **271**(33): p. 19664-7.
545. Tang, Y., H. Zhou, A. Chen, R.N. Pittman, and J. Field, *The Akt proto-oncogene links Ras to Pak and cell survival signals.* J Biol Chem, 2000. **275**(13): p. 9106-9.
546. Hofmann, C., M. Shepelev, and J. Chernoff, *The genetics of Pak.* J Cell Sci, 2004. **117**(Pt 19): p. 4343-54.
547. Molli, P.R., D.Q. Li, B.W. Murray, S.K. Rayala, and R. Kumar, *PAK signaling in oncogenesis.* Oncogene, 2009. **28**(28): p. 2545-55.
548. Baker, N.M., H. Yee Chow, J. Chernoff, and C.J. Der, *Molecular pathways: targeting RAC-p21-activated serine-threonine kinase signaling in RAS-driven cancers.* Clin Cancer Res, 2014. **20**(18): p. 4740-6.
549. Kumar, R., A.E. Gururaj, and C.J. Barnes, *p21-activated kinases in cancer.* Nat Rev Cancer, 2006. **6**(6): p. 459-71.
550. Ha, B.H., E.M. Morse, B.E. Turk, and T.J. Boggon, *Signaling, Regulation, and Specificity of the Type II p21-activated Kinases.* J Biol Chem, 2015. **290**(21): p. 12975-83.
551. Zeng, Y., et al., *Pak2 regulates hematopoietic progenitor cell proliferation, survival, and differentiation.* Stem Cells, 2015. **33**(5): p. 1630-41.
552. Beltran, L., C. Chaussade, B. Vanhaesebroeck, and P.R. Cutillas, *Calpain interacts with class IA phosphoinositide 3-kinases regulating their stability and signaling activity.* Proc Natl Acad Sci U S A, 2011. **108**(39): p. 16217-22.
553. Satelli, A. and S. Li, *Vimentin in cancer and its potential as a molecular target for cancer therapy.* Cell Mol Life Sci, 2011. **68**(18): p. 3033-46.
554. Chen, P.W. and G.S. Kroog, *Leupaxin is similar to paxillin in focal adhesion targeting and tyrosine phosphorylation but has distinct roles in cell adhesion and spreading.* Cell Adh Migr, 2010. **4**(4): p. 527-40.
555. Chew, V. and K.P. Lam, *Leupaxin negatively regulates B cell receptor signaling.* J Biol Chem, 2007. **282**(37): p. 27181-91.
556. Ding, L., et al., *FHL1 interacts with oestrogen receptors and regulates breast cancer cell growth.* J Cell Mol Med, 2011. **15**(1): p. 72-85.
557. Nayal, A., et al., *Paxillin phosphorylation at Ser273 localizes a GIT1-PIX-PAK complex and regulates adhesion and protrusion dynamics.* J Cell Biol, 2006. **173**(4): p. 587-9.
558. Hashimoto, S., A. Tsubouchi, Y. Mazaki, and H. Sabe, *Interaction of paxillin with p21-activated Kinase (PAK). Association of paxillin alpha with the kinase-inactive and the Cdc42-activated forms of PAK3.* J Biol Chem, 2001. **276**(8): p. 6037-45.
559. Galan-Diez, M., A. Cuesta-Dominguez, and S. Kousteni, *The Bone Marrow Microenvironment in Health and Myeloid Malignancy.* Cold Spring Harb Perspect Med, 2017.
560. Kumar, B., et al., *Acute myeloid leukemia transforms the bone marrow niche into a leukemia-permissive microenvironment through exosome secretion.* Leukemia, 2017.
561. Garcia, M. and C.C. Chen, *The bone marrow microenvironment-driver of leukemia evolution?* Stem Cell Investig, 2017. **4**: p. 11.
562. Liu, P., et al., *Overexpression of heme oxygenase-1 in bone marrow stromal cells promotes microenvironment-mediated imatinib resistance in chronic myeloid leukemia.* Biomed Pharmacother, 2017. **91**: p. 21-30.
563. Shen, Z., et al., *[Effects of SDF-1/CXCR4 signal pathway blockade by AMD3100 on the adhesion of leukemia cells to osteoblast niche and the drug resistance of leukemia cells].* Zhonghua Xue Ye Xue Za Zhi, 2015. **36**(5): p. 413-7.
564. Shen, Z.H., D.F. Zeng, P.Y. Kong, Y.Y. Ma, and X. Zhang, *AMD3100 and G-CSF disrupt the cross-talk between leukemia cells and the endosteal niche and enhance their sensitivity*

to chemotherapeutic drugs in biomimetic polystyrene scaffolds. Blood Cells Mol Dis, 2016. **59**: p. 16-24.
565. Ochoa, D., et al., *An atlas of human kinase regulation.* Mol Syst Biol, 2016. **12**(12): p. 888.
566. Olow, A., et al., *An Atlas of the Human Kinome Reveals the Mutational Landscape Underlying Dysregulated Phosphorylation Cascades in Cancer.* Cancer Res, 2016. **76**(7): p. 1733-45.
567. Shlush, L.I., et al., *Tracing the origins of relapse in acute myeloid leukaemia to stem cells.* Nature, 2017. **547**(7661): p. 104-108.
568. Hira, V.V.V., C.J.F. Van Noorden, H.E. Carraway, J.P. Maciejewski, and R.J. Molenaar, *Novel therapeutic strategies to target leukemic cells that hijack compartmentalized continuous hematopoietic stem cell niches.* Biochim Biophys Acta, 2017. **1868**(1): p. 183-198.
569. Shafat, M.S., B. Gnaneswaran, K.M. Bowles, and S.A. Rushworth, *The bone marrow microenvironment - Home of the leukemic blasts.* Blood Rev, 2017. **31**(5): p. 277-286.
570. Podar, K. and D. Jager, *Targeting the immune niche within the bone marrow microenvironment: The rise of immunotherapy in Multiple Myeloma.* Curr Cancer Drug Targets, 2017.
571. Schepers, H., et al., *STAT5 is required for long-term maintenance of normal and leukemic human stem/progenitor cells.* Blood, 2007. **110**(8): p. 2880-8.
572. Rozenveld-Geugien, M., I.O. Baas, D. van Gosliga, E. Vellenga, and J.J. Schuringa, *Expansion of normal and leukemic human hematopoietic stem/progenitor cells requires rac-mediated interaction with stromal cells.* Exp Hematol, 2007. **35**(5): p. 782-92.
573. Schepers, H., et al., *Reintroduction of C/EBPalpha in leukemic CD34+ stem/progenitor cells impairs self-renewal and partially restores myelopoiesis.* Blood, 2007. **110**(4): p. 1317-25.
574. Hanekamp, D., J. Cloos, and G.J. Schuurhuis, *Leukemic stem cells: identification and clinical application.* Int J Hematol, 2017. **105**(5): p. 549-557.
575. Mohammadi, S., et al., *Reciprocal Interactions of Leukemic Cells with Bone Marrow Stromal Cells Promote Enrichment of Leukemic Stem Cell Compartments in Response to Curcumin and Daunorubicin.* Asian Pac J Cancer Prev, 2017. **18**(3): p. 831-840.
576. Ito, S., et al., *Long term maintenance of myeloid leukemic stem cells cultured with unrelated human mesenchymal stromal cells.* Stem Cell Res, 2015. **14**(1): p. 95-104.
577. Kobari, L., A. Dubart, F. Le Pesteur, W. Vainchenker, and F. Sainteny, *Hematopoietic-promoting activity of the murine stromal cell line MS-5 is not related to the expression of the major hematopoietic cytokines.* J Cell Physiol, 1995. **163**(2): p. 295-304.
578. Hsu, H.C., et al., *Production of hematopoietic regulatory cytokines by peripheral blood mononuclear cells in patients with aplastic anemia.* Exp Hematol, 1996. **24**(1): p. 31-6.
579. Li, W.M., W.Q. Huang, Y.H. Huang, D.Z. Jiang, and Q.R. Wang, *Positive and negative hematopoietic cytokines produced by bone marrow endothelial cells.* Cytokine, 2000. **12**(7): p. 1017-23.
580. Scupoli, M.T., et al., *Bone marrow stromal cells and the upregulation of interleukin-8 production in human T-cell acute lymphoblastic leukemia through the CXCL12/CXCR4 axis and the NF-kappaB and JNK/AP-1 pathways.* Haematologica, 2008. **93**(4): p. 524-32.
581. Xiong, H., X.Y. Yang, J. Han, Q. Wang, and Z.L. Zou, *Cytokine expression patterns and mesenchymal stem cell karyotypes from the bone marrow microenvironment of patients with myelodysplastic syndromes.* Braz J Med Biol Res, 2015. **48**(3): p. 207-13.
582. Mbeunkui, F., B.J. Metge, L.A. Shevde, and L.K. Pannell, *Identification of differentially secreted biomarkers using LC-MS/MS in isogenic cell lines representing a progression of breast cancer.* J Proteome Res, 2007. **6**(8): p. 2993-3002.
583. Tape, C.J. and C. Jorgensen, *Cell-Specific Labeling for Analyzing Bidirectional Signaling by Mass Spectrometry.* Methods Mol Biol, 2017. **1636**: p. 219-234.

584. Krupka, C., et al., *CD33 target validation and sustained depletion of AML blasts in long-term cultures by the bispecific T-cell-engaging antibody AMG 330.* Blood, 2014. **123**(3): p. 356-65.
585. Li, X., et al., *Bone marrow microenvironment confers imatinib resistance to chronic myelogenous leukemia and oroxylin A reverses the resistance by suppressing Stat3 pathway.* Arch Toxicol, 2015. **89**(1): p. 121-36.
586. Soliman, A.H., *Diagnostic and Prognostic Relevance of Bone Marrow Microenvironment Components in Non Hodgkin's Lymphoma Cases Before and After Therapy.* Asian Pac J Cancer Prev, 2016. **17**(12): p. 5273-5280.
587. Tape, C.J., et al., *Cell-specific labeling enzymes for analysis of cell-cell communication in continuous co-culture.* Mol Cell Proteomics, 2014. **13**(7): p. 1866-76.
588. Li, X., et al., *A designed peptide targeting CXCR4 displays anti-acute myelocytic leukemia activity in vitro and in vivo.* Sci Rep, 2014. **4**: p. 6610.
589. Wang, J., et al., *BMP9 inhibits the growth and migration of lung adenocarcinoma A549 cells in a bone marrow stromal cellderived microenvironment through the MAPK/ERK and NF-kappaB pathways.* Oncol Rep, 2016. **36**(1): p. 410-8.
590. Nagasawa, T., Y. Omatsu, and T. Sugiyama, *Control of hematopoietic stem cells by the bone marrow stromal niche: the role of reticular cells.* Trends Immunol, 2011. **32**(7): p. 315-20.
591. Omatsu, Y., et al., *The essential functions of adipo-osteogenic progenitors as the hematopoietic stem and progenitor cell niche.* Immunity, 2010. **33**(3): p. 387-99.
592. Edmondson, R., J.J. Broglie, A.F. Adcock, and L. Yang, *Three-dimensional cell culture systems and their applications in drug discovery and cell-based biosensors.* Assay Drug Dev Technol, 2014. **12**(4): p. 207-18.
593. Breslin, S. and L. O'Driscoll, *The relevance of using 3D cell cultures, in addition to 2D monolayer cultures, when evaluating breast cancer drug sensitivity and resistance.* Oncotarget, 2016. **7**(29): p. 45745-45756.
594. Gerstung, M., et al., *Precision oncology for acute myeloid leukemia using a knowledge bank approach.* Nat Genet, 2017. **49**(3): p. 332-340.
595. Li, X., et al., *Improving chemotherapeutic efficiency in acute myeloid leukemia treatments by chemically synthesized peptide interfering with CXCR4/CXCL12 axis.* Sci Rep, 2015. **5**: p. 16228.
596. Guilbert, L.J. and E.R. Stanley, *Specific interaction of murine colony-stimulating factor with mononuclear phagocytic cells.* J Cell Biol, 1980. **85**(1): p. 153-9.
597. Husson, H., B. Mograbi, H. Schmid-Antomarchi, S. Fischer, and B. Rossi, *CSF-1 stimulation induces the formation of a multiprotein complex including CSF-1 receptor, c-Cbl, PI 3-kinase, Crk-II and Grb2.* Oncogene, 1997. **14**(19): p. 2331-8.
598. Bertacchini, J., et al., *Feedbacks and adaptive capabilities of the PI3K/Akt/mTOR axis in acute myeloid leukemia revealed by pathway selective inhibition and phosphoproteome analysis.* Leukemia, 2014. **28**(11): p. 2197-205.
599. Zarrinkar, P.P., et al., *AC220 is a uniquely potent and selective inhibitor of FLT3 for the treatment of acute myeloid leukemia (AML).* Blood, 2009. **114**(14): p. 2984-2992.
600. Espinoza, J.L., et al., *The simultaneous inhibition of the mTOR and MAPK pathways with Gnetin-C induces apoptosis in acute myeloid leukemia.* Cancer Lett, 2017. **400**: p. 127-136.
601. Carneiro, B.A., J.B. Kaplan, J.K. Altman, F.J. Giles, and L.C. Platanias, *Targeting mTOR signaling pathways and related negative feedback loops for the treatment of acute myeloid leukemia.* Cancer Biol Ther, 2015. **16**(5): p. 648-56.
602. Dick, J.E. and T. Lapidot, *Biology of normal and acute myeloid leukemia stem cells.* Int J Hematol, 2005. **82**(5): p. 389-96.
603. Craig, F.E. and K.A. Foon, *Flow cytometric immunophenotyping for hematologic neoplasms.* Blood, 2008. **111**(8): p. 3941-67.

604. Issaad, C., L. Croisille, A. Katz, W. Vainchenker, and L. Coulombel, *A murine stromal cell line allows the proliferation of very primitive human CD34++/CD38- progenitor cells in long-term cultures and semisolid assays.* Blood, 1993. **81**(11): p. 2916-24.
605. Namikawa, R., M.O. Muench, and M.G. Roncarolo, *Regulatory roles of the ligand for Flk2/Flt3 tyrosine kinase receptor on human hematopoiesis.* Stem Cells, 1996. **14**(4): p. 388-95.
606. Lisovsky, M., et al., *Flt3 ligand stimulates proliferation and inhibits apoptosis of acute myeloid leukemia cells: regulation of Bcl-2 and Bax.* Blood, 1996. **88**(10): p. 3987-97.
607. Thul, P.J. and C. Lindskog, *The human protein atlas: A spatial map of the human proteome.* Protein Sci, 2017.
608. Arai, F., A. Hirao, and T. Suda, *Regulation of hematopoietic stem cells by the niche.* Trends Cardiovasc Med, 2005. **15**(2): p. 75-9.
609. Ferrell, P.B., Jr., et al., *High-Dimensional Analysis of Acute Myeloid Leukemia Reveals Phenotypic Changes in Persistent Cells during Induction Therapy.* PLoS One, 2016. **11**(4): p. e0153207.
610. Abarrategi, A., et al., *Versatile humanized niche model enables study of normal and malignant human hematopoiesis.* J Clin Invest, 2017. **127**(2): p. 543-548.
611. Camacho, V., V. McClearn, S. Patel, and R.S. Welner, *Regulation of normal and leukemic stem cells through cytokine signaling and the microenvironment.* Int J Hematol, 2017. **105**(5): p. 566-577.
612. Abaza, Y., et al., *Long-term outcome of acute promyelocytic leukemia treated with all-trans-retinoic acid, arsenic trioxide, and gemtuzumab.* Blood, 2017. **129**(10): p. 1275-1283.
613. Tsitsipatis, D., et al., *Synergistic killing of FLT3ITD-positive AML cells by combined inhibition of tyrosine-kinase activity and N-glycosylation.* Oncotarget, 2017. **8**(16): p. 26613-26624.
614. Antar, A., et al., *Inhibition of FLT3 in AML: a focus on sorafenib.* Bone Marrow Transplant, 2017. **52**(3): p. 344-351.
615. Piddock, R.E., K.M. Bowles, and S.A. Rushworth, *The Role of PI3K Isoforms in Regulating Bone Marrow Microenvironment Signaling Focusing on Acute Myeloid Leukemia and Multiple Myeloma.* Cancers (Basel), 2017. **9**(4).
616. Huang, Y., et al., *MAPK/ERK2 phosphorylates ERG at serine 283 in leukemic cells and promotes stem cell signatures and cell proliferation.* Leukemia, 2016. **30**(7): p. 1552-61.
617. Sigismund, S., et al., *Clathrin-mediated internalization is essential for sustained EGFR signaling but dispensable for degradation.* Dev Cell, 2008. **15**(2): p. 209-19.
618. Barbieri, E., P.P. Di Fiore, and S. Sigismund, *Endocytic control of signaling at the plasma membrane.* Curr Opin Cell Biol, 2016. **39**: p. 21-7.
619. Cendrowski, J., A. Maminska, and M. Miaczynska, *Endocytic regulation of cytokine receptor signaling.* Cytokine Growth Factor Rev, 2016. **32**: p. 63-73.
620. Sorkin, A. and M. von Zastrow, *Endocytosis and signalling: intertwining molecular networks.* Nat Rev Mol Cell Biol, 2009. **10**(9): p. 609-22.
621. Kim, J.Y., et al., *Activity-Based Proteomics Reveals Heterogeneous Kinome and ATP-Binding Proteome Responses to MEK Inhibition in KRAS Mutant Lung Cancer.* Proteomes, 2016. **4**(2): p. 16.
622. Elenbaas, B. and R.A. Weinberg, *Heterotypic signaling between epithelial tumor cells and fibroblasts in carcinoma formation.* Exp Cell Res, 2001. **264**(1): p. 169-84.
623. Konig, H. and C.D. Santos, *Signal transduction in Acute Myeloid Leukemia - Implications for Novel Therapeutic Concepts.* Curr Cancer Drug Targets, 2015. **15**(9): p. 803-21.
624. Karigane, D. and K. Takubo, *Metabolic regulation of hematopoietic and leukemic stem/progenitor cells under homeostatic and stress conditions.* Int J Hematol, 2017. **106**(1): p. 18-26.
625. Farge, T., et al., *Chemotherapy-Resistant Human Acute Myeloid Leukemia Cells Are Not Enriched for Leukemic Stem Cells but Require Oxidative Metabolism.* Cancer Discov, 2017. **7**(7): p. 716-735.

626. Shafat, M.S., et al., *Leukemic blasts program bone marrow adipocytes to generate a protumoral microenvironment.* Blood, 2017. **129**(10): p. 1320-1332.
627. Testa, U., C. Labbaye, G. Castelli, and E. Pelosi, *Oxidative stress and hypoxia in normal and leukemic stem cells.* Exp Hematol, 2016. **44**(7): p. 540-60.
628. Luo, J., B.D. Manning, and L.C. Cantley, *Targeting the PI3K-Akt pathway in human cancer: rationale and promise.* Cancer Cell, 2003. **4**(4): p. 257-62.
629. Franke, T.F., D.R. Kaplan, and L.C. Cantley, *PI3K: downstream AKTion blocks apoptosis.* Cell, 1997. **88**(4): p. 435-7.
630. Furth, N. and Y. Aylon, *The LATS1 and LATS2 tumor suppressors: beyond the Hippo pathway.* Cell Death Differ, 2017. **24**(9): p. 1488-1501.
631. Taira, N., et al., *DYRK2 priming phosphorylation of c-Jun and c-Myc modulates cell cycle progression in human cancer cells.* J Clin Invest, 2012. **122**(3): p. 859-72.
632. Owen, H.C., et al., *Phytochemical Modulation of Apoptosis and Autophagy: Strategies to Overcome Chemoresistance in Leukemic Stem Cells in the Bone Marrow Microenvironment.* Int Rev Neurobiol, 2017. **135**: p. 249-278.
633. Tape, C.J., et al., *Oncogenic KRAS Regulates Tumor Cell Signaling via Stromal Reciprocation.* Cell, 2016. **165**(4): p. 910-20.
634. De Meyts, P., *The Insulin Receptor and Its Signal Transduction Network*, in *Endotext*, L.J. De Groot, et al., Editors. 2000: South Dartmouth (MA).
635. Le, Y., et al., *Adipogenic Mesenchymal Stromal Cells from Bone Marrow and Their Hematopoietic Supportive Role: Towards Understanding the Permissive Marrow Microenvironment in Acute Myeloid Leukemia.* Stem Cell Rev, 2016. **12**(2): p. 235-44.
636. Ford, A.M., et al., *Protracted dormancy of pre-leukemic stem cells.* Leukemia, 2015. **29**(11): p. 2202-7.
637. Gao, F.H., et al., *Protein kinase C-delta mediates down-regulation of heterogeneous nuclear ribonucleoprotein K protein: involvement in apoptosis induction.* Exp Cell Res, 2009. **315**(19): p. 3250-8.
638. Campbell, J., et al., *Large-Scale Profiling of Kinase Dependencies in Cancer Cell Lines.* Cell Rep, 2016. **14**(10): p. 2490-501.
639. Li, Y.H., et al., *The Human Kinome Targeted by FDA Approved Multi-Target Drugs and Combination Products: A Comparative Study from the Drug-Target Interaction Network Perspective.* PLoS One, 2016. **11**(11): p. e0165737.
640. Palumbo, A., Jr., O. Da Costa Nde, M.H. Bonamino, L.F. Pinto, and L.E. Nasciutti, *Genetic instability in the tumor microenvironment: a new look at an old neighbor.* Mol Cancer, 2015. **14**: p. 145.
641. Becker, P.S., *Dependence of acute myeloid leukemia on adhesion within the bone marrow microenvironment.* ScientificWorldJournal, 2012. **2012**: p. 856467.
642. Berger, A., et al., *PAK-dependent STAT5 serine phosphorylation is required for BCR-ABL-induced leukemogenesis.* Leukemia, 2014. **28**(3): p. 629-41.
643. Dierks, S., et al., *Leupaxin stimulates adhesion and migration of prostate cancer cells through modulation of the phosphorylation status of the actin-binding protein caldesmon.* Oncotarget, 2015. **6**(15): p. 13591-606.
644. Sahu, S.N., et al., *Association of leupaxin with Src in osteoclasts.* Am J Physiol Cell Physiol, 2007. **292**(1): p. C581-90.
645. Marx, V., *Finding the right antibody for the job.* Nat Methods, 2013. **10**(8): p. 703-7.
646. Manser, E. and L. Lim, *Roles of PAK family kinases.* Prog Mol Subcell Biol, 1999. **22**: p. 115-33.
647. Obermeier, A., et al., *PAK promotes morphological changes by acting upstream of Rac.* EMBO J, 1998. **17**(15): p. 4328-39.
648. Manser, E., et al., *PAK kinases are directly coupled to the PIX family of nucleotide exchange factors.* Mol Cell, 1998. **1**(2): p. 183-92.
649. Perkins, J.R., I. Diboun, B.H. Dessailly, J.G. Lees, and C. Orengo, *Transient protein-protein interactions: structural, functional, and network properties.* Structure, 2010. **18**(10): p. 1233-43.

650. Klomp, J.E., et al., *Mimicking transient activation of protein kinases in living cells.* Proc Natl Acad Sci U S A, 2016. **113**(52): p. 14976-14981.
651. Subbotin, R.I. and B.T. Chait, *A pipeline for determining protein-protein interactions and proximities in the cellular milieu.* Mol Cell Proteomics, 2014. **13**(11): p. 2824-35.
652. Mali, S., W.J. Moree, M. Mitchell, W. Widger, and S.J. Bark, *Observations on different resin strategies for affinity purification mass spectrometry of a tagged protein.* Anal Biochem, 2016. **515**: p. 26-32.
653. Bornhorst, J.A. and J.J. Falke, *Purification of proteins using polyhistidine affinity tags.* Methods Enzymol, 2000. **326**: p. 245-54.
654. Lobingier, B.T., et al., *An Approach to Spatiotemporally Resolve Protein Interaction Networks in Living Cells.* Cell, 2017. **169**(2): p. 350-360 e12.
655. Roux, K.J., D.I. Kim, and B. Burke, *BioID: a screen for protein-protein interactions.* Curr Protoc Protein Sci, 2013. **74**: p. Unit 19 23.
656. Krug, U., et al., *Therapy of older persons with acute myeloid leukaemia.* Leuk Res, 2017. **60**: p. 1-10.
657. Bullinger, L., K. Dohner, and H. Dohner, *Genomics of Acute Myeloid Leukemia Diagnosis and Pathways.* J Clin Oncol, 2017. **35**(9): p. 934-946.
658. Medeiros, B.C., et al., *Isocitrate dehydrogenase mutations in myeloid malignancies.* Leukemia, 2017. **31**(2): p. 272-281.
659. Duployez, N., et al., *Comprehensive mutational profiling of core binding factor acute myeloid leukemia.* Blood, 2016. **127**(20): p. 2451-9.
660. Zhu, L., et al., *ASH1L Links Histone H3 Lysine 36 Dimethylation to MLL Leukemia.* Cancer Discov, 2016. **6**(7): p. 770-83.
661. Miotto, B., *Kinases and chromatin structure: who regulates whom?* Epigenetics, 2013. **8**(10): p. 1008-12.
662. Ghiaur, G. and M. Levis, *Mechanisms of Resistance to FLT3 Inhibitors and the Role of the Bone Marrow Microenvironment.* Hematol Oncol Clin North Am, 2017. **31**(4): p. 681-692.
663. Pollyea, D.A. and C.T. Jordan, *Therapeutic targeting of acute myeloid leukemia stem cells.* Blood, 2017. **129**(12): p. 1627-1635.
664. Horak, P., S. Frohling, and H. Glimm, *Integrating next-generation sequencing into clinical oncology: strategies, promises and pitfalls.* ESMO Open, 2016. **1**(5): p. e000094.
665. Konig, H. and M. Levis, *Targeting FLT3 to treat leukemia.* Expert Opin Ther Targets, 2015. **19**(1): p. 37-54.